frontiers | Research Topics

Multimodal management of advanced gastric cancer.

Edited by
Pankaj Kumar Garg, Andreas Brandl and Luigi Marano

Published in
Frontiers in Oncology

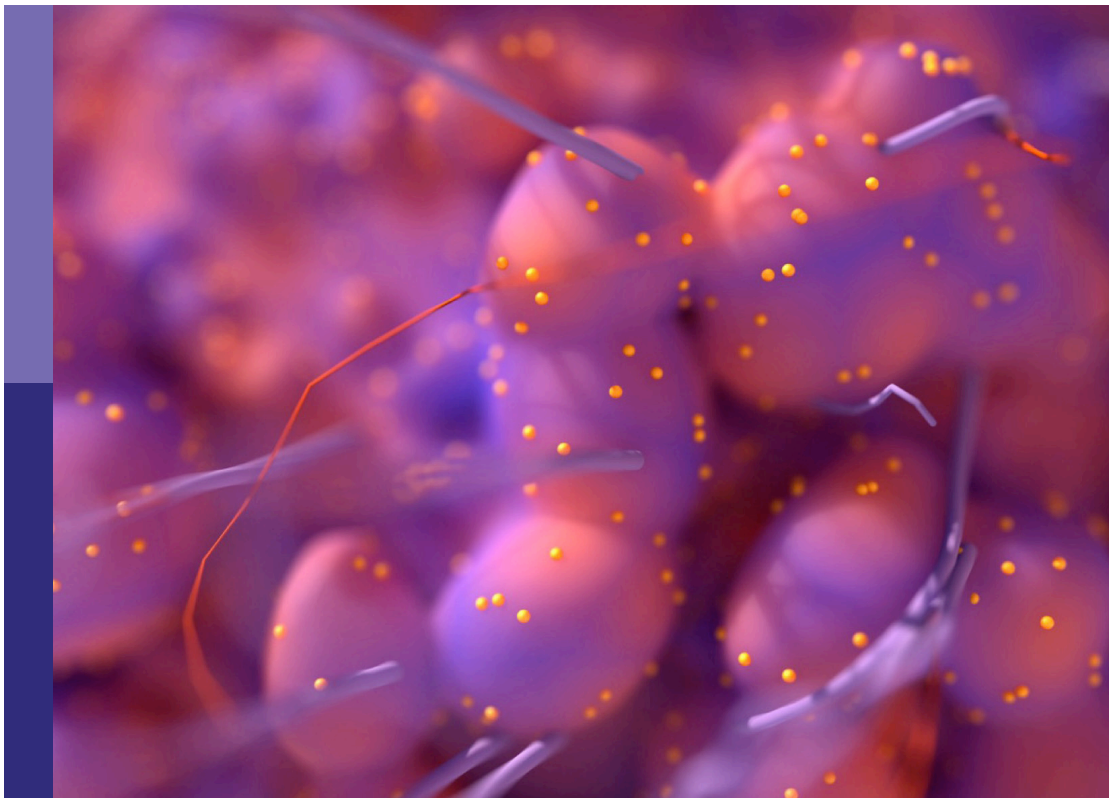

FRONTIERS EBOOK COPYRIGHT STATEMENT

The copyright in the text of individual articles in this ebook is the property of their respective authors or their respective institutions or funders. The copyright in graphics and images within each article may be subject to copyright of other parties. In both cases this is subject to a license granted to Frontiers.

The compilation of articles constituting this ebook is the property of Frontiers.

Each article within this ebook, and the ebook itself, are published under the most recent version of the Creative Commons CC-BY licence. The version current at the date of publication of this ebook is CC-BY 4.0. If the CC-BY licence is updated, the licence granted by Frontiers is automatically updated to the new version.

When exercising any right under the CC-BY licence, Frontiers must be attributed as the original publisher of the article or ebook, as applicable.

Authors have the responsibility of ensuring that any graphics or other materials which are the property of others may be included in the CC-BY licence, but this should be checked before relying on the CC-BY licence to reproduce those materials. Any copyright notices relating to those materials must be complied with.

Copyright and source acknowledgement notices may not be removed and must be displayed in any copy, derivative work or partial copy which includes the elements in question.

All copyright, and all rights therein, are protected by national and international copyright laws. The above represents a summary only. For further information please read Frontiers' Conditions for Website Use and Copyright Statement, and the applicable CC-BY licence.

ISSN 1664-8714
ISBN 978-2-83251-319-4
DOI 10.3389/978-2-83251-319-4

About Frontiers

Frontiers is more than just an open access publisher of scholarly articles: it is a pioneering approach to the world of academia, radically improving the way scholarly research is managed. The grand vision of Frontiers is a world where all people have an equal opportunity to seek, share and generate knowledge. Frontiers provides immediate and permanent online open access to all its publications, but this alone is not enough to realize our grand goals.

Frontiers journal series

The Frontiers journal series is a multi-tier and interdisciplinary set of open-access, online journals, promising a paradigm shift from the current review, selection and dissemination processes in academic publishing. All Frontiers journals are driven by researchers for researchers; therefore, they constitute a service to the scholarly community. At the same time, the *Frontiers journal series* operates on a revolutionary invention, the tiered publishing system, initially addressing specific communities of scholars, and gradually climbing up to broader public understanding, thus serving the interests of the lay society, too.

Dedication to quality

Each Frontiers article is a landmark of the highest quality, thanks to genuinely collaborative interactions between authors and review editors, who include some of the world's best academicians. Research must be certified by peers before entering a stream of knowledge that may eventually reach the public - and shape society; therefore, Frontiers only applies the most rigorous and unbiased reviews. Frontiers revolutionizes research publishing by freely delivering the most outstanding research, evaluated with no bias from both the academic and social point of view. By applying the most advanced information technologies, Frontiers is catapulting scholarly publishing into a new generation.

What are Frontiers Research Topics?

Frontiers Research Topics are very popular trademarks of the *Frontiers journals series*: they are collections of at least ten articles, all centered on a particular subject. With their unique mix of varied contributions from Original Research to Review Articles, Frontiers Research Topics unify the most influential researchers, the latest key findings and historical advances in a hot research area.

Find out more on how to host your own Frontiers Research Topic or contribute to one as an author by contacting the Frontiers editorial office: frontiersin.org/about/contact

Multimodal management of advanced gastric cancer.

Topic editors

Pankaj Kumar Garg — Shri Guru Ram Rai Institute of Medical and Health Sciences, India

Andreas Brandl — Charité Universitätsmedizin Berlin, Germany

Luigi Marano — University of Siena, Italy

Citation

Garg, P. K., Brandl, A., Marano, L., eds. (2023). *Multimodal management of advanced gastric cancer*. Lausanne: Frontiers Media SA. doi: 10.3389/978-2-83251-319-4

Table of contents

06 Editorial: Multimodal management of advanced gastric cancer
Pankaj Kumar Garg, Andreas Brandl and Luigi Marano

09 Neoadjuvant Chemotherapy *Versus* Direct Surgery for Locally Advanced Gastric Cancer With Serosal Invasion (cT4NxM0): A Propensity Score-Matched Analysis
Wei Xu, Lingquan Wang, Chao Yan, Changyu He, Sheng Lu, Zhentian Ni, Zichen Hua, Zhenglun Zhu, Birendra Kumar Sah, Zhongyin Yang, Yanan Zheng, Runhua Feng, Chen Li, Xuexin Yao, Mingmin Chen, Wentao Liu, Min Yan and Zhenggang Zhu

20 Is D2 Lymphadenectomy Alone Suitable for Gastric Cancer With Bulky N2 and/or Para-Aortic Lymph Node Metastases After Preoperative Chemotherapy?
Wei Xu, Wentao Liu, Lingquan Wang, Changyu He, Sheng Lu, Zhentian Ni, Zichen Hua, Zhenglun Zhu, Birendra Kumar Sah, Zhongyin Yang, Yanan Zheng, Runhua Feng, Chen Li, Xuexin Yao, Mingmin Chen, Chao Yan, Min Yan and Zhenggang Zhu

29 ^{18}F-FDG PET/CT Radiomics for Preoperative Prediction of Lymph Node Metastases and Nodal Staging in Gastric Cancer
Qiufang Liu, Jiaru Li, Bowen Xin, Yuyun Sun, Dagan Feng, Michael J. Fulham, Xiuying Wang and Shaoli Song

41 Extracellular Matrix Characterization in Gastric Cancer Helps to Predict Prognosis and Chemotherapy Response
Zhi Yang, Feifei Xue, Minhuan Li, Xingya Zhu, Xiaofeng Lu, Chao Wang, En Xu, Xingzhou Wang, Liang Zhang, Heng Yu, Chuanfu Ren, Hao Wang, Yizhou Wang, Jie Chen, Wenxian Guan and Xuefeng Xia

56 Comprehensive Analysis of IGFBPs as Biomarkers in Gastric Cancer
Qi Liu, Jianwu Jiang, Xiefu Zhang, Meixiang Zhang and Yang Fu

68 Long-Term Efficacy of Neoadjuvant Concurrent Chemoradiotherapy for Potentially Resectable Advanced Siewert Type II and III Adenocarcinomas of the Esophagogastric Junction
Yuan Tian, Jun Wang, Xueying Qiao, Jun Zhang, Yong Li, Liqiao Fan, Zhidong Zhang, Xuefeng Zhao, Bibo Tan, Dong Wang, Peigang Yang and Qun Zhao

78 The Impact of Tumor Mutation Burden on the Effect of Frontline Trastuzumab Plus Chemotherapy in Human Epidermal Growth Factor Receptor 2-Positive Advanced Gastric Cancers
Hye Ryeon Kim, Soomin Ahn, Hyunji Jo, Hongsik Kim, Joohyun Hong, Jeeyun Lee, Ho-Yeong Lim, Won Ki Kang and Seung Tae Kim

84 A Recombinant Human Adenovirus Type 5 (H101) Combined With Chemotherapy for Advanced Gastric Carcinoma: A Retrospective Cohort Study
Ran Zhang, Yanxin Cui, Xin Guan and Xiangjun Jiang

93 OncoVee™-MiniPDX-Guided Anticancer Treatment for Gastric Cancer Patients With Synchronous Liver Metastases: A Retrospective Cohort Analysis
Yutong Ge, Xin Zhang, Wei Liang, Cuiju Tang, Dongying Gu, Junfeng Shi and Xiaowei Wei

104 The Value of Perioperative Chemotherapy for Patients With Hepatoid Adenocarcinoma of the Stomach Undergoing Radical Gastrectomy
Kai Zhou, Anqiang Wang, Jingtao Wei, Ke Ji, Zhongwu Li, Xin Ji, Tao Fu, Ziyu Jia, Xiaojiang Wu, Ji Zhang and Zhaode Bu

113 Identification of a Four-Gene-Based SERM Signature for Prognostic and Drug Sensitivity Prediction in Gastric Cancer
Xiya Jia, Bing Chen, Ziteng Li, Shenglin Huang, Siyuan Chen, Runye Zhou, Wanjing Feng, Hui Zhu and Xiaodong Zhu

129 A Nomogram for Predicting the Risk of Radiotherapy-Related Esophageal Fistula in Esophageal Cancer Patients
Zhongxuan Gui, Huiquan Liu, Weijiong Shi, Yuechen Xu, Han Qian and Fan Wang

138 Case Report: Durable Clinical Response to Third-Line Pyrotinib After Resistance to Trastuzumab in a Gastric Cancer Patient
Junyi Wu, Lei Li, Jun Qin, Zhengqing Yan, Shiqing Chen, Tao Jin and Junming Xu

142 Superiority of Laparoscopic Gastrojejunostomy Combined With Multimodality Therapy for Gastric Outlet Obstruction Caused by Advanced Gastric Cancer
Chuandong Wang, Xiaojuan Zhang, Shengtao Lin, Changshun Yang, BiaoHuan Zhou, Yulong Mi, Rong Ye, Yifan Chen, Weijie Chen, Xiaojun Lin, Song Tan, Yuhang Zhou and Weihua Li

150 Identifying Prognostic Markers From Clinical, Radiomics, and Deep Learning Imaging Features for Gastric Cancer Survival Prediction
Degan Hao, Qiong Li, Qiu-Xia Feng, Liang Qi, Xi-Sheng Liu, Dooman Arefan, Yu-Dong Zhang and Shandong Wu

161 The Value of Whole-Tumor Histogram and Texture Analysis Using Intravoxel Incoherent Motion in Differentiating Pathologic Subtypes of Locally Advanced Gastric Cancer
Huan-Huan Li, Bo Sun, Cong Tan, Rong Li, Cai-Xia Fu, Robert Grimm, Hui Zhu and Wei-jun Peng

173 ω-3 and ω-6 Polyunsaturated Fatty Acids Regulate the Proliferation, Invasion and Angiogenesis of Gastric Cancer Through COX/PGE Signaling Pathway
Jiachi Ma, Chensong Zhang, Wanqing Liang, Lei Li, Jun Du, Chengwu Pan, Bangling Chen, Yuzhong Chen and Yuanpeng Wang

185 Comparison of the Efficacy of D2 Gastrectomy Plus Liver Radiofrequency Combined With Chemotherapy Versus Chemotherapy Alone in the Treatment of Advanced Gastric Cancer With Unresectable Synchronous Liver Metastases: A Multicenter Randomized Controlled Trial Protocol
Weidong Wang, Ruiqi Gao, Pengfei Yu, Zhenchang Mo, Danhong Dong, Xisheng Yang, Xiaohua Li and Gang Ji

194 Laparoscopic Gastrectomy for Cancer: Cut Down Complications to Unveil Positive Results of Minimally Invasive Approach
Milos Bjelovic, Milan Veselinovic, Dragan Gunjic, Zoran Bukumiric, Tamara Babic, Radmila Vlajic and Dario Potkonjak

203 Comparison of Treatment Efficacy and Survival Outcomes Between Asian and Western Patients With Unresectable Gastric or Gastro-Esophageal Adenocarcinoma: A Systematic Review and Meta-Analysis
Zhening Zhang, Zining Liu and Zeyang Chen

214 Conversion Surgery in Gastric Cancer Carcinomatosis
Paolo Morgagni, Leonardo Solaini, Luca Saragoni, Manlio Monti, Martina Valgiusti, Giovanni Vittimberga, Giovanni Luca Frassineti, Massimo Framarini and Giorgio Ercolani

220 Cost-Effectiveness of Nivolumab Plus Chemotherapy vs. Chemotherapy as First-Line Treatment for Advanced Gastric Cancer/Gastroesophageal Junction Cancer/Esophagel Adenocarcinoma in China
Yamin Shu, Yufeng Ding and Qilin Zhang

230 Patterns of Multimodality Management of Gastric Cancer—Single Institutional Experience of 372 Cases From a Tertiary Care Center in North India
Sunil Kumar, Naveen Kumar, Suryanarayana Deo, Sandeep Bhoriwal, Amitabha Mandal, Atul Sharma, Sushmita Pathy, Prasenjit Das, Sanjay Thulkar and Sushma Bhatnagar

238 Gastric Cancer With Peritoneal Metastasis—A Comprehensive Review of Current Intraperitoneal Treatment Modalities
Aruna Prabhu, Deepti Mishra, Andreas Brandl and Yutaka Yonemura

251 Cost-effectiveness analysis of nivolumab combination therapy in the first-line treatment for advanced esophageal squamous-cell carcinoma
Shixian Liu, Lei Dou, Kaixuan Wang, Zhao Shi, Ruixue Wang, Xiaohong Zhu, Zehua Song and Shunping Li

263 The prognostic role of circulating tumor cells in gastric cancer: A meta-analysis
Zuxi Li, Meijuan Song, Shangjun Han, Chuanwei Jin and Jing Yang

frontiers | Frontiers in Oncology

TYPE Editorial
PUBLISHED 29 December 2022
DOI 10.3389/fonc.2022.1113856

Check for updates

OPEN ACCESS

EDITED AND REVIEWED BY
Liang Qiao,
Westmead Institute for Medical Research, Australia

*CORRESPONDENCE
Pankaj Kumar Garg
dr.pankajgarg@gmail.com
Andreas Brandl
Andreas.Brandl@charite.de
Luigi Marano
luigi.marano@unisi.it

SPECIALTY SECTION
This article was submitted to Gastrointestinal Cancers: Gastric and Esophageal Cancers, a section of the journal Frontiers in Oncology

RECEIVED 01 December 2022
ACCEPTED 05 December 2022
PUBLISHED 29 December 2022

CITATION
Garg PK, Brandl A and Marano L (2022) Editorial: Multimodal management of advanced gastric cancer.
Front. Oncol. 12:1113856.
doi: 10.3389/fonc.2022.1113856

COPYRIGHT
© 2022 Garg, Brandl and Marano. This is an open-access article distributed under the terms of the Creative Commons Attribution License (CC BY). The use, distribution or reproduction in other forums is permitted, provided the original author(s) and the copyright owner(s) are credited and that the original publication in this journal is cited, in accordance with accepted academic practice. No use, distribution or reproduction is permitted which does not comply with these terms.

Editorial: Multimodal management of advanced gastric cancer

Pankaj Kumar Garg[1]*, Andreas Brandl[2]* and Luigi Marano[3]*

[1]Department of Surgical Oncology, Shri Guru Ram Rai Institute of Medical and Health Sciences, Dehradun, India, [2]Department of Surgery, Charité - Universitätsmedizin Berlin, Berlin, Germany, [3]Department of Medicine, Surgery, and Neurosciences, University of Siena, Siena, Italy

KEYWORDS

gastric cancer, gastrectomy, neoadjuvant chemotherapy, peritoneal metastases, HIPEC (heated intraperitoneal chemotherapy), adenocarcinoma

Editorial on the Research Topic
Multimodal management of advanced gastric cancer

As per the GLOBOCAN 2020 data, Gastric cancer is the fifth most common cancer and is the fourth major cause of cancer related death worldwide (1). The sheer magnitude of the gastric cancer cases has compelled the researchers across the globe to perform extensive research to demystify its etiopathogenesis to management strategies. As editors of the Research Topic on "*multimodality management of gastric cancer*", we enjoyed this academic journey of assessing a wide variety of submitted research articles.

The incidence and treatment of gastric cancer significantly varies across the globe. East-west divide is perhaps most apparent in the management of gastric cancer. While west has uniformly adopted the neoadjuvant chemotherapy (NACT) for local advanced gastric cancer (LAGC), many centres in the east still practice upfront surgery in all operable non-metastatic LAGC followed by adjuvant chemotherapy. Which multimodal treatment is best? Based on a Propensity Score-Matched analysis of 902 patients, Xu et al. concluded that NACT leads to improved overall survival and disease free survival without compromising the postoperative outcomes. In a large retrospective analysis of 372 patients treated between 1994 to 2021 in tertiary care centre in India, Kumar et al. highlighted that multimodality treatment is warranted in LAGC. Though there was an expected heterogeneity in the neoadjuvant/adjuvant strategies, the authors reported a 3-year disease-free survival and overall survival of 36.2% and 67.8% - the 5-year disease-free survival and overall survival were 30.1% and 37.7% after a follow-up of 50.16 months. The extent of surgery has been controversial in the locally advanced gastric cancer (2), especially in those patients who achieve good response following NACT. Xu et al. advocated that addition of para-aortic lymphadenectomy to standard gastrectomy improves survival in patients who had pre-NACT para-aortic metastasis. Moreover, tumour histology largely affects surgical approach concerning the extent of lymphadenectomy. Recent studies comparing D2 with D3 dissection in a clinical setting including both prophylactic and curative super-extended dissections, showed

that D3 offers a better locoregional control in advanced LAGC with diffuse histotype compared to D2 (10.1016/j.ejso.2015.01.023). However, D3 lymphadenectomy should only be performed in dedicated high-volume hospitals, due to the high risk of post-operative complications and mortality (10.1016/j.ejso.2010.03.008).

Recent improvements in surgical techniques – and locoregional control of peritoneal metastasis (PM) including hyperthermic intraperitoneal chemotherapy (HIPEC) and pressurized intra-peritoneal chemotherapy (PIPAC), as well as systemic chemotherapy has led to a paradigm change in the management of gastric cancer with PM (3, 4). Prabhu et al. presented a lucid and comprehensive review of various currently available intra-peritoneal treatment options; it generates a new hope for those patients with gastric cancer with PM, who once used to have dismal long-term survival. As the systemic chemotherapy continues to evolve, the benefit of adding surgery in a subgroup of metastatic gastric cancer (MGC) with isolated PM is being widely debated. In a retrospective series of 118 patients with MGC, who had isolated PM without any distant metastasis treated in a single centre in Italy, Morgagni et. al. reported impressive survival data in patients who had surgery plus HIPEC following systemic chemotherapy; the median OS was 60.4 months (9.2–60.4) in patients who had a complete response compared to a median OS 31.2 (15.8–64.0) who had a partial response.

Hepatoid adenocarcinoma of the stomach (HAS) is a rare type of gastric cancer that secretes alpha fetoprotein (AFP). Being a rare tumor, the management guidelines for HAS are not uniform. Zhou et al. analyzed 100 patients of HAS and concluded that upfront surgery followed by adjuvant chemotherapy seems an appropriate management strategy.

In order to further push the boundaries to improve survival in MGC with synchronous unresectable liver metastasis, Wang et al. submitted their protocol for a RCT to determine if addition of D2 gastrectomy plus radiofrequency ablation of liver lesions to systemic chemotherapy provide benefits to these patients compared to chemotherapy alone. The researchers have planned a multicentric trial with a large sample size of 200 patients. To open up another treatment frontier for gastric cancer, Zhang et al. evaluated the clinical outcomes of Human Adenovirus Type 5 (H101) combined with chemotherapy for advanced gastric carcinoma (GC) patients. Though the sample size was small, the authors highlighted that addition of H101 to chemotherapy leads to a significantly better disease control rate and overall rates compared to chemotherapy or H101 therapy alone. It definitely calls for further trials to assess if oncolytic virus therapy has a significant therapeutic potential in the management of gastric cancer.

Disease relapse – both loco-regional and systemic - is a major concern in the minds of both oncologists and patients prior to instituting the treatment. A number of clinic-pathological factors and disease stage helps us determine the chances of treatment failures. Li et al. performed a meta-analysis to evaluate the relationship between circulating tumor cells (CTC) and the prognosis of patients with gastric cancer. The meta-analysis included 14 retrospective cohort studies with 1053 patients and concluded that positive CTC suggest a poorer prognosis compared to those with CTC-negative tumors (HR=2.12, 95%CI 1.37, 3.29, P=0.0007).

A number of biomarkers are being studied all over the world for prognostication in gastric cancer. Insulin-like growth-factor-binding proteins (IGFBPs) play important roles in tumor occurrence and development by prolonging the half-life of the IGFs, controlling their access to IGF receptors (IGFRs), and promoting or inhibiting IGF downstream signaling pathways. There are two types of IGFBPs based on their different affinities for IGFs: high-affinity binding proteins (IGFBP1–6) and low-affinity binding proteins (IGFBP7–10). In a bioinformatic analysis study, Liu et al. described the involvement of IGFBPs, especially IGFBP7, in gastric cancer development through the extracellular matrix.

Financial toxicity of the treatment is another road-block in the optimum management of cancers including gastric cancer. Any oncological intervention must either lead to improvement in longevity or quality of life or both. Moreover, it must be cost effective as well so that the financial burden of the treatment for unknown/minimal benefit does not lead to bankruptcy of the caregivers destroying their social, emotional, family, and personal lives. Shu et al. evaluated the cost-effectiveness of nivolumab plus chemotherapy vs. chemotherapy as first-line therapy in patients with advanced gastric cancer/gastroesophageal junction cancer/esophageal adenocarcinoma from the perspective of the Chinese healthcare system. Their economic evaluation showed that the incremental effectiveness and cost of nivolumab plus chemotherapy versus chemotherapy alone were 0.28 QALYs and $78,626.53, resulting in an incremental cost-effectiveness ratio of $278,658.71/QALY which was much higher than the willingness-to-pay (WTP) threshold of China ($31,498.70/QALY). The authors highlighted that Nivolumab plus chemotherapy was clearly not a cost-effective treatment strategy compared with chemotherapy as first-line therapy for patients with advanced gastric cancer/gastroesophageal junction cancer/esophageal adenocarcinoma in China at current prices.

Though Trastuzumab for Gastric Cancer Trial established the role of Trastuzumab for Her2 positive gastric cancer, the benefit was marginal - 2.7 months in the overall median survival (HR 0.74, 95% CI 0.60–0.91; p value.0046) (5). In a study of 31 HER2-positive AGC patients who were treated with trastuzumab plus chemotherapy as first-line therapy for recurrent (n=8) or metastatic (n=23) tumors, Kim et al. correlated tumor mutation burden (TMB) with tumor response. The authors found that high TMB was associated with a favourable response rate compared to low TMB (75.0%, n=3/4 versus 59.3%, n=16/27).

We believe that the current research addressing all aspects of gastric cancer seems promising and provides hope for thousands of patients who are diagnosed with gastric cancer worldwide.

Author contributions

PG wrote the initial manuscript draft. AB and LM gave critical inputs. All the authors read the final manuscript and approved it for publication.

Acknowledgments

We thank the authors of the papers published in this Research Topic for their valuable contributions and the referees for their rigorous review. We are also thankful to Dr Kiran Turaga, Division Chief of Surgical Oncology in the Department of Surgery at Yale Cancer Center for his contribution to the initial planning of this Research Topic.

Conflict of interest

The authors declare that the research was conducted in the absence of any commercial or financial relationships that could be construed as a potential conflict of interest.

Publisher's note

All claims expressed in this article are solely those of the authors and do not necessarily represent those of their affiliated organizations, or those of the publisher, the editors and the reviewers. Any product that may be evaluated in this article, or claim that may be made by its manufacturer, is not guaranteed or endorsed by the publisher.

References

1. Garg PK, Jakhetiya A, Turaga KK, Kumar R, Brandl A, Rau B. Lack of oncological benefit from bursectomy in radical gastrectomy: A systematic review. *Visc Med* (2021) 37:511–20. doi: 10.1159/000517654

2. Garg PK, Jakhetiya A, Sharma J, Ray MD, Pandey D. Lymphadenectomy in gastric cancer: Contentious issues. *World J Gastrointest Surg* (2016) 8:294–300. doi: 10.4240/wjgs.v8.i4.294

3. Alberto M, Brandl A, Garg PK, Gül-Klein S, Dahlmann M, Stein U, et al. Pressurized intraperitoneal aerosol chemotherapy and its effect on gastric-cancer-derived peritoneal metastases: an overview. *Clin Exp Metastasis* (2019) 36:1–14. doi: 10.1007/s10585-019-09955-4

4. Garg PK, Jara M, Alberto M, Rau B. The role of pressurized IntraPeritoneal aerosol chemotherapy in the management of gastric cancer: A systematic review. *Pleura Peritoneum* (2019) 4:20180127. doi: 10.1515/pp-2018-0127

5. Garg PK, Jain BK. New cancer drugs at the cost of bankruptcy: will the oncologist tell the patients the benefit in terms of days/weeks added to life? *Oncologist* (2014) 19:1291. doi: 10.1634/theoncologist.2014-0263

frontiers in Oncology

ORIGINAL RESEARCH
published: 23 August 2021
doi: 10.3389/fonc.2021.718556

Neoadjuvant Chemotherapy *Versus* Direct Surgery for Locally Advanced Gastric Cancer With Serosal Invasion (cT4NxM0): A Propensity Score-Matched Analysis

Wei Xu†, Lingquan Wang†, Chao Yan†, Changyu He, Sheng Lu, Zhentian Ni, Zichen Hua, Zhenglun Zhu, Birendra Kumar Sah, Zhongyin Yang, Yanan Zheng, Runhua Feng, Chen Li, Xuexin Yao, Mingmin Chen, Wentao Liu, Min Yan* and Zhenggang Zhu**

Department of General Surgery, Shanghai Key Laboratory of Gastric Neoplasms, Shanghai Institute of Digestive Surgery, Ruijin Hospital, Shanghai Jiao Tong University School of Medicine, Shanghai, China

OPEN ACCESS

Edited by:
Andreas Brandl, Champalimaud Foundation, Portugal

Reviewed by:
Philipp Gehwolf, Medical University of Innsbruck, Austria
Alexander R. Novotny, Technical University of Munich, Germany
Ana Catarina Freitas, Champalimaud Foundation, Portugal

***Correspondence:**
Zhenggang Zhu
zzg1954@hotmail.com
Min Yan
ym10299@163.com
Wentao Liu
owenliu@sjtu.edu.cn

†These authors have contributed equally to this work

Specialty section:
This article was submitted to Gastrointestinal Cancers, a section of the journal Frontiers in Oncology

Received: *01 June 2021*
Accepted: *02 August 2021*
Published: *23 August 2021*

Citation:
Xu W, Wang L, Yan C, He C, Lu S, Ni Z, Hua Z, Zhu Z, Sah BK, Yang Z, Zheng Y, Feng R, Li C, Yao X, Chen M, Liu W, Yan M and Zhu Z (2021) Neoadjuvant Chemotherapy Versus Direct Surgery for Locally Advanced Gastric Cancer With Serosal Invasion (cT4NxM0): A Propensity Score-Matched Analysis. Front. Oncol. 11:718556. doi: 10.3389/fonc.2021.718556

Background: For locally advanced gastric cancer (LAGC) with serosal invasion (cT4NxM0), adjuvant chemotherapy (AC) after D2 gastrectomy is the standard therapy in Asia. However, perioperative chemotherapy (PCT) combined with D2 gastrectomy is mostly suggested in Europe and America. As a part of PCT, the value of neoadjuvant chemotherapy (NAC) is unclear. We investigated whether NAC could further improve survival and other outcomes for these patients.

Methods: Patients with cT4NxM0 gastric cancer who underwent D2 gastrectomy were analyzed. The patients were divided into two groups based on whether they received NAC: the neoadjuvant chemotherapy (NAC) and direct surgery (S) groups. After propensity score matching (1:1 ratio), survival and perioperative outcomes were analyzed between the two groups.

Results: A total of 902 patients met all the eligibility criteria and were enrolled. After propensity score matching, 221 matched pairs of patients were identified. The median overall survival (OS) and disease-free survival (DFS) of all patients were 75.10 and 43.67 months, respectively. The median OS of patients in the NAC and S groups were undefined and 29.80 months, respectively (P<0.0001). The median DFS of patients in the NAC and S groups were undefined and 22.60 months (P<0.0001). There were no significant differences in the radical degrees of operation between the two groups (P=0.07). However, there were significant differences in postoperative hospital stay (P<0.001) and complications (P=0.037) between the two groups.

Conclusion: This study suggested NAC can further improve prognosis and prevent recurrence in LAGC (cT4NxM0) patients. NAC is feasible and safe for LAGC (cT4NxM0) patients, and does not increase the risk of perioperative surgery.

Keywords: neoadjuvant chemotherapy, perioperative chemotherapy, locally advanced gastric cancer, gastrectomy, propensity score matching, real-world study

INTRODUCTION

Gastric cancer (GC) is one of the most common malignant tumors worldwide, with a high incidence and mortality rate. GC is the fifth most common cancer and the third leading cause of cancer-related deaths worldwide (1). In China, GC is the second most common cancer and the second leading cause of cancer death (2). Different stages of GC have different biological behaviors, treatment strategies and prognoses. For early gastric cancer (EGC), the primary treatment option is surgery (3–7). For advanced gastric cancer (AGC) with distant metastasis, comprehensive treatment based on systemic antitumor therapy is recommended to prolong the survival and improve the quality of life of patients (8–10). For locally advanced gastric cancer (LAGC), over the past few decades, the standard therapy has been D2 gastrectomy followed by adjuvant chemotherapy (AC), which was confirmed by several randomized controlled trials (RCTs) to improve disease-free survival (DFS) and overall survival (OS) compared with surgery alone (11, 12). The ACTS-GC and CLASSIC studies showed that AC with S-1 or XELOX could improve OS and DFS in patients with LAGC who had undergone curative D2 gastrectomy (11–14).

In recent years, more attention has been given to perioperative chemotherapy (PCT). PCT was widely accepted until a series of RCTs were performed to evaluate its value (15–17). The MAGIC trial was the first to show a survival benefit of surgery combined with PCT. The MAGIC trial showed that PCT with the ECF regimen decreased tumor size and stage and improved PFS and OS in patients with LAGC (15). However, less than 50% patients in the MAGIC trial underwent a D2 resection. Another RCT study (FNCLCC & FFCD trial) showed that PCT could increase the curative resection rate, DFS and OS in patients with LAGC (16). The two trials showed that PCT, on the basis of surgery, could further increase the 5-year OS rate by approximately 13~14% in LAGC. However, as a part of PCT, the value of neoadjuvant chemotherapy (NAC) in improving OS and DFS is unclear. It is unknown whether PCT is better than AC for LAGC patients who undergo D2 gastrectomy.

NAC is performed preoperatively and could result in disease progression during treatment. Although NAC has some theoretical advantages (15), it is unknown whether NAC could further improve the survival of LAGC on the basis of D2 gastrectomy followed by AC. Therefore, there are two ongoing RCTs addressing this issue, which were reported at the European Society for Medical Oncology (ESMO) 2019 conference. The PRODIGY study showed that the 3-year and 5-year DFS rates in the NAC (NAC + surgery + AC) group were significantly higher than those in the S (surgery +AC) group (18). The RESOLVE study showed that PCT improved the 3-year DFS rate compared with AC alone (19). In summary, PCT, the combination of AC and NAC, could increase the 3-year DFS rate by approximate 6~7% in LAGC compared with AC alone.

However, the value of NAC itself for LAGC patients in improving OS has not been reported. In China, NAC has not been used for all LAGC patients. Currently, NAC is mainly used in LAGC with serosal invasion (cT4NxM0). Therefore, we conducted our study to investigate whether the addition of NAC can further improve OS and other outcomes of LAGC (cT4NxM0) patients.

MATERIALS AND METHODS

Patient Selection

From our electronic medical record system which included all patients admitted to our gastric cancer professional group, we investigated 3228 patients with primary gastric cancer and without a history of other malignancies at Ruijin Hospital (Shanghai Jiao Tong University School of Medicine, Shanghai, China) between January 2013 and December 2018. The inclusion criteria were as follows: (1) pathologically proven gastric adenocarcinoma by gastroscopy before any treatment, (2) patients aged under 80 years old at their first gastroscopy, (3) patients without any antitumor therapy, (4) patients who provided consent for our treatment, (5) patients with pretreatment CT in our hospital, (6) patients with serosal invasion and without distant metastasis (cT4NxM0), (7) patients with no digestive tract obstruction, (8) patients with no active gastrointestinal bleeding, and (9) patients who underwent D2 gastrectomy and AC. Patients with clinical T stage 1~3, distant metastases, or changes in therapy regimen or without gastrectomy and AC were excluded from our study. According to whether the patients received NAC, all enrolled patients were divided into two groups: the NAC (NAC + surgery + AC) and S (surgery + AC) groups. The main difference between the two groups was the presence or absence of NAC.

In our database, we collected some pre-treatment information of patients, including sex, age, body mass index (BMI), hemoglobin, platelet, leukocyte, pre-albumin, total protein, albumin, blood tumor indicators (CA125, CA199, CA724, CEA, AFP), tumor differentiation, signet ring cell carcinoma component, Borrmann type and clinical TNM stage. Considering that there may be differences in baseline characteristics between the NAC and S groups, we performed propensity score matching analysis to match the NAC group to the S group at a ratio of 1:1.

Besides, we also collected some information during and after treatment, including therapy regimen, radical degrees of operation, postoperative complications, postoperative hospital stay, pathological TNM stage, disease recurrence time and death time. The radical degrees of operation were classified into three degrees: R0, macroscopically complete surgical resection with negative microscopic margins; R1, macroscopically complete surgical resection with positive microscopic margins; R2; macroscopically incomplete surgical resection.

This study was performed with the approval of the Ethics Committee of Ruijin Hospital affiliated to Shanghai Jiao Tong University School of Medicine. All patients were enrolled after signing an informed consent form.

Neoadjuvant Chemotherapy

In the NAC group, patients received NAC before D2 gastrectomy followed by AC. We performed NAC based on the guidelines of the National Comprehensive Cancer Network (NCCN) and Chinese Society of Clinical Oncology (CSCO). Due to the progress of new RCT research, the guidelines and NAC regimens have also changed over time. Even so, NAC regimens

are still based on the combination of 5-fluorouracil (5-FU) and platinum drugs, such as EOX (Epirubicin, Oxaliplatin and Capecitabine), XELOX (Oxaliplatin and Capecitabine), SOX (Oxaliplatin and S-1) and FLOT (Docetaxel, Oxaliplatin, Fluorouracil, and Leucovorin). All patients in the NAC group received average 3~4 cycles NAC. Before each cycle of NAC, patients were tested for hematological indicators, including blood routine, liver function, renal function, electrolyte, DIC and tumor markers.

Evaluation of Neoadjuvant Chemotherapy

There are two methods to evaluate the response to NAC in LAGC: imaging and pathology. Before surgery, the response to NAC can be assessed by imaging evaluation criteria. The most commonly used imaging evaluation criteria is the Response Evaluation Criteria In Solid Tumor (RECIST 1.1) (20), in which the response to NAC is divided into four grades: complete response (CR), partial response (PR), stable disease (SD), and progressive disease (PD).

After surgery, we assessed the response to NAC in the NAC group through pathological evaluation criterion. The tumor regression grade (TRG) system is an effective pathology evaluation criterion. There are several TRG systems used to assess the tumor pathological response to NAC, including the Mandard, Ninomiya, Becker and Ryan classification systems (21–24). In our study, we used the Ryan classification system, which is the most widely applied by the College of American Pathologists (CAP) and the Chinese Society of Clinical Oncology (CSCO), to assess the pathological response of tumors to NAC (8, 25). The TRG classification system is divided into four categories: grade 0 (complete response: no viable cancer cells), grade 1 (moderate response: single cells or small groups of cancer cells), grade 2 (minimal response: residual cancer outgrown by fibrosis) and grade 3 (poor response: minimal or no tumor cells killed; extensive residual cancer).

Surgery

For all enrolled patients in both the NAC and S groups, we performed D2 gastrectomy. All surgery were performed by the same surgical team of the gastric cancer specialized group in Ruijin hospital. The range of gastric resection and the method of reconstruction were determined by the patient's tumor location. Distal gastrectomy was the first choice for distal gastric cancer, and Billroth I stomach-duodenal anastomosis, Billroth II stomach-jejunal anastomosis or Roux-en-Y stomach-jejunal anastomosis could be used for reconstruction. Total gastrectomy was the first choice for proximal gastric cancer, and Roux-en-Y esophagus-jejunal anastomosis was used for reconstruction. No prophylactic splenectomy is performed in either distal gastrectomy or total gastrectomy. If the primary tumor involves spleen, transverse colon, pancreas, left liver and other organs around the stomach, combined organ resection should be decided by the same surgical team. Postoperative complications were graded using the Clavien-Dindo Complications Classification (CDCC) (26). In this study, postoperative complications of grade III or above were recorded.

Adjuvant Chemotherapy and Follow-Up

All patients received postoperative adjuvant chemotherapy. All chemotherapy regimens were based on NCCN and CSCO guidelines. There was no significant difference in chemotherapy regimens between the two NAC and S groups. The regimens of AC were basically based on 5-FU and platinum drugs.

Follow-Up

We followed up with the patients through outpatient visits and telephone calls. Outpatient follow-up mainly included physical examination, hematological examination, multidetector computed tomography (MDCT) and gastroscopy. Magnetic resonance imaging (MRI) and positron emission tomography/computed tomography (PET/CT) scan were additionally performed when necessary. Telephone follow-up was conducted almost every three months within two years after surgery. After two years, telephone follow-up was conducted every 6 months. The date of death and the first relapse were recorded. The primary endpoint of this study was the overall survival (OS). Disease-free survival (DFS) was the secondary endpoint. OS was measured from the date of initial diagnosis of gastric cancer to the date of death or the last follow-up. DFS was defined as the time from the date of D2 gastrectomy to the recurrence of gastric cancer or the last follow-up.

Statistical Analysis

To analyze the significance of enumeration data, chi-square test was used. For the measurement data, t-tests or the Mann-Whitney rank tests were used. Based on the differences between the NAC and S groups, we performed propensity score matching analysis to match the NAC group to the S group at a ratio of 1:1. We performed an exact match for region and used 2% caliper matching for the propensity score for the other variables. The Kaplan-Meier method was used to generate survival curves and analyze OS and DFS. All statistical tests were two-tailed, and the differences were statistically significant at $P<0.05$. Analyses were performed with SPSS version 26.0 (IBM Statistical Product and Service Solutions, Armonk, USA). GraphPad Prism version 8.0 (GraphPad, San Diego, CA, USA) was used to draw the survival curve and to calculate the survival rate and the median survival time.

RESULTS

Characteristics of the Patients

From January 2013 to December 2018, a total of 902 patients satisfied all the eligibility criteria and 2326 patients were excluded from the study (**Figure 1**). The last follow-up date was 30 August 2020, and the median follow-up time was 73.28 months (range 0.40 - 93.50 months). Of the 902 patients, 375 patients (41.57%) had died of GC, and 455 patients had experienced recurrence (50.44%) by the last follow-up day. A total of 51 (5.65%) patients were lost during the follow-up period. Of all eligible patients, 285 patients (31.60%) received NAC, and 617 patients (68.40%)

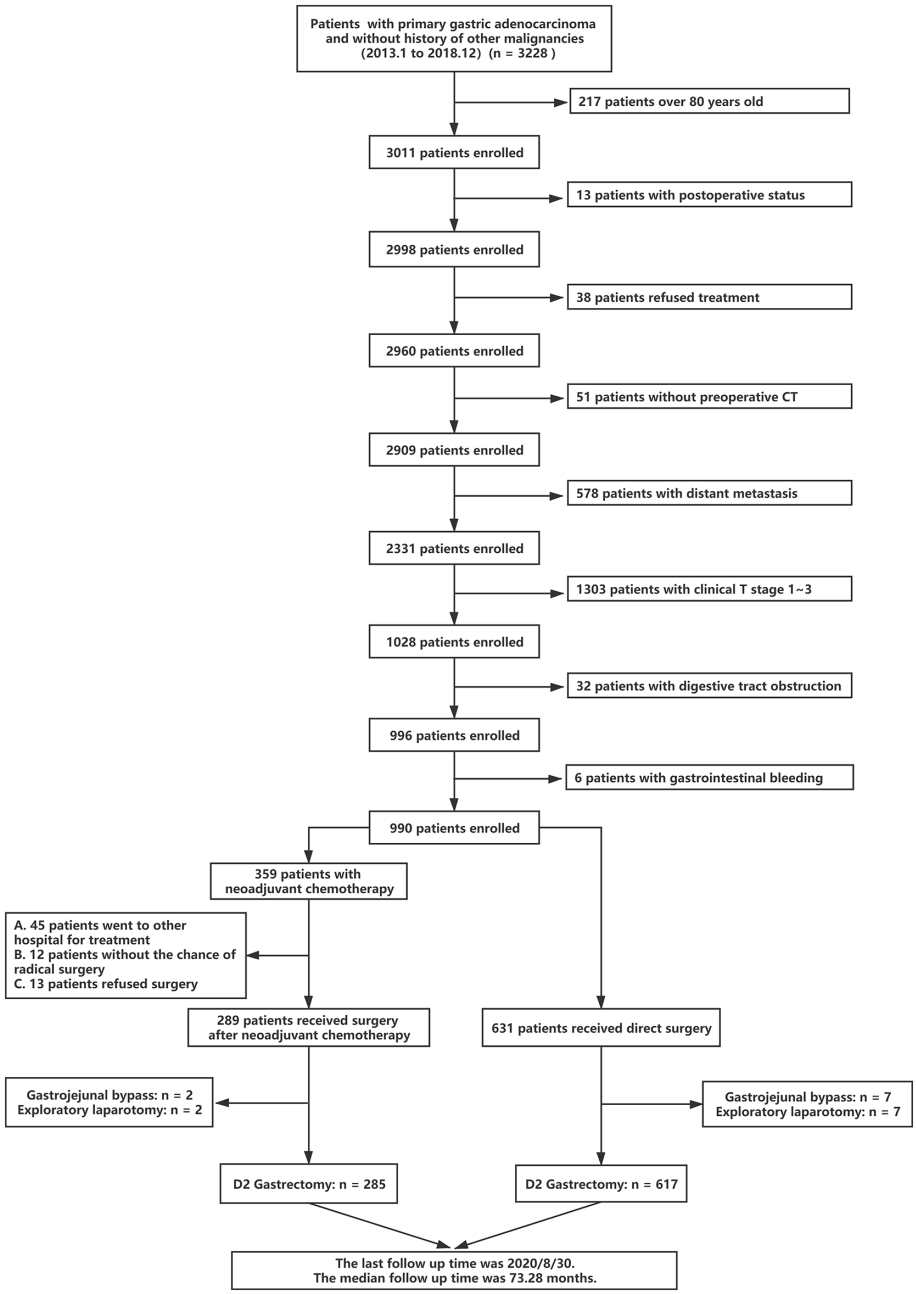

FIGURE 1 | Flowchart of patient selection process.

underwent D2 gastrectomy followed by AC alone. The pretreatment clinical characteristics of the 902 patients are summarized in **Table 1**. Between the NAC and S groups, several baseline characteristics had significant differences (P<0.05), including platelet, albumin, CA125, CA724, CEA, tumor differentiation, signet ring cell carcinoma component, Borrmann type and clinical N stage (**Table 1**). Three tumor markers (CA125, CA724 and CEA) in the NAC group were significantly higher than those in the S group (P<0.01). In the NAC group, there were 269 (94.39%) patients with Borrmann III/IV, which was significantly more than that in the S group (544, 88.17%, P<0.01). Regarding clinical N stage, in the NAC group, there were 61 (21.40%) patients with N0-1 stage disease, 139 (48.77%) patients with N2 stage disease and 85 (29.82%) patients with N3 stage disease. In the S group, there were 343 (55.59%) patients with N0-1 stage, 227 (36.79%) patients with N2 stage and 47 (7.62%) patients with N3 stage. These significant differences showed that patients in the NAC group experienced a

TABLE 1 | Pretreatment clinical characteristics of LAGC (cT4NxM0) patients before 1:1 matched.

Characteristics	Total (N = 902)	NAC (n = 285)	S (n = 617)	P
Sex (n[%])				0.050*
Male	618 (68.51)	208 (72.98)	410 (66.45)	
female	284 (31.49)	77 (27.02)	207 (33.55)	
Age (y)				0.624§
Median (range)	62 (21-80)	63 (21-80)	62 (26-80)	
BMI (kg/m^2)				0.358#
Median (range)	22.80 (13.97-33.20)	22.91 (14-33.20)	22.72 (13.97-32.89)	
Hemoglobin (g/L)				0.446§
Median (range)	124 (44-184)	123 (44-164)	124 (45-184)	
Leukocyte (10^9/L)				0.200§
Median(range)	5.70 (2.20-16.90)	5.70 (2.40-16.90)	5.70 (2.20-14.93)	
Platelet (10^9/L)				0.034§
Median (range)	216 (41-924)	223 (82-924)	211 (41-754)	
Prealbumin (g/L)				0.192*
Median (range)	208 (67-388)	206 (79-354)	211 (67-388)	
Total Protein (g/L)				0.990§
Median (range)	65 (41-82)	64 (46-78)	65 (41-82)	
Albumin (g/L)				0.040§
Median (range)	37 (21-48)	37 (21-47)	37 (21-48)	
CA125 (U/mL)				0.001§
Median (range)	10.90 (1.20-601.80)	12.10 (2.19-314.10)	10.25 (1.20-601.80)	
CA199 (U/mL)				0.646§
Median (range)	8.20 (0.80-20830)	8 (0.80-7424)	8.20 (0.80-20830)	
CA724 (U/mL)				0.005§
Median (range)	2.33 (0.06-300)	3.19 (0.06-300)	2.14 (0.20-300)	
CEA (ng/mL)				0.002§
Median (range)	2.24 (0.50-1803.83)	2.42 (0.50-1400.45)	2.16 (0.50-1803.83)	
AFP (ng/mL)				0.760§
Median (range)	2.55 (0.50-10783.52)	2.54 (0.65-10783.52)	2.56 (0.50-9017.75)	
Differentiation (n[%])				0.002*
Well	332 (36.81)	126 (44.21)	206 (33.39)	
poor	570 (63.19)	159 (55.79)	411 (66.61)	
Signet ring cell (n[%])				<0.001*
Yes	304 (33.70)	60 (21.05)	244 (39.55)	
No	598 (66.30)	225 (78.95)	373 (60.45)	
Borrmann (n[%])				0.004*
I/II	89 (9.87)	16 (5.61)	73 (11.83)	
III/IV	813 (90.13)	269 (94.39)	544 (88.17)	
cN stage (n[%])				<0.001*
0-1	404 (44.79)	61 (21.40)	343 (55.59)	
2	366 (40.58)	139 (48.77)	227 (36.79)	
3	132 (14.63)	85 (29.82)	47 (7.62)	

*χ^2 test (compares the counts of categorical responses between 2 or more independent groups).
§Mann-Whitney rank test (a nonparametric alternative to the 2 sample t test compares the means of 2 independent groups).
#T test (compare the means of 2 independent groups).

heavier tumor burden and advanced disease, which were associated with poor prognosis and could affect the OS and DFS of patients (27, 28). On the other hand, there were more well-differentiated tumors in the NAC group than the S group (44.21% *vs* 33.39%, P<0.01). In addition, there were fewer patients with signet ring cell carcinoma components in the NAC group than in the S group (21.05% *vs* 39.55%, P<0.001). It seemed that patients in the NAC group had better tumor differentiation which was considered to be associated with a better response to chemotherapy (29).

Propensity Score Matching Analysis

Owing to the differences in baseline characteristics between the NAC and S groups, we performed propensity score matching analysis to match the NAC group to the S group at a ratio of 1:1. There were 18 baseline parameters used for propensity score matching, including sex, age, BMI, hemoglobin, platelet, leukocyte, pre-albumin, total protein, albumin, CA125, CA199, CA724, CEA, AFP, tumor differentiation, signet ring cell carcinoma component, Borrmann type and clinical N stage. After propensity score match analysis, 221 matched pairs of patients were identified. There were no significant differences between the two groups. The comparison of the two groups is shown in **Table 2**. Between the 221 matched pairs of patients, there were 331 males and 111 females, with a male-to-female ratio of 2.98:1. The median age at diagnosis was 62.50 (range: 21-80) years. In the NAC group, 148 (66.97%) and 73 (33.03%) patients achieved PR and SD, respectively. In addition, twenty

TABLE 2 | Pre-treatment clinical characteristics of LAGC (cT4NxM0) patients after 1:1 matched.

Characteristics	Total (N = 442)	NAC (n = 221)	S (n = 221)	P
Sex (n[%])				0.443*
Male	331 (74.89)	162 (73.30)	169 (76.47)	
female	111 (25.11)	59 (26.70)	52 (23.53)	
Age (y)				0.350§
Median (range)	62.50 (21-80)	63 (21-80)	61 (36-80)	
BMI (kg/m^2)				0.741#
Median (range)	22.90 (14-33.20)	22.84 (14-33.20)	22.99 (14.98-31.59)	
Hemoglobin (g/L)				0.413§
Median (range)	123 (44-173)	125 (44-164)	121 (45-173)	
Leukocyte (10^9/L)				0.251§
Median(range)	5.80 (2.30-16.90)	5.70 (2.70-16.90)	5.80 (2.30-14.93)	
Platelet (10^9/L)				0.311§
Median (range)	218.50 (56-875)	216 (88-875)	226 (56-754)	
Prealbumin (g/L)				0.247#
Median (range)	206.50 (92-366)	203 (118-340)	212 (92-366)	
Total Protein (g/L)				0.953§
Median (range)	64 (41-82)	64 (46-77)	64 (41-82)	
Albumin (g/L)				0.712§
Median (range)	37 (21-48)	37 (21-47)	37 (21-48)	
CA125 (U/mL)				0.111§
Median (range)	10.95 (2.19-465.20)	11.60 (2.19-314.10)	10.40 (2.90-465.20)	
CA199 (U/mL)				0.488§
Median (range)	9.45 (0.80-7424)	8.70 (0.80-7424)	10.1 (0.80-3842.20)	
CA724 (U/mL)				0.419§
Median (range)	2.83 (0.46-300)	3.36 (0.46-300)	2.43 (0.66-300)	
CEA (ng/mL)				0.356§
Median (range)	2.40 (0.50-1400.45)	2.42 (0.50-1400.45)	2.38 (0.50-930.43)	
AFP (ng/mL)				0.326§
Median (range)	2.60 (0.77-9017.75)	2.46 (0.90-3220.19)	2.66 (0.77-9017.75)	
Differentiation (n[%])				0.702*
Well	196 (44.34)	100 (45.25)	96 (43.44)	
poor	246 (55.66)	121 (54.75)	125 (56.56)	
Signet ring cell (n[%])				0.586*
Yes	113 (25.57)	54 (24.43)	59 (26.70)	
No	329 (74.43)	167 (75.57)	162 (73.30)	
Borrmann (n[%])				0.208*
I/II	24 (5.43)	15 (6.79)	9 (4.07)	
III/IV	418 (94.57)	206 (93.21)	212 (95.93)	
cN stage (n[%])				0.742*
0-1	118 (26.70)	57 (25.79)	61 (27.60)	
2	244 (55.20)	126 (57.01)	118 (53.39)	
3	80 (18.10)	38 (17.19)	42 (19.01)	

*χ^2 test (compares the counts of categorical responses between 2 or more independent groups).
§Mann-Whitney rank test (a nonparametric alternative to the 2 sample t test compares the means of 2 independent groups).
#T test (compare the means of 2 independent groups).

patients obtained TRG 0 grade. For the regimens of NAC, 142 patients received EOX, 59 received SOX, 4 received XELOX, and 16 received FLOT.

Survival Analysis

Among the 442 matched patients, after a median follow-up of 53.25 months, 172 patients (38.91%) had died of gastric cancer and 206 patients had experienced disease recurrence (46.61%) by the last follow-up day. There were 66 and 140 patients with disease recurrence in the NAC and S groups, respectively. The details of the recurrence sites which were first found had been shown in **Table 3**. A total of 26 (5.88%) patients were lost during the follow-up period. The median overall survival of the patient population was 75.10 months (**Figure 2A**), and the median disease-free survival was 43.67 months (**Figure 2B**). The median OS of patients in the NAC and S groups was undefined and 29.80 months, respectively (P<0.0001, HR 0.34, 95% CI 0.25–0.46, **Figure 2C**). The 1-year, 3-year, and 5-year OS rates for patients in the NAC group were 93.59%, 78.82% and

TABLE 3 | Details of first recurrence site.

First Recurrence Site	Total (N = 206)	NAC (n = 66)	S (n = 140)
Local recurrence (n[%])	10 (4.85)	5 (7.58)	5 (3.57)
Distant recurrence (n[%])			
Peritoneal	149 (72.33)	42 (63.64)	107 (76.43)
Liver	17 (8.25)	7 (10.61)	10 (7.14)
Systemic lymph node	9 (4.37)	4 (6.06)	5 (3.57)
Ovarian	4 (1.94)	1 (1.52)	3 (2.14)
Bone	2 (0.97)	0 (0.00)	2 (1.43)
Multiple organs	15 (7.28)	7 (10.61)	8 (5.71)

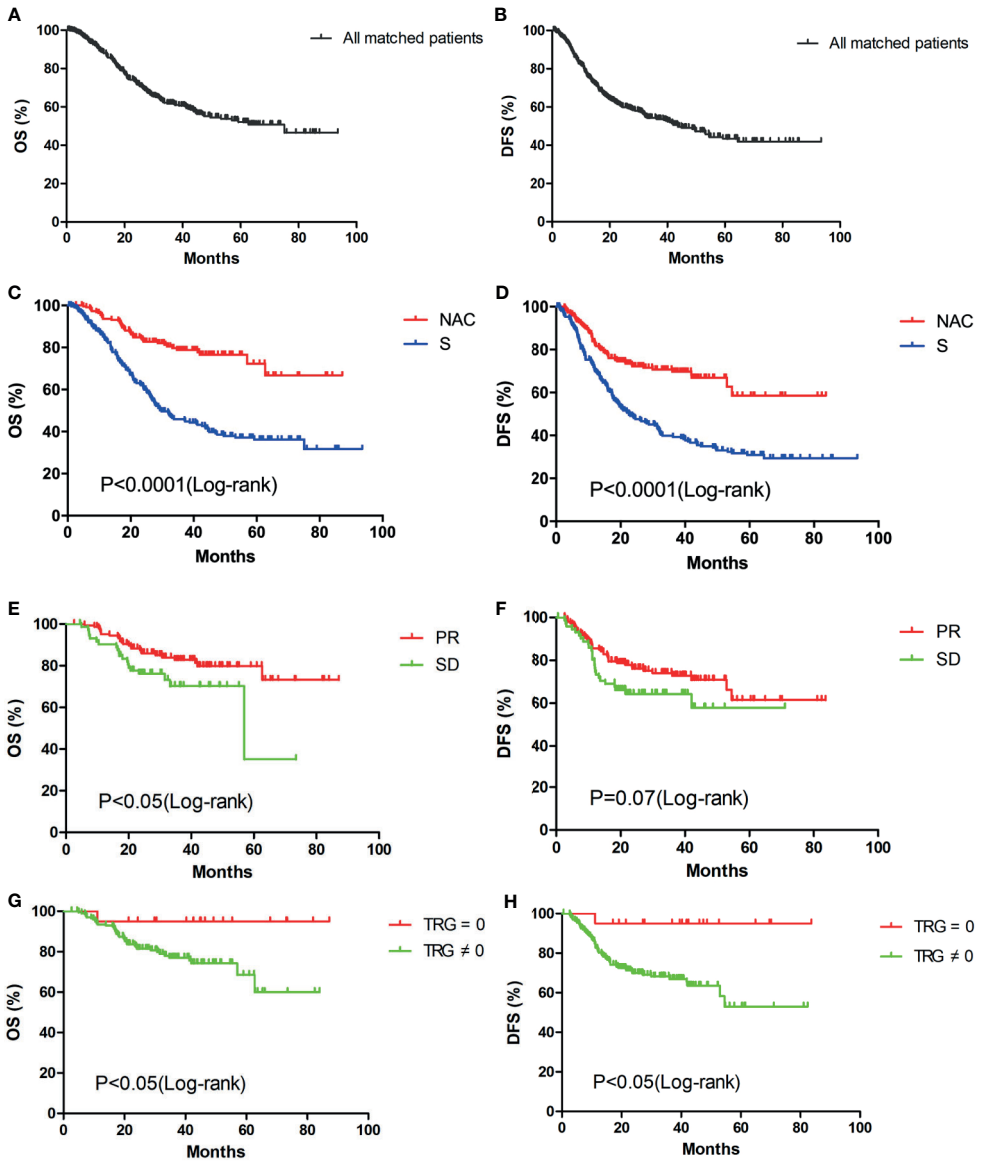

FIGURE 2 | Kaplan-Meier survival curves of overall survival and disease-free survival: OS **(A)** and DFS **(B)**analysis of all matched patients (n=442); OS **(C)** and DFS **(D)** analysis of patients in the NAC (n=221) and S (n=221) groups; OS **(E)** and DFS **(F)** analysis of patients in the PR (n=148) and SD (n=73) groups; OS **(G)** and DFS **(H)** analysis of patients in the TRG = 0 (n=20) and TRG ≠0 (n=201) groups.

72.29%, respectively. For patients in the S group, the 1-year, 3-year, and 5-year OS rates were 83.71%, 45.90% and 36.22%, respectively. In addition, the median DFS of patients in the NAC and S groups was undefined and 22.60 months, respectively (P<0.0001, HR 0.44, 95% CI 0.33 - 0.58, **Figure 2D**). The 1-year, 3-year, and 5-year DFS rates for patients in the NAC group were 82.53%, 69.74% and 58.53%, respectively. For patients in the S group, the 1-year, 3-year, and 5-year DFS rates were 70.44%, 39.86% and 30.87%, respectively.

Of all 902 patients, no patient achieved CR, and only 1 patient achieved PD after NAC. During propensity score matching, the PD patient in the NAC group was not matched in the S group. Therefore, according to the RECIST standard, 148 (66.97%) and 73 (33.03%) patients in the NAC group achieved PR and SD, respectively. We compared the survival between the PR and SD groups. The median OS of patients in the PR and SD groups was undefined and 56.97 months, respectively (P<0.05, **Figure 2E**). The 1-year, 3-year, and 5-year OS rates for patients in the PR group were 95.21%, 82.81% and 79.82%, respectively. For patients in the SD group, the 1-year, 3-year, and 5-year OS rates were 90.28%, 70.19% and 35.09%, respectively. The median DFS for PR and SD patients was undefined and was not significantly different (P=0.07, **Figure 2F**). The 1-year, 3-year, and 5-year DFS rates for patients in the PR group were 85.66%, 72.78% and 61.45%, respectively.

For patients in the SD group, the 1-year, 3-year, and 5-year DFS rates were 76.12%, 64.27% and 57.84%, respectively. Based on the TRG, 20 (9.05%) patients in the NAC group had TRG 0 grade. Significant differences in OS (P<0.05, **Figure 2G**) and DFS were observed between the TRG=0 and TRG ≠ 0 groups (P<0.05, **Figure 2H**). The 1-year, 3-year, and 5-year OS and DFS rates for patients in the TRG=0 group were all 95.00%. For patients in the TRG ≠ 0 group, the 1-year, 3-year, and 5-year OS rates were 93.45%, 77.02% and 68.57%, respectively. The 1-year, 3-year, and 5-year DFS rates were 81.27%, 66.98% and 53.03%, respectively.

Analysis of Perioperative Outcomes

In the NAC and S groups, 208 (94.12%) and 197 (89.14%) patients underwent R0 resection, respectively. In addition, 10 (4.52%) patients received R1 resection, and 3 (1.36%) patients received R2 resection in the NAC group. In the S group, 13 (5.88%) and 11 (4.98%) patients underwent R1 and R2 resection, respectively. The median of dissected lymph nodes numbers in the NAC and S groups were 34 and 38, respectively. There were no significant differences in the radical degrees of operation and numbers of dissected lymph nodes between the two groups (P=0.07 and P=0.124, **Table 4**).

Considering the postoperative hospital stays and postoperative complications, there were significant differences between the NAC and S groups (P<0.05, **Table 4**). The median postoperative hospital stays were 11 and 13 days in the NAC and S groups, respectively. The shortest postoperative hospital stay for both groups was 7 days. The longest postoperative hospital stays for the NAC and S groups were 68 and 75 days, respectively. The patient with a postoperative hospital stays of 68 days experienced intraperitoneal hemorrhage and underwent a second operation for hemostasis. The patient with a postoperative hospital stays of 75 days experienced anastomotic leakage, which was improved by conservative treatment.

From the perspective of postoperative complications, 15 (6.79%) patients in the NAC group experienced complications after the operation. Two patients underwent a second surgery due to the complications of anastomotic leakage and intraperitoneal hemorrhage. In the S group, 28 (12.67%) patients experienced postoperative complications. Four patients underwent a second surgery to treat complications, including anastomotic leakage, intraperitoneal hemorrhage, intestinal obstruction and pancreatic fistula. Details of the postoperative complications are given in **Table 5**.

DISCUSSION

Currently, the standard treatment for LAGC (cT4NxM0) is a combination of D2 gastrectomy and PCT. The chemotherapy regimens have changed over time. In the past decade, based on the results of MAGIC (15) and REAL-2 (30) studies, EOX had been the main NAC regimen in this study. In recent years, the German scholars advocated FLOT regimen (17, 31). Nowadays, FLOT has been recommended for NAC at a higher level than ECF and its modifications (8). Besides, SOX and XELOX are recommended at the same level as FLOT (Evidence 2A) (8). However, as a part of PCT, the value of NAC in improving OS and DFS is unclear. Therefore, we carried out this study to investigate this topic in China. In our study, a total of 902 patients were eligible for participation. The patients were divided into the following two groups according to whether they received NAC: the NAC (n=285) and S (n=617) groups. All patients underwent D2 gastrectomy and AC. The statistical analysis showed that there were several significant differences in the baseline characteristics between the two groups (**Table 1**). Because of these significant differences at baseline, we conducted propensity score matching (1:1 ratio) to

TABLE 5 | Details of the postoperative complications.

Postoperative Complications	NAC (n=15)	S (n=28)
Incision infection	3	3
Anastomotic leakage	3	9
Duodenal stump fistula	1	1
Pancreatic fistula	1	1
Lymphatic fistula	1	0
Intra-abdominal infection	2	1
Intraperitoneal hemorrhage	1	3
Gastroparesis	1	0
Intestinal obstruction	0	3
Anastomotic stenosis	1	0
Pleural effusion	1	1
Pulmonary infection	0	4
Deep venous thrombosis	0	2

TABLE 4 | Comparison of perioperative outcomes between NAC and S Groups after 1:1 matched.

Characteristics	Total (N = 442)	CSC (n = 221)	SC (n = 221)	P
Radical degrees (n[%])				0.072*
R0	405 (91.63)	208 (94.12)	197 (89.14)	
R1	23 (5.20)	10 (4.52)	13 (5.88)	
R2	14 (3.17)	3 (1.36)	11 (4.98)	
No. of dissected lymph nodes				0.124§
Median (range)	36 (0-121)	34 (0-104)	38 (9-121)	
Postoperative hospital stays (d)				<0.001§
Median (range)	12 (7-75)	11 (7-68)	13 (7-75)	
Postoperative complications (n[%])				0.037*
Yes	43 (9.73)	15 (6.79)	28 (12.67)	
No	399 (90.27)	206 (93.21)	193 (87.33)	

*χ^2 test (compares the counts of categorical responses between 2 or more independent groups).
§Mann-Whitney rank test (a nonparametric alternative to the 2 sample t test compares the means of 2 independent groups).

minimize the differences in underlying confounding factors between the two groups.

After propensity score matching, we obtained 221 matched pairs of patients and there were no significant differences between the NAC and S groups (P>0.05, **Table 2**). In the Kaplan-Meier analysis, the survival curve showed that the OS and DFS rates of patients in the NAC group were significantly higher than those in the S group (P<0.0001, **Figures 2C, D**). Compared to those patients in the S group, the 1-year, 3-year, and 5-year OS rates for patients in the NAC group were increased by 9.88%, 32.92% and 36.07%, respectively. The 1-year, 3-year, and 5-year DFS rates for patients in the NAC group were also increased by 12.09%, 29.88% and 27.66%, respectively. We consider that the difference in survival between the two groups is due to whether or not NAC was used. NAC can promote tumor downstaging, eliminate potential micrometastasis, and improve patients' prognosis. In our study, the 3-year DFS rate for patients in the NAC group was similar to the results in the PRODIGY (18) and RESOLVE (19) studies (69.74% *vs* 66.3% *vs* 62.02%). However, the 5-year OS rate for patients in the NAC group was significantly higher than that in the MAGIC (15) and FNCLCC & FFCD (16) trials (72.29% *vs* 36.6% *vs* 38%). The main reason for the difference in OS rate between studies may be the radical degrees of the operation. In our study, 94.12% of patients in the NAC group underwent R0 resection. In the MAGIC and FNCLCC & FFCD trials, only 69.3% and 84% of patients in the NAC groups obtained R0 resection, respectively.

In addition, subgroup analysis in the NAC group was conducted for further investigation. According to the RECIST, no one in the NAC group received CR in this study. Because it is difficult to distinguish a residual tumor from necrosis or fibrosis on imaging. Several patients received PD after NAC, but most of them did not receive surgery. One of the inclusion criteria in this study was that all patients received D2 gastrectomy. Therefore, only one PD patient was enrolled in this study, however this patient did not get matched during propensity score matching. Hence, survival was compared between PR and SD groups. The OS rate in the PR group was significantly higher than that in the SD group (P<0.05, **Figure 2E**) and no significant difference was found in the DFS rate between the two groups (P=0.07, **Figure 2F**). Compared with those for patients in the SD group, the 1-year, 3-year, and 5-year OS rates for patients in the PR group were increased by 4.93%, 12.62% and 44.73%, respectively. The OS and DFS rates in the PR and SD groups were all significantly higher than those in the S group (P<0.0001, **Figures 3A, B**). This result showed that patients

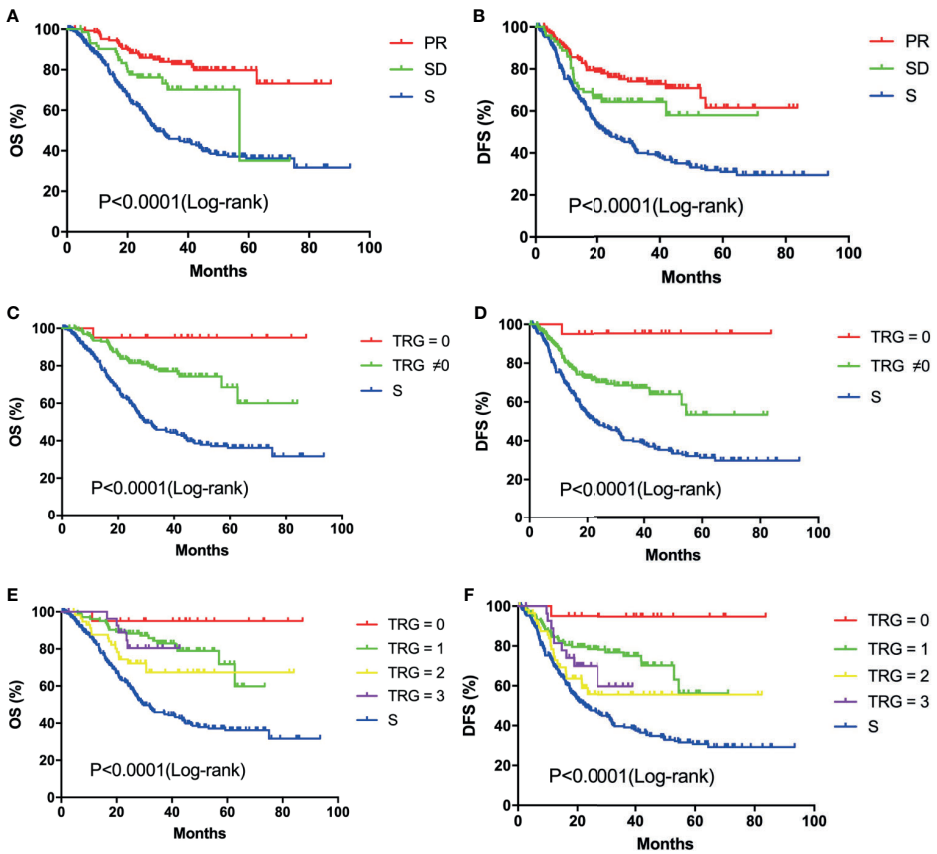

FIGURE 3 | Kaplan-Meier survival curves of overall survival and disease-free survival: OS **(A)** and DFS **(B)** analysis of patients in the PR (n=148), SD (n=73) and S (n=221) groups; OS **(C)** and DFS **(D)** analysis of patients in the TRG = 0 (n=20), TRG ≠0 (n=201) and S (n=221) groups; OS **(E)** and DFS **(F)** analysis of patients in the different TRG grade (0, n=20; 1, n=107; 2, n=62; 3, n=32) and S (n=221) groups;.

with LAGC who achieved a disease response or stable after NAC treatment could benefit from NAC.

In addition, survival analysis was conducted to compare the survival of patients in different TRG groups. Previous studies had shown that LAGC patients with a well TRG would have better survival than those with no response or minor pathologic changes (32, 33). TRG is considered as an important predictor of survival in LAGC. However, there are a lot of factors influencing patients' prognosis, such as the radical degree of surgery, adjuvant chemotherapy, postoperative complications and postoperative nutritional status. In this study, the OS and DFS rates of patients in the TRG=0 group were significantly higher than those in the TRG≠0 group ($P<0.05$, **Figures 2G, H**). For patients in the TRG=0 group, the 1-year, 3-year, and 5-year OS rates were improved by 1.55%, 17.98% and 26.43%, respectively, compared with those in the TRG≠0 group. The 1-year, 3-year, and 5-year DFS rates in the TRG=0 group were also increased by 13.73%, 28.02% and 41.97%, respectively. The OS and DFS rates in the different TRG grades were all significantly higher than those in the S group ($P<0.0001$, **Figures 3C–F**). This result suggested that better tumor regression in LAGC was associated with longer survival and lower rates of local recurrence.

When comparing perioperative outcomes between the NAC and S groups, the study showed that there was no significant difference in radical degrees of operation. However, patients in the NAC group had shorter postoperative hospital stays and lower postoperative complications than patients in the S group. This may be associated with improved nutritional status and reduced tumor burden after NAC, which are beneficial to postoperative recovery.

In conclusion, the results of our study showed that NAC can further improve prognosis and prevent recurrence in LAGC (cT4NxM0) patients. NAC is feasible and safe for LAGC (cT4NxM0) patients and does not increase the risk of perioperative surgery. Because our study is a retrospective study, it has certain limitations. A larger sample size of prospective, randomized, controlled clinical trial is necessary for the validation of this result.

DATA AVAILABILITY STATEMENT

The raw data supporting the conclusions of this article will be made available by the authors, without undue reservation.

ETHICS STATEMENT

The studies involving human participants were reviewed and approved by the Ethics Committee of Ruijin Hospital affiliated to Shanghai Jiao Tong University School of Medicine. The patients/participants provided their written informed consent to participate in this study.

AUTHOR CONTRIBUTIONS

WX conceived and designed the study, analyzed the data and wrote the paper. LW and CY participated in the design of the study and edited the final paper. CH, SL, ZN, ZH, ZLZ, BS, ZY, and YZ collected the clinicopathological factors of all patients. RF, CL, XY, and MC followed up the patient's survival status. WL revised the paper. MY and ZGZ gave professional guidance. All authors contributed to the article and approved the submitted version.

FUNDING

This work was supported by National Natural Science Foundation of China (NO. 81772518) and Multicenter Clinical Trial of Shanghai Jiao Tong University School of Medicine (DLY201602 and 2018CR003).

REFERENCES

1. Bray F, Ferlay J, Soerjomataram I, Siegel R, Torre L, Jemal A. Global Cancer Statistics 2018: GLOBOCAN Estimates of Incidence and Mortality Worldwide for 36 Cancers in 185 Countries. *CA: Cancer J Clin* (2018) 68 (6):394–424. doi: 10.3322/caac.21492
2. Chen W, Zheng R, Baade P, Zhang S, Zeng H, Bray F, et al. Cancer Statistics in China, 2015. *CA: Cancer J Clin* (2016) 66(2):115–32. doi: 10.3322/caac.21338
3. Isomoto H, Shikuwa S, Yamaguchi N, Fukuda E, Ikeda K, Nishiyama H, et al. Endoscopic Submucosal Dissection for Early Gastric Cancer: A Large-Scale Feasibility Study. *Gut* (2009) 58(3):331–6. doi: 10.1136/gut.2008.165381
4. Kim JJ, Lee JH, Jung HY, Lee GH, Cho JY, Ryu CB, et al. EMR for Early Gastric Cancer in Korea: A Multicenter Retrospective Study. *Gastrointest Endosc* (2007) 66(4):693–700. doi: 10.1016/j.gie.2007.04.013
5. Facciorusso A, Antonino M, Di Maso M, Muscatiello N. Endoscopic Submucosal Dissection *vs* Endoscopic Mucosal Resection for Early Gastric Cancer: A Meta-Analysis. *World J Gastrointest Endosc* (2014) 6(11):555–63. doi: 10.4253/wjge.v6.i11.555
6. Son T, Hyung WJ. Laparoscopic Gastric Cancer Surgery: Current Evidence and Future Perspectives. *World J Gastroenterol* (2016) 22(2):727–35. doi: 10.3748/wjg.v22.i2.727
7. Parisi A, Reim D, Borghi F, Nguyen NT, Qi F, Coratti A, et al. Minimally Invasive Surgery for Gastric Cancer: A Comparison Between Robotic, Laparoscopic and Open Surgery. *World J Gastroenterol* (2017) 23(13):2376–84. doi: 10.3748/wjg.v23.i13.2376
8. Wang FH, Shen L, Li J, Zhou ZW, Liang H, Zhang XT, et al. The Chinese Society of Clinical Oncology (CSCO): Clinical Guidelines for the Diagnosis and Treatment of Gastric Cancer. *Cancer Commun (Lond)* (2019) 39(1):10. doi: 10.1186/s40880-019-0349-9
9. Okines A, Verheij M, Allum W, Cunningham D, Cervantes AGroup EGW. Gastric Cancer: ESMO Clinical Practice Guidelines for Diagnosis, Treatment and Follow-Up. *Ann Oncol* (2010) 21 Suppl 5:v50–54. doi: 10.1093/annonc/mdq164
10. Ajani J, D'Amico T, Almhanna K, Bentrem D, Chao J, Das P, et al. Gastric Cancer, Version 3.2016, NCCN Clinical Practice Guidelines in Oncology. *J Natl Compr Cancer Network: JNCCN* (2016) 14(10):1286–312. doi: 10.6004/jnccn.2016.0137
11. Noh S, Park S, Yang H, Chung H, Chung I, Kim S, et al. Adjuvant Capecitabine Plus Oxaliplatin for Gastric Cancer After D2 Gastrectomy (CLASSIC): 5-Year Follow-Up of an Open-Label, Randomised Phase 3 Trial. *Lancet Oncol* (2014) 15(12):1389–96. doi: 10.1016/S1470-2045(14)70473-5
12. Sakuramoto S, Sasako M, Yamaguchi T, Kinoshita T, Fujii M, Nashimoto A, et al. Adjuvant Chemotherapy for Gastric Cancer With S-1, an Oral

Fluoropyrimidine. *New Engl J Med* (2007) 357(18):1810–20. doi: 10.1056/NEJMoa072252
13. Sasako M, Sakuramoto S, Katai H, Kinoshita T, Furukawa H, Yamaguchi T, et al. Five-Year Outcomes of a Randomized Phase III Trial Comparing Adjuvant Chemotherapy With S-1 *Versus* Surgery Alone in Stage II or III Gastric Cancer. *J Clin Oncol* (2011) 29(33):4387–93. doi: 10.1200/JCO.2011.36.5908
14. Bang YJ, Kim YW, Yang HK, Chung HC, Park YK, Lee KH, et al. Adjuvant Capecitabine and Oxaliplatin for Gastric Cancer After D2 Gastrectomy (CLASSIC): A Phase 3 Open-Label, Randomised Controlled Trial. *Lancet* (9813) 2012:315–21:379. doi: 10.1016/S0140-6736(11)61873-4
15. Cunningham D, Allum W, Stenning S, Thompson J, Van de Velde C, Nicolson M, et al. Perioperative Chemotherapy *Versus* Surgery Alone for Resectable Gastroesophageal Cancer. *New Engl J Med* (2006) 355(1):11–20. doi: 10.1056/NEJMoa055531
16. Ychou M, Boige V, Pignon J, Conroy T, Bouche O, Lebreton G, et al. Perioperative Chemotherapy Compared With Surgery Alone for Resectable Gastroesophageal Adenocarcinoma: An FNCLCC and FFCD Multicenter Phase III Trial. *J Clin oncology: Off J Am Soc Clin Oncol* (2011) 29 (13):1715–21. doi: 10.1200/JCO.2010.33.0597
17. Al-Batran S, Homann N, Pauligk C, Goetze T, Meiler J, Kasper S, et al. Perioperative Chemotherapy With Fluorouracil Plus Leucovorin, Oxaliplatin, and Docetaxel *Versus* Fluorouracil or Capecitabine Plus Cisplatin and Epirubicin for Locally Advanced, Resectable Gastric or Gastro-Oesophageal Junction Adenocarcinoma (FLOT4): A Randomised, Phase 2/3 Trial. *Lancet (London England)* (2019) 393(10184):1948–57. doi: 10.1016/S0140-6736(18)32557-1
18. Kang YK, Yook JH, Park YK, Kim YW, Kim J, Ryu MH, et al. Phase III Randomized Study of Neoadjuvant Chemotherapy (CT) With Docetaxel(D), Oxaliplatin(O) and S-1(S) (DOS) Followed by Surgery and Adjuvant S-1, *vs* Surgery and Adjuvant S-1, for Resectable Advanced Gastric Cancer (GC) (PRODIGY). *Ann Oncol* (2019) 30:v876–7. doi: 10.1093/annonc/mdz394.032
19. Ji J, Shen L, Li Z, Zhang X, Liang H, Xue Y, et al. Perioperative Chemotherapy of Oxaliplatin Combined With S-1 (SOX) *Versus* Postoperative Chemotherapy of SOX or Oxaliplatin With Capecitabine (XELOX) in Locally Advanced Gastric Adenocarcinoma With D2 Gastrectomy: A Randomized Phase III Trial (RESOLVE Trial). *Ann Oncol* (2019) 30:30. doi: 10.1093/annonc/mdz394.033
20. Eisenhauer E, Therasse P, Bogaerts J, Schwartz L, Sargent D, Ford R, et al. New Response Evaluation Criteria in Solid Tumours: Revised RECIST Guideline (Version 1.1). *Eur J Cancer (Oxford England: 1990)* (2009) 45(2):228–47. doi: 10.1016/j.ejca.2008.10.026
21. Mandard A, Dalibard F, Mandard J, Marnay J, Henry-Amar M, Petiot J, et al. Pathologic Assessment of Tumor Regression After Preoperative Chemoradiotherapy of Esophageal Carcinoma. Clinicopathologic Correlations. *Cancer* (1994) 73(11):2680–6. doi: 10.1002/1097-0142(19940601)73:11<2680::AID-CNCR2820731105>3.0.CO;2-C
22. Ninomiya Y, Yanagisawa A, Kato Y, Kitagawa T, Ishihara S, Nakajima T. Histological Indications of a Favorable Prognosis With Far-Advanced Gastric Carcinomas After Preoperative Chemotherapy. *J Cancer Res Clin Oncol* (1999) 125(12):699–706. doi: 10.1007/s004320050337
23. Becker K, Mueller J, Schulmacher C, Ott K, Fink U, Busch R, et al. Histomorphology and Grading of Regression in Gastric Carcinoma Treated With Neoadjuvant Chemotherapy. *Cancer* (2003) 98(7):1521–30. doi: 10.1002/cncr.11660
24. Ryan R, Gibbons D, Hyland J, Treanor D, White A, Mulcahy H, et al. Pathological Response Following Long-Course Neoadjuvant Chemoradiotherapy for Locally Advanced Rectal Cancer. *Histopathology* (2005) 47(2):141–6. doi: 10.1111/j.1365-2559.2005.02176.x
25. Chanjuan Shi M, Berlin J, Branton PA, Fitzgibbons PL, Frankel WL, Hofstetter WL, et al. Protocol for the Examination of Specimens From Patients With Carcinoma of the Stomach. *Coll Am Pathologists* (2020). Version: Stomach 4.1.0.0.
26. Dindo D, Demartines N, Clavien PA. Classification of Surgical Complications: A New Proposal With Evaluation in a Cohort of 6336 Patients and Results of a Survey. *Ann Surg* (2004) 240(2):205–13. doi: 10.1097/01.sla.0000133083.54934.ae
27. Song XH, Zhang WH, Kai L, Chen XL, Zhao LY, Chen XZ, et al. Prognostic Impact of Borrmann Classification on Advanced Gastric Cancer: A Retrospective Cohort From a Single Institution in Western China. *World J Surg Oncol* (2020) 18(1):204. doi: 10.1186/s12957-020-01987-5
28. Lazăr D, Tăban S, Dema A, Cornianu M, Goldis A, Ratiu I, et al. Gastric Cancer: The Correlation Between the Clinicopathological Factors and Patients' Survival (I). *Romanian J Morphol Embryol = Rev Roumaine Morphologie Embryologie* (2009) 50(1):41–50.
29. Wang L, Teng R, Jiang Z, Hu W, Dong M, Yuan X, et al. Clinicopathologic Variables Predicting Tumor Response to Neoadjuvant Chemotherapy in Patients With Locally Advanced Gastric Cancer. *J Surg Oncol* (2012) 105 (3):293–6. doi: 10.1002/jso.22085
30. Cunningham D, Starling N, Rao S, Iveson T, Nicolson M, Coxon F, et al. Capecitabine and Oxaliplatin for Advanced Esophagogastric Cancer. *N Engl J Med* (2008) 358(1):36–46. doi: 10.1056/NEJMoa073149
31. Al-Batran SE, Hofheinz RD, Pauligk C, Kopp HG, Haag GM, Luley KB, et al. Histopathological Regression After Neoadjuvant Docetaxel, Oxaliplatin, Fluorouracil, and Leucovorin *Versus* Epirubicin, Cisplatin, and Fluorouracil or Capecitabine in Patients With Resectable Gastric or Gastro-Oesophageal Junction Adenocarcinoma (FLOT4-AIO): Results From the Phase 2 Part of a Multicentre, Open-Label, Randomised Phase 2/3 Trial. *Lancet Oncol* (2016) 17(12):1697–708. doi: 10.1016/S1470-2045(16)30531-9
32. Neves Filho E, de Sant'Ana R, Nunes L, Pires A, da Cunha M. Histo pathological Regression of Gastric Adenocarcinoma After Neoadjuvant Therapy: A Critical Review. *APMIS: Acta pathologica microbiologica immunologica Scandinavica* (2017) 125(2):79–84. doi: 10.1111/apm.12642
33. Tomasello G, Petrelli F, Ghidini M, Pezzica E, Passalacqua R, Steccanella F, et al. Tumor Regression Grade and Survival After Neoadjuvant Treatment in Gastro-Esophageal Cancer: A Meta-Analysis of 17 Published Studies. *Eur J Surg oncology: J Eur Soc Surg Oncol Br Assoc Surg Oncol* (2017) 43(9):1607–16. doi: 10.1016/j.ejso.2017.03.001

Conflict of Interest: The authors declare that the research was conducted in the absence of any commercial or financial relationships that could be construed as a potential conflict of interest.

Publisher's Note: All claims expressed in this article are solely those of the authors and do not necessarily represent those of their affiliated organizations, or those of the publisher, the editors and the reviewers. Any product that may be evaluated in this article, or claim that may be made by its manufacturer, is not guaranteed or endorsed by the publisher.

Copyright © 2021 Xu, Wang, Yan, He, Lu, Ni, Hua, Zhu, Sah, Yang, Zheng, Feng, Li, Yao, Chen, Liu, Yan and Zhu. This is an open-access article distributed under the terms of the Creative Commons Attribution License (CC BY). The use, distribution or reproduction in other forums is permitted, provided the original author(s) and the copyright owner(s) are credited and that the original publication in this journal is cited, in accordance with accepted academic practice. No use, distribution or reproduction is permitted which does not comply with these terms.

frontiers in Oncology

ORIGINAL RESEARCH
published: 02 September 2021
doi: 10.3389/fonc.2021.709617

Check for updates

Is D2 Lymphadenectomy Alone Suitable for Gastric Cancer With Bulky N2 and/or Para-Aortic Lymph Node Metastases After Preoperative Chemotherapy?

Wei Xu†, Wentao Liu†, Lingquan Wang, Changyu He, Sheng Lu, Zhentian Ni, Zichen Hua, Zhenglun Zhu, Birendra Kumar Sah, Zhongyin Yang, Yanan Zheng, Runhua Feng, Chen Li, Xuexin Yao, Mingmin Chen, Chao Yan, Min Yan* and Zhenggang Zhu**

Department of General Surgery, Shanghai Key Laboratory of Gastric Neoplasms, Shanghai Institute of Digestive Surgery, Ruijin Hospital, Shanghai Jiao Tong University School of Medicine, Shanghai, China

OPEN ACCESS

Edited by:
Pankaj Kumar Garg, Shri Guru Ram Rai Institute of Medical and Health Sciences, India

Reviewed by:
Dharma Ram Poonia, All India Institute of Medical Sciences Jodhpur, India
Dillip Muduly, All India Institute of Medical Sciences Bhubaneswar, India
Tushar Mishra, All India Institute of Medical Sciences Bhubaneswar, India
Ashish Jakhetiya, Geetanjali Medical College, India
Madhabananda Kar, All India Institute of Medical Sciences Bhubaneswar, India

***Correspondence:**
Chao Yan
doctoryc@yeah.net
Min Yan
ym10299@163.com
Zhenggang Zhu
zzg1954@hotmail.com

†*These authors have contributed equally to this work*

Specialty section:
This article was submitted to Gastrointestinal Cancers, a section of the journal Frontiers in Oncology

Received: *14 May 2021*
Accepted: *16 August 2021*
Published: *02 September 2021*

Citation:
Xu W, Liu W, Wang L, He C, Lu S, Ni Z, Hua Z, Zhu Z, Sah BK, Yang Z, Zheng Y, Feng R, Li C, Yao X, Chen M, Yan C, Yan M and Zhu Z (2021) Is D2 Lymphadenectomy Alone Suitable for Gastric Cancer With Bulky N2 and/or Para-Aortic Lymph Node Metastases After Preoperative Chemotherapy? Front. Oncol. 11:709617. doi: 10.3389/fonc.2021.709617

Background: For gastric cancer (GC) with extensive lymph node metastasis (bulky N2 and/or para-aortic lymph node metastases), there is no standard therapy worldwide. In Japan, preoperative chemotherapy (PCT) followed by D2 gastrectomy plus para-aortic lymph node dissection (PAND) is considered the standard treatment for these patients. However, in China, the standard operation for GC patients with only bulky N2 metastases was D2 gastrectomy. Besides, after PCT, whether doing PAND improves survival or not is debatable for GC patients with para-aortic lymph node (PAN) metastases. Therefore, we conducted this study to investigate whether D2 lymphadenectomy alone is suitable for these patients after PCT.

Methods: We retrospectively collected data on patients from our electronic medical record system. GC patients with bulky N2 and/or PAN metastases who underwent D2 lymphadenectomy alone after PCT were enrolled. The survival outcomes and chemotherapy responses were analyzed and compared with the results of the JCOG0405 study.

Results: From May 2009 to December 2017, a total of 83 patients met all eligibility criteria and were enrolled. The median survival duration for all patients was 40.0 months. The 3-year and 5-year OS rates for all patients were 50.3% and 45.6%, respectively. For patients with only bulky N2 metastasis, the 3-year and 5-year OS rates were 77.1% and 71.6%, respectively, which were similar to the results of the JCOG0405 study (82.7% and 73.4%). For patients with only PAN metastases, the 3-year and 5-year OS rates were 50.0% and 50.0%, respectively, which seemed to be lower than those of the JCOG0405 study (64.3% and 57.1%). For patients with bulky N2 and PAN metastases, the 3-year and 5-year OS rates were 7.4% and 0.0%, respectively, which were lower than those of the JCOG0405 study (20.0% and 20.0%).

Conclusion: The results of our study suggest that D2 lymphadenectomy alone is suitable for GC patients with only bulky N2 metastasis after PCT. However, D2 lymphadenectomy alone perhaps is not suitable for patients with bulky N2 and PAN metastases after PCT.

Keywords: gastric cancer, preoperative chemotherapy, bulky N2 metastases, para-aortic lymph node metastases, D2 lymphadenectomy

INTRODUCTION

Gastric cancer (GC) is the fifth most common cancer and the third leading cause of cancer-related deaths worldwide (1). Surgery is the most effective and basic treatment for GC (2). Radical surgery includes gastrectomy and lymphadenectomy. Based on the 15-year results of a Dutch trial, D2 lymphadenectomy is considered the standard treatment for GC (3). Currently, most guidelines, including those established by the ESMO (4), NCCN (5), JGCA (6) and CSCO (7), have introduced D2 lymphadenectomy as the standard surgical procedure for GC. For advanced gastric cancer (AGC), however, the efficacy of surgery alone is limited. In recent years, more attention has been given to comprehensive treatment, particularly perioperative chemotherapy (preoperative and postoperative chemotherapy) (8–11). There is a special group of patients who have bulky N2 and/or para-aortic lymph node (PAN) metastases. Eastern and Western scholars have different opinions on the treatment of these patients. A bulky nodal lesion surrounding the coeliac artery and its branches with a diameter ≥ 3 cm or at least two adjacent tumors ≥ 1.5 cm are defined as bulky N2 metastases by the Japanese scholars (12, 13). In addition, PAN with a diameter ≥ 1 cm is considered PAN metastases (12, 13). The tumor node metastases (TNM) staging system considers PAN as distant metastases (M1) (14).

In Western countries, bulky N2 and/or PAN metastases are considered unresectable and warrant palliative chemotherapy. These patients can hardly survive for more than 3 years with chemotherapy alone or noncurative surgery followed by chemotherapy (15). Some previous studies showed that the addition of gastrectomy to chemotherapy might improve patient survival (median overall survival of 8.0-12.2 months with gastrectomy vs 2.4-6.7 months without gastrectomy) among GC patients with a single non-curable factor (16–23). The prognosis of these patients is still poor. In order to improve the prognosis of these patients, Japanese scholars conducted several studies to investigate new treatment strategies (12, 13, 24). The JCOG0001 study was the first clinical trial to evaluate the efficacy and safety of preoperative chemotherapy (PCT) followed by gastrectomy with D2 lymphadenectomy plus PAN dissection (PAND) for GC patients with bulky N2 and/or PAN metastasis (13). Although the JCOG0001 study was terminated because of a high number of treatment-related deaths, it provided a promising 3-year survival rate (27%). With the improvement of the PCT regimen, a similar study was conducted (JCOG0405) (12). The 3-year and 5-year survival rates in the JCOG0405 study were 59% and 53%, respectively. The study showed that PCT with the CS regimen (cisplatin and S-1) followed by gastrectomy with D2 lymphadenectomy plus PAND was safe and effective for GC patients with extensive lymph node metastasis. Recently, the JCOG1002 study also investigated the same subject with a different PCT regimen (DCS: docetaxel, cisplatin, and S-1) (24). The 3-year and 5-year survival rates in the JCOG1002 study were 62.7% and 54.9%, respectively, which were similar to those in the JCOG0405 study. At present, the standard therapy for these patients in Japan is still that stated in the JCOG0405 protocol. All three studies (JCOG0001, JCOG0405 and JCOG1002) combined PCT with D2 gastrectomy plus PAND. Therefore, the Japanese gastric cancer treatment guidelines suggested PCT with D2 gastrectomy plus PAND is the standard therapy for GC patients with bulky N2 and/or PAN metastases (**Figure 1A**) (6).

However, in China, for GC patients with only bulky N2 metastases, the standard treatment is D2 gastrectomy without PAND (7). Besides, for GC patients with PAN metastases, a phase II trial conducted by Chinese scholars showed that PCT with XELOX (capecitabine and oxaliplatin) followed by D2 gastrectomy alone also had a sufficient R0 resection rate (25). In addition, a real-world study conducted in China concluded that, for GC patients with PAN metastases that responds well to PCT, D2 gastrectomy alone is safe and effective (26).

For GC patients with bulky N2 and/or PAN metastases, it is unclear whether, on the basis of PCT, the addition of PAND would further improve prognosis compared to D2 lymphadenectomy alone. Therefore, we conducted this study to investigate whether D2 lymphadenectomy alone is suitable for GC patients with bulky N2 and/or para-aortic lymph node metastases after PCT.

MATERIALS AND METHODS

Patient Selection

Data on patients who were admitted to Ruijin Hospital (Shanghai Jiao Tong University School of Medicine, Shanghai, China) between May 2009 and December 2017 were collected retrospectively from the electronic medical record system. Eligibility criteria were as follows: (1) histologically proven gastric adenocarcinoma; (2) bulky N2 metastases and/or PAN metastases (Stations No. 16a2/16b1) confirmed by multidetector computed tomography (MDCT); (3) no distant metastases except for PAN confirmed by MDCT; (4) no history of other cancers; (5) patients received PCT before surgery; and (6) patients underwent D2 gastrectomy without PAND. According to the status of extensive lymph node metastases, all enrolled patients were divided into three groups: the Bulky N2+/PAN- group (only bulky N2 metastases without PAN metastases),

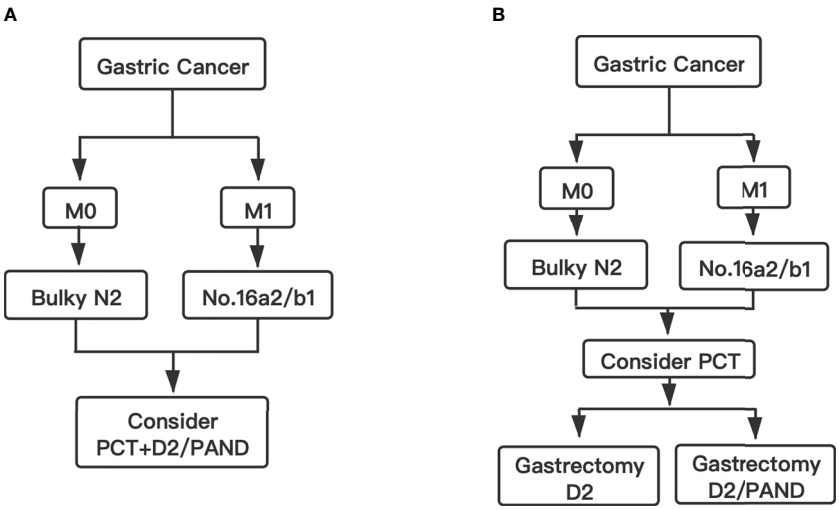

FIGURE 1 | Flow chart. **(A)** The standard therapy for GC patients with bulky N2 and/or PAN metastases in Japan. **(B)** The conclusion and suggested therapy for GC patients with bulky N2 and/or PAN metastases in this study.

the Bulky N2-/PAN+ group (only PAN metastases without bulky N2 metastases) and the Bulky N2+/PAN+ group (both bulky N2 and PAN metastases) group. This study was performed with approval from the Ethics Committee of Ruijin Hospital affiliated to the Shanghai Jiao Tong University School of Medicine. All patients were enrolled after signing an informed consent form.

Preoperative Chemotherapy

The preoperative chemotherapy regimen for all patients was EOX (epirubicin, oxaliplatin and capecitabine) (27). Epirubicin 50mg/m^2 and oxaliplatin 130mg/m^2 were administered on day 1, repeated every 3 weeks. Capecitabine (625mg/m^2) was given orally twice daily for the first two weeks of a 3-week cycle. Most patients received an average of three cycles of EOX chemotherapy before the imaging evaluation. A few patients received additional cycles. The National Cancer Institute Common Terminology Criteria for Adverse Events (CTCAE, 4.0) was applied for the evaluation of adverse effects.

Imaging Evaluation

The Response Evaluation Criteria In Solid Tumors (RECIST 1.1) was used to evaluate response of PCT in this study (28). The tumor responses were divided into 4 grades: complete response (CR), partial response (PR), stable disease (SD), and progressive disease (PD).

Surgery

All the operations were performed by the same surgical team of the gastric cancer specialized group in Ruijin hospital. For all enrolled patients, we performed open surgery for D2 gastrectomy without PAND. The radical degree of the operation was classified into three grades: R0, macroscopically complete surgical resection with negative microscopic margins; R1, macroscopically complete surgical resection with positive microscopic margins; and R2; macroscopically incomplete surgical resection. Surgical complications were graded using the Clavien-Dindo Complications Classification (CDCC) (29). In this study, surgical complications of grade III or above were recorded.

Pathological Evaluation

After the operation, the tumor specimens were evaluated pathologically. The tumor was staged in accordance with the Japanese Classifcation of Gastric Carcinoma (30). According to the proportion of tumors affected by degeneration or necrosis, the tumor regression grade (TRG) was divided into 4 degrees: grade 0, no part of the tumor affected; grade 1a, less than one-third affected; grade 1b, between one-third and two-thirds affected; grade 2, between two-thirds and the entire tumor affected; and grade 3, no residual tumor (pathological complete response, PCR) (6). The pathological evaluation was performed in the same manner as in the JCOG0001 (13), JCOG 0405 (12) and JCOG1002 (24)studies.

Postoperative Chemotherapy and Follow-up

The postoperative chemotherapy regimens for all patients were EOX or XELOX (oxaliplatin and capecitabine). According to the patient's postoperative physical status, we chose the three-drug regimen or the two-drug regimen. Most patients received an average of three cycles of postoperative chemotherapy. Through outpatient visits and telephone calls, we followed up all enrolled patients. Telephone calls was conducted every three months after surgery. Overall survival (OS) was measured from the date of the initial diagnosis of gastric cancer to the date of death or the last follow-up.

Statistical Analysis

The OS curve was estimated using the Kaplan-Meier method. To analyze baseline factors between different studies, the chi-square test was used. A two-sided P value<0.05 was considered

significantly different. Analyses were performed with SPSS version 26.0 (IBM Statistical Product and Service Solutions, Armonk, USA). GraphPad Prism version 8.0 (San Diego, CA, USA) was used to draw the survival curve.

RESULTS

Characteristics of the Patients

Between May 2009 and December 2017, 83 patients satisfied all eligibility criteria and were enrolled in this study. The study population comprised 59 males and 24 females, with a male-to-female ratio of 2.5:1. The median age at diagnosis was 61 years (range 31-80). In this study, 44 (53.0%), 12 (14.5%) and 27 (32.5%) patients comprised in the Bulky N2+/PAN-, Bulky N2-/PAN+ and Bulky N2+/PAN+ groups, respectively. The detailed characteristics of patients in three groups were also shown in **Table 1**, including sex, age ECOG, differentiation, body mass index (BMI), tumor location, Borrmann type, clinical nodal status, the diameter of the largest lymph node (LNmax) and the type of gastrectomy. The tumor location were classified into cardia, body, antrum and whole stomach. The LNmax was measured using multi-detector-row computed tomography (MDCT). The types of gastrectomy were divided into proximal, distal, total and multiorgan resection. A total of 4 patients received multiorgan resection. One patient in the Bulky N2+/PAN- group received total gastrectomy plus distal pancreatectomy and splenectomy. Two patients in the Bulky N2+/PAN+ group received gastrectomy plus left lateral hepatic lobectomy. One patient in the Bulky N2+/PAN+ group, from whom a constrictive metastatic lesion was found in the small intestine 30cm from the proximal ileocecal colon, received gastrectomy plus partial enterectomy (approximately 5cm of small intestine was resected).

Evaluation of Preoperative Chemotherapy

According to the CTCAE, one patient had grade 3 hematological adverse and three patients had grade 3 or 4 vomiting. Most of the hematological adverse effects and symptomatic adverse effects were acceptable for triplet chemotherapy. According to the RECIST, most patients in this study responsed well to PCT (**Table 2**).

All patients underwent D2 gastrectomy without PAND. Therefore, patients with PAN metastases did not receive R0

TABLE 1 | Characteristics of all enrolled patients.

Characteristics	Total (N = 83)	Bulky N2+/PAN- (n = 44)	Bulky N2-/PAN+ (n = 12)	Bulky N2+/PAN+ (n = 27)
Sex				
Male	59 (71.1%)	32 (72.7%)	9 (75.0%)	18 (66.7%)
female	24 (28.9%)	12 (27.3%)	3 (25.0%)	9 (33.3%)
Age (y)				
Median (range)	61 (31-80)	63.5 (31-80)	58.5 (40-74)	61 (43-76)
ECOG				
0	80 (96.4%)	41 (93.2%)	12 (100.0%)	27 (100.0%)
1	3 (3.6%)	3 (6.8%)	0 (0.0%)	0 (0.0%)
Differentiation				
Differentiated	41 (49.4%)	22 (50.0%)	6 (50.0%)	13 (48.1%)
Undifferentiated	42 (50.6%)	22 (50.0%)	6 (50.0%)	14 (51.9%)
BMI (kg/m^2)				
Median (range)	22.3 (17.0-31.7)	22.7 (17.0-30.5)	21.8 (18.1-31.7)	22.2 (17.2-27.8)
Location (n[%])				
Cardia	21 (25.3%)	16 (36.4%)	3 (25.0%)	2 (7.4%)
Body	20 (24.1%)	6 (13.6%)	5 (41.7%)	9 (33.3%)
Antrum	32 (38.6%)	19 (43.2%)	3 (25.0%)	10 (37.0%)
Whole stomach	10 (12.0%)	3 (6.8%)	1 (8.3%)	6 (22.2%)
Borrmann (n[%])				
I	3 (3.6%)	2 (4.5%)	1 (8.3%)	0 (0.0%)
II	7 (8.4%)	5 (11.4%)	2 (16.7%)	0 (0.0%)
III	67 (80.7%)	36 (81.8%)	8 (66.7%)	23 (85.2%)
IV	6 (7.2%)	1 (2.3%)	1 (8.3%)	4 (14.8%)
Nodal status				
cN0	0 (0.0%)	0 (0.0%)	0 (0.0%)	0 (0.0%)
cN1	8 (9.6%)	6 (13.6%)	2 (16.7%)	0 (0.0%)
cN2	26 (31.3%)	21 (47.7%)	1 (8.3%)	4 (14.8%)
cN3	49 (59.0%)	17 (38.6%)	9 (75.0%)	23 (85.2%)
LNmax (cm)				
Median (range)	2.1 (1.0-5.1)	2.6 (1.5-5.1)	1.4 (1.0-2.0)	1.9 (1.0-4.2)
Type of gastrectomy				
Proximal	1 (1.2%)	1 (2.3%)	0 (0.0%)	0 (0.0%)
Distal	27 (32.5%)	17 (38.6%)	3 (25.0%)	7 (25.9%)
Total	51 (61.4%)	26 (59.1%)	8 (66.7%)	17 (63.0%)
Multiorgan	4 (4.8%)	0 (0.0%)	1 (8.3%)	3 (11.1%)

TABLE 2 | Evaluation of preoperative chemotherapy.

Characteristics	Total (N = 83)	Bulky N2+/PAN- (n = 44)	Bulky N2-/PAN+ (n = 12)	Bulky N2+/PAN+ (n = 27)
RECIST				
CR	0 (0%)	0 (0%)	0 (0%)	0 (0%)
PR	63 (75.9%)	38 (86.4%)	7 (58.3%)	18 (66.7%)
SD	19 (22.9%)	5 (11.4%)	5 (41.7%)	9 (33.3%)
PD	1 (1.2%)	1 (2.3%)	0 (0%)	0 (0%)
Degree of gastrectomy				
R0	43 (51.8%)	43 (97.7%)	0 (0%)	0 (0%)
R1	0 (0%)	0 (0%)	0 (0%)	0 (0%)
R2	40 (48.2%)	1 (2.3%)	12 (100.0%)	27 (100.0%)
Depth of tumor invasion				
ypT0	12 (14.5%)	11 (25.0%)	1 (8.3%)	0 (0%)
ypT1	6 (7.2%)	4 (9.1%)	2 (16.7%)	0 (0%)
ypT2	14 (16.9%)	7 (15.9%)	3 (25.0%)	4 (14.8%)
ypT3	10 (12.0%)	4 (9.1%)	2 (16.7%)	4 (14.8%)
ypT4	41 (49.4%)	18 (40.9%)	4 (33.3%)	19 (70.4%)
Nodal status				
ypN0	26 (31.3%)	20 (45.5%)	3 (25.0%)	3 (11.1%)
ypN1	14 (16.9%)	8 (18.2%)	4 (33.3%)	2 (7.4%)
ypN2	14 (16.9%)	8 (18.2%)	1 (8.3%)	5 (18.5%)
ypN3	29 (34.9%)	8 (18.2%)	4 (33.3%)	17 (63.0%)
TRG				
Grade 0	4 (4.8%)	1 (2.3%)	1 (8.3%)	2 (7.4%)
Grade 1a	12 (14.5%)	3 (6.8%)	1 (8.3%)	8 (29.6%)
Grade 1b	10 (12.0%)	8 (18.2%)	1 (8.3%)	1 (3.7%)
Grade 2	45 (54.2%)	21 (47.7%)	8 (66.7%)	16 (59.3%)
Grade 3	12 (14.5%)	11 (25.0%)	1 (8.3%)	0 (0%)

resection. Besides, one patient in the Bulky N2+/PAN- group did not receive R0 resection. In this patient, metastatic nodules were found on the surface of the transverse colon and the root of the mesentery. Therefore, only 43 (51.8%) patients received R0 resection. An average of 37 (SD: 17.52, 95% CI: 33-41) lymph nodes were dissected in this study. For patients in the Bulky N2+/PAN-, Bulky N2-/PAN+ and Bulky N2+/PAN+ groups, the average numbers of lymph nodes dissected were 36, 31, and 41, respectively.

The pathological evaluations were also shown in **Table 2**. Patients with pathological grade ypT0 were considered to achieve a pathological complete response in the primary tumors. Patients with grade ypN0 were considered to achieve a pathological complete response in the lymph nodes. There were 11 patients received pathological complete response both in the primary tumors and lymph nodes. One patient achieved the pathological complete response in the primary tumors, but the lymph nodes did not get the pathological complete response. At last, 12 (14.5%) patients had complete tumor regression (TRG 3), and 45 (54.2%) patients had subtotal tumor regression (TRG 2) (**Table 2**).

Surgical Complications

Only two (2.4%) patients experienced grade III or above complications after surgery. Both patients were in the bulky N2+/PAN- group and had leakage. One patient underwent a second surgery due to anastomotic leakage. Another patient with duodenal stump leakage did not undergo a second surgery. There was no treatment-related or in-hospital death.

Survival Analysis

In this study, the last follow-up date was 22 December 2020, and the median follow-up time was 55.8 months (range 36.6–141.5 months). By the time of the last follow-up time, all patients had been followed up for 3 years and 28 patients had been followed up for 5 years. Among the 28 patients who had been followed up for 5 years, there were 20, 1, and 7 patients in the Bulky N2+/PAN-, Bulky N2-/PAN+ and Bulky N2+/PAN+ groups, respectively.

Survival curves for patients are shown in **Figure 2**. In this study, the median survival duration for all patients was 40.0 months. The 3-year and 5-year OS rates for all patients were 50.3% and 45.6%, respectively (**Figure 2A**). The median OS duration of patients in the Bulky N2+/PAN-, Bulky N2-/PAN+ and Bulky N2+/PAN+ groups were undefined, 77.1 and 15.9 months, respectively ($P<0.0001$, **Figure 2B**). The 3-year and 5-year OS rates for patients in the Bulky N2+/PAN- group were 77.1% and 71.6%, respectively. The 3-year and 5-year OS rates for patients in the Bulky N2-/PAN+ group were 50.0% and 50.0%, respectively. The 3-year and 5-year OS rates for patients in the Bulky N2+/PAN+ group were 7.4% and 0.0%, respectively.

After all patients were followed up for 3 years, 40 (48.2%) patients were still alive. For patients in the Bulky N2+/PAN- group, Bulky N2-/PAN+ and Bulky N2+/PAN+ groups, there were 32 (72.7%), 5 (41.7%) and 3 (11.1%) patients still alive, respectively.

In addition, in the Bulky N2+/PAN- group, 20 patients were followed up for 5 years and 7 patients died of cancer recurrence. In the Bulky N2-/PAN+ and Bulky N2+/PAN+ groups,

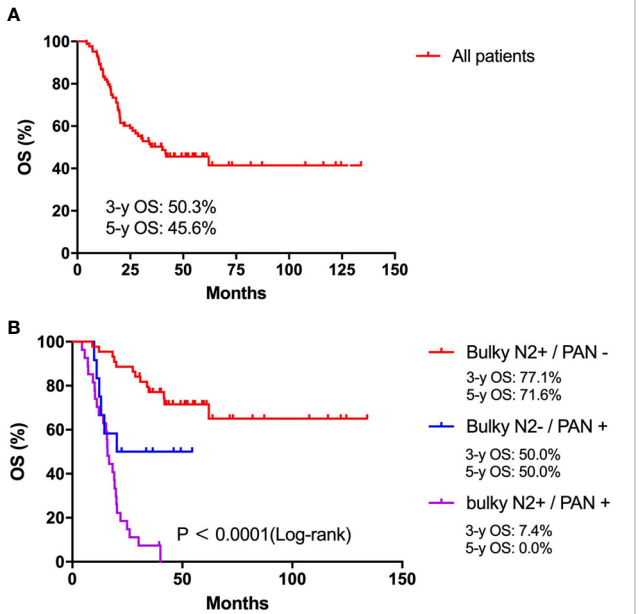

FIGURE 2 | Survival analysis. **(A)** Survival analysis for all patients with bulky N2 and/or para-aortic lymph node metastases. **(B)** Survival analysis for patients between the Bulky N2+/PAN-, Bulky N2-/PAN+ and Bulky N2+/PAN+ groups.

there were 1 and 7 patients followed up for 5 years and no one survived.

DISCUSSION

Currently, there is no standard treatment for gastric cancer with extensive lymph node metastases (bulky N2 and/or para-aortic lymph node metastases). In the West, these tumors are considered unresectable and tend to be treated with palliative chemotherapy. In Japan, PCT with the CS regimen followed by D2 gastrectomy plus PAND is considered the standard treatment for these tumors. Advances in research over recent years have focused only on regimen changes in PCT (12, 13, 24). However, it is unclear whether, on the basis of PCT, the addition of PAND could further improve prognosis compared to D2 lymphadenectomy alone. In China, PAND has not been widely carried out due to its highly technical difficulties, surgical complications and uncertain survival benefits. Therefore, we aimed to explore whether D2 lymphadenectomy alone is suitable for GC patients with bulky N2 and/or PAN metastases after PCT by comparing the results of our study and those from Japanese scholars.

The detailed OS rates of patients in the JCOG0001, JCOG0405, JCOG1002 studies and this study are showed in **Table 3**. The survival data were derived from analysis of 49 patients in JCOG0001 and 47 patients in JCOG0405 who underwent surgery, 52 eligible patients in JCOG1002 and all patients in this study. Integrated analysis demonstrated that the results of the JCOG0405 study were better than those of the JCOG0001 study for GC with extensive lymph node metastasis (31). In addition, the long-term outcomes of the JCOG1002 study also demonstrated that PCT with the CS regimen followed by D2 gastrectomy plus PAND remains the standard treatment for patients with extensive nodal metastases in Japan (32). Therefore, we mainly compared our study with the JCOG0405 study, in which 49 (92.5%) patients underwent surgery.

For patients in the Bulky N2+/PAN- group, the 3-year and 5-year OS rates in this study were 77.1% and 71.6%. The 3-year and 5-year OS rates in the JCOG0001 study were 37.5% and 29.2%. The 3-year and 5-year OS rates in the JCOG0405 study were 82.7% and 73.4%. The 3-year and 5-year OS rates in the JCOG1002 study were 62.1% and 57.1%. We found that the 5-year OS rate in this study (71.6%) were similar to those in the JCOG0405 (73.4%) and higher than those in the JCOG0001 (29.2%) and JCOG1002 (57.1%). On the other hand, there were obviously fewer surgical complications in this study than in the JCOG studies (**Table 4**, P<0.001). Besides, in a previous study of PCT followed by D2 lymphadenectomy for GC patients with PAN metastases, only one of the 28 patients had surgical complication (25). These results showed D2 gastrectomy alone is safer than surgery plus PAND. Based on the above analysis, we consider D2 lymphadenectomy alone is suitable for GC patients

TABLE 3 | Overall survival rates for different patients in four studies.

OS	Bulky N2+/PAN-		Bulky N2-/PAN+		Bulky N2+/PAN+	
	3-y	5-y	3-y	5-y	3-y	5-y
JCOG0001 (n=49)	37.5%	29.2%	22.2%	22.2%	25%	18.8%
JCOG0405 (n=47)	82.7%	73.4%	64.3%	57.1%	20%	20%
JCOG1002 (n=52)	62.1%	57.1%	50%	35.7%	77.8%	77.8%
This study (n=83)	77.1%	71.6%	50.0%	50.0%	7.4%	0%

TABLE 4 | Surgical complications in all operated patients.

Characteristics	JCOG0001 (n = 47)	JCOG0405 (n = 49)	JCOG1002 (n = 46)	This study (n = 83)	P
Leakage	1	3	2	2	
Pancreatic fistula	6	11	9	0	
Abdominal abscess	2	8	5	0	
Pneumonia	2	2	4	0	
Ileus	0	0	1	0	
Wound infection	2	0	2	0	
Anastomotic stenosis	1	0	1	0	
Cardiac failure	1	0	0	0	
Renal dysfunction	1	0	0	0	
Thromboembolic event	0	2	2	0	
Atelectasis	0	3	0	0	
Other	6	11	11	0	
Total	22	40	37	2	<0.001*

*χ^2 test (compares the counts of categorical responses between 2 or more independent groups).

TABLE 5 | Pathological evaluation for four studies.

Characteristics	JCOG0001 (n = 47)	JCOG0405 (n = 49)	JCOG1002 (n = 46)	This study (n = 83)	P
Depth of tumor invasion					<0.001*
ypT0	1 (2.1%)	2 (4.1%)	1 (2.2%)	12 (14.5%)	
ypT1	3 (6.4%)	7 (14.3%)	8 (17.4%)	6 (7.2%)	
ypT2	18 (38.3%)	23 (46.9%)	9 (19.6%)	14 (16.9%)	
ypT3	19 (40.4%)	16 (32.7%)	21 (45.6%)	10 (12.0%)	
ypT4	6 (12.8%)	1 (2.0%)	7 (15.2%)	41 (49.4%)	
Nodal status					<0.001*
ypN0	1 (2.1%)	8 (16.3%)	10 (21.7%)	26 (31.3%)	
ypN1	7 (14.9%)	5 (10.2%)	8 (17.4%)	14 (16.9%)	
ypN2	9 (19.1%)	21 (42.9%)	9 (19.6%)	14 (16.9%)	
ypN3	30 (63.8%)	15 (30.6%)	19 (41.3%)	29 (34.9%)	
Pathological response					<0.001*
Grade 0	6 (12.8%)	3 (6.1%)	3 (6.5%)	4 (4.8%)	
Grade 1a	33 (70.2%)	19 (38.8%)	17 (37.0%)	12 (14.5%)	
Grade 1b	2 (4.3%)	13 (26.5%)	8 (17.4%)	10 (12.0%)	
Grade 2	5 (10.6%)	13 (26.5%)	17 (37.0%)	45 (54.2%)	
Grade 3	1 (2.1%)	1 (2.0%)	1 (2.1%)	12 (14.5%)	

*χ^2 test (compares the counts of categorical responses between 2 or more independent groups).

with only bulky N2 metastases after PCT. Of course, further clinical studies are still needed to investigate whether D2 lymphadenectomy alone or the combination of D2 lymphadenectomy and PAND has a better survival benefit for these patients.

For patients with only PAN metastases, the 3-year and 5-year OS rates in this study were 50.0% and 50.0%, respectively. The 3-year and 5-year OS rates in the JCOG0001 study were 22.2% and 22.2%. The 3-year and 5-year OS rates in the JCOG0405 study were 64.3% and 57.1%. The 3-year and 5-year OS rates in the JCOG1002 study were 50% and 35.7%. We found that the 5-year OS rate in this study (50%) was similar to that in the JCOG0405 study (57.1%) and higher than those in the JCOG0001 (22.2%) and JCOG1002 (35.7%). This difference may be due to the number of false positives in patients with only PAN metastases. A previous study on PAND for GC with 1–3 involved PANs showed that the actual PAN metastases rate was 30.4% (33).

For patients with bulky N2 and PAN metastases, the 3-year and 5-year OS rates in this study were 7.4% and 0%. The 3-year and 5-year OS rates in the JCOG0001 study were 25% and 18.8%. The 3-year and 5-year OS rates in the JCOG0405 study were 20% and 20%. The 3-year and 5-year OS rates in the JCOG1002 study were 77.8% and 77.8%. We found that the 5-year OS rate in this study (0%)were lower than those in the JCOG0001 (18.8%), JCOG0405 (20%), and JCOG1002 (77.8%). According to the pathological evaluation, more patients in our study achieved grades of ypT0 and ypN0 and PCR than those in the JCOG0001, JCOG0405 and JCOG1002 studies (**Table 5**) which showed that the chemotherapy regimen in this study was effective and feasible. Therefore, the significant difference in survival for patients with bulky N2 and PAN metastases may be mainly due to the different surgeries. Therefore, we consider D2 lymphadenectomy alone is not suitable for GC patients with bulky N2 and PAN metastases after PCT.

There are some limitations to this study. This study was a retrospective study. Prospective studies are needed to further confirm the results. In addition, we did not have detailed data from the JCOG studies, and we can compare only our results with the data presented in their published articles. Since these studies were not conducted at the same time, there were some biases that could not be avoided. However, this study not only confirms our practice of not performing PAND in GC patients with only bulky N2 metastases, but also reminds us of the importance of PAND in the treatment of GC patients with bulky N2 and PAN metastases.

In conclusion, we consider D2 lymphadenectomy alone is suitable for GC patients with only bulky N2 metastases after PCT. However, for GC patients with bulky N2 and PAN metastases, D2 lymphadenectomy alone perhaps is not suitable. These patients need D2 lymphadenectomy plus PAND after PCT (**Figure 1B**).

DATA AVAILABILITY STATEMENT

The original contributions presented in the study are included in the article/supplementary material. Further inquiries can be directed to the corresponding authors.

ETHICS STATEMENT

The studies involving human participants were reviewed and approved by the Human Ethics Committee of Shanghai Jiao Tong University School of Medicine Ruijin Hospital. The patients/participants provided their written informed consent to participate in this study.

AUTHOR CONTRIBUTIONS

WX conceived and designed the study, analyzed the data and wrote the paper. WL participated in the design of the study

and edited the final paper. LW, CH, SL, ZN, ZH, ZLZ, ZY, BS, and YZ collected the clinicopathological factors of all patients. RF, CL, XY, and MC followed up the patient's survival status. CY revised the paper. MY and ZGZ gave professional guidance. All authors contributed to the article and approved the submitted version.

FUNDING

This work was supported by National Natural Science Foundation of China NO. 81772518 and clinical research project of Ruijin Hospital, Shanghai Jiao Tong University School of Medicine (DLY201602 and 2018CR003).

REFERENCES

1. Bray F, Ferlay J, Soerjomataram I, Siegel R, Torre L, Jemal A. Global Cancer Statistics 2018: GLOBOCAN Estimates of Incidence and Mortality Worldwide for 36 Cancers in 185 Countries. *CA: Cancer J Clin* (2018) 68 (6):394–424. doi: 10.3322/caac.21492
2. Agnes A, Biondi A, Laurino A, Persiani R, D'Ugo D. Global Updates in the Treatment of Gastric Cancer: A Systematic Review. Part 1: Staging, Classification and Surgical Treatment. *Updates Surg* (2020) 72(2):341–53. doi: 10.1007/s13304-020-00736-3
3. Songun I, Putter H, Kranenbarg EM-K, Sasako M, van de Velde CJH. Surgical Treatment of Gastric Cancer: 15-Year Follow-Up Results of the Randomised Nationwide Dutch D1D2 Trial. *Lancet Oncol* (2010) 11(5):439–49. doi: 10.1016/S1470-2045(10)70070-X
4. Smyth EC, Verheij M, Allum W, Cunningham D, Cervantes A, Arnold D. Gastric Cancer: ESMO Clinical Practice Guidelines for Diagnosis, Treatment and Follow-Up. *Ann Oncol* (2016) 27:v38–49. doi: 10.1093/annonc/mdw350
5. Ajani J, D'Amico T, Almhanna K, Bentrem D, Chao J, Das P, et al. Gastric Cancer, Version 3.2016, NCCN Clinical Practice Guidelines in Oncology. *J Natl Compr Cancer Network JNCCN* (2016) 14(10):1286–312. doi: 10.6004/jnccn.2016.0137
6. Japanese Gastric Cancer Association. Japanese Gastric Cancer Treatment Guidelines 2018 (5th Edition). *Gastric Cancer* (2021) 24(1):1–21. doi: 10.1007/s10120-020-01042-y
7. Wang FH, Shen L, Li J, Zhou ZW, Liang H, Zhang XT, et al. The Chinese Society of Clinical Oncology (CSCO): Clinical Guidelines for the Diagnosis and Treatment of Gastric Cancer. *Cancer Commun (Lond)* (2019) 39(1):10. doi: 10.1186/s40880-019-0349-9
8. Noh S, Park S, Yang H, Chung H, Chung I, Kim S, et al. Adjuvant Capecitabine Plus Oxaliplatin for Gastric Cancer After D2 Gastrectomy (CLASSIC): 5-Year Follow-Up of an Open-Label, Randomised Phase 3 Trial. *Lancet Oncol* (2014) 15(12):1389–96. doi: 10.1016/S1470-2045(14)70473-5
9. Sakuramoto S, Sasako M, Yamaguchi T, Kinoshita T, Fujii M, Nashimoto A, et al. Adjuvant Chemotherapy for Gastric Cancer With S-1, An Oral Fluoropyrimidine. *N Engl J Med* (2007) 357(18):1810–20. doi: 10.1056/NEJMoa072252
10. Cunningham D, Allum W, Stenning S, Thompson J, Van de Velde C, Nicolson M, et al. Perioperative Chemotherapy Versus Surgery Alone for Resectable Gastroesophageal Cancer. *N Engl J Med* (2006) 355(1):11–20. doi: 10.1056/NEJMoa055531
11. Ychou M, Boige V, Pignon J, Conroy T, Bouch O, Lebreton G, Ducourtieux M, Bedenne L, Fabre J, Saint-Aubert B, et al. Perioperative Chemotherapy Compared With Surgery Alone for Resectable Gastroesophageal Adenocarcinoma: An FNCLCC and FFCD Multicenter Phase III Trial. *J Clin Oncol Off J Am Soc Clin Oncol* (2011) 29(13):1715–21. doi: 10.1200/JCO.2010.33.0597
12. Tsuburaya A, Mizusawa J, Tanaka Y, Fukushima N, Nashimoto A, Sasako M. Stomach Cancer Study Group of the Japan Clinical Oncology G: Neoadjuvant Chemotherapy With S-1 and Cisplatin Followed by D2 Gastrectomy With Para-Aortic Lymph Node Dissection for Gastric Cancer With Extensive Lymph Node Metastasis. *Br J Surg* (2014) 101(6):653–60. doi: 10.1002/bjs.9484
13. Yoshikawa T, Sasako M, Yamamoto S, Sano T, Imamura H, Fujitani K, et al. Phase II Study of Neoadjuvant Chemotherapy and Extended Surgery for Locally Advanced Gastric Cancer. *Br J Surg* (2009) 96(9):1015–22. doi: 10.1002/bjs.6665
14. Amin MB ES, Greene FL, Brierley JD. *AJCC Cancer Staging Manual. 8th Ed*. New York: Springer (2017).
15. Miyagaki H, Fujitani K, Tsujinaka T, Hirao M, Yasui M, Kashiwazaki M, et al. The Significance of Gastrectomy in Advanced Gastric Cancer Patients With Non-Curative Factors. *Anticancer Res* (2008) 28(4C):2379–84.
16. Hartgrink HH, Putter H, Klein Kranenbarg E, Bonenkamp JJ, van de Velde CJ, Dutch Gastric Cancer G. Value of Palliative Resection in Gastric Cancer. *Br J Surg* (2002) 89(11):1438–43. doi: 10.1046/j.1365-2168.2002.02220.x
17. Bonenkamp JJ, Sasako M, Hermans J, van de Velde CJ. Tumor Load and Surgical Palliation in Gastric Cancer. *Hepatogastroenterology* (2001) 48(41):1219–21.
18. Kikuchi S, Arai Y, Morise M, Kobayashi N, Tsukamoto H, Shimao H, et al. Gastric Cancer With Metastases to the Distant Peritoneum: A 20-Year Surgical Experience. *Hepatogastroenterology* (1998) 45(22):1183–8.
19. Ouchi K, Sugawara T, Ono H, Fujiya T, Kamiyama Y, Kakugawa Y, et al. Therapeutic Significance of Palliative Operations for Gastric Cancer for Survival and Quality of Life. *J Surg Oncol* (1998) 69(1):41–4. doi: 10.1002/(SICI)1096-9098(199809)69:1<41::AID-JSO8>3.0.CO;2-K
20. Maekawa S, Saku M, Maehara Y, Sadanaga N, Ikejiri K, Anai H, et al. Surgical Treatment for Advanced Gastric Cancer. *Hepatogastroenterology* (1996) 43 (7):178–86.
21. Haugstvedt T, Viste A, Eide GE, Soreide O. The Survival Benefit of Resection in Patients With Advanced Stomach Cancer: The Norwegian Multicenter Experience. Norwegian Stomach Cancer Trial. *World J Surg* (1989) 13(5):617–21; discussion 621–12. doi: 10.1007/BF01658884
22. Bozzetti F, Bonfanti G, Audisio RA, Doci R, Dossena G, Gennari L, et al. Prognosis of Patients After Palliative Surgical Procedures for Carcinoma of the Stomach. *Surg Gynecol Obstet* (1987) 164(2):151–4.
23. Meijer S, De Bakker OJ, Hoitsma HF. Palliative Resection in Gastric Cancer. *J Surg Oncol* (1983) 23(2):77–80. doi: 10.1002/jso.2930230205
24. Ito S, Sano T, Mizusawa J, Takahari D, Katayama H, Katai H, et al. A Phase II Study of Preoperative Chemotherapy With Docetaxel, Cisplatin, and S-1 Followed by Gastrectomy With D2 Plus Para-Aortic Lymph Node Dissection for Gastric Cancer With Extensive Lymph Node Metastasis: JCOG1002. *Gastric Cancer* (2017) 20(2):322–31. doi: 10.1007/s10120-016-0619-z
25. Wang Y, Yu YY, Li W, Feng Y, Hou J, Ji Y, et al. A Phase II Trial of Xeloda and Oxaliplatin (XELOX) Neo-Adjuvant Chemotherapy Followed by Surgery for Advanced Gastric Cancer Patients With Para-Aortic Lymph Node Metastasis. *Cancer Chemother Pharmacol* (2014) 73(6):1155–61. doi: 10.1007/s00280-014-2449-1
26. Zheng XH, Zhang W, Yang L, Du CX, Li N, Xing GS, et al. Role of D2 Gastrectomy in Gastric Cancer With Clinical Para-Aortic Lymph Node Metastasis. *World J Gastroenterol* (2019) 25(19):2338–53. doi: 10.3748/wjg.v25.i19.2338
27. Sumpter K, Harper-Wynne C, Cunningham D, Rao S, Tebbutt N, Norman AR, et al. Report of Two Protocol Planned Interim Analyses in a Randomised Multicentre Phase III Study Comparing Capecitabine With Fluorouracil and Oxaliplatin With Cisplatin in Patients With Advanced Oesophagogastric Cancer Receiving ECF. *Br J Cancer* (2005) 92(11):1976–83. doi: 10.1038/sj.bjc.6602572
28. Eisenhauer E, Therasse P, Bogaerts J, Schwartz L, Sargent D, Ford R, et al. New Response Evaluation Criteria in Solid Tumours: Revised RECIST Guideline (Version 1.1). *Eur J Cancer (Oxford Engl 1990)* (2009) 45(2):228–47. doi: 10.1016/j.ejca.2008.10.026
29. Dindo D, Demartines N, Clavien PA. Classification of Surgical Complications: A New Proposal With Evaluation in a Cohort of 6336 Patients and Results of a Survey. *Ann Surg* (2004) 240(2):205–13. doi: 10.1097/01.sla.0000133083.54934.ae
30. Sano T, Aiko T. New Japanese Classifications and Treatment Guidelines for Gastric Cancer: Revision Concepts and Major Revised Points. *Gastric Cancer* (2011) 14(2):97–100. doi: 10.1007/s10120-011-0040-6
31. Katayama H, Tsuburaya A, Mizusawa J, Nakamura K, Katai H, Imamura H, et al. An Integrated Analysis of Two Phase II Trials (JCOG0001 and JCOG0405) of Preoperative Chemotherapy Followed by D3 Gastrectomy

for Gastric Cancer With Extensive Lymph Node Metastasis. *Gastric Cancer* (2019) 22(6):1301–7. doi: 10.1007/s10120-019-00981-5
32. Takahari D, Ito S, Mizusawa J, Katayama H, Terashima M, Sasako M, et al. Long-Term Outcomes of Preoperative Docetaxel With Cisplatin Plus S-1 Therapy for Gastric Cancer With Extensive Nodal Metastasis (JCOG1002). *Gastric Cancer* (2020) 23(2):293–9. doi: 10.1007/s10120-019-01007-w
33. Zhang C, He Y, Schwarz RE, Smith DD, Wang L, Liu F, et al. Evaluation of Para-Aortic Nodal Dissection for Locoregionally Advanced Gastric Cancer With 1-3 Involved Para-Aortic Nodes. *Chin Med J (Engl)* (2014) 127(3):435–41.

Conflict of Interest: The authors declare that the research was conducted in the absence of any commercial or financial relationships that could be construed as a potential conflict of interest.

Publisher's Note: All claims expressed in this article are solely those of the authors and do not necessarily represent those of their affiliated organizations, or those of the publisher, the editors and the reviewers. Any product that may be evaluated in this article, or claim that may be made by its manufacturer, is not guaranteed or endorsed by the publisher.

Copyright © 2021 Xu, Liu, Wang, He, Lu, Ni, Hua, Zhu, Sah, Yang, Zheng, Feng, Li, Yao, Chen, Yan, Yan and Zhu. This is an open-access article distributed under the terms of the Creative Commons Attribution License (CC BY). The use, distribution or reproduction in other forums is permitted, provided the original author(s) and the copyright owner(s) are credited and that the original publication in this journal is cited, in accordance with accepted academic practice. No use, distribution or reproduction is permitted which does not comply with these terms.

frontiers in Oncology

ORIGINAL RESEARCH
published: 13 September 2021
doi: 10.3389/fonc.2021.723345

^{18}F-FDG PET/CT Radiomics for Preoperative Prediction of Lymph Node Metastases and Nodal Staging in Gastric Cancer

Qiufang Liu[1,2†], Jiaru Li[3†], Bowen Xin[3], Yuyun Sun[1,2], Dagan Feng[3], Michael J. Fulham[3,4], Xiuying Wang[3] and Shaoli Song[1,2*]*

[1] Department of Nuclear Medicine, Fudan University Shanghai Cancer Center, Fudan University, Shanghai, China, [2] Department of Oncology, Shanghai Medical College, Fudan University, Shanghai, China, [3] School of Computer Science, The University of Sydney, Sydney, NSW, Australia, [4] Department of Molecular Imaging, Royal Prince Alfred Hospital, The University of Sydney, Sydney, NSW, Australia

OPEN ACCESS

Edited by:
Pankaj Kumar Garg, Shri Guru Ram Rai Institute of Medical and Health Sciences, India

Reviewed by:
Rajesh Pasricha, All India Institute of Medical Sciences Bhopal, India
Ajeet Kumar Tiwari, Sir Ganga Ram Hospital, India

***Correspondence:**
Shaoli Song
shaoli-song@163.com
Xiuying Wang
xiu.wang@sydney.edu.au

†These authors have contributed equally to this work and share first authorship

Specialty section:
This article was submitted to Gastrointestinal Cancers, a section of the journal Frontiers in Oncology

Received: *10 June 2021*
Accepted: *19 August 2021*
Published: *13 September 2021*

Citation:
Liu Q, Li J, Xin B, Sun Y, Feng D, Fulham MJ, Wang X and Song S (2021) ^{18}F-FDG PET/CT Radiomics for Preoperative Prediction of Lymph Node Metastases and Nodal Staging in Gastric Cancer. Front. Oncol. 11:723345. doi: 10.3389/fonc.2021.723345

Objectives: The accurate assessment of lymph node metastases (LNMs) and the preoperative nodal (N) stage are critical for the precise treatment of patients with gastric cancer (GC). The diagnostic performance, however, of current imaging procedures used for this assessment is sub-optimal. Our aim was to investigate the value of preoperative ^{18}F-FDG PET/CT radiomic features to predict LNMs and the N stage.

Methods: We retrospectively collected clinical and ^{18}F-FDG PET/CT imaging data of 185 patients with GC who underwent total or partial radical gastrectomy. Patients were allocated to training and validation sets using the stratified method at a fixed ratio (8:2). There were 2,100 radiomic features extracted from the ^{18}F-FDG PET/CT scans. After selecting radiomic features by the random forest, relevancy-based, and sequential forward selection methods, the BalancedBagging ensemble classifier was established for the preoperative prediction of LNMs, and the OneVsRest classifier for the N stage. The performance of the models was primarily evaluated by the AUC and accuracy, and validated by the independent validation methods. Analysis of the feature importance and the correlation were also conducted. We also compared the predictive performance of our radiomic models to that with the contrast-enhanced CT (CECT) and ^{18}F-FDG PET/CT.

Results: There were 185 patients—127 men, 58 women, with the median age of 62, and an age range of 22–86 years. One CT feature and one PET feature were selected to predict LNMs and achieved the best performance (AUC: 82.2%, accuracy: 85.2%). This radiomic model also detected some LNMs that were missed in CECT (19.6%) and ^{18}F-FDG PET/CT (35.7%). For predicting the N stage, four CT features and one PET feature were selected (AUC: 73.7%, accuracy: 62.3%). Of note, a proportion of patients in the validation set whose LNMs were incorrectly staged by CECT (57.4%) and ^{18}F-FDG PET/CT (55%) were diagnosed correctly by our radiomic model.

Conclusion: We developed and validated two machine learning models based on the preoperative ^{18}F-FDG PET/CT images that have a predictive value for LNMs and the

N stage in GC. These predictive models show a promise to offer a potentially useful adjunct to current staging approaches for patients with GC.

Keywords: lymph nodes metastases, PET/CT, radiomics, N stage, gastric cancer

1 INTRODUCTION

Gastric cancer (GC) is the fifth most common malignancy and the third leading cause of cancer death worldwide (1, 2). Clinical staging, based mainly on imaging, is critical in determining the best treatment. Involvement of regional lymph nodes with metastases (LNMs) is classified as N0 (no LNM), N1 (1–2 LNMs), N2 (3–6 LNMs), N3a (7–15 LNMs), and N3b (≥ 16 LNMs). The different nodal (N) stage then determines the treatment strategy. Various investigators showed that patients with LNMs have a poor prognosis and a high recurrence rate (3–5). According to the Japanese Gastric Cancer Treatment Guidelines (6), radical gastrectomy with level-2 extended lymphadenectomy (D2 resections) is the standard treatment for GC without LNMs. For patients with advanced stages who cannot undertake surgery, preoperative evaluation of LNMs could provide useful information for determining the appropriate adjuvant therapy, while for patients who are suitable for surgery, accurate detection of LNMs prior to surgery could help in determining the surgical approach and lymph node dissection range. Therefore, the accurate detection of LNMs prior to surgery is required for an appropriate decision-making in GC.

Currently, contrast-enhanced CT (CECT) is used for N staging. Kim et al. (7) reported that the accuracy of CT was 50%–70% for LNMs. Unlike CECT imaging, ^{18}F-fluorodeoxyglucose positron emission tomography-CT (^{18}F-FDG PET/CT) reflects the glucose metabolism in tumors and can detect disease in lymph nodes that are not enlarged, and may have a higher specificity (8). The PET/CT parameters, however, that include the maximum standardized uptake (SUVmax), metabolic volume (MTV), and total lesion glycolysis (TLG), are affected by the different uptake times (time from isotope injection to PET data acquisition), instrumentation differences (different scanners), and attenuation correction methods. Furthermore, the predictive performance of SUVmax has varied across different researchers (9, 10). Yun et al, albeit with a PET-only scanner, stated that the accuracy of ^{18}F-FDG PET/CT in identifying LNMs was unsatisfactory (for N1 metastases: PET: 56%, CT: 69%; for N2 metastases: PET: 72%, CT: 69%; for N3 metastases: both PET and CT: 95%) (11). Now, with the advent of new radiomics methods, we suggest that nodal staging in GC should be re-considered.

Radiomics is an imaging analysis method that maximizes the information obtaining from routine diagnostic images and may detect data that is not readily apparent from the images alone (12). Recent advances in radiomics have provided insights into the accurate prediction of the pre-operative clinical stage. Several studies have shown that a CT radiomics nomogram can predict the N staging in a variety of cancers (13–15). Feng et al. developed a computational clinical decision support system based on CT radiomics to predict the involved LNs in gastric cancer, yielding an accuracy of 71.3% (16). Jiang et al. (17) concluded that the radiomic signature was a powerful predictor of LNMs based on the significant association between the CT radiomic signature and the pathological LN stage in GC. When compared to CT, ^{18}F-FDG PET/CT offers an additional advantage of providing metabolic information. Recently, PET/CT radiomics studies have been published on predicting the treatment response, prognosis, and the pathology sub-types (18–20). The predictive value of ^{18}F-FDG PET/CT radiomics in the N staging of GC, to our knowledge, has not been widely investigated. In this study, our aim was to develop and validate predictive machine learning models based on ^{18}F-FDG PET/CT radiomics to predict the LNMs and specific N stage in GC.

2 MATERIALS AND METHODS

2.1 Patients Inclusion Criteria

This study was approved by the Ethics Committee of the Fudan University Shanghai Cancer Center (No. 1909207-14-1910), and the need for the written informed consent was waived. There were 185 patients diagnosed with GC who underwent a total or partial radical gastrectomy at Fudan University Shanghai Cancer Hospital, including 156 GC patients obtained from January 2019 to May 2020 and 29 GC patients recruited from May 2020 to June 2021. These patients were reviewed retrospectively. The TNM staging was conducted according to the American Joint Committee on Cancer TNM Staging Manual, Eighth Edition (21). The inclusion criteria were as follows: (1) patients diagnosed as GC on surgically resected specimens; (2) patients with available clinical features such as sex, age, and tumor size; (3) patients with available ^{18}F-FDG PET/CT scan data before surgery; and (4) patients who did not receive neoadjuvant therapy before surgery.

2.2 Imaging Protocols and Image Analysis

A total of 161 out of 185 GC patients received dynamic contrast scans with a multidetector spiral CT (Sensation 64; Siemens Medical Systems, Germany). Contrast images were acquired in

Abbreviations: AUC, area under the curve; CECT, contrast-enhanced computed tomography; CT, computed tomography; FDG, fluorodeoxyglucose; FN, false negative; FP, false positive; GC, gastric cancer; GLCM, gray-level co-occurrence matrix; GLSZM, gray-level size zone matrix; LIME, Local Interpretable Model-Agnostic Explanations model; LNMs, lymph node metastases; LoG, Laplacian of Gaussian; MTV, metabolic volume; N, nodal; NPV, negative predicted value; PET, positron emission tomography; PPV, positive predicted value; ROI, region of interest; sklearn, scikit-learn; SUV, standardized uptake value; SUVmax, the maximum standardized uptake value; TLG, total lesion glycolysis; VOI, volume of interest.

the arterial (delay time: 30–35 seconds) and portal phases (delay time: 65–70 seconds) after an intravenous injection of 90 ml of iohexol (Omnipaque 300; Amersham, Shanghai, China) at a rate of 3 ml/second. Images were obtained at 120 kV and 200 mA with a 1-mm slice thickness. CT findings of the tumor location, size, perigastric lymph nodes, degree and pattern of enhancement, and distant metastases were analyzed. The size of the tumor was determined according to the maximum diameter of the tumor on the axial/coronal/sagittal images in the contrast phase. Contrast enhancement was graded as mild (< 10 HU), moderate (10–40 HU), and marked (> 40 HU). A perigastric lymph node was considered positive if the shortest diameter was greater than 10 mm or if there was a marked enhancement. The TNM stage of each patient was recorded by two experienced radiologists, and the results were verified by a third radiologist.

^{18}F-FDG PET/CT scans were performed using two whole-body PET/CT scanners (Siemens Medical Systems, Biograph 16 mCT Flow, and Biograph 16 mCT) in the Department of Nuclear Medicine. Patients fasted for at least 6 h, and the blood glucose levels were <140 mg/dl. With the Biograph 16 mCT Flow Scanner, scans were acquired 1 h after an intravenous injection of ^{18}F-FDG (3.7 MBq/kg). Images were acquired from the skull base to the upper thighs. A low-dose CT scan (120 kV, 140 mA, 5-mm slice thickness) was performed first to provide attenuation correction and anatomical information. Then, PET scan data were obtained and reconstructed with a time-of-flight ordered subset expectation maximization algorithm (iterations 4; subsets 8; image size 168) (22). With the Biograph 16 mCT Scanner, the scan was acquired approximately 1 h after the intravenous administration of 5.18 MBq/kg of ^{18}F-FDG. The CT scans were conducted first (120 kVp, 150 mAs, 0.33 s per rotation, thickness of 3.0 mm) and reconstructed to a 512 × 512 matrix "(voxel size: 0.98 × 0.98 × 3.0 mm^3). Then, PET scans were performed with the parameters (2 min per bed, 2 iterations, 24 subsets, and 2 mm full width at half maximum) without filtering and smoothing to reconstruct the PET images. Two experienced nuclear medicine physicians evaluated the PET/CT images and measured the maximum standardized uptake value (SUVmax) of the primary tumor and any metastases.

2.3 PET/CT Radiomics Analysis With Machine Learning

The radiomics analysis workflow is shown in **Figure 1**. There were five principal modules: input image segmentation, radiomic feature extraction, representative feature selection, predictive model construction, and statistical analysis. Firstly, we applied the same input image segmentation and radiomic feature extraction procedure for two different classification tasks, including Task A, predicting the LNMs, and Task B, predicting the N stage. Due to the different nature of the problems, we derived two branches for these two different classification tasks for the remaining principal modules, including feature selection, predictive model construction, and statistical analysis.

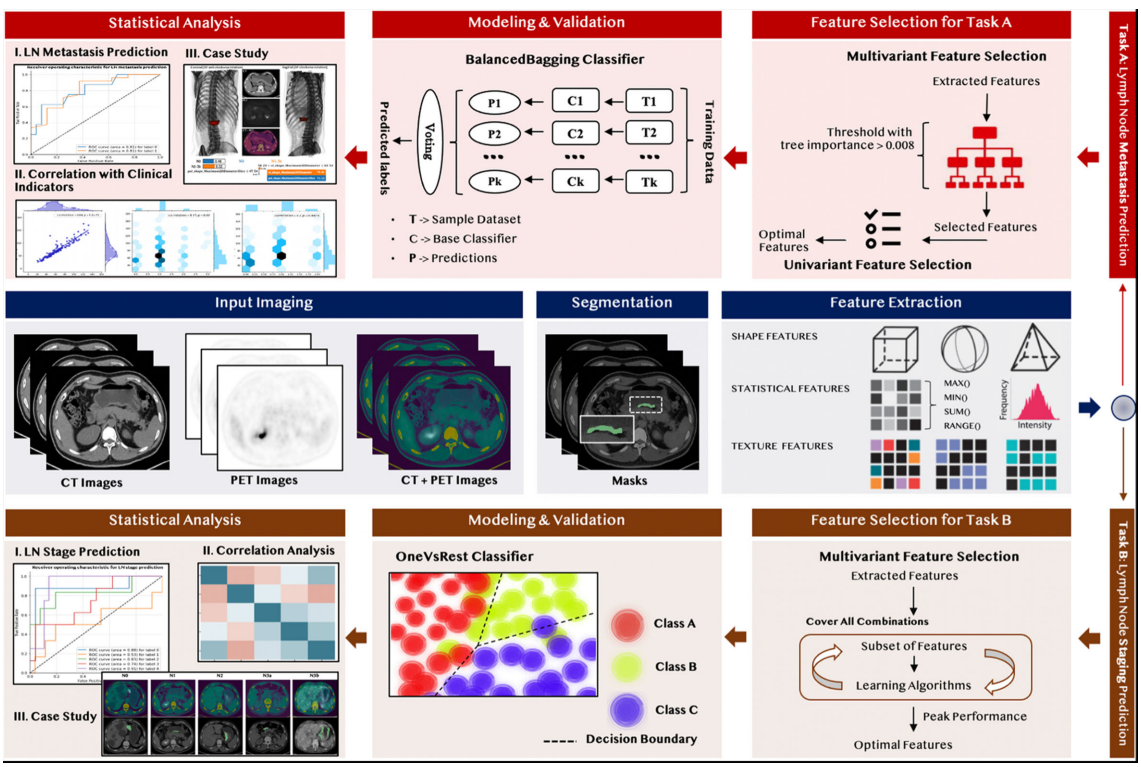

FIGURE 1 | Radiomic flowchart for the prediction of LNMs (task A) and the N stage (task B).

2.4 Medical Image Segmentation

The volume of interests (VOIs) in the tumor were delineated slice-by-slice with the ITK-SNAP software (version 3.6.0) (23) by the two senior nuclear medicine physicians. If a disagreement occurred, it was resolved by another experienced nuclear medicine physician. As the PET images and CT images were co-registered, only the VOIs of the PET images were individually segmented.

2.5 Radiomic Feature Extraction

There were 1,050 PET and 1,050 CT high-quantitative imaging features extracted from the corresponding VOIs. The 1,050 radiomic features included: (1) 18 first-order statistical features that were used to describe the distribution of individual voxel values within the image region defined by the mask through the commonly used and basic metrics without considering the spatial relationships (24); (2) 14 shape features used to describe the geometry properties and the shape of the region of interest (ROI) (25); (3) 56 texture features were extracted to measure the spatial arrangement of the voxel intensities and the intra-lesion heterogeneity, which could be derived from the grey-level co-occurrence matrix (GLCM) and grey-level size zone matrix (GLSZM) (25); and (4) 370 Laplacian of gaussian (LoG) filtered features and 592 wavelets filtered features; both were part of the higher-order statistical features obtained by applying the Laplacian of Gaussian (LoG) transformation and wavelets transformation, individually. Since the higher-order statistics features can suppress the noise and highlight the details in the original images, they are able to extract areas with increasingly coarse texture patterns in a more flexible way. The radiomic feature extraction process was implemented through the PyRadiomics package (24), an open-source package compliant with the Imaging biomarker standardization initiative (26).

2.6 Representative Feature Selection

We fused the 2,100 extracted radiomic features with 13 clinical features to form a feature pool before implementing the feature selection module. The feature selection strategy varied for different classification tasks, but both were mainly designed based on the output-driven model, with the aim of capturing the embedded patterns that were beneficial for each classification task.

As shown in **Figure 2A**, we applied a sequential combination of multivariant and univariant feature selection for predicting LNMs. In the multivariant feature selection, random forest feature selection (with tree importance > 0.008) was used due to its competitive predictive performance, low over-fitting, and easy interpretability. This interpretability was derived by computing the importance of each feature that contributed to the final decision. Then, univariant feature selection was deployed to select the final discriminative features through conducting the relevancy-based analysis using the Pearson correlation method among the selected features and the predicted class.

In predicting the N stage, we applied the sequential forward feature selection method in the multivariant feature selection. Since this algorithm comprehensively covered the combinations of the subsets and automatically selected a subset of the features

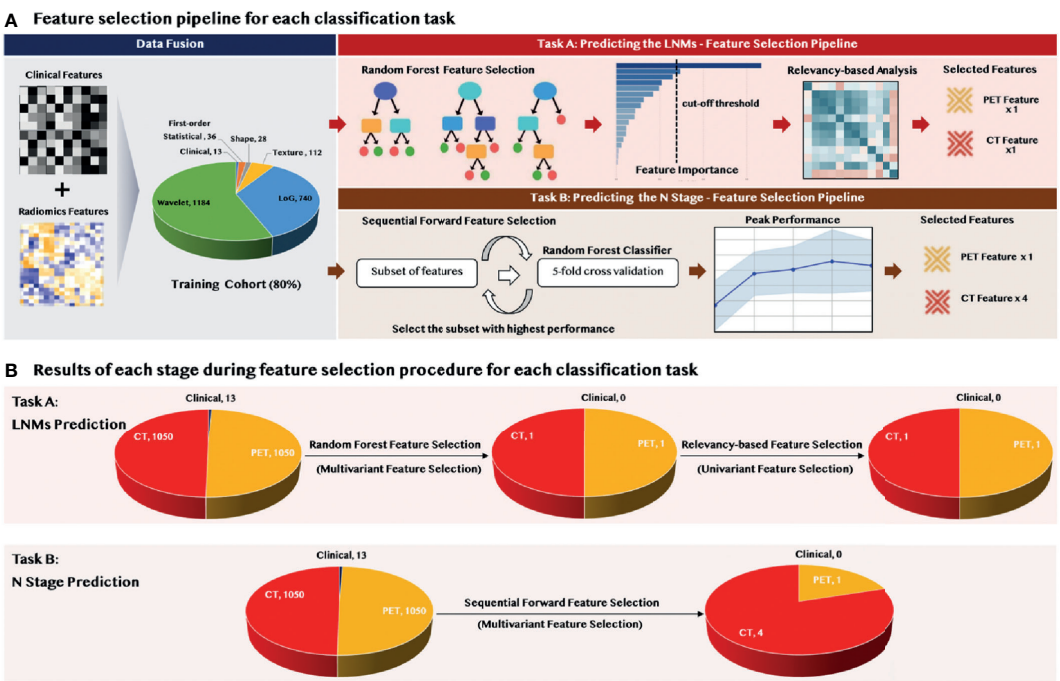

FIGURE 2 | Methodology and the results of feature selection: **(A)** feature selection pipeline, and **(B)** number of selected features during the selection procedure.

that offered the best performance on the training dataset, the univariant feature selection was not further required. The performance for each feature subset was evaluated by a 5-fold cross-validation to reduce the risk of overfitting, and the feature set that achieved the peak model performance was considered the final feature set.

2.7 Modeling and Validation

Patients, recruited from the 2019–2020 period (n = 156), were allocated into training and validation datasets using stratified methods at a fixed ratio to preserve the proportion of the targets in the original dataset; 80% of the 2019–2020 period patients were assigned to the training set, and the remaining 20% were assigned to the validation set. The 29 additional patients from 2020–2021 were further used to enlarge the independent validation cohorts.

For the prediction of LNMs, a BalancedBagging ensemble classifier (27) incorporated with Adaboost as the base classifier was constructed since it could improve the variance by voting the outcome from multiple base classifiers on variants of the training set and prevent overfitting. For the N stage, the OneVsRest classifier (27) was applied due to its high interpretability and the possibility of gaining knowledge about each class by inspecting its corresponding classes. Furthermore, we used 5-fold cross-validation methods on the training dataset and independent validation methods on the validation set to evaluate the performance and the robustness of each machine learning model. The performance of each model was primarily evaluated by the accuracy and the area under the curve (AUC); the confusion matrix also generated the sensitivity, specificity, positive predicted value (PPV), and negative predicted value (NPV) to detect the existence of bias within the model.

2.8 Statistical Analysis

Statistical analysis included a result interpretation of the machine learning model and correlation analysis of the selected radiomic features with pathological features. The Local Interpretable Model-Agnostic Explanations model (LIME) (28) was applied to explain the contribution of each selected feature through its derived weight coefficients to gain insights into the selected features and the predictive model. The LIME model estimated the weight coefficients by observing the changes in the results after eliminating several interpretable components. The changes were measured by the distance from the range center of the resulting changes in the prediction. The closer to the range center, the higher the weight coefficients would be assigned, indicating a better contribution to the final prediction.

We applied the Pearson correlation method that measured the strength and the direction of association between two continuous variables, to evaluate the correlation between the selected radiomic features and the pathological features. The Point-Biserial correlation method was used for the measurement between one continuous variable and one categorical variable. All statistical analyses were performed using the scikit-learn (sklearn) package (27) in Python version 3.6.4, and a two-sided P-value < 0.05 was considered statistically significant.

3 RESULTS

3.1 Demographics of Patients

The demographic information of 185 patients is summarized in **Table 1**. The included patients underwent open total gastrectomy (n = 103), distal gastrectomy (n = 79), and proximal gastrectomy (n = 3), with D2 lymphadenectomy in accordance with the Japanese guidelines [6], which included lymph node dissection (n > 15) of the perigastric and part of the suprapancreatic area. According to the pathological N stage (pN) of the TNM staging, LNM was divided into five categories: N0: no lymph node metastasis; N1: 1–2 lymph node metastases; N2: 3–6 lymph node metastases; N3a: 7-15 lymph node metastases; N3b: ≥ 16 lymph node metastases. The pathology in 77.8% of the patients was adenocarcinoma and mixed adenocarcinoma in the remainder. There were 136 patients with LNMs, and 49 patients without LNMs. There were 49 patients (26.4%) with N0 stage, 31 patients with N1 (16.8%), 31 patients (16.8%) with N2, 52 patients (28.1%) with N3a, and 22 patients (11.9%) with N3b stage. For ^{18}F-FDG PET/CT, the sensitivity was 68.7% and the specificity was 70%, while for CECT the sensitivity was 57.7% and the specificity was 66.7% (see **Table 2**). We maintained the same ratio between different predicted classes for the training set and the validation set as that in the original dataset, and there was no significant difference between the training set and validation set based on a two-sample t-test (p > 0.05).

3.2 Results of Feature Selection

As shown in **Figure 2B**, feature selection was applied to the 2,100 radiomic features extracted from PET and CT, and the 13 clinical features. Only two radiomic features—CT the Maximum3Ddiameter and PET the Maximum2DdiameterSlice—were selected during the multivariant feature selection for the prediction of LNMs. These two features remained through the relevancy-based feature selection and formed the final discriminative feature set used for the model construction. There were five radiomic features selected through the sequential forward feature selection method for the prediction of the N stage; these included four CT features (one shape; one LoG; two wavelet) and one for PET (wavelet).

3.3 Performance of Radiomic Features

Figures 3A, C show that during the validation process, the model had a good performance in predicting LNMs with an overall accuracy of 85.2% and AUC of 82.2%. More detailed information about the model performance, including sensitivity (73.3%) and specificity (89.1%), are shown in **Table 2**. Furthermore, the predictive model detected an additional 19.6% LNMs missed with CECT in the validation group, and 35.7% with ^{18}F-FDG PET/CT. The same evaluation procedure was applied for the model used to predict the N stage. The overall model accuracy was 62.3%, and the AUC was 73.7% (see **Figure 3B**). The model showed a competitive discrimination of the N stage (N0:72%, N1:96%, N2:77%, N3a:62%, and N3b:50%), and the detailed accuracy for each stage is outlined in **Figure 3D**. The overall accuracy for N stage prediction with CECT was 18.2%, and it was 35% for ^{18}F-FDG PET/CT in the validation set. In the validation group of N stage prediction, there were 57.4% that were incorrectly staged with CECT and 55% that

TABLE 1 | Demographic and clinical characteristics of the enrolled patients.

Characteristics		Total Population	N0	N1	N2	N3a	N3b
		(n = 185)	(n = 49)	(n = 31)	(n = 31)	(n = 52)	(n = 22)
Age, median (range)		62 (22–86)	61 (28–81)	63 (36–80)	62 (24–73)	62 (26–86)	66 (22–79)
Gender, n(%)		185	49	31	31	52	22
	Male	127 (68.6)	40 (81.6)	22 (71.0)	20 (64.5)	32 (61.5)	13 (59.1)
	Female	58 (31.4)	9 (18.4)	9 (29.0)	11 (35.5)	20 (38.5)	9 (40.9)
Histopathological Type, n (%)							
	adenocarcinoma	144 (77.8)	42 (85.7)	26 (83.9)	25 (80.6)	41 (78.8)	10 (45.5)
	mixed adenocarcinoma	41 (22.2)	7 (14.3)	5 (16.1)	6 (19.4)	11 (21.2)	12 (54.5)
Lauren Type, n (%)							
	intestinal type	64 (34.6)	23 (46.9)	14 (45.2)	12 (38.7)	14 (26.9)	1 (4.5)
	diffuse type	51 (27.6)	14 (28.6)	5 (16.1)	9 (29.0)	13 (25)	10 (45.5)
	mixed type	70 (37.8)	12 (24.5)	12 (38.7)	10 (32.3)	25 (48.1)	11 (50.0)
Differentiation, n (%)							
	low	85 (45.9)	18 (36.7)	10 (32.3)	12 (38.7)	28 (53.8)	17 (77.3)
	middle-low	58 (31.4)	11 (22.4)	10 (32.3)	13 (41.9)	19 (36.5)	5 (22.7)
	middle	36 (19.5)	16 (32.7)	11 (35.4)	5 (16.1)	4 (7.7)	0 (0.0)
	high	6 (3.2)	4 (8.2)	0 (0.0)	1 (3.3)	1 (2.0)	0 (0.0)
Vascular Tumor Thrombus, n (%)							
	not contain	34 (18.4)	25 (51)	8 (25.8)	1 (3.3)	0 (0.0)	0 (0.0)
	contain	126 (68.1)	12 (24.5)	18 (58.1)	25 (80.6)	51 (98.1)	20 (91.0)
	uncertain	22 (11.9)	12 (24.5)	4 (12.9)	5 (16.1)	0 (0.0)	1 (4.5)
	multiple tumors	3 (1.6)	0 (0.0)	1 (3.2)	0 (0.0)	1 (1.9)	1 (4.5)
Infiltration depth, n (%)							
	lamina propria or submucosa	31 (16.8)	20 (40.8)	5 (16.1)	3 (9.7)	2 (3.8)	1 (4.5)
	muscularis propria	23 (12.4)	9 (18.4)	6 (19.4)	3 (9.7)	4 (7.7)	1 (4.5)
	subserosa	54 (29.2)	10 (20.4)	9 (29.0)	13 (41.9)	17 (32.7)	5 (22.8)
	serosal layer	46 (24.8)	7 (14.3)	4 (12.9)	8 (25.8)	21 (40.4)	6 (27.3)
	fat tissue outside the serosal layer etc.	31 (16.8)	3 (6.1)	7 (22.6)	4 (12.9)	8 (15.4)	9 (40.9)
Nerve invasion, n (%)							
	+	104 (56.2)	16 (32.7)	17 (54.8)	19 (61.3)	37 (71.1)	15 (68.2)
	–	61 (33.0)	30 (61.2)	14 (45.2)	7 (22.6)	7 (13.5)	3 (13.6)
	uncertain	20 (10.8)	3 (6.1)	0 (0.0)	5 (16.1)	8 (15.4)	4 (18.2)
SUVmax_tumor, mean (std)		7.76 (5.93)	5.55 (4.41)	8.66 (5.61)	8.34 (5.02)	9.51 (7.57)	6.48 (3.87)
SUVmax_LN, mean (std)		2.92 (3.72)	1.56 (2.28)	3.32 (3.73)	3.07 (3.17)	3.58 (4.96)	3.60 (2.62)
maximum diameter, mean (std)		4.81 (2.97)	3.76 (2.48)	4.14 (2.43)	4.82 (2.10)	4.95 (2.85)	7.77 (3.89)

were incorrect with ^{18}F-FDG PET/CT, but which had the correct N stage with the radiomic model.

3.4 Feature Analysis and Interpretation

There were two features, one CT feature (ct_shape_Maximum3DDiameter) and one PET feature (pet_shape_Maximum2DDiameterSlice), which were identified by the sequentially combined multivariant and univariant feature selection process for predicting LNMs. The Maximum3DDiameter feature was used to define the largest pairwise Euclidean distance between the tumor surface mesh vertices. The Maximum2DDiameterSlice feature was a similar feature; however, it only defined the distance in the row-column (generally axis) plane. The statistics of these two selected quantitative features are summarized in **Supplementary Table S1**. The contribution of each selected feature in the prediction of LNMs is shown in **Figures 4A, B**, and **C** through the normalized importance calculated by the LIME model (28) in three different situations, including for: (1) all the patients in the validation set, (2) patients without metastases, and (3) patients with metastases. The CT feature had a higher contribution, when compared to the PET feature, in predicting LNMs in these three situations with the normalized importance of 86%, 90%, and 84%, sequentially.

TABLE 2 | Results for predicting lymph node metastases in independent validation cohorts.

Evaluation	Accuracy	AUC	Sensitivity	Specificity	PPV	NPV
CECT	0.602	–	0.577	0.667	**0.817**	0.380
^{18}F-FDG PET/CT	0.692	–	0.687	0.70	0.790	0.576
PET feature	0.770	0.724	0.563	0.844	0.563	0.844
CT feature	**0.852**	0.803	**0.769**	0.875	0.625	**0.933**
CT + PET	**0.852**	**0.822**	0.733	**0.891**	0.688	0.911

The bold feature value represented the combined radiomic features that achieved high prediction accuracy for both target classes, while the bold numerical value represented the highest value of each column.

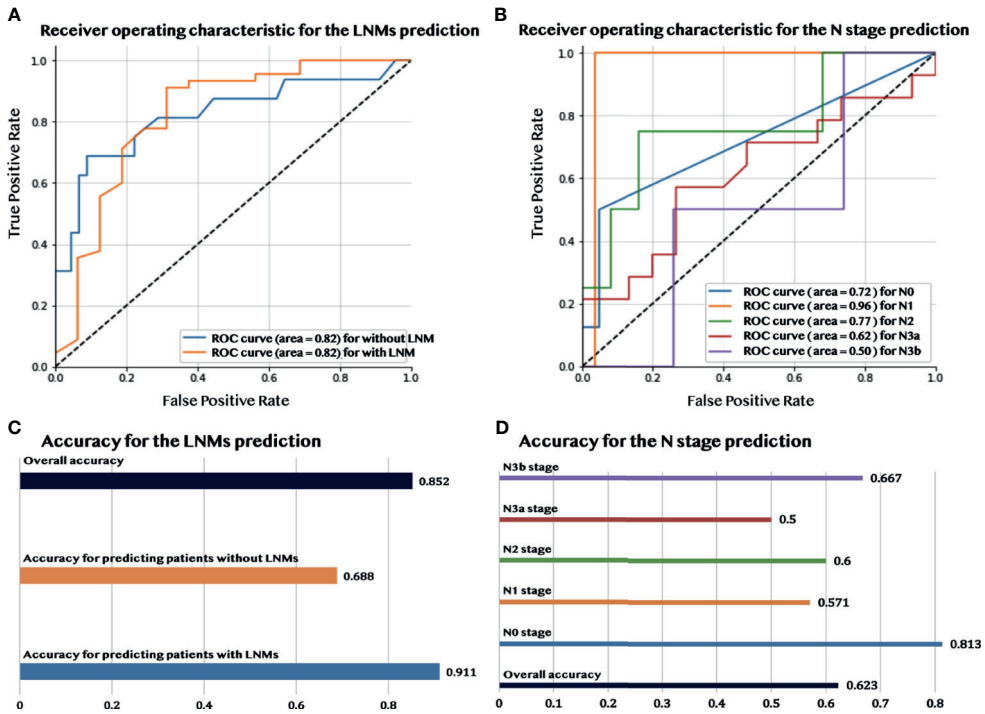

FIGURE 3 | The performance of predicting LNMs and the N stage. **(A)** The AUC curve for predicting LNMs. **(B)** The AUC curve for predicting the N stage. **(C)** Accuracy of the prediction of LNMs. **(D)** Accuracy of the prediction of the N stage.

We identified five features in the prediction of the N stage. These included four CT features and one PET wavelet feature. The detailed explanation of these features, including the definition and the calculated formula, are summarized in **Supplementary Table S2**. According to **Figure 4D**, the CT shape feature dominated the contribution to predicting the N stage in the validation set. The contribution of the CT shape feature was very similar to the only PET feature (see **Figures 4E–I**). Both features contributed more to predicting the N1 stage, N2 stage, and N3b stage with a lesser contribution to N0 and N3a.

3.5 Case Studies

Two typical cases were chosen by the domain experts—one patient with and one without metastases—to illustrate the performance of our model in predicting LNMs. The detailed medical information, including the CT and PET images and 3D models for each patient, are shown in **Figures 5A, B**. The value of the selected features for each patient is indicated in the table at the bottom of panels A and B. The contribution of each feature is explicitly revealed by the LIME model through the weight coefficients listed in the bar chart of each panel. The model quantitatively combined the selected features with their diverse weight coefficients for the final prediction and correctly predicted both cases. We also chose five cases to showcase the model performance for the prediction of the N stage. The PET/CT images and the segmentation section are shown in **Figure 5C**. In all five patients, our machine learning model predicted the N stage accurately. In comparison, ^{18}F-FDG PET/CT did not detect LNMs in all five patients, and CECT also did not stage the N stages correctly.

3.6 Correlation With Pathological Features

We computed the Pearson correlation between the selected radiomic features and the pathological features that were commonly used for the diagnosis of the LNMs to underline the reliability and the significance of two selected features in the prediction of the LNMs. The CT feature was significantly correlated to the vascular tumor thrombus, nerve invasion, histopathological type, differentiation, and infiltration depth ($p < 0.05$), which explained its high contribution to the final prediction, as shown in **Figure 6A**. The Pearson correlation between the five selected radiomic and pathological features used to predict the N stage is shown in **Figure 6B**. It showed that the PET/CT radiomic features were also significantly correlated ($p < 0.05$) to the pathological features such as infiltration depth. The detailed P-value for the correlation analysis were summarized in **Supplementary Figure S1**.

4 DISCUSSION

Our main findings are as follows: (1) We developed and validated (AUC 82.2%) a binary predictive model using two ^{18}F-FDG PET/CT radiomic features to predict LNMs preoperatively. This model might allow clinicians to identify patients with a high risk of LNMs and thus assist diagnosis and decision-making. (2) We developed and validated (AUC 73.7%) a radiomics multiclass predictive model using ^{18}F-FDG PET/CT to identify the N stage prior to surgery.

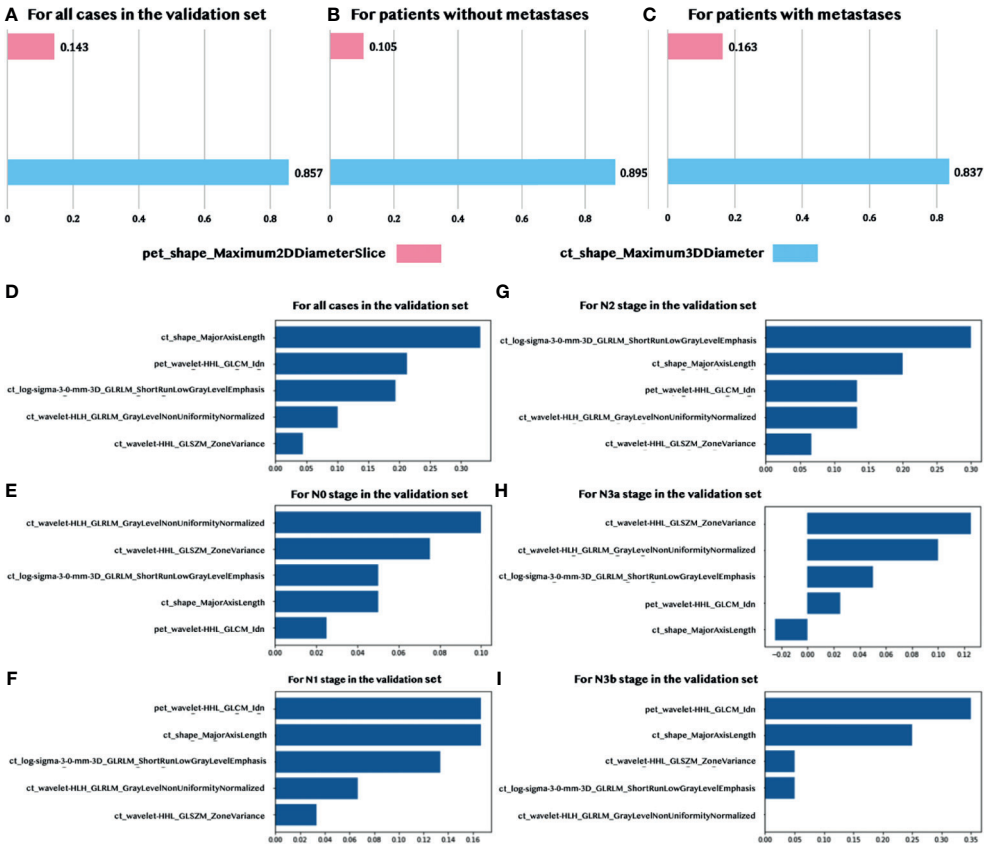

FIGURE 4 | Normalized feature importance. **(A–C)** Feature importance in predicting LNMs for all validation patients and patients with/without metastases. **(D–I)** Feature importance in predicting the N stage for all validation patients and patients with five N stages (N0, N1, N2, N3a, and N3b).

The reported sensitivity (57.7%) and specificity (66.7%) of CECT in our study were similar to a previous work (7). On CECT, enlarged lymphs were not always metastatic, and small lymph nodes could be metastatic, hence, the predictive performance of CECT in detecting LNMs is sub-optimal. Since ^{18}F-FDG PET/CT can detect disease in lymph nodes that are not enlarged, more recent clinical guidelines suggest that it might improve GC staging (29). Previous studies showed that a high ^{18}F-FDG uptake could be associated with LNMs (30–32). The thresholds of SUVmax, however, varied significantly across different studies. In our study, the performance of ^{18}F-FDG PET/CT in predicting LNMs was relatively inferior, especially with a low negative predicted value (NPV) of 57.6%. Our results were consistent with the previous study (33). The reasons might be that: (1) the resolution of ^{18}F-FDG PET was limited, which might miss some positive uptake of small LNs; (2) some LNMs presented no ^{18}F-FDG uptake because of the tumor heterogeneity and some histopathology type (such as signet-ring cell carcinoma and mixed adenocarcinoma); and (3) some perigastric LNs were masked by the high ^{18}F-FDG uptake of the primary tumor.

In the present study, the ^{18}F-FDG PET/CT-based radiomics model showed a superior performance in discriminating LNMs with an AUC of 82.2% in the independent validation. Moreover, it also detected some LNMs that were missed in CECT (19.6%) and ^{18}F-FDG PET/CT (35.7%), indicating that the PET/CT-based radiomics model could supplement ^{18}F-FDG PET/CT to optimize the diagnostic performance. The performance might be attributed to the quantification process of the radiomic model applied for the final prediction and the parameters that could not be obtained by routine visual analysis and measurement of lymph node size and metabolism. Additionally, the correlation analysis indicated that the selected features (CT feature: Maximum3DDiameter; PET feature: Maximum2DDiameterSlice) used to establish the predictive model were significantly correlated to the pathological features, including vascular tumor thrombus, nerve invasion, and infiltration depth ($p < 0.05$). Since these pathological features were strongly associated with tumor invasion and metastasis, it could further explain the outstanding performance of the radiomic models.

Feng et al. proposed a clinical decision support system for the preoperative prediction of LNMs in GC (16) with the support vector machine (SVM) classifier. However, since the SVM classifier works by placing data points above and below the classifying hyperplanes, it would be difficult to generate a probabilistic explanation for the classification. Furthermore, the SVM would underperform in cases where the number of features for each data point exceeded the number of training data samples, which might be the reason for a large number of applied features (13) in the classifier. in the

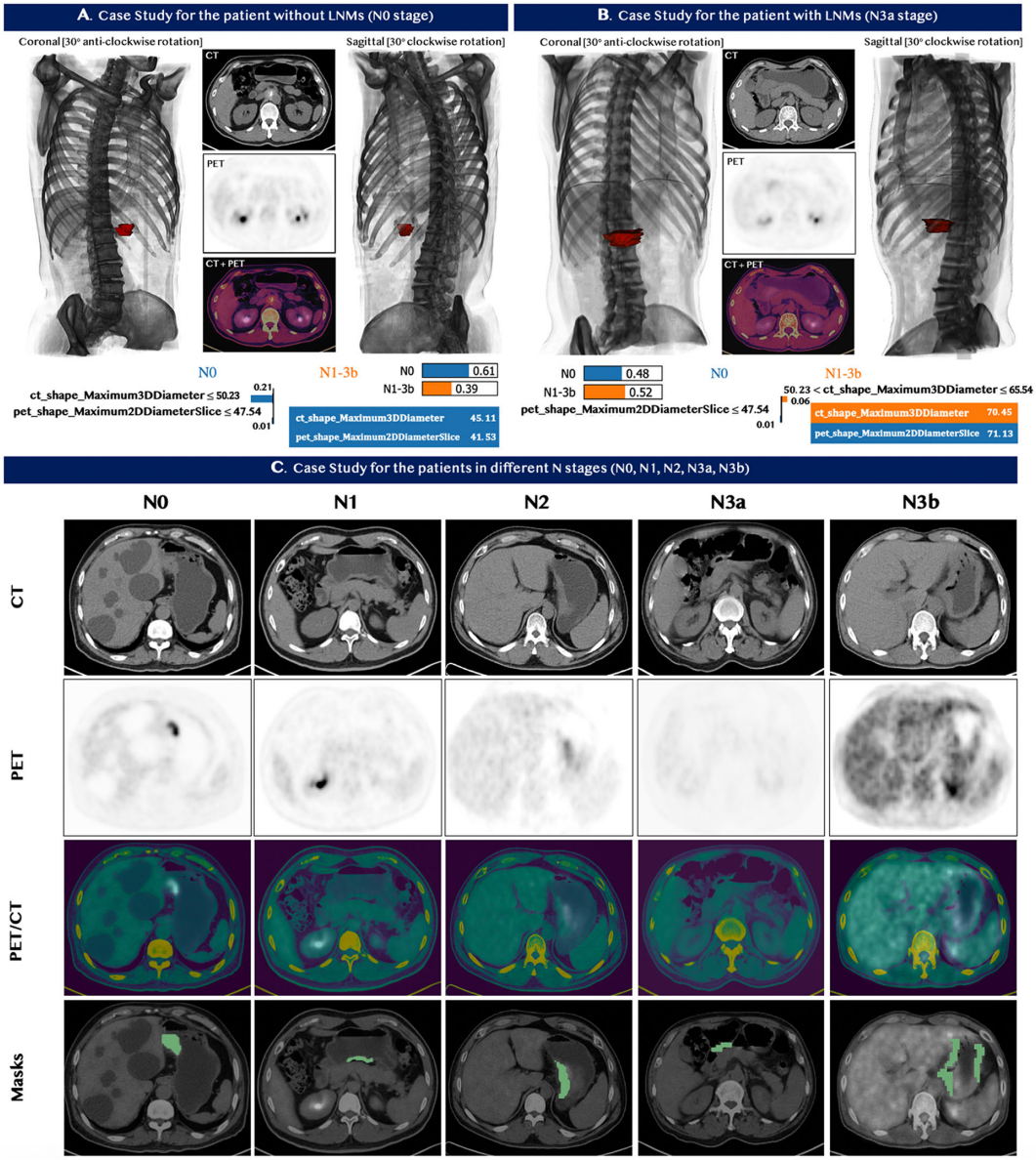

FIGURE 5 | Case studies for seven patients with GC. Top Panels: **(A)** patient with no lymph nodes metastases. **(B)** patient with lymph nodes metastases. The image at the bottom of **(A, B)** contains the feature value of the patients and the corresponding LIME interpretation. The top left and top right sections in panel **(A, B)** demonstrated the 3D model constructed based on the input CT and PET images from different viewpoints, while the red section represented the tumor of the patients. Our predictive model correctly identified the status for both patients in panel **(A, B)**. **(C)** Bottom Panel - Five patients with different stages N0, N1, N2, N3a, and N3b from left to right. Our machine learning model predicted the N stage of the five patients accurately. ^{18}F-FDG PET/CT, however, did not detect LNMs in all five patients; and CECT also did not assess the N stages correctly.

classifier. Our study employed an ensemble classifier to predict LNMs preoperatively. It improved the stability and the accuracy in the statistical classification and also helped reduce the variance to prevent overfitting. Thus, we achieved a better performance (accuracy 85.2% *vs.* 71.3%) with a smaller feature set (feature number 2 *vs.* 13) for the preoperative prediction of LNMs in GC.

Due to the low sensitivity and specificity, CECT and ^{18}F-FDG PET/CT missed and incorrectly identified some LNMs. As a result, the performance of the two imaging modalities in predicting the number of LNMs was inferior. In comparison, the machine learning model showed a better predictive performance, with an overall AUC of 73.7% and an accuracy of 62.3% in the validation group. In addition, a proportion of patients in the validation group, whose LNMs were incorrectly staged by CECT (57.4%) and ^{18}F-FDG PET/CT (55%), were then diagnosed correctly by our radiomic model, indicating that the

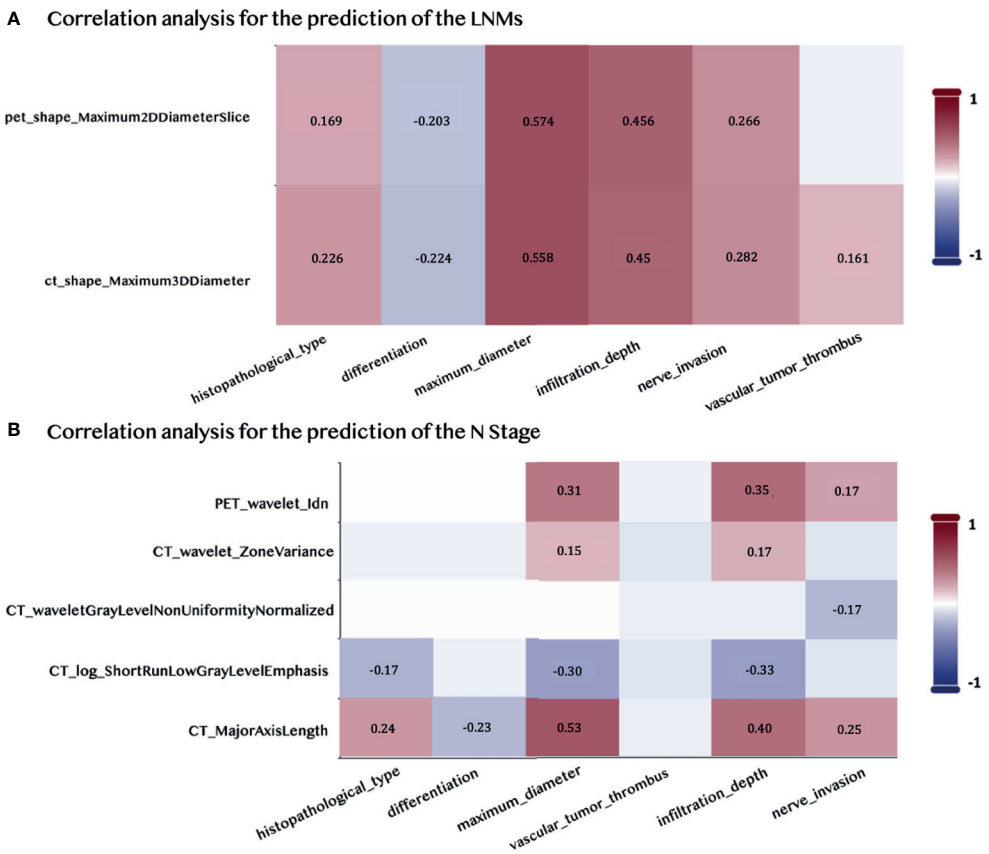

FIGURE 6 | Pearson Correlations between the selected PET/CT features and the pathological features. **(A)** Correlation analysis for predicting LNMs. **(B)** Correlation analysis for predicting the N stage. Pairwise correlations with $p < 0.05$ are shown in the figure.

radiomic model could supplement the current staging scheme. Dong et al. also reported a deep learning CT-radiomic model to predict the number of LNMs in GC with an overall C-index of 0.797 (0.771–0.823) (34). The model employed the deep learning features for delivering a high-quality result with the cost of the feature interpretability. Although with different methods, similar results indicated that the radiomic approach promised to facilitate an individualized prediction of N stages and help choose the best surgical approach with respect to resecting lymph nodes. Since the current study was a retrospective research, prospective research with GC patients recruited across multiple centers would be conducted in the future.

5 CONCLUSION

In this study in patients with GC, we successfully developed and validated machine learning models based on preoperative ^{18}F-FDG PET/CT radiomics to identify LNMs and stratify patients into the different N stages. The machine learning model might be an important adjunct to conventional imaging modalities to help select the most appropriate treatment for patients with GC.

DATA AVAILABILITY STATEMENT

The original contributions presented in the study are included in the article/**Supplementary Material**, further inquiries can be directed to the corresponding authors.

ETHICS STATEMENT

This study was approved by the Ethics Committee of the Fudan University Shanghai Cancer Center. The ethics committee waived the requirement of written informed consent for participation. Written informed consent was obtained from the individual(s) for the publication of any potentially identifiable images or data included in this article.

AUTHOR CONTRIBUTIONS

Methodology: QL, JL, and BX. Validation: JL, BX, and QL. Original draft preparation: QL and JL. Data collection: YS. Review and editing: MF. Visualization: all authors. Supervision

and project administration: SS and XW. Funding acquisition: SS. All authors contributed to the article and approved the submitted version.

FUNDING

This work was partially supported by the National Natural Science Foundation of China (Grant No. 82001866, 81971648, 81771861) and Shanghai Sailing Program (Grant No. 20YF1408400).

ACKNOWLEDGMENTS

We would like to thank all the members who participated in this work.

SUPPLEMENTARY MATERIAL

The Supplementary Material for this article can be found online at: https://www.frontiersin.org/articles/10.3389/fonc.2021.723345/full#supplementary-material

REFERENCES

1. Siegel RL, Miller KD, Goding Sauer A, Fedewa SA, Butterly LF, Anderson JC, et al. Colorectal Cancer Statistics, 2020. *CA: Cancer J Clin* (2020) 70:145–64. doi: 10.3322/caac.21601
2. Smyth EC, Nilsson M, Grabsch HI, van Grieken NC, Lordick F. Gastric Cancer. *Lancet* (2020) 396:635–48. doi: 10.1016/S0140-6736(20)31288-5
3. Saka M, Katai H, Fukagawa T, Nijjar R, Sano T. Recurrence in Early Gastric Cancer With Lymph Node Metastasis. *Gastric Cancer* (2008) 11:214–8. doi: 10.1007/s10120-008-0485-4
4. Bilici A, Selcukbiricik F, Seker M, Oven BB, Olmez OF, Yildiz O, et al. Prognostic Significance of Metastatic Lymph Node Ratio in Patients With Pn3 Gastric Cancer Who Underwent Curative Gastrectomy. *Oncol Res Treat* (2019) 42:204–11. doi: 10.1159/000496746
5. Morgan JW, Ji L, Friedman G, Senthil M, Dyke C, Lum SS. The Role of the Cancer Center When Using Lymph Node Count as a Quality Measure for Gastric Cancer Surgery. *JAMA Surg* (2015) 150:37–43. doi: 10.1001/jamasurg.2014.678
6. Association JGC. Japanese Gastric Cancer Treatment Guidelines 2010 (Ver 3). *Gastric Cancer* (2011) 14:113–23. doi: 10.1007/s10120-011-0042-4
7. Kim HJ, Kim AY, Oh ST, Kim JS, Kim KW, Kim PN, et al. Gastric Cancer Staging at Multi–Detector Row Ct Gastrography: Comparison of Transverse and Volumetric Ct Scanning. *Radiology* (2005) 236:879–85. doi: 10.1148/radiol.2363041101
8. Kawanaka Y, Kitajima K, Fukushima K, Mouri M, Doi H, Oshima T, et al. Added Value of Pretreatment 18f-Fdg Pet/Ct for Staging of Advanced Gastric Cancer: Comparison With Contrast-Enhanced Mdct. *Eur J Radiol* (2016) 85:989–95. doi: 10.1016/j.ejrad.2016.03.003
9. Tang L, Wang XJ, Baba H, Giganti F. Gastric Cancer and Image-Derived Quantitative Parameters: Part 2—A Critical Review of Dce-Mri and 18 F-Fdg Pet/Ct Findings. *Eur Radiol* (2020) 30:247–60. doi: 10.1007/s00330-019-06370-x
10. Liu Y, Zheng D, Liu JJ, Cui JX, Xi HQ, Zhang KC, et al. Comparing Pet/Mri With Pet/Ct for Pretreatment Staging of Gastric Cancer. *Gastroenterol Res Pract* (2019) 2019. doi: 10.1155/2019/9564627
11. Yun M, Lim JS, Noh SH, Hyung WJ, Cheong JH, Bong JK, et al. Lymph Node Staging of Gastric Cancer Using 18f-Fdg Pet: A Comparison Study With Ct. *J Nucl Med* (2005) 46:1582–8.
12. Davnall F, Yip CS, Ljungqvist G, Selmi M, Ng F, Sanghera B, et al. Assessment of Tumor Heterogeneity: An Emerging Imaging Tool for Clinical Practice? *Insights Imaging* (2012) 3:573–89. doi: 10.1007/s13244-012-0196-6
13. Wu S, Zheng J, Li Y, Yu H, Shi S, Xie W, et al. A Radiomics Nomogram for the Preoperative Prediction of Lymph Node Metastasis in Bladder Cancer. *Clin Cancer Res* (2017) 23:6904–11. doi: 10.1158/1078-0432.CCR-17-1510
14. Huang YQ, Liang CH, He L, Tian J, Liang CS, Chen X, et al. Development and Validation of a Radiomics Nomogram for Preoperative Prediction of Lymph Node Metastasis in Colorectal Cancer. *J Clin Oncol* (2016) 34:2157–64. doi: 10.1200/JCO.2015.65.9128
15. Wang Y, Liu W, Yu Y, Liu JJ, Xue HD, Qi YF, et al. Ct Radiomics Nomogram for the Preoperative Prediction of Lymph Node Metastasis in Gastric Cancer. *Eur Radiol* (2020) 30:976–86. doi: 10.1007/s00330-019-06398-z
16. Feng QX, Liu C, Qi L, Sun SW, Song Y, Yang G, et al. An Intelligent Clinical Decision Support System for Preoperative Prediction of Lymph Node Metastasis in Gastric Cancer. *J Am Coll Radiol* (2019) 16:952–60. doi: 10.1016/j.jacr.2018.12.017
17. Jiang Y, Wang W, Chen C, Zhang X, Zha X, Lv W, et al. Radiomics Signature on Computed Tomography Imaging: Association With Lymph Node Metastasis in Patients With Gastric Cancer. *Front Oncol* (2019) 9:340. doi: 10.3389/fonc.2019.00340
18. Dissaux G, Visvikis D, Da-Ano R, Pradier O, Chajon E, Barillot I, et al. Pretreatment 18f-Fdg Pet/Ct Radiomics Predict Local Recurrence in Patients Treated With Stereotactic Body Radiotherapy for Early-Stage non–Small Cell Lung Cancer: A Multicentric Study. *J Nucl Med* (2020) 61:814–20. doi: 10.2967/jnumed.119.228106
19. Li Y, Zhang Y, Fang Q, Zhang X, Hou P, Wu H, et al. Radiomics Analysis of [18 F] Fdg Pet/Ct for Microvascular Invasion and Prognosis Prediction in Very-Early-And Early-Stage Hepatocellular Carcinoma. *Eur J Nucl Med Mol Imaging* (2021), 48(8):1–16. doi: 10.1007/s00259-020-05119-9
20. Zhang N, Liang R, Gensheimer MF, Guo M, Zhu H, Yu J, et al. Early Response Evaluation Using Primary Tumor and Nodal Imaging Features to Predict Progression-Free Survival of Locally Advanced non-Small Cell Lung Cancer. *Theranostics* (2020) 10:11707. doi: 10.7150/thno.50565
21. Amin MB, Greene FL, Edge SB, Compton CC, Gershenwald JE, Brookland RK, et al. Ajcc Cancer Staging Manual. *AJCC Cancer Staging Manual* (2017) 67(2):93–9. doi: 10.3322/caac.21388
22. Zhu YM. Ordered Subset Expectation Maximization Algorithm for Positron Emission Tomographic Image Reconstruction Using Belief Kernels. *J Med Imaging* (2018) 5:044005. doi: 10.1117/1.JMI.5.4.044005
23. Yushkevich PA, Piven J, Hazlett HC, Smith RG, Ho S, Gee JC, et al. User-Guided 3d Active Contour Segmentation of Anatomical Structures: Significantly Improved Efficiency and Reliability. *Neuroimage* (2006) 31:1116–28. doi: 10.1016/j.neuroimage.2006.01.015
24. Van Griethuysen JJ, Fedorov A, Parmar C, Hosny A, Aucoin N, Narayan V, et al. Computational Radiomics System to Decode the Radiographic Phenotype. *Cancer Res* (2017) 77:e104–7. doi: 10.1158/0008-5472.CAN-17-0339
25. Rizzo S, Botta F, Raimondi S, Origgi D, Fanciullo C, Morganti AG, et al. Radiomics: The Facts and the Challenges of Image Analysis. *Eur Radiol Exp* (2018) 67(2):93–9. doi: 10.1186/s41747-018-0068-z
26. Zwanenburg A, Vallières M, Abdalah MA, Aerts HJ, Andrearczyk V, Apte A, et al. The Image Biomarker Standardization Initiative: Standardized Quantitative Radiomics for High-Throughput Image-Based Phenotyping. *Radiology* (2020) 295:328–38. doi: 10.1148/radiol.2020191145
27. Pedregosa F, Varoquaux G, Gramfort A, Michel V, Thirion B, Grisel O, et al. Scikit-Learn: Machine Learning in Python. *J Mach Learn Res* (2011) 12:2825–30.
28. Ribeiro MT, Singh S, Guestrin C. "Why Should I Trust You?" Explaining the Predictions of Any Classifier. In: *Proceedings of the 22nd ACM SIGKDD International Conference on Knowledge Discovery and Data Mining*. New York, NY, United States: Association for Computing Machinery (2016). p. 1135–44.
29. Smyth E, Verheij M, Allum W, Cunningham D, Cervantes A, Arnold D. Gastric Cancer: Esmo Clinical Practice Guidelines for Diagnosis,

Treatment and Follow-Up. *Ann Oncol* (2016) 27:v38–49. doi: 10.1093/annonc/mdw350
30. Bosch KD, Chicklore S, Cook GJ, Davies AR, Kelly M, Gossage JA, et al. Staging Fdg Pet-Ct Changes Management in Patients With Gastric Adenocarcinoma Who are Eligible for Radical Treatment. *Eur J Nucl Med Mol Imaging* (2020) 47:759–67. doi: 10.1007/s00259-019-04429-x
31. Wang X, Wei Y, Xue Y, Lu P, Yu L, Shen B. Predictive Role of the Number of 18f-Fdg-Positive Lymph Nodes Detected by Pet/Ct for Pre-Treatment Evaluation of Locally Advanced Gastric Cancer. *PLoS One* (2016) 11: e0166836. doi: 10.1371/journal.pone.0166836
32. Perlaza P, Ortín J, Pagès M, Buxó E, Fernández-Esparrach G, Colletti PM, et al. Should 18f-Fdg Pet/Ct Be Routinely Performed in the Clinical Staging of Locally Advanced Gastric Adenocarcinoma? *Clin Nucl Med* (2018) 43:402–10. doi: 10.1097/RLU.0000000000002028
33. Kim EY, Lee WJ, Choi D, Lee SJ, Choi JY, Kim BT, et al. The Value of Pet/Ct for Preoperative Staging of Advanced Gastric Cancer: Comparison With Contrast-Enhanced Ct. *Eur J Radiol* (2011) 79:183–8. doi: 10.1016/j.ejrad.2010.02.005
34. Dong D, Fang MJ, Tang L, Shan XH, Gao JB, Giganti F, et al. Deep Learning Radiomic Nomogram can Predict the Number of Lymph Node Metastasis in Locally Advanced Gastric Cancer: An International Multicenter Study. *Ann Oncol* (2020) 31:912–20. doi: 10.1016/j.annonc.2020.04.003

Conflict of Interest: The authors declare that the research was conducted in the absence of any commercial or financial relationships that could be construed as a potential conflict of interest.

Publisher's Note: All claims expressed in this article are solely those of the authors and do not necessarily represent those of their affiliated organizations, or those of the publisher, the editors and the reviewers. Any product that may be evaluated in this article, or claim that may be made by its manufacturer, is not guaranteed or endorsed by the publisher.

Copyright © 2021 Liu, Li, Xin, Sun, Feng, Fulham, Wang and Song. This is an open-access article distributed under the terms of the Creative Commons Attribution License (CC BY). The use, distribution or reproduction in other forums is permitted, provided the original author(s) and the copyright owner(s) are credited and that the original publication in this journal is cited, in accordance with accepted academic practice. No use, distribution or reproduction is permitted which does not comply with these terms.

frontiers in Oncology

ORIGINAL RESEARCH
published: 27 September 2021
doi: 10.3389/fonc.2021.753330

Extracellular Matrix Characterization in Gastric Cancer Helps to Predict Prognosis and Chemotherapy Response

Zhi Yang[1†], Feifei Xue[2†], Minhuan Li[3†], Xingya Zhu[1†], Xiaofeng Lu[1], Chao Wang[4], En Xu[4], Xingzhou Wang[4], Liang Zhang[1], Heng Yu[1], Chuanfu Ren[1], Hao Wang[1,4], Yizhou Wang[1], Jie Chen[5], Wenxian Guan[1,4*] and Xuefeng Xia[1,4*]*

[1] Department of General Surgery, Drum Tower Clinical Medical College of Nanjing Medical University, Nanjing, China, [2] Jiangsu Key Laboratory of Oral Diseases, Nanjing Medical University, Nanjing, China, [3] Department of Andrology, Drum Tower Clinical Medical College of Nanjing Medical University, Nanjing, China, [4] Department of General Surgery, Nanjing Drum Tower Hospital, The Affiliated Hospital of Nanjing University Medical School, Nanjing, China, [5] Department of Anesthesiology, Nanjing Drum Tower Hospital, The Affiliated Hospital of Nanjing University Medical School, Nanjing, China

The extracellular matrix (ECM) plays a central role in the formation of the tumor microenvironment. The deposition of the ECM is associated with poor prognosis in a variety of tumors. Aberrant ECM deposition could undermine the effect of chemotherapy and immunotherapy. However, there is no systematic analysis on the relationship between the ECM and prognosis or chemotherapy effect. In the present study, we applied the gene set variation analysis (GSVA) algorithm to score 2199 canonical pathways in 2125 cases of probe or sequencing data and identified the core matrisome as the driving factor in gastric cancer progression. We classified gastric cancer samples into three clusters according to the composition of the ECM and evaluated clinical and multi-omics characterization of ECM phenotypes. The ECM score was evaluated by GSVA score of core matrisome and a higher ECM score predicted poor prognosis of gastric cancer [Hazard Ratio (HR), 2.084; p-value $< 2 \times 10^{-16}$]. In The Cancer Genome Atlas (TCGA) cohort and KUGH, YUSH, and KUCM cohorts, we verified that patients with a low ECM score could benefit from chemotherapy. By contrast, patients with a high ECM score did not achieve satisfactory response from chemotherapy. Determining the characteristics of the ECM microenvironment might help to predict the prognosis and chemotherapy response of patients with gastric cancer, and help to resolve the enigma of chemoresistance acquisition, as well as providing inspiration to develop combination therapy.

Keywords: gastric cancer, ECM, prognostic factors, chemotherapy response, multi-omics

OPEN ACCESS

Edited by:
Andreas Brandl, Champalimaud Foundation, Portugal

Reviewed by:
Geoffroy Andrieux, Universität Freiburg, Germany
Linda Feldbrügge, Charité Universitätsmedizin, Germany

***Correspondence:**
Wenxian Guan
15850502391@163.com
Xuefeng Xia
danielxuefeng@hotmail.com
Jie Chen
jiechen028@163.com

†These authors have contributed equally to this work and share first authorship

Specialty section:
This article was submitted to Gastrointestinal Cancers: Gastric and Esophageal Cancers, a section of the journal Frontiers in Oncology

Received: *04 August 2021*
Accepted: *07 September 2021*
Published: *27 September 2021*

Citation:
Yang Z, Xue F, Li M, Zhu X, Lu X, Wang C, Xu E, Wang X, Zhang L, Yu H, Ren C, Wang H, Wang Y, Chen J, Guan W and Xia X (2021) Extracellular Matrix Characterization in Gastric Cancer Helps to Predict Prognosis and Chemotherapy Response. Front. Oncol. 11:753330. doi: 10.3389/fonc.2021.753330

INTRODUCTION

Gastric cancer (GC) is the third leading cause of cancer-related death and the fifth most common cancer diagnosed worldwide (1). Surgical resection has always been the mandatory backbone treatment for resectable stage II and III GC (1). However, the significant benefit from surgical resection alone is confined to early GC, while the rate of relapse remains high for advanced GC.

Multimodal therapies, including chemotherapy, chemoradiation, and immunotherapy, have been established to prevent recurrence and have improved the survival rates of patients after surgery (1). Although the receipt of adjunctive therapies could improve prognosis for some patients with GC patients to a certain extent, variations in clinical outcome have been detected for patients who received the same treatment (2–4). Multiple molecular subtypes and ingenious prognostic models based on multi-omics data have been established for patients with resectable GC. Stomach adenocarcinoma in The Cancer Genome Atlas (TCGA) was subdivided into five molecular subtypes on the basis of molecular profiles: microsatellite instable (MSI), genomically stable (GS), Epstein–Barr virus (EBV) associated, chromosomal instability (CIN) and hypermutated-single-nucleotide variant predominant (HM-SNV) (5, 6). And the Asian Cancer Research Group (ACRG) defined four molecular subtypes, including microsatellite stable (MSS)/epithelial–mesenchymal transition (EMT), MSI, MSS/$p53^+$, and MSS/$p53^-$ (7). Oh et al. (8)identified two distinct molecular subtypes: mesenchymal phenotype(MP) and epithelial phenotype (EP). These molecular subtypes show great tumor heterogeneity, distinct clinical outcome and different response to anti-tumor therapy. Additionally, Zeng et al. (9) depicted the comprehensive landscape of tumor microenvironment characteristics and established TMEscore based on tumor immune infiltration patterns to predict immunotherapy response in gastric cancer. Zhang et al. (10) characterized m^6A modification patterns in gastric cancer and constructed m6Ascore based on 21 m^6A regulators, which could also discriminate distinct TME and do well in predicting benefits from immunotherapy for patients with gastric cancer. Cheong et al. (11) developed and validated a model with four classifier genes (GZMB, WARS, SFRP4, and CDX1) for predicting adjuvant chemotherapy response in patients with resectable, stage II–III gastric cancer. Benefited from these classification and scoring system, the tumor heterogeneity could be defined, evaluated and precisely targeted.

The extracellular matrix (ECM) regulates tissue development and homeostasis (12). It consists of biochemically and biomechanically distinct macromolecules, including glycoproteins, collagens, and proteoglycans, which assemble into a three-dimensional supramolecular network that regulates cell growth, survival, motility, and differentiation (13). As a major component of the tumor microenvironment, the ECM could affect the hallmarks of cancer and is involved in all the cellular processes contributing to cancer initiation, progression, and dissemination (14, 15). Researchers found that increased ECM stiffness is required for the transformation of normal cells into tumor through YAP/TAZ mechanotransduction (16), and could also drive EMT, invasion and metastasis *via* TWIST1–G3BP2 mechanotransduction (17). In gastric cancer, the stiffness of the ECM could induce hypomethylation of the promoter region of mechanosensitive Yes-associated protein (YAP) and activate the oncogenic activity of YAP (18). Clinical observations also confirmed that an increased ECM content correlates with more aggressive tumors and poorer prognosis (Socovich and Naba 2019). Intriguingly, in pancreatic ductal adenocarcinoma, decreasing ECM with an anti–lysyl oxidase like-2 (anti-LOXL2) antibody in syngeneic orthotopic PDA mouse models accelerated tumor growth, resulting in diminished overall survival, which suggested a protective role of ECM (20). In addition, tumor ECM is also an affecting factor of cancer therapy. A pan-cancer analysis showed that ECM deposition induced by TGF-β signalling could predict failure of PD-1 blockade (21). On the contrary, inhibiting ECM deposition could soften metastases of colorectal cancer and increase the anti-angiogenic effects of bevacizumab (22). However, until recently, we were not aware of the whole picture of the complexity of the tumor ECM, nor had we determined, to what extent, the ECM is involved in cancer progression. Rapidly developing high throughput sequencing and bioinformatic technologies are of great help to precisely characterize the ECM composition in tumor microenvironments. In this study, we are going to characterize the landscape of ECM in gastric cancer and discuss its clinical implications.

MATERIALS AND METHODS

Gene Expression Data Gathering and Processing

We searched in The Cancer Genome Atlas (TCGA) database and Gene-Expression Omnibus (GEO) for open source gene-expression data with full clinical annotation of gastric cancer. Only those with a sample size greater than 50 and available survival information were included for further analysis. In total, 2125 gastric cancer samples were integrated, including 7 cohorts from the GEO database (https://www.ncbi.nlm.nih.gov/; geo accession numbers: GSE13861 [Yonsei University Severance Hospital (YUSH) cohort], GSE15459, GSE26253, GSE26942, GSE29272, GSE66229, GSE84437 [Asian Cancer Research Group (ACRG) cohort] and TCGA-STAD cohort (**Supplementary Table S1**). The GSE26942 cohort was merged with GSE26899 for the Korea University Guro Hospital (KUGH) cohort and with GSE26901 for the Kosin University College of Medicine (KUCM) cohort. In brief, primary microarray data sets downloaded from GEO were analyzed with background adjustment and normalized using the microarray data package in the R language environment (23). For the TCGA-STAD cohort, latest RNA-sequencing data (HTSeq-FPKM) were retrieved through the R package TCGAbiolinks 2.16.4, which was further transformed into transcripts per kilobase million (TPM) to make it more comparable with the microarray data. All the gene expression data sets were transformed into a log2 base before further analysis. To merge multiple gene expression data sets, a batch normalization algorithm was employed to remove batch effects using the R package sva 3.36.0.

Clinical and Genomic Data Collection

Up to date clinical information for the TCGA-STAD cohort was downloaded and prepared using the R package TCGAbiolinks

2.16.4 and that of other cohorts was directly downloaded as attached files from GEO database or from the **Supplementary Materials** in the related literature. Multi-omics data of the TCGA-STAD cohort, including somatic mutation, copy number variation (CNV), and DNA methylation (Illumina Human Methylation 450K), were obtained from UCSC Xena (https://xenabrowser.net/). All the multi-omics data analysis was limited to samples with available mRNA data; therefore, we analyzed 366 samples for somatic mutation, 374 samples for CNVs, and 336 samples for DNA methylation.

Gene Set Variation Analysis

We downloaded 2922 canonical pathways gene sets integrated from authoritative pathway databases, including the BioCarta pathway database, the Kyoto Encyclopedia of Genes and Genomes (KEGG) pathway database, the PID pathway database, the Reactome pathway database, and the WikiPathways pathway database, from the Molecular Signatures Database (MSigDB, https://www.gsea-msigdb.org/gsea/index.jsp) (24). The normalized GSVA score of each canonical pathway gene set was measured for each gastric cancer sample using the GSVA algorithm in the R package GSVA 1.36.2 (25). The ECM score was measured as the GSVA score of the core matrisome gene set downloaded from MatrisomeDB (http://www.pepchem.org/matrisomedb), an updated version with slight changes (26).

Gene Set Enrichment Analysis

The GSEA algorithm was used to analyze the enriched biological processes between different groups. In brief, the differential genes between two groups were measured with the R package limma 3.44.3, and were subsequently pre-ranked by log2 fold-change and submitted to the R package clusterProfiler 3.16.1 to run the GSEA. Results with a p-value < 0.05 and a q-value < 0.05 were considered statistically significant.

Consensus Clustering for the Extracellular Matrix Composition

To identify different ECM composition patterns and classify patients into distinct groups for further analysis, Unsupervised clustering analysis (based on the Euclidean distance and Ward's linkage) was carried out based on the expression of 274 kinds of ECM in the merged data set and the ACRG cohort. The R package ConsensuClusterPlus 1.52.0 was used to perform the clustering procedure and to determine the optimal number of clusters, which was repeated 1000 times to guarantee the stability of classification.

Estimation Tumor Microenvironment Cell Infiltration

To explore the immune cell infiltration composition of different ECM clusters, the CIBERSORT algorithm was used to analyze the proportions of 22 types of immune cells in each sample of the ACRG cohort using the R package CIBERSORT (27). CIBERSORT employed a deconvolution algorithm, along with support vector regression, to work on 547 specific immune cell-related genes and deconstructed 22 main types of immune cells, including $CD8^+$ T cells, regulatory T cells (Tregs), M0 macrophages, M1 macrophages, and M2 macrophages. 1,000 permutations were performed to achieve robust quantification of the relative abundance of each infiltrated immune cell.

Gene Silencing by Small Interfering RNA Transfection

AGS and Hs746T cells were seeded in 6-well plates at 2×10^5 cell per well overnight, and then treated with 2 μg of negative control small interfering RNA (siRNA), FBN1-siRNA (targeting FBN1 encoding fibrillin 1) and LAMC1-siRNA (targeting LAMC1 encoding laminin subunit gamma 1) constructed by Shanghai GenePharma Company (Shanghai, China) along with 5 μL siRNA interferin reagent (Polyplus, New York, NY, USA). After incubation at 37°C with 5% CO_2 for 48 h, the efficiency of gene silencing was determined using qRT-PCR.

Apoptosis Assay

For the apoptosis assay, cells were seeded into a six-well plate and subjected to different treatments. The cell apoptosis assay was operated according to the manual of the fluorescein isothiocyanate (FITC) Annexin V Apoptosis Detection Kit (BD Biosciences, San Jose, CA, USA). The results were analyzed using FlowJo 10 software (FlowJo, Ashland, OR, USA).

Transwell Invasion Assay

For the Transwell invasion assay, 5×10^4 cells in a volume of 200 μL of serum-free medium were added into a Transwell chamber containing a polycarbonate membrane with 8.0 μm pores (353097; BD Falcon) and covered with a layer of Matrigel matrix (56234; Corning Inc., Corning, NY, USA). The chamber was then placed in a 24-well plate containing 600 μL of medium with 10% fetal bovine serum and incubated at 37°C with 5% CO_2. After 24 h of incubation, non-migrated cells were wiped away and the remaining cells that had migrated through the bottom of the chamber were fixed in 4% paraformaldehyde followed by crystal violet staining and counting under a microscope.

Statistical Analysis

Unpaired Student t tests and Wilcoxon rank-sum tests were used to evaluate the statistical significance of normally distributed and non-normally distributed variables, respectively, when comparing two groups. Kruskal-Wallis tests and One-way analysis of variance (ANOVA) was used to conduct difference comparisons of more than two groups (28). Spearman and distance correlational analyses were conducted using the R package Hmisc 4.4.1. Objects with a Spearman correlation coefficient greater than 0.5 were deemed strongly correlated (29). The hazard ratios (HR) of all prognostic factors was calculated using a univariate Cox proportional hazards regression model. The "surv_cutpoint" function of the R package survminer 0.4.8 was used to estimate the best cut off point for prognostic factors according to their relationship with the patients' survival probability with the maximum rank statistic. For the ECM score, patients were then divided into ECM score low and ECM high groups according to the best cut off point. Then, survival curves were drawn using the Kaplan–Meier method. The statistical significance of the difference

in survival probability was estimated using the log-rank test. The R package forestplot 1.10 was used to show the univariate prognosis analyses of different groups of prognostic factors. The visualization of ECM clusters was facilitated by the R package umap 0.2.6., to perform dimensionality reduction. The networks of canonical signaling pathways were constructed using the software Cytoscape 3.7.2 and the hub pathway was estimated by the Cytoscape plug-in CytoHubba. The R package ComplexHeatmap 2.4.3 generated all the heat maps. A Waterfall Chart was used to exhibit the overview of gene mutation landscape, which was generated the R package maftools 2.4.12. The statistical difference of CNVs between the ECM low and ECM high group was determined using the R package cnvaq 0.1.3. Then, the IGV 2.8.2 software was employed to visualize the CNV landscape of the two groups.

All the above analyses were performed using the R 4.0.0 software. All the statistical analyses were two-sided and a p-value < 0.05 was considered statistically significant.

RESULTS

Identification of the Core Matrisome as the Major Factor Involved in Gastric Cancer Progression

In total, eight eligible GC cohorts (GSE13861, GSE15459, GSE26253, GSE26942, GSE29272, ACRG/GSE66229, GSE84437, and TCGA-STAD) were used in our study. Six cohorts with microarray data (GSE13861, GSE15459, GSE26942, GSE29272, ACRG/GSE66229, and GSE84437) were merged into a meta-cohort (n = 1323). GSE26253 was not merged because of its limited number of gene probes and the sequence data of TCGA-STAD cohort was dismissed because it was being incompatible with the microarray data for technical reasons. Then, we calculated the GSVA score of 2199 canonical pathways for all the cohorts engaged in our study. First, the hazard ratio (HR) of the canonical pathways for overall survival (OS) of patients with gastric cancer were calculated in the meta-cohort (**Figure 1A**). The Wnt signaling pathway, the common pathway of fibrin clot formation, and autophagy were among the top risk pathways, and the caspase pathway, tumor necrosis factor receptor 1 (TNFR1) pathway, and Fas signaling pathway were among the top favorable pathways (**Supplementary Figure S1B**).

Then, we computed the HR of all the canonical pathways for four cohorts with more than 300 tumor samples (TCGA-STAD, ACRG/GSE66229, GSE84437, and meta-cohort; GSE26253 was not engaged because of its limited number gene probes). The intersection of those pathways, 147 in total, were considered to correlate stably with patients' prognosis (**Figure 1B** and **Supplementary Table S2**). These 147 common pathways were further used to perform unsupervised hierarchical clustering for 1323 tumor samples in the meta-cohort. The result showed that these samples could be divided into three distinct subclusters, which displayed significant differences in survival (log-rank test, p-value < 0.001; **Figure 1D**).

To depict the biological processes that characterized the three pathway clusters, we performed GSEA for each cluster against the whole meta-cohort. The results showed that the top 10 gene ontology (GO) biological processes enriched in pathway cluster A primarily correlated with extracellular matrix organization and those of pathway cluster C were primarily correlated with mitosis and DNA replication (**Supplementary Figures S1C, D**), suggesting the importance of these pathways in gastric cancer progression. No pathway was enriched in pathway cluster B, implying it was intermediate between pathway cluster A and C.

To identify the core pathway involved in the OS of patients with gastric cancer, we calculated the Spearman correlation coefficient among the 147 common pathways in the four cohorts that had more than 300 tumor samples (**Supplementary Table S3**). Only those pathways with absolute value of the Spearman correlation coefficient greater than 0.5 were considered strongly correlated. The connectivity of each pathway in the correlation network was estimated for the four cohorts. Then, we constructed the clustering network of prognostic pathways for the meta cohort according to the intersection of these gene sets (**Figure 1C**). It showed that the most enriched pathways were extracellular matrix remodeling related pathways and glycosaminoglycan metabolism related pathways with higher degree and more closely related to prognosis followed by apoptosis related pathways. Moreover, the top 10 pathways ranked by degree for each cohort were estimated (**Supplementary Figures S1E–H**). The top four pathways with highest mean degree among the four cohorts were the core matrisome, ECM glycoproteins, ECM proteoglycans, and elastic fiber formation, all of which were included in the top 10 pathways in each of the four chosen cohorts, again indicating the key role of the ECM in gastric cancer progression.

Considering the striking performance of the ECM among all the prognostic pathways, we extracted the gene set of "core matrisome" from MatrisomeDB, consisting of all the ECM-related genes, including those encoding 195 ECM glycoproteins, 44 ECM collagens, and 35 proteoglycans (**Supplementary Table S4**). These ECM-related genes were then used to cluster the meta-cohort into three groups named ECM cluster A, ECM cluster B, and ECM cluster C (**Figure 1F**); the ECM clustering shared great similarity with the pathway clusters (**Supplementary Table S5**; Kappa value = 0.69, p-value < 0.0001). As expected, the three ECM clusters displayed significant differences in survival (**Figure 1E**; log-rank test, p-value < 0.001). In summary, this evidence strongly supported the core matrisome as the major pathway in gastric cancer progression.

Clinical and Different Biological Progress Traits of ECM Phenotypes in ACRG Cohort

To explore the clinical and transcriptomic characterization of ECM phenotypes, we chose the ACRG cohort for further study. Similarly, we clustered the 300 samples into three pathway clusters with 147 common prognostic pathways and three ECM clusters with 274 ECM genes (**Figures 2A, B** and **Supplementary Figures S2A–E**). There was high consistency between the pathway clusters and the ECM clusters (**Supplementary Table S6**; kappa value = 0.68, p-value < 0.0001), and different ECM clusters showed great differences in OS and relapse free survival (RFS) (**Figure 2C**, log-rank test, p-value = 7.4×10^{-7}; **Supplementary Figure S2H**, log-rank test, p-value = 7×10^{-7}). The most enriched biological processes still

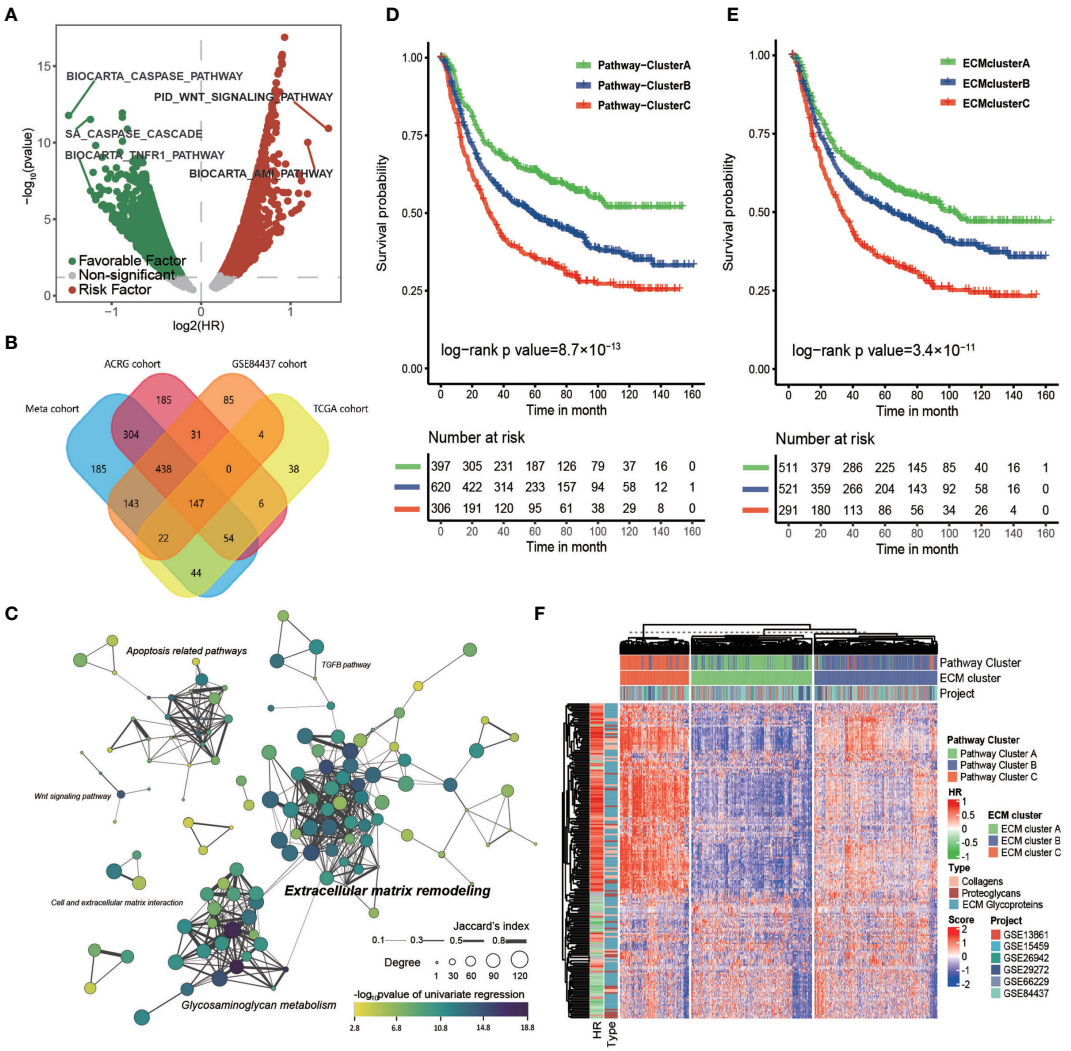

FIGURE 1 | The core matrisome is major pathway involved in gastric cancer progression. **(A)** Volcano plot of prognostic pathways. The x-axis shows the log2 transformed hazard ratio and the y-axis shows –log10 transformed log rank p-values. Red dots indicate risk pathways; green dots indicate favorable pathways; and Grey dots indicate non-prognostic pathways. **(B)** Venn plot of the prognostic pathways in the TCGA-STAD cohort, ACRG cohort, GSE84437 cohort, and the meta-cohort. **(C)** Network of prognostic pathways in the meta-cohort. Each dot represents a prognostic pathway in gastric cancer. A line connecting two pathways means the Jaccard's index between gene sets of the two pathways. The size of the dot represents the degree of the pathway in correlation network of these pathways. The color filling the dot shows the –log10 transformed p-value of univariate cox regression for the GSVA score of the corresponding gene set. **(D)** Kaplan–Meier curves for the overall survival of 1323 patients in the meta-cohort with 3 distinct pathway clusters. The sample size of pathway clusters A, B, and C were n = 397, n = 620, and n = 306, respectively. Log-rank test, p -value = 8.7×10^{-13}. **(E)** Kaplan–Meier curves for overall survival of 1323 patients in the meta-cohort with 3 distinct ECM clusters. The sample size of ECM clusters A, B, and C were n = 511, n = 521, and n = 291, respectively. Log-rank test, p-value = 3.4×10^{-11}. **(F)** Heat map showing the unsupervised clustering of 274 types of ECM for 1323 patients in the meta-cohort. The ECM clustering resembled the pathway clustering to a great extent. The hazard ratio and subtypes of ECM in the meta cohort are also shown in annotation on the right.

shared great similarity with those in the meta-cohort (**Supplementary Figures S2F, G**).

The GSVA score of the "core matrisome" was used as the ECM score for the gene set that consisted of all the ECM genes and could reflect the ECM deposition status. We also tried to shorten this list to obtain a more precise list of ECM-related genes by taking the intersection of differential genes between ECM score high and the ECM score low group in the above four cohorts (**Supplementary Table S7**). However, the shortened gene list was less competent in predicting prognosis. The three ECM clusters had distinct ECM scores (**Supplementary Figure S2I**). As expected, the ECM score could predict OS (**Figure 2D**; HR = 2.19, log-rank test, p-value = 2.8×10^{-6}) and RFS (**Supplementary Figure S2J**; HR = 2.47, log-rank test, p-value = 5.6×10^{-7}). Tumors at stage III/IV had higher ECM scores than those of tumors at stage I/II (**Figure 2E**). Molecular subtypes analysis showed that most of ECM cluster C overlapped with the EMT subtype and none of ECM cluster A belonged to

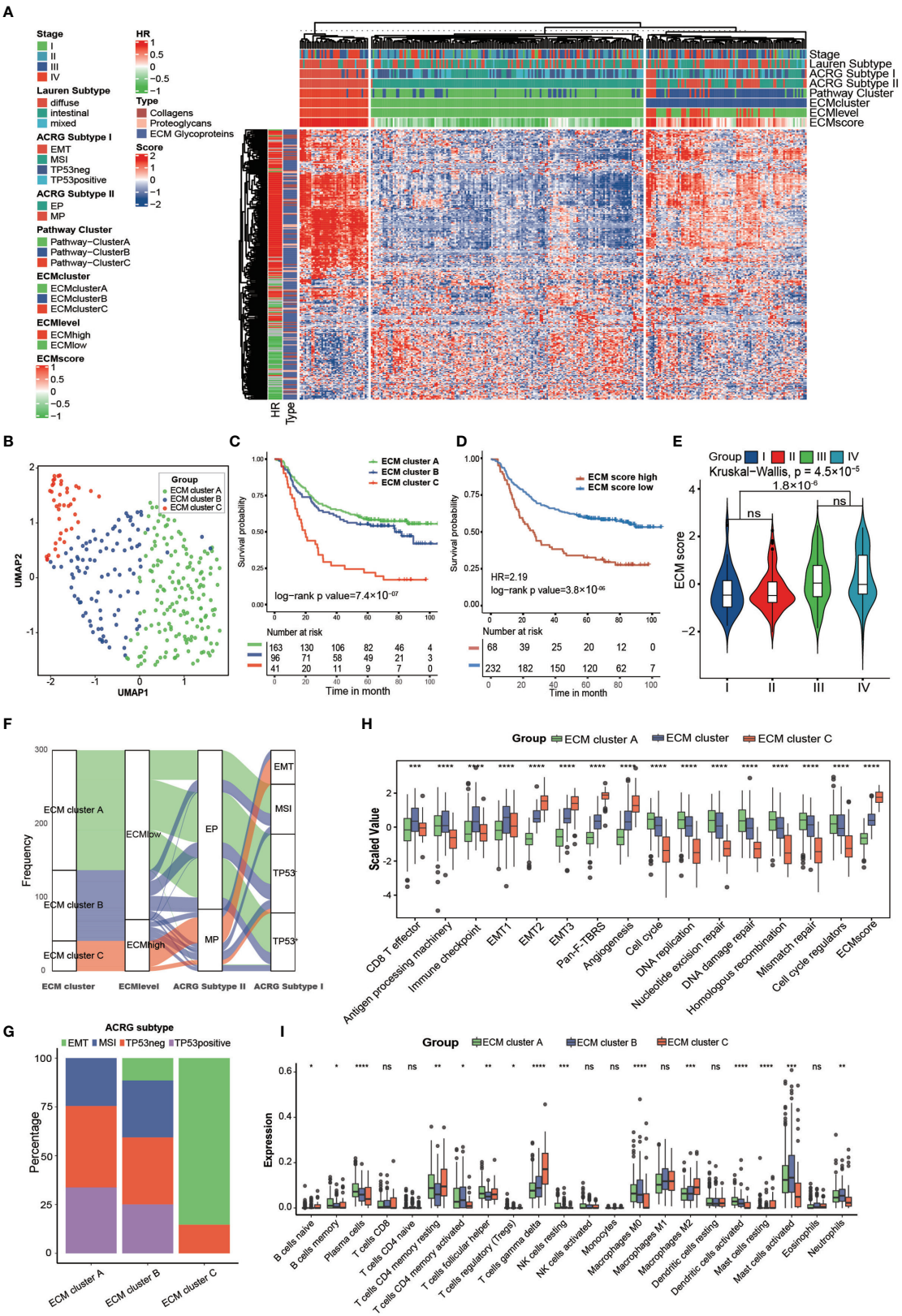

FIGURE 2 | Continued

FIGURE 2 | Clinical and transcriptome characteristics of ECM clusters in the ACRG cohort. **(A)** Heat map showing unsupervised clustering of 274 types of ECM for 300 patients in the ACRG cohort. Tumor stage, Lauren subtype, ACRG subtype I, ACRG subtype II, Pathway cluster, ECM level, and ECM score are shown as patient annotation. The hazard ratio and subtypes of ECM in the ACRG cohort are also shown in the ECM annotation. **(B)** A UMAP plot of 300 patients by dimensionality reduction of 274 types of ECM showing 3 distinct ECM clusters. **(C)** Kaplan–Meier curves for overall survival of 300 patients in the ACRG cohort with 3 distinct ECM clusters. The sample size of ECM clusters A, B, and C were n = 163, n =9 6, and n = 41, respectively. Log-rank test, p-value =7.4×10^{-7}. **(D)** Kaplan–Meier curves for the ECM score by the best cut off value in the ACRG cohort. The numbers of patients in the ECM score high and ECM score low groups were n = 68 and n = 232, respectively. Log-rank test, p-value = 3.8×10^{-6}. **(E)** Violin plot showing that the ECM scores are different among different tumor stages. Kruskal–Wallis test, p-value = 4.5×10^{-5}. The ECM score of stage I and II is lower than that in stage III and IV, Student's t test, p-value = 1.8×10^{-6}. **(F)** Alluvial diagram showing the different ECM clusters in the different ECM levels, ACRG subtype I, and ACRG subtype II. **(G)** Stacked bar chart showing the proportion of ACRG subtypes in the different ECM clusters. **(H, I)** Different biological status and immune cell infiltration patterns of ECM clusters. The top and bottom of the boxes represent the interquartile range of the values. The thick lines in the middle of the boxes represent the median values. The black dots show the outliers. The statistical differences among different ECM clusters were evaluated using the Kruskal–Wallis test. Statistical p-value (*P < 0.05; **P < 0.01; ***P < 0.001, ****P < 0.0001). ns, not significant.

the EMT subtype. Additionally, a higher ECM score was highly associated with a mesenchymal phenotype and diffuse type of Lauren class (**Figures 2F, G** and **Supplementary Figure S2K**) (8). Activation of the EMT program could permit tumors to enter the cancer stem cell (CSC) state, which is resistant to most conventional therapeutics and the major reason for failure of eradicating carcinoma (30, 31). Thus, we deduced that ECM deposition constructed the niche for CSC, which could hinder the efficacy of multiple therapeutics.

The core matrisome turned out to be the major factor in gastric cancer progression; therefore, we characterized the ECM phenotypes with relevant biological processes involved in cancer progression (**Supplementary Table S8**) (32). The results showed that almost all chosen biological processes exhibited significant differences among the three ECM clusters (**Figure 2H**). The ECM score correlated positively with EMT-related processes and negatively with processes involved in DNA replication and DNA repair, which happened to be the feature of CSCs (**Supplementary Figure S2A** and **Supplementary Table S9**). We also analyzed the expression of transforming growth factor beta (TGFβ)-EMT pathway-related genes (*VIM*, *COL4A1*, *PDGFRA*, *SMAD9*, *TGFB2*, *TWIST1*, *ZEB2*, *CDH1*), DNA damage repair-related genes (*BRCA1*, *BRCA2*, *MLH1*, *MSH2*, *MGMT*, *APEX1*, *FEN1*), and immune checkpoint-related genes (*CD80*, *CD86*, *CTLA4*, *HAVCR2*, *IDO1*, *LAG3*, *PD1*, *PDL1*, *TIGIT*, *TNFRSF9*) in the ECM clusters of the ACRG cohort. The results were consistent with the related biological processes (**Supplementary Figures S3C–E**).

Additionally, the results indicated that different ECM phenotypes showed different immunocompetences. Therefore, we analyzed the immune infiltration pattern of the ECM phenotypes. ECM cluster C showed highest level of M2 and T gamma delta cells, which were identified risk factors for the OS of patients with gastric cancer, and lowest level of activated dendritic cells, M0 macrophages, activated mast cells, and neutrophils, which were identified as favorable factors for the OS of patients with gastric cancer (**Figure 2I**) (9).

Clinical and Multi-Omics Traits of ECM Phenotypes in the TCGA Cohort

Benefitting from multi-omics data, the TCGA cohort contains data related to constructed comprehensive molecular subtypes for gastric cancer, including genome stable (GS), microsatellite instability (MSI), EBV infection, and chromosomal instability (CIN). A higher ECM score was associated with the GS subtype and unfavorable prognosis, whereas a lower ECM score was associated with the EBV or MSI subtypes and favorable prognosis (**Figure 3A**, log-rank test, p-value = 0.0046; **Figure 3B**).

Gene instability, evaluated using the tumor mutation burden (TMB), would result in more neo-antigens, increasing the opportunity for immune recognition and clearance (33, 34). Besides, chemotherapeutic drugs function through damaging DNA integrity of rapidly cycling cancer cells (35). Thus, evaluation of the gene mutation load is very important for the precise administration of medication. First, we found that the high ECM score group had a lower TMB than the low ECM score group in the TCGA cohort (**Figure 3C**; Wilcoxon rank sum test, p-value = 2.9×10^{-7}). In addition, the TMB correlated negatively with the ECM score (**Figure 3D**; Spearman correlation, r = −0.38, p-value = 6.4×10^{-14}). Subgroup analysis showed that the correlation between ECM score and TMB differed in different molecular subtypes (**Supplementary Figures S4A–E**), which was highest in GS group (Spearman correlation, r = −0.5, p-value = 0.0014) and insignificant in MSI group (p>0.05). Furthermore, the low ECM score group presented a more extensive TMB than the high ECM score group for the levels of individual altered genes in the top 30 most frequently mutated genes (**Figure 3E**). According to **Figure 2H**, the ECM score correlated negatively with DNA replication, which might explain why a higher ECM score was associated with a lower TMB. Similarly, the high ECM score group tended to have less gain or loss in copy number and more wild-type genes (**Figure 3F**). In addition, the total CNV was also correlated negatively with the ECM score (**Figure 3G**; Spearman correlation, r= −0.39, p-value = 8.1×10^{-15}), and the results in different molecular subtypes were about the same (**Supplementary Figures S4F–J**).

Epigenetic abnormalities are widespread among all tumor types, which also play an important role in drug resistance and immune surveillance (36–38). Therefore, we examined the association of the ECM score with DNA methylation. Interestingly, the high ECM score group had a lower level of DNA methylation in all DNA parts except for 3' untranslated region, and the CpG island and CpG shore, which are associated with inhibiting gene expression, were enriched in the low ECM score group (**Figure 3H** and **Supplementary Figures S4K–L**). Furthermore, we compared the CpG island abundance between the high ECM score and the low ECM score group. GSEA enrichment results showed that, in the high ECM score group, the most hypomethylated biological processes were synapse development and cell differentiation, which may lead to EMT

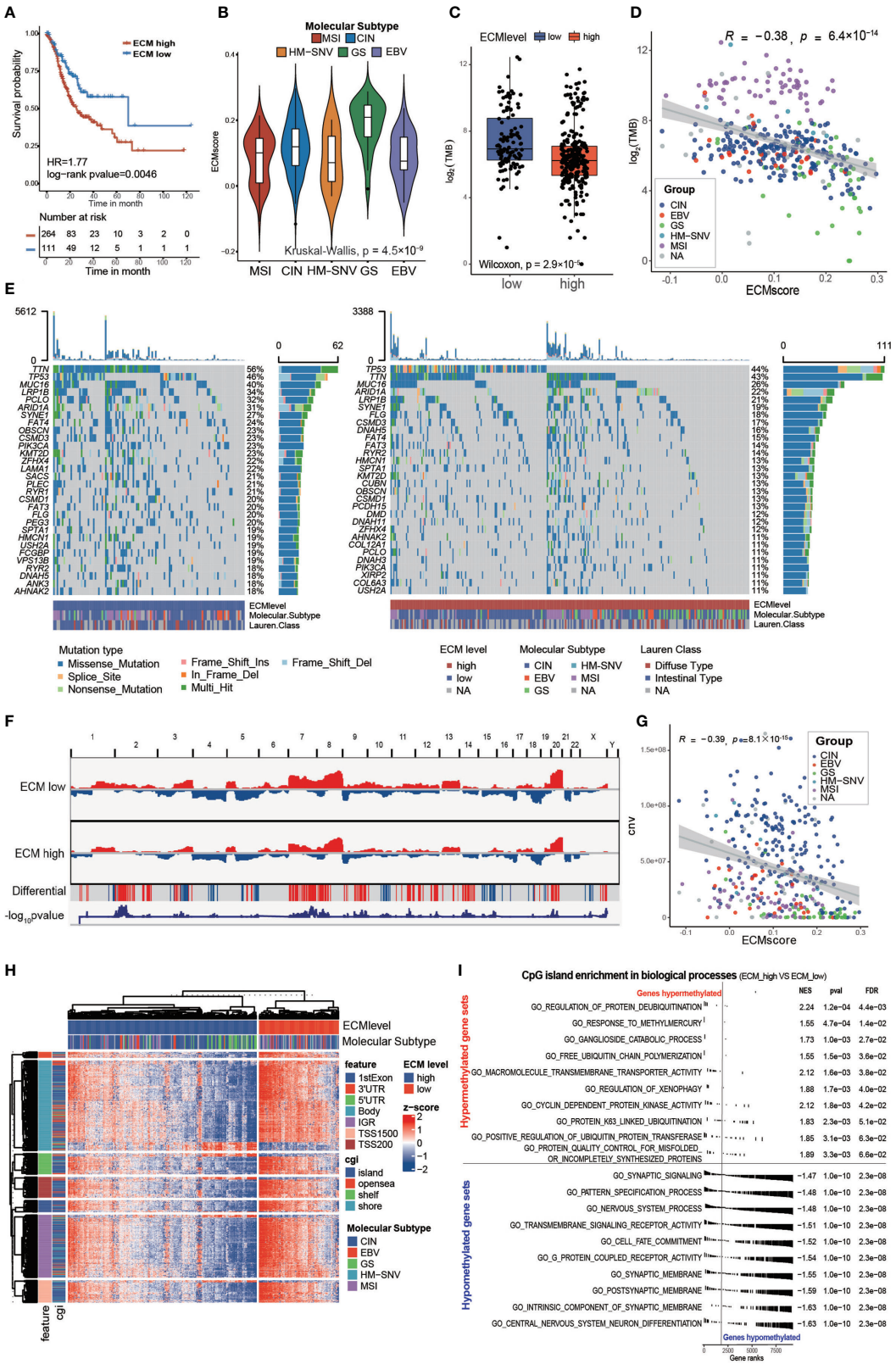

FIGURE 3 | Continued

FIGURE 3 | Characteristics of the ECM pattern in TCGA-STAD molecular subtypes and multi-omics level. **(A)** Kaplan–Meier curves for the ECM score by best cut off value in the TCGA-STAD cohort. The numbers of patients in the ECM score high and ECM score low groups were n = 264 and n = 111, respectively. Log-rank test, p-value = 0.0046. **(B)** Violin plot showing that the ECM scores are different among different molecular subtypes in the TCGA-STAD cohort. Kruskal–Wallis test, p-value = 4.5×10^{-9}. MSI (n = 61), CIN (n = 207), HM-SNV (n = 7), GS (n = 45), EBV (n = 27). **(C)** Difference in the TMB between the ECM high and ECM low groups. The scattered dots indicate the TMB of each sample. The top and bottom of the boxes represent the interquartile range of the values. The thick lines in the middle of the boxes represent the median value. Wilcoxon rank sum test, p-value = 2.9×10^{-7}. **(D)** Scatter plot depicting the correlation between the ECM score and the TMB. Spearman correlation analysis, R = −0.38, p-value = 6.4×10^{-14}. The color of the dots represents the molecular subtypes annotated by the legend. **(E)** An Oncoprint showing the gene mutation map of the ECM high (right, red) and ECM low (left, blue) groups. Each column represents a patient and the barplot in the right of each group indicates the gene mutation frequency of each gene in the corresponding group. The barplot on the top shows the TMB. The gene mutation types are annotated in the legend. Molecular subtypes and Lauren subtypes are also shown as patient annotation. **(F)** CNV pattern of the ECM high and ECM low groups. The length of the plot represents the whole genome and each vertical line represents a gene; red for gain of copy number and blue for loss of copy number. The penultimate line mark the genes with differential copy number between the two groups; a red stripe for higher and a blue stripe for lower copy number in the ECM high group. The last line indicates the –log10 transformed chi-squared test p-value of the copy number difference. **(G)** Scatter plot depicting the correlation between the ECM score and CNV. Spearman correlation analysis, R = −0.39, P = 8.1×10^{-15}. The color of the dots represents the molecular subtypes annotated by the legend. **(H)** Heat map exhibiting the DNA methylation pattern of the ECM high and ECM low groups. The locations of each DNA methylation site are indicated in the left annotation. The molecular subtype is shown as patient annotation. **(I)** GSEA enrichment of CpG islands in biological processes between ECM high group and ECM low groups. The upper part shows the top10 hypermethylated biological processes and the lower part shows the top10 hypomethylated biological processes. The enrichment plot, normalized enrichment score (NES), p value and false discovery rate (FDR) are shown in the right.

and cell stemness, and the most hypermethylated biological processes were less significant to be mentioned (**Figure 3I**). Global hypomethylation is an important feature of naïve pluripotent cells and complex regulation of the epigenome also promotes CSCs formation (39, 40). Therefore, we speculated that ECM deposition might promote CSC formation through an epigenetic mechanism.

The ECM Score Predicts Chemotherapeutic Benefits

Upon dividing the specific data sets by the best cutoff value of the ECM score, significant differences in OS were observed between the low and high ECM score groups for all gastric cancer data sets except GSE29272 (HR, 1.43; 95% CI, 0.99–2.07) (**Figure 4A** and **Supplementary Table S10**). Meanwhile, the prognostic value of the ECM score was also validated in five other independent data sets (GSE13861: HR, 3,21; 95% CI, 1.47–7.0; GSE15459: HR, 2.69; 95% CI, 1.57–4.6; GSE26253: HR, 2.19; 95% CI, 1.62-2.97; GSE26942: HR, 2.67; 95% CI, 1.75–4.08; GSE84437: HR, 2.15; 95% CI, 1.52–3.04; **Supplementary Figures S5C–G**). Moreover, the ECM score could also predict poor prognosis in each stage of gastric cancer (stage I: HR, 3.48; 95% CI, 1.91–6.34; stage II: HR, 2.16; 95% CI, 1.54–3.04; stage III: HR, 1.71; 95% CI, 1.40–2.09; and stage IV: HR, 2.03; 95% CI, 1.55–2.68). These results suggested that the ECM score could be prognostic factor that is independent of tumor stage in gastric cancer (**Supplementary Figures S5A, B**).

Next, we investigated the performance of the ECM score in pan-cancer. We evaluated the predictive value of the ECM score for 14 types of solid tumors in the TCGA cancer cohort, comprising 6251 samples in total (**Supplementary Table S11**). The results showed that the ECM score was a risk factors for eight types of cancer in the TCGA cohorts, including thyroid cancer, brain lower grade glioma, skin cutaneous melanoma, uterine corpus endometrial carcinoma, ovarian serous cystadenocarcinoma, glioblastoma, kidney renal clear cell carcinoma, and lung squamous cell carcinoma, but was irrelevant to other types of cancer, which indicated the biological heterogeneity of the ECM among distinct cancer types (**Figure 4B**).

Chemotherapy is a crucial treatment to supplement surgery in patients with gastric cancer. However, currently, there is no biomarker that can effectively predict a patient's chemotherapy response and even guide the choice of chemotherapeutic regimens. Our results demonstrated that a higher ECM score was associated with the EMT molecular subtype in the ACRG cohort and with the GS molecular subtype in the TCGA-STAD cohort, which were tolerant to chemotherapy. To explore the capacity of the ECM score to predict the chemotherapy response, we first evaluated the best cut off value of the ECM score for patients in the TCGA-STAD cohort who had received chemotherapy according to their prognosis, which could divide the TCGA-STAD cohort into ECM low and ECM high groups. Combined with the chemotherapeutic history, the best cut off value further stratified the TCGA-STAD cohort into $Chemo^+$/ECM high, $Chemo^-$/ECM high, $Chemo^+$/ECM low, $Chemo^-$/ECM score low groups. Interestingly, survival analysis indicated that patients with a low ECM score could benefit from chemotherapy (**Figure 4C**; log-rank test, p-value = 0.019), while there was no significant difference between the chemotherapy and non-chemotherapy group even when the sample size was larger (**Figure 4D**; log-rank test, p-value > 0.05). Besides, more patients with a low ECM score showed a complete response to chemotherapy and less progressive disease compared with patients with a high ECM score (**Supplementary Figure S5H**). To further verify this result, stage II, III, or IV gastric cancer without distant metastasis (n = 180) in three cohorts [GSE26899 for the KUGH cohort, GSE26901 for the KUCM cohort, and GSE13861 for the YUSH cohort; (**Supplementary Table S12**)] with complete chemotherapy information were integrated for survival analysis (log-rank test, p-value = 6.5×10^{-6}) Likewise, patients with a low ECM score could achieve a satisfactory chemotherapy response (**Figure 4E**; log-rank p-value = 0.00019), while patients with a high ECM score could not (**Figure 4F**; log-rank test, p-value > 0.05). Our results strongly supported the view that the ECM score could predict poor prognosis and the response to chemotherapy.

In Vitro Study Indicated That the ECM Could Influence the Invasion and Chemoresistance of Gastric Cancer Cells

To further verify our analysis, we chose two representative ECM genes for the *in vitro* experiment. Firstly, we conducted Spearman correlation analysis for two ECM genes according to their expression levels in the TCGA-STAD, ACRG/GSE66229,

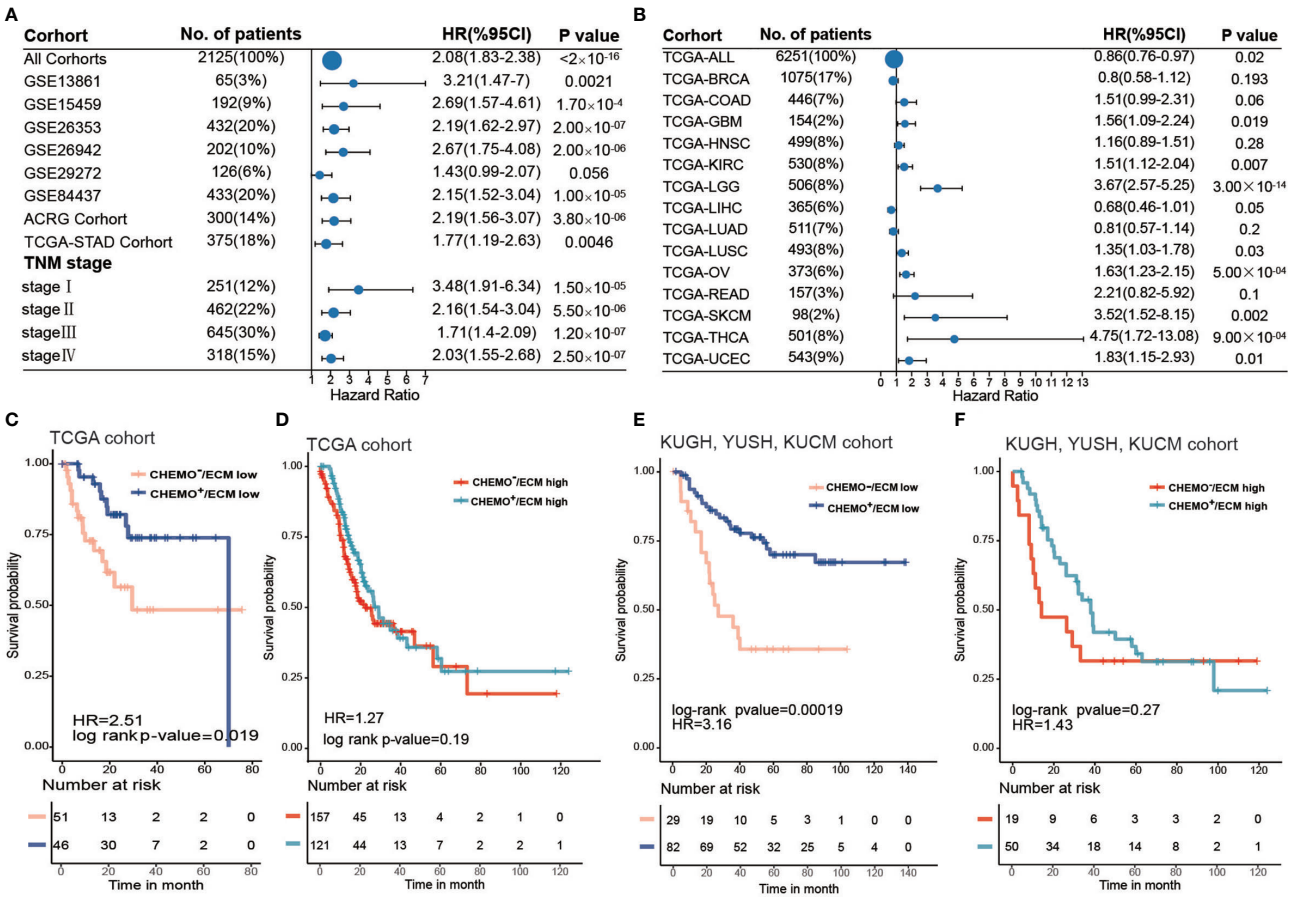

FIGURE 4 | ECM score is a prognostic biomarker and could predict chemotherapy response. **(A)** Forest plot showing the difference in prognosis between ECM high and low groups in independent gastric cancer cohorts and different tumor stages. The horizontal coordinates represent the hazard ratio of the ECM high group relative to the ECM low group and the horizontal line represents the 95% confident interval of the hazard ratio. The size of the dot indicates the sample size of the independent group. **(B)** Forest plot showing the difference in prognosis between the ECM high and low groups in 14 types of solid tumors from the TCGA datasets. The horizontal coordinates represent the hazard ratio of the ECM high group relative to the ECM low group and the horizontal line represents the 95% confident interval of hazard ratio. The size of the dot indicates the sample size of the independent group. **(C)** Kaplan–Meier curves for overall survival of the ECM high group in the TCGA-STAD cohort grouped by chemotherapeutic history. $CHEMO^-$/ECM high, n = 157; $CHEMO^+$/ECM high, n = 121. Log-rank test, p-value = 0.19. **(D)** Kaplan–Meier curves for overall survival of the ECM low group in the TCGA-STAD cohort grouped by chemotherapeutic history. $CHEMO^-$/ECM low, n = 51; $CHEMO^+$/ECM low, n = 46. Log-rank test, p-value = 0.019. **(E)** Kaplan–Meier curves for overall survival of the ECM high group in the KUGH, YUSH, and KUCM cohorts grouped by chemotherapeutic history. $CHEMO^-$/ECM high, n = 19; $CHEMO^+$/ECM high, n = 50. Log-rank test, p-value = 0.27. **(F)** Kaplan–Meier curves for overall survival of the ECM low group in the KUGH, YUSH, KUCM cohort grouped by chemotherapeutic history. $CHEMO^-$/ECM low, n = 29; $CHEMO^+$/ECM low, n = 82. Log-rank test, p-value = 0.00019.

GSE84437, and the meta-cohort and submitted the correlation networks to Cytoscape to find a hub gene for ECM deposition (**Supplementary Figures S6A–E** and **Supplementary Table S13**). *FBN1* was identified as the only common top 10 hub gene among all the cohorts. Fibrillin 1 serves as scaffold for elastic fibers and as a reservoir for growth factors like TGFβ (**Figure 5A**) (41, 42). Then, we performed univariate Cox regression for all the ECM genes in the meta-cohort and identified *LAMC1*, which encodes laminin subunit gamma 1, an essential component of the basement membrane that is involved in multiple types of cancer progression (43–46), as the risk factor with the lowest p-value (**Figure 5B**). Both genes correlated significantly with poor prognosis in the meta-cohort (**Figures 5C, D**; *LAMC1*: HR = 1.71, log-rank test, p-value < 0.0001; *FBN1*: HR = 1.74, log-rank test, p-value < 0.0001). After knocking down the expression of *LAMC1* and *FBN1* separately in Hs746T cells, a metastatic and mesenchymal like cell line, the invasiveness of Hs746T cells was compromised significantly. Similar but less conspicuous results were when the experiment was repeated in AGS cells, a primary and epithelial like cell line (**Figures 5E, F**). We speculated that relative lower expression of the targeted genes in AGS cells accounted for the less significant influence of treatment. However, it is plausible to claim that the ECM could have impact on the EMT phenotype. To check whether the ECM could influence the chemotherapeutic response, we treated Hs746T and AGS cells with 10 μM 5 fluorouracil (5FU), a first-line chemotherapy drug, (1) combined

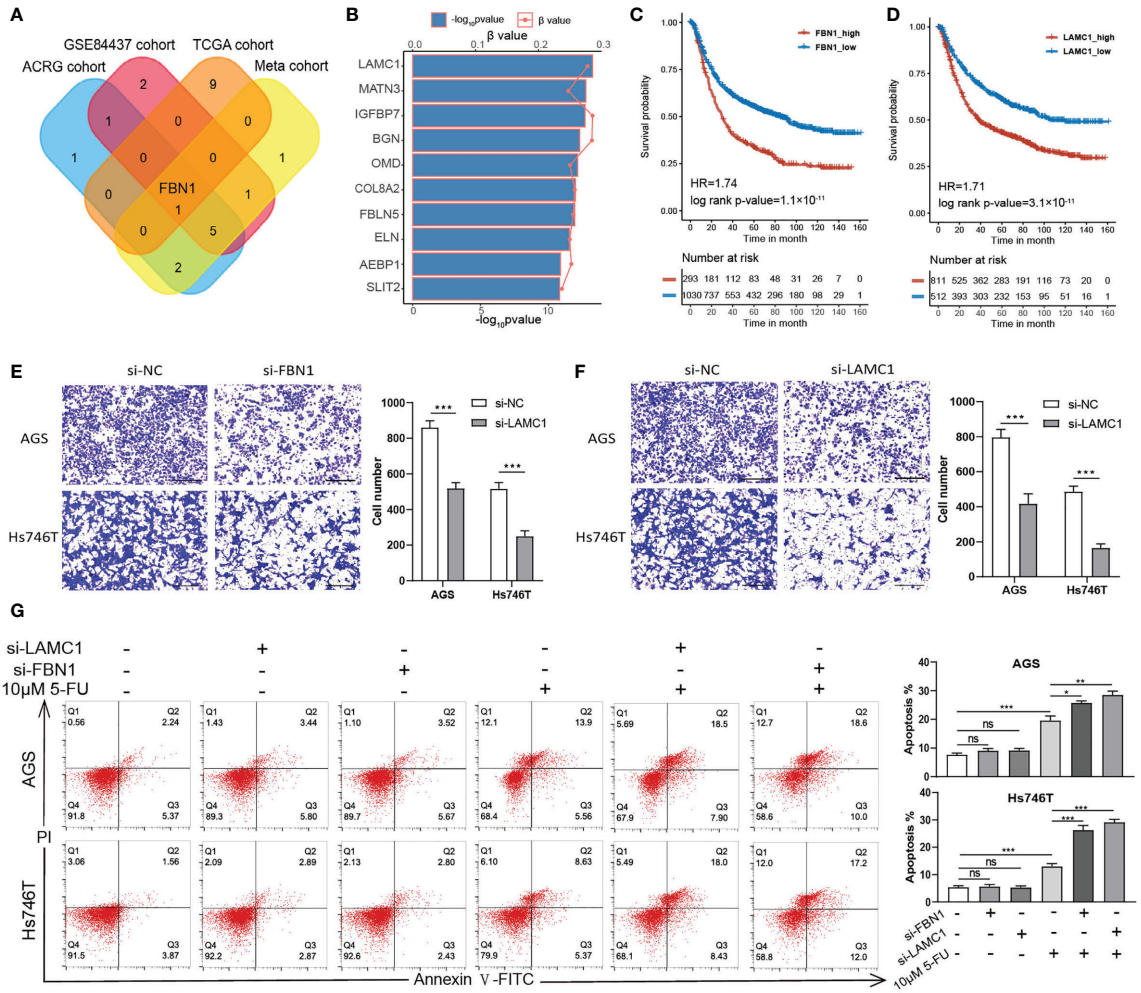

FIGURE 5 | ECM could influence the invasion and drug tolerance of gastric cancer cells. **(A)** A Venn diagram showing the intersection of top 10 hub ECM genes of four cohorts (TCGA-STAD, ACRG, GSE84437 and meta-cohort). *FBN1* is the only common hub ECM gene in the four cohorts. **(B)** Univariate Cox regression results of all ECM in the meta cohort. The top 10 ECM genes with the lowest p values are shown. The horizontal bars shows the $-\log_{10}$ p-value of the univariate Cox regression and the horizontal coordinates of the dots show the β value of univariate Cox regression. **(C, D)** Kaplan–Meier curves for *FBN1* and *LAMC1* by best cut off value in the meta cohort. *FBN1*: HR, 1.74, Log-rank p-value = 1.1×10^{-11}. *LAMC1*: HR, 1.71, Log-rank p-value = 3.1×10^{-11}. **(E, F)** Transwell invasion assay performed in AGS and Hs746T cells transfected with control siRNA, *FBN1* siRNA, or *LAMC1* siRNA. **(G)** Apoptosis was determined using fluorescence activated cell sorting (FACS) analysis by Annexin V-FITC and propidium iodide (PI) co-staining (left panel), and Annexin V^+ cell populations were defined as apoptotic (right panel). Statistical p-value (*P < 0.05; **P < 0.01; ***P < 0.001; ns, not significant).

with *LAMC1* or *FBN1* knockdown for 48 h. Knocking down *LAMC1* or *FBN1* did not influence the survival of Hs746T or AGS cells. However, knocking down *LAMC1* or *FBN1*, or both could sensitize Hs746T cells to 5-FU; the same phenomenon was observed in AGS cells but with less significance. In addition, the mesenchymal-like Hs746T cell line was more tolerant to 5-FU than the epithelial-like AGS cell line (**Figure 5G**).

DISCUSSION

Growing evidence suggests that the ECM is an indispensable but enigmatic component of the tumor microenvironment (13, 15). Aberrant constitution of the ECM is involved in all the cellular processes throughout cancer initiation, progression, and dissemination, and, in most cases, correlated with more aggressive tumors and poorer prognosis (19). In breast cancer, researchers found that decellularized ECM from tumor-bearing and obese mammary glands drives triple-negative breast cancer (TNBC) cell invasion, and collagen VI was found to be the driver protein by proteomic analysis (47). In colon cancer, Romero-López et al. (48) extracted and compared ECM from normal human colon and colon tumor that had metastasized to liver and even seeded tumor cells in these ECM. The results showed that cells seeded in tumor ECM had higher levels of free NADH along with glycolytic rate and more capable of inducing tumor-like

vasculature compared with those seeded in normal ECM. Contradictorily, in pancreatic ductal adenocarcinoma, decreasing ECM with an anti-LOXL2 antibody *in vivo* boosted tumor growth and diminished overall survival, suggesting a protective role of ECM (20). Also, in melanoma, there is evidence that aging fibroblasts were less capable of secreting ECM, especially HAPLN1, resulting in a more aligned ECM that promoted metastasis of melanoma cells (49). Hence, it seems that the ECM also share heterogeneity among different tumor types and the interplay between ECM and tumor cells is still intricate.

Additionally, the ECM is also an interference factor during anti-tumor therapy. Excessive ECM deposition and stiffening in solid tumors could also induce physical and biological barriers for chemotherapy, a major problem faced by current cancer research. For example, ECM deposition in liver metastasis of colorectal tumor could enhance angiogenesis and anti-angiogenic therapy resistance, while inhibiting ECM deposition with drugs targeting the renin-angiotensin system could reverse resistance to anti-angiogenic bevacizumab (22). Also, decreasing ECM stiffness with lysyl oxidase (LOX) inhibitors increased drug penetration and overcame chemotherapy resistance in triple negative breast cancer (50). However, to date, the clinical and multi-omics characterization of the ECM in gastric cancer and the potential of the ECM to predict prognosis and chemotherapy response had not yet been systematically explored, neither did any clinical trials investigate the role of ECM deposition in anti-tumor therapy resistance.

Exploiting GSVA algorithms, we scored all the gene set canonical pathways and ECM was identified as core factor in gastric cancer progression with highest degree among all prognostic pathways in the overlap of four cohort. Then, we resolved the ECM constitution pattern and depicted the overall landscape of the clinical and multi-omics characterization of the ECM in gastric cancer. Integrated analysis detected that the ECM score performed well to predict the prognosis and chemotherapy response in gastric cancer. The ECM score was a robust risk factor in different stage of gastric cancer and in different cohorts. It was verified in both the TCGA-STAD cohort and the KUGH, YUSH, and KUCM cohorts that chemotherapy showed a poor effect in patients with gastric cancer with a high ECM score, the result of which might be instructional for precision medicine.

In the ACRG cohort, the ECM score was exclusively high in patients with the EMT molecular subtype. Previous studies had identified EMT or a mesenchymal phenotype as predicators for poor prognosis and resistance to anti-cancer drug therapy in multiple cancer types (8, 30, 51–53). The EMT-like change could also enable cancer cells to acquire a cancer stem cell phenotype, which has received unanimous acceptance as the backbone of drug resistance (30). Counterintuitively, our results showed that cancers with a higher ECM score showed a remarkably low level of proliferation activity, which might be ascribed to the dominant state of CSCs. There is considerable evidence demonstrating that ECM remodeling could be the upstream signal that regulates the EMT or CSCs phenotype through a mechanochemical pathway in cancer cells (15, 54–56).

In the TCGA-STAD cohort, the ECM score was exclusively high in patients of the GS molecular subtype. The GS molecular subtype is characterized by a low TMB. Most chemotherapy imposes DNA damage on rapidly proliferating cancer cells that lack adequate DNA repair (35). Hence, we deduced that gene stability and relatively slow DNA replication could restrain the effectiveness of chemotherapeutic drugs, which happened to be the feature of those cancers with a high ECM score. Our results demonstrated that the ECM score was closely related to the TMB as well as CNV, further explaining its capacity to predict drug response.

The role of non-genetic or epigenetic mechanisms to regulate drug resistance is vital but poorly understood. Aberrant epigenetic regulation is common among all tumor types and has long been considered as a regulator of drug resistance, and several epigenetic therapies have been involved in preclinical trials (57–60). Our data indicated that ECM deposition in gastric cancer might alter epigenetic states, thus influencing the drug response. Determining the interconnection between ECM remodeling and epigenetic alteration would deepen our understanding of drug-tolerant cancer.

Increased use of immunotherapy has revealed the presence of immune tolerance (61–64). It is not surprising that in accordance with our results, the tumor-associated ECM could also have immune modulatory effects and could regulate the migration and localization of immune cells (65, 66). Actually, combined treatment targeting both the immune and stroma microenvironment could lead to remarkable therapeutic effects (67, 68). Finally, we chose two representative ECM genes, *LAMC1* and *FBN1*, to further verify our findings. Knocking down these two genes impaired the invasion ability of cancer cells and sensitized cancer cells to chemotherapeutic drugs, which, to some extent, corroborated our analyses.

In short, in the current study, gene expression analysis identified ECM as the driving factor involved in gastric cancer progression. Hence, we systematically discussed the landscape of clinical, biological, and multi-omics characterization of the ECM constitution pattern in gastric cancer and found a higher ECM score is tightly associated with an epithelial to mesenchyme transition (EMT) phenotype, a gene stable (GS) molecular subtype, markedly lower somatic mutation rates, and a lower level of DNA methylation. In addition, the ECM score was identified as robust prognostic biomarker and predictive factor for the response to chemotherapy resistance, which was further verified experimentally. Our findings imply that ECM may foster chemotherapy resistance in gastric cancer genetically and epigenetically. Further investigation would help to solve the enigma of chemoresistance acquisition. The establishment of ECM score could also help to design personalized and precise chemotherapy and provide inspiration to develop combination therapy. Nevertheless, our study has some limitations as well. Detailed information regarding the treatment history of the enrolled patients with gastric cancer was inadequate, such as the prescription and duration of the chemotherapy, and the receipt of any other treatment, which would interfere with the precise identification of the best cut off point. Further treatment information gathering would help to refine the prediction model. Additionally, tumor heterogeneity is the main cause of

chemotherapy tolerance, which means that sequencing of mixed tumor tissues might inevitably lead to bias. Standardized and sub-regional sample collection and, if conditional, single cell sequencing, would ensure an in-depth exploration of the role of the ECM in chemoresistance.

DATA AVAILABILITY STATEMENT

datasets presented in this study can be found in online repositories. The names of the repository/repositories and accession number(s) can be found in the article/**Supplementary Material**.

AUTHOR CONTRIBUTIONS

Conception and design of the study: XX, JC, and WG. Data collection and preprocessing: ML and XZ. Analysis and interpretation of data: ZY and FX. Manuscript writing: ZY, ML, and XZ. Study selection, *in vitro* experiment and statistical expertise: CW, EX, XW, LZ, HY, CR, HW, and YW. All authors contributed to the article and approved the submitted version.

FUNDING

This work was supported by the Nanjing Medical Science and Technology Development [No. YKK16117], the Nanjing Health Science and Technology Development Special Fund for Distinguished Young Scholar [No. JQX19001], the Key Research Plan and Social Development Project of Jiangsu Province, China [No. BE2016603], and the National Ministry of Science and Technology Project [No. 2016YFC0104105].

SUPPLEMENTARY MATERIAL

The Supplementary Material for this article can be found online at: https://www.frontiersin.org/articles/10.3389/fonc.2021.753330/full#supplementary-material

REFERENCES

1. Smyth EC, Nilsson M, Grabsch HI, van Grieken NC, Lordick F. Gastric Cancer. *Lancet* (2020) 396:635–48. doi: 10.1016/S0140-6736(20)31288-5
2. Kang YK, Boku N, Satoh T, Ryu MH, Chao Y, Kato K, et al. Nivolumab in Patients With Advanced Gastric or Gastro-Oesophageal Junction Cancer Refractory to, or Intolerant of, at Least Two Previous Chemotherapy Regimens (ONO-4538-12, ATTRACTION-2): A Randomised, Double-Blind, Placebo-Controlled, Phase 3 Trial. *Lancet* (2017) 390:2461–71. doi: 10.1016/S0140-6736(17)31827-5
3. Noh SH, Park SR, Yang HK, Chung HC, Chung IJ, Kim SW, et al. Adjuvant Capecitabine Plus Oxaliplatin for Gastric Cancer After D2 Gastrectomy (CLASSIC): 5-Year Follow-Up of an Open-Label, Randomised Phase 3 Trial. *Lancet Oncol* (2014) 15:1389–96. doi: 10.1016/S1470-2045(14)70473-5
4. Jiang Y, Li T, Liang X, Hu Y, Huang L, Liao Z, et al. Association of Adjuvant Chemotherapy With Survival in Patients With Stage II or III Gastric Cancer. *JAMA Surg* (2017) 152:e171087. doi: 10.1001/jamasurg.2017.1087
5. Liu Y, Sethi NS, Hinoue T, Schneider BG, Cherniack AD, Sanchez-Vega F, et al. Comparative Molecular Analysis of Gastrointestinal Adenocarcinomas. *Cancer Cell* (2018) 33:721–35.e8. doi: 10.1016/j.ccell.2018.03.010
6. Bass AJ, Thorsson V, Shmulevich I, Reynolds SM, Miller M, Bernard B, et al. Comprehensive Molecular Characterization of Gastric Adenocarcinoma. *Nature* (2014) 513:202–9. doi: 10.1038/nature13480
7. Cristescu R, Lee J, Nebozhyn M, Kim K-M, Ting JC, Wong SS, et al. Molecular Analysis of Gastric Cancer Identifies Subtypes Associated With Distinct Clinical Outcomes. *Nat Med* (2015) 21:449–56. doi: 10.1038/nm.3850
8. Oh SC, Sohn BH, Cheong J-H, Kim S-B, Lee JE, Park KC, et al. Clinical and Genomic Landscape of Gastric Cancer With a Mesenchymal Phenotype. *Nat Commun* (2018) 9:1777. doi: 10.1038/s41467-018-04179-8
9. Zeng D, Li M, Zhou R, Zhang J, Sun H, Shi M, et al. Tumor Microenvironment Characterization in Gastric Cancer Identifies Prognostic and Immunotherapeutically Relevant Gene Signatures. *Cancer Immunol Res* (2019) 7:737–50. doi: 10.1158/2326-6066.CIR-18-0436
10. Zhang B, Wu Q, Li B, Wang D, Wang L, Zhou YL. M6a Regulator-Mediated Methylation Modification Patterns and Tumor Microenvironment Infiltration Characterization in Gastric Cancer. *Mol Cancer* (2020) 19:53. doi: 10.1186/s12943-020-01170-0
11. Cheong J-H, Yang H-K, Kim H, Kim WH, Kim Y-W, Kook M-C, et al. Predictive Test for Chemotherapy Response in Resectable Gastric Cancer: A Multi-Cohort, Retrospective Analysis. *Lancet Oncol* (2018) 19:629–38. doi: 10.1016/S1470-2045(18)30108-6
12. Mammoto T, Ingber DE. Mechanical Control of Tissue and Organ Development. *Development* (2010) 137:1407–20. doi: 10.1242/dev.024166
13. Hynes RO. The Extracellular Matrix: Not Just Pretty Fibrils. *Science* (2009) 326:1216–9. doi: 10.1126/science.1176009
14. Hanahan D, Weinberg RA. Hallmarks of Cancer: The Next Generation. *Cell* (2011) 144:646–74. doi: 10.1016/j.cell.2011.02.013
15. Pickup MW, Mouw JK, Weaver VM. The Extracellular Matrix Modulates the Hallmarks of Cancer. *EMBO Rep* (2014) 15:1243–53. doi: 10.15252/embr.201439246
16. Panciera T, Citron A, Di Biagio D, Battilana G, Gandin A, Giulitti S, et al. Reprogramming Normal Cells Into Tumour Precursors Requires ECM Stiffness and Oncogene-Mediated Changes of Cell Mechanical Properties. *Nat Mater* (2020) 19:797–806. doi: 10.1038/s41563-020-0615-x
17. Wei SC, Fattet L, Tsai JH, Guo Y, Pai VH, Majeski HE, et al. Matrix Stiffness Drives Epithelial-Mesenchymal Transition and Tumour Metastasis Through a TWIST1-G3BP2 Mechanotransduction Pathway. *Nat Cell Biol* (2015) 17:678–88. doi: 10.1038/ncb3157
18. Jang M, An J, Oh SW, Lim JY, Kim J, Choi JK, et al. Matrix Stiffness Epigenetically Regulates the Oncogenic Activation of the Yes-Associated Protein in Gastric Cancer. *Nat BioMed Eng* (2021) 5:114–23. doi: 10.1038/s41551-020-00657-x
19. Socovich AM, Naba A. The Cancer Matrisome: From Comprehensive Characterization to Biomarker Discovery. *Semin Cell Dev Biol* (2019) 89:157–66. doi: 10.1016/j.semcdb.2018.06.005
20. Jiang H, Torphy RJ, Steiger K, Hongo H, Ritchie AJ, Kriegsmann M, et al. Pancreatic Ductal Adenocarcinoma Progression Is Restrained by Stromal Matrix. *J Clin Invest* (2020) 130:4704–9. doi: 10.1172/JCI136760
21. Chakravarthy A, Khan L, Bensler NP, Bose P. Carvalho DD De. TGF-β-Associated Extracellular Matrix Genes Link Cancer-Associated Fibroblasts to Immune Evasion and Immunotherapy Failure. *Nat Commun* (2018) 9:4692. doi: 10.1038/s41467-018-06654-8
22. Shen Y, Wang X, Lu J, Salfenmoser M, Wirsik NM, Schleussner N, et al. Reduction of Liver Metastasis Stiffness Improves Response to Bevacizumab in Metastatic Colorectal Cancer. *Cancer Cell* (2020) 37:800–17.e7. doi: 10.1016/j.ccell.2020.05.005
23. Bolstad BM, Irizarry RA, Astrand M. Speed TP. A Comparison of Normalization Methods for High Density Oligonucleotide Array Data Based on Variance and Bias. *Bioinformatics* (2003) 19:185–93. doi: 10.1093/bioinformatics/19.2.185
24. Liberzon A, Birger C, Thorvaldsdottir H, Ghandi M, Mesirov JP, Tamayo P. The Molecular Signatures Database (MSigDB) Hallmark Gene Set Collection. *Cell Syst* (2015) 1:417–25. doi: 10.1016/j.cels.2015.12.004

25. Hanzelmann S, Castelo R, Guinney J. GSVA: Gene Set Variation Analysis for Microarray and RNA-Seq Data. *BMC Bioinf* (2013) 14:7. doi: 10.1186/1471-2105-14-7
26. Shao X, Taha IN, Clauser KR, Gao YT, Naba A. MatrisomeDB: The ECM-Protein Knowledge Database. *Nucleic Acids Res* (2020) 48:D1136–44. doi: 10.1093/nar/gkz849
27. Newman AM, Liu CL, Green MR, Gentles AJ, Feng W, Xu Y, et al. Robust Enumeration of Cell Subsets From Tissue Expression Profiles. *Nat Methods* (2015) 12:453–7. doi: 10.1038/nmeth.3337
28. Hazra A, Gogtay N. Biostatistics Series Module 3: Comparing Groups: Numerical Variables. *Indian J Dermatol* (2016) 61:251–60. doi: 10.4103/0019-5154.182416
29. Cohen J. *Statistical Power Analysis for the Behavioral Sciences*. Hoboken: Taylor and Francis (2013).
30. Shibue T, Weinberg RA. EMT, CSCs, and Drug Resistance: The Mechanistic Link and Clinical Implications. *Nat Rev Clin Oncol* (2017) 14:611–29. doi: 10.1038/nrclinonc.2017.44
31. Holohan C, van Schaeybroeck S, Longley DB, Johnston PG. Cancer Drug Resistance: An Evolving Paradigm. *Nat Rev Cancer* (2013) 13:714–26. doi: 10.1038/nrc3599
32. Mariathasan S, Turley SJ, Nickles D, Castiglioni A, Yuen K, Wang Y, et al. Tgfβ Attenuates Tumour Response to PD-L1 Blockade by Contributing to Exclusion of T Cells. *Nature* (2018) 554:544–8. doi: 10.1038/nature25501
33. Klein O, Kee D, Markman B, Carlino MS, Underhill C, Palmer J, et al. Evaluation of TMB as a Predictive Biomarker in Patients With Solid Cancers Treated With Anti-PD-1/CTLA-4 Combination Immunotherapy. *Cancer Cell* (2021) 39:592–3. doi: 10.1016/j.ccell.2021.04.005
34. Samstein RM, Lee C-H, Shoushtari AN, Hellmann MD, Shen R, Janjigian YY, et al. Tumor Mutational Load Predicts Survival After Immunotherapy Across Multiple Cancer Types. *Nat Genet* (2019) 51:202–6. doi: 10.1038/s41588-018-0312-8
35. Bouwman P, Jonkers J. The Effects of Deregulated DNA Damage Signalling on Cancer Chemotherapy Response and Resistance. *Nat Rev Cancer* (2012) 12:587–98. doi: 10.1038/nrc3342
36. Morel D, Jeffery D, Aspeslagh S, Almouzni G, Postel-Vinay S. Combining Epigenetic Drugs With Other Therapies for Solid Tumours - Past Lessons and Future Promise. *Nat Rev Clin Oncol* (2020) 17:91–107. doi: 10.1038/s41571-019-0267-4
37. Brown R, Curry E, Magnani L, Wilhelm-Benartzi CS, Borley J. Poised Epigenetic States and Acquired Drug Resistance in Cancer. *Nat Rev Cancer* (2014) 14:747–53. doi: 10.1038/nrc3819
38. Jones PA, Ohtani H, Chakravarthy A, de Carvalho DD. Epigenetic Therapy in Immune-Oncology. *Nat Rev Cancer* (2019) 19:151–61. doi: 10.1038/s41568-019-0109-9
39. Leitch HG, Surani MA, Hajkova P. DNA (De)Methylation: The Passive Route to Naïvety? *Trends Genet* (2016) 32:592–5. doi: 10.1016/j.tig.2016.08.005
40. Wainwright EN, Scaffidi P. Epigenetics and Cancer Stem Cells: Unleashing, Hijacking, and Restricting Cellular Plasticity. *Trends Cancer* (2017) 3:372–86. doi: 10.1016/j.trecan.2017.04.004
41. Zilberberg L, Todorovic V, Dabovic B, Horiguchi M, Couroussé T, Sakai LY, et al. Specificity of Latent TGF-β Binding Protein (LTBP) Incorporation Into Matrix: Role of Fibrillins and Fibronectin. *J Cell Physiol* (2012) 227:3828–36. doi: 10.1002/jcp.24094
42. Godwin AR, Singh M, Lockhart-Cairns MP, Alanazi YF, Cain SA, Baldock C. The Role of Fibrillin and Microfibril Binding Proteins in Elastin and Elastic Fibre Assembly. *Matrix Biol* (2019) 84:17–30. doi: 10.1016/j.matbio.2019.06.006
43. Han Z-R, Jiang X-L, Fan W-C. LAMC1 s Related to the Poor Prognosis of Patients With Gastric Cancer and Facilitates Cancer Cell Malignancies. *Neoplasma* (2021) 8(4):711–8. doi: 10.4149/neo_2021_201117N1239
44. Liu J, Liu D, Yang Z, Yang Z. High LAMC1 Expression in Glioma s Associated With Poor Prognosis. *Onco Targets Ther* (2019) 12:4253–60. doi: 10.2147/OTT.S205333
45. Ye G, Qin Y, Wang S, Pan D, Xu S, Wu C, et al. Lamc1 Promotes the Warburg Effect in Hepatocellular Carcinoma Cells by Regulating PKM2 Expression Through AKT Pathway. *Cancer Biol Ther* (2019) 20:711–9. doi: 10.1080/15384047.2018.1564558
46. Kashima H, Wu R-C, Wang Y, Sinno AK, Miyamoto T, Shiozawa T, et al. Laminin C1 Expression by Uterine Carcinoma Cells s Associated With Tumor Progression. *Gynecol Oncol* (2015) 139:338–44. doi: 10.1016/j.ygyno.2015.08.025
47. Wishart AL, Conner SJ, Guarin JR, Fatherree JP, Peng Y, McGinn RA, et al. Decellularized Extracellular Matrix Scaffolds Identify Full-Length Collagen VI as a Driver of Breast Cancer Cell Invasion in Obesity and Metastasis. *Sci Adv* (2020) 6(43):eabc3175. doi: 10.1126/sciadv.abc3175
48. Romero-López M, Trinh AL, Sobrino A, Hatch MM, Keating MT, Fimbres C, et al. Recapitulating the Human Tumor Microenvironment: Colon Tumor-Derived Extracellular Matrix Promotes Angiogenesis and Tumor Cell Growth. *Biomaterials* (2017) 116:118–29. doi: 10.1016/j.biomaterials.2016.11.034
49. Kaur A, Ecker BL, Douglass SM, Kugel CH, Webster MR, Almeida FV, et al. Remodeling of the Collagen Matrix in Aging Skin Promotes Melanoma Metastasis and Affects Immune Cell Motility. *Cancer Discov* (2019) 9:64–81. doi: 10.1158/2159-8290.CD-18-0193
50. Saatci O, Kaymak A, Raza U, Ersan PG, Akbulut O, Banister CE, et al. Targeting Lysyl Oxidase (LOX) Overcomes Chemotherapy Resistance in Triple Negative Breast Cancer. *Nat Commun* (2020) 11:2416. doi: 10.1038/s41467-020-16199-4
51. Byers LA, Diao L, Wang J, Saintigny P, Girard L, Peyton M, et al. An Epithelial-Mesenchymal Transition Gene Signature Predicts Resistance to EGFR and PI3K Inhibitors and Identifies Axl as a Therapeutic Target for Overcoming EGFR Inhibitor Resistance. *Clin Cancer Res* (2013) 19:279–90. doi: 10.1158/1078-0432.ccr-12-1558
52. Farmer P, Bonnefoi H, Anderle P, Cameron D, Wirapati P, Wirapati P, et al. A Stroma-Related Gene Signature Predicts Resistance to Neoadjuvant Chemotherapy in Breast Cancer. *Nat Med* (2009) 15:68–74. doi: 10.1038/nm.1908
53. Zheng X, Carstens JL, Kim J, Scheible M, Kaye J, Sugimoto H, et al. Epithelial-To-Mesenchymal Transition Is Dispensable for Metastasis But Induces Chemoresistance in Pancreatic Cancer. *Nature* (2015) 527:525–30. doi: 10.1038/nature16064
54. Plotnikov SV, Pasapera AM, Sabass B, Waterman CM. Force Fluctuations Within Focal Adhesions Mediate ECM-Rigidity Sensing to Guide Directed Cell Migration. *Cell* (2012) 151:1513–27. doi: 10.1016/j.cell.2012.11.034
55. Vogel V. Unraveling the Mechanobiology of Extracellular Matrix. *Annu Rev Physiol* (2018) 80:353–87. doi: 10.1146/annurev-physiol-021317-121312
56. Kesh K, Gupta VK, Durden B, Garrido V, Mateo-Victoriano B, Lavania SP, et al. Therapy Resistance, Cancer Stem Cells and ECM in Cancer: The Matrix Reloaded. *Cancers (Basel)* (2020) 12(10):3067. doi: 10.3390/cancers12103067
57. Baylin SB, Jones PA. A Decade of Exploring the Cancer Epigenome - Biological and Translational Implications. *Nat Rev Cancer* (2011) 11:726–34. doi: 10.1038/nrc3130
58. Glasspool RM, Teodoridis JM, Brown R. Epigenetics as a Mechanism Driving Polygenic Clinical Drug Resistance. *Br J Cancer* (2006) 94:1087–92. doi: 10.1038/sj.bjc.6603024
59. Easwaran H, Tsai H-C, Baylin SB. Cancer Epigenetics: Tumor Heterogeneity, Plasticity of Stem-Like States, and Drug Resistance. *Mol Cell* (2014) 54:716–27. doi: 10.1016/j.molcel.2014.05.015
60. Zhang Y-W, Zheng Y, Wang J-Z, Lu X-X, Wang Z, Chen L-B, et al. Integrated Analysis of DNA Methylation and mRNA Expression Profiling Reveals Candidate Genes Associated With Cisplatin Resistance in Non-Small Cell Lung Cancer. *Epigenetics* (2014) 9:896–909. doi: 10.4161/epi.28601
61. Sharma P, Hu-Lieskovan S, Wargo JA, Ribas A. Primary, Adaptive, and Acquired Resistance to Cancer Immunotherapy. *Cell* (2017) 168:707–23. doi: 10.1016/j.cell.2017.01.017
62. Lovly CM, Shaw AT. Molecular Pathways: Resistance to Kinase Inhibitors and Implications for Therapeutic Strategies. *Clin Cancer Res* (2014) 20:2249–56. doi: 10.1158/1078-0432.CCR-13-1610
63. Kalbasi A, Ribas A. Tumour-Intrinsic Resistance to Immune Checkpoint Blockade. *Nat Rev Immunol* (2020) 20:25–39. doi: 10.1038/s41577-019-0218-4
64. Aldea M, Andre F, Marabelle A, Dogan S, Barlesi F, Soria J-C. Overcoming Resistance to Tumor-Targeted and Immune-Targeted Therapies. *Cancer Discov* (2021) 11:874–99. doi: 10.1158/2159-8290.cd-20-1638
65. Salmon H, Franciszkiewicz K, Damotte D, Dieu-Nosjean M-C, Validire P, Trautmann A, et al. Matrix Architecture Defines the Preferential Localization and Migration of T Cells Into the Stroma of Human Lung Tumors. *J Clin Invest* (2012) 122:899–910. doi: 10.1172/JCI45817
66. Gajewski TF, Schreiber H, Fu Y-X. Innate and Adaptive Immune Cells in the Tumor Microenvironment. *Nat Immunol* (2013) 14:1014–22. doi: 10.1038/ni.2703

67. Ravi R, Noonan KA, Pham V, Bedi R, Zhavoronkov A, Ozerov IV, et al. Bifunctional Immune Checkpoint-Targeted Antibody-Ligand Traps That Simultaneously Disable Tgfβ Enhance the Efficacy of Cancer Immunotherapy. *Nat Commun* (2018) 9:741. doi: 10.1038/s41467-017-02696-6
68. Lan Y, Zhang D, Xu C, Hance KW, Marelli B, Qi J, et al. Enhanced Preclinical Antitumor Activity of M7824, a Bifunctional Fusion Protein Simultaneously Targeting PD-L1 and TGF-β. *Sci Transl Med* (2018) 10(424):eaan5488. doi: 10.1126/scitranslmed.aan5488

Conflict of Interest: The authors declare that the research was conducted in the absence of any commercial or financial relationships that could be construed as a potential conflict of interest.

Publisher's Note: All claims expressed in this article are solely those of the authors and do not necessarily represent those of their affiliated organizations, or those of the publisher, the editors and the reviewers. Any product that may be evaluated in this article, or claim that may be made by its manufacturer, is not guaranteed or endorsed by the publisher.

Copyright © 2021 Yang, Xue, Li, Zhu, Lu, Wang, Xu, Wang, Zhang, Yu, Ren, Wang, Wang, Chen, Guan and Xia. This is an open-access article distributed under the terms of the Creative Commons Attribution License (CC BY). The use, distribution or reproduction in other forums is permitted, provided the original author(s) and the copyright owner(s) are credited and that the original publication in this journal is cited, in accordance with accepted academic practice. No use, distribution or reproduction is permitted which does not comply with these terms.

frontiers in Oncology

ORIGINAL RESEARCH
published: 21 October 2021
doi: 10.3389/fonc.2021.723131

Comprehensive Analysis of IGFBPs as Biomarkers in Gastric Cancer

Qi Liu[1], *Jianwu Jiang*[1], *Xiefu Zhang*[1], *Meixiang Zhang*[2*] and *Yang Fu*[1*]

[1] Department of Gastrointestinal Surgery, The First Affiliated Hospital of Zhengzhou University, Zhengzhou, China, [2] Center for Reproductive Medicine, Henan Key Laboratory of Reproduction and Genetics, The First Affiliated Hospital of Zhengzhou University, Zhengzhou, China

Objective: Gastric cancer is the fifth most common cancer worldwide and the third leading cause of cancer-related deaths. Insulin-like growth-factor-binding proteins (IGFBPs) were initially identified as passive inhibitors that combined with insulin-like growth factors (IGFs) in serum. However, more recent data have shown that they have different expression patterns and a variety of functions in the development and occurrence of cancers. Thus, their various roles in cancer still need to be elucidated. This study aimed to explore the IGFBPs and their prognostic value as markers in gastric cancer.

Methods: Oncomine, Gene Expression Profiling Interactive Analysis (GEPIA), Kaplan–Meier Plotter, cBioPortal, GeneMANIA, and TIMER were used to analyze the differential expression, prognostic value, genetic alteration, and association with immune cell infiltration of IGFPBs in gastric cancer.

Results: Expression levels of IGFBP3, IGFBP4, and IGFBP7 were significantly elevated in gastric cancer tissues, whereas those of IGFBP1 were reduced in normal tissues. IGFBP1/5/7 expression was significantly associated with overall survival whereas IGFBP6/7 expression was significantly correlated with disease-free survival in gastric cancer patients. IGFBP3/5/6/7 were associated with clinical cancer stage. Gene ontology and Kyoto Encyclopedia of Genes and Genome analyses showed that IGFBP3/5/7 were mainly enriched in focal adhesion, extracellular matrix structural constituent, cell-substratist junction, extracellular structure, and matrix organization. Stomach adenocarcinoma (STAD) and gastric cancer had more IGFBP1–7 mutations than other tumor types. Hub gene analysis showed that TP53 and IGF2 expression was significantly elevated in STAD patients; PLG, PAPPA, AFP, and CYR61 were associated with overall survival rate; and IGFALS, PLG, IGF1, AHSG, and FN1 were associated with disease-free survival. Finally, IGFBP3–7 were all associated with cancer-associated fibroblast infiltration in STAD, colon adenocarcinoma, and rectal adenocarcinoma.

Conclusion: Our study provides a comprehensive analysis and selection of IGFBPs as prognostic biomarkers in STAD. This was the first bioinformatic analysis study to describe the involvement of IGFBPs, especially IGFBP7, in gastric cancer development through the extracellular matrix.

Keywords: gastric cancer, insulin-like growth factor-binding protein, prognostic biomarker, bioinformatics analysis, stomach adenocarcinoma (STAD)

OPEN ACCESS

Edited by:
Luigi Marano,
University of Siena, Italy

Reviewed by:
Zhangya Pu,
Central South University, China
Fei Ma,
Zhengzhou University, China

***Correspondence:**
Yang Fu
fuyang@zzu.edu.cn
Meixiang Zhang
mxz329@163.com

Specialty section:
This article was submitted to Gastrointestinal Cancers, a section of the journal Frontiers in Oncology

Received: *10 June 2021*
Accepted: *29 September 2021*
Published: *21 October 2021*

Citation:
Liu Q, Jiang J, Zhang X, Zhang M and Fu Y (2021) Comprehensive Analysis of IGFBPs as Biomarkers in Gastric Cancer. Front. Oncol. 11:723131. doi: 10.3389/fonc.2021.723131

INTRODUCTION

Stomach cancer is the fifth most common cancer worldwide (1). More than 900,000 gastric cancer cases are diagnosed each year, with higher incidences among males and in developing countries (2). Most gastric cancers are already at an advanced stage when they are diagnosed; thus, gastric cancer has become the third leading cause of cancer-related deaths, causing 784,000 deaths globally in 2018 (3). Ninety percent of gastric cancers are gastric adenocarcinomas in terms of pathological type. However, their biological behaviors and histopathological structures vary, as do patients' outcomes.

The pathogenesis of gastric cancer is unclear; infections, genetic mutations, and unhealthy lifestyles are the main causes. *Helicobacter pylori* infection is the best-described risk factor for non-cardia gastric cancer. Chronic *H. pylori* infection leads to atrophic gastritis and intestinal metaplasia, which are considered to be precancerous lesions (4). Familial aggregation appears in approximately 10% of all gastric cancer cases, and germline mutations are found in 1%–3% of gastric cancer patients (5). For instance, a pathogenic gene in STAD, Ecadherin-coding gene CDH1, appears in 30%–40% of hereditary diffuse gastric cancer patients (6). CTNNA1, a cell matrix αEcatenin-coding gene, has an exon 1B point mutation also found in families with hereditary diffuse gastric cancer (7, 8). APC, a tumor suppressor and Wnt signaling pathway antagonist-coding gene, also plays a part in gastric adenocarcinoma by altering cell migration and adhesion (9). These two genes indicate the importance of the tumor microenvironment (TME), which contains multiple cell types that enable the sustained growth, invasion, and metastasis of cancers. With respect to lifestyle, cigarette smoking, alcohol consumption, salty food intake, and older age are risk factors for gastric cancer, whereas a high intake of vegetables and fruit and a low-salt diet will reduce the risk (10).

Insulin-like growth-factor-binding proteins IGFBPs are a series of cystine-rich proteins that act as combiners of insulin growth factors (IGFs) in serum. They have important roles in tumor occurrence and development, prolonging the half-life of the IGFs, controlling their access to IGF receptors (IGFRs), and promoting or inhibiting IGF downstream signaling pathways (11). Recent studies have indicated that these growth factors are also involved in interaction with ECM proteins and proteolytic enzymes (12). This regulation process is also called the IGF–IGFR–IGFBP axis. IGFBPs can be divided into two groups according to their different affinities for IGFs: high-affinity binding proteins (IGFBP1–6) and low-affinity binding proteins (IGFBP7–10). Our study focused on the prognostic value of IGFBP1–6 in gastric cancer; however, IGFBP7 is also significantly upregulated in STAD patients and closely related to prognosis (13). Thus, we also included IGFBP7 in the analysis.

MATERIALS AND METHODS

Oncomine

IGFBP1–7 mRNA levels in diverse cancer types were analyzed using Oncomine (www.oncomine.org), which provides microarray information for 65 gene expression datasets comprising most major cancer types (14). In this study, a p-value <0.01, a fold change of 2, and a gene rank in the top 10% were set as the significance thresholds. Student's t-test was applied to determine the differences in expression of IGFBP1–7 in gastric cancer.

Gene Expression Profiling Interactive Analysis

Gene Expression Profiling Interactive Analysis (GEPIA) (http://gepia.cancer-pku.cn) is an interactive web server using a standard procession pipeline to analyze 9,736 tumor tissues and 8,587 normal samples from The Cancer Genome Atlas (TCGA) and the GTEx project (15). In this study, IGFBP1–7 expression in normal and tumor tissues was compared by Student's t-test. IGFBP1–7 expression between different stages was compared with one-way analysis of variance. Survival analysis was performed with Kaplan–Meier curves. Comparisons of normal and tumor tissues and survival analysis were also performed for hub genes of IGFBP1–7 by GEPIA.

cBioPortal

cBioPortal (www.cbioportal.org) is a comprehensive cancer data analysis tool. It provides online analysis of data types including gene mutation, copy number variation, mRNA expression, and protein phosphorylation (16). In this study, genetic alterations (structure variant, mutation, and copy number variant data) of IGFBP1–7 from 11,084 samples (from 11,070 patients in 35 studies) were obtained from cBioPortal.

STRING

STRING (https://string-db.org/) is a database of protein–protein interactions (PPIs), which can be used to predict a comprehensive and global network for a customized protein list (17). In this study, IGFBP1–7 PPI network analysis was performed with STRING.

TIMER

TIMER (https://cistrome.shinyapps.io/timer/) is a web resource that can be used to evaluate immune cell infiltration and its clinical effects (18). IGFBP1–7 immune cell infiltration levels in STAD were analyzed and visualized using scatterplots with TIMER.

Other Bioinformatic Analyses

Gene expression data for STAD in HTSeq-FPKM format were downloaded from TCGA, and 407 patients were selected for analysis. The R package "pROC" was used for ROC analysis, and "ggplot2" was used for visualization. Genes co-expressed with IGFBP3/5/7 were screened from TCGA data with R package "stat" using Pearson correlation with coefficient $|r| > 0.4$ and $p < 0.001$. Gene ontology (GO) and Kyoto Encyclopedia of Genes and Genome (KEGG) analysis were performed on co-expressed genes with the R package "clusterProfiler" to explore possible biological functions and signaling pathways affected by IGFBP1–7. GO analysis included biological process, cell composition, and molecular function ($p < 0.05$ was considered to indicate statistical significance) (19).

RESULTS

Differential Expression of IGFBP1–7 in Gastric Cancer

IGFBP1–7 expression data were analyzed in the Oncomine database. Expression of IGFBP3/4/7 was significantly elevated in gastric cancer samples, whereas IGFBP1 expression was decreased in normal tissues. Specific fold change and p-values are listed in **Table 1**. Based on the Oncomine data, the following expression fold change values relative to the corresponding normal tissues were obtained: 4.577 (p = 9.92E-09) for IGFBP3 in gastric mixed adenocarcinoma; 3.73 (p = 6.31E-06) for IGFBP4 in gastric cancer; 4.217 (p = 6.31E-13) for IGFBP7 in diffuse gastric adenocarcinoma; 2.333 (p = 6.19E-19) for gastric intestinal type adenocarcinoma; 4.141 (p = 1.24E-05) for gastric mixed adenocarcinoma (20); and 2.926 (p = 7.51E-06) for gastric mixed adenocarcinoma (21). That is, IGFBP3, IGFBP4, and IGFBP7 expression levels were higher in gastric cancer patients *vs.* normal in the Oncomine data (**Figure 1A**). In TCGA data, the average IGFBP1/3/7 expression levels in STAD were significantly higher than those in normal tissue, while IGFBP2/5/6 expression was significantly lower in tumor tissue (**Figure 1B**). Analysis of TCGA STAD data showed that 4%–6% of STAD patients had high expression of IGFBP1–7. These data suggest that IGFBP1/3/7 might have key roles in gastric cancer.

Prognostic Value of mRNA Expression of IGFBP1–7 in STAD Patients

To investigate the prognostic value of IGFBP1–7 in STAD patients, area under the curve (AUC) analysis was performed for IGFBP1–7 in TCGA STAD mRNA data. The respective AUCs for IGFBP1–7 were 0.844, 0.662, 0.871, 0.487, 0.597, 0.793, and 0.721 (**Figure 2A**). Kaplan–Meier Plotter was used for survival analysis with GEPIA; IGFBP1/5/7 mRNA levels were found to be significantly associated with overall survival (**Figure 2B**), whereas IGFBP6/7 mRNA levels were significantly correlated with disease-free survival rates (**Figure 2C**). All these data indicated significant roles of IGFBP1/5/6/7 in STAD. Prognostic value of IGFBPs were also validated in another cohort (20), but IGFBP1/3/5 expression was not significantly associated with overall survival.

TABLE 1 | IGFBP1–7 expression in STAD patients from the cBioPortal database.

	Type of gastric cancer *versus* normal gastric tissue	Fold change	p value	t test	Source and/or reference	
IGFBP1	Gastric intestinal type adenocarcinoma *vs*. normal	1.068	2.96E-08	6.685	Deng Gastric	PMID: 22315472
	Diffuse gastric adenocarcinoma *vs*. normal	1.033	1.02E-05	4.845	Deng Gastric	PMID: 22315472
	Gastric mixed adenocarcinoma *vs*. normal	1.051	0.009	2.807	Deng Gastric	PMID: 22315472
	Gastric cancer *vs*. normal	1.057	9.27E-05	4.099	Deng Gastric	PMID: 22315472
	Gastric adenocarcinoma *vs*. normal	1.045	3.01E-05	4.293	Deng Gastric	PMID: 22315472
	Gastric intestinal type adenocarcinoma *vs*. normal	1.13	4.04E-08	6.545	TCGA	
	Mucinous gastric adenocarcinoma *vs*. normal	1.078	0.002	3.518	TCGA	
	Diffuse gastric adenocarcinoma *vs*. normal	1.078	9.35E-06	4.798	TCGA	
	Gastric tubular adenocarcinoma *vs*. normal	1.123	6.52E-05	4.387	TCGA	
	Gastric adenocarcinoma *vs*. normal	1.101	1.88E-15	8.638	TCGA	
IGFBP2	Gastric adenocarcinoma *vs*. normal	1.017	0.001	3.172	Deng Gastric	PMID: 22315472
IGFBP3	Gastric mixed adenocarcinoma *vs*. normal	4.577	9.92E-09	11.971	Chen Gastric	PMID: 12925757
	Gastric intestinal type adenocarcinoma *vs*. normal	2.319	7.89E-11	7.202	Chen Gastric	PMID: 12925758
	Gastric intestinal type adenocarcinoma *vs*. normal	1.068	2.96E-08	6.685	Deng Gastric	PMID: 22315472
	Diffuse gastric adenocarcinoma *vs*. normal	1.033	1.02E-05	4.845	Deng Gastric	PMID: 22315472
	Gastric mixed adenocarcinoma *vs*. normal	1.051	0.009	2.807	Deng Gastric	PMID: 22315472
	Gastric cancer *vs*. normal	1.057	9.27E-05	4.099	Deng Gastric	PMID: 22315472
	Gastric adenocarcinoma *vs*. normal	1.045	3.01E-05	4.293	Deng Gastric	PMID: 22315472
	Gastric intestinal type adenocarcinoma *vs*. normal	1.13	4.04E-08	6.545	TCGA	
	Mucinous gastric adenocarcinoma *vs*. normal	1.078	0.002	3.518	TCGA	
	Diffuse gastric adenocarcinoma *vs*. normal	1.078	9.35E-06	4.798	TCGA	
	Gastric tubular adenocarcinoma *vs*. normal	1.123	6.52E-05	4.387	TCGA	
	Gastric adenocarcinoma *vs*. normal	1.101	1.88E-15	8.638	TCGA	
IGFBP4	Gastric cancer *vs*. normal	3.731	6.31E-06	5.498	Wang Gastric	PMID: 21132402
	Diffuse gastric adenocarcinoma *vs*. normal	1.84	2.01E-05	4.526	Cho Gastric	PMID: 21447720
	Gastric adenocarcinoma *vs*. normal	1.965	0.021	2.993	Cho Gastric	PMID: 21447720
	Gastric intestinal type adenocarcinoma *vs*. normal	1.73	0.01	2.483	Cho Gastric	PMID: 21447720
	Gastric mixed adenocarcinoma *vs*. normal	1.647	0.018	2.379	Cho Gastric	PMID: 21447720
IGFBP5	Diffuse gastric adenocarcinoma *vs*. normal	1.78	0.000557	3.678	Chen Gastric	PMID: 12925758
IGFBP6	NA					
IGFBP7	Diffuse gastric adenocarcinoma *vs*. normal	4.217	6.31E-13	14.986	Chen Gastric	PMID: 12925758
	Gastric intestinal type adenocarcinoma *vs*. normal	2.333	6.19E-19	11.245	Chen Gastric	PMID: 12925758
	Gastric mixed adenocarcinoma *vs*. normal	4.141	1.24E-05	8.377	Chen Gastric	PMID: 12925758
	Gastric cancer *vs*. normal	2.926	7.51E-06	5.352	Wang Gastric	PMID: 21132402
	Gastric mixed adenocarcinoma *vs*. normal	4.669	1.54E-06	7.154	DErrico Gastric	PMID: 19081245
	Gastric intestinal type adenocarcinoma *vs*. normal	2.721	3.26E-09	7.102	DErrico Gastric	PMID: 19081245
	Diffuse gastric adenocarcinoma *vs*. normal	2.238	4.16E-06	4.998	Cho Gastric	PMID: 21447720
	Gastric cancer *vs*. normal	1.466	0.000307	3.497	Cui Gastric	PMID: 20965966

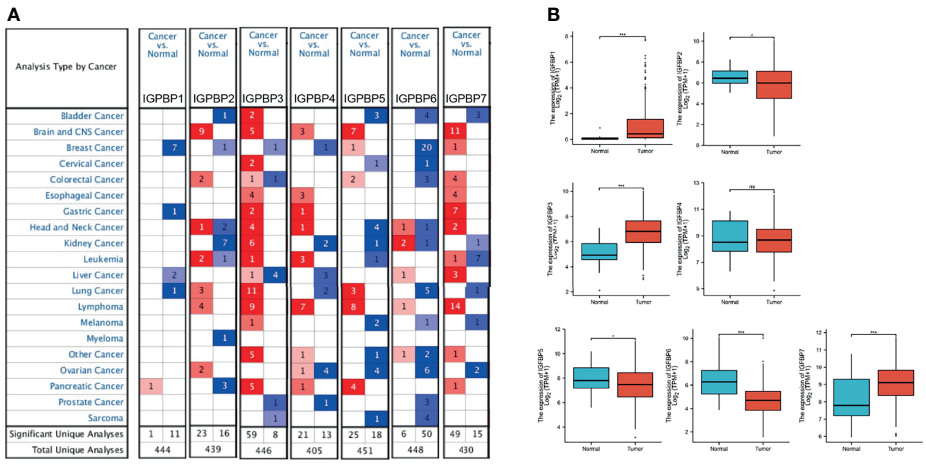

FIGURE 1 | IGFBP1–7 expression in STAD patients. **(A)** mRNA expression of IGFBP1–7 in different cancer types from Oncomine. The graphic shows the numbers of datasets with statistically significant alterations in the mRNA expression of the target gene: upregulated (red) and downregulated (blue). The following criteria were used: p-value: 0.01, fold change: 2, gene rank: 10%, data type: mRNA, analysis type: cancer *vs*. normal tissue. As shown in the green frame, transcriptional levels of IGFBP3/4/7 were significantly elevated while transcriptional levels of IGFBP1 were reduced in gastric cancer. **(B)** Expression of IGFBP1–7 in the TCGA database. *p < 0.05, ***p < 0.001.

To investigate the relationships between IGFBP1–7 expression and clinicopathological parameters in STAD patients, we analyzed mRNA levels in patients of different gender, age, *H. pylori* infection status, metastasis, pathological stage, lymphatic metastasis, and T stage. The results showed that IGFBP1–7 expression was not related to patients' age, gender, *H. pylori* infection status, metastasis, or lymphatic metastasis; however, IGFBP3/5/6/7 expression was significantly elevated in pathological stages II–IV compared with pathological stage I. IGFBP3/5/7 expression was also significantly increased in advanced T-stage patients. These results suggest that IGFBP3/5/6/7 may have roles in tumor progression (**Table 2**). Cox multivariate regression analysis showed that besides tumor stages, IGFBP1 and IGFBP7 were independent predictors in STAD patients (**Supplementary Table 1**).

Correlations Between IGPBP1–7 Expression and Tumor Stage in STAD Patients

To further study the functions of IGFBP1–7 in tumor progression, we analyzed their expression levels at different stages using TCGA data. Violin plots of IGFBP1–7 expression at different tumor stages showed an upward trend with increasing T stages. This trend was significant for IGFBP3/4/5/6/7 (**Figure 3**). Based on these results, combined with those of

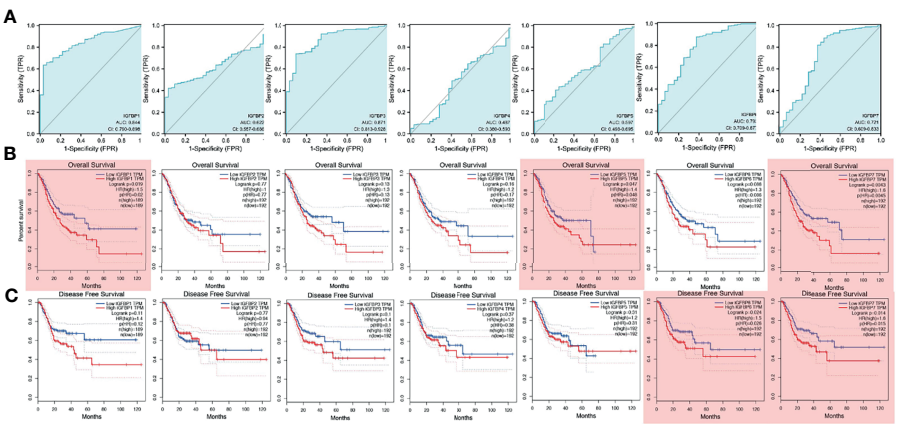

FIGURE 2 | Survival analysis and diagnostic value of IGFBP1–7 in STAD patients. **(A)** Diagnostic value of IGFBP1–7 in STAD patients. **(B)** Overall survival curve for IGFBP1–7 in STAD patients. **(C)** Disease-free survival curve for IGFBP1–7 in STAD patients. Results with p < 0.05 are marked with red shadow.

TABLE 2 | The relationships between IGFBP1/3/5/7 with clinicopathological parameters in STAD patients.

Clinicopathological parameters	N	IGFBP1 expression		IGFBP2 expression		IGFBP3 expression		IGFBP4 expression		IGFBP5 expression		IGFBP6 expression		IGFBP7 expression	
		Mean ±SD	P value	Mean ±SD	P value	Mean ±SD	P value	Mean ±SD	P value	Mean ±SD	P value	Mean ±SD	P value	Mean ±SD	P value
Tissue			<0.001		0.022*		<0.001		0.803*		0.069		<0.001*		<0.001
Normal	32	0.095 ±0.162		6.539 ±0.727		5.052 ±1.010		8.791 ±1.246		7.918 ±1.253		6.383 ±1.602		8.138 ±1.302	
Tumor	375	1.071 ±1.402		5.762 ±1.872		6.787 ±1.199		8.695 ±1.286		7.407 ±1.415		4.706 ±1.216		9.128 ±1.048	
Gender			0.826*		0.691*		0.867		0.626		0.809		0.596*		0.845
Female	134	1.044 ±1.331		5.722 ±1.830		6.773 ±1.235		8.652 ±1.372		7.384 ±1.428		4.654 ±1.255		9.113 ±1.104	
Male	241	1.087 ±1.443		5.785 ±1.898		6.795 ±1.181		8.72 ±1.238		7.421 ±1.41		4.735 ±1.196		9.136 ±1.019	
Age(years)			0.107*		0.006*		0.509		0.294		0.166		<0.001*		0.107*
≤65	164	0.893 ±1.176		6.088 ±1.707		6.827 ±1.23		8.776 ±1.359		7.521 ±1.396		4.941 ±1.215		9.236 ±1.147	
>65	207	1.22 ±1.555		5.489 ±1.967		6.744 ±1.184		8.634 ±1.237		7.316 ±1.42		4.53 ±1.191		9.04 ±0.968	
H pylori infection			0.438*		0.123*		0.904		0.197		0.376		0.344		0.008
Yes	18	0.742 ±0.889		5.389 ±1.308		6.479 ±1.098		8.729 ±1.027		7.372 ±1.37		4.612 ±1.013		9.348 ±0.81	
No	145	1.139 ±1.442		5.866 ±1.864		6.517 ±1.274		8.34 ±1.221		7.045 ±1.486		4.345 ±1.134		8.701 ±0.983	
Metastasis			0.305*		0.134*		0.744		0.348		0.987		0.975		0.847*
No	330	1.039 ±1.415		5.725 ±1.889		6.763 ±1.203		8.66 ±1.292		7.398 ±1.425		4.71 ±1.237		9.117 ±1.043	
Yes	25	1.320 ±1.424		6.217 ±2.003		6.845 ±1.156		8.911 ±1.219		7.403 ±1.512		4.718 ±1.18		9.250 ±1.204	
Pathological stage			0.758*		0.414*		0.001		0.053		<0.001		0.002		<0.001
I	53	1.190 ±1.637		5.599 ±2.156		6.274 ±1.414		8.393 ±1.488		6.563 ±1.585		4.25 ±1.316		8.608 ±1.128	
II-IV	150	1.062 ±1.367		5.843 ±1.833		6.857 ±1.14		8.76 ±1.228		7.55 ±1.336		4.82 ±1.195		9.215 ±1.008	
Lymphatic metastasis			0.631*		0.775*		0.608*		0.844		0.055		0.993		0.613
No	111	1.094 ±1.580		5.732 ±2.064		6.769 ±1.274		8.722 ±1.376		7.197 ±1.475		4.716 ±1.368		9.086 ±1.176	
Yes	246	1.063 ±1.340		5.829 ±1.803		6.788 ±1.165		8.693 ±1.226		7.505 ±1.368		4.718 ±1.153		9.147 ±0.984	
T stage			0.958*		0.828*		0.015		0.043		<0.001		0.081		<0.001
T1-T2	99	1.105 ±1.540		5.839 ±1.982		6.523 ±1.337		8.465 ±1.355		6.963 ±1.507		4.496 ±1.258		8.799 ±1.064	
T3-T4	268	1.055 ±1.352		5.784 ±1.824		6.866 ±1.138		8.771 ±1.248		7.549 ±1.355		4.787 ±1.208		9.231 ±1.025	

IGF, Insulin-like growth factor-binding protein; STAD, Stomach adenocarcinoma.
**samples do not meet the normal distribution, use Mann-Whitney U test.*

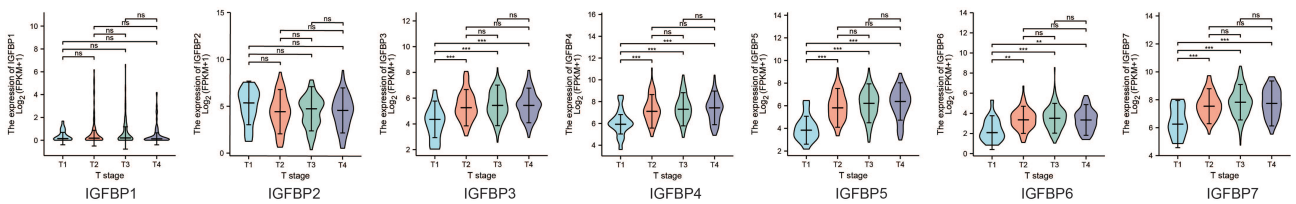

FIGURE 3 | Difference between IGPBP1–7 expression and tumor stage in STAD patients from the TCGA database.

the mRNA expression analysis, IGFBP3/5/7 were chosen for further study of the mechanisms of tumor progression.

Analysis of Genes Co-Expressed With IGFBP3/5/7 in STAD Patients

To further understand the possible molecular mechanisms of IGFBP3/5/7 in tumor progression, we selected the top 10 genes positively and negatively co-expressed with IGFBP3/5/7 based on TCGA data and constructed a heatmap (**Figures 4A–C**). The thresholds for gene co-expression genes were $|r| > 0.4$ and $p < 0.001$. We found 449 genes co-expressed with IGFBP3, 2,295 with IGFBP5, and 2,643 with IGFBP7; 407 genes overlapped the three co-expression groups (**Figure 4D**, all genes listed in **Supplementary Table 2**). GO (**Figure 4E**) and KEGG (**Figure 4F**) analyses were performed for all four groups of genes with R package "clusterProfiler" (**Supplementary Table 3**). Collagen-containing extracellular matrix (ECM), extracellular structure organization, ECM organization, and ECM structural constituent were the most significant terms in the GO analysis. In the KEGG analysis, ECM–receptor interaction, focal adhesion, and PI3K-Akt signaling pathway were the most significant pathways. These results suggest that IGFBP3/5/7 might be involved in tumor progression *via* interactions with the ECM. Besides, the association between tumor stage and IGFBP expression was also validated in the other two cohorts (20, 22) (**Supplementary Figure 2**).

Genetic Alterations of IGFBP1–7 in STAD Patients

Pathogenic mutations increase the risk of tumorigenesis, including that of gastric cancer. We analyzed the genetic alterations of IGFBP1–7 in STAD patients using cBioPortal; 35 datasets and 11,070 patients were included in this analysis. The results showed that STAD patients had the highest rates of IGFBP1–7 genetic alterations compared with other cancer types, with 80 of 440 patients (18.8%) having such alterations according to TCGA data. In the OncoSG (2018) database, 25 of 147 gastric cancer patients (17.1%) had such genetic mutations (**Figure 5**). These results further confirmed the importance of IGFBP1–7 in gastric cancer (specific mutation types are listed in **Supplementary Table 4**). However, mutations were not associated with prognosis in STAD patients (**Supplementary Figure 3**).

Interactions of IGFBPs in STAD and Hub Hene Analyses

Next, we performed a correlation analysis for IGFBP1–7 and found that IGFBP3/4/5/6/7 had strong correlations with each other (**Figure 6A**). Then, we put all seven molecules into STRING and constructed a PPI network (**Figure 6B**, the interaction score was >0.4) with IGFBP1/3/4/5/7 in the center and another 10 hub genes (TP53, IGFALS, PLG, IGF1, IGF2, PAPPA, AHSG, FN1, AFP, and CYR61) around them. We performed GO analysis for all these

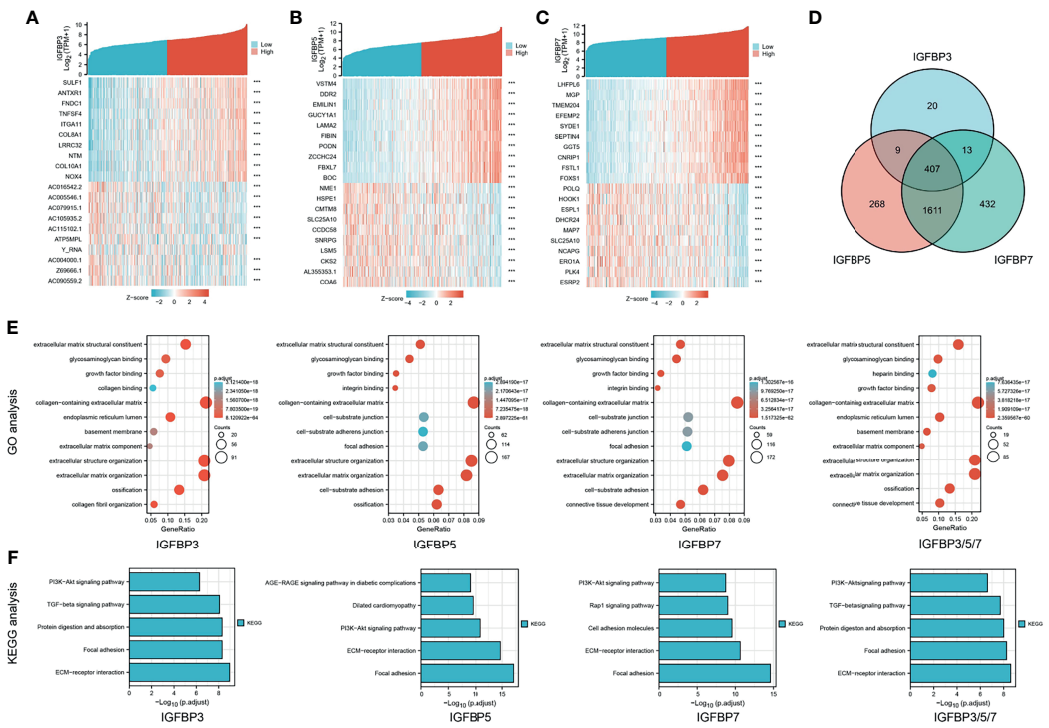

FIGURE 4 | Heat map, Venn diagram, and GO/KEGG analysis of IGFBP3/5/7. Heat map and Venn diagram showing top 10 genes with positive and negative co-expression with IGFBP3 **(A)**, IGFBP5 **(B)**, and IGFBP7 **(C)** in STAD patients from the TCGA database. **(D)** Intersection of genes co-expressed with IGFBP3/5/7. $|r| > 0.4$, $p < 0.001$. **(E)** GO analysis of IGFBP3, IGFBP5, IGFBP7, and IGFBP3/5/7 (407 overlap genes); **(F)** KEGG analysis of IGFBP3, IGFBP5, IGFBP7, and IGFBP3/5/7 (407 overlap genes).

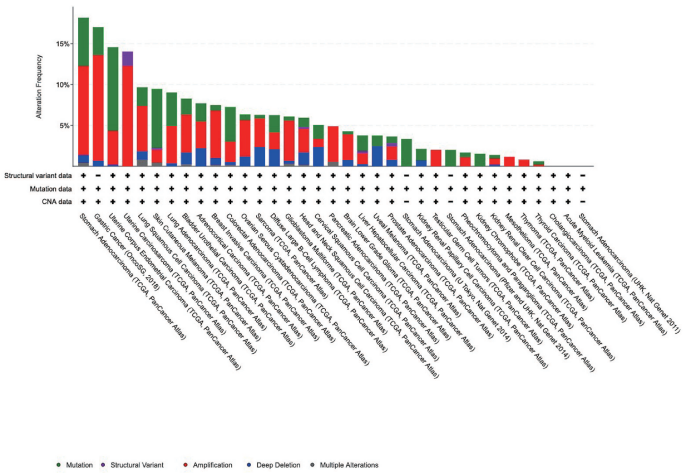

FIGURE 5 | Genetic alterations of IGFBP1–7 in different cancer patients from cBioPortal database.

genes and found that they encoded proteins involved in the PI3K-Akt signaling pathway and ECM–reception interaction (**Figure 6C**). Expression level and survival analyses were also performed on these hub genes (**Figure 6D**). TP53 and IGF2 expression were significantly elevated in STAD patients, but they were not associated with overall (**Figure 6E**) or disease-free survival (**Figure 6F**). PLG, PAPPA, AFP, and CYR61 were associated with overall survival, whereas IGFALS, PLG, IGF1, AHSG, and FN1 were associated with disease-free survival. The immunohistochemical verification from Human Protein Atlas data is shown in **Figure 6G**.

Association of Immune Cell Infiltration With IGFBP1–7 in STAD Patients

Immune cell infiltration creates a microenvironment for the tumor that facilitates cancer cell proliferation and progression. The relationships between IGFBP1–7 expression and immune cell infiltration were analyzed using the TIMER database (18, 23). Using the EPIC, MCPCOUNTER, XCELL, and TIDE algorithms, we found that IGFBP3/4/5/6/7 were all associated with cancer-associated fibroblast (CAF) infiltration in STAD, COAD (colon adenocarcinoma), and READ (rectal adenocarcinoma) (**Figure 7A**). **Figure 7B** shows some examples of specific correlations of IGFBP with CAFs in STAD. These results further indicate that IGFBP3–7 have important roles in the TME. The correlation of IGFBP expression and other subtypes of immune cell infiltration including B cells, CD4+T cells, CD8+T cells, neutrophils, macrophages, and dendritic cells in patients with gastric cancer is shown in **Supplementary Figure 4**.

DISCUSSION

Gastric cancer is the third most common cause of cancer-related deaths worldwide, with a particularly high incidence in Asian populations. Many studies have been devoted to investigating the pathogenesis of gastric cancer and identifying prognostic biomarkers. Among such markers, IGFBPs have been shown to modulate cell proliferation, migration, and autophagy *via* temporal and spatial regulation of IGF and IGFR levels (24). However, their roles in the occurrence and development of gastric cancer remained controversial. The results of this study showed that IGFBP1/3/7 expression levels in STAD tissue were significantly higher than those in normal tissues. IGFBP1/5/7 expression was significantly associated with overall survival, whereas IGFBP6/7 expression was significantly correlated with disease-free survival. IGFBP3/5/6/7 expression was significantly elevated in pathological stages II–IV compared with pathological stage I. IGFBP3/5/7 expression was also significantly increased in advanced T-stage patients and was associated with tumor progression in STAD. Collagen-containing ECM, extracellular structure organization, ECM organization, and ECM structural constituents were the main GO/KEGG terms correlated with IGFBP3/5/7 genes. STAD and gastric cancer had the most IGFBP1–7 mutations compared with other tumors. In the hub gene analysis, expression levels of TP53 and IGF2 were significantly elevated in STAD patients; PLG, PAPPA, AFP, and CYR61 were associated with overall survival rate; and IGFALS, PLG, IGF1, AHSG, and FN1 were associated with disease-free survival rate. Finally, IGFBP3-7 expression levels were all correlated with CAF infiltration in STAD, COAD, and READ.

IGFBPs show variable expressions in gastric cancer tissues and cell lines, and there has been no comprehensive evaluation of IGFBPs as biomarkers in gastric cancer. A study of 11 gastric cancer cell lines demonstrated that IGFBP1 expression levels were extremely low in all cell lines, whereas IGFBP2 and IGFBP4 were expressed in 10 and 9 cell lines, respectively, and IGFBP3, IGFBP5, and IGFBP6 were expressed in half of all cell lines (25). Among these IGFBPs, IGFBP3, and IGFBP5 have received more research focus than others. Our data showed higher IGFBP3 expression levels in STAD patients' tumor tissues but no

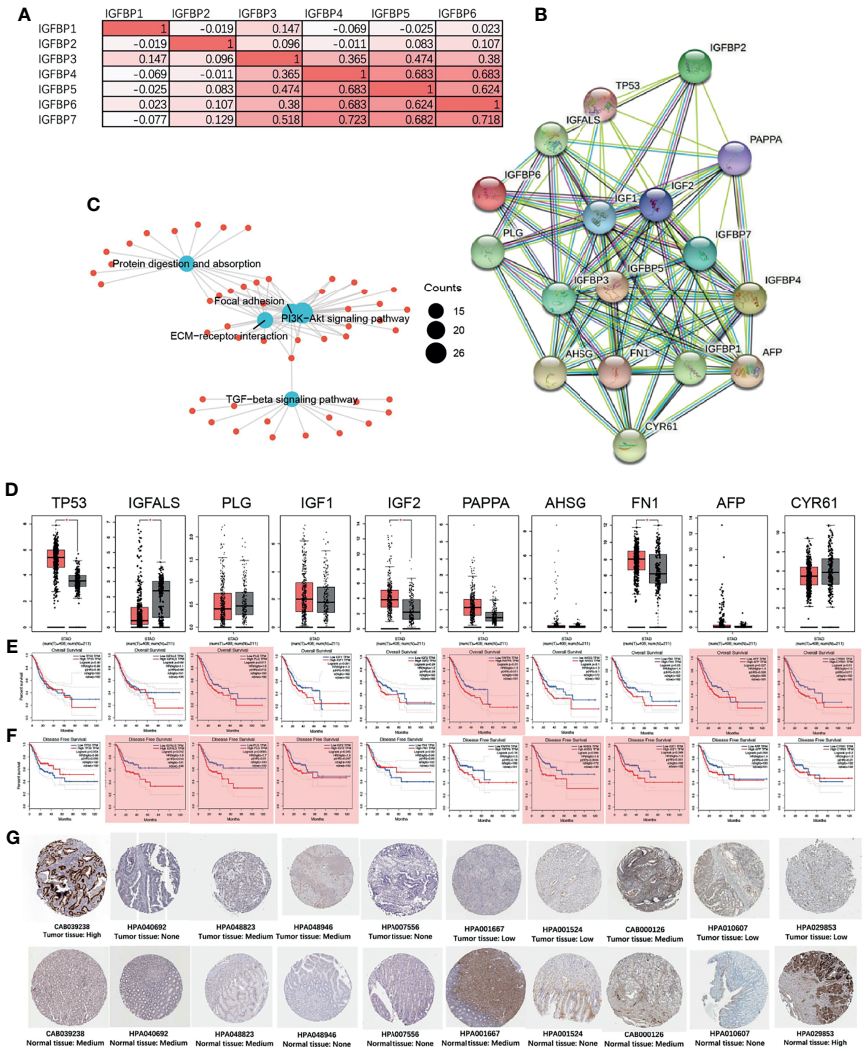

FIGURE 6 | IGFBP1–7 gene expression correlation and protein network interactions (STRING), and hub gene expression and survival analysis of STAD based on GEPIA database. **(A)** Correlations among IGFBP1–7 in STAD patients from the TCGA database. **(B)** PPI network of IGFBP1–7. **(C)** GO analysis of interacting proteins from **(B)**. **(D)** Expression levels of 10 hub genes of IGFBP1–7 in STAD patients. **(E)** Overall survival analysis for the 10 hub genes in GEPIA database. **(F)** Disease-free survival analysis for the 10 hub genes in the GEPIA database. *p < 0.05 (bar plot); p < 0.05 marked as red shadow (survival analysis). **(G)** The immunohistochemical verification of IGFBP1–7 in patients' tissue from Human Protein Atlas data (antibody name and tissue type are listed below the immunohistochemical figure).

relationship with OS. Other studies found that serum IGFBP3 levels were similar between cancer and control groups, but surgery could reduce serum IGFBP3 levels by decreasing IGFBP3 protease activity (26). Another study examined tumor tissues and adjacent tumor-free tissues from 86 STAD patients; the results showed that IGFBP3 expression was higher in the tumor-free tissues, and high IGFBP3 expression predicted better prognosis (27). All these studies illustrate the complex relationship between IGFBP3 and gastric cancer. Studies of other tumor types have provided some insight into the specific mechanisms of IGFBP3. For example, cancer-related gene vasohibin-2 induced proliferation of breast cancer cells by activating IGFBP3 and IGFBP6 (28).

This study first proposed that IGFBP7 might affect gastric cancer development by modulating the ECM. IGFBP7 is upregulated in gastric cancer and located in the cytoplasm of the majority of cancer cells, fibroblasts, and lymphocytes, and its expression is significantly correlated with indicators of pathological stage including tumor invasion depth, lymph node metastasis, and distant metastasis/recurrence (29). Regarding pathological typing, IGFBP7 has been shown to be upregulated in undifferentiated compared with differentiated tumors (13). The cell matrix is widely understood to be involved in cancer occurrence, progression, and metabolism (30). Disruption of the normal structure and function of gastric epithelia eventually leads to gastric cancer progression. However, few studies have

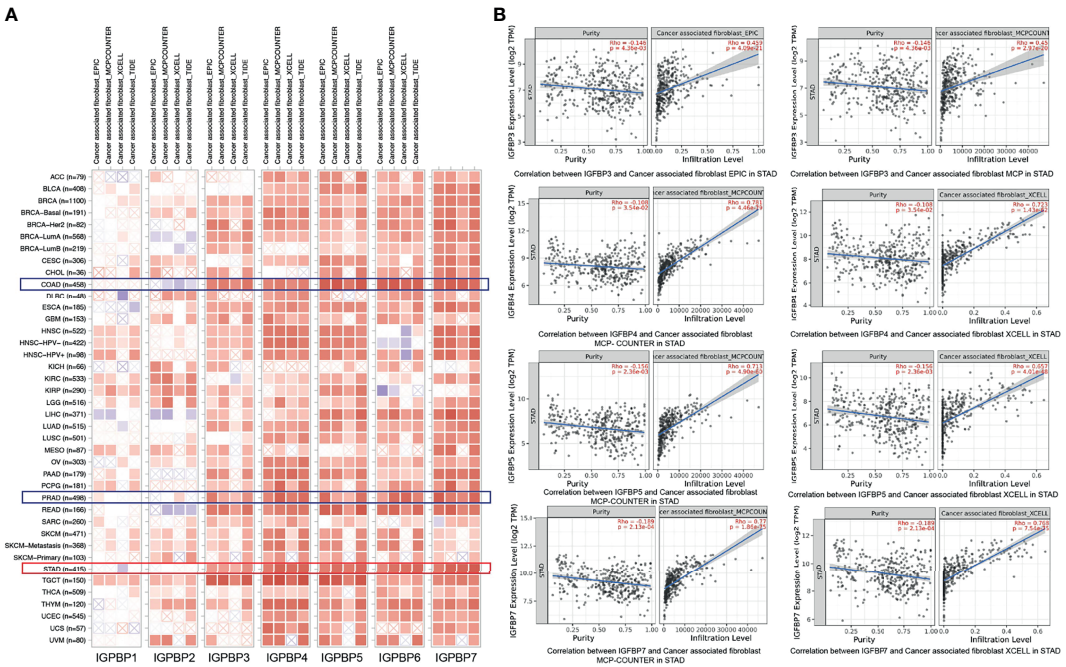

FIGURE 7 | Correlations between differentially expressed IGFBPs and immune cell infiltration (TIMER). **(A)** Correlations between abundance of immune cells and expression of IGFBP1–7 in 40 different cancer types. **(B)** Examples of IGFBP3/4/5/7-related tumor immune cell infiltration in STAD patients.

investigated the relationship between IGFBP7 and collagen-containing ECM formation in gastric cancer. A study compared premalignant and malignant stomach lesions and found that collagen-related genes COL11A1 and COL1A1 involved the focal adhesion pathway (31). In our study, COL1A1 was found to be co-expressed with IGFBP7 in STAD patients with |r| = 0.55355494 and p = 1.71475E-31. COL4A1 overexpression has previously been shown to be correlated with overall survival in gastric cancer (32); it was correlated with IGFBP7 with p = 6.99147E-33 in our study. Another overexpressed collagen gene, COL6A3 (33), was correlated with IGFBP7 with p = 1.48823E-40. COL12A1 was upregulated in gastric cancer and positively associated with tumor invasion and clinical stage and was also significantly correlated with IGFBP7 (|r| = 0.426016684, p = 5.75765E-18). Although collagen and IGFBP7 were all closely related to cancer progression, few studies have focused on the contribution of IGFBP7 in gastric cancer. However, research from other perspectives has demonstrated a relationship between IGFBP7 and collagen. Human endometrium cells formed a mesh-like structure in human uterus as well as on Matrigel *in vitro*. Knockdown of IGFBP7 could inhibit the formation of this mesh-like structure by interfering with protein kinase A and the MAPK signaling pathway (34). In a wound healing study, wound healing mediators including TGF-β1 and chemokines IL-6, IL-8, MCP-1, and RANTES in mesenchymal stem cells were identified, as well as IGFBP7, indicating that IGFBP7 contributes to the formation of the ECM (35).

In recent years, the TME has become a research hot spot. Accumulating evidence shows that carcinomas modify their environment by expressing growth factors, altering ECM gene expression to increase fibroblast proliferation, and changing immune cell infiltration, as well as by cross-talking with each other (36). During this process, growth factors and CAFs play important parts (37). IGFBP7 was identified as a fibroblast marker in CAFs and significantly stimulated fibroblast proliferation and migration (38). In gastric cancer, the abnormal expression of FGF9 in lymph node CAFs was correlated with poor prognosis (39). *H. pylori* infection was shown to elevate VCAM1 expression in CAFs, which indicated tumor invasion and progression (40). IGFBPs facilitate binding of IGF1 to ECM prote*in vitro*nectin to stimulate proliferation and migration of skin keratinocytes and fibroblasts (12). IGFs independently stimulate IGFBP3 and reduce IGFBP4 in human fibroblasts and epidermal cells (41). Knockout of Igfbp7 increased the proliferation of mouse hepatocytes and embryonic fibroblasts, whereas its overexpression inhibited hepatocytes in syngeneic immunocompetent mice, indicating its immune-mediated function (42). However, there has been a lack of studies focusing on IGFBPs in CAFs in gastric cancer, although these molecules have been shown to have an important role in fibroblasts. The mechanism by which IGFBPs participate in gastric cancer progression and metastasis *via* CAFs is worth further exploration. In addition, stromal cells are much more stable than cancer cells, which makes them attractive therapeutic targets for gastric cancer treatment (37, 43).

This study had some limitations. All data were downloaded from online databases and analyzed by computer algorithms; further studies including cell and animal experiments are

required to validate the results. However, the mechanism of IGFBPs' involvement in tumor progression could become a new research direction and provide promising treatment targets.

CONCLUSION

In conclusion, we systematically analyzed the transport protein IGFBP1–7 in gastric cancer. With collection of the gene expression data of cancer *vs.* normal patients, tumor *vs.* adjacent tumor tissue, and IGFBP mutations in all cancer types and immune infiltration data, we provided a relative complete analysis for IGFBP1–7 in gastric cancer. Our results screened out the meaningful IGFBPs in gastric cancer clinical prognosis, tumor staging, and immune infiltration and provided directions for the future research on gastric cancer. To better elucidate how these molecules get involved in specific mechanisms of gastric cancer occurrence, progression, and metastasis, further efforts might be focused on the research of IGFBPs in the tumor microenvironment and extracellular matrix.

DATA AVAILABILITY STATEMENT

The datasets presented in this study can be found in online repositories. The names of the repository/repositories and accession number(s) can be found in the article/**Supplementary Material**.

AUTHOR CONTRIBUTIONS

QL and YF designed the study and performed the bioinformatics analysis. QL and MXZ collected TCGA data and participated in the writing of the manuscript and did the main revision. All authors contributed to manuscript revision and read and approved the submitted version.

FUNDING

This project was supported by the National Natural Science Foundation of China (No. 8210061367) for MXZ, (No. 81871995) for YF, Henan Health Department (No. YXKC2020029) and the Excellent Youth Fund of Henan Natural Science Foundation (No. 212300410075) for YF, Henan Province Medical Science and Technology Co-construction Project for QL, JWJ and MXZ.

ACKNOWLEDGMENTS

We acknowledge assistance with the access of analytic instruments from Translational Medical Center at The First Affiliated Hospital of Zhengzhou University.

SUPPLEMENTARY MATERIAL

The Supplementary Material for this article can be found online at: https://www.frontiersin.org/articles/10.3389/fonc.2021.723131/full#supplementary-material

Supplementary Figure 1 | Validation of survival analysis of IGFBP1, IGFBP3, IGFBP7 in STAD patients from Chen's data [PMID: 12925757]. There was no significant difference in IGFBP1/3/7.

Supplementary Figure 2 | Validation of IGPBP1–7 expression and tumor stage in STAD patients from Cho's data and Chen's data. **(A)** The expression difference of IGFBP1-7 between T stage II and T stage III from Cho's data [PMID: 19798449]. **(B)** The expression difference of ten hub genes between T stage II and T stage III from Cho's data. **(C)** The expression difference of IGFBP1, IGFBP3, IGFBP7, TP53, PLG, IGF2, PAPPA, AHSG, FN1, AFP, CYR1 between T stage I, II, III, IV from Chen's data [PMID: 12925757].

Supplementary Figure 3 | Survival curves of IGFBP associated mutations in STAD patients.

Supplementary Figure 4 | Correlation of IGFBPs expression immune cell infiltration including B cells, CD4+ cells, CD8+ cells, macrophages, neutrophils and dendritic cells in gastric cancer.

Supplementary Table 1 | Cox multivariate regression analysis for IGFBP1/3/5/7 in STAD patients with TCGA database.

Supplementary Table 2 | IGFBP3/5/7 co-expressed genes and overlapping genes of three co-expression groups.

Supplementary Table 3 | GO and KEGG analysis of IGFBP3/5/7 co-expressed genes.

Supplementary Table 4 | Specific mutation sites of genetic alterations of IGFBP1–7 in STAD patients.

REFERENCES

1. Smyth EC, Nilsson M, Grabsch HI, van Grieken NC, Lordick F. Gastric Cancer. *Lancet* (2020) 396:635–48. doi: 10.1016/S0140-6736(20)31288-5
2. McGuire S. World Cancer Report 2014. Geneva, Switzerland: World Health Organization, International Agency for Research on Cancer, WHO Press, 2015. *Adv Nutr* (2016) 7:418–9. doi: 10.3945/an.116.012211
3. Bray F, Ferlay J, Soerjomataram I, Siegel RL, Torre LA, Jemal A. Global Cancer Statistics 2018: GLOBOCAN Estimates of Incidence and Mortality Worldwide for 36 Cancers in 185 Countries. *CA Cancer J Clin* (2018) 68:394–424. doi: 10.3322/caac.21492
4. Quezada-Marin JI, Lam AK, Ochiai A, Odze RD, Washington KM, Fukayama M, et al. Gastrointestinal Tissue-Based Molecular Biomarkers: A Practical Categorisation Based on the 2019 World Health Organization Classification of Epithelial Digestive Tumours. *Histopathology* (2020) 77:340–50. doi: 10.1111/his.14120
5. Oliveira C, Pinheiro H, Figueiredo J, Seruca R, Carneiro F. Familial Gastric Cancer: Genetic Susceptibility, Pathology, and Implications for Management. *Lancet Oncol* (2015) 16:e60–70. doi: 10.1016/S1470-2045(14)71016-2
6. van der Post RS, Vogelaar IP, Carneiro F, Guilford P, Huntsman D, Hoogerbrugge N, et al. Hereditary Diffuse Gastric Cancer: Updated Clinical Guidelines With an Emphasis on Germline CDH1 Mutation Carriers. *J Med Genet* (2015) 52:361–74. doi: 10.1136/jmedgenet-2015-103094
7. Donner I, Kiviluoto T, Ristimaki A, Aaltonen LA, Vahteristo P. Exome Sequencing Reveals Three Novel Candidate Predisposition Genes for Diffuse Gastric Cancer. *Fam Cancer* (2015) 14:241–6. doi: 10.1007/s10689-015-9778-z

8. Fewings E, Larionov A, Redman J, Goldgraben MA, Scarth J, Richardson S, et al. Germline Pathogenic Variants in PALB2 and Other Cancer-Predisposing Genes in Families With Hereditary Diffuse Gastric Cancer Without CDH1 Mutation: A Whole-Exome Sequencing Study. *Lancet Gastroenterol Hepatol* (2018) 3:489–98. doi: 10.1016/S2468-1253(18)30079-7
9. Li J, Woods SL, Healey S, Beesley J, Chen X, Lee JS, et al. Point Mutations in Exon 1B of APC Reveal Gastric Adenocarcinoma and Proximal Polyposis of the Stomach as a Familial Adenomatous Polyposis Variant. *Am J Hum Genet* (2016) 98:830–42. doi: 10.1016/j.ajhg.2016.03.001
10. Tsugane S, Sasazuki S. Diet and the Risk of Gastric Cancer: Review of Epidemiological Evidence. *Gastric Cancer* (2007) 10:75–83. doi: 10.1007/s10120-007-0420-0
11. Kashyap MK. Role of Insulin-Like Growth Factor-Binding Proteins in the Pathophysiology and Tumorigenesis of Gastroesophageal Cancers. *Tumour Biol* (2015) 36:8247–57. doi: 10.1007/s13277-015-3972-3
12. Murekatete B, Shokoohmand A, McGovern J, Mohanty L, Meinert C, Hollier BG, et al. Targeting Insulin-Like Growth Factor-I and Extracellular Matrix Interactions in Melanoma Progression. *Sci Rep* (2018) 8:583. doi: 10.1038/s41598-017-19073-4
13. Takeno A, Takemasa I, Doki Y, Yamasaki M, Miyata H, Takiguchi S, et al. Integrative Approach for Differentially Overexpressed Genes in Gastric Cancer by Combining Large-Scale Gene Expression Profiling and Network Analysis. *Br J Cancer* (2008) 99:1307–15. doi: 10.1038/sj.bjc.6604682
14. Rhodes DR, Yu J, Shanker K, Deshpande N, Varambally R, Ghosh D, et al. ONCOMINE: A Cancer Microarray Database and Integrated Data-Mining Platform. *Neoplasia* (2004) 6:1–6. doi: 10.1016/S1476-5586(04)80047-2
15. Tang Z, Li C, Kang B, Gao G, Li C, Zhang Z. GEPIA: A Web Server for Cancer and Normal Gene Expression Profiling and Interactive Analyses. *Nucleic Acids Res* (2017) 45:W98–102. doi: 10.1093/nar/gkx247
16. Gao J, Aksoy BA, Dogrusoz U, Dresdner G, Gross B, Sumer SO, et al. Integrative Analysis of Complex Cancer Genomics and Clinical Profiles Using the Cbioportal. *Sci Signal* (2013) 6:pl1. doi: 10.1126/scisignal.2004088
17. Szklarczyk D, Gable AL, Lyon D, Junge A, Wyder S, Huerta-Cepas J, et al. STRING V11: Protein-Protein Association Networks With Increased Coverage, Supporting Functional Discovery in Genome-Wide Experimental Datasets. *Nucleic Acids Res* (2019) 47:D607–13. doi: 10.1093/nar/gky1131
18. Li T, Fan J, Wang B, Traugh N, Chen Q, Liu JS, et al. TIMER: A Web Server for Comprehensive Analysis of Tumor-Infiltrating Immune Cells. *Cancer Res* (2017) 77:e108–10. doi: 10.1158/0008-5472.CAN-17-0307
19. Yu G, Wang LG, Han Y, He QY. Clusterprofiler: An R Package for Comparing Biological Themes Among Gene Clusters. *OMICS* (2012) 16:284–7. doi: 10.1089/omi.2011.0118
20. Chen X, Leung SY, Yuen ST, Chu KM, Ji J, Li R, et al. Variation in Gene Expression Patterns in Human Gastric Cancers. *Mol Biol Cell* (2003) 14:3208–15. doi: 10.1091/mbc.e02-12-0833
21. Wang Q, Wen YG, Li DP, Xia J, Zhou CZ, Yan DW, et al. Upregulated INHBA Expression is Associated With Poor Survival in Gastric Cancer. *Med Oncol* (2012) 29:77–83. doi: 10.1007/s12032-010-9766-y
22. Ooi CH, Ivanova T, Wu J, Lee M, Tan IB, Tao J, et al. Oncogenic Pathway Combinations Predict Clinical Prognosis in Gastric Cancer. *PloS Genet* (2009) 5:e1000676. doi: 10.1371/journal.pgen.1000676
23. Li T, Fu J, Zeng Z, Cohen D, Li J, Chen Q, et al. TIMER2.0 for Analysis of Tumor-Infiltrating Immune Cells. *Nucleic Acids Res* (2020) 48:W509–14. doi: 10.1093/nar/gkaa407
24. Bach LA. IGF-Binding Proteins. *J Mol Endocrinol* (2018) 61:T11–28. doi: 10.1530/JME-17-0254
25. Yi HK, Hwang PH, Yang DH, Kang CW, Lee DY. Expression of the Insulin-Like Growth Factors (IGFs) and the IGF-Binding Proteins (IGFBPs) in Human Gastric Cancer Cells. *Eur J Cancer* (2001) 37:2257–63. doi: 10.1016/S0959-8049(01)00269-6
26. Lee DY, Yang DH, Kang CW, Kim SJ, Joo CU, Cho SC, et al. Serum Insulin-Like Growth Factors (IGFs) and IGF Binding Protein (IGFBP)-3 in Patients With Gastric Cancer: IGFBP-3 Protease Activity Induced by Surgery. *J Korean Med Sci* (1997) 12:32–9. doi: 10.3346/jkms.1997.12.1.32
27. Xue M, Fang Y, Sun G, Zhuo W, Zhong J, Qian C, et al. IGFBP3, a Transcriptional Target of Homeobox D10, is Correlated With the Prognosis of Gastric Cancer. *PloS One* (2013) 8:e81423. doi: 10.1371/journal.pone.0081423
28. Tu M, Liu X, Han B, Ge Q, Li Z, Lu Z, et al. Vasohibin2 Promotes Proliferation in Human Breast Cancer Cells *via* Upregulation of Fibroblast Growth Factor2 and Growth/Differentiation Factor15 Expression. *Mol Med Rep* (2014) 10:663–9. doi: 10.3892/mmr.2014.2317
29. Sato Y, Inokuchi M, Takagi Y, Otsuki S, Fujimori Y, Yanaka Y, et al. Relationship Between Expression of IGFBP7 and Clinicopathological Variables in Gastric Cancer. *J Clin Pathol* (2015) 68:795–801. doi: 10.1136/jclinpath-2015-202987
30. Moreira AM, Pereira J, Melo S, Fernandes MS, Carneiro P, Seruca R, et al. The Extracellular Matrix: An Accomplice in Gastric Cancer Development and Progression. *Cells* (2020) 9:394. doi: 10.3390/cells9020394
31. Zhao Y, Zhou T, Li A, Yao H, He F, Wang L, et al. A Potential Role of Collagens Expression in Distinguishing Between Premalignant and Malignant Lesions in Stomach. *Anat Rec (Hoboken)* (2009) 292:692–700. doi: 10.1002/ar.20874
32. Zhang QN, Zhu HL, Xia MT, Liao J, Huang XT, Xiao JW, et al. A Panel of Collagen Genes Are Associated With Prognosis of Patients With Gastric Cancer and Regulated by microRNA-29c-3p: An Integrated Bioinformatics Analysis and Experimental Validation. *Cancer Manag Res* (2019) 11:4757–72. doi: 10.2147/CMAR.S198331
33. Xie X, Liu X, Zhang Q, Yu J. Overexpression of Collagen VI Alpha3 in Gastric Cancer. *Oncol Lett* (2014) 7:1537–43. doi: 10.3892/ol.2014.1910
34. Kutsukake M, Tamura K, Yoshie M, Tachikawa E. Knockdown of IGF-Binding Protein 7 Inhibits Transformation of the Endometrial Gland in an *In Vitro* Model. *Mol Reprod Dev* (2010) 77:265–72. doi: 10.1002/mrd.21143
35. Walter MN, Wright KT, Fuller HR, MacNeil S, Johnson WE. Mesenchymal Stem Cell-Conditioned Medium Accelerates Skin Wound Healing: An *In Vitro* Study of Fibroblast and Keratinocyte Scratch Assays. *Exp Cell Res* (2010) 316:1271–81. doi: 10.1016/j.yexcr.2010.02.026
36. Quail DF, Joyce JA. Microenvironmental Regulation of Tumor Progression and Metastasis. *Nat Med* (2013) 19:1423–37. doi: 10.1038/nm.3394
37. Bhowmick NA, Neilson EG, Moses HL. Stromal Fibroblasts in Cancer Initiation and Progression. *Nature* (2004) 432:332–7. doi: 10.1038/nature03096
38. Komiya E, Furuya M, Watanabe N, Miyagi Y, Higashi S, Miyazaki K. Elevated Expression of Angiomodulin (AGM/IGFBP-Rp1) in Tumor Stroma and its Roles in Fibroblast Activation. *Cancer Sci* (2012) 103:691–9. doi: 10.1111/j.1349-7006.2012.02203.x
39. Wang R, Sun Y, Yu W, Yan Y, Qiao M, Jiang R, et al. Downregulation of miRNA-214 in Cancer-Associated Fibroblasts Contributes to Migration and Invasion of Gastric Cancer Cells Through Targeting FGF9 and Inducing EMT. *J Exp Clin Cancer Res* (2019) 38:20. doi: 10.1186/s13046-018-0995-9
40. Shen J, Zhai J, You Q, Zhang G, He M, Yao X, et al. Cancer-Associated Fibroblasts-Derived VCAM1 Induced by H. Pylori Infection Facilitates Tumor Invasion in Gastric Cancer. *Oncogene* (2020) 39:2961–74. doi: 10.1038/s41388-020-1197-4
41. Neely EK, Rosenfeld RG. Insulin-Like Growth Factors (IGFs) Reduce IGF-Binding Protein-4 (IGFBP-4) Concentration and Stimulate IGFBP-3 Independently of IGF Receptors in Human Fibroblasts and Epidermal Cells. *Endocrinology* (1992) 130:985–93. doi: 10.1210/endo.130.2.1370799
42. Akiel M, Guo C, Li X, Rajasekaran D, Mendoza RG, Robertson CL, et al. IGFBP7 Deletion Promotes Hepatocellular Carcinoma. *Cancer Res* (2017) 77:4014–25. doi: 10.1158/0008-5472.CAN-16-2885
43. Kalluri R. The Biology and Function of Fibroblasts in Cancer. *Nat Rev Cancer* (2016) 16:582–98. doi: 10.1038/nrc.2016.73

Conflict of Interest: The authors declare that the research was conducted in the absence of any commercial or financial relationships that could be construed as a potential conflict of interest.

The reviewer FM declared a shared affiliation with the authors to the handling editor at the time of the review.

Publisher's Note: All claims expressed in this article are solely those of the authors and do not necessarily represent those of their affiliated organizations, or those of the publisher, the editors and the reviewers. Any product that may be evaluated in

this article, or claim that may be made by its manufacturer, is not guaranteed or endorsed by the publisher.

Copyright © 2021 Liu, Jiang, Zhang, Zhang and Fu. This is an open-access article distributed under the terms of the Creative Commons Attribution License (CC BY). The use, distribution or reproduction in other forums is permitted, provided the original author(s) and the copyright owner(s) are credited and that the original publication in this journal is cited, in accordance with accepted academic practice. No use, distribution or reproduction is permitted which does not comply with these terms.

frontiers in Oncology

ORIGINAL RESEARCH
published: 11 November 2021
doi: 10.3389/fonc.2021.756440

Long-Term Efficacy of Neoadjuvant Concurrent Chemoradiotherapy for Potentially Resectable Advanced Siewert Type II and III Adenocarcinomas of the Esophagogastric Junction

*Yuan Tian[1], Jun Wang[2], Xueying Qiao[2], Jun Zhang[2], Yong Li[1], Liqiao Fan[1], Zhidong Zhang[1], Xuefeng Zhao[1], Bibo Tan[1], Dong Wang[1], Peigang Yang[1] and Qun Zhao[1]**

[1] Third Surgery Department, The Fourth Hospital of Hebei Medical University, Shijiazhuang, China, [2] Department of Radiation, The Fourth Hospital of Hebei Medical University, Shijiazhuang, China

OPEN ACCESS

Edited by:
Pankaj Kumar Garg,
Shri Guru Ram Rai Institute of Medical and Health Sciences, India

Reviewed by:
Tushar Mishra,
All India Institute of Medical Sciences Bhubaneswar, India
Rahul Kumar,
All India Institute of Medical Sciences, Rishikesh, India

***Correspondence:**
Qun Zhao
zhaoqun@hebmu.edu.cn

Specialty section:
This article was submitted to Gastrointestinal Cancers: Gastric Esophageal Cancers, a section of the journal Frontiers in Oncology

Received: 10 August 2021
Accepted: 25 October 2021
Published: 11 November 2021

Citation:
Tian Y, Wang J, Qiao X, Zhang J, Li Y, Fan L, Zhang Z, Zhao X, Tan B, Wang D, Yang P and Zhao Q (2021) Long-Term Efficacy of Neoadjuvant Concurrent Chemoradiotherapy for Potentially Resectable Advanced Siewert Type II and III Adenocarcinomas of the Esophagogastric Junction. Front. Oncol. 11:756440. doi: 10.3389/fonc.2021.756440

Background: Reports have shown that neoadjuvant concurrent chemoradiotherapy (nCRT) increases the R0 resection rate for patients with Siewert type II or III adenocarcinoma of the gastroesophageal junction (AEG). However, the long-term efficacy of nCRT for AEG patients remains unclear. In this multicenter study, we investigated the long-term results of AEG patients treated with nCRT.

Methods: A total of 149 patients with potentially resectable advanced AEG (T3/4, Nany, M0) were randomly divided into two groups: the nCRT-treated group (treated group) (n = 76) and the surgery group (control group) (n = 73). The primary endpoint was disease-free survival (DFS), and the secondary outcome indexes included the R0 resection rate, HER-2 expression, tumor regression grade (TRG), objective response rate (ORR), disease control rate (DCR), overall survival (OS), and adverse events.

Results: In the treated group, the overall therapeutic efficacy rate was 40.8%, and the pathological complete response (pCR) rate was 16.9%. The rates of patients who underwent R0 resection in the treated and control groups were 97.0% and 87.7%, respectively ($p < 0.05$). The toxic effects were mainly graded 1–2 in the treated group. The median DFS times in the treated and control groups were 33 and 27 months, respectively ($p = 0.08$), whereas the median OS times were 39 and 30 months, respectively ($p = 0.01$). The median DFS times of patients with positive and negative HER-2 expression in the treated group were 13 and 43 months, respectively ($p = 0.01$), and the median OS times were 27 and 41 months, respectively ($p = 0.01$).

Conclusion: Surgery after nCRT improved the efficacy of treatment for AEG patients and thus provided a better prognosis.

Clinical Trial Registration: The trial is registered with ClinicalTrials.gov (number NCT01962246).

Keywords: neoadjuvant chemoradiotherapy, potentially resectable, advanced, Siewert II and III, adenocarcinoma of esophagogastric junction, treatment

INTRODUCTION

In recent years, the incidence of adenocarcinoma of the esophagogastric junction (AEG) has been increasing worldwide (1–3). Due to the uniqueness of AEG, treatment for this condition has attracted increasing attention from scholars. Most clinicians believe that appropriate perioperative treatments should be used for AEG, and regarding this topic, an increasing number of researchers are trying preoperative concurrent chemoradiotherapy for AEG (4, 5). Undoubtedly, the Chemoradiotherapy for Oesophageal Cancer Followed by Surgery Study (CROSS) trial (6) is a milestone of preoperative concurrent chemoradiotherapy on AEG, but it still has some deficiencies, such as the inclusion of patients not only with AEG but also with lower esophageal cancer and squamous cell carcinoma and the inclusion of patients mostly in the early and middle stages. Trials on the treatment of Siewert type II and III AEGs are lacking. Siewert types II and III are representative of AEG, and the effect of neoadjuvant chemoradiotherapy (nCRT) is currently a research hotspot. The "Preoperative Concurrent Chemoradiotherapy for Potentially Resectable Adenocarcinoma of Esophagogastric Junction (NCT01962246)" trial conducted by our center has reported mid-term results (7) and verified a satisfactory surgical R0 resection rate and tolerable safety. The present study further summarizes the long-term follow-up data for this trial. We conclude that accurate clinical staging, target area delineation and radiation dose selection, efficacy evaluation, chemotherapy regimen and operation time after drug withdrawal, and perioperative nutritional support influence the treatment of Siewert type II and III AEGs. Based on these data, we attempted to provide a more reasonable solution for the preoperative treatment of AEG.

MATERIALS AND METHODS

The patient inclusion criteria for this study consisted of the following: (1) gastroscopy- and computed tomography (CT)-confirmed Siewert type II or III AEG with a long diameter of the primary tumor ≤8 cm prior to surgery; (2) American Joint Committee on Cancer (AJCC) 2010 classification of progressive gastric cancer before surgery (T3/4, Nany, M0) with no evidence of metastatic lesions in the liver, lung, brain, bone or other organs; (3) no prior antitumor therapy; (4) no contradictions to chemotherapy or surgery; (5) a Karnofsky Performance Scale (KPS) score >60 and an Eastern Cooperative Oncology Group (ECOG) score 0–2; and (6) informed consent obtained before enrollment in the study. All enrolled patients were randomly assigned to the concurrent chemoradiotherapy group or surgery group by using an interactive web-response system (IWRS). Patients were enrolled by authorized individuals who requested randomization with an IWRS integrated into the electronic case report forms (eCRF). Assignment to trial groups was completed on the server of the independent data management providers (Bioknow, Beijing, China) *via* a validated assignment program, which underlies strict access control. The randomization system assigned each patient a unique identification number and sent the researchers a message containing the results of the assignment.

Regimen for Chemotherapy

The following XELOX regimen was applied for chemotherapy: capecitabine was administered at 1,000 mg/m^2 twice daily for 14 days (day 1 to day 14); oxaliplatin was intravenously administered at 130 mg/m^2 on day 1, and all subjects were treated for two cycles. Two cycles of chemotherapy were administered prior to surgery, and six cycles were administered after surgery. Eight cycles were administered after surgery in the control group.

Regimen for Radiotherapy

(1) Radiotherapy planning CT scans were obtained with the patient in the supine position in a body mold to ensure setup reproducibility.

(2) CT simulation with intravenous (IV) contrast was performed to help guide the gross tumor volume (GTV) target, particularly for lymph nodes.

(3) The treating physicians utilized the following information to delineate active disease: barium meal, esophagoscopy/gastroscopy, and magnetic resonance imaging (MRI) scanning.

(4) Radiation targets included AEG, any perigastric extension, and lymph nodes (perigastric, celiac, portal hepatis, splenic hilar) with adequate margins. The standard GTV-t to clinical target volume (CTV)-t expansions were 2 cm in the superior-inferior direction and 0.8 cm laterally and anteroposteriorly. CTV-nd included CTV-nd and involved the field; 0.8–1.0 cm was added so that CTV+ 0.8–1.0 cm = planning target volume (PTV).

(5) Intensity-modulated radiation therapy (IMRT) was used and delivered by a linear accelerator as multiple shaped beams of 6 MV X-rays in five daily fractions of 1.8 Gy per week for 5 weeks (total PTV dose: 45 Gy).

Determination of Therapeutic Efficacy

Therapeutic efficacy was determined according to the Response Evaluation Criteria in Solid Tumors (RECIST version 1.1).

The response was made up of four classifications: complete response (CR), partial response (PR), stable disease (SD), and progressive disease (PD). The total efficacy [response rate (RR)] was calculated as the sum of CR and PR, and the tumor control rate was calculated as the sum of CR, PR, and SD. Tumor-node-metastasis (TNM) staging was performed according to the criteria developed by the AJCC (7th edition).

A tumor volume reduction rate of 12.5% was measured by CT as an effective threshold for evaluating neoadjuvant therapy (8).

Tumor volume reduction rate after chemotherapy = (tumor volume before chemotherapy − tumor volume after chemotherapy)/tumor volume before chemotherapy × 100%.

Surgery

Laparoscopic exploration was performed 6–8 weeks after the end of concurrent chemoradiotherapy. Surgical treatment involved total gastrectomy and subsequent extended lymph node dissection (D2 resection). Reconstruction of the digestive tract involved Roux-en-Y esophagojejunostomy.

Nutritional Support

The treated group started with 500 ml of the enteral nutrition (EN) suspension (total protein fiber, TPF) (Nutrison Fiber®), an oral nutrition supplementation (ONS) (500 ml per bottle containing energy 500 kcal, protein 20 g, fat 19.45 g, and carbohydrate 61.5 g), 7 days before surgery in addition to a routine preoperative diet (35 kcal/kg/day) according to dietary guidance. Patients in this group also received TPF 48 h after surgery *via* a nasojejunal tube placed during surgery. The feeding speed increased from the initial 30 ml/h according to the tolerance of the patients' intestinal tracts. In general, nutritional support was shifted to the total EN 3–5 days after surgery, where patients were expected to start a semiliquid diet 4 days later. Consequently, the amounts of energy and protein were 25–30 kcal/kg/day and 1.0–1.5 g/kg/day, respectively, with the insufficient component supplemented with parenteral nutrition (9).

Pathological Analysis

The pathological examination included the detection of tumor size, depth of invasion, number of metastatic lymph nodes, surgical margins, HER-2 expression, and tumor regression grade (TRG).

TRG was defined as follows: grade 0 (complete remission), no cancer cells; grade 1 (partial remission), single cells or a small group of cancer cells; grade 2 (low efficacy), residual cancer outgrown by fibrosis; and grade 3 (poor efficacy), minimum or no treatment effect with extensive residual cancer cells.

Follow-Up

During the first year after treatment completion, patients received regular check-ups every 3 months. In the second year, regular follow-ups took place every 6 months and annually thereafter until 5 years after treatment. Additional interim visits were scheduled if complaints, such as renewed dysphagia and unexplained weight loss or pain, arose before the next scheduled visit. Diagnostic investigations were only undertaken as necessary measures during follow-up. No data on adverse events were collected beyond the initial report of this trial.

Statistical Analysis

Statistical analysis was performed with SPSS version 19.0 software and GraphPad Prism version 7. Quantitative data were compared using the chi-square test. Qualitative data were compared using the *t*-test and are expressed as the mean ± standard deviation. The Kaplan–Meier method was used to calculate overall survival (OS) and disease-free survival (DFS). A p-value < 0.05 was considered statistically significant.

RESULTS

Patient Data

A total of 149 patients with AEG who were admitted to the Fourth Hospital of Hebei Medical University between August 2012 and January 2016 were enrolled in this study. Patients were randomized at a 1:1 ratio using a stratified method (HER2 expression): a concurrent chemoradiotherapy group (n = 76) or a surgery group (n = 73). Patients in the concurrent chemoradiotherapy group (68 males and 8 females, median age 64 years, range: 43–75 years) received concurrent chemoradiotherapy and subsequent surgery. Patients in the surgery group (63 males and 10 females, median age 65 years, range: 42–74 years) were treated with surgery without chemoradiotherapy preoperatively. The general clinical characteristics of the patients in the two groups are shown in **Table 1**. After the end of concurrent chemoradiotherapy, 11 patients did not undergo surgery, 3 patients due to disease progression and 8 patients due to poor tolerance or economic reasons (**Figure 1**).

Clinical Efficacy

In the treated group, evaluation according to RECIST 1.1 revealed CR in 0 patients, PR in 31 patients, SD in 42 patients, and PD in 3 patients. The RR in the treated group was 40.8% (31/76), and the tumor control rate was 96.1% (73/76).

The tumor volume was 53.23 ± 21.57 cm^3 before nCRT, and the tumor volume was 45.26 ± 22.39 cm^3 after nCRT. Based on CT measurements of tumor volume reduction, the effective rate was 47.4%.

Safety Evaluation

The hematologic toxic effects included leukopenia, neutropenia, anemia, thrombocytopenia, and abnormal liver function. The incidence of neutropenia in the treated group was greater than that in the control group, and the difference was statistically significant (65.8% *vs.* 38.4%, p = 0.034). The nonhematologic toxic effects included nausea, vomiting, diarrhea, constipation, hand–foot syndrome, and fatigue. These toxic effects were mainly graded 1–2. The incidence of nausea in the treated group was greater than that in the control group, and the difference was statistically significant (67.1% *vs.* 47.9%, p = 0.032). The incidence of fatigue in the treated group was greater than that in the control group, and the difference was statistically significant (61.8% *vs.* 39.7%, p = 0.022).

TABLE 1 | General clinical characteristics of patients in the two groups.

	Concurrent chemoradiotherapy (*n* = 76)	Surgery alone (*n* = 73)	*p*
Age (years)	64 (43–75)	65 (42–74)	0.823
Sex [*n* (%)]			0.553
M	68 (89.5)	63 (86.3)	
F	8 (10.5)	10 (13.7)	
Vertical axis diameter of the tumor (cm)	4.6 (3–7)	4.4 (3–7)	0.757
HER2 expression			0.723
0	21 (27.6)	19 (26)	
1+	23 (30.3)	26 (35.6)	
2+ (FISH: negative)	23 (30.3)	17 (23.3)	
3+ (or FISH: positive)	9 (11.8)	11 (15.1)	
Clinical T stage [*n* (%)]			0.603
cT3	27 (35.5)	23 (31.5)	
cT4	49 (64.5)	50 (68.5)	
Clinical N stage [*n* (%)]			0.950
cN0	21 (27.6)	20 (27.4)	
cN1	20 (26.3)	18 (24.7)	
cN2	24 (31.6)	26 (35.6)	
cN3	11 (14.5)	9 (12.3)	
ECOG score [*n* (%)]			0.597
0	30 (39.5)	23 (31.5)	
1	36 (47.4)	39 (53.4)	
2	10 (13.1)	11 (15.1)	

The incidences of grade 3–4 hematologic and nonhematologic toxicities were low in the two groups, and the difference was not statistically significant ($p > 0.05$). Radiation gastritis/esophagitis and pneumonitis were unique to the treated group, with incidence rates of 43.4% and 13.2%, respectively, and these toxic effects were mainly grade 1–2 (**Table 2**).

Perioperative Complications

The incidence of wound infection, anastomotic bleeding, anastomotic leakage, abdominal infection, and intestinal obstruction was low, and the difference between groups was not statistically significant ($p > 0.05$). The incidence of pleural effusion in the treated group was higher than that in the control

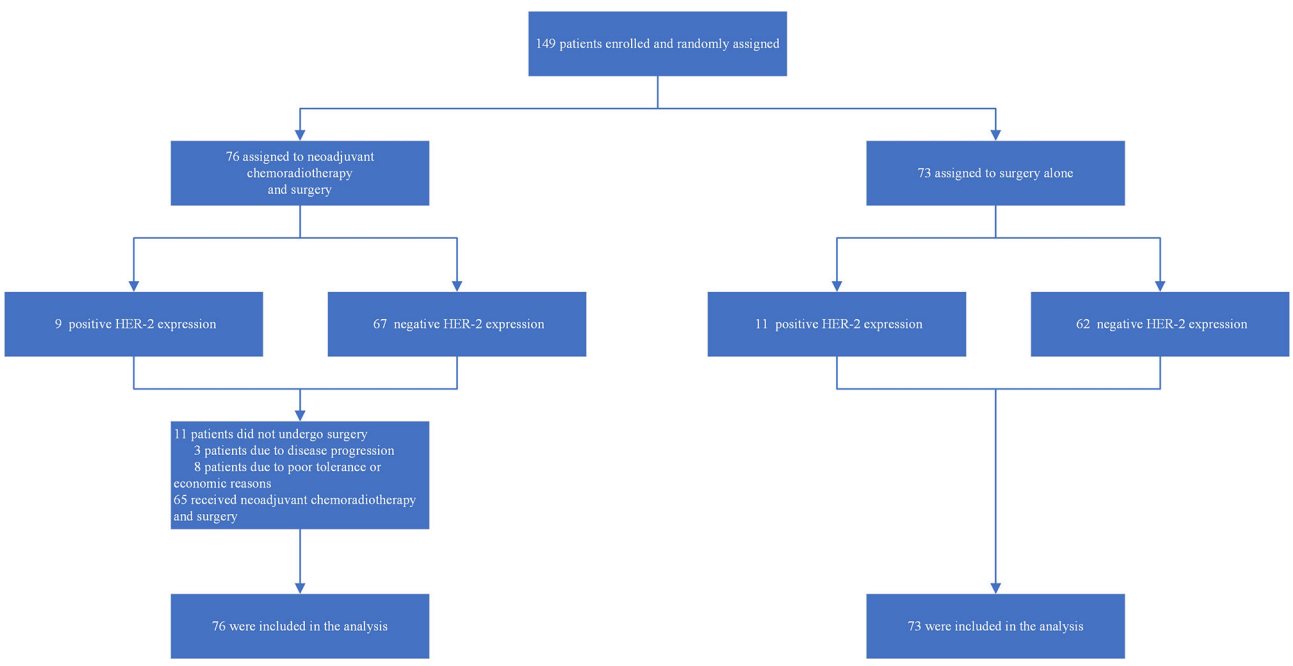

FIGURE 1 | Trial profile.

TABLE 2 | Toxic effects of concurrent chemoradiotherapy/adjuvant chemotherapy in the two groups [*n* (%)].

	Concurrent chemoradiotherapy: incidence rate (*n*, %)			Surgery alone: incidence rate (*n*, %)			*p*	
	Grade 1	Grade 2	Grade 3-4	Grade 1	Grade 2	Grade 3–4	Grade 1–4	Grade 3–4
Hematologic								
Anemia	30 (39.5)	7 (9.2)	3 (3.9)	23 (31.5)	7 (9.6)	1 (1.4)	0.340	0.611
Neutropenia	25 (32.8)	21 (27.6)	4 (5.3)	17 (23.3)	10 (13.7)	1 (1.4)	0.034	1.000
Thrombocytopenia	25 (32.8)	9 (11.8)	2 (2.6)	16 (21.9)	5 (6.8)	–	0.078	0.486
Liver dysfunction	17 (22.4)	2 (2.6)	–	13 (17.8)	3 (4.1)	–	0.374	–
Non-hematologic								
Nausea	28 (36.8)	19 (25)	4 (5.3)	18 (24.7)	13 (17.8)	4 (5.5)	0.032	1.000
Vomit	13 (17.1)	7 (9.2)	2 (2.6)	10 (13.7)	5 (6.8)	1 (1.4)	0.662	0.785
Diarrhea	9 (11.8)	6 (7.9)	4 (5.3)	9 (12.3)	4 (5.5)	3.6 (2/56)	0.374	0.673
Constipation	7 (9.2)	3 (3.9)	2 (2.6)	7 (9.6)	4 (5.5)	1 (1.4)	1.000	1.000
Hand–foot syndrome	14 (18.4)	6 (7.9)	4 (5.3)	13 (17.8)	8 (11)	1 (1.4)	1.000	0.354
Weak	40 (52.6)	7 (9.2)	–	26 (35.6)	3 (4.1)	–	0.022	–
Radiation gastritis/esophagitis	9 (11.8)	13 (17.1)	11 (14.5)	–	–	–	0.000	0.001
Radiation pneumonia	7 (9.2)	3 (3.9)	–	–	–	–	0.009	–

group, and this difference was statistically significant (23.08% *vs.* 6.85%, $p = 0.007$). The incidence of lung infection in the treated group was higher than that in the control group, and this difference was statistically significant (24.62% *vs.* 8.22%, $p = 0.009$). One patient in the treated group died during the perioperative period due to severe pulmonary infection (**Tables 3**, **4**). In the intention-to-treat analysis, the incidences of pleural effusion and pneumonia were also significantly different between the two groups (19.74% *vs.* 6.85%, $p = 0.021$; 21.05% *vs.* 8.22%, $p = 0.027$).

Surgery and Pathological Evaluation

The R0 resection rates in the treated group and the control group were 97% (63/65) and 87.7% (64/73), respectively, and this difference was statistically significant ($\chi^2 = 4.012$, $p = 0.045$). In the treated group, the pathological complete response (pCR) rate was 16.9% (11/65), and the total pathological response rate (grade 1 + grade 0) was 47.7% (31/65). The pathological lymph node metastasis rate and positivity rate were 43.1% and 3.9%, respectively, in the treated group and 76.7% and 20.9%, respectively, in the control group (**Table 5**). In the intention-to-treat analysis, there was no significant difference in the R0 resection rate between the two groups (86.3% *vs.* 87.7%, $p = 0.806$).

Follow-Up

The median follow-up time was 52 months (27–77) in all patients, and the median DFS times in the treated group and the control group were 33 and 27 months, respectively (HR 0.68, [95% confidence interval (CI) 0.44–1.05], $p = 0.08$) (**Figure 2**). In the treated group, 30 patients had recurrence and metastasis, 8 patients had local recurrence, 27 patients had distant metastasis, and 5 patients had two or more recurrent metastases; therefore, the rate of total recurrence/distant metastases was 39.5% (30/76). In the control group, 39 patients had recurrence and metastasis, 20 patients had local recurrence, 26 patients had distant metastasis, and 7 patients had two or more recurrent metastases. Therefore, the rate of total recurrence/distant metastases was 53.4% (39/73) (**Table 6**). The median OS times were 39 and 30 months (HR 0.59, [95% CI 0.38–0.91], $p = 0.01$) (**Figure 3**), and the survival rates were 43.94% and 36.92% ($\chi^2 = 0.83$, $p = 0.362$).

The median DFS times of patients with positive or negative HER-2 expression in the treated group were 13 and 43 months, respectively (HR 0.36, [95% CI 0.09–1.33], $p = 0.01$), and the median OS times were 27 and 41 months, respectively (HR 0.35, [95% CI 0.09–1.30], $p = 0.01$) (**Figures 4**, **5**). The median DFS times of patients with positive and negative HER-2 expression in the control group were 22 and 30 months, respectively (HR 0.57, [95% CI 0.24–1.39], $p = 0.17$), and the median OS times were 24 and 31.5 months, respectively (HR 0.59, [95% CI 0.23–1.49], $p = 0.16$) (**Figures 6**, **7**).

DISCUSSION

The efficacy of nCRT has been investigated in numerous clinical trials (10–12). Our results showed that patients with AEG who received nCRT benefitted more than those who received direct

TABLE 3 | Peri-operative complications in the two groups [*n* (%)].

	Concurrent chemoradiotherapy	Surgery alone	*p*
Incisional infection	4.62% (3/65)	2.74% (2/73)	0.556
Anastomotic bleeding	1.54% (1/65)	1.37% (1/73)	0.934
Anastomotic leakage	3.08% (2/65)	1.37% (1/73)	0.492
Abdominal infection	0% (0/65)	1.37% (1/73)	0.344
Intestinal obstruction	3.08% (2/65)	1.37% (1/73)	0.492
Pleural effusion	23.08% (15/65)	6.85% (5/73)	0.007
Pulmonary infection	24.62% (16/65)	8.22% (6/73)	0.009

TABLE 4 | Grade III and above perioperative complications in the two groups [*n* (%)].

Complication	Concurrent chemoradiotherapy	Surgery alone	*p*
Grade III	5 (Pleural effusion) 1 (Anastomotic bleeding)	2 (Pleural effusion)	
Grade IV	1 (Pulmonary infection)	1 (Pulmonary infection)	
Grade V	1 (Pulmonary infection)	0	
Incidence of grade III and above	12.31% (8/65)	4.1% (3/73)	0.065

surgery according to the R0 resection rate and long-term survival. On this basis, we intended to seek a more efficient and safe treatment plan to prolong patient survival. Therefore, we performed preoperative nCRT on AEG patients according to the anatomical features of the esophagogastric junction.

In terms of the clinical and pathological evaluations, the effective rate was 40.8% in the treated group according to RECIST 1.1. At present, there are certain limitations associated with the clinical TNM staging system and RECIST, and the cTNM staging system differs from the pTNM staging system. RECIST can be used to evaluate solid tumors. However, for hollow organs, fluctuations in the degree of organ filling and the method used to select the longest diameter are obvious. Therefore, our center selected the tumor volume reduction rate after neoadjuvant treatment as the curative effect. The effective rate of nCRT was 47.4%, and although it was not completely consistent with the number of patients who received a pathological evaluation, it was similar to pathological efficiency (48.4%). However, tumor volume measurements, laparoscopic exploration and pathological HER-2 results could be used to supplement the clinical stage to select a more suitable treatment and predict prognosis.

There are significant differences in the delineation, dose, and range of radiotherapy for AEG (13–15). Although the European Organisation for Research and Treatment of Cancer (EORTC) elaborated on the delineation of preoperative radiotherapy target areas of AEG, there are some differences between the EORTC and National Comprehensive Cancer Network (NCCN) guidelines in the recommended high-risk lymph node prophylaxis areas. According to the literature reports, the difficulty of radiotherapy technology for AEG is mainly attributed to determining the boundary of the GTV, the reasonable expansion of the CTV, and the irradiation range of high-risk lymph node areas. Until recently, there have been few related studies and a lack of data on pathological results. There is no accepted standard for preoperative radiotherapy target area delineation. In this study, the water filling method was used for CT simulation, and the CTV range was mainly determined by the thickening of lesions displayed on enhanced CT images and the results of upper gastrointestinal angiography and gastroscopy. Standard GTV-t to CTV-t expansions were 2 cm in the superior–inferior direction and 0.8 cm laterally and anteroposteriorly. CTV-nd included CTV-nd and involved fields; 0.8–1.0 cm was added so that CTV + 0.8–1.0 cm = PTV. This radiotherapy program can achieve a better pCR rate, reduce the lymph node metastasis rate, and increase the R0 resection rate. The incidence of acute radiation inflammatory reactions is low, and the tolerance is good.

The pCR rate in this study was 16.9% (11/65), which was close to that of the PreOperative therapy in Esophagogastric adenocarcinoma Trial (POET) (14.3%) (5). A European study on the time interval between nCRT and surgery for esophageal or junctional cancer (16) showed that 906 (29%) of 3,091 patients achieved a pCR. In this study, we confirmed that the pCR rate was mainly related to the pathological type, duration of surgery or nCRT, and cT stage. An interval of ≥10 weeks for adenocarcinoma and ≥13 weeks for squamous cell carcinoma between nCRT and esophagectomy was associated with a higher probability of achieving pCR. The 30-day/in-hospital mortality rate was higher in patients with extended intervals (10–12 and ≥15 weeks). In this study, for adenocarcinoma of the esophagogastric junction, the percentage of patients who achieved a pCR was 15%–17% with an interval of 6–9 weeks, which was similar to the results of our study. In terms of safety, the incidence of pleural effusion increased significantly, which might be related to tissue edema caused by radiotherapy. The incidence of pulmonary infection in the perioperative period also significantly increased, and one patient died due to pulmonary infection. Therefore, lung function and the respiratory system should be fully evaluated in patients who receive nCRT before surgery. Lung function should be examined early after surgery to anticipate early detection and early treatment. Precise nutritional

TABLE 5 | Surgery and pathological evaluation in the two groups [*n* (%)].

	Concurrent chemoradiotherapy (%/*N*)	Surgery alone (%/*N*)	*p*
R0 resection rate	97 (63/65)	87.7 (64/73)	0.045
pCR rate	16.9 (11/65)		
TRG			
0	16.9 (11/65)		
1	30.8 (20/65)		
2	46.2 (30/65)		
3	6.1 (4/65)		
Lymph node metastasis rate	43.1 (28/65)	76.7 (56/73)	0.000
Lymph node positive rate	3.9 (73/1853)	20.9 (424/2031)	<0.05

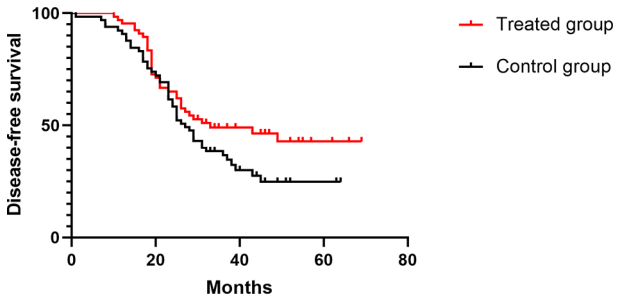

FIGURE 2 | Comparison of DFS in the two groups.

TABLE 6 | Metastatic site in the two groups.

	Concurrent chemoradiotherapy (*N*/%)	Surgery alone (*N*/%)
Local recurrence		
Anastomotic/residual stomach	6 (7.9)	14 (19.1)
Regional tissue	2 (2.6)	6 (8.2)
Distant metastasis		
Lung	1 (1.3)	0
Liver	3 (3.9)	6 (8.2)
Bone	1 (1.3)	1 (1.4)
Brain	0	1 (1.4)
Peritoneum	17 (22.4)	15 (10.5)
Distant lymph node	5 (6.6)	3 (4.1)
Total recurrence/distant metastases	30 (39.5)	39 (53.4)

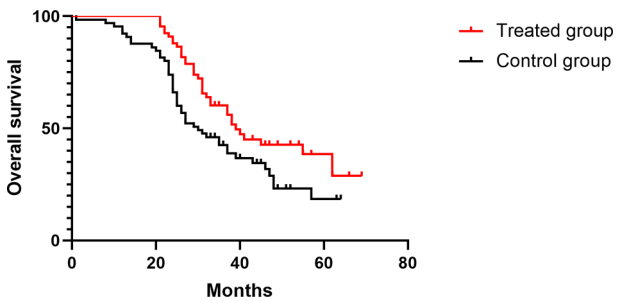

FIGURE 3 | Comparison of OS in the two groups.

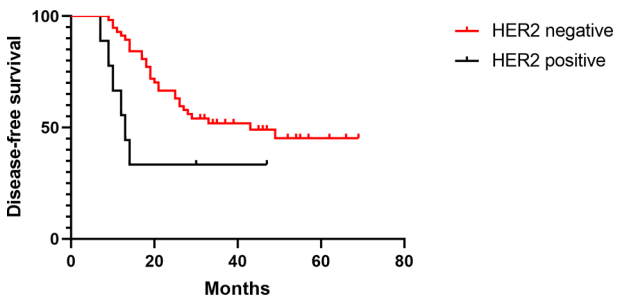

FIGURE 4 | DFS of HER-2-positive and -negative patients in the test group.

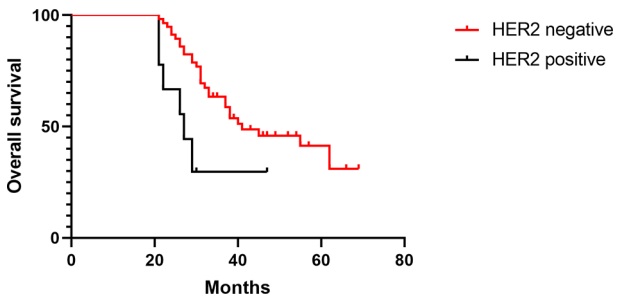

FIGURE 5 | OS of HER-2-positive and -negative patients in the test group.

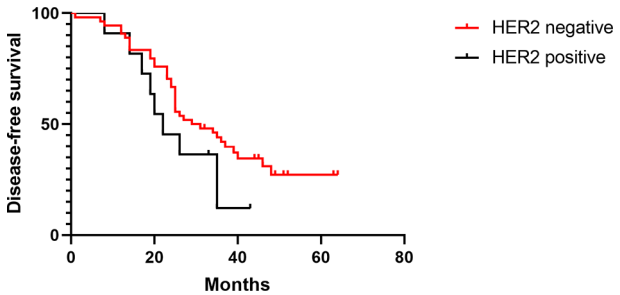

FIGURE 6 | DFS of HER-2-positive and -negative patients in the control group.

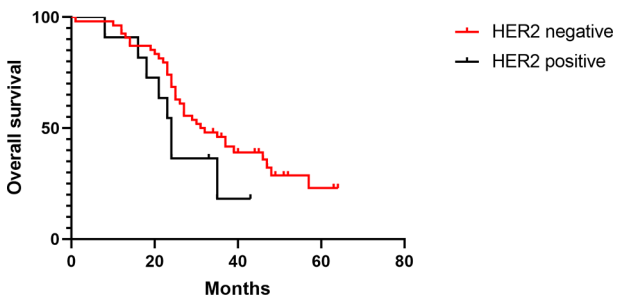

FIGURE 7 | OS of HER-2-positive and -negative patients in the control group.

therapy for the perioperative period can improve postoperative complications (9).

Based on the successful experience of preoperative concurrent chemoradiotherapy for esophageal adenocarcinoma (17), the clinical possibilities of nCRT for AEG (14, 18) are endless, and the CROSS and POET trials (5, 6, 19, 20) confirmed the effect of nCRT on reducing recurrence and metastasis and improving survival and quality of life in AEG patients. In this study, neoadjuvant concurrent chemoradiotherapy significantly improved OS, especially for patients with local recurrence. The addition of radiotherapy is one of the main reasons for the decrease in the local recurrence rate. The most frequent type of distant metastasis in the two groups was peritoneal metastasis, which may be related to the fact that the inclusion criteria did not require a cytological examination of abdominal exfoliation. In addition, it is worth noting that some studies (21, 22) showed that HER-2 overexpression suggested a poor prognosis. In the subgroup analysis of this study, we also found that DFS and OS were significantly different between patients in the treated group with HER-2 overexpression and those with negative HER-2 expression, providing insights into our subsequent in-depth study. We have provided different targeted therapies for

patients with different HER-2 expression statuses based on nCRT, and we expect reports on the effectiveness and safety of this trial in the future.

At present, nCRT is effective and relatively safe for patients with locally advanced Siewert type II and III AEGs and can be used as a standard treatment mode.

DATA AVAILABILITY STATEMENT

The raw data supporting the conclusions of this article will be made available by the authors, without undue reservation.

ETHICS STATEMENT

The studies involving human participants were reviewed and approved by the Ethical Review Committee of Hebei Medical University. The patients/participants provided their written informed consent to participate in this study.

AUTHOR CONTRIBUTIONS

QZ designed the research. QZ, YT, JW, JZ, and XQ collected clinical data and performed the research. YL, LF, PY, ZZ, XZ, DW and BT performed the experiments. BT and YT analyzed the data. QZ and YT wrote the paper. All authors contributed to the article and approved the submitted version.

FUNDING

This study was supported by the University Research Project of Hebei Province (grant no. ZD2019139) and the Medical Research Project of Hebei Province (grant no. 20201137).

REFERENCES

1. Liu K, Yang K, Zhang W, Chen X, Chen X, Zhang B, et al. Changes of Esophagogastric Junctional Adenocarcinoma and Gastroesophageal Reflux Disease Among Surgical Patients During 1988-2012: A Single-Institution, High-Volume Experience in China. *Ann Surg* (2016) 263:88–95. doi: 10.1097/SLA.0000000000001148
2. Buas MF, Vaughan TL. Epidemiology and Risk Factors for Gastroesophageal Junction Tumors: Understanding the Rising Incidence of This Disease. *Semin Radiat Oncol* (2013) 23:3–9. doi: 10.1016/j.semradonc.2012.09.008
3. Colquhoun A, Arnold M, Ferlay J, Goodman KJ, Forman D, Soerjomataram I. Global Patterns of Cardia and non-Cardia Gastric Cancer Incidence in 2012. *Gut* (2015) 64:1881–8. doi: 10.1136/gutjnl-2014-308915
4. Brücher BLDM, Kitajima M, Siewert JR. Undervalued Criteria in the Evaluation of Multimodal Trials for Upper GI Cancers. *Cancer Investig* (2014) 32:497–506. doi: 10.3109/07357907.2014.958497
5. Stahl M, Walz MK, Riera-Knorrenschild J, Stuschke M, Sandermann A, Bitzer M, et al. Preoperative Chemotherapy *Versus* Chemoradiotherapy in Locally Advanced Adenocarcinomas of the Oesophagogastric Junction (POET): Long-Term Results of a Controlled Randomised Trial. *Eur J Cancer* (2017) 81:183–90. doi: 10.1016/j.ejca.2017.04.027
6. Shapiro J, van Lanschot JJB, Hulshof MCCM, van Hagen P, van Berge Henegouwen MI, Wijnhoven BPL, et al. Neoadjuvant Chemoradiotherapy Plus Surgery *Versus* Surgery Alone for Oesophageal or Junctional Cancer (CROSS): Long-Term Results of a Randomised Controlled Trial. *Lancet Oncol* (2015) 16:1090–8. doi: 10.1016/S1470-2045(15)00040-6
7. Zhao Q, Li Y, Wang J, Zhang J, Qiao X, Tan B, et al. Concurrent Neoadjuvant Chemoradiotherapy for Siewert II and III Adenocarcinoma at Gastroesophageal Junction. *Am J Med Sci* (2015) 349:472–6. doi: 10.1097/MAJ.0000000000000476
8. Zhao Q, Lian C, Huo Z, Li M, Liu Y, Fan L, et al. The Efficacy and Safety of Neoadjuvant Chemotherapy on Patients With Advanced Gastric Cancer: A Multicenter Randomized Clinical Trial. *Cancer Med* (2020) 9:5731–45. doi: 10.1002/cam4.3224
9. Zhao Q, Li Y, Yu B, Yang P, Fan L, Tan B, et al. Effect of Postoperative Precision Nutrition Therapy on Postoperative Recovery for Advanced Gastric Cancer After Neoadjuvant Chemotherapy. *Chin J Oncol* (2018) 40:127–32. doi: 10.3760/cma.j.issn.0253-3766.2018.02.009
10. Ronellenfitsch U, Schwarzbach M, Hofheinz R, Kienle P, Kieser M, Slanger TE, et al. Preoperative Chemo(Radio)Therapy *Versus* Primary Surgery for Gastroesophageal Adenocarcinoma: Systematic Review With Meta-Analysis Combining Individual Patient and Aggregate Data. *Eur J Cancer* (2013) 49:3149–58. doi: 10.1016/j.ejca.2013.05.029
11. Ychou M, Boige V, Pignon JP, Conroy T, Bouché O, Lebreton G, et al. Perioperative Chemotherapy Compared With Surgery Alone for Resectable Gastroesophageal Adenocarcinoma: An FNCLCC and FFCD Multicenter Phase III Trial. *J Clin Oncol* (2011) 29:1715–21. doi: 10.1200/JCO.2010.33.0597
12. Davies AR, Gossage JA, Zylstra J, Mattsson F, Lagergren J, Maisey N, et al. Tumor Stage After Neoadjuvant Chemotherapy Determines Survival After Surgery for Adenocarcinoma of the Esophagus and Esophagogastric Junction. *J Clin Oncol* (2014) 32:2983–90. doi: 10.1200/JCO.2014.55.9070
13. van Hagen P, Hulshof MCCM, van Lanschot JJB, Steyerberg EW, Henegouwen MIB, Wijnhoven BPL, et al. Preoperative Chemoradiotherapy for Esophageal or Junctional Cancer. *N Engl J Med* (2012) 366:2074–84. doi: 10.1056/NEJMoa1112088
14. Burmeister BH, Smithers BM, Gebski V, Fitzgerald L, Simes RJ, Devitt P, et al. Surgery Alone *Versus* Chemoradiotherapy Followed by Surgery for Resectable Cancer of the Oesophagus: A Randomised Controlled Phase III Trial. *Lancet Oncol* (2005) 6:659–68. doi: 10.1016/S1470-2045(05)70288-6
15. Tepper J, Krasna MJ, Niedzwiecki D, Hollis D, Reed CE, Goldberg R, et al. Phase III Trial of Trimodality Therapy With Cisplatin, Fluorouracil, Radiotherapy, and Surgery Compared With Surgery Alone for Esophageal Cancer: CALGB 9781. *J Clin Oncol* (2008) 26:1086–92. doi: 10.1200/JCO.2007.12.9593
16. van der Werf LR, Dikken JL, van der Willik EM, van Berge HMI, Nieuwenhuijzen GAP, Wijnhoven BPL, et al. Time Interval Between Neoadjuvant Chemoradiotherapy and Surgery for Oesophageal or Junctional Cancer: A Nationwide Study. *Eur J Cancer* (2018) 91:76–85. doi: 10.1016/j.ejca.2017.12.009
17. Sjoquist KM, Burmeister BH, Smithers BM, Zalcberg JR, Simes RJ, Barbour A, et al. Survival After Neoadjuvant Chemotherapy or Chemoradiotherapy for Resectable Oesophageal Carcinoma: An Updated Meta-Analysis. *Lancet Oncol* (2011) 12:681–92. doi: 10.1016/S1470-2045(11)70142-5
18. Nakamura K, Kato K, Igaki H, Ito Y, Mizusawa J, Ando N, et al. Three-Arm Phase III Trial Comparing Cisplatin Plus 5-FU (CF) *Versus* Docetaxel, Cisplatin Plus 5-FU (DCF) *Versus* Radiotherapy With CF (CF-RT) as Preoperative Therapy for Locally Advanced Esophageal Cancer (JCOG1109, Next Study). *Jpn J Clin Oncol* (2013) 43:752–5. doi: 10.1093/jjco/hyt061
19. Oppedijk V, van der Gaast A, van Lanschot JJB, van Hagen P, van Os R, van Rij CM, et al. Patterns of Recurrence After Surgery Alone *Versus* Preoperative Chemoradiotherapy and Surgery in the CROSS Trials. *J Clin Oncol* (2014) 32:385–91. doi: 10.1200/JCO.2013.51.2186
20. Noordman BJ, Verdam MGE, Lagarde SM, Hulshof M, van Hagen P, van Berge Henegouwen MI, et al. Effect of Neoadjuvant Chemoradiotherapy on Health-Related Quality of Life in Esophageal or Junctional Cancer: Results

From the Randomized CROSS Trial. *J Clin Oncol* (2018) 36:268–75. doi: 10.1200/JCO.2017.73.7718
21. Liang JW, Zhang JJ, Zhang T, Zheng ZC. Clinicopathological and Prognostic Significance of HER2 Overexpression in Gastric Cancer: A Meta-Analysis of the Literature. *Tumor Biol* (2014) 35:4849–58. doi: 10.1007/s13277-014-1636-3
22. Gravalos C, Jimeno A. HER2 in Gastric Cancer: A New Prognostic Factor and a Novel Therapeutic Target. *Ann Oncol* (2008) 19:1523–9. doi: 10.1093/annonc/mdn169

Conflict of Interest: The authors declare that the research was conducted in the absence of any commercial or financial relationships that could be construed as a potential conflict of interest.

Publisher's Note: All claims expressed in this article are solely those of the authors and do not necessarily represent those of their affiliated organizations, or those of the publisher, the editors and the reviewers. Any product that may be evaluated in this article, or claim that may be made by its manufacturer, is not guaranteed or endorsed by the publisher.

Copyright © 2021 Tian, Wang, Qiao, Zhang, Li, Fan, Zhang, Zhao, Tan, Wang, Yang and Zhao. This is an open-access article distributed under the terms of the Creative Commons Attribution License (CC BY). The use, distribution or reproduction in other forums is permitted, provided the original author(s) and the copyright owner(s) are credited and that the original publication in this journal is cited, in accordance with accepted academic practice. No use, distribution or reproduction is permitted which does not comply with these terms.

frontiers in Oncology

ORIGINAL RESEARCH
published: 02 December 2021
doi: 10.3389/fonc.2021.792340

The Impact of Tumor Mutation Burden on the Effect of Frontline Trastuzumab Plus Chemotherapy in Human Epidermal Growth Factor Receptor 2-Positive Advanced Gastric Cancers

*Hye Ryeon Kim[1,2], Soomin Ahn[3], Hyunji Jo[1], Hongsik Kim[1], Joohyun Hong[1], Jeeyun Lee[1], Ho-Yeong Lim[1], Won Ki Kang[1] and Seung Tae Kim[1]**

[1] Division of Hematology-Oncology, Department of Medicine, Samsung Medical Center, Sungkyunkwan University School of Medicine, Seoul, South Korea, [2] Department of Internal Medicine, Dong-A University College of Medicine, Busan, South Korea, [3] Department of Pathology, Samsung Medical Center, Sungkyunkwan University School of Medicine, Seoul, South Korea

OPEN ACCESS

Edited by:
Pankaj Kumar Garg,
Shri Guru Ram Rai Institute of Medical and Health Sciences, India

Reviewed by:
Jonathan Abraham Demma,
Hadassah-Hebrew University Medical Center, Israel
Mert Tanal,
Tekirdag Ismail Fehmi Cumalioglu State Hospital, Turkey

***Correspondence:**
Seung Tae Kim
seungtae1.kim@samsung.com

Specialty section:
This article was submitted to Gastrointestinal Cancers: Gastric Esophageal Cancers, a section of the journal Frontiers in Oncology

Received: 10 October 2021
Accepted: 16 November 2021
Published: 02 December 2021

Citation:
Kim HR, Ahn S, Jo H, Kim H, Hong J, Lee J, Lim H-Y, Kang WK and Kim ST (2021) The Impact of Tumor Mutation Burden on the Effect of Frontline Trastuzumab Plus Chemotherapy in Human Epidermal Growth Factor Receptor 2-Positive Advanced Gastric Cancers. Front. Oncol. 11:792340. doi: 10.3389/fonc.2021.792340

Background: Trastuzumab is a HER2-trargeted humanized monoclonal antibody that has been studied as a first-line treatment for patients with HER2-positive advanced gastric cancer (AGC). The effect of anti-HER2 therapy according to tumor mutational burden (TMB) in HER2-positive AGC remains unclear.

Methods: We performed next-generation sequencing (NGS), including TMB analysis, in 31 HER2-positive AGC patients with trastuzumab plus chemotherapy as first-line therapy for recurrent (n=8) or metastatic (n=23) tumors. The TruSight Oncology 500 Assay from Illumina (San Diego, CA, USA) was used to evaluate TMB.

Results: Among 31 patients, 30 had tumors with immunohistochemistry (IHC) 3+, and one was IHC 2+ and silver *in situ* hybridization (SISH) positive. The median age was 57.0 years old (range, 35-76), and the majority had tumors with low TMB (87.1%, n=27/31). Only four (12.9%) had tumors with high TMB. Of these four, three achieved complete response (CR) or partial response (PR) to treatment, and the remaining patient was not evaluable for tumor response. Objective response rate (ORR) to trastuzumab plus chemotherapy showed a favorable trend in patients with high TMB (75.0%, n=3/4) compared to patients with low TMB (59.3%, n=16/27) (P=0.546). The median progression-free survival (PFS) was not reached in the TMB-high group but was 8.0 months (95% CI, 7.6-8.5) in the TMB-low group (P=0.019)

Conclusion: The status of TMB could be a novel biomarker in predicting the efficacy of trastuzumab plus chemotherapy in HER2-positive AGCs.

Keywords: trastuzumab, advanced gastric cancer, HER2, tumor mutational burden, biomarker

INTRODUCTION

Gastric cancer (GC) is the sixth most common cancer and has the third-highest global mortality rate in 2018 (1). In Korea, the stomach is the second most common site of cancer following lung, and GC is the fifth-highest mortality following lung, liver, colorectal, and pancreas cancers (2). The frequency of human epidermal growth factor receptor 2 (HER2) overexpression in gastric and gastroesophageal cancer varies by study, with a mean of 18%, and is a significant predictor of poor survival (3–5). Trastuzumab, a monoclonal antibody targeting HER2, inhibits HER2-mediated signaling and prevents cleavage of the extracellular domain of HER2 (6). In a previous study, trastuzumab plus chemotherapy showed a survival advantage in HER2-positive advanced gastric and gastroesophageal junction cancers (7). However, the overall response rate (ORR) was 47%, with a complete response (CR) of only 5%, and the available data demonstrated that high dose trastuzumab is not associated with efficacy improvement (7, 8). Thus, there is a need for potential biomarkers regarding the efficacy of anti-HER2 therapy.

Tumor mutational burden (TMB) means the total number of mutations per coding area of a tumor genome. There is a strong relationship between the TMB and the activity of immune checkpoint inhibitors (ICIs) across multiple cancers (9–12). Hu et al. suggested that TMB could predict the response to trastuzumab rather than HER2 status in patients with advanced gastric cancer (AGC) (13). However, few studies have been performed on the relationship between TMB and the efficacy of anti-HER2 therapies.

Herein, we analyzed the efficacy of anti-HER2 therapy in patients with HER2-positive AGC according to TMB.

PATIENTS AND METHODS

Patients

Patients, who had started trastuzumab plus chemotherapy for metastatic or recurrent HER2-positive AGC at Samsung Medical Center between April 2019 and June 2021, were retrospectively analyzed. The patients had to be tested prospectively for molecular aberrations, including TMB, with the TruSight Oncology 500 assay. Either metastatic or recurrent tumor tissues had to show HER2 positivity as IHC 3+ or IHC 2+ with ERBB2 gene amplification by silver *in situ* hybridization (SISH). The prior palliative systemic chemotherapy was not allowed, but adjuvant chemotherapy was allowed. The patients received trastuzumab, capecitabine, and cisplatin (HXP) as first-line therapy. This study was reviewed and approved by our institutional review board (IRB number: 2021-08-123-001).

TruSight Oncology 500 Assay

Forty (40) ng of DNA was quantified with the Qubit dsDNA HS Assay (Thermo Fisher Scientific, Inc., Waltham, MA, USA) on the Qubit 2.0 Fluorometer (Thermo Fisher Scientific) and then sheared using a Coraris E220 focused-ultrasonicator (Woburn, MA, USA) and the 8 microTUBE–50 Strip AFA Fiber V2 following the manufacturer's instructions. The treatment time was optimized for formalin fixed paraffin embedded (FFPE) material. The treatment settings were as follows: peak incident power (W): 75; duty factor: 15%; cycles per burst: 500; treatment time (s): 360; temperature (°C): 7; water level: 6. For DNA library preparation and enrichment, the TruSight Oncology 500 Kit (Illumina) was used following the manufacturer's instructions. Post-enriched libraries were quantified, pooled, and sequenced on a NextSeq 500 (Illumina Inc., San Diego, CA, USA). The quality of the NextSeq 500 (Illumina) sequencing runs was assessed with the Illumina Sequencing Analysis Viewer (Illumina). Sequencing data were analyzed with the TruSight Oncology 500 Local App Version 1.3.0.39 (Illumina), a comprehensive tumor profiling assay designed to identify known and emerging tumor biomarkers, including small variants, splice variants, and fusions. Importantly, the TruSight Oncology 500 measures tumor mutational burden (TMB) and microsatellite instability (MSI), features that are potential key biomarkers for immunotherapy. TMB was reported as mutations per megabase (Mb) sequenced, and high TMB was defined as more than 10 mutations per Mb (≥10Mut/Mb).

Statistics

Descriptive statistics are reported as proportion and median. Data are presented as numbers (%) for categorical variables. Response categories were assessed according to Response Evaluation Criteria In Solid Tumors (RECIST) 1.1. Duration of response (DOR) was analyzed in patients who achieved CR or PR and was calculated from the date of CR or PR to the date of progression or death. Progression-free survival (PFS) was defined as the time from the date of anti-HER2 treatment to the date of disease progression. Overall survival (OS) was defined as the time from the date of anti-HER2 treatment and the date of death from any cause. Analyses of PFS and OS were censored at the date of the last follow-up visit. The survival analysis was performed using the Kaplan-Meier method and comparative analysis was performed by the log-rank test and Fisher's exact test. A P value of less than 0.05 was considered statistically significant. Statistical analysis was performed using IBM SPSS statistics version 27 (Armonk, NY, USA).

RESULTS

Patients

A total of 31 patients were analyzed retrospectively in this study. The median age was 57.0 years old (range, 35-76), and the number of males and females was 25 (80.6%) and six (19.4%), respectively. Twenty-four (77.4%) patients were diagnosed with tubular adenocarcinoma, and the degree of differentiation was moderate in 16 (51.6%). All patients had microsatellite stable disease (MSS). Thirty (96.8%) patients had IHC 3+ tumors, and only one patient had IHC 2+ and SISH positive tumors. Twenty-seven (87.1%) and four (12.9%) patients had low and high TMB

disease, respectively. Only one patient in the TMB-low group was positive for Epstein-Barr virus (EBV)-status. Fifteen (48.4%) had programmed death-ligand 1 (PD-L1) positivity, one in the TMB-high group and 14 in the TMB-low group. Twenty-three (74.2%) patients were first diagnosed with metastatic AGC, and eight (25.8%) patients had the recurrent disease at the time of HXP administration. Among eight with the recurred disease, one patient had locally recurred TMB-high tumor, and seven with systemic recurrence (**Table 1**).

Efficacy and Survival

The median follow-up duration was 10.8 months (range, 1.7-20.9). The median number of treatment cycles was 7.0 (range, 2-20), and the median treatment duration was 4.7 months (range, 0.7-14.2). In all patients, the ORR was 61.3%, including 1 (3.2%) CR and 18 (58.1%) of PR. Four (12.9%) patients had stable disease (SD), and the other four (12.9%) had progressive disease (PD). In four patients with TMB-high tumor, three achieved CR or PR, and the other patient was not evaluated for tumor response due to short treatment duration. In 27 patients with TMB-low tumor, ORR was 59.3%, and four (14.8%) patients had PD. The ORR to trastuzumab plus chemotherapy showed a favorable trend in patients with TMB-high tumor (75%, n=3/4) compared to patients with TMB-low tumor (59.3%, n=16/27) (*P*=0.546) (**Table 2**).

In patients with CR or PR, the median DOR was 6.1 months (IQR, 3.4-9.6). The median PFS was 9.0 months (95% confidence interval [CI], 7.1-10.8), and the median OS was not achieved in all populations (**Figures 1A, B**). According to TMB status, the median PFS was not reached in patients with TMB-high tumor but was 8.0 months (95% CI, 7.6-8.5) in patients with TMB-low tumor (*P*=0.019) (hazard ratio [HR], 0.122; 95% CI, 0.016-0.954). The median OS was not achieved in patients with TMB-high tumor but was 14.5 months (95% CI, 10.3-18.7) in patients with TMB-low tumor (*P*=0.117) (HR, 0.034; 95% CI, 0-31.208) (**Figures 2A, B**). The computed tomography (CT)

TABLE 1 | Patient characteristics.

Variables	Total (n = 31)	TMB-high (n = 4)	TMB-low (n = 27)
Median age (y) (range)	57.0 (35-76)	60.5 (42-76)	57.0 (35-76)
Sex			
Male	25 (80.6%)	4 (100%)	21 (77.8%)
Female	6 (19.4%)	–	6 (22.2%)
Disease classification			
Metastatic	23 (74.2%)	2 (50.0%)	21 (77.8%)
Recurrent	8 (25.8%)	2 (50.0%)†	6 (22.2%)
Histologic subtype			
Adenocarcinoma	5 (16.1%)	2 (50.0%)	3 (11.1%)
Tubular adenocarcinoma	24 (77.4%)	2 (50.0%)	22 (81.5%)
Signet ring cell carcinoma	2 (6.5%)	–	2 (7.4%)
Differentiation			
Well	2 (6.5%)	–	2 (7.4%)
Moderately	16 (51.6%)	2 (50.0%)	14 (51.9%)
Poorly	12 (38.7%)	2 (50.0%)	10 (37.0%)
Unknown	1 (3.2%)*	–	1 (3.7%)
HER2			
IHC 3+	30 (96.8%)	4 (100%)	26 (96.3%)
IHC 2+, SISH positive	1 (3.2%)	–	1 (3.7%)
EBV			
Positive	1 (3.2%)	–	1 (3.7%)
Negative	19 (61.3%)	2 (50.0%)	17 (63.0%)
Unknown	11 (35.5%)	2 (50.0%)	9 (33.3%)
PD-L1			
<1%	4 (12.9%)	–	4 (14.8%)
1-20%	15 (48.4%)	1 (25.0%)	14 (51.9%)
Unknown	12 (38.7%)	3 (75.0%)	9 (33.3%)
MSI			
MSI-high	–	–	–
MSS	31 (100%)	4 (100%)	27 (100%)
Previous treatment			
Gastrectomy	10 (32.3%)	2 (50.0%)	8 (29.6%)‡
Adjuvant chemotherapy	4 (12.9%)	–	4 (14.8%)₮
Palliative radiotherapy	2 (6.5%)	4 (100%)	2 (7.4%)

**The patient was diagnosed with gastric cancer by biopsy of a metastatic brain lesion from the stomach. †In the TMB-high group, two patients had recurrent disease, including one with local recurrence. ‡Among eight patients who had received gastrectomy, six patients received radical gastrectomy at the first diagnosis, one received radical gastrectomy after second lines of chemotherapy, and one received palliative surgery. ₮Adjuvant chemotherapy was completed more than 6 months before the treatment started.*

TMB, tumor mutational burden; HER2, human epidermal growth factor receptor 2; IHC, immunohistochemistry; SISH, silver in-situ hybridization; EBV, Epstein-Barr virus; PD-L1, programmed death-ligand 1; MSI, microsatellite instability; MSS, microsatellite stable.

TABLE 2 | Best response – No. of patients (%).

	Total patients (n = 31)	TMB-high (n = 4)	TMB-low (n = 27)
CR	1 (3.2%)	1 (25.0%)	–
PR	18 (58.1%)	2 (50.0%)	16 (59.3%)
ORR	19 (61.3%)	3 (75.0%)	16 (59.3%)
SD	4 (12.9%)	–	4 (14.8%)
PD	4 (12.9%)	–	4 (14.8%)
NE*	4 (12.9%)	1 (25.0%)	3 (11.1%)

*Four patients were prior to the first response assessment due to short treatment duration. TMB, tumor mutational burden; CR, complete response; PR, partial response; ORR, objective response rate; SD, stable disease; PD, progressive disease; NE, non-evaluable.

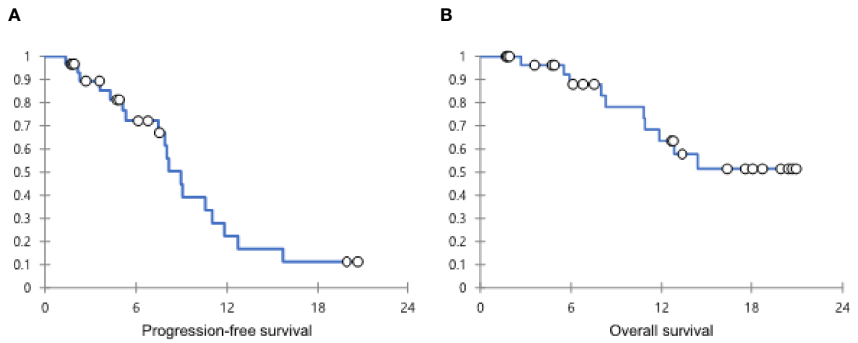

FIGURE 1 | The Kaplan-Meier curves showing PFS **(A)** and OS **(B)** in all patients. PFS, progression-free survival; OS, overall survival.

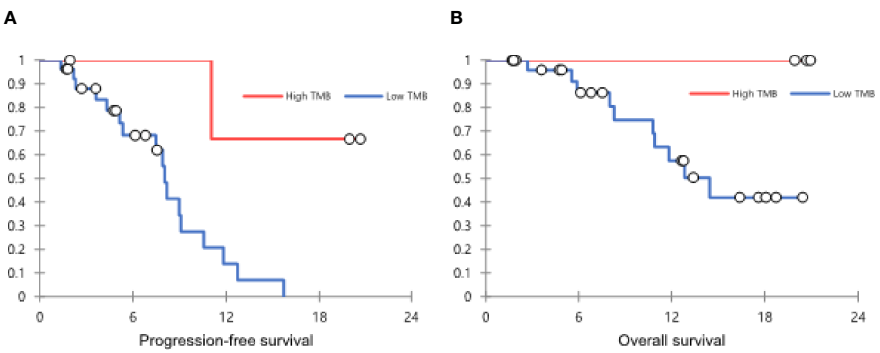

FIGURE 2 | The Kaplan-Meier curves showing PFS **(A)** and OS **(B)** according to the TMB status. PFS, progression-free survival; OS, overall survival; TMB, tumor mutational burden.

imaging before and after HXP treatment of the patient who achieved CR was presented in **Figure 3**.

DISCUSSION

In this study, we retrospectively analyzed the relationship between TMB and response to trastuzumab plus chemotherapy as first-line treatment in metastatic or recurrent GC. There was no difference in ORR and OS between the TMB-high and low groups (P=0.546 and 0.117, respectively). However, PFS in the TMB-high group was longer than that in the TMB-low group with statistically a significant difference (P=0.019).

GC has a molecular heterogeneity and has been classified to diffuse and intestinal subtypes according to Lauren classification (14). In 2014, The Cancer Genome Atlas (TCGA) genomically separated GC into four subtypes, such as EBV-associated tumors, microsatellite instability-high (MSI-H) tumors, genomically stable tumors, and tumors with chromosomal instability (15). In the era of immunotherapy, pembrolizumab, PD-L1 monoclonal antibody, showed a durable response rate in patients with advanced gastric or gastroesophageal cancer that had progressed after second-line

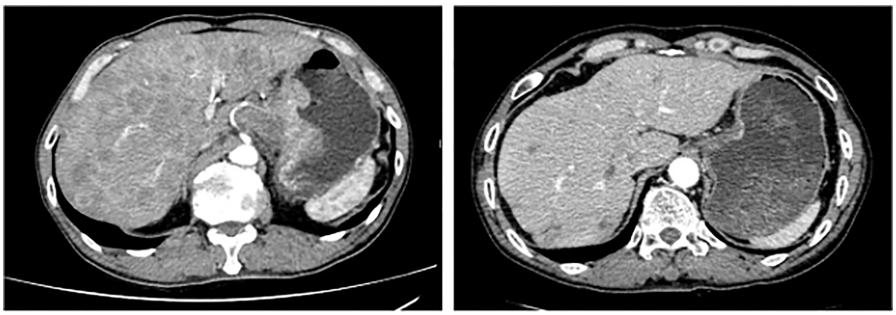

FIGURE 3 | Computed tomography (CT) scan in a HER2-positive patient with high TMB achieving CR to HXP. The image on the left was at the time of treatment start, and the image on the right was at the time of CR achievement. HER2, human epidermal growth factor receptor 2; TMB, tumor mutational burden; CR, complete response; HXP, trastuzumab, capecitabine, and cisplatin.

treatment (16). Especially in a previous study, EBV-positive and/or MSI-high GC had a higher response to an anti-PD-L1 therapy compared to other subtypes according to TCGA (17). A recent study showed that nivolumab, the first programmed cell death-1 (PD-1) inhibitor, plus chemotherapy had superior OS and PFS with tolerable toxicity profile in patients with previously untreated advanced gastric, gastroesophageal junction, or esophageal adenocarcinoma (18). However, this study included only non-HER2-positive disease, and the importance of trastuzumab is still emphasized in patients with HER2-positive gastric or gastroesophageal cancers.

Despite the development of targeted therapy, surgical resection is still the only curable treatment option for GC, and preoperative chemo-radiotherapy or perioperative chemotherapy is needed to improve the outcomes for locally advanced disease (clinically T2-4 or positive lymph node). In the metastatic setting, the first-line chemotherapy consists of platinum-based doublet or triplet with or without trastuzumab according to HER2 status (19). In ToGA (Trastuzumab for Gastric Cancer) trial, trastuzumab plus chemotherapy showed significantly longer OS (18.6 *versus* 17.1 months; HR 0.74 [95% CI 0.60-0.91]; *P*=0.0046) than the chemotherapy alone for HER2-positive gastric or gastroesophageal junction cancer. And the ORR and CR were 47% (n=139/294) and 5% (n=16/294), respectively (7).

Considering that high TMB correlates with a greater probability of displaying tumor neoantigens on human leukocyte antigen molecules on the surface of tumor cells (20, 21), it was suggested that the tumors with higher TMB are more likely to respond to immunotherapy. In several previous studies, the benefit of high TMB on response to immunotherapy has been reported in many cancer types, including melanoma, non-small cell lung cancer, and bladder cancer (9–12). Furthermore, a previous case report suggested that TMB could be a predictor of the response to trastuzumab in patients with HER2-positive AGCs (13). However, as far as we know, there was no clinical trial to evaluate the value of TMB as a predictor of efficacy of trastuzumab in HER2-positive AGCs.

This study had several limitations. First, it had a small sample size, was retrospective in nature, and utilized a heterogeneous population, all conductive to bias. Second, in patients with low TMB, anti-HER2 therapy showed a useful effect. This suggests that the status of TMB is not a sufficient biomarker for selecting patients likely to benefit from HXP. Third, only Asian patients with HER2-positive AGC were analyzed in the study, limiting the generalizability because of differences in molecular profiles and clinical features between Western and Eastern patients with HER2-positive AGC.

Therefore, study findings for high TMB as a novel biomarker should be interpreted with caution and make it difficult to draw definite conclusions. Further prospective clinical trials are required to determine whether high TMB could be a novel predictive or prognostic biomarker for anti-HER2 therapy in HER2-positive AGC. Furthermore, as next-generation sequencing (NGS) is available in the biomarker-based trials are in practice (22).

DATA AVAILABILITY STATEMENT

The original contributions presented in the study are included in the article. Further inquiries can be directed to the corresponding author.

ETHICS STATEMENT

The studies involving human participants were reviewed and approved by the Institutional Review Board Samsung Medical Center. Written informed consent for participation was not required for this study in accordance with the national legislation and the institutional requirements.

AUTHOR CONTRIBUTIONS

The conception and design of the study: HRK and STK. Acquisition of data: HRK, SA, HJ, HK, JH, JL,

H-YL, WK, and STK. Analysis and interpretation of data: HRK and STK. Drafting the article or revising it critically for important intellectual content: HRK and STK. Final approval of the version to be submitted: HRK and STK. All authors contributed to the article and approved the submitted version.

ACKNOWLEDGMENT

This research was supported by a grant of the Korea Health Technology R&D Project through the Korea Health Industry Development Institute (KHIDI), funded by the Ministry of Health & Welfare, Republic of Korea (grant number: HR20C0025).

REFERENCES

1. Bray F, Ferlay J, Soerjomataram I, Siegel RL, Torre LA, Jemal A. Global Cancer Statistics 2018: GLOBOCAN Estimates of Incidence and Mortality Worldwide for 36 Cancers in 185 Countries. *CA Cancer J Clin* (2018) 68 (6):394–424. doi: 10.3322/caac.21492
2. Jung KW, Won YJ, Hong S, Kong HJ, Lee ES. Prediction of Cancer Incidence and Mortality in Korea, 2020. *Cancer Res Treat* (2020) 52(2):351–8. doi: 10.4143/crt.2020.203
3. Park DI, Yun JW, Park JH, Oh SJ, Kim HJ, Cho YK, et al. HER-2/Neu Amplification Is an Independent Prognostic Factor in Gastric Cancer. *Dig Dis Sci* (2006) 51(8):1371–9. doi: 10.1007/s10620-005-9057-1
4. Begnami MD, Fukuda E, Fregnani JH, Nonogaki S, Montagnini AL, da Costa WL, et al. Prognostic Implications of Altered Human Epidermal Growth Factor Receptors (HERs) in Gastric Carcinomas: HER2 and HER3 Are Predictors of Poor Outcome. *J Clin Oncol* (2011) 29(22):3030–6. doi: 10.1200/JCO.2010.33.6313
5. Abrahao-Machado LF, Scapulatempo-Neto C. HER2 Testing in Gastric Cancer: An Update. *World J Gastroenterol* (2016) 22(19):4619–25. doi: 10.3748/wjg.v22.i19.4619
6. Hudis CA. Trastuzumab–mechanism of Action and Use in Clinical Practice. *N Engl J Med* (2007) 357(1):39–51. doi: 10.1056/NEJMra043186
7. Bang YJ, Van Cutsem E, Feyereislova A, Chung HC, Shen L, Sawaki A, et al. Trastuzumab in Combination With Chemotherapy Versus Chemotherapy Alone for Treatment of HER2-Positive Advanced Gastric or Gastro-Oesophageal Junction Cancer (ToGA): A Phase 3, Open-Label, Randomised Controlled Trial. *Lancet* (2010) 376(9742):687–97. doi: 10.1016/S0140-6736(10)61121-X
8. Shah MA, Xu RH, Bang YJ, Hoff PM, Liu T, Herráez-Baranda LA, et al. HELOISE: Phase IIIb Randomized Multicenter Study Comparing Standard-Of-Care and Higher-Dose Trastuzumab Regimens Combined With Chemotherapy as First-Line Therapy in Patients With Human Epidermal Growth Factor Receptor 2-Positive Metastatic Gastric or Gastroesophageal Junction Adenocarcinoma. *J Clin Oncol* (2017) 35(22):2558–67. doi: 10.1200/JCO.2016.71.6852
9. Yarchoan M, Hopkins A, Jaffee EM. Tumor Mutational Burden and Response Rate to PD-1 Inhibition. *N Engl J Med* (2017) 377(25):2500–1. doi: 10.1056/NEJMc1713444
10. Rizvi NA, Hellmann MD, Snyder A, Kvistborg P, Makarov V, Havel JJ, et al. Cancer Immunology. Mutational Landscape Determines Sensitivity to PD-1 Blockade in Non-Small Cell Lung Cancer. *Science* (2015) 348(6230):124–8. doi: 10.1126/science.aaa1348
11. Snyder A, Wolchok JD, Chan TA. Genetic Basis for Clinical Response to CTLA-4 Blockade. *N Engl J Med* (2015) 372(8):783. doi: 10.1056/NEJMc1415938
12. Rosenberg JE, Hoffman-Censits J, Powles T, van der Heijden MS, Balar AV, Necchi A, et al. Atezolizumab in Patients With Locally Advanced and Metastatic Urothelial Carcinoma Who Have Progressed Following Treatment With Platinum-Based Chemotherapy: A Single-Arm, Multicentre, Phase 2 Trial. *Lancet* (2016) 387(10031):1909–20. doi: 10.1016/S0140-6736(16)00561-4
13. Hu CT, Zhou YC, Zu LD, Fu GH, Li Q. High Tumor Mutation Burden in a Patient With Metastatic Gastric Cancer Sensitive to Trastuzumab: A Case Report. *Ann Palliat Med* (2021) 10(5):5846–52. doi: 10.21037/apm-20-132
14. Lauren P. The Two Histological Main Types of Gastric Carcinoma: Diffuse and So-Called Intestinal-Type Carcinoma. An Attempt at a Histo-Clinical Classification. *Acta Pathol Microbiol Scand* (1965) 64:31–49. doi: 10.1111/apm.1965.64.1.31
15. Network CGAR. Comprehensive Molecular Characterization of Gastric Adenocarcinoma. *Nature* (2014) 513(7517):202–9. doi: 10.1038/nature13480
16. Fuchs CS, Doi T, Jang RW, Muro K, Satoh T, Machado M, et al. Safety and Efficacy of Pembrolizumab Monotherapy in Patients With Previously Treated Advanced Gastric and Gastroesophageal Junction Cancer: Phase 2 Clinical KEYNOTE-059 Trial. *JAMA Oncol* (2018) 4(5):e180013. doi: 10.1001/jamaoncol.2018.0013
17. Kim ST, Cristescu R, Bass AJ, Kim KM, Odegaard JI, Kim K, et al. Comprehensive Molecular Characterization of Clinical Responses to PD-1 Inhibition in Metastatic Gastric Cancer. *Nat Med* (2018) 24(9):1449–58. doi: 10.1038/s41591-018-0101-z
18. Janjigian YY, Shitara K, Moehler M, Garrido M, Salman P, Shen L, et al. First-Line Nivolumab Plus Chemotherapy Versus Chemotherapy Alone for Advanced Gastric, Gastro-Oesophageal Junction, and Oesophageal Adenocarcinoma (CheckMate 649): A Randomised, Open-Label, Phase 3 Trial. *Lancet* (2021) 398(10294):27–40. doi: 10.1016/S0140-6736(21)00797-2
19. Network NCC. *Gastric Cancer (Version 5.2021)* (November 5, 2021). Available at: https://www.nccn.org/professionals/physician_gls/pdf/gastric.pdf.
20. Peggs KS, Segal NH, Allison JP. Targeting Immunosupportive Cancer Therapies: Accentuate the Positive, Eliminate the Negative. *Cancer Cell* (2007) 12(3):192–9. doi: 10.1016/j.ccr.2007.08.023
21. Segal NH, Parsons DW, Peggs KS, Velculescu V, Kinzler KW, Vogelstein B, et al. Epitope Landscape in Breast and Colorectal Cancer. *Cancer Res* (2008) 68(3):889–92. doi: 10.1158/0008-5472.CAN-07-3095
22. Nakamura Y, Shitara K, Lee J. The Right Treatment of the Right Patient: Integrating Genetic Profiling Into Clinical Decision Making in Advanced Gastric Cancer in Asia. *Am Soc Clin Oncol Educ Book* (2021) 41):e166–e73. doi: 10.1200/edbk_321247

Conflict of Interest: The authors declare that the research was conducted in the absence of any commercial or financial relationships that could be construed as a potential conflict of interest.

Publisher's Note: All claims expressed in this article are solely those of the authors and do not necessarily represent those of their affiliated organizations, or those of the publisher, the editors and the reviewers. Any product that may be evaluated in this article, or claim that may be made by its manufacturer, is not guaranteed or endorsed by the publisher.

Copyright © 2021 Kim, Ahn, Jo, Kim, Hong, Lee, Lim, Kang and Kim. This is an open-access article distributed under the terms of the Creative Commons Attribution License (CC BY). The use, distribution or reproduction in other forums is permitted, provided the original author(s) and the copyright owner(s) are credited and that the original publication in this journal is cited, in accordance with accepted academic practice. No use, distribution or reproduction is permitted which does not comply with these terms.

frontiers in Oncology

ORIGINAL RESEARCH
published: 09 December 2021
doi: 10.3389/fonc.2021.752504

A Recombinant Human Adenovirus Type 5 (H101) Combined With Chemotherapy for Advanced Gastric Carcinoma: A Retrospective Cohort Study

*Ran Zhang, Yanxin Cui, Xin Guan and Xiangjun Jiang**

Department of Gastroenterology, Qingdao Municipal Hospital, Qingdao University, Qingdao, China

OPEN ACCESS

Edited by:
Pankaj Kumar Garg, Shri Guru Ram Rai Institute of Medical and Health Sciences, India

Reviewed by:
Deepa Joseph, All India Institute of Medical Sciences, Rishikesh, India
Jyoti Sharma, All India Institute of Medical Sciences, India
Amit Sehrawat, All India Institute of Medical Sciences, Rishikesh, India

***Correspondence:**
Xiangjun Jiang
drjxj@163.com

Specialty section:
This article was submitted to Gastrointestinal Cancers: Gastric & Esophageal Cancers, a section of the journal Frontiers in Oncology

Received: *03 August 2021*
Accepted: *16 November 2021*
Published: *09 December 2021*

Citation:
Zhang R, Cui Y, Guan X and Jiang X (2021) A Recombinant Human Adenovirus Type 5 (H101) Combined With Chemotherapy for Advanced Gastric Carcinoma: A Retrospective Cohort Study. Front. Oncol. 11:752504. doi: 10.3389/fonc.2021.752504

Background: This retrospective cohort study aimed to evaluate the clinical outcomes of H101 combined with chemotherapy for advanced gastric carcinoma (GC) patients.

Methods: The advanced GC patients, who were treated with H101 and/or chemotherapy, were enrolled and divided into three groups according to treatment method. The clinical characteristics of patients, clinical short-term and long-term outcomes, followed up, and complication were analyzed.

Results: A total of 95 patients (30 patients in group A were treated with H101, 33 in group B patients were treated with chemotherapy, 32 patients in group C were treated with H101 combined with chemotherapy) were retrospectively reviewed. The disease control rate (DCR) and overall response rate (ORR) were significantly greater in group C (81.3% and 50.0%) than in groups A (63.3% and 30.0%) and B (66.7% and 33.3%, all $p < 0.05$). The 1- and 2-year survival rates and progression-free survival were significantly greater in group C than in groups A and B (all $p < 0.05$). There was no significant difference in complication among the three groups. At dose levels of 0.5×10^{12} vp/day, 1.0×10^{12} vp/day, and 1.5×10^{12} vp/day, complications were not increased as increased of dose.

Conclusions: H101 combined with chemotherapy may be a potential therapeutic option for patients with advanced GC, and prospective studies with proper assessment of toxicity will be needed in the future.

Keywords: H101, chemotherapy, advanced gastric carcinoma, survival, response rate

INTRODUCTION

Gastric carcinoma (GC) is one of the most common malignant tumors in digestive system. In 2020, the new and death cases of GC were approximately 1,090,000 and 770,000 worldwide, respectively, making it the fifth most commonly diagnosed cancer and the third most common cause of cancer death globally (1). Especially, in China, according to the Global Cancer Observatory in 2020, 478,000 new cases and 374,000 death cases of GC occurred in China, accounting for 44% and 49% of

the new and death cases worldwide, respectively (2). The high mortality is mainly due to most patients were with late-stage GC when diagnosed (3). Presently, the treatment modalities of GC mainly include surgery, chemotherapy, targeted therapy, and immunotherapy. The early-stage GC patients is recommended surgery as a curative approach, while advanced GC are mainly treated by chemotherapy, but with a poor prognosis, only 25%–30% 5-year overall survival (OS) rate (4, 5). Many available targeted drugs are limited in efficacy and cannot maintain for long time, due to complicated tumor microenvironment and instability of genes (6). Immunotherapy needs to select appropriate population according to specific molecular markers, and some GC patients have good clinical efficacy after initial immunotherapy, but may have recurrence (7). These drawbacks indicate the new strategies for advanced GC are urgently needed. Oncolytic virus (OV) therapy is poised to be one of the leading treatments for cancer, due to OVs offering the attractive therapeutic combination of tumor-specific cell lysis together with immune stimulation to kill cancer cells, leaving nonmalignant cells unharmed (8).

Wild-type *p53* gene, as a tumor suppressor gene, plays an important role in maintaining normal growth and inhibiting malignant cell proliferation. For *p53* gene mutations, they could lead to an inability to promote apoptosis and the loss of inhibiting cell proliferation and cause excessive cell proliferation and blocks DNA damage repair (9, 10). Previous studies have reported that *p53* mutations were more frequently found in GC, especially in advanced GC or metastasis GC (11). The *p*53 mutations have been related to the worse prognosis and resistance to standard chemotherapeutics in most tumor types, including GC (11, 12). The *p*53 has been extensively studied because of its inhibitory effect on tumorigenesis and is considered to be a promising treatment for cancers. ONYX-015, for example, as an E1B gene-defective adenovirus, was the first genetically engineered OV to be tested in humans; it would selectively replicate and destroy tumor cells carrying mutations of the *p*53 tumor suppressor gene. Furthermore, some studies revealed that ONYX-015 is remarkably safe and effective in the treatment of head and neck cancer, and that the antitumor efficacy could be further enhanced in combination with chemotherapy (13–15). H101, as a recombinant human adenovirus type 5, is similar to ONYX-015, in which the gene encoding the 55-kDa E1B protein responsible for *p53* binding and inactivation has been deleted (16). The H101 also contains a deletion of a 78.3–85.8-μm gene segment in the E3 region. The E3 region is related to the inhibition of host immunity, which enhances the virus replication and spread in the tumor (**Figure 1**) (17, 18).

In 1998, H101, produced by Shanghai Sunway Biotech, initiated the preclinical study in China (19). In a phase II clinical trial, H101 resulted in tumor regression of advanced cancers, with the activated host immune system and enhanced cell-medicated immune responses, indicating that H101 may exert its antitumor effect by promoting the host immune system, especially the cell-medicated immune responses (20). Previously, Wang et al. (18) have summarized the detailed clinical trial of H101 in head and neck cancer, providing information of other ongoing OV clinical trials in China. Recently, some clinical studies have shown that H101 is effective in the treatment of esophageal carcinoma, nasopharyngeal carcinoma, lung carcinoma, and liver carcinoma (21–25). Moreover, the combination of H101 with chemotherapy is superior to chemotherapy alone in delaying the progression of advanced malignant tumors and extending the survival of patients with advanced carcinoma (26, 27). Although the anticancer activity of H101 has been confirmed by extensive intratumoral injection, its clinical efficacy on GC is rarely reported. Therefore, this retrospective cohort study was conducted to evaluate the clinical outcomes of H101 intratumor injection with or without combination with chemotherapy in the treatment of advanced GC.

MATERIALS AND METHODS

Patients

The study was approved by the Ethics Committee of Qingdao Municipal Hospital and performed in accordance with the Helsinki Declaration of 1975 (No. 2018-030). Written informed consent was obtained from all patients before treatment. The patients who were diagnosed with advanced GC and treated with H101 and/or chemotherapy as an initial therapy at the Department of Gastroenterology of Qingdao University Affiliated Qingdao Municipal Hospital (Qingdao, China) between September 5, 2012 and May 20, 2018 were retrospectively studied. Diagnosis of GC was based on the histological assessment of biopsies taken during upper endoscopy. Inclusion criteria include the following: (1) patients were 18–80 years old; (2) patients were unable or refused to undergo surgical treatment; and (3) the lesion site was suitable for intratumoral injection. The patients were excluded if they met the following criteria: (1) had uncontrolled active infection, coagulation abnormality, or serious liver, kidney, or other organ dysfunction; (2) failed to complete the treatment; (3) received surgery, targeted therapy, immunotherapy, or other therapy after H101 and/or chemotherapy. Patients were divided into three groups according to treatment methods: group A, H101 alone; group B, chemotherapy alone; and group C, H101 combined with chemotherapy.

Treatment Procedures

The treatments were performed according to the uniform protocols recommended by the National Comprehensive Cancer Network (NCCN) practice guidelines for gastric cancer (28). Before endoscopy, all patients underwent laboratory tests and electrocardiogram with fasting, administration of proton pump inhibitors, and nutrition supplementation. The tumor size and the number of lesions were evaluated by endoscopy. H101 (–20°C, Shanghai Sunway Biotech, Shanghai, China) was then dissolved with normal saline to 30% of the estimated tumor volume at room temperature, was peritumorally injected *via* endoscopy according to the manufacturer's instructions, and these injections were

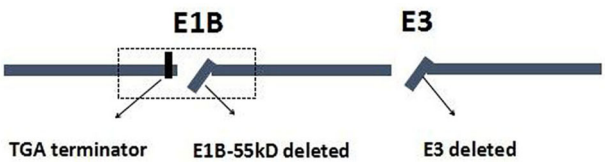

FIGURE 1 | Schematic diagram of constructed adenovirus (H101). E, early region of adenovirus genome.

repeated 21 days as one treatment cycle. The specifications of H101, including the titer, sterility, and general safety, were tested by the National Institute for the Control of Pharmaceutical and Biological Products (Beijing, China) that followed the standard biosecurity and institutional safety procedures (29).

The doses of H101 depended on tumor size and the number of lesions: (1) 0.5×10^{12} virus particles (vp)/day (1 unit) for patients with one lesion with a maximum diameter of ≤5 cm; (2) 1.0×10^{12} vp/day (2 units) for patients with one lesion with a maximum diameter of 5–10 cm or two lesions with a sum of the diameters of 5–10 cm; (3) 1.5×10^{12} vp/day (3 units) for patients with one lesion with a maximum diameter >10 cm or ≥ three lesions; (4) for patients with two or more lesions, the dose of H101 for each lesion was further decided by the proportion and size of the different lesions. The number of cycles of H101 was determined according to the instructions for the use of H101 and patients' effect after injection. After injection of H101, renin (0.1 mg/ml) and thrombin (10–100 unit/mL) were sprayed to stop the bleeding.

For chemotherapy method, oxaliplatin, 130 mg/m^2, was administered by intravenous drip on day 1 and Tegafur (Tegafur, Qilu Pharmaceutical (Hainan) Co., Ltd, Haikou, China), 80 mg/m^2, was taken orally after meals twice a day on days 1–14 in a row with 21 days for a cycle for three cycles. For H101 combined with chemotherapy method, the above mentioned procedures were followed.

Clinical Evaluation and Follow-Up

Short-term outcome was assessed based on the new Response Evaluation Criteria in Solid Tumors (RECIST) (30), which include complete response (CR, disappearance of all target lesions), a partial response (PR, the sum of all of the length-to-diameter ratio of the target lesion was reduced by 30% or more), stable disease (SD, all of the target lesions changed between PR and PD), and progressive disease (PD, the sum of all of the length to diameter ratio of the target lesion increased by at least 20%, and the absolute value of total length to diameter increased more than 5 mm, or new lesions appear). The disease control rate (DCR) was the proportion of the total number of CR+PR+SD patients treated to the total number of cases. The overall response rate (ORR) was the proportion of the total number of CR+PR patients treated compared to the total number of cases. After treatment, CT scanning and gastrointestinal endoscopy were performed for all patients, and the RECIST was to evaluate the tumor response. Long-term outcome was analyzed by calculating 1- and 2-year overall survival (OS) and progression-free survival (PFS), the median OS and median PFS, the upper quartile (Q_3) and lower quartile (Q_1) of OS and PFS, and the interquartile range (IQR = Q_3–Q_1) of OS and PFS. The complications, which were defined as any manifestations that occurred during the period of treatment or follow-up, were recorded. All patients were followed up at least every 2 months in the first year after treatment and every 3 months until death or loss of follow-up. The latest follow-up date for this study was September 28, 2018.

Statistical Analysis

Data were expressed as mean ± standard deviation (SD) or median (range), where appropriate. SPSS version 21 software (SPSS Inc., Chicago, IL, USA) was used to analyze the data. Analysis of variance was used to compare the difference in numerical variables with least significant difference as the *post-hoc* test. The Chi-square test was used to compare the differences between the categorical variables in the groups. Moreover, Kaplan-Meier analysis was used to compare the survival between the groups. A p-value <0.05 was considered statistically significant.

RESULTS

Patients' Characteristics

Between September 5, 2012 and May 20, 2018, a total of 220 patients were diagnosed with advanced GC and received H101 and/or chemotherapy. Among these patients, 53 patients had uncontrolled active infection, coagulation abnormality, and liver and kidney function damage; 18 patients failed to complete the treatment; and 54 patients received surgery, targeted therapy, immunotherapy, and other therapy after H101 and/or chemotherapy. Finally, 95 patients, 56 males and 39 females aged 45–80 years (67.2 ± 9.8), were included (**Figure 2**). The main clinical symptoms of patients were difficulty eating, upper gastrointestinal bleeding, weight loss, fatigue, appetite loss, nausea and vomiting, and abdominal pain. All patients were at stage III/IV GC and not suitable for surgical resection: 30 cases were treated with H101, including 17 males and 13 females, aged from 47 to 78 years (group A); 33 cases received chemotherapy, including 19 males and 14 females, aged 45–76 years (group B); and 32 cases were treated with H101 combined with chemotherapy, including 20 males and 12 females, aged 48 to 80 years (group C). The main characteristics of the study population are shown in **Table 1**. There was no significant

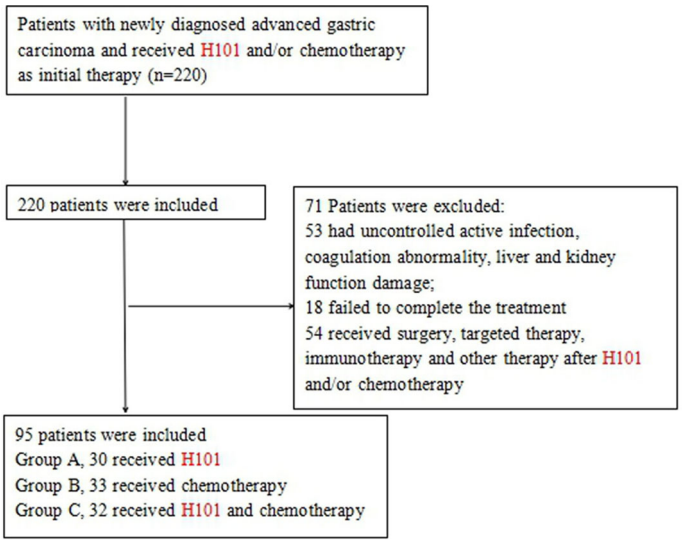

FIGURE 2 | Flowchart of the patient selection process.

TABLE 1 | Clinical characteristics of patients treated with recombinant human adenovirus type 5, chemotherapy and H101 combined with chemotherapy (*n* = 95).

Clinical characteristics	Total (*n* = 95)	Group A (*n* = 30)	Group B (*n* = 33)	Group C (*n* = 32)	*p*-value
Age (year)	67.2 ± 9.8	66.7 ± 7.4	65.0 ± 8.8	69.9 ± 6.8	0.846
Gender (*n*)					0.879
Male	56 (58.9%)	17 (56.7%)	19 (57.6%)	20 (62.5%)	
Female	39 (41.1%)	13 (43.3%)	14 (42.4%)	12 (37.5%)	
Primary tumor location (*n*)					0.701
Fundus	18 (18.9%)	6 (20.0%)	7 (21.2%)	5 (15.6%)	
Body	28 (29.5%)	9 (30.0%)	9 (27.3%)	10 (31.3%)	
Pylorus	49 (51.6%)	15 (50.0%)	17 (51.5%)	17 (53.1%)	
Pathological type (*n*)					0.837
Adenocarcinoma	85 (89.5%)	26 (86.7%)	30 (90.9%)	29 (90.6%)	
Signet-ring cell carcinoma	10 (10.5%)	4 (13.3%)	3 (9.1%)	3 (9.4%)	
Depth of invasion (*n*)					0.619
T3	27 (28.4%)	7 (23.3%)	9 (27.3%)	11 (34.4%	
T4	68 (71.6%)	23 (76.7%)	24 (72.7%)	21 (65.6%	
Lymph node metastasis (*n*)					0.947
N1	24 (25.3%)	8 (26.7%)	7 (21.2%)	9 (28.1%)	
N2	41 (43.2%)	13 (43.3%)	14 (42.4%)	14 (43.8%)	
N3	30 (31.5%)	9 (30.0%)	12 (36.4%)	9 (28.1%)	
Hepatic metastasis (*n*)					0.935
Yes	50 (52.6%)	15 (50.0%)	18 (54.5%)	17 (53.1%)	
No	45 (47.4%)	15 (50.0%)	15 (45.5%)	15 (46.9%)	
Stage of gastric carcinoma (*n*)					0.710
III	35 (36.8%)	10 (33.3%)	14 (42.4%)	11 (34.4%)	
IV	60 (63.2%)	20 (66.7%)	19 (57.6%)	21 (65.6%)	

Group A, H101 alone; group B, chemotherapy alone; group C, H101 combined with chemotherapy; N1, 1–2 lymph node metastasis; N2, 3-6 lymph node metastasis; N3, ≥7 lymph node metastasis.

difference among the three groups in terms of age, gender, primary tumor location, pathological type, depth of invasion hepatic metastasis, and GC stage.

Clinical Outcomes and Follow-Up

Overall, 95 patients were evaluable. In group A (*n* = 30 cases) with effective H101 injection, there were one CR and 11 PDs for the control lesions, respectively. Whereas, the combination of H101 injection with chemotherapy in group C (*n* = 32 cases, four CRs and six PDs) was more effective than H101 injection alone in group A (all $p < 0.05$, **Table 2**). The DCR and ORR were 63.3%, 66.7%, and 81.3% and 30.0%, 33.3%, and 50.0%, respectively, in groups A, B, and C, with the rates being significantly greater in group C than in groups A and B (both $p < 0.05$, **Table 2**). After treatment, most

TABLE 2 | Short-term outcomes of H101, chemotherapy, and H101 combined with chemotherapy for advanced gastric carcinoma.

	Group A (n = 30)	Group B (n = 33)	Group C (n = 32)	p-value
Response assessment after treatment				
Complete response	1 (3.3%)	2 (6.1%)	4 (12.5%)*	0.022
Partial response	8 (26.7%)	9 (27.3%)	12 (37.5%)	0.168
Stable disease	10 (33.3%)	11 (33.3%)	10 (31.3%)	0.941
Progressive diseases	11 (36.7%)	11 (33.3%)	6 (18.7%)*	0.014
Disease control rate	19 (63.3%)	22 (66.7%)	26 (81.3%)*	0.014
Overall response rate	9 (30.0%)	11 (33.3%)	16 (50.0%)*	0.007

*Group A, H101; Group B, chemotherapy; Group C, H101 combined with chemotherapy. *$p < 0.05$ compared with group A.*

patients had tumors involving pylorus lead to symptoms of obstruction, which was significantly improved in three groups, meanwhile H101 or/and chemotherapy had antitumor effect on metastatic lesions. **Figure 3** shows the regression/response after the injection of H101 in one typical case.

As of September 28, 2018, five, four, and four patients were known to be dead and three, four, and three patients were lost to follow-up in groups A, B, and C, respectively. Thus, 22, 25, and 25 cases in groups A, B, and C, respectively, were followed up for 2 years and longer. Generally, patients in group C survived longer than those in groups A and B, as analyzed by the Kaplan-Meier method (**Figure 4**). Furthermore, as **Table 3** shows, in 1- and 2-year OS and PFS, the median OS and median PFS in group C were significantly greater than those in the other two groups (all $p < 0.05$). In addition, Q_3 and Q_1 of OS and PFS of group C were significantly higher (OS: $Q_3 = 37.5$, $Q_1 = 19.5$, PFS: $Q_3 = 20.5$, $Q_1 = 7.0$) than that of group A (OS: $Q_3 = 25.5$, $Q_1 = 8.75$, PFS: $Q_3 = 11.375$, $Q_1 = 4.0$) and group B (OS: $Q_3 = 26.5$, $Q_1 = 9.0$, PFS: $Q_3 = 11.15$, $Q_1 = 5.0$) (all $p < 0.05$). They were not significantly different between groups A and B. IQR of PFS was significantly higher in group C (13.5) than in group A (7.375) and group B (6.15); IQR of OS was not significantly different in three groups (**Figure 5**).

Complications

No serious complication or severe toxicity was reported during the treatment or follow-up period. The complication rates of the three groups are summarized in **Table 4**. Fever was more frequently observed in groups A and C than in group B, whereas nausea and vomiting, constipation, granulocytopenia, anemia, and hair loss occurred more commonly in groups B and C than in group A but without significant differences between groups B and C. All complications were alleviated by symptomatic treatment. Furthermore, the incidence of complications did not vary with the dosage changes (0.5×10^{12} vp/day, 1.0×10^{12} vp/day, and 1.5×10^{12} vp/day), correspondingly (**Table 5**).

DISCUSSION

In this retrospective cohort study, the clinical outcomes of three treatment modalities of advanced GC were compared. Regarding short-term outcomes, the rates of CR and PR were significantly higher in patients treated with H101 combined with chemotherapy than in those treated with chemotherapy alone or H101 alone, whereas there was no significant difference in the rate of SD among the three groups. Correspondingly, the rate of PD was less in patients treated with H101 combined with chemotherapy than in the other two groups. Therefore, the DCR and ORR were both higher in patients treated with H101 combined with chemotherapy than in those treated with H101 alone or chemotherapy alone. These findings indicated that H101 combined with chemotherapy was beneficial in terms of short-term clinical outcome in the treatment of advanced GC. However, H101 alone had no obvious advantage regarding short-term outcomes compared with chemotherapy alone. In this study, the DCR of patients who were treated with H101 combined with chemotherapy was higher than that of a previous study reported (81.3% vs. 73.44%) by Lu et al. (20), which might indicate when combined with chemotherapy, the short-term outcomes of H101 through upper endoscopy appears to be better than intravenous drips combined with chemotherapy.

Oxaliplatin is a diaminocyclohexane-containing third-generation platinum compound; it was first patented in 1976 and approved for medical use in 1996 (31). Oxaliplatin has clinical activity as a monosubstance, but it is usually used in combination with other chemotherapeutic drugs to form some of the most common chemotherapeutic schemes in modern oncology (32). Tegafur, which is widely used in Asia, has a similar effect with other chemotherapy regimens. One previous meta-analysis has summarized the effect of a tegafur-based regimen compared with a surgery-alone control, it is suggested that chemotherapy with a tegafur-based agent after surgery can improve the survival of patients with curatively resected GC (33). The mechanism of action of H101 in killing tumor cells is different from that of chemotherapy, but they have synergistic effect. The clinical study has shown that H101 combined with traditional chemotherapy is effective in the treatment of various solid tumors, and the efficacy is better than that of chemotherapy alone (20). However, the efficacy and safety of endoscopic tumor injection of H101 in the treatment of gastric cancer have not been reported. H101 can change its biological activity after acting on tumor cells, making it easier for chemotherapy drugs to enter tumor cells and increasing the effect of chemotherapy to kill tumors. In this study, for advanced GC patients who were treated with the H101 combined with chemotherapy (oxaliplatin + tegafur), H101 was injected into the tumor locally and uniformly under endoscopic operation. After treatment, it was observed visually under an endoscope that the lesion volume of the patient was smaller than before, the congestion and edema of local tissues were reduced, the patient's self-conscious obstruction caused by tumor was significantly reduced, and the

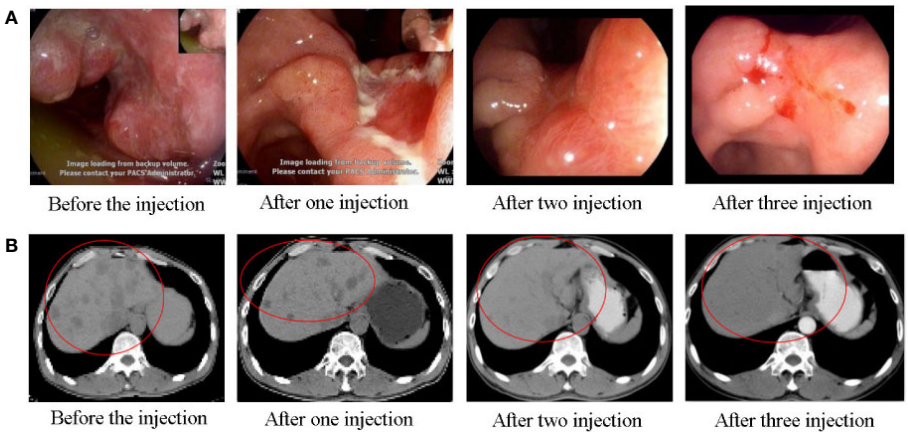

FIGURE 3 | A 51-year-old male patient was diagnosed with T2N1M1 stage gastric carcinoma (GC), involving the entire gastric angle and anterior wall of lesser curvature of gastric antrum. **(A)** The gastroscopy showed that there were huge ulcer-like tumors in the whole gastric angle and the anterior wall of the lesser curvature of the gastric antrum. The bottom of the tumor was uneven, nodular, and covered with white moss, and the edge was raised, with erosion, hyperemia, edema, poor peristalsis, and hard texture. After treatment, the huge ulcer-like tumor was reduced and healed, and the mucosa was gathered, the edge was raised, congestion and edema were reduced, and the tumor volume was significantly reduced. **(B)** Contrast-enhanced CT of the upper abdomen, before endoscopic injection treatment, revealed multiple low-density foci in the liver parenchyma before endoscopic injection, with unclear boundaries, the largest of which was about 2.5 cm in diameter. After the treatment, CT examination showed that the multiple metastases in the liver were significantly reduced and smaller than before and some of the low-density lesions in the liver disappeared.

feeding condition was improved. All the above further proved the H101 combined with chemotherapy was effective to treat GC.

According to a report by Peng et al. (34), the median OS and PFS of advanced GC patients with conventional chemotherapy was 6.2 and 11.5 months. Furthermore, a multiple-center phase II study has reported that the oxaliplatin combining with oral tegafur-uracil (uracil combined with tegafur in a 4:1 ratio) could produce a 50% response rate, PFS of 177 days and OS of 331 days, and showed acceptable activity and manageable toxicity in treating patients with advanced GC (35). In this study, some patients who only received the chemotherapeutic combination of oxaliplatin and tegafur achieved a 33% response rate, 8.5 months PFS and 17.2 months OS. Patients treated with H101 combined with chemotherapy had extended survival compared with those treated with H101 alone or chemotherapy alone; the median OS and PFS with H101 combined with chemotherapy were 29.6 and 14.8 months, respectively, which

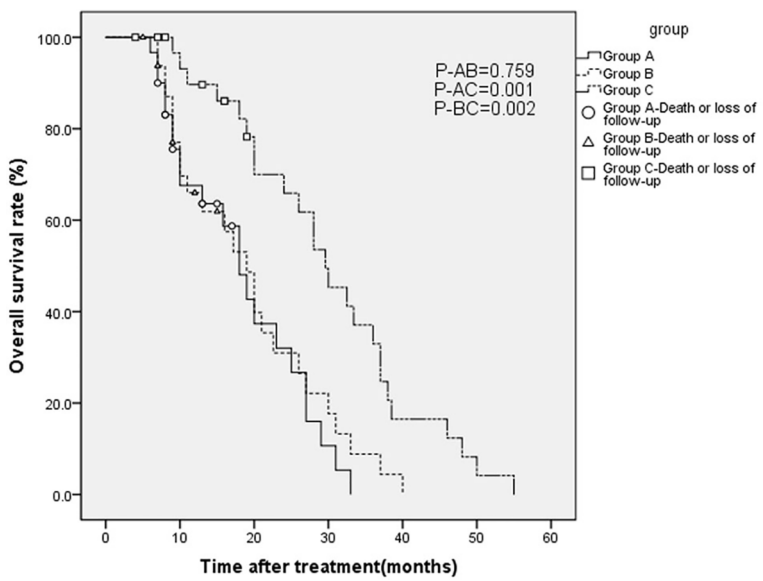

FIGURE 4 | Overall survival (OS) curves estimated by the Kaplan-Meier method for patients with advanced gastric carcinoma who were treated with H101 and/or chemotherapy.

TABLE 3 | Long-term outcomes of H101, chemotherapy, and H101 combined with chemotherapy for advanced gastric carcinoma.

	Group A (*n* = 30)	Group B (*n* = 33)	Group C (*n* = 32)	*p*-value
Overall survival				
Median (months)	16.9 (13.0–20.9)	17.2 (12.5–19.4)	29.6 (22.1–31.2)*	
1-year (%)	59.1	60.0	88.0*#	0.000
2-year (%)	27.3	28.0	60.0*#	0.000
Progression-free survival				
Median (months)	7.8 (6.1–10.5)	8.5 (6.9–11.7)	14.8 (9.4–15.3)*	
1-year (%)	22.7	24.0	52.0*#	0.000
2-year (%)	4.5	8.0	20.0*#	0.001

*Group A, H101; Group B, chemotherapy; Group C, H101 combined with chemotherapy. *$p < 0.05$ compared with group A; #$p < 0.05$ compared with group B.*

were nearly twice those with H101 alone or chemotherapy alone. The Q_1 of OS of patients with H101 combined with chemotherapy were more than twice those with H101 alone or chemotherapy alone, the Q_3 of OS and PFS and Q_1 of PFS with H101 combined with chemotherapy were clearly increased than the other groups. Moreover, the IQR of PFS with H101 combined with chemotherapy, H101 alone, and chemotherapy alone were 13.5, 7.38, and 6.15 months, respectively. This might indicate the PFS of H101 alone and chemotherapy alone is more concentrated. These findings indicated that H101 combined with chemotherapy might have substantially better long-term outcomes than H101 alone and chemotherapy alone.

One study has reported that low toxicity was observed in patients with the squamous cell carcinoma of the head and neck after they received intratumoral H101 injection in a dose-escalation manner (from 5.0×10^7 to 1.5×10^{12} vp/day) for 5 consecutive days. The most frequent complications were fever, flulike symptoms, and pain at the injection site (19). In our study, fever was also frequently observed in groups A and C, which was higher than that in group B. All complications in groups A and C were not increased following the increasing of H101 dose (0.5×10^{12} vp/day, 1.0×10^{12} vp/day, and 1.5×10^{12} vp/day), which was were similar to previous reports (19, 29). This study further proved H101 combined with chemotherapy can effectively control the growth of gastric malignant tumors and improve the survival rate without increasing complications. The upper endoscopic procedure is relatively simple, and H101 through upper endoscopy combined with chemotherapy has positive clinical value that is worthy of clinical promotion and application. Moreover, the present study also provides a relevant basis for a therapeutic adenovirus combined with chemotherapy in the treatment of GC.

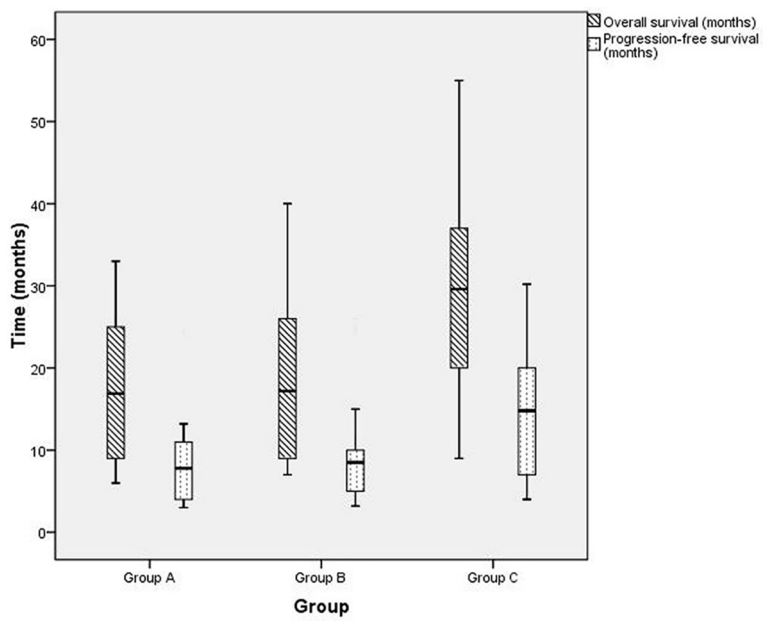

FIGURE 5 | The box plot of overall survival (OS) and progression-free survival (PFS) for patients with advanced gastric carcinoma who were treated with H101 and/or chemotherapy. Group A (OS: $Q_3 = 25.5$, $Q_1 = 8.75$, median OS = 16.9, PFS: $Q_3 = 11.375$, $Q_1 = 4.0$, median PFS = 7.8, IQR = 7.375), group B (OS: $Q_3 = 26.5$, $Q_1 = 9.0$, median OS = 17.2, PFS: $Q_3 = 11.15$, $Q_1 = 5.0$, median PFS = 8.5, IQR=6.15), group C (OS: $Q_3 = 37.5$, $Q_1 = 19.5$*, median OS = 29.6*, PFS: $Q_3 = 20.5$, $Q_1 = 7.0$, median PFS = 14.8*, IQR = 13.5*). *$p < 0.05$ compared with group A or B.

TABLE 4 | Complications of H101, chemotherapy, and H101 combined with chemotherapy for advanced gastric carcinoma.

Complications	Group A (n = 30)	Group B (n = 33)	Group C (n = 32)	p-value
Nausea and vomiting	8 (26.7%)	25 (75.8%)*	24 (75.0%)*	0.000
Diarrhea	13 (43.3%)	14 (42.4%)	13 (40.7%)	0.960
Constipation	4 (13.3%)	11 (33.3%)*	12 (37.5%)*	0.000
Granulocytopenia	1 (3.3%)	18 (54.5%)*	19 (59.4%)*	0.000
Anemia	2 (6.6%)	15 (45.5%)*	16 (50.0%)*	0.000
Hair loss	0 (0.0%)	17 (51.5%)*	17 (53.1%)*	0.000
Fever	25 (83.3%)	14 (42.4%)*	27 (84.4%)#	0.000
Overall	25(83.3%)	31 (93.9%)*	29 (90.6%)	0.034
Alleviated	25 (100%)	31 (100%)	29 (100%)	–

*Group A, H101; Group B, chemotherapy; Group C, H101 combined with chemotherapy. *$p < 0.05$ compared with group A. #$p < 0.05$ compared with group B.*

TABLE 5 | Complications of the three dose levels of recombinant human adenovirus type 5 (H101) in groups A and C.

Complications	Group A at various doses (vp/day) (n = 30)				Group C at various doses (vp/day) (n = 32)			
	0.5×10^{12} (n = 5)	1.0×10^{12} (n = 13)	1.5×10^{12} (n = 12)	p-value	0.5×10^{12} (n = 3)	1.0×10^{12} (n = 15)	1.5×10^{12} (n = 14)	p-value
Nausea and vomiting	1 (20.0)	4 (30.1)	3 (25.0)	0.503	2 (66.7)	12 (80.0)	10 (71.4)	0.107
Diarrhea	2 (40.0)	6 (46.2)	5 (41.7)	0.683	1 (33.3)	6 (40.0)	6 (42.3)	0.389
Constipation	0 (0.0)	2 (15.4)	2 (16.7)	0.000	1 (33.3)	7 (46.7)	4 (33.3)	0.062
Granulocytopenia	0 (0.0)	1 (7.7)	0 (0.0)	0.000	2 (66.7)	8 (53.3)	9 (64.2)	0.101
Anemia	0 (0.0)	1 (7.7)	1 (8.3)	0.015	1 (33.3)	8 (53.3)	7 (50.0)	0.009
Hair loss	0 (0.0)	0 (0.0)	0 (0.0)	–	1 (33.3)	8 (53.3)	8 (57.1)	0.001
Fever	4 (80.0)	11 (84.6)	10 (83.3)	0.643	3 (100.0)	12 (80.0)	12 (85.7)	0.000
Overall	4 (80.0)	11 (84.6)	11 (91.7)	0.052	3 (100.0)	13 (86.7)	13 (92.9)	0.048

Data were expressed as number (percentage). Group A, H101; Group C, H101 combined with chemotherapy.

However, this study has some inherent limitations due to being a retrospective study. First, selection bias might be present but cannot be fully assessed for such an observational study. Second, the subjects were all from one hospital, the sample size was relatively small, which weakened the statistical power of the analyses. Third, due to its relatively high cost and patients having doubts about its efficacy and safety, patients' acceptance of H101 is still relatively low and the clinical application of H101 is not very common. Therefore, a prospective randomized controlled trial with larger samples is urgently needed to obtain more robust clinical data and more convincing results to guide clinical treatment.

In conclusion, H101 combined with chemotherapy may be a potential therapeutic option for patients with advanced GC, and prospective studies with proper assessment of toxicity will be needed in the future.

DATA AVAILABILITY STATEMENT

The original contributions presented in the study are included in the article/supplementary material. Further inquiries can be directed to the corresponding author.

ETHICS STATEMENT

The studies involving human participants were reviewed and approved by Qingdao Municipal Hospital, Qingdao Affiliated to Qingdao University. The patients/participants provided their written informed consent to participate in this study.

AUTHOR CONTRIBUTIONS

Conception and design: RZ. Administrative support: XJ. Provision of study materials or patients: XJ. Collection and assembly of data: RZ, YC and XG. Data analysis and interpretation: RZ and YC. Manuscript writing: all authors. All authors contributed to the article and approved the submitted version.

ACKNOWLEDGMENTS

We thank Dr. Harry H-X Xia of Medjaden Bioscience Limited for writing assistance.

REFERENCES

1. Ferlay J, Colombet M, Soerjomataram I, Parkin DM, Pineros M, Znaor A, et al. Cancer Statistics for the Year 2020: An Overview. *Int J Cancer* (2021). doi: 10.1002/ijc.33588
2. WHO. Globocan 2020 Stomach. In: *WHO, Globocan 2020 China*. China: International Agency for Research on Cancer. March 2021. Available at: https://gco.iarc.fr/today/data/factsheets/cancers/7-Stomach-fact-sheet.pdf2.
3. Chen W, Zheng R, Baade PD, Zhang S, Zeng H, Bray F, et al. Cancer Statistics in China, 2015. *CA Cancer J Clin* (2016) 66:115–32. doi: 10.3322/caac.21338
4. Kim HS, Kim JH, Kim JW, Kim BC. Chemotherapy in Elderly Patients With Gastric Cancer. *J Cancer* (2016) 7:88–94. doi: 10.7150/jca.13248
5. Farran B, Muller S, Montenegro RC. Gastric Cancer Management: Kinases as a Target Therapy. *Clin Exp Pharmacol Physiol* (2017) 44:613–22. doi: 10.1111/1440-1681.12743

6. Wang X, Su C, Cao H, Li K, Chen J, Jiang L, et al. A Novel Triple-Regulated Oncolytic Adenovirus Carrying P53 Gene Exerts Potent Antitumor Efficacy on Common Human Solid Cancers. *Mol Cancer Ther* (2008) 7:1598–603. doi: 10.1158/1535-7163.MCT-07-2429
7. Fujiwara T, Urata Y, Tanaka N. Telomerase-Specific Oncolytic Virotherapy for Human Cancer With the hTERT Promoter. *Curr Cancer Drug Targets* (2007) 7:191–201. doi: 10.2174/156800907780058835
8. Lawler SE, Speranza MC, Cho CF, Chiocca EA. Oncolytic Viruses in Cancer Treatment: A Review. *JAMA Oncol* (2017) 3:841–9. doi: 10.1001/jamaoncol.2016.2064
9. Wang P, Wang Z, Zhou Z. Roles of P53 in the Interaction With Digestive Malignant Tumors. *Pract Oncol J* (2016) 30:468–72. doi: 10.11904/j.issn.1002-3070.2016.05.017.
10. Zhang ML, Liu S, Liu YJ, Wang SL. Research Advances in the Antitumor Drugs Targeting P53. *J Int Pharm Res* (2018) 45:88–93. doi: 10.13220/j.cnki.jipr.2018.02.002.
11. Busuttil RA, Zapparoli GV, Haupt S, Fennell C, Wong SQ, Pang JM, et al. Role of P53 in the Progression of Gastric Cancer. *Oncotarget* (2014) 5:12016–26. doi: 10.18632/oncotarget.2434
12. Li CH, Xu HY, Otolaryngolog DO. The Influence of Human Recombinant Adenovirus Type 5 Local Injections Combined Chemoradiation on the Prognosis of Patients with Nasopharyngeal Carcinoma and Tumor Malignant Degree. *J Clin Exp Med* (2016) 15:2022–5. doi: 10.3969/j.issn.1671-4695.2016.20.019
13. Nemunaitis J, Khuri F, Ganly I, Arseneau J, Posner M, Vokes E, et al. Phase II Trial of Intratumoral Administration of ONYX-015, a Replication-Selective Adenovirus, in Patients With Refractory Head and Neck Cancer. *J Clin Oncol* (2001) 19:289–98. doi: 10.1200/JCO.2001.19.2.289
14. Khuri FR, Nemunaitis J, Ganly I, Arseneau J, Tannock IF, Romel L, et al. A Controlled Trial of Intratumoral ONYX-015, a Selectively-Replicating Adenovirus, in Combination With Cisplatin and 5-Fluorouracil in Patients With Recurrent Head and Neck Cancer. *Nat Med* (2000) 6:879–85. doi: 10.1038/78638
15. Heise C, Sampson-Johannes A, Williams A, McCormick F, Von Hoff DD, Kirn DH. ONYX-015, an E1B Gene-Attenuated Adenovirus, Causes Tumor-Specific Cytolysis and Antitumoral Efficacy That can be Augmented by Standard Chemotherapeutic Agents. *Nat Med* (1997) 3:639–45. doi: 10.1038/nm0697-639
16. Dobner T, Horikoshi N, Rubenwolf S, Shenk T. Blockage by Adenovirus E4orf6 of Transcriptional Activation by the P53 Tumor Suppressor. *Science* (1996) 272:1470–3. doi: 10.1126/science.272.5267.1470
17. Benedict CA, Norris PS, Prigozy TI, Bodmer JL, Mahr JA, Garnett CT, et al. Three Adenovirus E3 Proteins Cooperate to Evade Apoptosis by Tumor Necrosis Factor-Related Apoptosis-Inducing Ligand Receptor-1 and -2. *J Biol Chem* (2001) 276:3270–8. doi: 10.1074/jbc.M008218200
18. Yu W, Fang H. Clinical Trials With Oncolytic Adenovirus in China. *Curr Cancer Drug Targets* (2007) 7:141–8. doi: 10.2174/156800907780058817
19. Liang M. Oncorine, the World First Oncolytic Virus Medicine and its Update in China. *Curr Cancer Drug Targets* (2018) 18:171–6. doi: 10.2174/1568009618666171129221503
20. Lu W, Zheng S, Li XF, Huang JJ, Zheng X, Li Z. Intra-Tumor Injection of H101, a Recombinant Adenovirus, in Combination With Chemotherapy in Patients With Advanced Cancers: A Pilot Phase II Clinical Trial. *World J Gastroenterol* (2004) 10:3634–8. doi: 10.3748/wjg.v10.i24.3634
21. Zhang J, Guo XC, Lv GX. Clinical Curative Effects of Local Injection of Recombinant Oncolytic Adenovirus Type 5 Combined With Radiochemotherapy in the Treatment of Advanced Nasopharyngeal Carcinoma. *Chin J Exp Clin Virol* (2015) 29:71–3. doi: 10.3760/cma.j.issn.1003-9279.2015.01.024
22. Hou B, Cui K, Jiang L. Intraoperative Infiltration Injection of Recombinant Human Adenovirus Type 5 in the Treatment of 22 Cases of Esophageal Cancer. *China Pharmaceuticals* (2012) 21:89. doi: 10.3969/j.issn.1006-4931.2012.05.056
23. Tang X, Wang GH, Wang WM, Oncology DO. Analysis of Effect by Human Recombinant Type 5 Adenovirus Through Intrapleural Injection in the Treatment of Advanced Lung Cancer Malignant Pleural Effusion. *Chin J Modern Drug Appl* (2017) 11:91–3. doi: 10.14164/j.cnki.cn11-5581/r.2017.05.044.
24. Li LL, Zhang X, Jin XX, Wang CL, Chen R, Medicine SO, et al. Inhibitory Effect of Recombinant Adenovirus H101 Combined With Sorafenib Against Hepatocellular Carcinoma HepG2 Cells In Vitro. *J Southeast Univ (MedicalSci Edition)* (2016) 35:673–7. doi: 10.3969/j.issn.1671-6264.2016.05.006
25. Lin XJ, Li QJ, Lao XM, Yang H, Li SP. Transarterial Injection of Recombinant Human Type-5 Adenovirus H101 in Combination With Transarterial Chemoembolization (TACE) Improves Overall and Progressive-Free Survival in Unresectable Hepatocellular Carcinoma (HCC). *BMC Cancer* (2015) 15:707. doi: 10.1186/s12885-015-1715-x
26. Wang D, Yang ZX, Zhang QH, Wang G, Jing F, Yang ZZ, et al. The Clinical Observation of Effect of Recombinant Human Ad-P53–Gendicine Combined With Chemotherapy or Radiotherapy in Advanced Cancer Patients. *Chin Clin Oncol* (2008) 10:896–900. doi: 10.3969/j.issn.1009-0460.2008.10.008.
27. Liu XJ, Peng JX, Jing-Chang LU. Perfusion of Recombinant Human Adenovirus Type 5 Injection in Pleural Cavity to Patients With Lung Cancer Combining Malignant Pleural Effusions. *J Clin Pulm Med* (2010) 15:1539–40. doi: 10.3969/j.issn.1009-6663.2010.11.007.
28. Ajani J, D'Amico TA, Hayman JA, Meropol NJ, Minsky BNational Comprehensive Cancer N. Gastric Cancer. Clinical Practice Guidelines in Oncology. *J Natl Compr Canc Netw* (2003) 1:28–39. doi: 10.6004/jnccn.2003.0005
29. Gong L, Gong K, Yu Z, Wu F, Xu Y. Efficacy and Safety of Intravenous Administration of Recombinant Human Adenovirus Type 5. *Med Inf* (2013) 000:577–8. doi: 10.3969/j.issn.1006-1959.2013.27.796
30. Eisenhauer EA, Therasse P, Bogaerts J, Schwartz LH, Sargent D, Ford R, et al. New Response Evaluation Criteria in Solid Tumours: Revised RECIST Guideline (Version 1.1). *Eur J Cancer* (2009) 45:228–47. doi: 10.1016/j.ejca.2008.10.026
31. Wong NS, Fernando NH, Bendell JC, Morse MA, Blobe GC, Honeycutt W, et al. A Phase II Study of Oxaliplatin, Dose-Intense Capecitabine, and High-Dose Bevacizumab in the Treatment of Metastatic Colorectal Cancer. *Clin Colorectal Cancer* (2011) 10:210–6. doi: 10.1016/j.clcc.2011.03.018
32. Fritsch R, Hoeppner J. Oxaliplatin in Perioperative Chemotherapy for Gastric and Gastroesophageal Junction (GEJ) Adenocarcinoma. *Expert Rev Gastroenterol Hepatol* (2019) 13:285–91. doi: 10.1080/17474124.2019.1573143
33. Oba K. Efficacy of Adjuvant Chemotherapy Using Tegafur-Based Regimen for Curatively Resected Gastric Cancer: Update of a Meta-Analysis. *Int J Clin Oncol* (2009) 14:85–9. doi: 10.1007/s10147-009-0877-4
34. Peng XT, Wang SB. Comparison of Efficacy Between Oxaliplatin CombinedWith Sergio and Oxaliplatin Combined With Capecitabine in First-LineTreatment of Advanced Gastric Cancer. *Clin J Chin Med* (2019) 11:77–9. doi: CNKI:SUN:ZYLY.0.2019-06-042
35. Chen JS, Rau KM, Chen YY, Huang JS, Yang TS, Lin YC, et al. A Multiple-Center Phase II Study of Biweekly Oxaliplatin and Tegafur-Uracil/Leucovorin for Chemonaive Patients With Advanced Gastric Cancer. *Cancer Chemother Pharmacol* (2009) 63:819–25. doi: 10.1007/s00280-008-0797-4

Conflict of Interest: The authors declare that the research was conducted in the absence of any commercial or financial relationships that could be construed as a potential conflict of interest.

Publisher's Note: All claims expressed in this article are solely those of the authors and do not necessarily represent those of their affiliated organizations, or those of the publisher, the editors and the reviewers. Any product that may be evaluated in this article, or claim that may be made by its manufacturer, is not guaranteed or endorsed by the publisher.

Copyright © 2021 Zhang, Cui, Guan and Jiang. This is an open-access article distributed under the terms of the Creative Commons Attribution License (CC BY). The use, distribution or reproduction in other forums is permitted, provided the original author(s) and the copyright owner(s) are credited and that the original publication in this journal is cited, in accordance with accepted academic practice. No use, distribution or reproduction is permitted which does not comply with these terms.

frontiers in Oncology

ORIGINAL RESEARCH
published: 03 January 2022
doi: 10.3389/fonc.2021.757383

OncoVee™-MiniPDX-Guided Anticancer Treatment for Gastric Cancer Patients With Synchronous Liver Metastases: A Retrospective Cohort Analysis

Yutong Ge[1†], Xin Zhang[2†], Wei Liang[1], Cuiju Tang[1], Dongying Gu[1], Junfeng Shi[1‡] and Xiaowei Wei[1*‡]*

[1] Department of Oncology, Nanjing First Hospital, Nanjing Medical University, Nanjing, China,
[2] Department of Gastrointestinal Surgery, Qilu Hospital of Shandong University, Jinan, China

Background: It is estimated that 35% of gastric cancer patients appear with synchronous distant metastases—the vast majority of patients presenting with metastatic hepatic disease. How to choose the most appropriate drugs or regimens is crucial to improve the prognosis of patients. We conducted this retrospective cohort analysis to evaluate the efficacy of OncoVee™-MiniPDX-guided treatment for these patients.

Methods: Gastric cancer patients with liver metastases (GCLM) were enrolled. Patients were divided into MiniPDX and control group according to their wishes. In the observation group, the OncoVee™-MiniPDX model was conducted to screen the most sensitive drug or regimens to determine the clinical administration. Meanwhile, patients were treated with regular medications in the control group according to the guidelines without the MiniPDX model. The primary endpoint was overall survival (OS), and the secondary outcomes included objective response rate (ORR), disease control rate (DCR), and progression-free survival (PFS).

Results: A total of 68 patients with GCLM were included, with the observation and control groups of 21 and 47 patients, respectively. The baseline characteristics of patients were balanced between these two groups. MiniPDX drug sensitivity tests were associated with the increased use of targeted drugs when compared with the control group (33.3 *vs.* 0%, p=0.032). Median OS was estimated to be 9.4 (95% CI, 7.9–11.2) months and 7.9 (95% CI, 7.2–8.7) months in the observation and control group, respectively. Both univariate (control group *vs.* MiniPDX group: HR=2.586, 95% CI= 1.362–4.908, p=0.004) and multivariate regression analyses (Control group *vs.* MiniPDX group: adjusted HR (aHR)=4.288, 95% CI= 1.452–12.671, p=0.008) showed the superiority of the observation group on OS. Similarly, MiniPDX-based regiments significantly improve the PFS of these cases (median PFS 6.7 months *vs.* 4.2 months, aHR=2.773, 95% CI=1.532–3.983, p=0.029). ORR and DCR were

OPEN ACCESS

Edited by:
Andreas Brandl, Champalimaud Foundation, Portugal

Reviewed by:
Miguel Alberto, Charité University Medicine Berlin, Germany
Ana Clara, Champalimaud Foundation, Portugal

***Correspondence:**
Xiaowei Wei
gswxw@njmu.edu.cn
Junfeng Shi
junfengshi1984@njmu.edu.cn

[†]These authors have contributed equally to this work and share first authorship

[‡]These authors jointly supervised this work

Specialty section:
This article was submitted to Gastrointestinal Cancers: Gastric & Esophageal Cancers, a section of the journal Frontiers in Oncology

Received: *12 August 2021*
Accepted: *03 December 2021*
Published: *03 January 2022*

Citation:
Ge Y, Zhang X, Liang W, Tang C, Gu D, Shi J and Wei X (2022) OncoVee™-MiniPDX-Guided Anticancer Treatment for Gastric Cancer Patients With Synchronous Liver Metastases: A Retrospective Cohort Analysis. Front. Oncol. 11:757383. doi: 10.3389/fonc.2021.757383

also improved in MiniPDX group comparing with control group (ORR, 57.14 *vs.* 25.53%, p=0.029; DCR: 85.71 *vs.* 68.08%, p=0.035).

Conclusion: OncoVee™-MiniPDX model, which was used to select drugs to guide antitumor treatment, was promising to prolong survival and improve the response rate of patients with GCLM. Further well-designed studies are needed to confirm the clinical benefits of MiniPDX.

Keywords: MiniPDX, gastric cancer, hepatic metastases, survival, response, OncoVee

1 INTRODUCTION

Gastric cancer (GC) is one of the most common malignant tumors and the fifth leading cause of cancer-related death worldwide (1). The situation is even grimmer in China, which accounts for about half of the morbidity and mortality associated with stomach disease (1, 2). Although the age-adjusted incidence and mortality rates in gastric cancer have decreased during the last decades, the relative survival has only witnessed a modest increase compared to improvements in many other gastrointestinal cancers (3). Metastatic spread is fatal to patients by leading to mass-effects and failures of physiological homeostasis. During the last two decades, the proportion of gastric cancer patients with synchronous metastases has increased to over 35–40% (4), with the vast majority of patients presenting with metastatic hepatic disease.

Hepatic resection should always be considered as an option for gastric cancer patients with liver metastases. However, some patients with GC are not suitable for hepatic resection, for whom adjuvant chemotherapy or molecular targeted therapy would be a choice. Newly developed cytotoxic agents represented by S-1 show promising activity for patients with metastases (5). How to choose the most sensitive antitumor drugs is crucial to improve the prognosis of patients.

Cancer research relies on interrogation model systems that reflect the biology of human tumors. Primary cell culture from human tumors has been a traditional approach to cancer research, but significant differences between *in vitro* cell culture environments and *in vivo* tumor environments have raised concerns that these cell lines may not be fully representative of human tumors (6). Patient-derived xenograft (PDX) model, injecting the tumor fragments from the patient into immunodeficient mice directly, has become a powerful method for preclinical drug evaluation (7–9). The advantage of PDX models to cell lines or genetically engineered mouse models is to obtain the heterogeneity and the molecular and histopathologic characteristics of the parent primary tumors (10, 11). Moreover, the drug response characteristics of PDX are closely related to the patients' clinical responses. PDX models have been reported in the treatment of many different types of solid tumors (12). It has been certified that PDX models can predict the patients' chemotherapy response and provide guidance for informed clinical decision-making (13). So far, about 300 cases of 13 tumor types have been evaluated, and the overall agreement between the clinical and treatment response of PDX patients is 70 to 100% (14, 15). Although PDX has significant advantages, limitations prevent them from being widely used in personalized medicine. Tumor xenotransplantation takes too long, usually 4 to 8 months, and it takes extra time to generate enough tissue to test the treatment options in mice (16). Additionally, in many cancer types, the implantation rate in mouse models is usually less than 50%, and even lower in breast, prostate, and renal cell carcinoma (17). As a result, many patients with rapidly developing diseases are unable to benefit from PDX studies, and a fast and reliable alternative drug sensitivity assessment method is particularly urgent (18).

A rapid and accurate *in vivo* drug response detection method has been developed using hollow fiber implantation technology, which can effectively and realistically predict patients' clinical responses to targeted therapy and chemotherapy. MiniPDX analysis provides a rapid and effective alternative to the PDX model for evaluating cancer treatment response that mimics the patients' clinical treatment response. The simplified conditions in MiniPDX analysis enable tumor cells, especially primary tumor cells of various cancer types, to survive and grow in the body, thus achieving a high success rate (19–21). A PDX model establishment is a prerequisite for *in vivo* PDX analysis, usually takes several months, with the success rate usually much lower than 50%. However, MiniPDX analysis does not require establishing a PDX model in advance. This study will adopt the MiniPDX model from patients with gastric cancer with liver metastases (GCLM), screening sensitive drugs for patients with liver metastases from gastric cancer.

PATIENTS AND METHODS

Patients Eligibility

Patients who were histologically confirmed with GCLM in Nanjing First Hospital and Qilu Hospital of Shandong University from January 2018 to June 2019 were enrolled consecutively in this cohort analysis. The criteria were as follow (1): 18 years of age or older (2); unresectable lesions with the necessity of systematic treatment (3); HER2 were negative (4); relapse or refractory to prior line treatment (4); Child-Pugh class A-B (5); ECOG PS of 0–2 (6); adequate organ function (white blood cell $\geq 3.9\times10^9$/L, absolute neutrophil count $\geq 1.5\times10^9$/L, platelets $\geq 100\times10^9$/L, bilirubin ≤2 mg/dl; hemoglobin ≥10g/dl, and serum creatinine ≤150 mmol/L) (7); life expectancy of ≥3 months; and (6) received at least one response evaluation by CT

or US. The exclusion criteria were as follows (1): patients who are indicated for liver resection (2), women with pregnancy or lactation (3), patients with a previous cerebrovascular event and active infectious disease (4), patients with clinically significant liver failure (i.e., encephalopathy or ascites found clinically).

This study was approved by the ethics committee of Nanjing First Hospital (KY20180604-05-KS-01). This research was conducted following the Declaration of Helsinki. All patients signed an informed consent.

OncoVee™-MiniPDX Model

The chemotherapy regimens for patients in the MiniPDX group were based on drug sensitivity assay results in mice. The MiniPDX assay was performed using the OncoVee™-MiniPDX kit (LIDE Biotech Co., Ltd, Shanghai, China). Briefly, the tumor cell suspension from patients' tumor tissues or biopsy samples was transferred to HBSS-washed capsules made of a hollow fiber membrane with an aperture of less than 500 kDa. The fiber system delivered the media to cells in a manner similar to blood delivery through the capillary network *in vivo*.

BALB/c nude mice (4–6 weeks of age) (SLARC Inc., Shanghai, China) weighing 15–20 g were selected for subcutaneous implantation. A small skin incision was made, and the OncoVee™-MiniPDX capsules were embedded in the subcutaneous tissues. One day after inoculation of tumor cells, the tumor-bearing mice were given the following drugs for 7 days [eg. gemcitabine, 60 mg/kg, ip, every 4 days; docetaxel, 10 mg/kg, ip, every 4 days; nab-paclitaxel, 20 mg/kg, intravenously (iv), every 4 days]. Normal saline was used as a control. Tumor cell viability was assessed based on relative fluorescence units (RFU) using CellTiter-Glo® Luminescent Cell Viability Assay (Promega, Madison, WI, USA) to demonstrate the antitumor activity of each drug. The equation for calculating proliferation rate was as follows:

$$\text{Relative proliferation rate (T/C ratio)} = \frac{(\text{RFUD7} - \text{RFUD0})\text{drug}}{(\text{RFUD7} - \text{RFUD0})\text{placebo}}$$

T/C ratio was defined as the relative proliferation rate of the treatment group compared with the control group 7 days after drug administration. A T/C ratio less than 50% was considered as the cutoff value to indicate response, which was proven before (22). The research flow chart is shown in **Figure 1**. All procedures were performed in accordance with the guidelines for the Care and Use of Laboratory Animals of the National Institutes of Health in the absence of specific pathogens.

Conventional Chemotherapy

Patients in the conventional group were treated with chemotherapy regimens according to National Comprehensive Cancer Network (NCCN) Clinical Practice Guidelines in Oncology, version 1.2018. Treatment regimens were decided by at least two independent medical professionals.

Outcomes and Measurement

The primary endpoint was the overall survival (OS) of included patients. The secondary endpoints included progression-free survival (PFS), objective response rate (ORR), disease control rate (DCR), and biomarkers response status. During the treatment, patients were followed up every month, then every 3 months after treatment till death or loss. The follow-up evaluations consisted of history, physical examination, hematology and blood chemistry panels, including serum tumor markers. Progression-free survival (PFS) and OS were measured as the time between treatment initiation and documented disease progression (PFS) or death (OS). OS refers to the time from treatment initiation to death. PFS is the time from treatment initiation to disease progression or death. All patients underwent conventional CT scans of liver by Somatom PLUS-S CT scanner (Siemens Medical Systems, Erlangen, Germany) at baseline and during follow-up. CT images were processed using 3D slice software package (Version 4.7). At least two radiologists with more than 10 years of work experience and an assistant researcher completed the entire process together. Radiographic assessments of short-term efficacy were performed every two cycles until disease progression or death during chemotherapy as per RECIST v1.1, and patients were classified into four subgroups: complete remission (CR), partial remission (PR), stable disease (SD), and progressive disease (PD). ORR was defined as the percent of patients with CR and PR from all the patients. And DCR was defined as the percent of the patients who achieved CR, PR, and SD.

Statistical Analysis

All the data analyses and plots were conducted using the statistical software of STATA Version 13.0 (College Station, TX, USA). Our data were described as the mean ± SD for normally distributed data or median with range for non-normally distributed data. Continuous variables with normally distributed were analyzed using unpaired Student's t-test. For multiple comparisons, the Tukey-Kramer honestly significant difference test was applied following ANOVA. OS analysis of patients was conducted by the Kaplan-Meier method. Potential independent risk factors for survival were evaluated by univariate analysis (log-rank test) and multivariate analysis (Cox proportional hazards model). P-value < 0.05 indicated statistical significance. The OS and PFS were analyzed using the Kaplan-Meier method and log-rank test. The correlations between clinical-pathological variables and drug sensitivity were analyzed using the Pearson $\chi 2$ test. $P<0.05$ was considered to indicate a statistically significant difference.

RESULTS

Baseline Characteristics of Patients

According to the inclusion criteria, 21 patients who received OncoVee™-MiniPDX drug sensitivity test were included. As a control group, 47 cases who received experimental treatment according to the NCCN guidance without the results of the

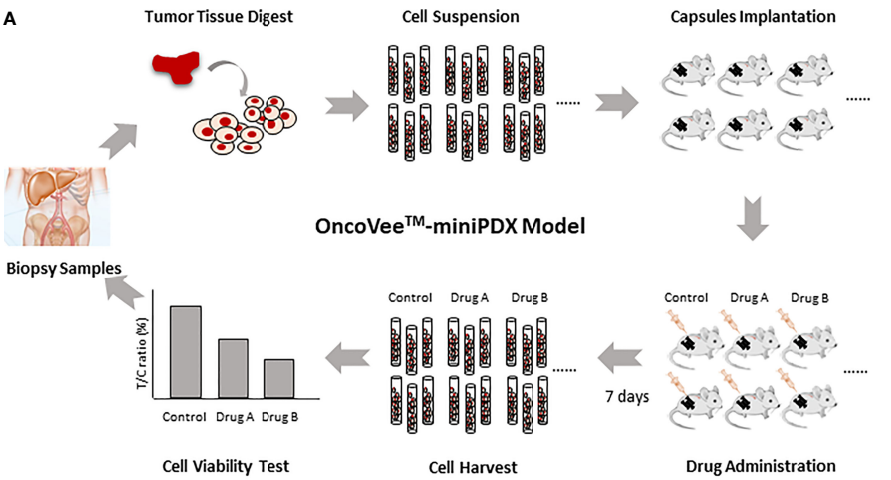

B

Drugs	1	2	3	4	5	6	7	8	9	10	11	12	13	14	15	16	17	18	19	20	21	Mean	Median
5-FU				55	22		39	55		82		78	55		49	34				43		51.2	52
Anlotinib	59	83						45	82	49	45			77		47		33			65	58.5	54
Apatinib	47		41			17	67			22			34				42		68			42.3	41.5
Capecitabine		27	59		91			36		89	39		63			72						59.5	61
Docetaxel			62		60		59		44	67			37	50		77			100	68		62.4	61
Gemcitabine		77		52	86				65		44	49		72	62			53		33		59.3	57.5
Irinotecan	63	62	44	59		23	43	52	44			49			47	21	42		62		63	48.1	48
Oxaliplatin		47	66	54	44	64	42		26			11		72			33	42	77	30	57	47.5	45.5
Paclitaxel	94					81					39				67		72	65		88	91	74.6	76.5
Regorafenib		59						48			89		41	92		34			72			62.1	59
S-1	33			72			42			72		31			44		77	49			72	54.7	49

C

Drugs	MiniPDX Scheme
5-FU	25mpk,ip,qd×5
Anlotinib	3mpk,po,qd×7
Apatinib	100mpk,po,qd×7
Gemcitabine	60mpk,ip,q4d×2
Irinotecan	50mpk,ip,q4d×2
Capecitabine	400mpk,po,qd×7
Oxaliplatin	5mpk,ip,q4d×2
Paclitaxel	20mpk,ip,q4d×2
Regorafenib	30mpk,po,qd×7
S-1	10mpk,po,qd×5
Docetaxel	20mpk,ip,q4d×2

D

Clinical medication	MiniPDX-guided group (n=21)	Experimental treatment group (n=47)	p-value
5-FU	7	9	0.203
Anlotinib	2	0	0.066
Apatinib	3	0	0.041
Gemcitabine	1	0	0.085
Irinotecan	8	15	0.618
Capecitabine	3	18	0.048
Oxaliplatin	6	22	0.158
Paclitaxel	1	6	0.316
Regorafenib	2	0	0.066
S-1	4	8	0.840
Docetaxel	2	9	0.319

P=0.032*

FIGURE 1 | OncoVee™-MiniPDX flow diagram and the medication administration. **(A)** OncoVee™-MiniPDX flow diagram was as follows: Tumor cells, digested from biopsy samples (sometimes from fresh tissue), were loaded into three capsules and subcutaneously implanted in 4-week-old BALB/c nude mice. Then, 7 days after drug or placebo administration intraperitoneally or orally, capsules were harvested to evaluate drug sensitivity *via* cell viability test. According to the results of MiniPDX, the optimal regimens were selected for personalized chemotherapy. **(B)** Medication compliance and medication frequency were different from the control group. **(C)** Specific dosages, administration routes and cycles of drugs recommended by MiniPDX. * represents the multiplication sign, indicating the total number of days. **(D)** Assessment of the medication regimens of these two groups to evaluate the influence of MiniPDX on drug selection in clinical practice. * represents statistical significance, $p < 0.05$.

MiniPDX model were concurrently selected. As present in **Table 1**, the baseline characteristics of these two cohorts were balanced without statistical difference. The previous line treatments include SP (S-1 and cisplatin), CP (irinotecan and cisplatin), DCF (Docetaxel and cisplatin and 5-FU), FP (5-FU and cisplatin), FOLFIRI (5-FU and leucovorin and irinotecan), XELOX (oxaliplatin and capecitabine), in which SP or CP was mainly used (60%). Relapse disease count for 38% of all these patients, with a median time to relapse of 3.2 (range:0.5–5.8) months.

TABLE 1 | Patients' demography and tumor characteristics.

Characteristics	MiniPDX-guided group (n = 21)	Experimental treatment group (n = 47)	p-value
Age, years			0.270
Median (range)	62 (28–83)	63 (32–86)	
<65, n (%)	8	20	
≥65	13	27	
Sex			0.612
Male	13	26	
Female	8	21	
ECOG PS			0.560
0–1	17	35	
2	4	12	
Primary gastric tumors size			0.763
Mean (SE), cm	5.76 (2.35)	5.49 (2.96)	
<5 cm	9	22	
≥5 cm	12	25	
Differentiation of primary tumor			0.954
Well	3	8	
Moderate	15	32	
Poor	3	7	
T-stage of primary tumor[&]			0.934
pT1	2	7	
pT2	5	11	
pT3	11	22	
pT 4	3	7	
N-stage of Primary tumor[&]			0.908
N0	3	7	
N1	9	19	
N2	6	11	
N3	3	10	
Number of metastases			0.634
Median (range)	4 (1–9)	4 (1–11)	
Solitary n (%)	9	22	
2–5, n (%)	9	15	
>5, n (%)	3	10	
Metastases tumors size			0.793
Median (range), cm	4.77 (2.18)	4.06 (2.69)	
<5 cm	10	24	
≥5 cm	11	23	
Metastases lesions location			0.914
Left lobe, n (%)	5	10	
Right lobe, n (%)	6	12	
Both, n (%)	10	25	
Interruption of hepatic hilum			0.243
Yes	5	18	
No	16	29	
Relapse or refractory disease			0.600
Relapse	9	17	
Refractory	12	30	
CEA level*			0.210
Mean ± SE, ng/ml	47.66 ± 29.06	54.01 ± 33.72	
Negative	4	16	
Positive	17	31	
CA199[#]			0.349
Mean ± SE, U/ml	3879.2 ± 1823.3	4211.3 ± 2201.3	
Negative	6	19	
Positive	15	28	

[&]Tumor stage was defined according to the American Joint Committee on Cancer (AJCC) TNM staging system (AJCC 7th edition).

**CEA levels were measured in 16 and 38 patients, respectively, in MiniPDX-guided and experimental treatment groups. A CEA level of <5 ng/ml was considered as negative.*

[#]CA19-9 levels were measured in 17 and 40 patients, respectively, in MiniPDX-guided and experimental treatment groups. A CA19-9 level of <37 U/ml was considered as negative.

CA19-9, carbohydrate antigen 19-9; CEA, carcinoma embryonic antigen; ECOG PS, Eastern Cooperative Oncology Group physical status; PDX, patient-derived xenograft.

Efficacy Prediction and Medication Regimens by MiniPDX Model

As presented in **Figure 1B**, the sensitivity of 11 kinds of drugs, including 5-FU, Anlotinib, Apatinib, Capecitabine, Docetaxel, Gemcitabine, Irinotecan, Oxaliplatin, Paclitaxel, Regorafenib, and S-1, was tested in patients in the MiniPDX-guided group. Based on the results of MiniPDX, Apalitinib, Irinotecan, and Oxaliplatin seemed to show potential efficacy in the susceptibility tests, with both mean and median pooled T/C ratio less than 50%.

When patients were taken as subjects for analysis, 17 out of 21 patients were clinically administrated according to the results of MiniPDX tests, in whom at least one kind of drug with T/C less than 50%, which were considered the potential efficacy drugs (except for case #4, case #14, case #19, and case #21) (**Figures 1B, C**). The medication compliance to MiniPDX from physicians or patients was estimated to be 80.95%.

In addition, the medication regimens of these two groups were also assessed to evaluate the influence of MiniPDX on drug selection in clinical practice. With the exception of capecitabine (marginal difference P =0.048), the results showed no statistical difference between the MiniPDX group and patients receiving experimental treatment (**Figure 1D**). However, seven patients in the MiniPDX group received targeted drugs, including Anlotinib, Apatinib, and Regofenib, compared with no administration in the control group. Chi test showed significant difference (33.3 *vs.* 0%, P =0.032). The increased use of targeted drugs might contribute to the survival benefit.

Survival Outcomes and Subgroup Analysis

The median OS of the MiniPDX-guided group was estimated to be 9.4 months with 95% confidence interval (CI) of 7.9–11.2 months. Meanwhile, patients with experimental treatment had a median OS of 7.9 (95% CI: 7.2–8.7) months (**Figure 2A**). Log-rank test revealed a statistical difference between these two groups (HR=2.586, 95% CI=1.362–4.908, p=0.004) (**Table 2**). The 6- and 12-month survival rates were 78.9, 36.9, and 55.7, 17.8%, respectively, in the minPDX group and control group.

To explore the survival outcomes in more detail, subgroup analyses based on the baseline characteristics were conducted

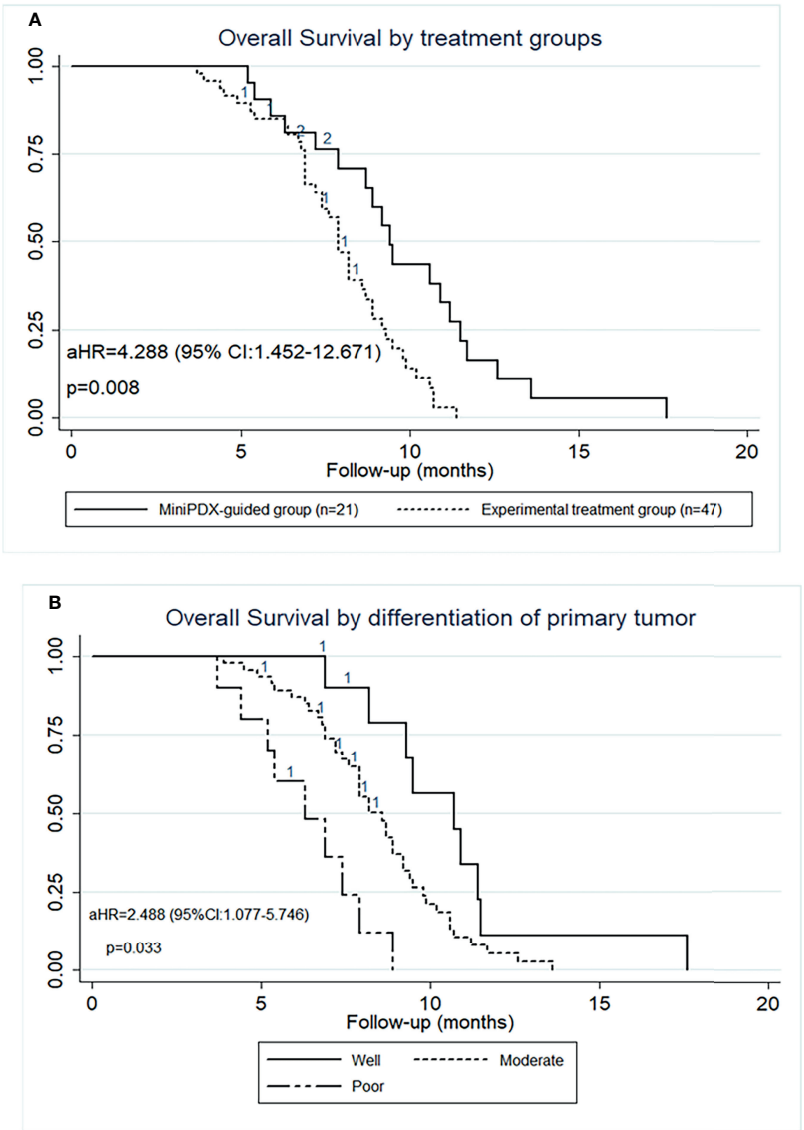

FIGURE 2 | OS outcomes of patients included in this study. **(A)** OS was significantly prolonged in cases who received the MiniPDX-guided regimens compared with the control group. **(B)** The poor-differentiation primary tumor was an independent risk factor for poor prognosis.

(**Table 2**). The univariate analysis revealed that patients who received MiniPDX-guided treatment, with primary tumor size less than 5 cm, with well- or moderated-differentiation tumor, and with hepatic metastases less than 5 cm were associated with improved survival outcomes of patients. Multivariate regression analyses suggested that treatment without MiniPDX test, poor-differentiation of the primary tumor (**Figure 2B**), N3 stage of the primary tumor were independent risk factors for the poor prognosis.

RECIST Response Status and Biomarkers Response

All the patients in these two groups received at least one RECIST evaluation after systematic treatment. Seventeen out of all 21 patients in the MiniPDX group was indicated at least one kind of potential drug use based on drug sensitivity tests. The correlation of the response rate between the MiniPDX test and the clinical response status was 70.6% (11/17) in these patients. ORR of the MiniPDX-guided group was 57.14%, which was significantly higher than 25.53% in the control group (p=0.029). Similarly, the DCR was also considerably improved in the MiniPDX group (85.71 *vs.* 68.08%, p=0.035). In addition, more patients experienced a CEA response in the MiniPDX-guided group (62.50 *vs.* 37.84%). However, the difference did not reach statistical significance (p=0.174). Meanwhile, treatment with MiniPDX-guided drugs was associated with improved CA19-9 response

TABLE 2 | Univariate and multivariate Cox proportional hazards regression analysis of overall survival.

Characteristics	Median OS months	Univariate HR (95% CI)	P-value	Multivariate aHR[&](95% CI)	P-value[&]
Treatment		2.586 (1.362–4.908)	0.004	4.288 (1.452–12.671)	0.008
MiniPDX-guided group, n=21	9.4 (7.9–11.2)				
Experimental treatment group, n=47	7.9 (7.2–8.7)				
Age		1.613 (0.947–2.747)	0.078	NA	NA
<65, n=31	8.9 (7.9–9.5)				
≥65, n=37	7.4 (6.9–8.7)				
Sex		0.747 (0.442–1.263)	0.277	NA	NA
Male, n=39	8.2 (6.9–9.2)				
Female, n=29	8.6 (7.9–9.9)				
ECOG PS		1.294 (0.710–2.359)	0.400	NA	NA
0–1, n=52	8.7 (7.4–9.2)				
2, n=16	8.2 (7.2–9.5)				
Primary gastric tumors size		2.008 (1.163–3.469)	0.012	1.624 (0.674–3.915)	0.280
<5 cm, n=31	8.9 (8.2–10.2)				
≥5 cm, n=37	7.6 (6.9–8.9)				
Differentiation of primary tumor		2.780 (1.612–4.791)	0.000	2.488 (1.077–5.746)	0.033
Well, n=11	10.7 (6.9–11.5)				
Moderate, n=47	8.6 (7.6–9.2)				
Poor, n=10	6.3 (3.7–7.9)				
T-stage of primary tumor		1.211 (0.887–1.654)	0.277	NA	NA
pT1, n=9	8.9 (7.2–10.6)				
pT2, n=16	8.9 (6.9–10.7)				
pT3, n=33	8.2 (7.4–9.2)				
pT4, n=10	6.9 (5.3–8.7)				
N-stage of primary tumor		1.441 (1.087–1.912)	0.011	1.467 (1.007–2.138)	0.046
N0, n=10	9.3 (6.9–10.9)				
N1, n=28	8.2 (7.4–9.4)				
N2, n=17	7.9 (6.3–9.5)				
N3, n=13	7.6 (4.9–8.7)				
Number of metastases		1.149 (0.820–1.639)	0.426	NA	NA
Solitary, n=31	9.8 (6.3–11.2)				
2–5, n=24	9.2 (6.8–9.9)				
>5, n=13	8.2 (7.4–8.9)				
Metastases tumors size		1.830 (1.078–3.107)	0.025	1.351 (0.589–3.103)	0.478
<5 cm, n=34	9.2 (7.9–9.9)				
≥ 5cm, n=34	7.6 (6.4–8.7)				
Metastases lesions location		0.876 (0.627–1.224)	0.438	NA	NA
Left lobe, n=15	7.9 (4.9–9.8)				
Right lobe, n=18	8.2 (7.9–8.9)				
Both, n=35	8.6 (7.2–9.5)				
Interruption of hepatic hilum		0.599 (0.335–1.071)	0.084	NA	NA
Yes, n=24	7.9 (6.8–8.2)				
No, n=44	8.9 (7.9–9.4)				
Relapse or refractory disease		1.136 (0.736–1.563)	0.535	NA	NA
Relapse, n=26	8.6 (6.8–10.7)				
Refractory, n=42	8.2 (7.4–9.9)				
CEA level*		0.810 (0.461–1.425)	0.466	NA	NA
Negative, n=16	8.6 (6.9–9.2)				
Positive, n=38	8.2 (7.4–9.4)				
CA199[#]		1.021 (0.585–1.781)	0.942	NA	NA
Negative, n=17	8.6 (7.6–9.3)				
Positive, n=40	7.9 (7.2–9.4)				

**CEA levels were measured in 16 and 38 patients, respectively, in MiniPDX-guided and experimental treatment groups. A CEA level of <5 ng/ml was considered as negative.*

[#]CA19-9 levels were measured in 17 and 40 patients, respectively, in MiniPDX-guided and experimental treatment groups. A CA19-9 level of <37 U/ml was considered as negative.

[&]These results were adjusted by multiple variables identified in univariate analyses, including treatment group, primary gastric tumors size, differentiation of primary tumor, N-stage of primary tumor, metastases tumors size.

CA19-9, carbohydrate antigen 19-9; CEA, carcinoma embryonic antigen; ECOG PS, Eastern Cooperative Oncology Group physical status; PDX, patient-derived xenograft; OS, overall survival; NA, not applicated.

status compared with the control group (p=0.009) (**Table 3**). **Figure 3** shows the CT images and the CA19-9 response status of one 67-year-old patient who received MiniPDX-guided regimen.

DISCUSSION

Most gastric cancer patients with concomitant liver metastases were excluded from being candidates for curative surgery

TABLE 3 | Metrics of RECIST response, CEA response, and CA 19-9 response to different groups.

Characteristics	MiniPDX-guided group (n = 21)	Experimental treatment group (n = 47)	p-value
RECIST 1.1			0.038
CR	0	0	
PR	12 (57.14%)	12 (25.53%)	
SD	6 (28.57%)	20 (42.55%)	
PD	3 (14.29%)	15 (31.91%)	
ORR	12 (57.14%)	12 (25.53%)	0.029
DCR	18 (85.71%)	32 (68.08%)	0.035
CEA parameters*			0.174
Decrease >50%	10 (62.50%)	14 (37.84%)	
Decrease >20%	4 (25.00%)	12 (32.43%)	
Decrease <20% or increase	2 (12.50%)	11 (29.73%)	
CA 19-9 parameters#			0.009
Decrease >50%	12 (70.59%)	12 (30.0%)	
Decrease >20%	2 (11.76%)	18 (45.00%)	
Decrease <20% or increase	3 (17.65%)	10 (25.00%)	

**CEA levels were evaluated in 16 and 37 patients, respectively, in the MiniPDX-guided and control groups.*

#CA19-9 levels were tested in 17 and 40 patients, respectively, in the MiniPDX-guided and control groups.

CA19-9, carbohydrate antigen 19-9; CEA, carcinoma embryonic antigen; CR, complete response; DCR, disease control rate; ECOG PS, Eastern Cooperative Oncology Group physical status; ORR, objective response rate; PD, progressive disease; PDX, patient-derived xenograft; PR, partial response; SD, stable disease.

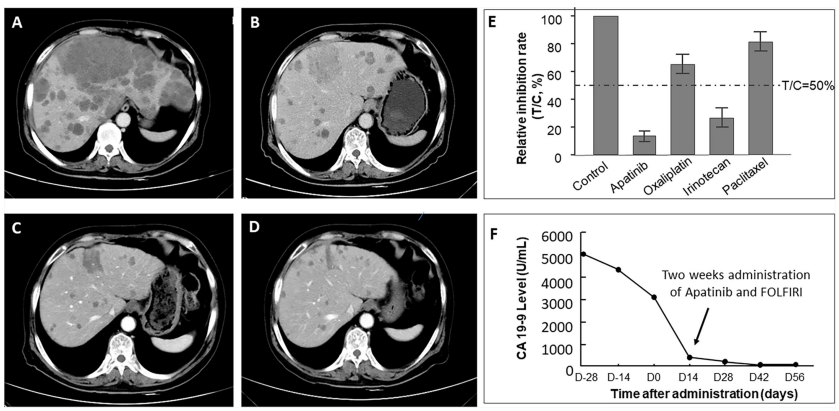

FIGURE 3 | CT images of one 67-year-old patient who received MiniPDX-guided regimen. **(A)** The patient suffered a progressive disease after six cycles of XELOX as first-line treatment. **(E)** The MiniPDX test revealed that this patient was resistant to Paclitaxel and Oxaliplatin and was sensitive to Irinotecan and Apatinib. **(B)** Two cycles after second-line Apatinib and FOLFIRI (Irinotecan and 5-FU) treatment, hepatic metastases shrank obviously. **(C)** Three cycles and **(D)** four cycles after Apatinib and FOLFIRI administration, lesions in the liver continue to shrink. **(F)** CA19-9 levels significantly decrease to negative (<37 U/ml) after 2 weeks of Apatinib and FOLFIRI administration and maintain low levels in the follow-up period.

accompanied by hepatic resection due to the simultaneous presence of incurable factors such as peritoneal dissemination, widespread lymph nodal metastasis, and direct invasion to adjacent structures (23). In fact, hepatic metastases to gastric cancer usually represent only a fraction of the broader spread of the primary tumor. In our research, tumor cells were enriched from biopsy samples of 21 patients with GCLM, followed by establishing a MiniPDX model and the formulation of individualized chemotherapy regimens based on drug sensitivity test results. The results confirmed that MiniPDX-guided chemotherapy was more beneficial to GCLM patients than conventional treatment, which might have some implications for oncologists making informed decisions about individualized chemotherapy.

For patients who relapsed or were refractory to first-line treatment (e.g., 5-FU and platinum), second-line chemotherapy regimes, including SPA (S-1 and Paclitaxel) (24), XELOX (capecitabine and oxaliplatin) (25, 26), DOCOX (Docetaxel plus oxaliplatin) (27), S-1 monotherapy, XELIRI (capecitabine and irinotecan) (28), and some newly developed targeted drugs (e.g., Apatinib monotherapy) (29), have failed to show an adequate response to them. The OS and PFS were pooled to be approximately 7.0 and 4.5 months, respectively, in advanced gastric cancer. Our results on the control group showed a median OS and PFS of 7.9 and 4.2 months, which is in accordance with previous results, and indirectly confirmed the robust results of this study.

PDX models, either heterotopic or orthotopic implantation, allow invaluable assessment of human tumor biology, therapeutic targets, and drug evaluation based on the principle of biological stability and accurately reflecting the tumor characteristic of patients (30–32). But lengthy test period and unsatisfactory engraftment rate prevent the wide application of PDX in some high-grade malignant tumors, especially in gastric cancer (33). MiniPDX is a rapid, systematic *in vivo* assay to measure drug sensitivity of tumor cells and takes only 7 days. As Zhang et al. reported, MiniPDX could overcome the limitations of PDX and retain the accuracy and efficiency, compared to PDX models, with 92% of positive value, 81% negative value, 80% sensitivity, and 90% specificity (19).

The clinical application of MiniPDX has become more prevalent in recent years; increasing encouraging results on MiniPDX were reported (34). Zhan et al. used MiniPDX to guide the selection of chemotherapeutic regimens in patients with gallbladder carcinoma, who had significantly longer median PFS (17.6 months *vs.* 12.0 months, P=0.014) and overall survival (18.6 months *vs.* 13.9 months, P=0.030) than patients with conventional chemotherapy (20). In another case reported by Zhao et al., personalized treatment based on MiniPDX and whole-exome sequencing in a patient with metastatic duodenal adenocarcinoma demonstrated that this combination could rapidly assess drug sensitivity and reveal significant genetic alterations (21). Also, the study by Yang et al. showed a significant benefit from the MiniPDX test than the control group in hepatocellular carcinoma (DFS: 25.8 months *vs.* 18.2 months, P=0.022) (35). Similar results were validated in ovarian cancer (36) and lung cancer (37). In our study, individual chemotherapy based on MiniPDX also showed superiority to prolong the OS and PFS of patients with GCLM, which could consider solid validation evidence for previous studies.

In terms of the response status, our study showed that ORR and DCR were also higher in the MiniPDX group than in the experimental treatment group. Moreover, the biomarkers' levels of CEA and CA19-9 have also achieved a better response status in the MiniPDX group. The correlation of the response rate between the MiniPDX test and the clinical response status was estimated to be 70.6% in those MiniPDX, indicating a T/C ratio of less than 50%. Considering the other four cases, two patients did not achieve a clinical response with drugs in the test list.

It should be noted that the MiniPDX test significantly increased the selection of targeted drugs, including Apatinib, Anlotinib, and Regorafenib. It might contribute to the response and survival benefit of patients who received MiniPDX-guided therapy. This suggested that MiniPDX is not about finding the more potent drugs, but about finding the more appropriate drugs for individuals. This concept is to fully respect the tumor heterogeneity of the patients to achieve personalized treatment. The difference between these two groups was not significant to each drug individually, which may be due to the limited sample size and statistical power. Moreover, based on the baseline tumor characteristics in the present study, we found that our enrolled patients had predominantly moderately to poorly differentiated tumors in both observasion and control groups (18/21 *vs.* 40/47), which indicates a poor prognosis in clinical practices. Subsequent multivariate analysis also showed that moderately to poorly differentiated tumor was an independent risk factor for poor prognosis after adjustment by the MiniPDX application (P =0.033). The above results suggested that MiniPDX, although showing statistically promising results for the overall cohort, did not overcome the inherent independent risk factors, like moderately or poorly differentiated tumors, similarly, N-stage of N1 to N3.

Some limitations of this research should be acknowledged. Firstly, the limited number of participants, especially in the MiniPDX group, may affect the reliability and statistical power of this analysis. Secondly, the timing of MiniPDX testing, whether it should be performed in first-line or second-line therapy, needs further discussion. Therefore, the conclusions of this study need to be further verified in a randomized controlled clinical trial with a larger sample size. Nevertheless, our research indicated the MiniPDX-guided chemotherapy regimen selected the most effective drugs or regimens to treat GCLM patients and could effectively improve patient outcomes. Our results might provide a meaningful and exploratory basis for the precise treatment of GCLM and even other solid tumors in the future.

In conclusion, treatment based on MiniPDX is promising to improve the survival and response of GCLM patients in this preliminary study. OncoVee™-MiniPDX models have potential in the treatment of other aggressive tumors. However, further well-designed clinical trials with a larger sample size are necessary to verify the results of this study.

DATA AVAILABILITY STATEMENT

The raw data supporting the conclusions of this article will be made available by the authors, without undue reservation.

ETHICS STATEMENT

The studies involving human participants were reviewed and approved by the ethics committee of Nanjing First Hospital. The patients/participants provided their written informed consent to participate in this study. The animal study was reviewed and approved by the ethics committee of Nanjing First Hospital. Written informed consent was obtained from the individual(s) for the publication of any potentially identifiable images or data included in this article.

AUTHOR CONTRIBUTIONS

All authors contributed to the conception and design. XW and JS supervised the study. Material preparation, data collection, and analysis were performed by YG and XZ. YG, XZ, WL, CT, and

DG drafted the manuscript. XW and JS critically revised the manuscript for important intellectual content. All our authors contributed to the article and approved the submitted version.

FUNDING

This study was supported by the National Natural Science Foundation of China (No. 81773240), the Nanjing Medical Science and Technique Development Foundation (No. QRX17062), and the Nanjing Health Science and Technology Development Foundation (No. JQX18004).

ACKNOWLEDGMENTS

We appreciate Dr. Danyi Wen (LIDE Biotech Inc.) for providing technical support on OncoVee™-MiniPDX models.

REFERENCES

1. Sung H, Ferlay J, Siegel RL, Laversanne M, Soerjomataram I, Jemal A, et al. Global Cancer Statistics 2020: GLOBOCAN Estimates of Incidence and Mortality Worldwide for 36 Cancers in 185 Countries. *CA Cancer J Clin* (2021) 71(3):209–49. doi: 10.3322/caac.21660
2. Zhao LL, Huang H, Wang Y, Wang TB, Zhou H, Ma FH, et al. Lifestyle Factors and Long-Term Survival of Gastric Cancer Patients: A Large Bidirectional Cohort Study From China. *World J Gastroenterol* (2020) 26 (14):1613–27. doi: 10.3748/wjg.v26.i14.1613
3. Klint A, Engholm G, Storm HH, Tryggvadottir L, Gislum M, Hakulinen T, et al. Trends in Survival of Patients Diagnosed With Cancer of the Digestive Organs in the Nordic Countries 1964-2003 Followed Up to the End of 2006. *Acta Oncol* (2010) 49(5):578–607. doi: 10.3109/02841861003739330
4. Riihimaki M, Hemminki A, Sundquist K, Sundquist J, Hemminki K. Metastatic Spread in Patients With Gastric Cancer. *Oncotarget* (2016) 7 (32):52307–16. doi: 10.18632/oncotarget.10740
5. Kakeji Y, Morita M, Maehara Y. Strategies for Treating Liver Metastasis From Gastric Cancer. *Surg Today* (2010) 40(4):287–94. doi: 10.1007/s00595-009-4152-0
6. Cheung ST, Chan SL, Lo KW. Contaminated and Misidentified Cell Lines Commonly Use in Cancer Research. *Mol Carcinog* (2020) 59(6):573–4. doi: 10.1002/mc.23189
7. Williams JA. Using PDX for Preclinical Cancer Drug Discovery: The Evolving Field. *J Clin Med* (2018) 7(3):41. doi: 10.3390/jcm7030041
8. Jeong SY, Cho YJ, Ryu JY, Choi JJ, Hwang JR, Kim B, et al. Establishment and Preclinical Application of a Patient-Derived Xenograft Model for Uterine Cancer. *Gynecol Oncol* (2021) 162(1):173–81. doi: 10.1016/j.ygyno.2021.04.028
9. Jiang W, Xie S, Liu Y, Zou S, Zhu X. The Application of Patient-Derived Xenograft Models in Gynecologic Cancers. *J Cancer* (2020) 11(18):5478–89. doi: 10.7150/jca.46145
10. Lai Y, Wei X, Lin S, Qin L, Cheng L, Li P. Current Status and Perspectives of Patient-Derived Xenograft Models in Cancer Research. *J Hematol Oncol* (2017) 10(1):106. doi: 10.1186/s13045-017-0470-7
11. Kita K, Fukuda K, Takahashi H, Tanimoto A, Nishiyama A, Arai S, et al. Patient-Derived Xenograft Models of Non-Small Cell Lung Cancer for Evaluating Targeted Drug Sensitivity and Resistance. *Cancer Sci* (2019) 110 (10):3215–24. doi: 10.1111/cas.14171
12. van Weerden WM. Patient-Derived Xenograft Models in Cancer Research. *Cancers (Basel)* (2021) 13(4):815. doi: 10.3390/cancers13040815
13. Hidalgo M, Bruckheimer E, Rajeshkumar NV, Garrido-Laguna I, De Oliveira E, Rubio-Viqueira B, et al. A Pilot Clinical Study of Treatment Guided by Personalized Tumorgrafts in Patients With Advanced Cancer. *Mol Cancer Ther* (2011) 10(8):1311–6. doi: 10.1158/1535-7163.MCT-11-0233
14. Stebbing J, Paz K, Schwartz GK, Wexler LH, Maki R, Pollock RE, et al. Patient-Derived Xenografts for Individualized Care in Advanced Sarcoma. *Cancer* (2014) 120(13):2006–15. doi: 10.1002/cncr.28696
15. Fujii E, Kato A, Suzuki M. Patient-Derived Xenograft (PDX) Models: Characteristics and Points to Consider for the Process of Establishment. *J Toxicol Pathol* (2020) 33(3):153–60. doi: 10.1293/tox.2020-0007
16. Shi J, Li Y, Jia R, Fan X. The Fidelity of Cancer Cells in PDX Models: Characteristics, Mechanism and Clinical Significance. *Int J Cancer* (2020) 146 (8):2078–88. doi: 10.1002/ijc.32662
17. Risbridger GP, Lawrence MG, Taylor RA. PDX: Moving Beyond Drug Screening to Versatile Models for Research Discovery. *J Endocr Soc* (2020) 4(11):bvaa132. doi: 10.1210/jendso/bvaa132
18. Annibali D, Leucci E, Hermans E, Amant F. Development of Patient-Derived Tumor Xenograft Models. *Methods Mol Biol* (2019) 1862:217–25. doi: 10.1007/978-1-4939-8769-6_15
19. Zhang F, Wang W, Long Y, Liu H, Cheng J, Guo L, et al. Characterization of Drug Responses of Mini Patient-Derived Xenografts in Mice for Predicting Cancer Patient Clinical Therapeutic Response. *Cancer Commun (Lond)* (2018) 38(1):60. doi: 10.1186/s40880-018-0329-5
20. Zhan M, Yang RM, Wang H, He M, Chen W, Xu SW, et al. Guided Chemotherapy Based on Patient-Derived Mini-Xenograft Models Improves Survival of Gallbladder Carcinoma Patients. *Cancer Commun (Lond)* (2018) 38(1):48. doi: 10.1186/s40880-018-0318-8
21. Zhao P, Chen H, Wen D, Mou S, Zhang F, Zheng S. Personalized Treatment Based on Mini Patient-Derived Xenografts and WES/RNA Sequencing in a Patient With Metastatic Duodenal Adenocarcinoma. *Cancer Commun (Lond)* (2018) 38(1):54. doi: 10.1186/s40880-018-0323-y
22. Li C, Sun YD, Yu GY, Cui JR, Lou Z, Zhang H, et al. Integrated Omics of Metastatic Colorectal Cancer. *Cancer Cell* (2020) 38(5):734–47.e9. doi: 10.1016/j.ccell.2020.08.002
23. Cavanna L, Bodini FC, Stroppa EM, Banchini F, Michieletti E, Capelli P, et al. Advanced Gastric Cancer With Liver and Lymph Node Metastases Successfully Resected After Induction Chemotherapy With Docetaxel, Cisplatin and 5-Fluorouracil. *Chemotherapy* (2014) 60(4):224–7. doi: 10.1159/000375156
24. Zheng Y, Fang W, Mao C, Qian J, Zhao P, Zhang X, et al. Biweekly S-1 Plus Paclitaxel (SPA) as Second-Line Chemotherapy After Failure From Fluoropyrimidine and Platinum in Advanced Gastric Cancer: A Phase II Study. *Cancer Chemother Pharmacol* (2014) 74(3):503–9. doi: 10.1007/s00280-014-2537-2
25. Kim C, Lee JL, Ryu MH, Chang HM, Kim TW, Lim HY, et al. A Prospective Phase II Study of Cetuximab in Combination With XELOX (Capecitabine and Oxaliplatin) in Patients With Metastatic and/or Recurrent Advanced Gastric Cancer. *Invest New Drugs* (2011) 29(2):366–73. doi: 10.1007/s10637-009-9363-0
26. Wang Y, Cheng X, Cui YH, Hou J, Ji Y, Sun YH, et al. Efficacy After Preoperative Capecitabine and Oxaliplatin (XELOX) Versus Docetaxel, Oxaliplatin and S1 (DOS) in Patients With Locally Advanced Gastric Adenocarcinoma: A Propensity Score Matching Analysis. *BMC Cancer* (2018) 18(1):702. doi: 10.1186/s12885-017-3767-6
27. Zhong H, Zhang Y, Ma S, Ying JE, Yang Y, Yong D, et al. Docetaxel Plus Oxaliplatin (DOCOX) as a Second-Line Treatment After Failure of Fluoropyrimidine and Platinum in Chinese Patients With Advanced Gastric Cancer. *Anticancer Drugs* (2008) 19(10):1013–8. doi: 10.1097/CAD.0b013e328314b5ab
28. Luo HY, Wang ZQ, Wang FH, Qiu MZ, Teng KY, Ruan DY, et al. Phase 2 Study of Capecitabine and Irinotecan Combination Chemotherapy (Modified XELIRI Regimen) in Patients With Advanced Gastric Cancer. *Am J Clin Oncol* (2011) 34(6):555–60. doi: 10.1097/COC.0b013e3181f47ac1
29. Scott LJ. Apatinib: A Review in Advanced Gastric Cancer and Other Advanced Cancers. *Drugs* (2018) 78(7):747–58. doi: 10.1007/s40265-018-0903-9
30. Hidalgo M, Amant F, Biankin AV, Budinska E, Byrne AT, Caldas C, et al. Patient-Derived Xenograft Models: An Emerging Platform for Translational Cancer Research. *Cancer Discovery* (2014) 4(9):998–1013. doi: 10.1158/2159-8290.CD-14-0001
31. Byrne AT, Alferez DG, Amant F, Annibali D, Arribas J, Biankin AV, et al. Interrogating Open Issues in Cancer Precision Medicine With Patient-Derived Xenografts. *Nat Rev Cancer* (2017) 17(4):254–68. doi: 10.1038/nrc.2016.140

32. Lorz A, Lorenzi T, Clairambault J, Escargueil A, Perthame B. Modeling the Effects of Space Structure and Combination Therapies on Phenotypic Heterogeneity and Drug Resistance in Solid Tumors. *Bull Math Biol* (2015) 77(1):1–22. doi: 10.1007/s11538-014-0046-4
33. Reddavid R, Corso S, Moya-Rull D, Giordano S, Degiuli M. Patient-Derived Orthotopic Xenograft Models in Gastric Cancer: A Systematic Review. *Updates Surg* (2020) 72(4):951–66. doi: 10.1007/s13304-020-00751-4
34. Wang J, Sun T, Meng Z, Wang L, Li M, Chen J, et al. XPO1 Inhibition Synergizes With PARP1 Inhibition in Small Cell Lung Cancer by Targeting Nuclear Transport of FOXO3a. *Cancer Lett* (2021) 503:197–212. doi: 10.1016/j.canlet.2021.01.008
35. Yang L, Yuan Z, Zhang Y, Cui Z, Li Y, Hou J, et al. MiniPDX-Guided Postoperative Anticancer Treatment can Effectively Prolong the Survival of Patients With Hepatocellular Carcinoma. *Cancer Chemother Pharmacol* (2021) 87(1):125–34. doi: 10.1007/s00280-020-04182-1
36. Huang Y, Xu J, Li K, Wang J, Dai Y, Kang Y. A Novel, Personalized Drug-Screening System for Platinum-Resistant Ovarian Cancer Patients: A Preliminary Clinical Report. *Cancer Manag Res* (2021) 13:2849–67. doi: 10.2147/CMAR.S276799
37. Wang X, Sun Y, Xu Y, Wen D, An N, Leng X, et al. Mini-Patient-Derived Xenograft Assay Based on Microfluidic Technology Promises to be an Effective Tool for Screening Individualized Chemotherapy Regimens for Advanced Non-Small Cell Lung Cancer. *Cell Biol Int* (2021) 45(9):1887–96. doi: 10.1002/cbin.11622

Conflict of Interest: The authors declare that the research was conducted in the absence of any commercial or financial relationships that could be construed as a potential conflict of interest.

Publisher's Note: All claims expressed in this article are solely those of the authors and do not necessarily represent those of their affiliated organizations, or those of the publisher, the editors and the reviewers. Any product that may be evaluated in this article, or claim that may be made by its manufacturer, is not guaranteed or endorsed by the publisher.

Copyright © 2022 Ge, Zhang, Liang, Tang, Gu, Shi and Wei. This is an open-access article distributed under the terms of the Creative Commons Attribution License (CC BY). The use, distribution or reproduction in other forums is permitted, provided the original author(s) and the copyright owner(s) are credited and that the original publication in this journal is cited, in accordance with accepted academic practice. No use, distribution or reproduction is permitted which does not comply with these terms.

frontiers in Oncology

ORIGINAL RESEARCH
published: 10 January 2022
doi: 10.3389/fonc.2021.789104

The Value of Perioperative Chemotherapy for Patients With Hepatoid Adenocarcinoma of the Stomach Undergoing Radical Gastrectomy

Kai Zhou[1†], Anqiang Wang[1†], Jingtao Wei[1†], Ke Ji[1], Zhongwu Li[2], Xin Ji[1], Tao Fu[1], Ziyu Jia[1], Xiaojiang Wu[1], Ji Zhang[1] and Zhaode Bu[1]*

[1] Gastrointestinal Cancer Center, Key Laboratory of Carcinogenesis and Translational Research (Ministry of Education), Peking University Cancer Hospital and Institute, Beijing, China, [2] Department of Pathology, Key Laboratory of Carcinogenesis and Translational Research (Ministry of Education), Peking University Cancer Hospital and Institute, Beijing, China

OPEN ACCESS

Edited by:
Luigi Marano, University of Siena, Italy

Reviewed by:
Juan Liao, Sichuan University, China
Jinping Lai, Kaiser Permanente Sacramento Medical Center, United States

***Correspondence:**
Zhaode Bu
buzhaode@cjcrcn.org

[†]These authors have contributed equally to this work and share first authorship

Specialty section:
This article was submitted to Gastrointestinal Cancers: Gastric & Esophageal Cancers, a section of the journal Frontiers in Oncology

Received: *04 October 2021*
Accepted: *20 December 2021*
Published: *10 January 2022*

Citation:
Zhou K, Wang A, Wei J, Ji K, Li Z, Ji X, Fu T, Jia Z, Wu X, Zhang J and Bu Z (2022) The Value of Perioperative Chemotherapy for Patients With Hepatoid Adenocarcinoma of the Stomach Undergoing Radical Gastrectomy. Front. Oncol. 11:789104. doi: 10.3389/fonc.2021.789104

Background: Hepatoid adenocarcinoma of the stomach (HAS) is a rare type of gastric cancer, but the role of perioperative chemotherapy is still poorly understood. The aim of this retrospective study was to investigate the associations between perioperative chemotherapy and prognosis of HAS.

Method: We retrospectively analyzed patients with locally advanced HAS who received radical surgery in Peking University Cancer Hospital between November 2009 and October 2020. Patients were divided into neoadjuvant chemotherapy-first (NAC-first) group and surgery-first group. The relationships between perioperative chemotherapy and prognosis of HAS were analyzed using univariate, multivariate survival analyses and propensity score matching analysis (PSM).

Results: A total of 100 patients were included for analysis, including 29 in the NAC-first group and 71 in the surgery-first group. The Her-2 amplification in HAS patients was 22.89% (19/83). For NAC-first group, 4 patients were diagnosed as tumor recession grade 1 (TRG1), 4 patients as TRG 2, and 19 patients as TRG 3. No significant difference in prognosis between the surgery-first group and the NAC-first group (P=0.108) was found using PSM analysis. In the surgery-first group, we found that the survival rate was better in group of ≥6 cycles of adjuvant chemotherapy than that of <6 cycles (P=0.013).

Conclusion: NAC based on platinum and fluorouracil may not improve the Overall survival (OS) and Disease-free survival time (DFS) of patients with locally advanced HAS. Patients who received ≥6 cycles of adjuvant chemotherapy had better survival. Therefore, the combination treatment of radical gastrectomy and sufficient adjuvant chemotherapy is recommended for patients with locally advanced HAS.

Keywords: hepatoid adenocarcinoma of stomach, neoadjuvant chemotherapy, adjuvant chemotherapy, prognosis, propensity score matching

INTRODUCTION

Hepatoid adenocarcinoma is characterized as histologically resembling hepatocellular carcinoma (HCC) with enteroblastic differentiation (1, 2). Hepatoid adenocarcinoma has been found in many extrahepatic organs, such as the stomach, ovary, gallbladder, colon, bladder, renal pelvis, lung, duodenum and pancreas, among which the stomach is the most prevalent (3–8). During the development of the human embryo, both the stomach and liver are primitive foregut derivatives and originate from the endoderm. Some gastric cancer cells may differentiate into early embryonic hepatocytes and then form hepatoid carcinoma of the stomach (HAS) (9, 10). Bourreille et al. reported the first case in 1970, a unique entity of gastric malignant tumor producing alpha-fetoprotein (AFP) with liver metastasis (11). Kodama et al. found that gastric cancer with AFP production had a well-differentiated papillary or tubular type and medullary type, and the latter was considered as hepatocellular carcinoma (12). In 1985, Ishikura et al. eventually expressly provided the term "hepatoid carcinoma of the stomach" (HAS) (13).

HAS is a rare subtype of gastric cancer (GC) that was previously reported to account for 0.38-1.6% of GC (5, 14). HAS mostly occurs in elderly male individuals without specific clinical manifestations and imaging features (15–17). HAS is mainly located in the gastric antrum and is prone to vascular invasion and early metastasis, specifically to the lymph nodes, liver and lung (15, 18, 19). According to current research, the treatment strategy for HAS is similar to gastric adenocarcinoma (15, 18). Radical surgery and adjuvant therapy are the standard treatments for resectable HAS (15, 20, 21). However, early disease recurrence and poor patient prognosis were still observed despite radical surgery with free margins (22, 23). Drugs for gastric cancer have been used as adjuvant chemotherapy (AC) or neoadjuvant chemotherapy (NAC) for a limited number of patients with HAS (5, 23, 24), and there are no definitive specific chemotherapy regimens that are beneficial for patients with HAS. In summary, there is no unanimous conclusion on the most appropriate therapeutic strategy for HAS (16).

Theoretically, NAC can resolve micrometastatic lesions (25) and alleviate disease development, thus reducing the overall mortality rate of patients with cancer. NAC provides a valuable opportunity to evaluate the effectiveness of chemotherapy, which is one of the standard treatments for advanced gastric cancer (26). However, the true effect of NAC for gastric cancer is unknown (27). The results of some studies have suggested that NAC may lead to short-term postoperative complications, which delay the implementation of AC after surgery. If the NAC protocol is ineffective against GC, there is a risk of cancer progression during the period of NAC treatment (28). However, due to the scarcity of the literature, there is minimal information available on the role of perioperative chemotherapy for HAS. Accordingly, we conducted a single-center retrospective study to elucidate the effects of NAC and AC in patients with HAS and the prognostic factors related to HAS.

MATERIALS AND METHODS

Enrollment of Patients

We consecutively enrolled patients with HAS who underwent curative total or partial gastrectomy with D2 lymph nodes (LNs) dissection between November 2009 and October 2020. We selected patients who were pathologically diagnosed with HAS after radical gastrectomy and with clinical stage T3/T4 or N+ disease. The exclusion criteria were as follows: (1) perioperative death, (2) R0 resection was not performed, (3) preoperative or postoperative radiotherapy, (4) clinical stage IVb, and (5) pathological stage I patients without high risk factors, which included age below 40 years old, poor differentiation and lymphovascular invasion. Patients who received preoperative chemotherapy were defined as neoadjuvant chemotherapy-first (NAC-first) group, and patients who did not receive preoperative treatment were defined as surgery-first group. Clinicopathological features were retrospectively collected and all patients were followed up. We used abdominal and pelvic computed tomography (CT) to assess the clinical stage using the American Joint Committee on Cancer/Union for International Cancer Control 8th classification system. Enlarged LNs over 8 mm at their largest axis or with internal necrosis were classified as cN+. This retrospective study was performed according to the tenets of the Declaration of Helsinki and was approved by the Institutional Review Board of Peking University Cancer Hospital.

A total of 125 HAS patients were eligible for the study. Twenty-five patients were excluded, of whom 13 patients were diagnosed with distant metastases, 2 patients had postoperative residual lesions, 4 patients accepted perioperative radiotherapy, one patient died perioperatively and 5 patients were diagnosed with pathological stage I without high risk factors or other types of tumor differentiation. Eventually, 29 patients were included in the NAC-first group and 71 patients were included in the surgery-first group, for a total of 100 patients (**Figure 1**).

Pathological Diagnosis and Treatment Evaluation

Pathological diagnosis was based on morphological features and immunohistochemistry, including hepatoid and/or adenocarcinoma components, by two independent pathologists (**Supplementary Figure 1**). Clinical responses to NAC were assessed based on CT scans according to the Response Assessment Criteria for Solid Tumors version 1.1 (29). The assessment of target lesions was divided into the following four categories: complete remission (CR), partial remission (PR), stable disease (SD), and progressive disease (PD). According to the NCCN guidelines for gastric cancer (2018), the pathological response was graded according to the 3-point tumor regression grading (TRG) system (30). The tumors were divided into the following four grades: grade 0 (no visible cancer cells), grade 1 (single cells or small groups of cancer cells), grade 2 (residual cancer outgrown by fibrosis) and grade 3 (significant fibrosis outgrown by cancer or no fibrosis with extensive residual cancer). We also evaluated the toxicities related to NAC by the WHO standard criteria.

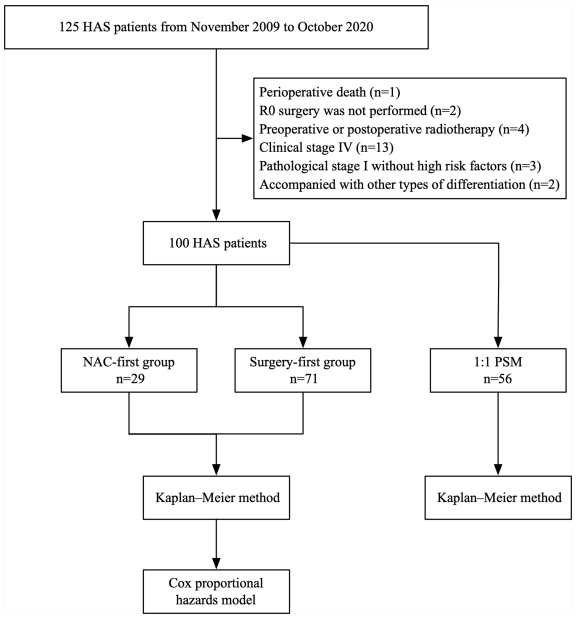

FIGURE 1 | Schematic of the study design. The chart showed the selection of patients and study methods.

Follow-Up

The patients underwent follow-up gastroscopy, abdominal and pelvic computed tomography, chest radiography and tumor biomarkers at our hospital or local hospital 3 months after the operation and every 3 or 6 months thereafter. Overall survival time (OS) was defined as the length of time from the date of first NAC treatment or radical gastrectomy to the date of the last follow-up or the date of death from any cause. Disease-free survival time (DFS) was defined as the length of time from the date of first NAC treatment or radical gastrectomy to the date of disease recurrence, metastasis or death from any cause or the date of last follow-up. The mean follow-up time was 30.5 months, ranging from 2.4 to 102.6 months.

Statistical Analysis

To compare the clinicopathological features of the NAC-first and surgery-first groups, SPSS 23.0 was used for statistical analysis. Independent sample *t*-tests were used for continuous variables. The chi-square test or Mann-Whitney *U* test was used for categorical variables. Propensity score matching analysis (PSM) was used to reduce the impact of possible confounding factors. The 1:1 PSM method (match tolerance 0.2) was conducted to compare the NAC-first and surgery-first groups. To estimate the long-term OS and DFS outcomes, the Kaplan–Meier method and a log-rank test were used. To evaluate the independent predictors of OS and DFS, variables with $P<0.10$ in univariate survival analyses or with clinical significance were entered into the multiple regression analysis using the Cox proportional hazards model. $P<0.05$ was considered statistically significant. GraphPad Prism 5 was used to draw the Kaplan-Meier survival curve.

RESULTS

Clinicopathologic Features of Included Patients and PSM

We found that there were differences in sex, tumor location, clinical T, N, TNM stage, lymphovascular invasion, nerve invasion, PDL-1 and SALL4 expression between the NAC-first group and the surgery-first group ($P<0.1$). The positive expression rate of Her-2 (staining by immunohistochemistry 3+ or with positive fluorescence *in situ* hybridization) in HAS patients was 22.89% (19/83). In the surgery-first group, 23% (14/61) of the patients were Her-2 positive. In the NAC-first group, 22.7% (5/22) of the patients were Her-2 positive. In addition, 91.7% (88/96) of the patients had AFP-positive cells as determined by immunohistochemistry. The number of patients with stage cIII/IVa disease in the NAC-first group was substantially higher than that in the surgery-first group (100% versus 78.9%, $P=0.01$). However, lymphovascular invasion were more prevalent in the surgery-first group than in the NAC-first group (67.6% vs 44.8%, $P=0.03$) (**Table 1**). Nerve invasion levels were also similar (63.4% vs 41.4%, $P=0.04$) (**Table 1**). To reduce confounding bias, 1:1 PSM was performed, and 56 patients were ultimately included. Most clinicopathological features were not significantly different between the two groups after 1:1 PSM (**Table 1**).

Regimens, Cycles, Adverse Effects and Clinical Response to NAC

In our study, 29 patients underwent NAC. Of these, 19 patients received S-1+oxaliplatin (SOX), 6 patients received oxaliplatin + capecitabine (XELOX), one received SOX+ paclitaxel + trastuzumab, one received XELOX+ trastuzumab, one received docetaxel+ cisplatin+ fluorouracil (DCF) and one received oxaliplatin+ calcium folinate+ fluorouracil (mFOLFOX). The median course of NAC was 3 cycles (1-5 cycles).

In the SOX regimen, one patient developed grade 1 gastrointestinal discomfort, and the main clinical manifestation was nausea and vomiting. One patient developed grade 1 gastrointestinal discomfort and neurotoxicity. Fourteen patients did not exhibit side effects during NAC. In the XELOX regimen, one patient experienced grade 3 gastrointestinal discomfort and grade 2 thrombocytopenia. One patient developed grade 1 neutropenia and leukopenia, grade 2 thrombocytopenia and slight numbness in the extremities. In the SOX+ paclitaxel + trastuzumab, DCF and mFOLFOX regimens, no toxicities were observed during NAC.

In the NAC-first group, a total of 6 patients achieved partial remission (PR), 20 patients achieved stable disease (SD), 1 patient had progressive disease (PD) and none achieved complete remission (CR). In the SOX regimen, pathological responses of TRG 1, 2 and 3 were observed in 2, 2 and 13 patients, respectively. In the XELOX regimen, TRG 1, 2 and 3 were observed in 0, 0, and 6 patients, respectively. Pathological responses of other chemotherapy regimens were shown in **Table 2**.

TABLE 1 | Baseline demographics of the study population before and after propensity score matching.

Clinicopathological features		Before PSM			After 1:1 PSM		
		Surgery-first N=71	NAC-first N=29	P value	Surgery-first N=28	NAC-first N=28	P value
Age (year)		61.056 ± 10.70	59.379 ± 7.50	0.44	62 ± 8.2642	59.714 ± 7.423	0.28
Gender	Female	22 (31)	3 (10.3)	0.03	3 (10.7)	2 (7.1)	1.00
	Male	49 (69)	26 (89.7)		25 (89.3)	26 (92.9)	
KPS score	80	2 (2.8)	0 (0)	0.92	–	–	0.32
	90	14 (19.7)	7 (24.1)		4 (14.3)	7 (25)	
	100	55 (77.5)	22 (75.9)		24 (85.7)	21 (75)	
Location of tumor	GEJ	15 (21.10)	13 (44.8)	0.02	9 (32.1)	13 (46.4)	0.27
	Non-GEJ	56 (78.9)	16 (55.2)		19 (67.9)	15 (53.6)	
Family history of cancer	No	56 (78.9)	22 (75.9)	0.74	22 (78.6)	21 (75)	0.75
	Yes	15 (21.1)	7 (24.1)		6 (21.4)	7 (25)	
Clinical T stage	1	2 (2.8)	0 (0)	0.01	–	–	0.17
	2	3 (4.2)	0 (0)		–	–	
	3	34 (47.9)	8 (27.6)		13 (46.4)	8 (28.6)	
	4a/b	32 (45.1)	21 (72.4)		15 (53.6)	20 (71.4)	
Clinical N stage	–	11 (15.5)	0 (0)	0.03	1 (3.6)	0 (0)	0.32
	+	60 (84.5)	29 (100)		27 (96.4)	28 (100)	
Clinical TNM stage	IIa	5 (7)	0 (0)	0.01	–	–	0.32
	IIb	10 (14.1)	0 (0)		1 (3.6)	0 (0)	
	III	55 (77.5)	28 (96.6)		27 (96.4)	28 (100)	
	IVa	1 (1.4)	1 (3.4)		–	–	
Number of lymph node dissection	<16	0 (0)	2 (6.9)	0.42	0 (0)	2 (7.1)	0.21
	16-30	30 (42.3)	12 (41.4)		9 (32.1)	11 (39.3)	
	>30	41 (57.7)	15 (51.7)		19 (67.9)	15 (53.6)	
AC	No	7 (10.3)	3 (10.7)	1.00	0 (0)	3 (11.1)	0.24
	Yes	61 (89.7)	25 (89.3)		27 (100)	24 (88.9)	
Cycles of perioperative chemotherapy	0	7 (10.3)	0 (0)	0.617			0.535
	<6	14 (20.6)	8 (28.6)		6 (22.2)	8 (29.6)	
	≥6	47 (69.1)	20 (71.4)		21 (77.8)	19 (70.4)	
Borrmann type	I	4 (7)	1 (4.2)	0.84	3 (13.6)	1 (4.3)	0.95
	II	15 (26.3)	6 (25)		4 (18.2)	6 (26.1)	
	III	36 (63.2)	17 (70.8)		14 (63.6)	16 (69.6)	
	IV	2 (3.5)	0 (0)		1 (4.5)	0 (0)	
Degree of differentiation	High/middle differentiation	43 (60.6)	17 (58.6)	0.86	19 (67.9)	16 (57.1)	0.41
	Low/undifferentiation	28 (39.4)	12 (41.4)		9 (32.1)	12 (42.9)	
Lauren type	Intestinal type	35 (49.3)	19 (65.5)	0.26	13 (46.4)	19 (67.9)	0.08
	Diffuse type	12 (16.9)	2 (6.9)		1 (3.6)	2 (7.1)	
	Mixed type	24 (33.8)	8 (27.6)		14 (50)	7 (25)	
Surgery type	Proximal gastrectomy	3 (4.2)	2 (6.9)	0.74	0 (0)	2 (7.1)	0.79
	Distal gastrectomy	37 (52.1)	13 (44.8)		14 (50)	12 (42.9)	
	Total gastrectomy	31 (43.7)	14 (48.3)		14 (50)	14 (50)	
Lymphovascular invasion	–	23 (32.4)	16 (55.2)	0.03	13 (46.4)	15 (53.6)	0.59
	+	48 (67.6)	13 (44.8)		15 (53.6)	13 (46.4)	
Nerve invasion	–	26 (36.6)	17 (58.6)	0.04	15 (53.6)	16 (57.1)	0.79
	+	45 (63.4)	12 (41.4)		13 (46.4)	12 (42.9)	
Postoperative metastasis	no	60 (84.50)	21 (72.4)	0.16	24 (85.7)	20 (71.4)	0.19
	yes	11 (15.5)	8 (27.6)		4 (14.3)	8 (28.6)	
C-met	–	8 (11.6)	2 (7.7)	0.99	3 (10.7)	2 (8)	0.79
	+	37 (53.6)	15 (57.7)		14 (50)	14 (56)	
	++	19 (27.5)	9 (34.6)		9 (32.1)	9 (36)	
	+++	5 (7.2)	0 (0)		2 (7.1)	0 (0)	
EGFR	–	2 (2.9)	1)3.8)	0.18	0 (0)	1 (4)	0.90
	+	10 (14.5)	2 (7.7)		1 (3.6)	2 (8)	
	++	38 (55.1)	12 (46.2)		18 (64.3)	12 (48)	
	+++	19 (27.5)	11 (42.3)		9 (32.1)	10 (40)	
HER-2	-/±	47 (68.1)	17 (63)	0.54	19 (67.9)	16 (61.5)	0.53
	++	8 (11.6)	5 (18.5)		3 (10.7)	5 (19.2)	
	+++	14 (20.3)	5 (18.5)		6 (21.4)	5 (19.2)	
MMR	pMMR	58 (98.3)	24 (100)	1.00	22 (95.7)	23 (100)	0.32
	dMMR	1 (1.7)	0 (0)		1 (4.3)	0 (0)	
PDL1	≤5%	39 (88.6)	9 (64.3)	0.09	19 (95)	9 (64.3)	0.02

(Continued)

TABLE 1 | Continued

Clinicopathological features		Before PSM			After 1:1 PSM		
		Surgery-first N=71	NAC-first N=29	P value	Surgery-first N=28	NAC-first N=28	P value
	>5%	5 (11.4)	5 (35.7)		1 (5)	5 (35.7)	
Ki-67	<25%	3 (4.4)	0 (0)	0.23	–	–	0.79
	25-49%	6 (8.8)	1 (3.8)		1 (3.7)	1 (4)	
	50-75%	27 (39.7)	10 (38.5)		12 (44.4)	10 (40)	
	>75%	32 (47.1)	15 (57.7)		14 (51.9)	14 (56)	
SALL4	<25%	45 (68.2)	21 (91.3)	0.04	15 (53.6)	20 (90.9)	0.01
	25-49%	6 (9.1)	0 (0)		3 (10.7)	0 (0)	
	50-75%	10 (15.2)	1 (4.3)		7 (25)	1 (4.5)	
	>75%	5 (7.6)	1 (4.3)		3 (10.7)	1 (4.5)	
AFP	–	5 (7.2)	3 (11.1)	0.84	0 (0)	3 (11.5)	0.11
	+	64 (92.8)	24 (88.9)		28 (100)	23 (88.5)	
CEA (ng/ml)	0-5	44 (64.7)	15 (55.6)	0.41	17 (60.7)	14 (53.8)	0.61
	>5	24 (35.3)	12 (44.4)		11 (39.3)	12 (46.2)	
CA199 (U/ml)	0-37	58 (85.3)	25 (92.60	0.34	24 (85.7)	24 (92.3)	0.45
	>37	10 (14.7)	2 (7.4)		4 (14.3)	2 (7.7)	
CA242 (U/ml)	0-20	37 (88.1)	11 (84.6)	0.74	11 (84.6)	11 (84.6)	1.00
	>20	5 (11.9)	2 (15.4)		2 (15.4)	2 (15.4)	
CA72.4 (U/ml)	0-6.7	59 (86.8)	25 (92.6)	0.43	25 (89.3)	24 (92.3)	0.71
	>6.7	9 (13.2)	2 (7.4)		3 (10.7)	2 (7.7)	
AFP (ng/ml)	0-7	25 (48.1)	8 (40)	0.54	7 (38.9)	8 (40)	0.95
	>7	27 (51.9)	12 (60)		11 (61.1)	12 (60)	

KPS, Karnofsky Performance Status; GEJ, Gastroesophageal junction; AC, Adjuvant chemotherapy; PSM, Propensity score matching analysis; MMR, Mismatch repair.

No Significant Prognostic Difference Was Associated With NAC in HAS

The OS time of the surgery-first group was better than that of the NAC-first group (**Figure 2A**, *P*=0.02). In particular, the 1- and 3-year survival rates of the NAC-first group were 92.7% and 68.2%, respectively. The 1- and 3-year survival rates of the surgery-first group were 97% and 83.4%, respectively. And univariate survival analysis was demonstrated in **Supplementary Material**. Multivariate Cox regression analysis indicated that clinical T4 (*P*=0.015), proximal gastrectomy (*P*=0.021), lymphovascular invasion (*P*=0.030) and CA199 (*P*=0.007) were independent risk factors for poor OS outcomes in HAS patients (**Table 3**). However, no significant difference in OS times was found between the NAC-first group and the surgery-first group after PSM analysis, although the surgery-first group had a tendency toward better OS rates than the NAC-first group (**Figure 2B**, *P*=0.105).

To explore the relationship between NAC and the recurrence of HAS, we also conducted a univariate survival analysis of the DFS rates. The most common site of metastases was the liver. In the NAC-first group, 5 patients had postoperative liver metastasis with a median time of 5 months (1-58 months), 1 patient had lung metastasis at 1 month after surgery, and 2 patients metastasized to other sites. In the surgery-first group, postoperative liver metastasis occurred in 6 patients, with a median time of 7.5 months (4-26 months). In addition, 2 patients had lung metastasis at an average time of 10.5 months after surgery, 1 patient had ovarian metastasis at 18 months after gastrectomy, and 2 patients had metastases to other sites. The DFS time of the surgery-first group was substantially longer than that of the NAC-first group (**Figure 2A**, *P*=0.022). Specifically, the 1- and 3-year DFS rates of the NAC-first group were 80.4% and 71.5%, respectively. The 1- and 3-year DFS rates of the surgery-first group were 97% and 83.8%, respectively. Multivariate Cox regression analysis also revealed that clinical T4 (*P*=0.023) and lymphovascular invasion (*P*=0.046) was significant predictor of DFS outcomes (**Table 3**). However, a difference in the DFS rates between the NAC-first group and the surgery-first group was not found after PSM analysis (**Figure 2B**, *P*=0.108).

We also analyzed the relationship between the number of adjuvant chemotherapy cycles and the prognosis of HAS patients. Among the 61 patients who underwent surgery first, we found that the OS of the ≥6 cycles group were better than that of the <6 cycles group (**Figure 3**, *P*=0.023) and the DFS also had similar results (**Figure 3**, *P*=0.013).

Prognostic Factors of HAS

As the clinical TNM stage was included in the survival analysis before and after PSM, there was confounding bias present. To reduce the confounding bias resulting from disease stage, we divided 100 patients into two groups, 29 patients in the NAC-first group and 71 patients in the surgery-first group. Their pathological TNM stages (pTNM, ypTNM) were used for univariate and multivariate survival analyses. In the NAC-first group, the results showed that the radiological response (P<0.01), the type of surgery (P = 0.032), and EGFR status (P=0.005) were related to the OS rate in the NAC-first group. Radiological response (P<0.01), number of LNs dissected (P = 0.039) and EGFR status (P=0.032) were related to the DFS rate (**Supplementary Table 1**). Multivariate Cox regression analysis showed that EGFR status was an independent risk factor for poor

TABLE 2 | Evaluation of radiological response, TRG, and main toxicity occurring of NAC.

NAC regimen		SOX (n=19)	XELOX (n=6)	SOX+ Paclitaxel + Trastuzumab (n=1)	XELOX+ Trastuzumab (n=1)	DCF (n=1)	Mfolfox (n=1)
Radiological response	CR	0 (0)	0 (0)	0 (0)	0 (0)	0 (0)	0 (0)
	PR	3 (15.8)	2 (33.3)	1 (100)	0 (0)	0 (0)	0 (0)
	SD	14 (73.7)	3 (50.0)	0 (0)	1 (100)	1 (100)	1 (100)
	PD	0 (0)	1 (16.7)	0 (0)	0 (0)	0 (0)	0 (0)
	Unknown	2 (10.5)	0 (0)	0 (0)	0 (0)	0 (0)	0 (0)
TRG	0	0 (0)	0 (0)	0 (0)	0 (0)	0 (0)	0 (0)
	1	2 (10.5)	0 (0)	1 (100)	1 (100)	0 (0)	0 (0)
	2	2 (10.5)	0 (0)	0 (0)	0 (0)	1 (100)	1 (100)
	3	13 (68.5)	6 (100)	0 (0)	0 (0)	0 (0)	0 (0)
	Unknown	2 (10.5)	0 (0)	0 (0)	0 (0)	0 (0)	0 (0)
Adverse event[a]	Gastrointestinal discomfort	2 (10.5)	1 (16.7)	0 (0)	0 (0)	0 (0)	0 (0)
	Myelosuppression	0 (0)	1 (16.6)	0 (0)	0 (0)	0 (0)	0 (0)
	No	14 (73.7)	1 (16.6)	1 (100)	0 (0)	1 (100)	1 (100)
	Unknown	3 (15.8)	3 (50.0)	0 (0)	1 (100)	0 (0)	0 (0)

[a]*The main toxicity occurring of NAC were recorded, and the secondary side effects were not taken into account.*

NAC, neoadjuvant chemotherapy; CR, complete remission; PR, partial remission; SD, stable disease; PD, progressive disease; TRG, tumor regression grade; XELOX, oxaliplatin + capecitabine; SOX, S-1+oxaliplatin; DCF, Docetaxel+ cisplatin+ fluorouracil.

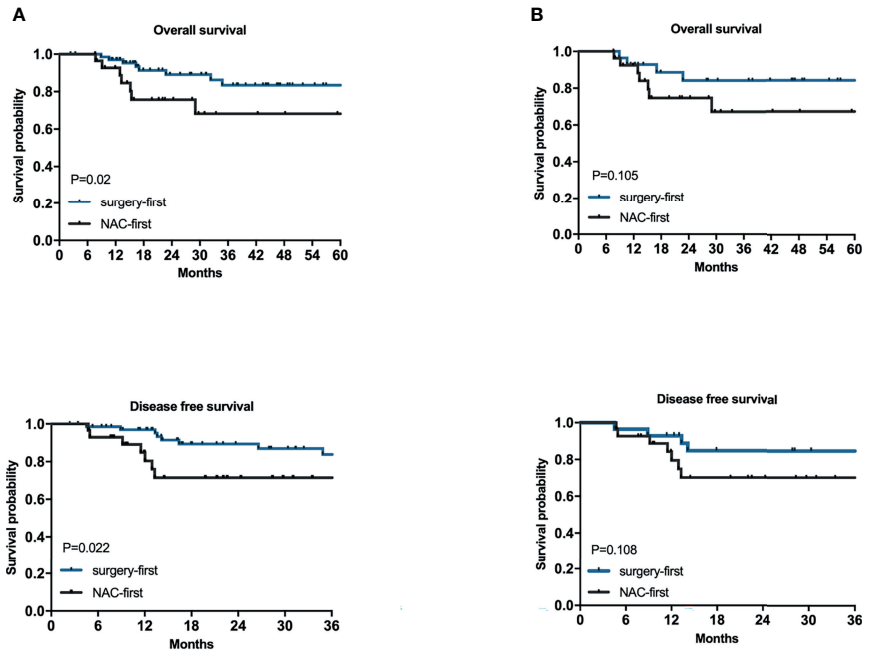

FIGURE 2 | The relationships between NAC and the prognosis of HAS. Kaplan–Meier survival plots for NAC-first and surgery-first groups for 100 patients **(A)** and for after 1:1 PSM of 56 patients **(B)**. P values were calculated by the log-rank test.

OS (P=0.006) and DFS outcomes (P=0.036) (**Supplementary Table 2**). In the surgery-first group, univariate survival analysis showed that age (p=0.03), lymphovascular invasion (P=0.045), CEA (P=0.044), and CA199 (P=0.003) were associated with the OS rate. Age (P=0.028), lymphovascular invasion (P=0.039), cycles of perioperative chemotherapy (P=0.029) and CA199 (P=0.001) were associated with the DFS rate (**Supplementary Table 3**). Multivariate Cox regression analysis showed that age (P=0.049) and CA199 (P=0.001) were independent risk factors for the DFS outcome (**Supplementary Table 4**).

DISCUSSION

Our research revealed that neoadjuvant chemotherapy (mainly platinum + fluorouracil) was not associated with increased survival of HAS patients undergoing radical surgery. However, our result was inconsistent with that of a previous study reported by Zeng et al, who declared that the DFS and disease-specific survival rates of patients in the NAC-first group were significantly higher than those in the surgery-first group (15). The conflicting results may be attributable to the different

TABLE 3 | Multivariate analysis of overall survival (OS) and disease-free survival time (DFS) before propensity score matching analysis.

Clinicopathological features		OS			DFS		
		P value	HR	95%CI	*P* value	HR	95%CI
Age(year)		0.091			0.104		
Location of tumor GEJ vs non-GEJ		0.164					
Clinical T stage	T1/2/3 vs T4	0.015	8.945	1.542-51.872	0.023	3.630	1.190-11.077
Clinical N stage	N- vs N+	0.437			0.641		
Clinical TNM stage	IIa	0.943			0.411		
	IIb	0.624			0.913		
	III	0.533			0.958		
	IVa	0.763			0.441		
NAC	No vs Yes	0.115			0.265		
AC	No vs Yes	0.417			0.405		
Surgery type	Proximal gastrectomy	0.021			0.140		
	Distal gastrectomy	0.006	0.027	0.002-0.352	0.078		
	Total gastrectomy	0.034	0.068	0.006-0.813	0.051		
Number of lymph node dissection		0.349			0.478		
Degree of differentiation	High/middle differentiation vs Low/undifferentiation	0.547			0.969		
Lymphovascular invasion	- vs +	0.030	11.239	1.258-100.394	0.046	3.547	1.023-12.295
Never invasion	- vs +	0.452			0.969		
CEA(ng/ml)	0-5 vs >5	0.081	3.075	0.875-10.866	0.760		
CA199(U/ml)	0-37 vs>37	0.007	9.046	1.830-44.716	0.075		

KPS, Karnofsky Performance Status; GEJ, Gastroesophageal junction; AC, Adjuvant chemotherapy; NAC, Neoadjuvant chemotherapy.

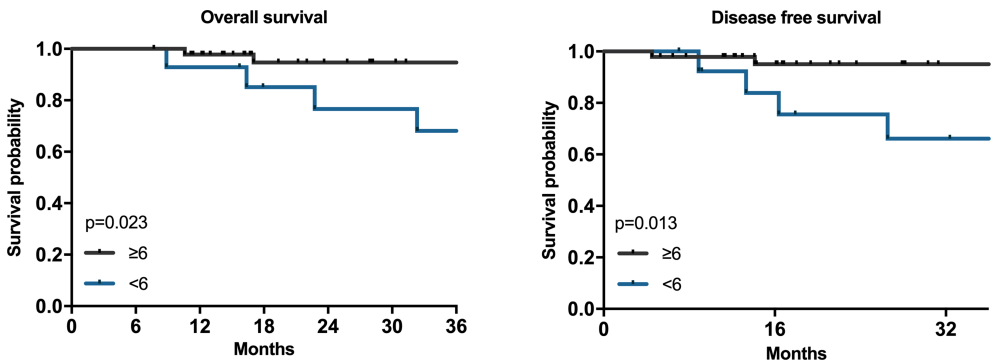

FIGURE 3 | The associations between adjuvant chemotherapy circles and prognosis of HAS. Kaplan–Meier survival plots for adjuvant chemotherapy cycles ≥6 and<6 for 61 patients. P values were calculated by the log-rank test.

proportions of preoperative distant metastases. No patient was diagnosed with preoperative distant metastasis in our study, however, the proportion reached 70.5% in the Zeng et al. study (15). According to the result of our study, radical surgery was recommended for HAS patients without distant metastasis. However, the benefits of NAC with different regimens are still worthy of further research.

In our study, AC and lymphovascular invasion were two of the independent risk factors for DFS outcomes, which is similar to the conclusion of Zeng et al. (15). In a study by Qu, it was revealed that the survival time was not associated with sex, the disease location, or the serum AFP level (cutoff value: 40 ng/L), which is in agreement with our results (4). Similar to other studies of HAS, the results of Yang et al. indicated that pTNM is an independent risk factor for HAS (5, 24). In our study, the clinical or pathological stage was not an independent risk factor for prognosis. The statistical results might have been affected by the small sizes of the subgroups for pTNM stage, especially in the NAC-first group. The relatively short follow-up time may be another explanation. To understand the relationship between clinicopathological characteristics and the prognosis of HAS, it is still necessary to conduct multicenter studies with more samples to further study the treatment of HAS.

Our study demonstrated that AC was one of the independent factors for the prognosis of patients with HAS, similar to the findings of other studies (23, 31). However, few researchers have explored the optimal number of cycles of adjuvant chemotherapy that benefits patients with gastric cancer (32). As far as we know, the current research on HAS is blank. Due to the toxicity and side effects of neoadjuvant/adjuvant chemotherapy, it is necessary to

determine the appropriate number of chemotherapy cycles to minimize side effects and maintain oncological efficacy, especially for patients with severe side effects. In our study, we found that patients who received ≥ 6 cycles of adjuvant chemotherapy had a better survival outcome than patients who received < 6 cycles, which is consistent with a multicenter retrospective study of gastric cancer (32). Accordingly, adjuvant chemotherapy is still advised, and more than 6 cycles of chemotherapy are preferable.

The incidence of Her-2 amplification in gastric cancer ranges from 6.0% to 29.5%; the variation may result from different testing methods and objective criteria (33). In our study, we found that the Her-2-positive expression rate of HAS was 22.89%, which is consistent with the results of previous studies that revealed a positivity rate of 25% (31). The negative prognostic value of Her-2 amplification for breast cancer is clear, however, opinions on its prognostic relationship with gastric cancer are still contradictory. In the ToGA study, researchers found that the OS and DFS of patients treated with trastuzumab combined with chemotherapy were better than those of patients treated with chemotherapy alone. Similarly, some researchers have suggested that trastuzumab combined with chemotherapy could improve OS outcomes (34). In our study, we also found that the two patients treated with chemotherapy and trastuzumab had the most satisfactory pathological response rate. Therefore, Her-2 inhibitors such as trastuzumab could be considered for NAC and the systematic treatment of HAS.

As the largest retrospective study on HAS treated with radical surgery, our study still had several limitations. Although 100 patients represent the largest sample size studied to date, this number was still small for statistical analysis. Furthermore, the chemotherapy regimens were various, especially for NAC, which may affect the results of NAC on HAS. Therefore, the conclusions drawn in our research should be adopted with caution.

CONCLUSIONS

NAC based on platinum and fluorouracil may not improve the OS and DFS of patients with HAS treated with radical surgery. Patients who received more than 6 cycles of postoperative adjuvant chemotherapy had improved outcomes compared with the patient outcomes in other treatment groups. Therefore, the combination treatment of radical gastrectomy and sufficient adjuvant chemotherapy is recommended for patients with locally advanced HAS.

DATA AVAILABILITY STATEMENT

The original contributions presented in the study are included in the article/**Supplementary Material**. Further inquiries can be directed to the corresponding author.

ETHICS STATEMENT

The studies involving human participants were reviewed and approved by Institutional Review Board of Peking University Cancer Hospital. The patients/participants provided their written informed consent to participate in this study. Written informed consent was obtained from the individual(s) for the publication of any potentially identifiable images or data included in this article.

AUTHOR CONTRIBUTIONS

KZ, methodology, data curation, investigation, formal analysis, writing - original draft, and writing - review and editing. AW, conceptualization, methodology, writing - review and editing, and funding acquisition. JW, conceptualization, data curation, investigation, and writing - review and editing. ZL, resources, data curation, and investigation. KJ, XJ, TF, ZJ, XW, and JZ, resources and investigation. ZB, conceptualization, resources, project administration, supervision, and writing - review and editing. All authors contributed to the article and approved the submitted version.

FUNDING

This work was supported by the Peking University Clinical Scientist Program (BMU2019LCKXJ011), National Science Foundation for Young Scientists of China (No. 81802735), Beijing Youth Talent Plan (No. QML20191101), Science Foundation of Peking University Cancer Hospital (No. 2020-11) and Beijing Municipal Administration of Hospitals Clinical Medicine Development of Special Funding Support (XMLX202119).

SUPPLEMENTARY MATERIAL

The Supplementary Material for this article can be found online at: https://www.frontiersin.org/articles/10.3389/fonc.2021.789104/full#supplementary-material

REFERENCES

1. Søreide JA, Greve OJ, Gudlaugsson E, Størset S. Hepatoid Adenocarcinoma of the Stomach–Proper Identification and Treatment Remain a Challenge. *Scand J Gastroenterol* (2016) 51(6):646–53. doi: 10.3109/00365521.2015.1124286
2. Fujii H, Ichikawa K, Takagaki T, Nakanishi Y, Ikegami M, Hirose S, et al. Genetic Evolution of Alpha Fetoprotein Producing Gastric Cancer. *J Clin Pathol* (2003) 56(12):942–9. doi: 10.1136/jcp.56.12.942
3. Chen J, Rocken C, Treiber G, Jentsch-Ulrich K, Malfertheiner P, Ebert MP. Clinical Implications of Alpha-Fetoprotein Expression in Gastric Adenocarcinoma. *Dig Dis* (2003) 21(4):357–62. doi: 10.1159/000075360
4. Qu BG, Bi WM, Qu BT, Qu T, Han XH, Wang H, et al. PRISMA-Compliant Article: Clinical Characteristics and Factors Influencing Prognosis of Patients With Hepatoid Adenocarcinoma of the Stomach in China. *Med (Baltimore)* (2016) 95(15):e3399. doi: 10.1097/MD.0000000000003399
5. Yang J, Wang R, Zhang W, Zhuang W, Wang M, Tang C. Clinicopathological and Prognostic Characteristics of Hepatoid Adenocarcinoma of the Stomach. *Gastroenterol Res Pract* (2014) 2014:140587. doi: 10.1155/2014/140587
6. Liu Q, Bannan M, Melamed J, Witkin GB, Nonaka D. Two Cases of Hepatoid Adenocarcinoma of the Intestine in Association With Inflammatory Bowel Disease. *Histopathology* (2007) 51(1):123–5. doi: 10.1111/j.1365-2559.2007.02715.x

7. Gakiopoulou H, Givalos N, Liapis G, Agrogiannis G, Patsouris E, Delladetsima I. Hepatoid Adenocarcinoma of the Gallbladder. *Dig Dis Sci* (2007) 52(12):3358–62. doi: 10.1007/s10620-007-9807-3
8. Ogbonna OH, Sakruti S, Sulieman M, Ali A, Shokrani B, Oneal P. Hepatoid Adenocarcinoma of the Duodenum: An Unusual Location. *Case Rep Oncol* (2016) 9(1):182–7. doi: 10.1159/000444746
9. Akiyama S, Tamura G, Endoh Y, Fukushima N, Ichihara Y, Aizawa K, et al. Histogenesis of Hepatoid Adenocarcinoma of the Stomach: Molecular Evidence of Identical Origin With Coexistent Tubular Adenocarcinoma. *Int J Cancer* (2003) 106(4):510–5. doi: 10.1002/ijc.11246
10. Lin CY, Yeh HC, Hsu CM, Lin WR, Chiu CT. Clinicopathologial Features of Gastric Hepatoid Adenocarcinoma. *BioMed J* (2015) 38(1):65–9. doi: 10.4103/2319-4170.126860
11. Bourreille J, Metayer P, Sauger F, Matray F, Fondimare A. Existence of Alpha Feto Protein During Gastric-Origin Secondary Cancer of the Liver. *Presse Med* (1970) 78(28):1277–8.
12. Kodama T, Kameya T, Hirota T, Shimosato Y, Ohkura H, Mukojima T, et al. Production of Alpha-Fetoprotein, Normal Serum Proteins, and Human Chorionic Gonadotropin in Stomach Cancer: Histologic and Immunohistochemical Analyses of 35 Cases. *Cancer* (1981) 48(7):1647–55. doi: 10.1002/1097-0142(19811001)48:7<1647::aid-cncr2820480729>3.0.co;2-v
13. Ishikura H, Fukasawa Y, Ogasawara K, Natori T, Tsukada Y, Aizawa M. An AFP-Producing Gastric Carcinoma With Features of Hepatic Differentiation. A Case Report. *Cancer* (1985) 56(4):840–8. doi: 10.1002/1097-0142(19850815)56:4<840::aid-cncr2820560423>3.0.co;2-e
14. Inoue M, Sano T, Kuchiba A, Taniguchi H, Fukagawa T, Katai H. Long-Term Results of Gastrectomy for Alpha-Fetoprotein-Producing Gastric Cancer. *Br J Surg* (2010) 97(7):1056–61. doi: 10.1002/bjs.7081
15. Zeng XY, Yin YP, Xiao H, Zhang P, He J, Liu WZ, et al. Clinicopathological Characteristics and Prognosis of Hepatoid Adenocarcinoma of the Stomach: Evaluation of a Pooled Case Series. *Curr Med Sci* (2018) 38(6):1054–61. doi: 10.1007/s11596-018-1983-1
16. Wang Y, Sun L, Li Z, Gao J, Ge S, Zhang C, et al. Hepatoid Adenocarcinoma of the Stomach: A Unique Subgroup With Distinct Clinicopathological and Molecular Features. *Gastric Cancer* (2019) 22(6):1183–92. doi: 10.1007/s10120-019-00965-5
17. Liu X, Cheng Y, Sheng W, Lu H, Xu X, Xu Y, et al. Analysis of Clinicopathologic Features and Prognostic Factors in Hepatoid Adenocarcinoma of the Stomach. *Am J Surg Pathol* (2010) 34(10):1465–71. doi: 10.1097/PAS.0b013e3181f0a873
18. Liu X, Sheng W, Wang Y. An Analysis of Clinicopathological Features and Prognosis by Comparing Hepatoid Adenocarcinoma of the Stomach With AFP-Producing Gastric Cancer. *J Surg Oncol* (2012) 106(3):299–303. doi: 10.1002/jso.23073
19. Wang XL. Hepatoid Adenocarcinoma of the Stomach. *Zhonghua Zhong Liu Za Zhi [Chinese J Oncology]* (1988) 10(6):455–7.
20. National Health Commission Of The People's Republic Of China. Chinese Guidelines for Diagnosis and Treatment of Gastric Cancer 2018 (English Version). *Chin J Cancer Res* (2019) 31(5):707–37. doi: 10.21147/j.issn.1000-9604.2019.05.01
21. Wang W, Zheng C, Fang C, Li P, Xie J, Lin J, et al. Time Trends of Clinicopathologic Features and Surgical Treatment for Gastric Cancer: Results From 2 High-Volume Institutions in Southern China. *Surgery* (2015) 158(6):1590–7. doi: 10.1016/j.surg.2015.04.038
22. Su JS, Chen YT, Wang RC, Wu CY, Lee SW, Lee TY. Clinicopathological Characteristics in the Differential Diagnosis of Hepatoid Adenocarcinoma: A Literature Review. *World J Gastroenterol* (2013) 19(3):321–7. doi: 10.3748/wjg.v19.i3.321
23. Zhang JF, Shi SS, Shao YF, Zhang HZ. Clinicopathological and Prognostic Features of Hepatoid Adenocarcinoma of the Stomach. *Chin Med J (Engl)* (2011) 124(10):1470–6.
24. Baek SK, Han SW, Oh DY, Im SA, Kim TY, Bang YJ. Clinicopathologic Characteristics and Treatment Outcomes of Hepatoid Adenocarcinoma of the Stomach, a Rare But Unique Subtype of Gastric Cancer. *BMC Gastroenterol* (2011) 11:56. doi: 10.1186/1471-230x-11-56
25. Reddavid R, Sofia S, Chiaro P, Colli F, Trapani R, Esposito L, et al. Neoadjuvant Chemotherapy for Gastric Cancer. Is it a Must or a Fake? *World J Gastroenterol* (2018) 24(2):274–89. doi: 10.3748/wjg.v24.i2.274
26. Hashemzadeh S, Pourzand A, Somi MH, Zarrintan S, Javad-Rashid R, Esfahani A. The Effects of Neoadjuvant Chemotherapy on Resectability of Locally-Advanced Gastric Adenocarcinoma: A Clinical Trial. *Int J Surg* (2014) 12(10):1061–9. doi: 10.1016/j.ijsu.2014.08.349
27. Li W, Qin J, Sun YH, Liu TS. Neoadjuvant Chemotherapy for Advanced Gastric Cancer: A Meta-Analysis. *World J Gastroenterol* (2010) 16(44):5621–8. doi: 10.3748/wjg.v16.i44.5621
28. Coccolini F, Nardi M, Montori G, Ceresoli M, Celotti A, Cascinu S, et al. Neoadjuvant Chemotherapy in Advanced Gastric and Esophago-Gastric Cancer. Meta-Analysis of Randomized Trials. *Int J Surg* (2018) 51:120–7. doi: 10.1016/j.ijsu.2018.01.008
29. Watanabe H, Okada M, Kaji Y, Satouchi M, Sato Y, Yamabe Y, et al. [New Response Evaluation Criteria in Solid Tumours-Revised RECIST Guideline (Version 1.1)]. *Gan To Kagaku Ryoho* (2009) 36 (13):2495501.
30. Ryan R, Gibbons D, Hyland JM, Treanor D, White A, Mulcahy HE, et al. Pathological Response Following Long-Course Neoadjuvant Chemoradiotherapy for Locally Advanced Rectal Cancer. *Histopathology* (2005) 47(2):141–6. doi: 10.1111/j.1365-2559.2005.02176.x
31. Xia R, Zhou Y, Wang Y, Yuan J, Ma X. Hepatoid Adenocarcinoma of the Stomach: Current Perspectives and New Developments. *Front Oncol* (2021) 11:633916. doi: 10.3389/fonc.2021.633916
32. Jeong SH, Yoo MW, Son YG, Oh SJ, Kim JH, Kim HI, et al. Appropriate Number of Adjuvant Chemotherapy Cycles for Patients With Stage 2 or 3 Gastric Cancer After Curative Gastrectomy: A Multicenter Cohort Study. *Ann Surg Oncol* (2021) 28(8):4458–70. doi: 10.1245/s10434-020-09504-4
33. Boku N. HER2-Positive Gastric Cancer. *Gastric Cancer* (2014) 17(1):1–12. doi: 10.1007/s10120-013-0252-z
34. Hofmann M, Stoss O, Shi D, Büttner R, van de Vijver M, Kim W, et al. Assessment of a HER2 Scoring System for Gastric Cancer: Results From a Validation Study. *Histopathology* (2008) 52(7):797–805. doi: 10.1111/j.1365-2559.2008.03028.x

Conflict of Interest: The authors declare that the research was conducted in the absence of any commercial or financial relationships that could be construed as a potential conflict of interest.

Publisher's Note: All claims expressed in this article are solely those of the authors and do not necessarily represent those of their affiliated organizations, or those of the publisher, the editors and the reviewers. Any product that may be evaluated in this article, or claim that may be made by its manufacturer, is not guaranteed or endorsed by the publisher.

Copyright © 2022 Zhou, Wang, Wei, Ji, Li, Ji, Fu, Jia, Wu, Zhang and Bu. This is an open-access article distributed under the terms of the Creative Commons Attribution License (CC BY). The use, distribution or reproduction in other forums is permitted, provided the original author(s) and the copyright owner(s) are credited and that the original publication in this journal is cited, in accordance with accepted academic practice. No use, distribution or reproduction is permitted which does not comply with these terms.

frontiers in Oncology

ORIGINAL RESEARCH
published: 12 January 2022
doi: 10.3389/fonc.2021.799223

Identification of a Four-Gene-Based SERM Signature for Prognostic and Drug Sensitivity Prediction in Gastric Cancer

Xiya Jia[1,2†], *Bing Chen*[1,2†], *Ziteng Li*[1,2], *Shenglin Huang*[1,2], *Siyuan Chen*[1,2], *Runye Zhou*[1,2], *Wanjing Feng*[1,2], *Hui Zhu*[1,2*] *and Xiaodong Zhu*[1,2*]

[1] *Department of Medical Oncology, Fudan University Shanghai Cancer Center, Shanghai, China,* [2] *Department of Oncology, Shanghai Medical College of Fudan University, Shanghai, China*

OPEN ACCESS

Edited by:
Luigi Marano, University of Siena, Italy

Reviewed by:
Wei Cao, Shanghai Jiao Tong University, China
Ahmet Acar, Middle East Technical University, Turkey

***Correspondence:**
Hui Zhu
huizhu171717@163.com
Xiaodong Zhu
xddr001@163.com

†*These authors have contributed equally to this work and share first authorship*

Specialty section:
This article was submitted to Gastrointestinal Cancers: Gastric & Esophageal Cancers, a section of the journal Frontiers in Oncology

Received: *21 October 2021*
Accepted: *14 December 2021*
Published: *12 January 2022*

Citation:
Jia X, Chen B, Li Z, Huang S, Chen S, Zhou R, Feng W, Zhu H and Zhu X (2022) Identification of a Four-Gene-Based SERM Signature for Prognostic and Drug Sensitivity Prediction in Gastric Cancer. Front. Oncol. 11:799223. doi: 10.3389/fonc.2021.799223

Background: Gastric cancer (GC) is a highly molecular heterogeneous tumor with poor prognosis. Epithelial-mesenchymal transition (EMT) process and cancer stem cells (CSCs) are reported to share common signaling pathways and cause poor prognosis in GC. Considering about the close relationship between these two processes, we aimed to establish a gene signature based on both processes to achieve better prognostic prediction in GC.

Methods: The gene signature was constructed by univariate Cox and the least absolute shrinkage and selection operator (LASSO) Cox regression analyses by using The Cancer Genome Atlas (TCGA) GC cohort. We performed enrichment analyses to explore the potential mechanisms of the gene signature. Kaplan-Meier analysis and time-dependent receiver operating characteristic (ROC) curves were implemented to assess its prognostic value in TCGA cohort. The prognostic value of gene signature on overall survival (OS), disease-free survival (DFS), and drug sensitivity was validated in different cohorts. Quantitative reverse transcription polymerase chain reaction (RT-qPCR) validation of the prognostic value of gene signature for OS and DFS prediction was performed in the Fudan cohort.

Results: A prognostic signature including SERPINE1, EDIL3, RGS4, and MATN3 (SERM signature) was constructed to predict OS, DFS, and drug sensitivity in GC. Enrichment analyses illustrated that the gene signature has tight connection with the CSC and EMT processes in GC. Patients were divided into two groups based on the risk score obtained from the formula. The Kaplan-Meier analyses indicated high-risk group yielded significantly poor prognosis compared with low-risk group. Pearson's correlation analysis indicated that the risk score was positively correlated with carboplatin and 5-fluorouracil IC50 of GC cell lines. Multivariate Cox regression analyses showed that the gene signature was an independent prognostic factor for predicting GC patients' OS, DFS, and susceptibility to adjuvant chemotherapy.

Conclusions: Our SERM prognostic signature is of great value for OS, DFS, and drug sensitivity prediction in GC, which may give guidance to the development of targeted therapy for CSC- and EMT-related gene in the future.

Keywords: gastric cancer, cancer stem cells, epithelial-mesenchymal transition, prognostic signature, drug sensitivity prediction

INTRODUCTION

Gastric cancer (GC) is one of the most common malignant tumors which have high morbidity and mortality, and it is the fourth leading cause of cancer-related death. A total of 1,089,103 people were diagnosed with GC worldwide in 2020, and new deaths increased to 768,793 which accounted for 7.7% of cancer-related death (1, 2). Although overall GC incidence rates continue to decrease in the majority of countries, including high-incidence countries such as China, Korea, and Japan, the absolute number of newly diagnosed GC cases and the incidence in younger age groups (below age 50 years) are predicted to continue to increase in both low- and high-risk countries (3). Nowadays, different classification and staging systems such as TNM staging, Lauren classification, and Borrmann classification are extensively used to predict the outcomes and plan personalized treatment strategies for GC patients in clinical practice. However, the outcomes can vary significantly for the patients with similar clinicopathological characteristics because molecular heterogeneity has been shown in similar stages and classifications, suggesting the current classification system is insufficient to achieve precise prognostication and risk stratification. Hence, novel strategies providing more precise predictive value are strongly demanded for making individualized treatment strategies.

Recently, some literature reports that the molecular heterogeneity (gene expression, gene amplification, epigenetic changes, chromosomal aberrations) between GC patients can be used to develop molecular classification systems to stratify patients to different molecular subtypes with different outcomes. The Asian Cancer Research Group (ACRG) proposed a molecular classification containing 4 molecular subtypes: MSS/TP53 activation, MSS/TP53 loss, microsatellite instability (MSI), and MSS/EMT. The result of survival analysis between different molecular subtypes illustrated that the MSI group had a better prognosis and the MSS/EMT group had the worst prognosis (4). Next-generation sequencing for tumor tissue has been widely used in clinical practice to detect genetic alterations. The most widely used molecular classification of GC is based on the human epidermal growth factor receptor 2 (HER2) expression level, which is the basis for selecting anti-HER2-targeted therapy. Anti-HER2-targeted drugs have revolutionized the treatment of HER2-positive GC and improved its outcome over the last decade. However, although HER2-positive patients account for only around 10% of all GC patients, it is necessary to develop novel molecular biomarkers to guide targeted treatments in GC.

Epithelial-mesenchymal transition (EMT) is a biological process allowing the epithelial cells to transform into mesenchymal cells, and EMT plays a role in physiological and pathological processes, which include embryonic evolution, wound healing, tumor cell metastasis, and drug resistance (5, 6). Different signaling pathways are involved in EMT: transforming growth factor-beta (TGF-β) signaling pathway, Hedgehog signaling pathway, Wnt/β-catenin signaling pathway, and Notch signaling pathway (7–9). The changes of molecular expression levels in these pathways could modulate the EMT-related transcription factors such as Snail, Twist, Slug, and Zeb, leading to an increased expression of mesenchymal cell markers (8). The EMT process could speed up the invasion, dissemination, and migration rates of cancer cells, which contributes to the rapid deterioration of disease and chemotherapeutic resistance. EMT markers were proven to be a critical prognosticator for different tumors, including glioma, endometrial cancer, and also GC (10–12).

Cancer stem cells (CSCs) are a small population of tumor cells playing a pivotal role in tumor progression, drug resistance, and survival of tumor cells. CSCs cause chemotherapeutic resistance and tumor recurrence through different mechanisms such as exporting cytotoxic drugs out of the cell through multidrug resistance (MDR) pumps, developing stronger DNA repair mechanisms, and reducing sensitivity to redox stress to prevent senescence (13–15). CSCs have been discovered to predict poor prognosis in many solid malignancies, including GCs, and inhibition of the CSC population may be an appropriate therapeutic strategy to prevent tumor recurrence and metastasis (16).

Literature surveys have revealed that there is an overlap between EMT stimuli and CSCs; activation of EMT-related transcription factors could increase the expression level of genes involved in prompting CSC transformation. Vesna et al. demonstrated that breast cancer cells would develop CSC phenotypes under the influence of TWIST overexpression (17). The tight connection between the EMT process and CSCs is observed in GC as well. Yoon et al. reported that activation of RTK-RAS signaling promoted EMT in GC cells, thus leading to the acquisition of CSC phenotypes (enrichment of CD44 expression) and invasive capabilities (18). There is mounting evidence suggesting that two processes may share common signaling pathways including TGF-β, Wnt/β-catenin, Hedgehog, Notch, and STAT3 (19). Considering the close relationship between these two processes in regulating each other and the common pathways they share, identifying molecular biomarkers related to both processes can achieve higher prognostic value and aid in the discovery of targeted treatment options.

Malta et al. used an innovative one-class logistic regression machine learning algorithm (OCLR) to calculate mRNA expression-based stemness index (mRNAsi), which indirectly

reflected the activity of CSCs and the tumor differentiation state (20). Previous studies demonstrated that mRNAsi was a prognostic factor for GC (21). Therefore, it was reasonable to screen differentially expressed genes (DEGs) between high- and low-mRNAsi groups to identify stemness-related prognostic genes. The SERM signature for prognostic and drug sensitivity prediction was then developed by screening overlapped genes of CSC and EMT processes through statistical analyses, followed by the construction of a nomogram by integrating the signature and other clinical parameters.

MATERIALS AND METHODS

Data Collection and Processing

RNA-sequencing matrix and clinical data of GC samples were downloaded from TCGA database (https://portal.gdc.cancer.gov/). "HT-Seq COUNT" and "HT-Seq FPKM" workflow types of TCGA stomach adenocarcinoma (TCGA-STAD) were downloaded, which included a total of 375 GC tissue samples and 32 adjacent normal samples. Clinical information was constituted by age, sex, TNM level, pathological stage, grade, survival time, and survival states. The mRNAsi of TCGA-STAD were obtained from Malta's previous studies (20). Patients who met the following criteria were included in the subsequent analyses: (1) RNA-seq matrix sample ID name can be matched to mRNAsi ID name from the literature; (2) patients with completed clinical data for further analyses; and (3) clinical follow-up time no less than 30 days. Thus, 296 patients (296 tumor samples and corresponding mRNAsi level) were included in constructing CSC- and EMT-related prognostic gene signature (**Supplementary Table S1**). The microarray matrix and clinical data of GSE66229, GSE15459, and GSE26942 were downloaded from the GEO database (https://www.ncbi.nlm.nih.gov/geo/). We extracted the data of GC cell lines mRNA expression level and the information of different antineoplastic drugs IC50 of 32 GC cell lines from the CCLE database (https://sites.broadinstitute.org/ccle/).

Identification of CSC- and EMT-Related Genes

Patients were categorized into low- and high-mRNAsi groups based on the median value of mRNAsi. The differentially expressed genes (DEGs) between low- and high-mRNAsi groups were screened using the "edgeR" R package with false discovery rate (FDR) <0.05 and $|\log_2$ fold change$|$ >1. The heatmap and volcano plot were drawn by the R package "ggplot2" and "tinyarray" to visualized the differential analysis. The gene set HALLMARK_EPITHELIAL_MESENCHYMAL_TRANSITION was downloaded from the Molecular Signatures Database (MsigDB), which included the EMT-related genes for further analysis. To decipher gene signatures related to both CSCs and EMT, we screened overlapped genes between filtered DEGs and the EMT gene set. Based on the aforementioned strategies, 60 genes representing CSC and EMT crosstalk were finally identified.

Construction of a 4-Gene-Based Prognostic Signature

A total number of 296 STAD patients with complete clinical data were enrolled in the construction of the CSC- and EMT-relevant prognostic signature. The univariate Cox regression analyses were conducted on CSC- and EMT-related genes and of which a *p*-value of less than 0.05 were considered the genes that significantly impact the survival of GC patients. The aforementioned genes were collected and pooled into the least absolute shrinkage and selection operator (LASSO) Cox regression algorithm, which minimized multicollinearity between different genes, to further reduce selected genes with the "survival" and "glmnet" R package. A risk prognosis model composed of 4 genes was established based on the linear combination of regression coefficients obtained from multivariate Cox regression analyses and gene expression values. The risk score of each patient was calculated by the formula that Risk score = sum of coefficients × gene expression level. The median value of risk score was used to separate samples into high- and low-risk groups in TCGA cohort. The same cutoff value was applied in the validation cohorts.

Exploration of the Potential Biological Pathways for the Prognostic Signature in GC

To further explore the significant biological pathways potentially involved in the high-risk patients compared with low-risk patients, we conducted gene set enrichment analysis (GSEA) by "clusterProfiler" R package in the TCGA-STAD and GSE66229 cohorts between high- and low-risk patients. When adjust *p*-value <0.05 and FDR <0.25 after performing 1,000 permutations in GSEA analysis, gene sets were considered to be dramatically enriched. "Hallmark gene sets" were downloaded from the MsigDB for GSEA analysis. We then chose the upregulated genes in high-risk group to perform Kyoto Encyclopedia of Genes and Genomes (KEGG) enrichment analyses using "clusterProfiler" R package with a *p*-value <0.05 and a *q*-value <0.05.

To demonstrate the close relationship between the gene signature and EMT processes, we compared the risk score level among four GC molecular subtypes (MSS/TP53 activation, MSS/TP53 loss, MSI, and MSS/EMT) associated with distinct clinical outcomes (4). Furthermore, Pearson's correlation analysis was performed between the risk score and the mRNA expression level of EMT markers (TWIST1, TWIST2, CDH2, FN1, SNAI1, SNAI2, MMP2, MMP9, ZEB1) (22).

Assessment and Validation of the Prognostic Value of the Gene Signature on OS and DFS in the Public Database

Kaplan-Meier survival analyses and log-rank tests were implemented to evaluate the predictive value of the signature by using the R package "survival." With "survival ROC" R package, time-dependent receiver operating characteristic (ROC) curves were conducted to determine the sensitivity and specificity of the risk score by measuring the area under the curve

(AUC) (23). Univariate and multivariate Cox regression analyses of clinical characteristics and risk score were applied to evaluate whether the risk model was an independent prognostic factor for OS. The prognostic value of the established gene signature was validated in external validation cohorts GSE66229 and GSE15459.

Except for OS, DFS is also a crucial indicator for evaluating the disease progression, especially for the early stage of GC. The precise and accurate prediction of DFS could guide clinicians in formulating subsequent treatment plans. We wonder if the prognostic gene signature could be applied to predict the DFS of GC patients. In the GSE66229 cohort, survival curves between high- and low-risk groups of patients were depicted and compared using Kaplan-Meier estimates and log-rank test, respectively. Whether the risk score was an independent outcome predictor linked with DFS was determined by univariate and multivariate Cox analyses.

Application of Quantitative Reverse Transcription Polymerase Chain Reaction in GC Cell Lines and Tissues

To further validate the prognostic value of gene signature, we collected 126 GC patients who were diagnosed between 2007 and 2011 with complete clinical information from Fudan University Shanghai Cancer Center. In these cases, the expression level of genes that were included in the CSC- and EMT-related prognostic signature was validated by quantitative reverse transcription polymerase chain reaction (RT-qPCR) in gastric cancer tissues of 126 patients. The clinical information and RT-qPCR results of patients in our cohort are presented in **Supplementary Table S2**. We also explored the mRNA expression levels of four genes in eight human GC cell lines (HGC-27, MKN-28, SGC-7901, BGC-823, MGC-803, AGS, NCI-N87, MKN45) and gastric mucosal cell line GES-1. Total RNAs were extracted from the GC cell lines and clinical tissue specimens using TRIzol reagent (Invitrogen, Waltham, MA, USA). First-strand cDNA was synthesized using the Evo M-MLV RT Premix kit for qPCR (Accurate Biology, Hunan, China) according to the manufacturer's instructions. Relative RNA levels determined by RT-qPCR were measured on a 7900 Real-Time PCR System with the SDS 2.3 software sequence detection system (Applied Biosystems, Waltham, MA, USA) using the SYBR Green (Accurate Biology, Hunan, China) method. β-Actin was employed as the internal control to quantify the mRNA levels of model genes. The relative levels of RNA were calculated using the comparative CT($2-\Delta\Delta CT$) method. We listed the specific primers for SERPINE1, EDIL3, RGS4, MATN3, and β-actin in **Supplementary Table S3**.

Clinical Subgroup Analysis of the Prognostic Signature

To investigate whether the prognostic gene signature had the predictive power for OS and DFS in subgroups of patients with different clinical characteristics, patients were divided into subgroups based on age, gender, T stage, N stage, and TNM stage. The *p*-value of the log-rank test obtained by comparing survival outcomes between different risk levels of patients was used to measure the prognostic value of gene signature in each clinical subgroup.

Construction and Assessment of the Signature-Based Nomogram

A nomogram including age, gender, pathological parameters, and risk score was constructed by "rms" R package to predict the 1-, 3-, and 5-year OS of GC patients. The concordance index (C-index) and AUC of the nomogram were calculated by "rms" R package to reflect the discrimination ability of the model. The concordance between the predicted outcome and actual survival outcome was reflected by plotting the nomogram calibration curves. Decision curve analyses (DCA) were conducted to evaluate the net benefit of nomogram at different threshold values compared with other simple or complex models by "ggDCA" R packages (24). We applied the same methods to validate the accuracy of nomogram in the external validation cohort GSE66229.

Assessment of the Gene Signature Prognostic Value on Antineoplastic Drug Sensitivity

Research advances have provided solid evidence for the contribution of EMT and CSC activation to primary and developed chemotherapeutic drug resistance (25). Therefore, we speculated that the gene signature we developed, which was related to CSC and EMT process, could predict the GC patients' susceptibility to chemotherapeutic drug treatment. We downloaded the data of GC cell line mRNA expression level and the information of different antineoplastic drugs IC50 of GC cell lines from the CCLE database. The risk score of each GC cell line was calculated by the formula we developed. The relationship between IC50 of drugs and risk score was then analyzed by conducting Pearson's correlation analyses. The GSE26942 cohort, which was based on GPL6947 (Illumina HumanHT-12 V3.0 expression beadchip) contained 202 GC patients' samples, including 106 patients treated with adjuvant chemotherapy and 96 patients untreated after surgery. To analyze the capacity of the signature on predicting chemotherapeutic drug sensitivity, we chose the patients who accepted the adjuvant chemotherapy for further analysis. The previous formula was used to compute each patient's risk score, and patients were divided into high- and low-risk groups based on the same cutoff applied in TCGA cohort. To test the prognostic value of gene signature on chemotherapeutic drug susceptibility, we applied Kaplan-Meier analyses between high- and low-risk groups. We conducted multivariate Cox regression analyses of clinical characteristics and risk score to assess whether the gene signature was an independent prognostic factor for drug sensitivity.

Statistical Analyses

R 4.1.0 software (https://www.R-project.org) and GraphPad Prism 7 were used for statistical analysis and graphing in this article. Wilcoxon test and Kruskal-Wallis were used for risk score comparisons between EMT and non-EMT groups. Pearson's

correlation analysis was implemented to analyze the correlation between risk score and EMT markers and calculate the correlation coefficient. Kaplan-Meier curve analysis with log-rank test was conducted to compare survival differences between different groups of patients. Statistical significance was considered $p < 0.05$, and all p-values were two tailed.

RESULTS

Construction of the SERM Prognostic Signature

We conducted this study methodically based on the steps presented in the flow chart (**Figure 1**). We screened 1,315 DEGs (1,100 downregulated, 215 upregulated) between high- and low-mRNAsi group; heatmap reflecting differential gene expression patterns and volcano plot which directly identify significantly differentially expressed genes among two groups were exhibited in **Figure 2A, B**. PCA plot presented the differences in gene expression between high- and low-mRNAsi groups (**Figure 2C**). The Venn diagram indicated the overlapped genes between DEGs and EMT gene set (**Figure 2D**). Univariate Cox regression was applied on overlapped genes with p-value less than 0.05 (**Supplementary Table S4**), after which, 29 genes were subjected to LASSO Cox regression analyses to construct a prognostic signature based on CSC and EMT processes for evaluating the prognosis of GC patients (**Figures 2E, F**). Ultimately, a prognostic gene signature including SERPINE1, EDIL3, RGS4, and MATN3 four genes (SERM signature) was constructed. The formula of calculating prognostic risk score could be indicated as: 0.211372 × (expression level of SERPINE1) + 0.103095 × (expression level of EDIL3) + 0.071508 × (expression level of RGS4) + 0.210286 × (expression level of MATN3). The coefficients of the four genes in the prognostic model were all greater than zero, which indicated that they were all predictors of poor prognosis. GC patients in the TCGA-STAD cohort were split into high- and low-risk groups based on the median risk score which was identified as −0.018421. Patients in validation cohorts were separated into two groups based on the same cutoff value.

Enrichment and Statistical Analysis Revealed the Potential Mechanisms of the SERM Signature

We obtained ranked gene lists between high- and low-risk groups by using "limma" R package and then conducted GSEA analysis using "hallmark gene sets" downloaded from MsigDB. GSEA analysis indicated that in addition to powerful activation of EMT process, the enrichment of angiogenesis process, hypoxia, TGF-β pathway, Hedgehog pathway, and KRAS signaling pathways was observed in the high-risk group of GC patients in both TCGA and GSE66229 cohorts (**Figure 3A**). Accumulating evidence indicates that TGF-β and Hedgehog pathways play significant roles in EMT process and formation of CSCs, suggesting that the signature has a strong association with both processes (19, 26, 27). What is more, KRAS signaling pathway, hypoxia, and angiogenesis processes were demonstrated to accelerate tumorigenesis and metastasis, thus leading to disease progression and poor prognosis in GC (18, 28, 29). The results of KEGG enrichment analyses for gene signature are shown in **Figure 3B**. Protein digestion and absorption, focal adhesion, ECM-receptor interaction, complement, coagulation cascades, and PI3K-Akt pathways were five top significant KEGG pathways related to high-risk group in both cohorts.

To further elucidate and demonstrate the close relationship between the gene signature and EMT process, we performed a Kruskal-Wallis test to investigate the differential risk score value among four molecular subtypes (MSS/TP53 activation, MSS/TP53 loss, MSI, and MSS/EMT) proposed by the ACRG group in TCGA-STAD cohort. Wilcoxon test was used to compare the risk score value between MSS/EMT group and other subtypes. In the TCGA-STAD cohort, the risk score level was significantly higher in the MSS/EMT group compared with MSS/TP53 activation, MSS/TP53 loss, and MSI subtypes ($p < 0.05$) (**Figure 3C**). To make the results more reliable, we applied the same analyses in the GSE66229 cohort and the results turned out

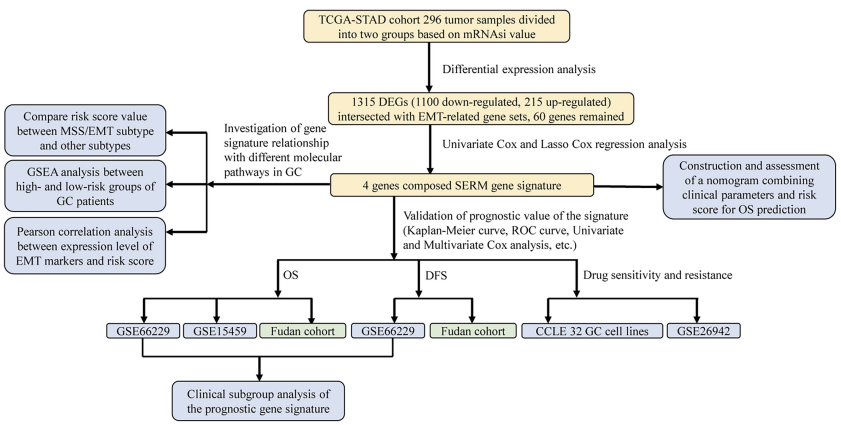

FIGURE 1 | The flowchart presenting the procedure and processes of our study.

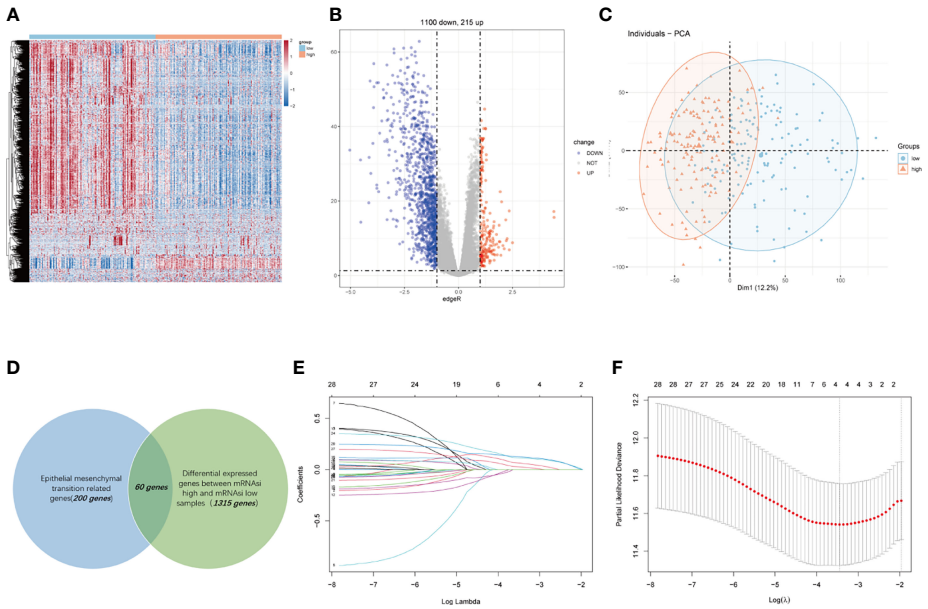

FIGURE 2 | Construction of a four-gene-based SERM prognostic signature for GC. **(A, B)** Heatmap **(A)** and volcano plot **(B)** reflected DEGs between high- and low-mRNAsi groups. **(C)** PCA plot presented the differences in overall gene expression level between high- and low-mRNAsi group. **(D)** Venn diagram indicated the overlapped genes between DEGs and EMT gene set. **(E)** LASSO coefficient profiles of 29 prognostic genes. **(F)** Ten-fold crossvalidation for tuning parameter selection in the LASSO model.

to be identical with TCGA cohort (**Figure 3D**). Furthermore, we conducted ROC analysis to further elucidate the remarkably differential risk score value between EMT and non-EMT subtypes. The result of ROC analysis illustrated that the established gene signature based on CSC and EMT processes showed good discriminatory ability between EMT and non-EMT subtypes (**Figure 3E**). Additionally, we computed the correlation index between the mRNA expression level of EMT markers and risk score value in the TCGA and GSE66229 cohorts using "ggpubr" R package by Pearson's correlation analysis. Recent studies have shown the signaling pathways involved in the EMT process change the gene expression through modulating the transcription factors such as Snail, Twist, and ZEB (8). The changes of EMT-related transcription factors could increase the expression level of mesenchymal cell markers and matrix metalloproteinases (MMP), especially MMP-2 and MMP-9 (30). Therefore, We chose EMT-related transcription factors and their downstream proteins as EMT markers in our study. The results were presented in **Supplementary Figure S1**. We could conclude that the mRNA expression level of all EMT markers we investigated in our study showed obvious positive correlations with risk score ($p < 0.001$).

Assessment and Validation of the Prognostic Value of SERM Signature on OS and DFS in the Public Database

The result of survival analysis between high- and low-risk groups is presented in **Figure 4A**, the high-risk group exhibited significantly shorter OS compared with the low-risk group ($p < 0.0001$). The predictive value of the four-gene-based model was evaluated by calculating the AUC value under the time-dependent ROC curve. The 1-, 3-, and 5-year AUCs were 0.621, 0.664, and 0.749, respectively (**Figure 4D**). To validate the prognostic ability of gene signature, the risk score was calculated by the same formula in the GSE66229 and GSE15459 cohorts. To divide patients into different groups, the same cutoff of risk score was used in two validation cohorts. In the GSE66229 cohort, 162 patients belonged to the low-risk group and the remaining 138 patients were categorized as high-risk group. Two groups owned the same number of patients in the GSE15459 cohort, which meant 96 patients were included in each group. The difference in survival time between high- and low-risk groups was also statistically significant in two validation cohorts (**Figures 4B, C**). In the GSE66229 cohort, the AUCs of 1-, 3-, and 5-year ROC were 0.663, 0.655, and 0.647, respectively. The 1-, 3-, and 5-year AUCs were 0.657, 0.699, and 0.716 in GSE15459, showing a good prognostic discrimination of the SERM signature (**Figures 4E, F**). Univariate Cox regression analysis of risk score showed that it was an adverse prognostic factor for GC. Furthermore, multivariate Cox analysis in three cohorts indicated that the risk score was an independent prognostic factor for GC patient OS (**Supplementary Tables S5**-**S7**). These results demonstrated that the gene signature we derived by LASSO Cox regression for OS prediction could be used as a valuable prognostic marker. The distributions of risk score, survival status, and heatmap of gene signature expression levels of the TCGA-STAD, GSE66229, and GSE15459 cohorts are shown in **Figures 4G–I**.

We tested the prognostic value of SERM signature on DFS of GC patients in the GSE66229 cohort. The same cutoff value (−0.018421) was used for dividing GC patients in the GSE66229

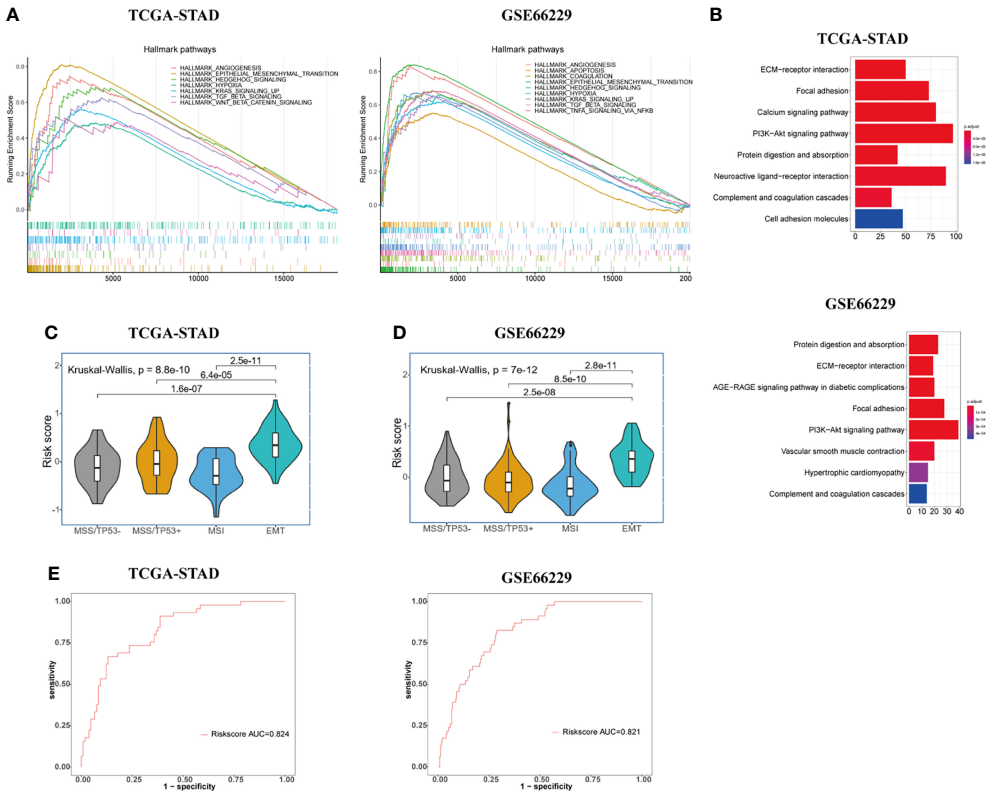

FIGURE 3 | Exploration of the potential biological pathways for the prognostic signature in GC. **(A)** GSEA analysis was carried out to investigate the enrichment score and *p*-value of hallmark gene sets between the high- and low-risk groups in TCGA-STAD and GSE66229 cohorts. **(B)** KEGG enrichment analysis for upregulated genes in the high-risk group. **(C, D)** Risk score value were evaluated among four molecular subtypes (MSS/TP53 activation, MSS/TP53 loss, MSI, and MSS/EMT) in both TCGA-STAD **(C)** and GSE66229 **(D)** cohorts. **(E)** The ROC curves were used to testify the ability of risk score level in discriminating EMT and non-EMT molecular subtypes in the TCGA-STAD and GSE66229 cohorts.

cohort into high- and low-risk groups to analyze the survival differences between two groups by Kaplan-Meier plot with the log-rank test. The result is shown in **Supplementary Figure S2A**, which suggested the SERM signature owning a strong predictive power for DFS of GC patients who undergo a radical operation. We then performed time-dependent ROC analysis to evaluate the prognostic accuracy of the model and observed the values of 1-, 3-, and 5-year AUC were 0.653, 0.66, 0.695, respectively (**Supplementary Figure S2B**). Multivariate Cox regression indicated the risk score was an independent prognostic factor for predicting DFS of GC patients (**Supplementary Figure S2C**). The distributions of risk score, survival status, and heatmap of gene signature expression levels of the GSE66229 cohort are shown in **Supplementary Figure S2D**.

RT-qPCR Validation of SERM Signature Gene Expression in Both GC Cell Lines and the Fudan Cohort

We measured the mRNA expression level of EDIL3, SERPINE1, RGS4, and MATN3 with RT-qPCR in GC cell lines and Fudan cohort. The results for members of SERM signature gene expression level in different GC cell lines are presented in **Supplementary Figure S3**, which to some extent would provide guidance for us to choose GC cell lines for underlying molecular biological mechanism detection in further study. To validate the prognostic ability of gene signature on OS prediction, the risk score was calculated for each patient in our cohort according to the formula and coefficient obtained from multivariate Cox regression analysis in the TCGA cohort. We applied the same cutoff of the risk score in our validation cohort. In total, 52 and 74 patients were divided into high- and low-risk groups, respectively. The Kaplan-Meier analysis between the two groups demonstrated that compared with the low-risk group, the OS in the high-risk group was significantly poorer (**Figure 5A**). Univariate Cox regression analysis indicated risk score was an important marker influencing the OS of GC patients ($p < 0.001$). Multivariate Cox regression analysis based on risk score with other clinical parameters suggested risk score was an independent poor prognostic marker for OS (**Figure 5B**). The prognostic value of the risk model on DFS prediction in Fudan cohort was also analyzed. The risk score was computed for each patient in our cohort with the formula and coefficient obtained from TCGA cohort. Patients were separated into high- and low-risk groups

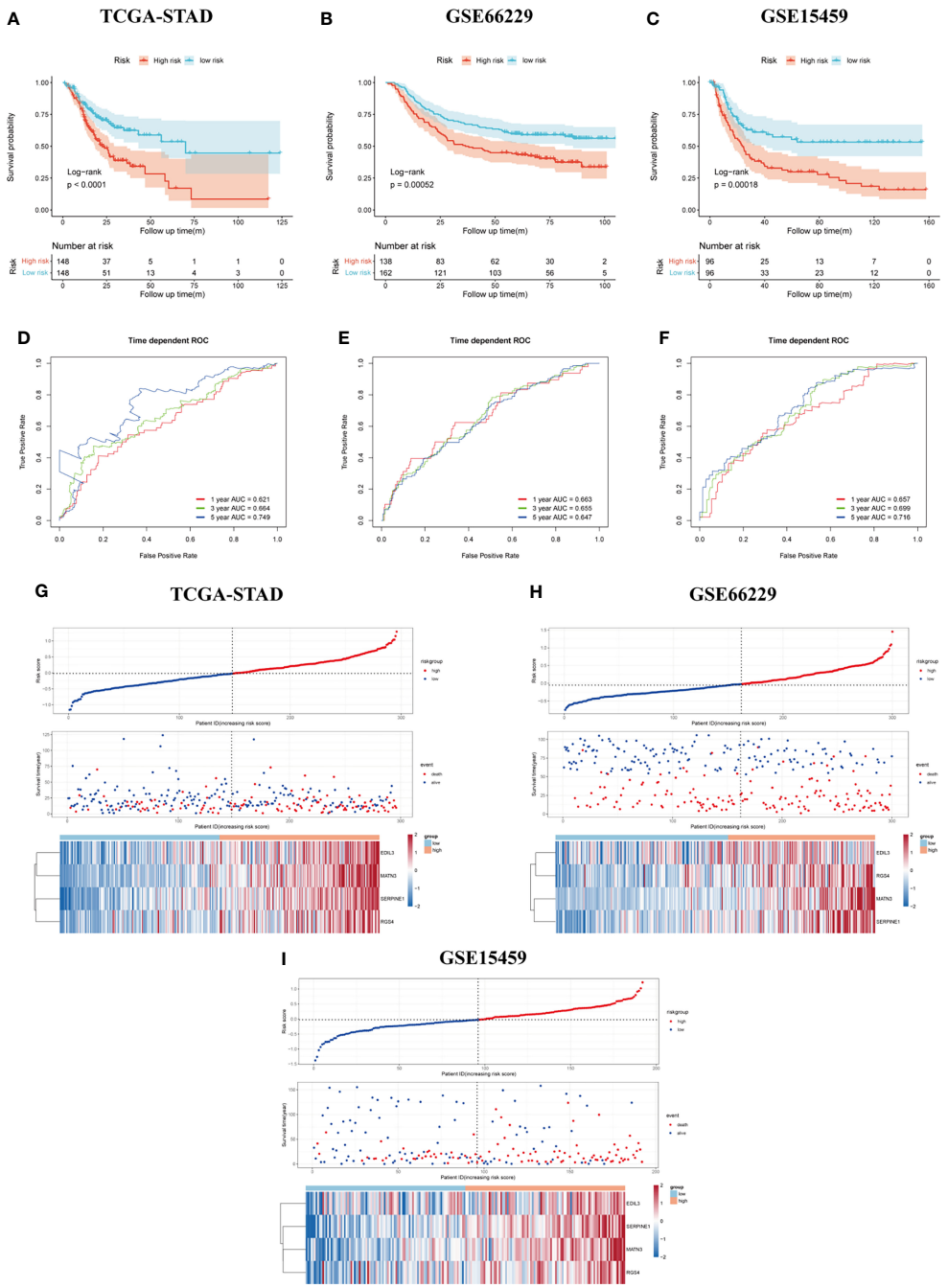

FIGURE 4 | Assessment and validation of the SERM prognositc signature on OS prediction. **(A–C)** Kaplan-Meier analysis of OS between the high- and low-risk groups based on the SERM signature in the TCGA-STAD **(A)**, GSE66229 **(B)**, and GSE15459 **(C)** cohorts. **(D–F)** Time-dependent ROC curves of the SERM signature in the TCGA-STAD **(D)**, GSE66229 **(E)**, and GSE15459 **(F)** cohorts. **(G–I)** The distributions of risk score, survival status, and heatmap of the SERM signature expression levels in the TCGA-STAD **(G)**, GSE66229 **(H)**, and GSE15459 **(I)** cohorts.

according to the same cutoff and each group owned 29 and 41 patients, respectively. Furthermore, we conducted the Kaplan-Meier analysis between two groups, and the results indicated the DFS in the high-risk group was significantly poorer compared with the low-risk group (**Figure 5D**). The *p*-values of the risk score of univariate and multivariate Cox analyses were both lower than 0.001, indicating it was an independent prognostic marker for DFS (**Figure 5E**). Time-dependent ROC analysis suggested the signature's good performance on predicting OS and DFS in GC patients (**Figures 5C, F**).

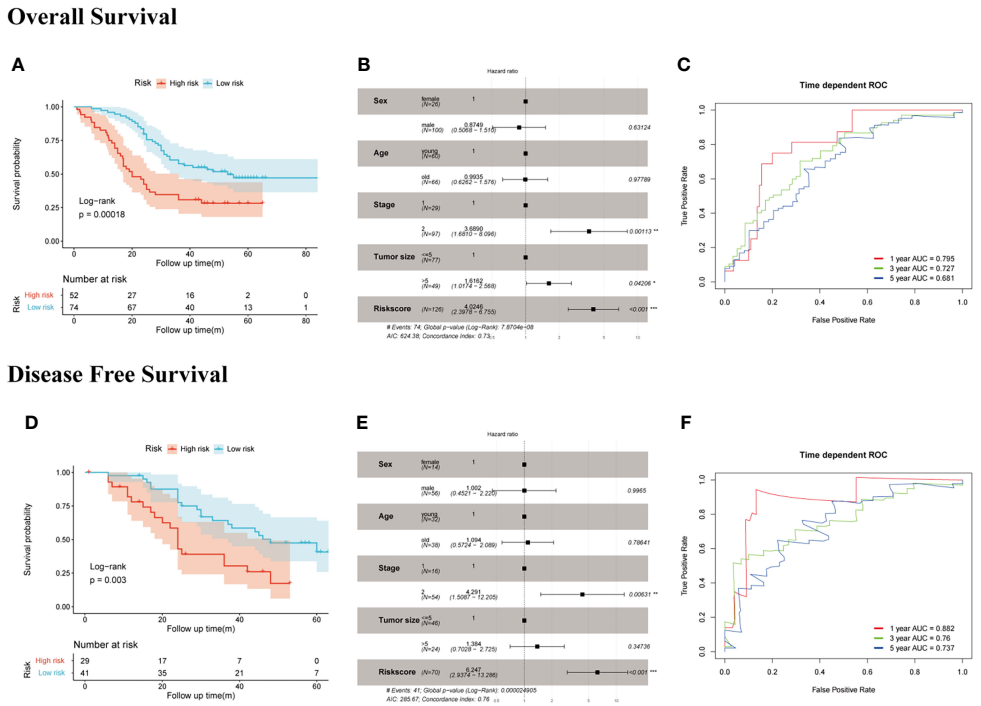

FIGURE 5 | Evaluation of the prognostic value of SERM signature on OS and DFS prediction in Fudan cohort. OS: **(A)** Kaplan-Meier analysis of OS according to risk score value. **(B)** Multivariate Cox regression analysis of clinical parameters and risk score. **(C)** Time-dependent ROC curves of the SERM signature for 1-, 3-, and 5-year OS prediction. DFS: **(D)** Kaplan-Meier analysis of DFS according to risk score value. **(E)** Multivariate Cox regression analysis of clinical parameters and risk score. **(F)** Time-dependent ROC curves of the SERM signature for 1-, 3-, and 5-year DFS prediction.

Assessment of the Prediction Power of the SERM Prognostic Signature in Clinical Subgroups by Kaplan-Meier Plot

We demonstrated the predictive power of gene signature in different clinical subgroups based on age, gender, T stage, N stage, and TNM stage in the GSE66229 cohort. According to the previous risk score cutoff, patients in subgroups were split into high- and low-risk groups, and the Kaplan-Meier analyses were conducted to detect if the signature could be used as a prognostic indicator for OS and DFS in clinical subgroups. As shown in **Figures 6A–J**, patients with high risk had a worse prognosis of OS than patients with low risk in patients >65 years ($p < 0.001$), female ($p = 0.0015$), male ($p = 0.043$), T1-2 ($p = 0.02$), N0-1 ($p = 0.048$), N2-3 ($p = 0.0084$), stage III-IV ($p = 0.013$) subgroups; however, the prognostic signature was incompetent in distinguishing the OS of the high risk from the low-risk group in age ≤65 years ($p = 0.054$), T3-4 ($p = 0.18$), and stages I–II ($p = 0.37$) subgroups. In **Figures 6K–R**, patients with high risk had a worse prognosis of DFS than patients with low risk in patients >65 years ($p = 0.0014$), ≤65 years ($p < 0.001$), male ($p < 0.001$), female ($p = 0.0012$), T1-2 ($p < 0.001$), N0-1 ($p < 0.001$), stages I–II ($p = 0.011$), and stages III–IV ($p = 0.0098$). While in T3-4 and N2-3 subgroups, p-values of the Kaplan-Meier plot were 0.092 and 0.19, respectively.

Construction and Validation of the SERM Signature-Based Nomogram for OS Prediction in GC

To make the model more applicable in clinical use, we next established a nomogram, which integrates age, gender, TNM stage, and risk score to achieve the purpose of optimizing current indicators for long-term OS prediction by multivariate Cox regression in TCGA-STAD cohort (**Figure 7A**). The validation cohort GSE66229 was used to test the predictive accuracy of the nomogram. The nomogram-combined clinical characteristics and the SERM signature were used to predict 1-, 3-, and 5-year survival probabilities. Each patient would get a unique score based on the constructed nomogram, and the higher the score was, the worse the prognosis. The discrimination degree, concordance, and clinical usefulness of the nomogram were quantified by time-dependent ROC curve, nomogram calibration curve, and DCA.

For the constructed nomogram in the training cohort, the C-index of the nomogram for survival prediction was 0.70 and the AUCs of 1-, 3- and 5-year ROC were 0.719, 0.722 and 0.815, respectively (**Figure 7B**). The C-index of nomogram built with age, gender, TNM stage, and risk score in the GSE66229 cohort was 0.72. The AUC values of ROC were 0.787 at 1 year, 0.762 at 3 years, and 0.759 at 5 years (**Figure 7C**). The nomogram

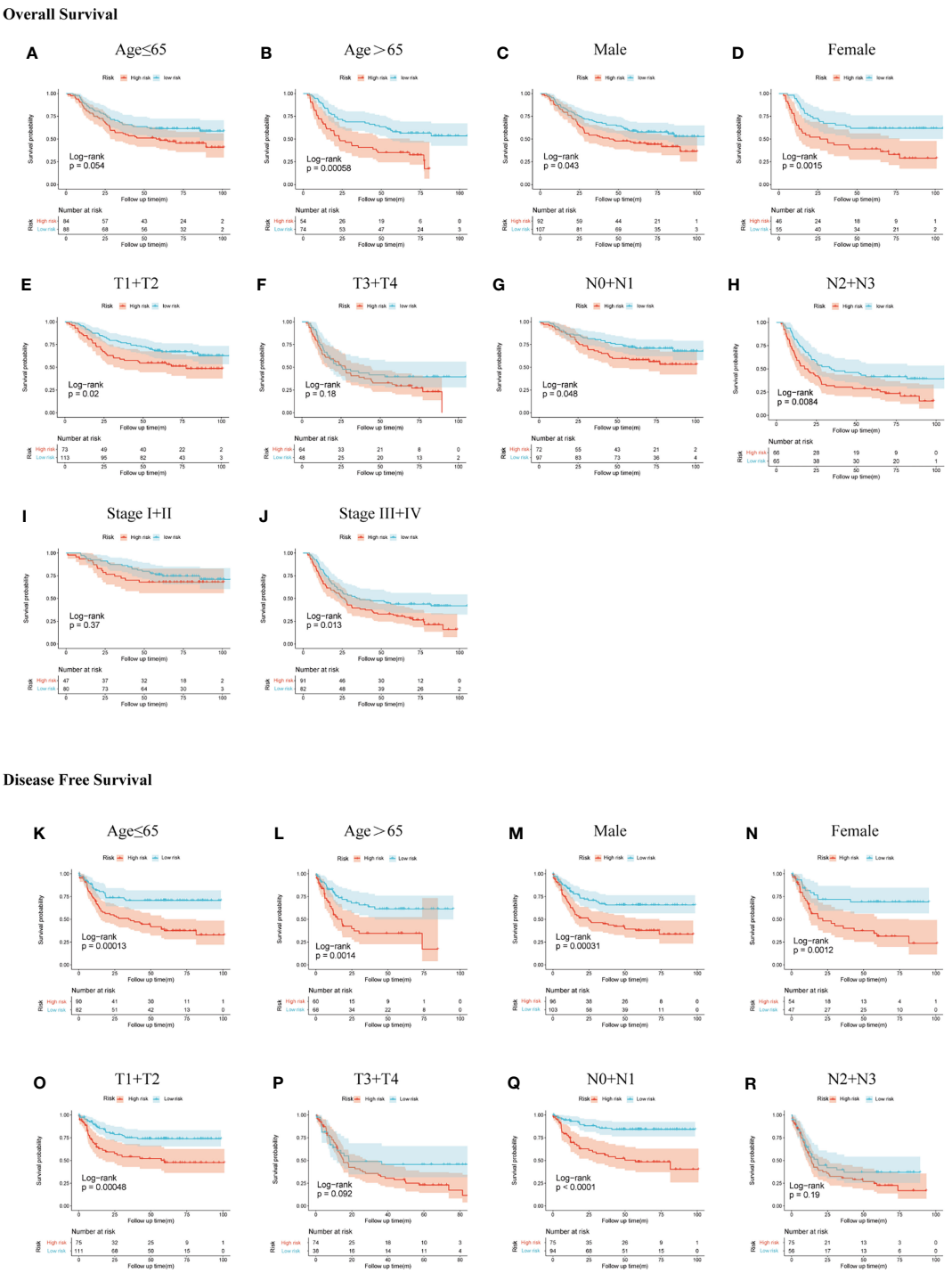

FIGURE 6 | Subgroup analysis of OS and DFS in the GSE66229 cohort. OS Kaplan-Meier plot: **(A)** age ≤65, **(B)** age >65, **(C)** male, **(D)** female, **(E)** T1 + T2, **(F)** T3 + T4, **(G)** N0 + N1, **(H)** N2 + N3, **(I)** stage I + II, and **(J)** stage III + IV; DFS Kaplan-Meier plot: **(K)** age ≤65, **(L)** age >65, **(M)** male, **(N)** female, **(O)** T1 + T2, **(P)** T3 + T4, **(Q)** N0 + N1, and **(R)** N2 + N3.

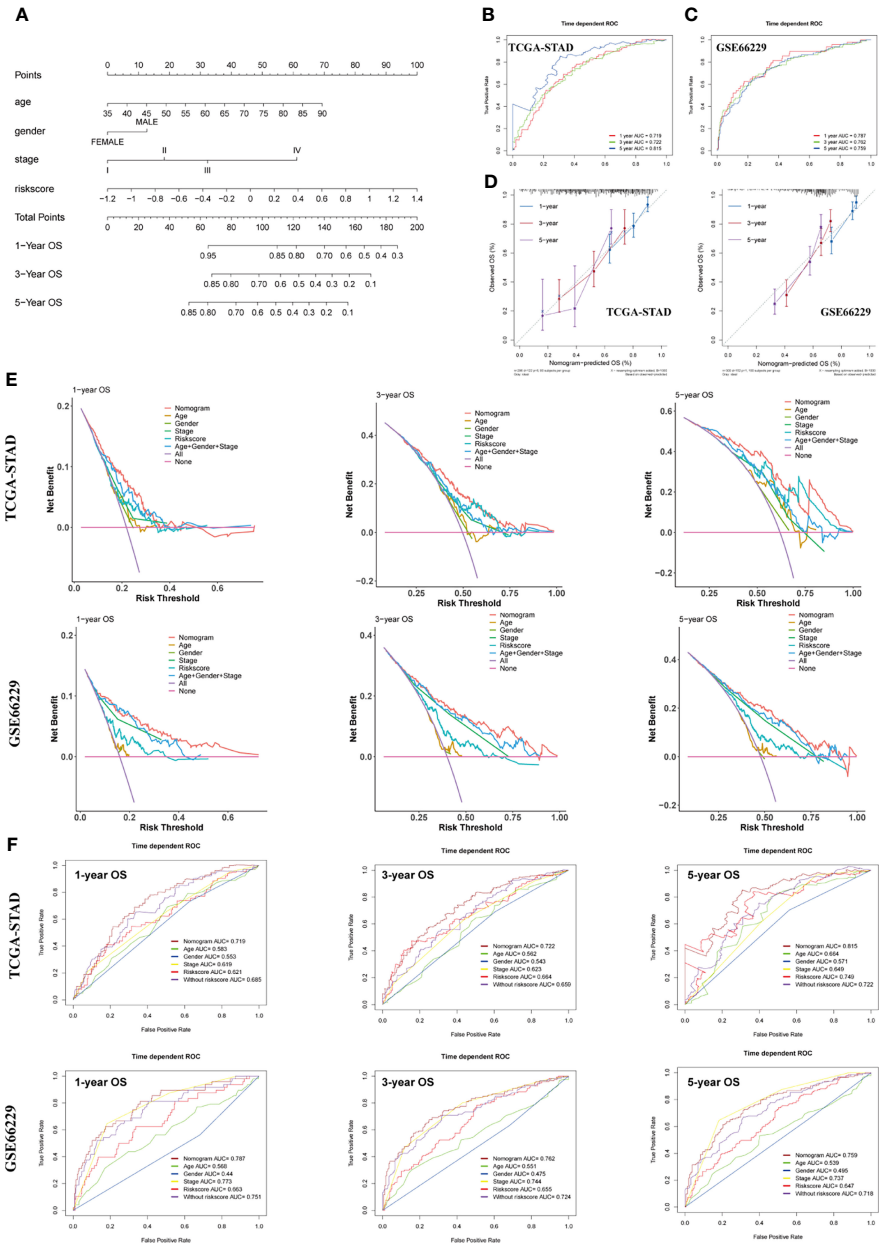

FIGURE 7 | Construction and assessment of a nomogram for OS prediction. **(A)** A nomogram integrating age, gender, TNM stage, and risk score was constructed in the TCGA-STAD cohort. **(B, C)** Time-dependent ROC curves of the nomogram for 1-, 3-, and 5-year OS prediction in the TCGA-STAD **(B)** and GSE66229 cohorts **(C)**. **(D)** Calibration curves of the nomogram for 1-, 3-, and 5-year OS prediction in the TCGA-STAD and GSE66229 cohorts. **(E)** DCA curves were performed to evaluate the net benefit of the nomogram, age, gender, pathological characteristics, and risk score in the TCGA-STAD and GSE66229 cohorts. **(F)** Time-dependent ROC curves of the nomogram, age, gender, TNM stage, risk score, and model without risk score for 1-, 3-, and 5-year OS prediction in the TCGA-STAD and GSE66229 cohorts.

calibration curves of training and validation cohorts presented in **Figure 7D** exhibited a good consistency between nomogram-predicted OS and the actual observation at 1-, 3-, and 5-year OS, which further demonstrated the accuracy of the nomogram. Shown by the DCA curve in **Figure 7E**, the nomogram yielded a better net benefit compared with individual predictive factors and the model without risk score, illustrating the combined nomogram could give guidance to clinicians to make a better prediction on patient OS prognosis. Compared with age, gender, TNM stage, and model without risk score, the combined nomogram exhibited the largest AUC for 1-, 3-, and 5-year OS prediction in both training and validation cohort, suggesting integrating risk score into Cox model could improve the discrimination capacity of the model (**Figure 7F**).

The Developed SERM Signature Could Predict Antineoplastic Drug Sensitivity in GC Cell Lines and GC Patients

Pieces of evidence have demonstrated that phenotypical changes associated with EMT process and stem cell characteristics lead to a reduced response of GC to chemotherapy. The upregulation of EMT markers (vimentin and N-cadherin), which may be regulated by the activation of TGF-β pathway, was reported to cause a worse response of GC to 5-FU (31). CD133 has been identified as a significant marker of CSCs in various cancers, including GC. GC patients with a high expression level of CD133 treated with an adjuvant cisplatin/5-FU therapy had shorter OS and DFS than those CD133-low patients, which indicated that CD133 seemed to contribute to chemoresistance in GC (32). Thus, we reasonably speculated that the established SERM signature could predict GC patients' susceptibility to chemotherapeutic drugs. To confirm our conjecture, we analyzed the prognostic value of gene signature on drug sensitivity in both GC cell lines and patients. Pearson's correlation tests were used to assess the relationship between antineoplastic drugs IC50 and riskscore of 32 GC cell lines. We screened the results of Pearson's correlation test with a *p*-value <0.1; the results showed that the risk score was positively related to IC50 of most antineoplastic drugs, which indicated that the higher level of risk score was associated with drug resistance (**Figure 8A**). As shown by **Figures 8B, C**, IC50 of carboplatin and 5-FU chemotherapeutic drug was positively correlated with the risk score value. Additionally, We chose 106 patients who were treated with adjuvant chemotherapy in GSE26942 cohort to assess the capacity of the signature on predicting chemotherapeutic drug sensitivity. We selected DFS as an indicator reflecting patients' response to adjuvant chemotherapy. The distributions of risk score, survival status, and heatmap of gene signature expression levels of the GSE26942 cohort were shown in **Figure 8D**. The Kaplan-Meier plot illustrated that the patients with high risk score had shorter DFS compared with patients with low-risk score (p = 0.054) (**Figure 8E**). The results of Kaplan-Meier analysis for 3- and 5-year DFS between high- and low-risk groups are presented in **Figure 8F** (p = 0.040) and **Figure 8G** (p = 0.033), respectively. The result of univariate (p = 0.012) and multivariate Cox analyses suggested the signature was an independent prognostic factor for predicting GC patients' susceptibility to adjuvant chemotherapy (**Figure 8H**).

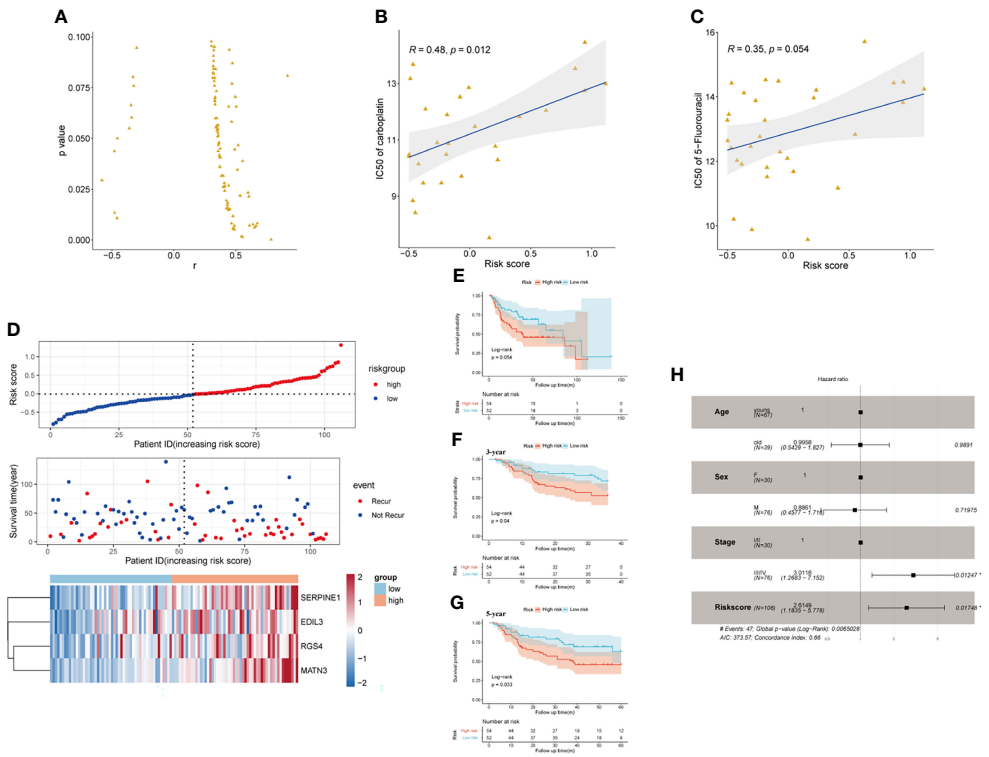

FIGURE 8 | The prognostic value of the signature on drug sensitivity in GC cell lines and GSE26942. **(A)** Risk score was positively related to IC50 of most antineoplastic drugs in GC cell lines. **(B, C)** Risk score was positively related to IC50 of carboplatin **(B)** and 5-flurouracil **(C)**. **(D)** The distributions of risk score, survival status, and heatmap of CSCs and EMT-related gene signature expression levels in GSE26942. **(E)** Kaplan-Meier analysis of DFS for patients who received adjuvant chemotherapy between high- and low-risk groups in GSE26942 cohort. **(F, G)** Kaplan-Meier analysis for 3- **(F)** and 5- year **(G)** DFS prediction between high- and low-risk groups in patients received adjuvant chemotherapy. **(H)** Multivariate Cox regression analysis of clinical parameters and risk score in the GSE26942 cohort.

DISCUSSION

The traditional prognostic systems such as TNM staging systems could be inaccurate under some conditions for predicting GC patients' survival, so exploring specific and sensitive markers for survival prediction of GC patients remains an exigency. Evidence shows that EMT is closely related to the function of CSCs in addition to playing an important role in the metastasis of various tumors. Moreover, under the influence of the EMT process, tumor cells may acquire cancer stem-like properties, which leads to drug resistance, increased relapse, and metastasis in multiple kinds of tumors (26, 33). In addition, accumulating evidence verifies that there is an overlap between pathways mediating two processes, including TGF-β, Hedgehog, Wnt/β catenin, and Notch pathways (19). Choi et al. reported that the expression level of EMT markers (E-cadherin, β-catenin, Snail, vimentin) was correlated with stem cell marker expression level (34). CSC and EMT processes were proven to cause disease progression, poor prognosis, and drug resistance in lung cancer, esophageal cancer, breast cancer, and also GC (35–38). Thus, considering the common pathways and mechanisms two processes share and the same clinical impact they have, identification of transcriptional markers for these two processes will achieve a better prognosis and may give guidance to targeted therapies in GC patients.

In this study, we screened out CSC- and EMT-related mRNAs and identified a novel four-gene-based SERM signature and validated the prognostic value of signature in both public and Fudan cohorts. We calculated the risk score of patients using the formula we mentioned in the *Results* part. Patients were then divided into high- and low-risk groups based on the median value of risk score. The results of Kaplan-Meier survival analyses and time-dependent ROC curves in different cohorts indicated that the signature could effectively predict the survival and drug sensitivity to adjuvant chemotherapy of GC patients. To improve the clinical use of the gene signature, we combined clinical parameters with the risk score and build a nomogram to predict each GC patient's OS in 1, 3, and 5 years. Discrimination degree, concordance, and clinical usefulness of nomogram were evaluated in TCGA and GEO cohorts, the results of which suggest its potential application values in patient's risk stratification.

Four members in the signature were related to adverse clinical outcomes of GC patients, and they all have been reported as EMT-related negative predictors in various kinds of tumors. GSEA results in our study indicated that four members involved in the gene signature may have a crucial role in regulating TGF-β, Hedgehog, and Wnt pathways to promote the formation of CSCs through the EMT process in GC patients. Except for the mentioned pathways, we noticed the enrichment of angiogenesis process, hypoxia, and KRAS signaling pathways in the high-risk group. Literature demonstrated the compact association between these pathways and EMT or CSC-related processes. Twist1 was a transcription factor playing a crucial role in EMT and cancer stemness; Chen et al. indicated that in addition to traditional angiogenesis, the activation of the Twist-Jagged1-KLF4 axis could induce tumor-associated endothelial differentiation (39, 40). Previous literature indicated that the concurrent activated KRAS and depletion of p53 could reprogram EMT-like phenotypes and increase the expression of cancer stemness genes including CD133, EpCAM, and CD24 in prostate cancer (41). Changhwan et al. demonstrated the RTK-RAS signaling could enhance the activation of EMT signal and promote the expression of stemness-related transcription factors in human tumor-derived GC cells (18). Of note, hypoxia-inducible factor-1α (HIF-1α) were proven to regulate expression of EMT markers and EMT transcriptional factors (42). Recent studies conducted by Komal et al. discovered CSC accumulation in hypoxic niches and the anoxic conditions promoted the self-renewal ability of CSCs (43). We observed the upregulation of PI3K-Akt pathway-related genes in KEGG enrichment analysis, and previous studies indicated that this pathway was involved in both CSC and EMT processes (44). The results of GSEA and KEGG enrichment analyses revealed the potential molecular mechanisms of the gene signature, which might give guidance to the development of targeted therapy. SERPINE1 gene encodes a protein called plasminogen activator inhibitor-1 (PAI-1), which is a key regulator of the urokinase-type plasminogen activator (uPA) system. Previous reports demonstrated that the upregulation of SERPINE1 in breast cancer and pancreatic cancer tissue could be induced by TGF-β pathway activation (45–47). However, the pathway influencing SERPINE1 expression level in GC needs more investigation. Bhat-Nakshatri et al. discovered all-trans retinoic acid (ATRA) reduced the mammosphere-forming ability of cell lines by reducing the expression level of SERPINE1 in CSCs, suggesting SERPINE1 may be a pivotal molecule related to CSC formation (48). Increasing sherds of evidences have revealed that SERPINE1 was significantly upregulated in GC tissues compared with normal tissues and could lead to a poor prognosis. McCann et al. pointed out the poor prognosis caused by overexpression of SERPINE1 was related to the imbalance between fibrin deposition and fibrin degradation, inhibiting PAI-1 expression with miR-30c imitated enhanced plasmin activity by fibrin zymograms (49). EDIL3 is an extracellular matrix protein containing three EGF-like domains and the second domain could allow the interaction of EDIL3 with integrins. EDIL3 acts as a proangiogenic factor, a mediator of angiogenesis, and a regulator of endothelial cell adhesion and migration (50–52). The overexpression of EDIL3 was observed in several tumor types, including breast, bladder, liver, and lung carcinomas, and it associates with drug resistance and poor prognosis (53–56). Overexpression of EDIL3 in hepatocellular carcinoma could induce the phosphorylation of SRC, ERK, and SMAD2, leading to the activation of ERK and TGF-β signaling. The activation of these pathways could increase the transcription efficiency of mesenchymal markers and integrins, resulting in cell acquisition of the molecular and morphologic changes of CSCs and EMT (57). RGS4, is a kind of regulator of G-protein signaling (RGS) proteins that catalyze the dephosphorylation of guanosine triphosphate into guanosine diphosphate. Guda et al. found that silencing RGS4 in glioma cancer stem cells (GSCs) decreased the expression, secretion, and activity of MMP2, suggesting decreased invasive and migratory abilities of GSCs (58). However, Cheng et al. suggested that overexpression of RGS4 in NSCLC cells inhibits

MM2/9 expression, thus leading to decreased invasion and migration (59). It was verified that RGS4 was upregulated in mesenchymal stem cells compared with diffuse-type GC, which may suggest that increased expression level of RGS4 may lead to cell EMT transition (60). The prognostic value of RGS4 in GC is not yet clear. MATN3 is a protein-coding gene encoding a member of von Willebrand factor A domain containing protein family, which is involved in the formation of filamentous networks in the extracellular matrix (61). Wu et al. performed bioinformatics and immunohistochemistry to prove that compared with a normal control group, MATN3 protein expression level was significantly higher in the GC tissue group. Furthermore, they found MATN3 was an independent factor to predict unfavorable prognosis in GC patients (62).

Although the prognostic signature was tested and validated in several different cohorts and the results turned out to be stable, our study still has some limitations. Firstly, the TNM stages recorded in TCGA and GEO cohorts were not computed according to the latest edition of AJCC staging system. It was difficult for us to unify the standard of the TNM stages because of the insufficient data recording. Secondly, although we developed a prognostic gene signature related to both CSC and EMT processes and demonstrated its accuracy, scientists should carry out more research on how these genes influence both pathways and how they are connected in GC. A legible understanding of biological mechanisms can give better guidance for clinical use. Thirdly, the GSE26942 cohort we used to demonstrate the prognostic value of gene signature on drug sensitivity and resistance only contained the microarray data before adjuvant chemotherapy treatment, so the change of gene expression level after treatment remained unknown. Therefore, it was difficult for us to analyze the relationship between the signature and developed drug resistance. Furthermore, the prognostic effect of the gene signature on chemotherapeutic resistance for advanced GC patients who received palliative chemotherapy needs more exploration. Of note, GC patients always received combination chemotherapy, or sometimes with targeted agents, so the mechanism of chemoresistance will be quite complicated and elusive. Consequently, we should attach more importance to the exploration of basic biological mechanisms for chemotherapeutic resistance in GC. Fourthly, except for mRNA level, the protein expression level of genes could also be powerful prognostic markers of patient survival. Further investigations and researches are needed to explore the relationship between the protein expression level of four genes and GC patients' survival.

In conclusion, we developed the SERM prognostic signature related to CSC and EMT processes for predicting OS, DFS, and drug sensitivity in GC patients. Enrichment analysis to some extent unmasked a part of molecular mechanisms of the gene signature in GC, which might give guidance for developing targeted therapies. The nomogram-combined clinical characteristics and gene signature for OS prediction could improve the prognostic accuracy of the traditional TNM staging system. We anticipate that the SERM signature will offer a brand-new reference for current prognostic prediction and give more guidance in developing tailored therapy in GC patients.

DATA AVAILABILITY STATEMENT

The datasets presented in this study can be found in online repositories. The names of the repository/repositories and accession number(s) can be found in the article/**Supplementary Material**.

ETHICS STATEMENT

Ethical review and approval was not required for the study on human participants in accordance with the local legislation and institutional requirements. Written informed consent for participation was not required for this study in accordance with the national legislation and the institutional requirements.

AUTHOR CONTRIBUTIONS

XJ, BC, and ZL contributed to the conception and design of the project. XJ, BC, ZL, SC, and RZ participated in the data collection, data analyses, and manuscript writing. XJ and BC made all the figures and tables. SH provided advice for the study and reviewed the manuscript. XZ and HZ edited the manuscript and supervised the project. All the authors read and approved the final manuscript. All authors contributed to the article and approved the submitted version.

FUNDING

This work was funded by The National Key Research and Development Program of China (2017YFC1308900) and the Science and Technology Commission of Shanghai Municipality (grant number: STCSM18411953000) granted to HZ.

SUPPLEMENTARY MATERIAL

The Supplementary Material for this article can be found online at: https://www.frontiersin.org/articles/10.3389/fonc.2021.799223/full#supplementary-material

Supplementary Table S1 | Clinical characteristics and mRNAsi of 296 samples in the TCGA cohort.

Supplementary Table S2 | Clinical characteristics and RT-qPCR results of 126 patients in our cohort.

Supplementary Table S3 | Primers of SERPINE1, EDIL3, RGS4, MATN3 and β-catenin used for RT-qPCR.

Supplementary Table S4 | Univariate Cox regression analysis of 60 overlapped genes.

Supplementary Table S5 | Univariate and Multivariate Cox regression of TCGA cohort with different clinical parameters and Risk score.

Supplementary Table S6 | Univariate and Multivariate Cox regression of GSE66229 cohort with different clinical parameters and Risk score.

Supplementary Table S7 | Univariate and Multivariate Cox regression of GSE15459 cohort with different clinical parameters and risk score.

Supplementary Figure S1 | Pearson's correlation analyses between mRNA expression level of EMT markers and risk score value in TCGA-STAD and GSE66229 cohorts.

Supplementary Figure S2 | Assessment of prognostic value of gene signature on GC DFS in GSE66229 cohort. **(A)** Kaplan-Meier analysis of DFS between high- and low-risk groups based on CSCs and EMT-related gene signature. **(B)** Risk score time dependent 1-, 3-, 5- year ROC of DFS. **(C)** Multivariate Cox regression analysis of clinical parameters and risk score. **(D)** The distributions of risk score, survival status, and heatmap of CSCs and EMT-related gene signature expression levels.

Supplementary Figure S3 | RT-qPCR result of SERPINE1 **(A)**, EDIL3 **(B)**, RGS4 **(C)**, MATN3 **(D)** mRNA expression levels in eight GC cell lines (HGC-27, MKN-28, SGC-7901, BGC-823, MGC-803, AGS, NCI-N87, MKN-45) and gastric mucosal cell line GES1.

REFERENCES

1. Machlowska J, Baj J, Sitarz M, Maciejewski R, Sitarz R. Gastric Cancer: Epidemiology, Risk Factors, Classification, Genomic Characteristics and Treatment Strategies. *Int J Mol Sci* (2020) 21(11):4012. doi: 10.3390/ijms21114012
2. Sung H, Ferlay J, Siegel RL, Laversanne M, Soerjomataram I, Jemal A, et al. Global Cancer Statistics 2020: GLOBOCAN Estimates of Incidence and Mortality Worldwide for 36 Cancers in 185 Countries. *CA Cancer J Clin* (2021) 71(3):209–49. doi: 10.3322/caac.21660
3. Arnold M, Park JY, Camargo MC, Lunet N, Forman D, Soerjomataram I. Is Gastric Cancer Becoming a Rare Disease? A Global Assessment of Predicted Incidence Trends to 2035. *Gut* (2020) 69(5):823–9. doi: 10.1136/gutjnl-2019-320234
4. Cristescu R, Lee J, Nebozhyn M, Kim KM, Ting JC, Wong SS, et al. Molecular Analysis of Gastric Cancer Identifies Subtypes Associated With Distinct Clinical Outcomes. *Nat Med* (2015) 21(5):449–56. doi: 10.1038/nm.3850
5. Babaei G, Aziz SG, Jaghi NZZ. EMT, Cancer Stem Cells and Autophagy; The Three Main Axes of Metastasis. *BioMed Pharmacother* (2021) 133:110909. doi: 10.1016/j.biopha.2020.110909
6. Wilson MM, Weinberg RA, Lees JA, Guen VJ. Emerging Mechanisms by Which EMT Programs Control Stemness. *Trends Cancer* (2020) 6(9):775–80. doi: 10.1016/j.trecan.2020.03.011
7. Gonzalez DM, Medici D. Signaling Mechanisms of the Epithelial-Mesenchymal Transition. *Sci Signal* (2014) 7(344):re8. doi: 10.1126/scisignal.2005189
8. Lamouille S, Xu J, Derynck R. Molecular Mechanisms of Epithelial-Mesenchymal Transition. *Nat Rev Mol Cell Biol* (2014) 15(3):178–96. doi: 10.1038/nrm3758
9. Yeo CD, Kang N, Choi SY, Kim BN, Park CK, Kim JW, et al. The Role of Hypoxia on the Acquisition of Epithelial-Mesenchymal Transition and Cancer Stemness: A Possible Link to Epigenetic Regulation. *Korean J Intern Med* (2017) 32(4):589–99. doi: 10.3904/kjim.2016.302
10. Dai W, Xiao Y, Tang W, Li J, Hong L, Zhang J, et al. Identification of an EMT-Related Gene Signature for Predicting Overall Survival in Gastric Cancer. *Front Genet* (2021) 12:661306. doi: 10.3389/fgene.2021.661306
11. Ning W, Qiu Z, Ji X, Wang X, An Y, Wang S, et al. The Prognostic Value of EMT in Glioma and its Role in the Glioma Immune Microenvironment. *J Mol Neurosci* (2020) 70(10):1501–11. doi: 10.1007/s12031-020-01583-y
12. Tanaka Y, Terai Y, Kawaguchi H, Fujiwara S, Yoo S, Tsunetoh S, et al. Prognostic Impact of EMT (Epithelial-Mesenchymal-Transition)-Related Protein Expression in Endometrial Cancer. *Cancer Biol Ther* (2013) 14 (1):13–9. doi: 10.4161/cbt.22625
13. Kathawala RJ, Gupta P, Ashby CRJr., Chen ZS. The Modulation of ABC Transporter-Mediated Multidrug Resistance in Cancer: A Review of the Past Decade. *Drug Resist Update* (2015) 18:1–17. doi: 10.1016/j.drup.2014.11.002
14. Korkaya H, Liu S, Wicha MS. Breast Cancer Stem Cells, Cytokine Networks, and the Tumor Microenvironment. *J Clin Invest* (2011) 121(10):3804–9. doi: 10.1172/jci57099
15. Korkaya H, Liu S, Wicha MS. Regulation of Cancer Stem Cells by Cytokine Networks: Attacking Cancer's Inflammatory Roots. *Clin Cancer Res* (2011) 17 (19):6125–9. doi: 10.1158/1078-0432.CCR-10-2743
16. Brungs D, Aghmesheh M, Vine KL, Becker TM, Carolan MG, Ranson M. Gastric Cancer Stem Cells: Evidence, Potential Markers, and Clinical Implications. *J Gastroenterol* (2016) 51(4):313–26. doi: 10.1007/s00535-015-1125-5
17. Vesuna F, Lisok A, Kimble B, Raman V. Twist Modulates Breast Cancer Stem Cells by Transcriptional Regulation of CD24 Expression. *Neoplasia* (2009) 11 (12):1318–28. doi: 10.1593/neo.91084
18. Yoon C, Till J, Cho SJ, Chang KK, Lin JX, Huang CM, et al. KRAS Activation in Gastric Adenocarcinoma Stimulates Epithelial-To-Mesenchymal Transition to Cancer Stem-Like Cells and Promotes Metastasis. *Mol Cancer Res* (2019) 17(9):1945–57. doi: 10.1158/1541-7786.MCR-19-0077
19. Cai Z, Cao Y, Luo Y, Hu H, Ling H. Signalling Mechanism(s) of Epithelial-Mesenchymal Transition and Cancer Stem Cells in Tumour Therapeutic Resistance. *Clin Chim Acta* (2018) 483:156–63. doi: 10.1016/j.cca.2018.04.033
20. Malta TM, Sokolov A, Gentles AJ, Burzykowski T, Poisson L, Weinstein JN, et al. Machine Learning Identifies Stemness Features Associated With Oncogenic Dedifferentiation. *Cell* (2018) 173(2):338–54 e15. doi: 10.1016/j.cell.2018.03.034
21. Mao D, Zhou Z, Song S, Li D, He Y, Wei Z, et al. Identification of Stemness Characteristics Associated With the Immune Microenvironment and Prognosis in Gastric Cancer. *Front Oncol* (2021) 11:626961. doi: 10.3389/fonc.2021.626961
22. Yang JD, Ma L, Zhu Z. SERPINE1 as a Cancer-Promoting Gene in Gastric Adenocarcinoma: Facilitates Tumour Cell Proliferation, Migration, and Invasion by Regulating EMT. *J Chemother* (2019) 31(7-8):408–18. doi: 10.1080/1120009X.2019.1687996
23. Kamarudin AN, Cox T, Kolamunnage-Dona R. Time-Dependent ROC Curve Analysis in Medical Research: Current Methods and Applications. *BMC Med Res Methodol* (2017) 17(1):53. doi: 10.1186/s12874-017-0332-6
24. Van Calster B, Wynants L, Verbeek JFM, Verbakel JY, Christodoulou E, Vickers AJ, et al. Reporting and Interpreting Decision Curve Analysis: A Guide for Investigators. *Eur Urol* (2018) 74(6):796–804. doi: 10.1016/j.eururo.2018.08.038
25. Shibue T, Weinberg RA. EMT, CSCs, and Drug Resistance: The Mechanistic Link and Clinical Implications. *Nat Rev Clin Oncol* (2017) 14(10):611–29. doi: 10.1038/nrclinonc.2017.44
26. Wang SS, Jiang J, Liang XH, Tang YL. Links Between Cancer Stem Cells and Epithelial-Mesenchymal Transition. *Onco Targets Ther* (2015) 8:2973–80. doi: 10.2147/OTT.S91863
27. Singh A, Settleman JEMT. Cancer Stem Cells and Drug Resistance: An Emerging Axis of Evil in the War on Cancer. *Oncogene* (2010) 29 (34):4741–51. doi: 10.1038/onc.2010.215
28. Ding X, Huang R, Zhong Y, Cui N, Wang Y, Weng J, et al. CTHRC1 Promotes Gastric Cancer Metastasis *via* HIF-1alpha/CXCR4 Signaling Pathway. *BioMed Pharmacother* (2020) 123:109742. doi: 10.1016/j.biopha.2019.109742
29. Sammarco G, Varricchi G, Ferraro V, Ammendola M, De Fazio M, Altomare DF, et al. Mast Cells, Angiogenesis and Lymphangiogenesis in Human Gastric Cancer. *Int J Mol Sci* (2019) 20(9):2106. doi: 10.3390/ijms20092106
30. S. Kaufhold BB. Central Role of Snail1 in the Regulation of EMT and Resistance in Cancer: A Target for Therapeutic Intervention. *J Exp Clin Cancer Res* (2014) 33(1):62. doi: 10.1186/s13046-014-0062-0
31. Zhang H, Ren L, Ding Y, Li F, Chen X, Ouyang Y, et al. Hyaluronan-Mediated Motility Receptor Confers Resistance to Chemotherapy *via* TGFbeta/Smad2-Induced Epithelial-Mesenchymal Transition in Gastric Cancer. *FASEB J* (2019) 33(5):6365–77. doi: 10.1096/fj.201802186R

32. Lee HH, Seo KJ, An CH, Kim JS, Jeon HM. CD133 Expression is Correlated With Chemoresistance and Early Recurrence of Gastric Cancer. *J Surg Oncol* (2012) 106(8):999–1004. doi: 10.1002/jso.23178
33. Song Y, Chen Y, Li Y, Lyu X, Cui J, Cheng Y, et al. Resveratrol Suppresses Epithelial-Mesenchymal Transition in GBM by Regulating Smad-Dependent Signaling. *BioMed Res Int* (2019) 2019:1321973. doi: 10.1155/2019/1321973
34. Choi JE, Bae JS, Kang MJ, Chung MJ, Jang KY, Park HS, et al. Expression of Epithelial-Mesenchymal Transition and Cancer Stem Cell Markers in Colorectal Adenocarcinoma: Clinicopathological Significance. *Oncol Rep* (2017) 38(3):1695–705. doi: 10.3892/or.2017.5790
35. Groza IM, Braicu C, Jurj A, Zanoaga O, Lajos R, Chiroi P, et al. Cancer-Associated Stemness and Epithelial-To-Mesenchymal Transition Signatures Related to Breast Invasive Carcinoma Prognostic. *Cancers (Basel)* (2020) 12 (10):3053. doi: 10.3390/cancers12103053
36. Stark TW, Hensley PJ, Spear A, Pu H, Strup SS, Kyprianou N. Predictive Value of Epithelial-Mesenchymal-Transition (EMT) Signature and PARP-1 in Prostate Cancer Radioresistance. *Prostate* (2017) 77(16):1583–91. doi: 10.1002/pros.23435
37. Yi L, Huang P, Zou X, Guo L, Gu Y, Wen C, et al. Integrative Stemness Characteristics Associated With Prognosis and the Immune Microenvironment in Esophageal Cancer. *Pharmacol Res* (2020) 161:105144. doi: 10.1016/j.phrs.2020.105144
38. Zhao M, Chen Z, Zheng Y, Liang J, Hu Z, Bian Y, et al. Identification of Cancer Stem Cell-Related Biomarkers in Lung Adenocarcinoma by Stemness Index and Weighted Correlation Network Analysis. *J Cancer Res Clin Oncol* (2020) 146(6):1463–72. doi: 10.1007/s00432-020-03194-x
39. Yang MH, Hsu DS, Wang HW, Wang HJ, Lan HY, Yang WH, et al. Bmi1 is Essential in Twist1-Induced Epithelial-Mesenchymal Transition. *Nat Cell Biol* (2010) 12(10):982–92. doi: 10.1038/ncb2099
40. Chen HF, Wu KJ. Endothelial Transdifferentiation of Tumor Cells Triggered by the Twist1-Jagged1-KLF4 Axis: Relationship Between Cancer Stemness and Angiogenesis. *Stem Cells Int* (2016) 2016:6439864. doi: 10.1155/2016/6439864
41. Weng CC, Ding PY, Liu YH, Hawse JR, Subramaniam M, Wu CC, et al. Mutant Kras-Induced Upregulation of CD24 Enhances Prostate Cancer Stemness and Bone Metastasis. *Oncogene* (2019) 38(12):2005–19. doi: 10.1038/s41388-018-0575-7
42. Yang MH, Wu MZ, Chiou SH, Chen PM, Chang SY, Liu CJ, et al. Direct Regulation of TWIST by HIF-1alpha Promotes Metastasis. *Nat Cell Biol* (2008) 10(3):295–305. doi: 10.1038/ncb1691
43. Qureshi-Baig K, Kuhn D, Viry E, Pozdeev VI, Schmitz M, Rodriguez F, et al. Hypoxia-Induced Autophagy Drives Colorectal Cancer Initiation and Progression by Activating the PRKC/PKC-EZR (Ezrin) Pathway. *Autophagy* (2020) 16(8):1436–52. doi: 10.1080/15548627.2019.1687213
44. Deng J, Bai X, Feng X, Ni J, Beretov J, Graham P, et al. Inhibition of PI3K/Akt/mTOR Signaling Pathway Alleviates Ovarian Cancer Chemoresistance Through Reversing Epithelial-Mesenchymal Transition and Decreasing Cancer Stem Cell Marker Expression. *BMC Cancer* (2019) 19(1):618. doi: 10.1186/s12885-019-5824-9
45. Xu J, Zhang W, Tang L, Chen W, Guan X. Epithelial-Mesenchymal Transition Induced PAI-1 is Associated With Prognosis of Triple-Negative Breast Cancer Patients. *Gene* (2018) 670:7–14. doi: 10.1016/j.gene.2018.05.089
46. Massagué J. How Cells Read TGF-Beta Signals. *Nat Rev Mol Cell Biol* (2000) 1 (3):169–78. doi: 10.1038/35043051
47. Radke DI, Ling Q, Hasler R, Alp G, Ungefroren H, Trauzold A. Downregulation of TRAIL-Receptor 1 Increases TGFbeta Type II Receptor Expression and TGFbeta Signalling *Via* MicroRNA-370-3p in Pancreatic Cancer Cells. *Cancers (Basel)* (2018) 10(11):399. doi: 10.3390/cancers10110399
48. Bhat-Nakshatri P, Goswami CP, Badve S, Sledge GWJr., Nakshatri H. Identification of FDA-Approved Drugs Targeting Breast Cancer Stem Cells Along With Biomarkers of Sensitivity. *Sci Rep* (2013) 3:2530. doi: 10.1038/srep02530
49. McCann JV, Xiao L, Kim DJ, Khan OF, Kowalski PS, Anderson DG, et al. Endothelial miR-30c Suppresses Tumor Growth *via* Inhibition of TGF-Beta-Induced Serpine1. *J Clin Invest* (2019) 129(4):1654–70. doi: 10.1172/JCI123106
50. Aoki M, Kanamori M, Ohmori K, Takaishi M, Huh NH, Nogami S, et al. Expression of Developmentally Regulated Endothelial Cell Locus 1 was Induced by Tumor-Derived Factors Including VEGF. *Biochem Biophys Res Commun* (2005) 333(3):990–5. doi: 10.1016/j.bbrc.2005.06.009
51. Luo J-H, Ren B, Keryanov S, Tseng GC, Rao UNM, Monga SP, et al. Transcriptomic and Genomic Analysis of Human Hepatocellular Carcinomas and Hepatoblastomas. *Hepatology* (2006) 44(4):1012–24. doi: 10.1002/hep.21328
52. Choi EY, Chavakis E, Czabanka MA, Langer HF, Fraemohs L, Economopoulou M, et al. Del-1, an Endogenous Leukocyte-Endothelial Adhesion Inhibitor, Limits Inflammatory Cell Recruitment. *Science* (2008) 322(5904):1101–4. doi: 10.1126/science.1165218
53. Damhofer H, Medema JP, Veenstra VL, Badea L, Popescu I, Roelink H, et al. Assessment of the Stromal Contribution to Sonic Hedgehog-Dependent Pancreatic Adenocarcinoma. *Mol Oncol* (2013) 7(6):1031–42. doi: 10.1016/j.molonc.2013.08.004
54. Beckham CJ, Olsen J, Yin PN, Wu CH, Ting HJ, Hagen FK, et al. Bladder Cancer Exosomes Contain EDIL-3/Del1 and Facilitate Cancer Progression. *J Urol* (2014) 192(2):583–92. doi: 10.1016/j.juro.2014.02.035
55. Lee SJ, Lee J, Kim WW, Jung JH, Park HY, Park JY, et al. Del-1 Expression as a Potential Biomarker in Triple-Negative Early Breast Cancer. *Oncology* (2018) 94(4):243–56. doi: 10.1159/000485658
56. Jeong D, Ban S, Oh S, Jin Lee S, Yong Park S, Koh YW. Prognostic Significance of EDIL3 Expression and Correlation With Mesenchymal Phenotype and Microvessel Density in Lung Adenocarcinoma. *Sci Rep* (2017) 7(1):8649. doi: 10.1038/s41598-017-08851-9
57. Xia H, Chen J, Shi M, Gao H, Sekar K, Seshachalam VP, et al. EDIL3 is a Novel Regulator of Epithelial-Mesenchymal Transition Controlling Early Recurrence of Hepatocellular Carcinoma. *J Hepatol* (2015) 63(4):863–73. doi: 10.1016/j.jhep.2015.05.005
58. Guda MR, Velpula KK, Asuthkar S, Cain CP, Tsung AJ. Targeting RGS4 Ablates Glioblastoma Proliferation. *Int J Mol Sci* (2020) 21(9):3300. doi: 10.3390/ijms21093300
59. Cheng C, Yue W, Li L, Li S, Gao C, Si L, et al. Regulator of G-Protein Signaling 4: A Novel Tumor Suppressor With Prognostic Significance in non-Small Cell Lung Cancer. *Biochem Biophys Res Commun* (2016) 469(3):384–91. doi: 10.1016/j.bbrc.2015.11.110
60. Tanabe S, Aoyagi K, Yokozaki H, Sasaki H. Regulated Genes in Mesenchymal Stem Cells and Gastric Cancer. *World J Stem Cells* (2015) 7(1):208–22. doi: 10.4252/wjsc.v7.i1.208
61. Zhang Y, Wang ZK, Luo JM, Kanbe K, Chen Q. Multiple Functions of the Von Willebrand Factor A Domain in Matrilins: Secretion, Assembly, and Proteolysis. *J Orthop Surg Res* (2008) 3:21. doi: 10.1186/1749-799X-3-21
62. Wu PL, He YF, Yao HH, Hu B. Martrilin-3 (MATN3) Overexpression in Gastric Adenocarcinoma and its Prognostic Significance. *Med Sci Monit* (2018) 24:348–55. doi: 10.12659/msm.908447

Conflict of Interest: The authors declare that the research was conducted in the absence of any commercial or financial relationships that could be construed as a potential conflict of interest.

Publisher's Note: All claims expressed in this article are solely those of the authors and do not necessarily represent those of their affiliated organizations, or those of the publisher, the editors and the reviewers. Any product that may be evaluated in this article, or claim that may be made by its manufacturer, is not guaranteed or endorsed by the publisher.

Copyright © 2022 Jia, Chen, Li, Huang, Chen, Zhou, Feng, Zhu and Zhu. This is an open-access article distributed under the terms of the Creative Commons Attribution License (CC BY). The use, distribution or reproduction in other forums is permitted, provided the original author(s) and the copyright owner(s) are credited and that the original publication in this journal is cited, in accordance with accepted academic practice. No use, distribution or reproduction is permitted which does not comply with these terms.

frontiers in Oncology

ORIGINAL RESEARCH
published: 18 January 2022
doi: 10.3389/fonc.2021.785850

A Nomogram for Predicting the Risk of Radiotherapy-Related Esophageal Fistula in Esophageal Cancer Patients

Zhongxuan Gui, Huiquan Liu, Weijiong Shi, Yuechen Xu, Han Qian and Fan Wang *

Department of Radiation Oncology, The First Affiliated Hospital of Anhui Medical University, Hefei, China

Background: To construct and validate a nomogram for predicting the risk of esophageal fistula in esophageal cancer patients receiving radiotherapy.

Methods: A retrospective nested case–control study was performed, in which a total of 81 esophageal fistula patients and 243 controls from 2014 to 2020 in the First Affiliated Hospital of Anhui Medical University were enrolled. Factors included in the nomogram were determined by univariate and multiple logistic regression analysis. The following methods including ROC curve, C-index, calibration curves, Brier score, and decision curve analysis (DCA) were adopted to evaluate this nomogram.

Results: Multivariate logistic regression analysis showed that T4 stage, level 4 stenosis, ulcerative esophageal cancer, prealbumin, and maximum diameters of GTV and NLR were the independent risk factors of esophageal fistula. Accordingly, a nomogram incorporating the aforementioned six parameters was constructed. The AUC was 0.848 (95% CI 0.901–0.895), indicating a high prediction accuracy of this nomogram. Further evaluation of this model showed that the C-index was 0.847, while the bias-corrected C-index after internal validation was 0.833. The Brier score was 0.127. The calibration curves presented good concordance, and the DCA revealed promising clinical application.

Conclusions: The nomogram presents accurate and applicable prediction for the esophageal fistula risk in esophageal cancer patients receiving radiotherapy.

Keywords: esophageal cancer, radiotherapy, esophageal fistula, risk factors, nomogram

OPEN ACCESS

Edited by:
Luigi Marano,
University of Siena, Italy

Reviewed by:
Jian Bin Li,
Shandong Cancer Hospital, China
Ludovico Carbone,
University of Siena, Italy

***Correspondence:**
Fan Wang
wangfan1965@126.com

Specialty section:
This article was submitted to Gastrointestinal Cancers: Gastric Esophageal Cancers, a section of the journal Frontiers in Oncology

Received: *29 September 2021*
Accepted: *20 December 2021*
Published: *18 January 2022*

Citation:
Gui Z, Liu H, Shi W, Xu Y, Qian H and Wang F (2022) A Nomogram for Predicting the Risk of Radiotherapy-Related Esophageal Fistula in Esophageal Cancer Patients. Front. Oncol. 11:785850. doi: 10.3389/fonc.2021.785850

INTRODUCTION

Esophageal cancer (EC) is the seventh most common malignancy worldwide leading to estimated 544,000 deaths in 2020 (1). Patients with EC are usually diagnosed at the advanced or metastatic stage due to the lack of early symptoms and the rapid progression of carcinoma. Thus, a considerable proportion of EC patients are considered inoperable or surgically contraindicated at the initial visit. Radiotherapy, especially the intensity-modulated radiation therapy (IMRT), plays a critical role in the treatment of locally advanced inoperable EC (2). It is remarkable that esophageal fistula (EF), a fatal treatment-related complication, may occur during and after radiotherapy.

The incidence of EF in EC patients receiving chemoradiotherapy is about 4.3%–22% according to previous studies (3–10). The common clinical symptoms of EF include bucking, back/chest/abdominal pain, fever, hydrothorax, dysphagia, and empyema (11). Therefore, early prediction of EF and appropriate intervention are important to enhance clinical outcomes and increase quality of life.

Previous literature (6, 8, 12) described that several clinical parameters are closely correlated with the occurrence of EF, including age, T stage, N stage, stenosis, ulceration, low serum cholesterol level, and body mass index (BMI). However, a unified diagnosis criterion for esophageal stenosis has not been unified, and the majority of studies defined stenosis solely based on symptoms (4, 8, 13). To date, there are still no reliable clinical standards for predicting high-risk EF. In this study, we further refined several EF-associated parameters and explored a clinically applicable nomogram to predict EF risk for EC patients receiving radiotherapy.

MATERIALS AND METHODS

Study Design

We retrospectively studied the medical records of EC patients receiving radiotherapy in the First Affiliated Hospital of Anhui Medical University, between October 19, 2014, and June 15, 2020. Follow-up was carried out since the radiotherapy stated until the EF occurred or until June 15, 2021, ensuring that each patient was followed for sufficient time to accurately assess the occurrence of EF. The enrolled EC patients with previous malignancies, history of esophageal surgery, already formed fistula before treatment, and lost follow-up were excluded. The inclusion criteria for EF patients are applied: (1) histologically proved squamous cell carcinoma, adenocarcinoma, or small cell carcinoma of the esophagus; (2) complete record of the necessary clinical characteristics; (3) clinically confirmed EF or esophageal perforation which were detected by endoscopy, computed tomography (CT), or esophagography; and (4) no EF before radiotherapy. The diagnostic standards of EF were as follows: (i) iodine examination shows that contrast media leak out from the patient's fistula, or into the patient's chest, mediastinum; (ii) CT scan findings include mediastinal air surrounding the esophagus, abscess cavities adjacent to the esophagus in the pleural space, mediastinal air, pleural effusion, pneumothorax, and subdiaphragmatic air(11). To improve the comparison and the stability of the results, the cases and controls were matched by age, gender, and diagnosis time at a ratio of 1:3. This retrospective nested case–control study was approved by the institutional research ethics committee of Anhui Medical University.

Data Collection

In this single-centered, retrospective study, we obtained the demographic characteristics, laboratory data, radiological examinations, and therapeutic strategy from electronic medical records. The following clinical characteristics were collected before radiotherapy: general characteristics (gender, age, body mass index (BMI), smoking history, hypertension, diabetes (DM)), tumor characteristics (stage, location, ulcerative EC, esophageal stenosis), treatment characteristics (re-radiotherapy, radiotherapy dose, chemotherapy, gross tumor volume (GTV), maximum diameter of GTV, length of GTV, treatment response), and hematological data (albumin, hemoglobin, prealbumin, neutrophil count, lymphocyte count).

The pretreatment clinical staging was on the basis of the American Joint Committee on Cancer (AJCC) 8th edition staging system (14). GTV was defined by the planning physicians as the primary tumor (GTVp) and involved mediastinal and hilar nodes (GTVn) found by computed tomography (CT) or positron emission tomography/computed tomography (PET/CT) before treatment. The NLR was defined as the absolute neutrophil count divided by the absolute lymphocyte count. The treatment response was assessed 30 days after radiotherapy by enhanced CT based on Response Evaluation Criteria in Solid Tumors (RECIST) version 1.1, and it was classified as clinically complete response (CR), partial response (PR), stable disease (SD), or progressive disease (PD). CR was defined as the disappearance of all target lesions, PR as reduction by 30% or more in maximum diameter of target lesion, PD as increase by 20% or more in the longest tumor diameter of target lesion or appearance of new lesions, and SD as other than CR, PD, and PR.

To determine the stenosis of esophagus, we reviewed the esophagography image obtained before radiotherapy and measured the lumen diameter at the widest part of the oral side (**Figure 1A**) and the narrowest part of the lesion (**Figure 1B**). The stenosis ratio was calculated as following formula: c = (a - b)/a * 100%. The severity of esophageal stenosis (stenosis ratio) was evaluated and classified as the following grades: grade I, 0%–24%; grade II, 25%–49%; grade III, 50%–74%; grade IV, 75%–100%.

Statistical Analyses

Odds ratios (OR) with 95% confidence intervals (CI) were used to evaluate the relationship between the clinical parameters and EF, and the best cutoff values to predict EF risk were determined using receiver operating characteristic (ROC) curves. We investigated all the clinical factors by univariable logistic regression for paired samples, and the significant factors were included in the multivariable logistic-regression model. Statistical analyses were performed using IBM SPSS 22.0 software. A nomogram integrating independent risk factors of EF was created using R software (version 3.6.1). The receiver operating characteristic (ROC) curve and the area under the ROC curve (AUC) were applied to assess the discrimination of the model. We adopted three methods, including C-index for discrimination, calibration curves, and Brier score to evaluate this nomogram. The established nomogram was further internally validated by bootstrapping (1,000 bootstrap replicates) to obtain bias-corrected predictive parameters. Significance was defined as 2-sided p-value of < 0.05.

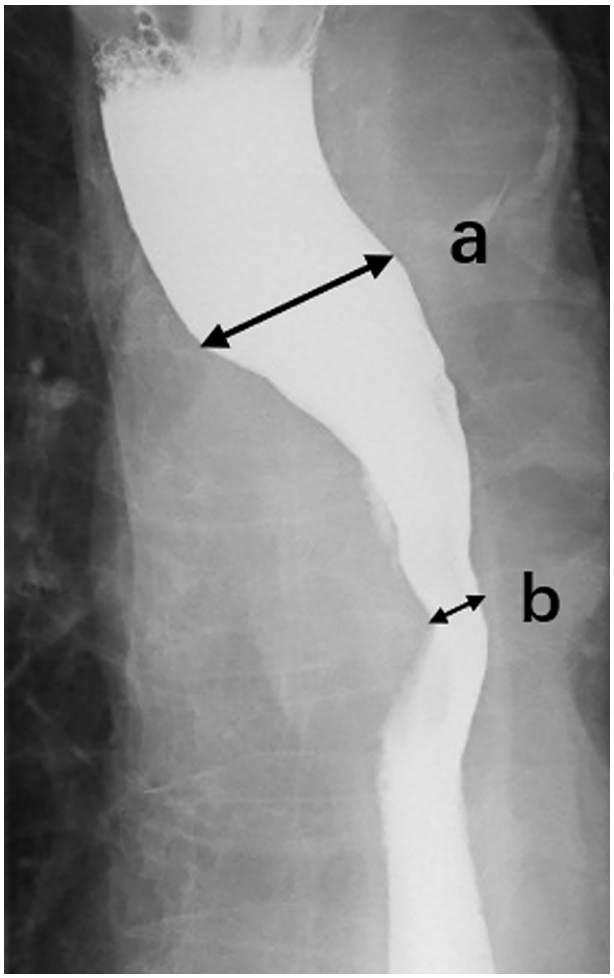

FIGURE 1 | Esophagography image. We reviewed the esophagography image obtained before radiotherapy and measured the lumen diameter at the widest part **(A)** of the oral side and the narrowest part **(B)** of the lesion, then calculated the stenotic ratio (c = (a - b)/a * 100).

RESULTS

Characteristics of Participants

Between October 19, 2014, and June 15, 2020, 1,894 cases who had undergone radiotherapy were identified in our database and 711 cases were excluded based on our exclusion criteria. Among the 1,183 EC patients, 81 (6.85%) had developed EF before June 15, 2021. After matching by age, gender, and diagnosis time, a total of 324 EC patients, including those 81 (25.0%) EF cases and 243 (75.0%) controls, were enrolled for the subsequent analyses. The follow-up period ranged from 2.3 to 82.6 months, and the median time was 51.7 months. The median age of these participants was 70.0 years, and the male-to-female ratio is 3.3:1. Middle thoracic (40.7%) EC was more common than upper thoracic (31.1%) and lower thoracic (28.0%) EC. Of these patients who developed EF, 12 patients suffered perforation during RT, while 69 patients developed this complication after RT. The median intervals between the end of radiotherapy and the EF onset were 4.60 months (95% CI: 3.50–5.64). Among all the 81 cases with EF, 46 cases developed esophagomediastinal fistula, 28 cases developed esophagotracheal fistula, 2 cases developed esophagoarterio fistulas, and 5 cases suffered both esophagomediastinal and esophagotracheal fistula. Managements of fistula included nutrient canal in 61 patients (75.3%), esophageal stent in 16 patients (19.7%), and parenteral nutrition in 4 patients (4.9%). The patient characteristics are listed in **Table 1**.

Risk Factors for EF

As shown in **Table 2**, univariate analysis revealed that BMI < 20 kg/m^2, N1–3 stage, T4 stage, NLR, hemoglobin, prealbumin, re-radiotherapy, ulcerative EC, stenosis, length of GTV, and maximum diameter of GTV were significantly correlated with the occurrence of EF (p-value < 0.05). The other clinical parameters including age, albumin, tumor location, M stage, total dose > 60 Gy, single dose, GTV volume, chemotherapy, treatment response (PR+CR vs. SD+PD), smoking history, diabetes, and hypertension were not significant for their association with EF. Multivariate analysis showed that T4 stage, level 4 stenosis, ulcerative EC, prealbumin, and maximum diameters of GTV and NLR remained significant (p-value < 0.05), which indicated that these clinical characteristics were independent risk factors for the occurrence of EF (**Table 2**).

Predictive Nomogram for EF

According to the results of multivariate analysis, a nomogram incorporating the 6 independent risk factors was constructed to predict EF (**Figure 2**). The total point was calculated with the use of T4, NLR, ulcerative EC, level 4 stenosis, prealbumin, and maximum diameter of GTV. The point of each of these variables was given a score on the point scale axis. A total score could be easily calculated by adding each single score, and by projecting the total score to the lower total point scale, we were able to estimate the probability of EF.

Evaluation and Validation the Nomogram

The AUC was 0.848 (95% CI 0.901–0.895) (**Figure 3A**), indicating robust discrimination. The Brier score of the nomogram was 0.127, which was close to 0, indicating great predictive ability (**Figure 3B**). As shown in **Figure 3C**, the calibration plot showed good conformity between predicted and actual probability for EF. The uncorrected concordance index (C-index) was 0.847, and the corrected C-index generated by internal validation was 0.833 (**Figure 3C**). Finally, we performed a decision curve analysis (DCA) to evaluate the clinical utility of the nomogram and its effective threshold ranged from approximately 7% to 91%, showing that using this nomogram was more effective than the "treat-all" or the "treat-none" strategy in predicting EF when the prediction probability was within this range (**Figure 3D**).

DISCUSSION

The EF, a severe complication, deteriorates the quality of life and shortens survival in EC patients. Predicting EF risk is crucial for developing individual therapeutic strategies. In this study, we

TABLE 1 | The characteristics of patients with radiotherapy-related esophageal fistula.

Characteristics	No esophageal fistula	Esophageal fistula
Gender		
Male	186 (0.77)	62 (0.77)
Female	57 (0.23)	19 (0.23)
Age (years)		
<60	41 (0.17)	20 (0.25)
≥60	202 (0.83)	61 (0.75)
History of smoking		
No	168 (0.69)	48 (0.59)
Yes	75 (0.31)	33 (0.41)
History of hypertension		
No	212 (0.87)	67 (0.83)
Yes	31 (0.13)	14 (0.17)
History of diabetes		
No	235 (0.97)	76 (0.94)
Yes	8 (0.03)	5 (0.06)
BMI (kg/m^2)		
<20	93 (0.38)	43 (0.53)
≥20	150 (0.62)	38 (0.47)
T stage		
T1–3	224 (0.92)	55 (0.68)
T4	19 (0.08)	26 (0.32)
N stage		
N0	104 (0.43)	25 (0.31)
N1–3	139 (0.57)	56 (0.69)
M stage		
M0	189 (0.78)	66 (0.81)
M1	54 (0.22)	15 (0.19)
Location of primary tumor		
Upper thoracic esophagus	74 (0.30)	27 (0.33)
Middle thoracic esophagus	95 (0.39)	37 (0.46)
Lower thoracic esophagus	74 (0.30)	17 (0.21)
Ulcerative tumor		
No	191 (0.79)	34 (0.42)
Yes	52 (0.21)	47 (0.58)
Maximum diameter of GTV (cm)		
≤2.5	72 (0.30)	7 (0.09)
>2.5	171 (0.70)	74 (0.91)
Length of GTV (cm)		
≤5.5	141 (0.58)	28 (0.35)
>5.5	102 (0.42)	53 (0.65)
GTV volume (cm^3)		
≤60	151 (0.62)	36 (0.44)
>60	92 (0.38)	45 (0.56)
Fraciton dose (Gy)		
1.8	17 (0.07)	10 (0.12)
2.0	226 (0.93)	71 (0.88)
Total radiation dose		
<60	148 (0.58)	36 (0.54)
≥60	92 (0.42)	45 (0.46)
Re-radiotherapy		
No	231 (0.95)	70 (0.86)
Yes	12 (0.05)	11 (0.14)
Treatment modalities		
Concurrent CRT	127 (0.52)	38 (0,47)
Sequential CRT	103 (0.42)	39 (0.48)
Without CT	13 (0.05)	4 (0.05)
Treatment response		
SD+PD	106 (0.44)	31 (0.38)
CR+PR	137 (0.56)	50 (0.62)
Stenosis before radiotherapy		
Levels 1–3	151 (0.62)	18 (0.22)
Level 4	92 (0.38)	63 (0.78)

(Continued)

TABLE 1 | Continued

Characteristics	No esophageal fistula	Esophageal fistula
Hemoglobin (g/L)		
<120	89 (0.37)	42 (0.52)
≥120	154 (0.63)	39 (0.48)
Albumin (g/L)		
<35	50 (0.21)	23 (0.28)
≥35	193 (0.79)	58 (0.72)
Prealbumin (mg/L)		
<180	66 (0.27)	37 (0.46)
≥180	177 (0.73)	44 (0.54)
NLR		
<3.2	130 (0.53)	30 (0.37)
≥3.2	113 (0.47)	51 (0.63)
PLR		
<155	135 (0.56)	27 (0.33)
≥155	108 (0.44)	54 (0.67)

BMI, body mass index; GTV, gross tumor volume; CRT, chemoradiotherapy; CT, chemotherapy; SD, stable disease; PD, progressive disease; CR, complete response; PR, partial response; NLR, neutrophil to lymphocyte ratio; PLR, platelet to lymphocyte ratio.

comprehensively evaluated the fistula-related parameters and identified several new independent risk factors. For dosimetry-related indicators, we found that the incidence of fistula was 28.9% in the group of GTV maximum diameters ≤2.5 cm, while the incidence decreased to 14.6% in the group of maximum diameter of GTV > 2.5 cm. To some extent, the maximum diameter of GTV indicated the severity of local radiation damage and the depth of tumor invasion. These results suggest that for the high-risk EF patients, moderate shrinks of GTV are needed.

The status when esophageal carcinoma invades adjacent structures, such as the pleura, pericardium, azygos vein, diaphragm, peritoneum, aorta, vertebral body, and airway, is defined as T4 stage in the 8th Edition of the AJCC TNM Staging System (15). Recently, Chen et al. (16)revealed that the incidence rate of EF was 30.1% in EC patients (stage T4b) and the median overall survival was only 6.9 months. It is easy to understand that if the space-occupying lesions were eliminated speedily by chemoradiotherapy without sufficient tissue repair, the fistula might form between the esophageal lumen and contiguous structures. Formation of a fistula between the esophagus and the mediastinum was suspected.

We believe that EC with external esophageal invasion should receive individualized radiotherapy not only to kill the tumor cells but also to maximize normal tissue repair. Additionally, we also characterized ulcerative lesion as an independent factor of EF, which was consistent with previous studies (8, 16). In our study, we observed that the incidence rate of ulcerative-type carcinoma diagnosed before radiotherapy in the EF group was nearly three times that in the control group (58.0% vs. 21.3%). Ulcerative esophageal cancer has a deep invasion and thin wall, reaching or penetrating the muscular layer, and then the perforation may occur due to increased luminal pressure during swallowing or severe coughing.

It is estimated that more than half of EC patients suffer from malnutrition (17). Cancer-associated dysphagia and anorexia are the leading causes of malnutrition, while radiation-induced mucositis makes matters worse. Malnutrition and cachexia restrain the damage repair, reduce therapeutic effects, and increase mortality (17, 18). In this study, we also explored the risk factors from the perspective of nutrition and found that BMI, hemoglobin, and prealbumin were significantly associated with the occurrence of EF. Meanwhile, multivariable analysis demonstrated that low prealbumin was an independent risk factor, which was not previously reported. Previous studies have shown that prealbumin is considered to be more sensitive than albumin in the nutritional assessment of patients undergoing radiotherapy (19). Serum prealbumin with a half-life of 2 to 3 days in the human body is a good clinical marker of protein balance and nutritional status (20, 21). These results indicate that nutritional support, such as oral nutritional supplements, promisingly prevents the occurrence of EF.

Most of the published articles investigated esophageal stenosis based on symptoms and did not define its degree of severity. The NCCN guidelines noted that the most common cause of dysphagia is obstruction, but it may also be associated with cancer-related dysmotility (22), which may affect the assessment of esophageal stenosis. Thus, we used a specific criterion to evaluate and grade the stenosis by esophageal barium meal examination before treatment. Intriguingly, our results showed that esophageal stenosis at level 4 was a significant independent risk factor in fistula formation. It is speculated that the internal pressure was associated with severity of the esophageal stenosis and caused expansionary damage to esophageal wall. As a result, it is appropriate to identify the esophageal stenosis before radiotherapy, so as to make dietary adjustments and palliative management, such as endoscopic stenting and endoscopic dilation (23, 24).

Malignant tumors usually trigger an intrinsic inflammatory response to establish a tumorigenic microenvironment (25, 26). The NLR as a marker of systemic inflammatory response has received great attention because of its accessibility. In clinical practice, the NLR is increasingly used to predict bacteremia, peptic ulcer perforation, severe cholecystitis, acute cholecystitis, acute pancreatitis, acute coronary syndrome and community-acquired infections, and even the survival of cancer patients (27–30). Systemic inflammatory responses have been proved to

TABLE 2 | Univariate and multivariate analysis of the factors associated with esophageal fistula.

Characteristics	Univariate			Multivariate		
	OR	95% CI	*p*-value	OR	95% CI	*p*-value
Age (years)						
<60	0.621	0.338–1.143	0.126			
≥60						
History of smoking						
No	0.990	0.565–1.737	0.973			
Yes						
History of hypertension						
No	0.574	0.249–1.324	0.193			
Yes						
History of diabetes						
No	2.000	0.626–6.393	0.242			
Yes						
BMI (kg/m^2)						
<20	0.560	0.339–0.924	0.924	0.872	0.404–1.882	0.728
≥20						
T stage						
T1–3	5.278	2.687–10.366	<0.001	5.357	2.052–13.983	0.001
T4						
N stage						
N0	1.787	1.001–3.188	0.049	1.160	0.5–2.691	0.730
N1–3						
M stage						
M0	0.801	0.427–1.504	0.491			
M1						
Location of primary tumor						
Upper thoracic esophagus	1.000		1.000			
Middle thoracic esophagus	1.050	0.590–1.866	0.869			
Lower thoracic esophagus	0.591	0.288–1.214	0.152			
Ulcerative tumor						
No	5.504	3.015–10.049	<0.001	3.102	1.536–6.265	0.002
Yes						
Maximum diameters of GTV (cm)						
≤2.5	4.611	1.999–10.633	<0.001	3.675	1.432–9.433	0.007
>2.5						
Length of GTV (cm)						
≤5.5	2.553	1.510–4.318	<0.001	1.297	0.623–2.698	0.487
>5.5						
GTV volume (cm^3)						
≤60	2.048	1.226–3.421	0.008	1.378	0.678–2.8	0.375
>60						
Fraction dose (Gy)						
1.8	0.492	0.202–1.198	0.118			
2.0						
Total radiation dose						
<60	1.149	0.695–1.899	0.589			
≥60						
Re–radiotherapy						
No	2.887	1.244–6.702	0.014	2.599	0.707–9.548	0.150
Yes						
Treatment modalities						
Concurrent CRT	1.000					
Sequential CRT	1.038	0.319–3.373	0.951			
Without CT	1.258	0.737–2.146	0.400			
Treatment response						
SD+PD	1.217	0.732–2.023	0.449			
CR+PR						
Stenosis before radiotherapy						
Level 1–3	5.631	3.069–10.331	<0.001	6.549	2.984–14.373	<0.001
Level 4						
Hemoglobin (g/dL)						
<120	0.528	0.311–0.898	0.018	0.834	0.4–1.738	0.627

(Continued)

TABLE 2 | Continued

Characteristics	Univariate			Multivariate		
	OR	95% CI	*p*-value	OR	95% CI	*p*-value
≥120						
Albumin(g/dL)						
<35	0.678	0.388–1.185	0.173			
≥35						
Prealbumin (mg/L)						
<180	0.439	0.257–0.749	0.003	0.399	0.189–0.842	0.016
≥180						
NLR						
<3.2	1.953	1.158–3.293	0.012	2.326	1.12–4.831	0.024
≥3.2						
PLR						
<155	2.657	1.516–4.659	0.001	1.492	0.609–3.657	0.382
≥155						

BMI, body mass index; GTV, gross tumor volume; CRT, chemoradiotherapy; CT, chemotherapy; SD, stable disease; PD, progressive disease; CR, complete response; PR, partial response; NLR, neutrophil to lymphocyte ratio; PLR, platelet to lymphocyte ratio.

influence the motility, invasiveness, and survival of malignant cells through upregulating cytokines, such as IL-1β, IL-6, IL-7, IL-8, and IL-12. The host-cellular response to IL-8 released by cancer cells enhances neutrophil infiltration, which promotes remodeling of the extracellular matrix and tumor progression (31). High NLR represents more severe inflammation and more advanced disease with aggressive clinical characteristics. In this study, we preliminarily explored the significant association of high NLR with EF. Further research is needed to explore the specific mechanism and the application of NLR in EF.

The nomogram is a kind of visual graph based on the multiple regression model. It integrates several parameters and consists of different length line segments. In this study, we screened out six independent risk factors by multiple regression to establish a personalized prediction model. Further validation proved that this nomogram has good predictive accuracy and clinical application potential. This is the first and comprehensive calculable tool consisting of systemic inflammatory status, nutritional status, and radiation-related parameters to predict EF risk. However, our current study has certain drawbacks that merit discussion. First, as a retrospective, single-center study, it was inevitable to have potential bias. Second, only internal validation was carried out due to limited EF cases. External validation from other centers is necessary to confirm the clinical value of this nomogram. Lastly, the interaction between inflammation and fistula remains obscure, and more trials are needed to clarify the underlying mechanisms. In view of these limitations, we are now planning to expand the sample size of EF patients, further explore predictors with clinical practicability, and improve the model on the basis of the current findings to optimize the prediction of EF.

In summary, we characterized several new clinical parameters as the independent risk factors of EF. A nomogram was accordingly constructed and visualized to facilitate the prediction of EF risk. This calculable tool is promisingly applied in clinical practice to participate in determining individual therapeutic strategies for EC patients.

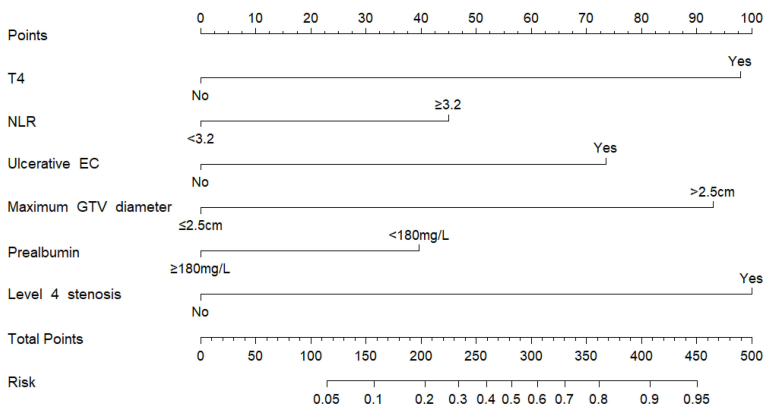

FIGURE 2 | Nomogram for the individualized prediction of radiation-related esophageal fistula in esophageal cancer patients. The nomogram was developed in the cohort, using T4, level 4 stenosis, ulcerative EC, prealbumin, and maximum diameters of GTV and NLR. GTV, gross tumor volume; NLR, neutrophil-to-lymphocyte ratio.

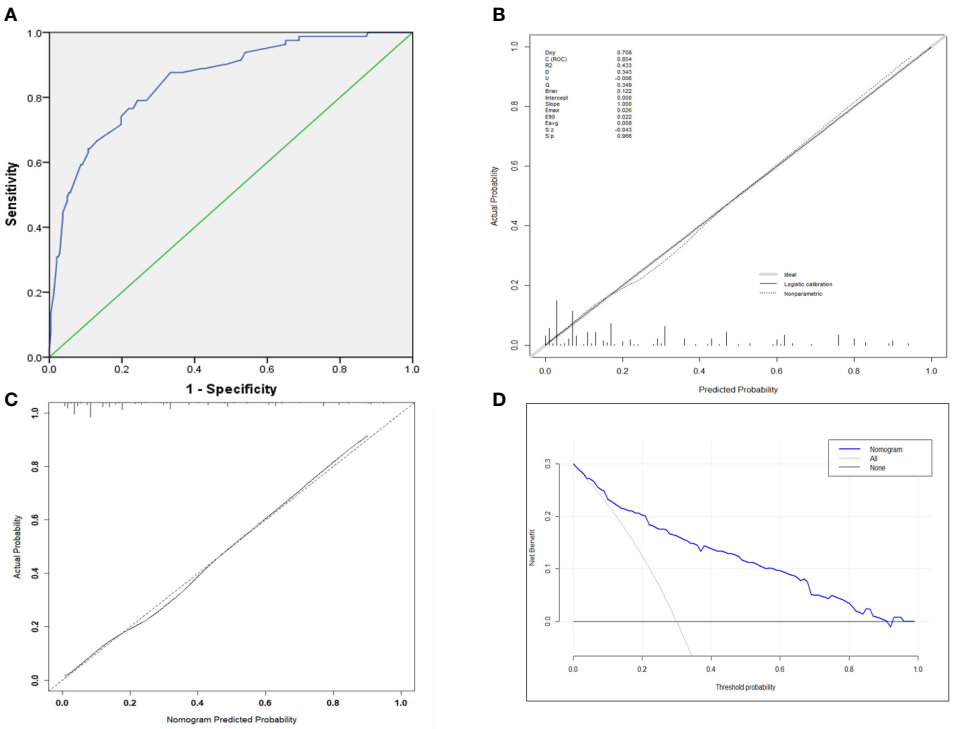

FIGURE 3 | **(A)** ROC curve for the prediction nomogram. **(B)** The Brier score for the prediction nomogram. **(C)** Calibration curve showing nomogram-predicted EF probabilities compared with the actual EF. **(D)** The decision curve analysis of the nomogram.

DATA AVAILABILITY STATEMENT

The original contributions presented in the study are included in the article/supplementary material. Further inquiries can be directed to the corresponding author.

ETHICS STATEMENT

The studies involving human participants were reviewed and approved by the Institutional Review Board of the First Affiliated Hospital of Anhui Medical University. Written informed consent for participation was not required for this study in accordance with the national legislation and the institutional requirements.

AUTHOR CONTRIBUTIONS

ZG and HL conceived and designed this study. WS, YX, and HQ processed the data analysis. ZG wrote the article. FW revised the final manuscript. All authors contributed to the article and approved the submitted version.

ACKNOWLEDGMENTS

The authors appreciate the esophagography images provided by the Department of Medical Imaging at the First Affiliated Hospital of Anhui Medical University.

REFERENCES

1. Sung H, Ferlay J, Siegel RL. Global Cancer Statistics 2020: GLOBOCAN Estimates of Incidence and Mortality Worldwide for 36 Cancers in 185 Countries. *CA Cancer J Clin* (2021) 71(3):209–49. doi: 10.3322/caac.21660
2. Wang SX, Marshall MB. Chemoradiation Therapy as Definitive Treatment of Esophageal Cancer. *Surg Clin North Am* (2021) 101(3):443–51. doi: 10.1016/j.suc.2021.03.006
3. Chen Y, Lu Y, Wang Y, Yang H, Xia Y, Chen M, et al. Comparison of Salvage Chemoradiation Versus Salvage Surgery for Recurrent Esophageal Squamous Cell Carcinoma After Definitive Radiochemotherapy or Radiotherapy Alone. *Dis Esophagus* (2014) 27(2):134–40. doi: 10.1111/j.1442-2050.2012.01440.x
4. Han D, Zhang J, Zhao J, Lei T, Chen X, Zhang T, et al. Platelet-To-Lymphocyte Ratio Is an Independent Predictor of Chemoradiotherapy-Related Esophageal Fistula in Esophageal Cancer Patients. *Ann Transl Med* (2020) 8(18):1163. doi: 10.21037/atm-20-4053
5. Hihara J, Hamai Y, Emi M, Murakami Y, Kenjo M, Nagata Y, et al. Role of Definitive Chemoradiotherapy Using Docetaxel and 5-Fluorouracil in Patients With Unresectable Locally Advanced Esophageal Squamous Cell Carcinoma: A Phase II Study. *Dis Esophagus* (2016) 29(8):1115–20. doi: 10.1111/dote.12433
6. Pao TH, Chen YY, Chang WL, Chang JS, Chiang NJ, Lin CY, et al. Esophageal Fistula After Definitive Concurrent Chemotherapy and Intensity Modulated Radiotherapy for Esophageal Squamous Cell Carcinoma. *PLOS ONE* (2021) 16(5):e0251811. doi: 10.1371/journal.pone.0251811

7. Sun X, Han S, Gu F, Lin G, Wang Z, Wang Y, et al. A Retrospective Comparison of Taxane and Fluorouracil-Based Chemoradiotherapy in Patients With Inoperable Esophageal Squamous Cell Carcinoma. *J Cancer* (2016) 7(9):1066–73. doi: 10.7150/jca.13547
8. Tsushima T, Mizusawa J, Sudo K, Honma Y, Kato K, Igaki H, et al. Risk Factors for Esophageal Fistula Associated With Chemoradiotherapy for Locally Advanced Unresectable Esophageal Cancer: A Supplementary Analysis of JCOG0303. *Med (Baltimore)* (2016) 95(20):e3699. doi: 10.1097/md.0000000000003699
9. Watanabe S, Ogino I, Kunisaki C, Hata M. Relationship Between Nutritional Status and Esophageal Fistula Formation After Radiotherapy for Esophageal Cancer. *Cancer Radiother* (2019) 23(3):222–7. doi: 10.1016/j.canrad.2018.10.005
10. Zhou ZG, Zhen CJ, Bai WW, Zhang P, Qiao XY, Liang JL, et al. Salvage Radiotherapy in Patients With Local Recurrent Esophageal Cancer After Radical Radiochemotherapy. *Radiat Oncol* (2015) 10:54. doi: 10.1186/s13014-015-0358-z
11. Carrascosa MF, Herreras-Martínez R, Trugeda-Carrera S, Terán Á., Fernández-Díaz MJ, Concha ST, et al. Oesophageal Perforation. *Lancet Gastroenterol Hepatol* (2018) 3(9):654. doi: 10.1016/s2468-1253(18)30179-1
12. Xu Y, Wang L. Development and Validation of a Risk Prediction Model for Radiotherapy-Related Esophageal Fistula in Esophageal Cancer. *Radiat Oncol* (2019) 14: (1):181. doi: 10.1186/s13014-019-1385-y
13. Zhang Y, Li Z, Zhang W, Chen W, Song Y. Risk Factors for Esophageal Fistula in Patients With Locally Advanced Esophageal Carcinoma Receiving Chemoradiotherapy. *Onco Targets Ther* (2018) 11:2311–7. doi: 10.2147/ott.s161803
14. Rice TW, Patil DT, Blackstone EH. 8th Edition AJCC/UICC Staging of Cancers of the Esophagus and Esophagogastric Junction: Application to Clinical Practice. *Ann Cardiothorac Surg* (2017) 6(2):119–30. doi: 10.21037/acs.2017.03.14
15. Daiko H, Kato K. Updates in the 8th Edition of the TNM Staging System for Esophagus and Esophagogastric Junction Cancer. *Jpn J Clin Oncol* (2020) 50 (8):847–51. doi: 10.1093/jjco/hyaa082
16. Chen B, Deng M, Yang C, Dragomir MP, Zhao L, Bai K, et al. High Incidence of Esophageal Fistula on Patients With Clinical T4b Esophageal Squamous Cell Carcinoma Who Received Chemoradiotherapy: A Retrospective Analysis. *Radiother Oncol* (2021) 158:191–9. doi: 10.1016/j.radonc.2021.02.031
17. Mariette C, De Botton ML, Piessen G. Surgery in Esophageal and Gastric Cancer Patients: What is the Role for Nutrition Support in Your Daily Practice? *Ann Surg Oncol* (2012) 19(7):2128–34. doi: 10.1245/s10434-012-2225-6
18. Jordan T, Mastnak DM, Palamar N, Kozjek NR. Nutritional Therapy for Patients With Esophageal Cancer. *Nutr Cancer* (2018) 70(1):23–9. doi: 10.1080/01635581.2017.1374417
19. Unal D, Orhan O, Eroglu C, Kaplan B. Prealbumin is a More Sensitive Marker Than Albumin to Assess the Nutritional Status in Patients Undergoing Radiotherapy for Head and Neck Cancer. *Contemp Oncol (Pozn)* (2013) 17 (3):276–80. doi: 10.5114/wo.2013.35281
20. Geisler JP, Linnemeier GC, Thomas AJ, Manahan KJ. Nutritional Assessment Using Prealbumin as an Objective Criterion to Determine Whom Should Not Undergo Primary Radical Cytoreductive Surgery for Ovarian Cancer. *Gynecol Oncol* (2007) 106(1):128–31. doi: 10.1016/j.ygyno.2007.03.008
21. Guerra LT, Rosa AR, Romani RF, Gurski RR, Schirmer CC, Kruel CD. Serum Transferrin and Serum Prealbumin as Markers of Response to Nutritional Support in Patients With Esophageal Cancer. *Nutr Hosp* (2009) 24(2):241–2.
22. Ajani JA, Barthel JS, Bentrem DJ, D'Amico TA, Das P, Denlinger CS, et al. Esophageal and Esophagogastric Junction Cancers. *J Natl Compr Canc Netw* (2011) 9(8):830–87. doi: 10.6004/jnccn.2011.0072
23. Halpern AL, McCarter MD. Palliative Management of Gastric and Esophageal Cancer. *Surg Clin North Am* (2019) 99(3):555–69. doi: 10.1016/j.suc.2019.02.007
24. Kim JY, Kim SG, Lim JH, Im JP, Kim JS, Jung HC. Clinical Outcomes of Esophageal Stents in Patients With Malignant Esophageal Obstruction According to Palliative Additional Treatment. *J Dig Dis* (2015) 16(10):575–84. doi: 10.1111/1751-2980.12280
25. Gonzalez H, Hagerling C, Werb Z. Roles of the Immune System in Cancer: From Tumor Initiation to Metastatic Progression. *Genes Dev* (2018) 32: (19-20):1267–84. doi: 10.1101/gad.314617.118
26. Greten FR, Grivennikov SI. Inflammation and Cancer: Triggers, Mechanisms, and Consequences. *Immunity* (2019) 51(1):27–41. doi: 10.1016/j.immuni.2019.06.025
27. Han F, Liu Y, Cheng S, Sun Z, Sheng C, Sun X, et al. Diagnosis and Survival Values of Neutrophil-Lymphocyte Ratio (NLR) and Red Blood Cell Distribution Width (RDW) in Esophageal Cancer. *Clin Chim Acta* (2019) 488:150–8. doi: 10.1016/j.cca.2018.10.042
28. Lee SK, Lee SC, Park JW, Kim SJ. The Utility of the Preoperative Neutrophil-to-Lymphocyte Ratio in Predicting Severe Cholecystitis: A Retrospective Cohort Study. *BMC Surg* (2014) 14:100. doi: 10.1186/1471-2482-14-100
29. Suppiah A, Malde D, Arab T, Hamed M, Allgar V, Smith AM, et al. The Prognostic Value of the Neutrophil-Lymphocyte Ratio (NLR) in Acute Pancreatitis: Identification of an Optimal NLR. *J Gastrointest Surg* (2013) 17(4):675–81. doi: 10.1007/s11605-012-2121-1
30. Tanrikulu Y, Sen Tanrikulu C, Sabuncuoglu MZ, Kokturk F, Temi V, Bicakci E. Is the Neutrophil-to-Lymphocyte Ratio a Potential Diagnostic Marker for Peptic Ulcer Perforation? A Retrospective Cohort Study. *Am J Emerg Med* (2016) 34(3):403–6. doi: 10.1016/j.ajem.2015.11.009
31. De Larco JE, Wuertz BR, Furcht LT. The Potential Role of Neutrophils in Promoting the Metastatic Phenotype of Tumors Releasing Interleukin-8. *Clin Cancer Res* (2004) 10(15):4895–900. doi: 10.1158/1078-0432.ccr-03-0760

Conflict of Interest: The authors declare that the research was conducted in the absence of any commercial or financial relationships that could be construed as a potential conflict of interest.

Publisher's Note: All claims expressed in this article are solely those of the authors and do not necessarily represent those of their affiliated organizations, or those of the publisher, the editors and the reviewers. Any product that may be evaluated in this article, or claim that may be made by its manufacturer, is not guaranteed or endorsed by the publisher.

Copyright © 2022 Gui, Liu, Shi, Xu, Qian and Wang. This is an open-access article distributed under the terms of the Creative Commons Attribution License (CC BY). The use, distribution or reproduction in other forums is permitted, provided the original author(s) and the copyright owner(s) are credited and that the original publication in this journal is cited, in accordance with accepted academic practice. No use, distribution or reproduction is permitted which does not comply with these terms.

frontiers in Oncology

CASE REPORT
published: 27 January 2022
doi: 10.3389/fonc.2021.780577

Case Report: Durable Clinical Response to Third-Line Pyrotinib After Resistance to Trastuzumab in a Gastric Cancer Patient

Junyi Wu[1†], Lei Li[1†], Jun Qin[1], Zhengqing Yan[2], Shiqing Chen[2], Tao Jin[1] and Junming Xu[1*]*

[1] Department of General Surgery, Shanghai General Hospital, Shanghai Jiaotong University School of Medicine, Shanghai, China, [2] The Medical Department, 3D Medicines Inc., Shanghai, China

Background: Trastuzumab plus chemotherapy remains the standard first-line treatment strategy for HER2-positive gastric cancer (GC). Trastuzumab resistance, on the other hand, remains a significant issue. There are a few effective anti-HER2 agents for patients who develop resistance to trastuzumab.

Case Presentation: A 49-year-old female was diagnosed with stage IV GC with liver and lung metastasis in July 2017. She underwent gastrostomy, and the immunohistochemistry (IHC) result of postoperative tissue demonstrated HER2 (3+). She received first-line treatment of trastuzumab (440 mg), oxaliplatin (200 mg), and S-1 (40 mg). After treatment for 6 months, the patient achieved complete response (CR) with PFS up to 21 months. After progression, she subsequently received trastuzumab (440 mg) plus oxaliplatin (200 mg) as second-line treatment. However, the patient developed resistance to trastuzumab after 12 months of treatment. She started to receive third-line treatment of irinotecan (200 mg d1) and capecitabine (60 mg bid) plus pyrotinib (400 mg/day). After 2 months of treatment, the tumor is evaluated as partial response with PFS of 12 months.

Conclusions: We presented a patient with HER2-positive GC who benefited from the pyrotinib-based treatment after two lines of trastuzumab-based therapies failed. Further research is required to validate such conclusions.

Keywords: gastric cancer, HER2, trastuzumab, resistance, pyrotinib

OPEN ACCESS

Edited by:
Luigi Marano, University of Siena, Italy

Reviewed by:
Antonio Rozzi, CHIC Compiégne-Noyon, France
Pankaj Kumar Garg, Shri Guru Ram Rai Institute of Medical and Health Sciences, India

****Correspondence:***
Tao Jin
empiric_taojin@163.com
Junming Xu
xujunming183@163.com

†These authors share first authorship

Specialty section:
This article was submitted to Gastrointestinal Cancers: Gastric & Esophageal Cancers, a section of the journal Frontiers in Oncology

Received: *21 September 2021*
Accepted: *13 December 2021*
Published: *27 January 2022*

Citation:
Wu J, Li L, Qin J, Yan Z, Chen S, Jin T and Xu J (2022) Case Report: Durable Clinical Response to Third-Line Pyrotinib After Resistance to Trastuzumab in a Gastric Cancer Patient. Front. Oncol. 11:780577. doi: 10.3389/fonc.2021.780577

INTRODUCTION

Gastric cancer (GC) ranks the third among the leading causes of cancer deaths worldwide (1, 2). The survival outcomes in unresectable or advanced GC patients are poor with generally a 5-year survival rate of less than 20%. Although many clinical trials for GC treatment have been investigating the novel treatment strategies, most of them failed. Among various molecular biomarkers, human epidermal growth factor receptor 2 (HER2) remains a critical biomarker and accounted for ~5% to 36% GC (3). Although conflicting, some studies reported that HER2-positive related to the aggressive disease and poor outcomes.

Trastuzumab in combination with chemotherapy remains the standard first-line treatment strategy for HER2-positive GC. However, trastuzumab cardiotoxicity and resistance are two tricky issues (4, 5). Previous studies show that compensatory signal transduction of other HER receptors belong to a critical drug-resistance mechanism of trastuzumab (6). Currently, there are few effective anti-HER2 agents for patients who develop resistance to trastuzumab.

Pyrotinib, as a novel irreversible EGFR/HER2 dual tyrosine kinase inhibitor (TKI), has been approved by the National Medical Products Administration (NMPA) for HER2−positive breast cancer (7–9). A phase III randomized controlled trial demonstrated that pyrotinib plus capecitabine, compared with lapatinib plus capecitabine, could significantly prolong progression-free survival (PFS) (12.5 vs. 6.8 months) in patients with HER2-positive advanced breast cancer (10). Notably, patients achieved benefits from pyrotinib therapy, no matter whether trastuzumab was administered previously. Nine patients with HER2-positive GC were enrolled to receive pyrotinib-based therapy with a median OS of 5.9 months (95% CI: 4.0–9.6 months) (11). Currently, it is still unclear whether pan-HER inhibitor pyrotinib is an effective agent for trastuzumab-resistant GC. Herein, we presented a HER2-postive advanced GC that achieved durable clinical response to third-line pyrotinib, after two lines of trastuzumab-based treatments failed.

CASE PRESENTATION

A 49-year-old female was diagnosed with stage IV GC with liver and lung metastasis in July 2017 (**Figure 1A**). She suffered gastrostomy and the immunohistochemistry (IHC) result of postoperative tissue demonstrated HER2 (3+). She received first-line treatment of trastuzumab (440 mg), oxaliplatin (200 mg), and S-1 (40 mg). After 6 months of treatment, the patient achieved complete response (CR) with PFS up to 21 months (**Figure 1B**). In March 2019, enlarged hepatic portal lymph nodes were observed. Liver metastasis lesion was curatively resected (R0) and subsequently second-line treatment of trastuzumab (440 mg) plus oxaliplatin (200 mg) was administrated (**Figure 1C**). The PFS was 12 months with enlarged peritoneal lymph nodes in March 2020, which suggested that the patient developed resistance to trastuzumab. Regardless of pre-resistance or post-resistance, both the tumors were HER2-positive (**Figure 1D**). The NGS results of the

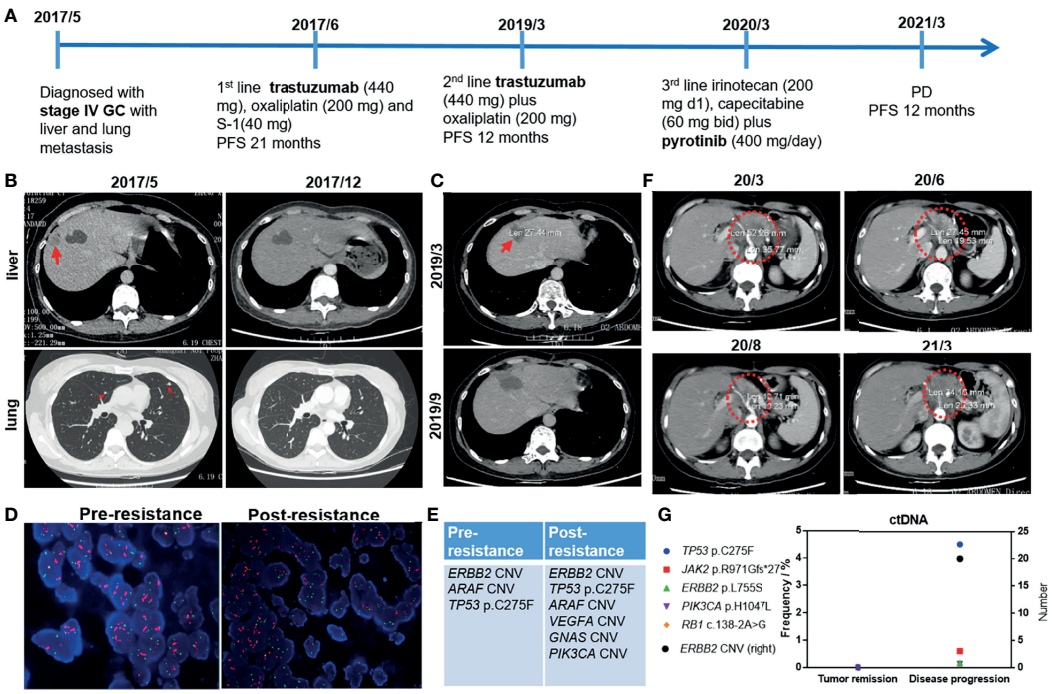

FIGURE 1 | **(A)** The treatment procedure of the 49-year-old female with stage IV GC. GC, gastric cancer; PFS, progression-free survival; PD, progressive disease. **(B)** The results of chest computed tomography (CT) scans suggested that liver and lung lesions were reduced in size after first-line treatment. **(C)** CT results at first relapse in March 2019 and after surgical operation (R0 resection) in September 2019. **(D)** Fluorescence *in situ* hybridization (FISH) images demonstrated HER2 amplification. **(E)** NGS analysis of tumor tissue at diagnosis (pre-resistance) and first relapse (post-resistance). **(F)** The CT results following second relapse suggested the tumor shrank with third-line treatment. March 2020, Baseline; June and August 2020, during tumor remission; March 2021, tumor progression. **(G)** The ctDNA status during tumor remission and disease progression.

primary and liver lesions are shown in **Figure 1E**, respectively. The primary lesion harbored *HER2* copy number variation (CNV), *ARAF* CNV, and *TP53* p.C275F. Besides, *VEGFA*, *GNAS*, and *PIK3CA* CNVs were also found in the liver metastasis. The adverse effect (AE) was bone marrow suppression (Grade 2) during the treatment of trastuzumab plus chemotherapy. After multi-disciplinary team (MDT) discussion, she started to receive third-line treatment of irinotecan (200 mg d1) and capecitabine (60 mg bid) plus pyrotinib (400 mg/day). After 2 months of treatment, the tumor is evaluated as partial response (PR, **Figure 1F**). No ctDNA alterations are detected at tumor remission (**Figure 1G**). The AEs were diarrhea (Grade 1) and bone marrow suppression (Grade 2) during the third-line treatment. Until March 2021, progressive disease was observed with PFS of 12 months and the maximum allele frequency (MAF) of ctDNA was up to 4.53%. The patient was administrated trastuzumab + anti-PD-1 + chemotherapy as fourth-line treatment. Until the last follow-up in November 2021, no progressive disease was observed. Currently, close follow-up is still ongoing.

DISCUSSION

In this work, a pyrotinib-based regime was administered as third-line treatment for a HER2-positive GC patient who developed resistance to trastuzumab, and this patient achieved partial response. During treatment, ctDNA was used for monitoring tumor development. Interestingly, no ctDNA was detected during tumor remission. In contrast, the maximum allele frequency (MAF) of ctDNA was up to 4.53% (*TP53* p. C275F) during progression. Such results supported that ctDNA might be an alternative clinical biomarker for disease monitoring in GC.

With the development of non-invasive ctDNA sequencing technology, real-time monitoring tumor load is becoming an effective complement for tissue testing (12–14). Such technology has been used to monitor minimal residual disease (MRD), as well as tumor recurrence in various cancers, such as NSCLC and CRC (15, 16). Additionally, ctDNA response could be used to evaluate therapeutic effect and to explore potential resistance mechanisms for targeted drugs (17, 18). Considering the high heterogeneity characteristic of GC, ctDNA was used as an important tool for monitoring disease progression (19, 20). The appearance of ctDNA could predict tumor recurrence earlier than routine imaging examination. Previous work reported that ctDNA appearance during longitudinal post-operative follow-up was associated with worse DFS (HR = 14.78) and OS (HR = 7.664) (21). Furthermore, the clearance of ctDNA was associated with better clinical outcomes in advanced solid cancers, especially for the patients who were treated with pembrolizumab (14). In this work, no ctDNA was detected during tumor remission, and the maximum allele frequency (MAF) was up to 4.53% (*TP53* p. C275F) during progression. The present work highlighted that monitoring ctDNA might be a viable alternative to tissue-based genotyping in the metastatic setting.

Currently, HER2-targeted regimes have been widely used in various tumor treatments. HER2 protein plays a critical role in the tumorigenesis, tumor progression, and tumor metastasis (22). The ToGA trial suggested that trastuzumab combined with chemotherapy could significantly improve survival outcomes for advanced HER2-positive GC (23). However, the heterogeneity of GC and trastuzumab resistance limited the therapeutic effect of trastuzumab in clinical practice. Currently, some novel anti-HER2 agents (e.g., lapatinib, afatinib, neratinib, dacomitinib, pertuzumab, and ado-trastuzumab emtansine) are being investigated in HER2-positive GC, especially for those patients who progressed on or after trastuzumab-based therapy (24). Besides HER2, pan-HER inhibitors could induce sustained inhibition of HER3 or EGFR, which might overcome intrinsic or acquired resistance of trastuzumab. Such differences might support durable clinical response to pyrotinib in trastuzumab-resistant GC. Previous work reported that HER2-positive GC who received trastuzumab-based therapy also could benefit from 8th-line treatment of pyrotinib, a novel irreversible pan-HER TKI inhibitor (25). In this case, pyrotinib was administrated after two lines of trastuzumab, which might explain the efficacy of pyrotinib in trastuzumab-resistant GC better.

Previous studies indicated that bypass activation represented an important resistance mechanism for trastuzumab resistance (6). The RAS or PI3K signaling pathway, as a downstream signaling pathway of the HER2 receptor, is associated with intrinsic and/or acquired trastuzumab resistance and poor survival outcomes in patients who received trastuzumab treatment. In this case, *VEGFA*, *GNAS*, and *PIK3CA* CNVs were observed in tissue during trastuzumab resistance. The new emerging gene alterations *PIK3CA* p.H1047L, *HER2* p.L755S, *JAK2* p.R971Gfs*27, and *RB1* c.138-2A>G were observed in ctDNA during pyrotinib progression. Such results indicated that the resistance mechanism of trastuzumab and pyrotinib might be different. Furthermore, exploring their exact resistance mechanism is important and necessary. In view of the nature of case reports, such results should be further explored in larger cohorts.

CONCLUSION

In this case, a pyrotinib-based regime was used as third-line therapy for a HER2-positive GC patient who developed resistance to trastuzumab, and the patient achieved a partial response. Furthermore, longitudinal ctDNA sequencing could be used to investigate drug resistance mechanisms and guide the precision treatment for GC patients. Further research is required to validate such conclusions.

ETHICS STATEMENT

Written informed consent was obtained from the patient for the publication of any potentially identifiable images or data included in this article.

AUTHOR CONTRIBUTIONS

JX and TJ contributed to the planning and organization. JW and LL collected clinical data and supervised the findings of this work. JQ aided in the data collection and the supervision. ZY and SC analyzed the results and prepared the manuscript. All authors contributed to the article and approved the submitted version.

REFERENCES

1. Song Z, Wu Y, Yang J, Yang D, Fang X. Progress in the Treatment of Advanced Gastric Cancer. *Tumour Biol* (2017) 39:1010428317714626. doi: 10.1177/1010428317714626
2. Smyth EC, Nilsson M, Grabsch HI, van Grieken NCT, Lordick F. Gastric Cancer. *Lancet* (2020) 396:635–48. doi: 10.1016/S0140-6736(20)31288-5
3. Boku N. HER2-Positive Gastric Cancer. *Gastric Cancer* (2014) 17:1–12. doi: 10.1007/s10120-013-0252-z
4. Soo Park J, Youn JC, Shim CY, Hong GR, Lee CK, Kim JH, et al. Cardiotoxicity of Trastuzumab in Patients With HER2-Positive Gastric Cancer. *Oncotarget* (2017) 8:61837–45. doi: 10.18632/oncotarget.18700
5. Kelly CM, Janjigian YY. The Genomics and Therapeutics of HER2-Positive Gastric Cancer-From Trastuzumab and Beyond. *J Gastrointest Oncol* (2016) 7:750–62. doi: 10.21037/jgo.2016.06.10
6. Janjigian YY, Sanchez-Vega F, Jonsson P, Chatila WK, Hechtman JF, Ku GY, et al. Genetic Predictors of Response to Systemic Therapy in Esophagogastric Cancer. *Cancer Discov* (2018) 8:49–58. doi: 10.1158/2159-8290.CD-17-0787
7. Li X, Yang C, Wan H, Zhang G, Feng J, Zhang L, et al. Discovery and Development of Pyrotinib: A Novel Irreversible EGFR/HER2 Dual Tyrosine Kinase Inhibitor With Favorable Safety Profiles for the Treatment of Breast Cancer. *Eur J Pharm Sci* (2017) 110:51–61. doi: 10.1016/j.ejps.2017.01.021
8. Huang T, Luo X, Wu B, Peng P, Dai Y, Hu G, et al. Pyrotinib Enhances the Radiosensitivity of HER2overexpressing Gastric and Breast Cancer Cells. *Oncol Rep* (2020) 44:2634–44. doi: 10.3892/or.2020.7820
9. Gao Z, Song C, Li G, Lin H, Lian X, Zhang N, et al. Pyrotinib Treatment on HER2-Positive Gastric Cancer Cells Promotes the Released Exosomes to Enhance Endothelial Cell Progression, Which Can Be Counteracted by Apatinib. *Onco Targets Ther* (2019) 12:2777–87. doi: 10.2147/OTT.S194768
10. Xu B, Yan M, Ma F, Hu X, Feng J, Ouyang Q, et al. Pyrotinib Plus Capecitabine Versus Lapatinib Plus Capecitabine for the Treatment of HER2-Positive Metastatic Breast Cancer (PHOEBE): A Multicentre, Open-Label, Randomised, Controlled, Phase 3 Trial. *Lancet Oncol* (2021) 22:351–60. doi: 10.1016/S1470-2045(20)30702-6
11. Yin Y, Yang H, Liu Z, Tan J, Zhu C, Chen M, et al. Studies on the Safety and Efficacy of Pyrotinib in the Treatment of HER2- Positive Advanced Solid Tumors Excluding Breast Cancer. *Cancer Manage Res* (2020) 12:13479–87. doi: 10.2147/CMAR.S281765
12. Kim ST, Cristescu R, Bass AJ, Kim KM, Odegaard JI, Kim K, et al. Comprehensive Molecular Characterization of Clinical Responses to PD-1 Inhibition in Metastatic Gastric Cancer. *Nat Med* (2018) 24:1449–58. doi: 10.1038/s41591-018-0101-z
13. Jin Y, Chen DL, Wang F, Yang CP, Chen XX, You JQ, et al. The Predicting Role of Circulating Tumor DNA Landscape in Gastric Cancer Patients Treated With Immune Checkpoint Inhibitors. *Mol Cancer* (2020) 19:154. doi: 10.1186/s12943-020-01274-7
14. Bratman SV, Yang SYC, Iafolla MAJ, Liu Z, Hansen AR, Bedard PL, et al. Personalized Circulating Tumor DNA Analysis as a Predictive Biomarker in Solid Tumor Patients Treated With Pembrolizumab. *Nat Cancer* (2020) 1:873–81. doi: 10.1038/s43018-020-0096-5
15. Reinert T, Henriksen TV, Christensen E, Sharma S, Salari R, Sethi H, et al. Analysis of Plasma Cell-Free DNA by Ultradeep Sequencing in Patients With Stages I to III Colorectal Cancer. *JAMA Oncol* (2019) 5:1124–31. doi: 10.1001/jamaoncol.2019.0528
16. Pellini B, Szymanski J, Chin RI, Jones PA, Chaudhuri AA. Liquid Biopsies Using Circulating Tumor DNA in Non-Small Cell Lung Cancer. *Thorac Surg Clin* (2020) 30:165–77. doi: 10.1016/j.thorsurg.2020.01.005
17. Wang DS, Liu ZX, Lu YX, Bao H, Wu X, Zeng ZL, et al. Liquid Biopsies to Track Trastuzumab Resistance in Metastatic HER2-Positive Gastric Cancer. *Gut* (2019) 68:1152–61. doi: 10.1136/gutjnl-2018-316522
18. Wang Y, Zhao C, Chang L, Jia R, Liu R, Zhang Y, et al. Circulating Tumor DNA Analyses Predict Progressive Disease and Indicate Trastuzumab-Resistant Mechanism in Advanced Gastric Cancer. *EBioMedicine* (2019) 43:261–9. doi: 10.1016/j.ebiom.2019.04.003
19. Zhang C, Chen Z, Chong X, Chen Y, Wang Z, Yu R, et al. Clinical Implications of Plasma ctDNA Features and Dynamics in Gastric Cancer Treated With HER2-Targeted Therapies. *Clin Transl Med* (2020) 10:e254. doi: 10.1002/ctm2.254
20. Leal A, van Grieken NCT, Palsgrove DN, Phallen J, Medina JE, Hruban C, et al. White Blood Cell and Cell-Free DNA Analyses for Detection of Residual Disease in Gastric Cancer. *Nat Commun* (2020) 11:525. doi: 10.1038/s41467-020-14310-3
21. Yang J, Gong Y, Lam VK, Shi Y, Guan Y, Zhang Y, et al. Deep Sequencing of Circulating Tumor DNA Detects Molecular Residual Disease and Predicts Recurrence in Gastric Cancer. *Cell Death Dis* (2020) 11:346. doi: 10.1038/s41419-020-2531-z
22. Yu GZ, Chen Y, Wang JJ. Overexpression of Grb2/HER2 Signaling in Chinese Gastric Cancer: Their Relationship With Clinicopathological Parameters and Prognostic Significance. *J Cancer Res Clin Oncol* (2009) 135:1331–9. doi: 10.1007/s00432-009-0574-8
23. Bang Y-J, Van Cutsem E, Feyereislova A, Chung HC, Shen L, Sawaki A, et al. Trastuzumab in Combination With Chemotherapy Versus Chemotherapy Alone for Treatment of HER2-Positive Advanced Gastric or Gastro-Oesophageal Junction Cancer (ToGA): A Phase 3, Open-Label, Randomised Controlled Trial. *Lancet* (2010) 376:687–97. doi: 10.1016/S0140-6736(10)61121-X
24. Yoshioka T, Shien K, Namba K, Torigoe H, Sato H, Tomida S, et al. Antitumor Activity of Pan-HER Inhibitors in HER2-Positive Gastric Cancer. *Cancer Sci* (2018) 109:1166–76. doi: 10.1111/cas.13546
25. Huang LT, Ma JT, Zhang SL, Li XH, Sun L, Jing W, et al. Durable Clinical Response to Pyrotinib After Resistance to Prior Anti-HER2 Therapy for HER2-Positive Advanced Gastric Cancer: A Case Report. *Front Oncol* (2019) 9:1453. doi: 10.3389/fonc.2019.01453

Conflict of Interest: Authors ZY and SC were employed by the company 3D Medicines Inc.

The remaining authors declare that the research was conducted in the absence of any commercial or financial relationships that could be construed as a potential conflict of interest.

Publisher's Note: All claims expressed in this article are solely those of the authors and do not necessarily represent those of their affiliated organizations, or those of the publisher, the editors and the reviewers. Any product that may be evaluated in this article, or claim that may be made by its manufacturer, is not guaranteed or endorsed by the publisher.

Copyright © 2022 Wu, Li, Qin, Yan, Chen, Jin and Xu. This is an open-access article distributed under the terms of the Creative Commons Attribution License (CC BY). The use, distribution or reproduction in other forums is permitted, provided the original author(s) and the copyright owner(s) are credited and that the original publication in this journal is cited, in accordance with accepted academic practice. No use, distribution or reproduction is permitted which does not comply with these terms.

frontiers in Oncology

ORIGINAL RESEARCH
published: 28 January 2022
doi: 10.3389/fonc.2022.814283

Superiority of Laparoscopic Gastrojejunostomy Combined With Multimodality Therapy for Gastric Outlet Obstruction Caused by Advanced Gastric Cancer

Chuandong Wang[1,2†], Xiaojuan Zhang[3,4†], Shengtao Lin[1,2], Changshun Yang[1,2], BiaoHuan Zhou[1,2], Yulong Mi[1,2], Rong Ye[1,2], Yifan Chen[1,2], Weijie Chen[1,2], Xiaojun Lin[1,2], Song Tan[1,2], Yuhang Zhou[1,2] and Weihua Li[1,2]*

[1] Shengli Clinical Medical College of Fujian Medical University, Fuzhou, China, [2] Department of Surgical Oncology, Fujian Provincial Hospital, Fuzhou, China, [3] Fuzong Clinical Medical College of Fujian Medical University, Fuzhou, China, [4] Department of Radiology, 900th Hospital Logistic Support Forces of PLA, Fuzhou, China

Background: Data are limited concerning the survival outcomes of patients with gastric outlet obstruction (GOO) caused by advanced gastric cancers according to laparoscopic gastrojejunostomy (LGJ) combined with multimodality therapy (MMT). Therefore, the purpose of this study was to examine the feasibility and efficacy of these therapies.

Methods: This single-centered, retrospective analysis included data of 184 patients with GOO due to advanced gastric cancer (AGC). Treatment models were: laparoscopic gastrojejunostomy combined with multimodality therapy (LGJ+MMT), endoscopic metal stent placement combined with multimodality therapy (EMSP+MMT), and multimodality therapy (MMT).

Results: Improved oral intake, better nutritional indices, and better response to chemotherapy were observed in the LGJ+MMT group. Subsequent gastrectomy was performed in 43 (61.4%) patients in the LGJ+MMT group, 23 (37.7%) in the EMSP+MMT group, and 11 (20.8%) in the MMT group (P<0.001). LGJ+MMT was associated with better long-term prognosis. As confirmed by propensity scores and multivariate analyses, the 3-year survival rates in the three treatment models were 31.4% with LGJ+MMT, 0% with EMSP+MMT, and 0% with MMT in conversion therapy, and 50.0% with LGJ+MMT, 33.3% with EMSP+MMT, and 23.5% with MMT in NAC. A forest plot revealed that LGJ+MMT was related to a decreased risk of death.

Conclusions: LGJ combined with MMT was associated with better nutritional status, higher rates of subsequent gastrectomy, and good prognosis. LGJ combined with MMT may improve the long-term survival of patients with GOO caused by AGC.

Keywords: gastric cancer, gastrojejunostomy, endoscopy, neoadjuvant chemotherapy, conversion therapy

OPEN ACCESS

Edited by:
Pankaj Kumar Garg,
Shri Guru Ram Rai Institute of Medical and Health Sciences, India

Reviewed by:
Tushar Mishra,
All India Institute of Medical Sciences Bhubaneswar, India
Naveen Sharma,
All India Institute of Medical Sciences Jodhpur, India

****Correspondence:***
Weihua Li
liwh@fjmu.edu.cn

†These authors have contributed equally to this work

Specialty section:
This article was submitted to Gastrointestinal Cancers: Gastric and Esophageal Cancers, a section of the journal Frontiers in Oncology

Received: *13 November 2021*
Accepted: *10 January 2022*
Published: *28 January 2022*

Citation:
Wang C, Zhang X, Lin S, Yang C, Zhou B, Mi Y, Ye R, Chen Y, Chen W, Lin X, Tan S, Zhou Y and Li W (2022) Superiority of Laparoscopic Gastrojejunostomy Combined With Multimodality Therapy for Gastric Outlet Obstruction Caused by Advanced Gastric Cancer. Front. Oncol. 12:814283. doi: 10.3389/fonc.2022.814283

INTRODUCTION

Gastric cancer is frequently diagnosed at an advanced stage with a poor prognosis (1). Multimodality therapy (MMT), which is defined as neoadjuvant chemotherapy (NAC) therapy or conversion therapy, is a therapeutic regimen for advanced gastric cancer (AGC) (2–4).

Several landmark clinical trials have revealed the survival benefits of MMT for advanced gastric cancer. The MAGIC trial showed an improved 5-year survival rate (23% to 36%) for advanced gastric cancer treated with perioperative chemotherapy, revealing the era of neoadjuvant chemotherapy (5). In addition, some patients with initially unresectable tumors who responded to palliative chemotherapy underwent conversion surgery in the REGATTA trial, with a better long-term outcome (6). Similar findings have been reported in numerous investigations, and each of these trials demonstrated prolonged survival of AGC treated with MMT (2, 4, 7–12). However, gastric outlet obstruction (GOO) is a common and detrimental complication of AGC (3, 13), which deprives patients the opportunity to undergo MMT with deteriorated nutritional and metabolic patterns (3). To address this issue, alleviating GOO plays a vital role in the application of MMT. Laparoscopic gastrojejunostomy (LGJ) is a promising option in restoring oral intake with small incisions, reduced immunosuppression, and enhanced compliance with chemotherapies (13, 14). Our institution recently published two studies on MMT with LGJ followed by conversion therapy and demonstrated higher conversion surgery completion rates in patients with GOO caused by incurable AGC (48.6% and 47.9%) (15, 16). However, little is known regarding treatment models with LGJ followed by neoadjuvant therapy in patients with GOO due to AGC. Moreover, there remains no head-to-head comparison of LGJ and endoscopic stenting in patients with GOO receiving MMT.

Therefore, the purpose of the present research was to compare MMT completion rates and prognosis in these treatment models and identify factors associated with survival to verify the feasibility and efficacy of these treatments.

METHOD

Patient Selection

We retrospectively reviewed clinical data of patients with GOO due to AGC in Fujian Provincial Hospital between June 2015 and June 2020. We retrieved data of eligible patients for analysis based on the following criteria: histologic and radiologic confirmation of AGC; endoscopic confirmation of GOO with difficulty in oral intake; at least two cycles of chemotherapy before gastrectomy; 20–80 years of age; good tolerance of general anesthesia; Eastern Cooperative Oncology Group performance status (PS) score of 0–2; and no prior chemotherapy, targeted therapy, or radiotherapy. We included patients with initial unresectable and locally advanced gastric cancer who had indications for NAC and conversion therapy. Patients with early stage (T1N0) disease, gastric cancer perforation, active bleeding, combined with other malignant tumors, altered chemotherapy regimen, and incomplete data were excluded. This study was reviewed and approved by the Ethics Committee of Fujian Provincial Hospital. Data were anonymized, and the requirement for informed consent from the patients was waived. All study procedures were performed in accordance with the Helsinki Declaration of 1964 and later versions.

Procedural Details

A multidisciplinary team consisting of oncology, nutrition, and surgery experts determined the strategy for each patient. Patients with a GOOSS score of 2 were categorized into the MMT group, while patients with a GOOSS score of 0 or 1 were categorized into LGJ+MMT or EMSP+MMT. After LGJ or EMSP, enteral nutrition and early parenteral nutrition was initiated. All patients received additional enteral nutrition support during the hospitalization. On postoperative day 1, patients were encouraged to drink 500–1000 ml of clear fluid. The amount of fluid intake was increased as tolerated by patients. Parenteral nutrition was discontinued when oral intake reached 2000–2500 ml/day. All patients received nutrition (protein 4.0 g, fat 3.0 g, carbohydrate 12.1 g, caloric value 1.0 kcal/ml) at a temperature of 40°C in the hospital. The calorie and protein intake were 25–30 kcal/kg/day and 1–2 g/kg/day, respectively, supplemented by parenteral nutrition (15, 16). EOX therapy was applied 7–14 days after LGJ or EMSP, which consisted of oxaliplatin 130 mg/m^2 intravenously on day 1 and epirubicin 100 mg/m^2 intravenously on day 1, with fluoropyrimidine capecitabine 825 mg/m^2 orally twice daily on days 1–14. Preoperative chemotherapy was generally continued for 2–4 cycles in patients treated with NAC and 6–8 cycles in patients treated with conversion therapy. Tumor response was evaluated using abdominal enhanced computed tomography every two cycles of chemotherapy. Treatment was discontinued in cases of tumor progression, patient refusal, and unacceptable chemotherapy toxicity. The multidisciplinary team determines the criteria for gastrectomy when CR or PR is generally observed (10). Adjuvant chemotherapy was determined by the attending physicians in a clinical setting.

Data Collection

Patient information and clinical and pathological characteristics were obtained from the electronic medical records. Demographic and preoperative variables were acquired, including age, sex, performance status (PS), body mass index (BMI), nutritional and inflammatory status, clinical stages, and GOOSS. GOOSS is defined as follows: 0, no oral intake; 1, liquid only; 2, soft food; and 3, low-residue or full diet (14). Nutritional status was estimated using Onodera's prognostic nutritional index (PNI) and BMI. Inflammatory status was estimated by the neutrophil-to-lymphocyte ratio (NLR) and platelet-to-lymphocyte ratio (PLR). According to previous studies, we divided patients into two groups based on PNI (<45 or ≥45), PLR (<162 or ≥162), and NLR (<2.5 or ≥2.5) (17–21). Clinical and pathological stages were determined according to the National Comprehensive Cancer Network (NCCN) guidelines (22). Response to chemotherapy was classified according to the Response Evaluation Criteria in Solid Tumors guidelines (version 1.0) (12).

Statistical Analysis

Statistical analyses were conducted using SPSS software (IBM SPSS Statistics for Windows, version 22.0, Armonk, NY, USA). Two-tailed *P* values <0.05 were considered significant. Wilcoxon rank-sum tests were used for continuous variables and the Pearson chi-square test was used for categorical variables. Prognostic factors of overall survival (OS) were analyzed using univariate and multivariate logistic regression. OS rates were calculated using the Kaplan–Meier method. A propensity score-matched analysis was conducted to avoid confounding bias (performance status) with a small caliper of 0.2. Subgroup analyses were used to evaluate the impact of treatment models on OS after LGJ+MMT vs. EMSP+MMT.

RESULT

Baseline Characteristics

During the study period, we identified 224 patients with GOO caused by AGC. Forty patients were excluded due to an altered chemotherapy regimen (n=13), less than two cycles of chemotherapy (n=11), missing data (n=8), and other treatments (n=8). We obtained data on 70 patients who received LGJ+MMT, 61 patients who received EMSP+MMT, and 53 patients who received MMT only (**Table 1**). The EMSP+MMT group had a lower performance status (*P*<0.001). More than three-quarters (82.0%) of the EMSP+MMT group had a preoperative PS of 2, in contrast to only 37.1% in the LGJ+MMT and 54.7% in the MMT group. Significant differences were not found in ratios of PNI≥45, which represent nutritional status, and the ratios of PLR <162 and NLR <2.5, which represent the inflammatory status, in these treatment models (17–23). There was also no significant difference in the distribution of tumor stages, non-curable factors, and MMT regimens.

Clinical and Pathologic Outcomes

Table 2 summarizes the clinical outcomes of each treatment model, which were collected after two cycles of chemotherapy. Significant improvements in oral intake were observed after treatment with LGJ and EMSP. GOOSS 3 was achieved in 98.6% of the LGJ+MMT group and 86.9% of the EMSP+MMT group after the intervention. However, none of the patients in the MMT group had a restored full diet. Patients treated with LGJ +MMT received more cycles of chemotherapy, especially in conversion therapy (six cycles vs. two cycles vs. three cycles, *P*<0.001). In addition, the proportion of patients with PNI ≥45 was significantly higher in the LGJ+MMT group than in the other groups (64.3% vs. 54.1% vs. 35.8%, *P*=0.007). These results were attributed to 61.4% of the LGJ+MMT group who displayed a major response (5.7% complete response and 55.7% partial response). Notably, no significant differences were found in chemotherapy cycles of patients treated with NAC. In contrast, higher rates of PLR <162 and NLR <2.5 were observed in the MMT group (34.3% vs. 19.7% vs. 60.4%, and 55.7% vs. 34.4% vs. 73.6%, respectively, *P<0.001*).

TABLE 1 | Baseline Patients Characteristics.

	LGJ+MMT (n=70)	EMSP+MMT (n=61)	MMT (n=53)	*P value*
Age (year)	62 (33-80)	67 (32-80)	57 (28-77)	0.073
Sex (male/female)	48/22 (68.6/31.4)	46/15 (75.4/24.6)	35/18 (66.0/44.0)	0.518
PS (0/1/2)	8/36/26 (11.4/51.4/37.1)	3/8/50 (4.9/13.1/82.0)	4/20/29 (7.5/37.7/54.7)	<0.001
BMI	21.3 (17.3-26.4)	21.6 (17.7-27.8)	22.5 (18.2-29.0)	0.078
GOOSS (0/1/2)	29/41/0 (41.4/58.6/0)	39/22/0 (63.9/36.1/0)	0/0/53 (0/0/100)	<0.001
PNI				0.970
<45	51 (72.9)	45 (73.8)	38 (71.7)	
≥45	19 (27.1)	16 (26.2)	15 (28.3)	
PLR				0.413
<162	21 (30.0)	21 (34.4)	22 (41.5)	
≥162	49 (70.0)	40 (65.6)	31 (58.5)	
NLR				0.144
<2.5	19 (27.1)	16 (26.2)	22 (41.5)	
≥2.5	51 (72.9)	45 (73.8)	31 (58.5)	
cT				0.928
T2	1 (1.4)	1 (1.6)	1 (1.9)	
T3	10 (14.3)	12 (19.7)	7 (13.2)	
T4a	51 (72.9)	41 (67.2)	41 (77.4)	
T4b	8 (11.4)	7 (11.5)	4 (7.5)	
cN (+)	70 (100)	61 (100)	53 (100)	–
Non-curable factor				
Infiltration to adjacent organs	3 (4.3)	5 (8.2)	4 (7.5)	0.623
Peritoneal metastasis	34 (48.6)	24 (39.3)	19 (35.8)	0.326
Hepatic metastasis	10 (14.3)	8 (13.1)	9 (17.0)	0.839
Distant lymph node metastasis	28 (40.0)	23 (37.7)	23 (43.4)	0.825
MMT (NAC/Conversion)	18/52 (25.7/74.3)	12/49 (19.7/80.3)	17/36 (32.1/67.9)	0.317

PS, Performance status; GOOSS, Gastric outlet obstruction scoring system; PNI, Prognostic Nutritional Index; BMI, Body mass index; PLR, Platelet to lymphocyte ratio; NLR, Neutrophil to lymphocyte ratio; MMT, multimodality therapy.

TABLE 2 | Clinical outcomes after treatment models.

	LGJ+MMT (n=70)	EMSP+MMT (n=61)	MMT (n=53)	*P* value
GOOSS 3 achieved	69 (98.6)	53 (86.9)	0 (0)	<0.001
Chemotherapy cycles				
NAC	4 (2-4)	4 (2-4)	4 (1-4)	0.251
Conversion	6 (2-10)	2 (2-8)	3 (2-6)	<0.001
BMI	21.2 (17.4-27.7)	21.6 (17.7-27.8)	22.2 (18.0-27.8)	0.322
PNI				0.007
<45	25 (35.7)	28 (45.9)	34 (64.2)	
≥45	45 (64.3)	33 (54.1)	19 (35.8)	
PLR				<0.001
<162	24 (34.3)	12 (19.7)	32 (60.4)	
≥162	46 (65.7)	49 (80.3)	21 (39.6)	
NLR				<0.001
<2.5	39 (55.7)	21 (34.4)	39 (73.6)	
≥2.5	31 (44.3)	40 (65.6)	14 (26.4)	
Response				
Complete response	4 (5.7)	2 (3.3)	0 (0)	
Partial response	39 (55.7)	21 (34.4)	11 (20.8)	
Stable disease	5 (7.1)	21 (34.4)	25 (47.2)	
Progressive disease	22 (31.4)	17 (27.9)	17 (32.0)	
ORR (%)	61.4	37.7	20.8	<0.001
Subsequent resection	43 (61.4)	23 (37.7)	11 (20.8)	<0.001

GOOSS, Gastric outlet obstruction scoring system; NAC, Neoadjuvant chemotherapy; PNI, Prognostic Nutritional Index; BMI, Body mass index; PLR, Platelet to lymphocyte ratio; NLR, Neutrophil to lymphocyte ratio; MMT, multimodality therapy; ORR, Objective response rate.

Subsequent gastrectomy was performed in 43 (61.4%) patients in the LGJ+MMT group, 23 (37.7%) in the EMSP+MMT group, and 11 (20.8%) in the MMT group. There were 12 and six cases of peritoneal metastasis in the LGJ+MMT and EMSP+MMT groups, respectively, which disappeared after chemotherapy. In the LGJ+MMT group, three and four patients with hepatic metastasis underwent additional radiofrequency ablation and combined partial hepatectomy, respectively. Additional radiofrequency ablation and combined partial hepatectomy were performed in one and three cases in the EMSP+MMT group, respectively. Among patients with organ infiltrations, one case of infiltration lesion disappeared and two patients underwent partial pancreatectomy in the LGJ+MMT group. In contrast, two patients in the EMSP+MMT group underwent partial pancreatectomy. None of the patients with non-curable factors treated with conversion therapy underwent subsequent resection in the MMT group. In patients treated with NAC, 17 (94.4%), 9 (75.0%), and 11 (64.7%) patients received subsequent gastrectomy in the LGJ+MMT, EMSP+MMT, and MMT groups, respectively. No significant differences were found in the pathological outcomes of the treatment models (**Table 3**).

Survival Analysis

We compared the OS between the three groups, and significant differences in median survival time (MST) were found in patients treated with NAC (37.4 vs. 28.2 vs. 20.3 months, *P*=0.0039),

TABLE 3 | Surgical and pathological findings after treatments models.

	LGJ+MMT (n=43)	EMSP+MMT (n=23)	MMT (n=11)	*P* value
Resection margin				0.945
R0	38 (88.4)	20 (87.0)	10 (90.9)	
R1	5 (11.6)	3 (13.0)	1 (9.1)	
Pathological response				0.204
0	4 (9.3)	3 (13.0)	0 (0)	
1	18 (41.9)	13 (56.6)	4 (36.4)	
2	10 (23.3)	4 (17.4)	6 (54.5)	
3	11 (25.6)	3 (13.0)	1 (9.1)	
pT				0.147
T0	4 (9.3)	1 (4.3)	0 (0)	
T2	1 (2.3)	3 (13.0)	3 (27.3)	
T3	8 (18.6)	6 (26.1)	1 (9.1)	
T4a	30 (69.8)	13 (56.6)	7 (63.6)	
pN				0.109
N0	25 (58.2)	9 (39.2)	6 (54.5)	
N1	8 (18.6)	11 (47.8)	1 (9.1)	
N2	5 (11.6)	2 (8.7)	3 (27.3)	
N3	5 (11.6)	1 (4.3)	1 (9.1)	

conversion therapy (13.8 vs. 6.9 vs. 4.7 months, $P < 0.0001$), and both treatments (25.4 vs. 7.6 vs. 6.4 months, $P<0.0001$). We performed propensity score matching to reduce the selection bias (**Figure 1**). Outcomes data after matching also demonstrated that the LGJ+MMT group had a better prognosis ($P<0.05$). In addition, the 3-year survival rates were noteworthy across the three treatment models: 31.4% with LGJ+MMT, 0% with EMSP+MMT, and 0% with MMT in conversion therapy, and 50.0% with LGJ+MMT, 33.3% with EMSP+MMT, and 23.5% with MMT in NAC. Regardless of treatment models, patients who completed subsequent gastrectomy had improved OS compared to those who did not finish the treatment (MST: 32.8 vs. 6.5 months, $P<0.001$). This was confirmed again in the univariate and multivariate analyses (HR, 48.783: 95% CI: 19.546–121.754, $P<0.001$). Compared with LGJ+MMT, EMSP +MMT (HR, 2.242; 95% CI: 1.460–3.441, $P<0.001$) and MMT (HR, 2.199; 95% CI: 1.395–3.468, $P=0.001$) were associated with an increased risk of death. An additional factor that increased the risk of death was conversion therapy (HR, 1.589; 95% CI 1.030–2.452, $P=0.036$) (**Table 4**). A forest plot revealed that LGJ+MMT was related to a decreased risk of death in all subgroups (**Figure 2**).

DISCUSSION

The survival benefits of MMT have been demonstrated in numerous large, multicentered, prospective trials of AGC (5, 6). Significantly improved survival of more than 40 months could be achieved in patients with incurable AGC treated with conversion therapy (4). However, the major challenge in these trials was the ability of patients to receive the intended MMT (2). GOO, a common complication of distal AGC, impairs the ability to receive MMT (13). We previously showed that LGJ combined with conversion therapy is an independent prognostic factor of OS in patients with GOO caused by incurable AGC. However, whether such treatment could prolong survival in all patients with GOO due to AGC has not been clarified. To the best of our knowledge, the present study is the first to compare the long-term prognosis of different methods to alleviate GOO immediately before MMT and evaluate the effect of these treatment models on OS. Our study revealed a marked improvement in eating practices and better nutritional status, and response to chemotherapy after LGJ, similar to findings of previous studies (15, 16). Furthermore, the MST of the LGJ +MMT group was also higher than that of the EMSP+MMT and MMT groups for both NAC and conversion therapy. Multivariate analysis identified that EMSP+MMT and MMT were associated with an increased risk of death, compared with LGJ+MMT. These findings suggest that LGJ combined with MMT could achieve better long-term survival in these patients.

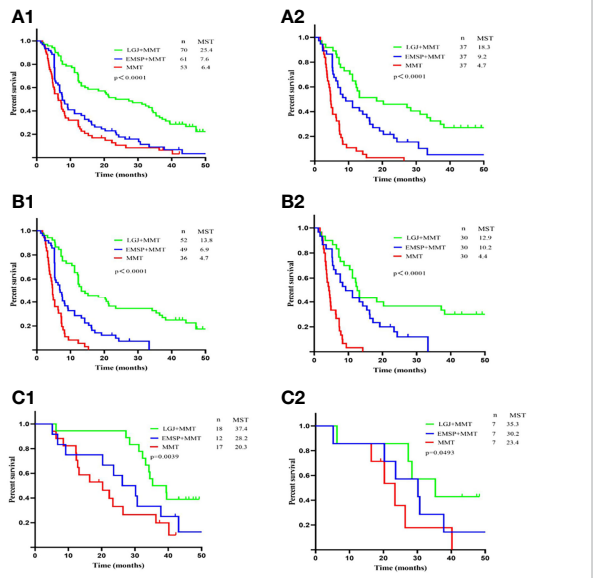

FIGURE 1 | Overall survival according to treatment models. **(A1)** OS for patients treated by NAC and conversion therapy. **(A2)** OS for patients treated by NAC and conversion therapy after propensity score matching. **(B1)** OS for patients treated by conversion therapy. **(B2)** OS for patients treated by conversion therapy after propensity score matching. **(C1)** OS for patients treated by NAC therapy. **(C2)** OS for patients treated by NAC therapy after propensity score matching.

Previous studies on GOO made more efforts on short-term outcomes, including restoration of oral intake, postoperative complications, and luminal patency duration. The reported advantages of EMSP include rapid resumption of oral intake and shorter hospital stay, which are more likely to be used in patients with physical deterioration. Several studies have also demonstrated longer luminal patency durations and lower intervention rates after surgery (3, 13, 24). In addition, with the advancement of laparoscopy, the median time of resumption of oral intake reduces to 2 and 4 days, as reported by some studies (25–27). However, these studies, under consideration for palliative purposes, did not address long-term survival. Furthermore, many investigators have revealed that completion of MMT, especially curative surgery, plays a vital role in the long-term prognosis of AGC (2, 4–12). Yoshio et al. (3) conducted a multicentered cohort study on patients with GOO receiving stents and gastrojejunostomy, and found that only 1% and 15% of patients underwent subsequent resection, respectively. In addition, Tanaka et al. (14) demonstrated that only 13.3% of patients with GOO underwent conversion surgery after LGJ. This may suggest that long-term malnutrition caused by GOO impairs the ability of patients to undertake subsequent treatments, especially in conversion therapy, which requires more cycles of chemotherapy. The true advantages of these interventions hinge on the restoration of nutritional and metabolic status. In this current study, LGJ+MMT have significantly improved subsequent resection rates compared with EMSP+MMT and MMT (61.4% vs. 37.7% vs. 20.8%, *P<0.0001*), in addition to higher rates of PNI ≥45 (64.3% vs. 54.1% with EMSP+MMT and 35.8% with MMT), lower rates of PLR <162 (34.3% vs. 19.7% with EMSP+MMT), and lower rates of NLR <2.5% (55.7% vs. 34.4% with EMSP+MMT). This phenomenon may be related to the immediate application of

TABLE 4 | Univariate and multivariate analyses for OS.

Variable	Hazard ratio	95% CI	*P* value
Univariate analysis			
Age (≥65/<65)	0.837	0.614-1.141	0.260
Sex (male/female)	1.283	0.917-1.795	0.145
PS (2/0 or 1)	0.490	0.356-0.676	<0.001
BMI (≥18.5/<18.5)	1.340	0.705-2.545	0.372
PNI (≥45/<45)	1.008	0.710-1.431	0.967
PLR (≥162/<162)	1.166	0.843-1.613	0.353
NLR (≥2.5/<2.5)	0.891	0.639-1.243	0.396
Subsequent resection (yes/no)	67.736	27.536-166.623	<0.001
MMT (NAC/conversion)	2.366	1.623-3.450	<0.001
Treatment selection			
LGJ+MMT	Ref	Ref	Ref
EMSP+MMT	2.424	1.646-3.569	<0.001
MMT	3.195	2.135-4.780	<0.001
Multivariate analysis			
PS (2/0 or 1)	0.775	0.542-1.108	0.163
Subsequent resection (yes/no)	48.783	19.546-121.754	<0.001
MMT (NAC/conversion)	1.589	1.030-2.452	0.036
Treatment selection			
LGJ+MMT	Ref	Ref	Ref
EMSP+MMT	2.242	1.460-3.441	<0.001
MMT	2.199	1.395-3.468	0.001

PS, Performance status; PNI, Prognostic Nutritional Index; BMI, Body mass index; PLR, Platelet to lymphocyte ratio; NLR, Neutrophil to lymphocyte ratio; MMT, multimodality therapy.

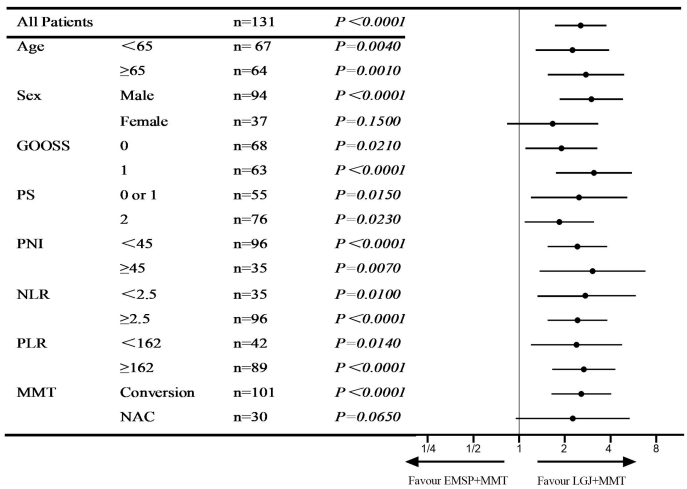

FIGURE 2 | Hazard ratio for overall survival. Forest plot evaluating the impact of treatment models on OS after LGJ+MMT vs EMSP+MMT.

enteral nutrition after LGJ or EMSP combined with early parenteral nutrition. Interestingly, reduced inflammatory status was observed in the MMT group, which may result from myelosuppressive effects of cytotoxic anticancer chemotherapy, especially in patients with a lower nutritional status (28).

In survival analysis, LGJ+MMT offers a survival benefit over EMSP+MMT and MMT in patients with obstructive AGC, and propensity score matching strengthens this hypothesis (*P<0.05*). In addition, multivariate analysis identified that treatment with EMSP+MMT (HR, 2.242; 95% CI: 1.460–3.441, *P*<0.001) and MMT (HR, 2.199; 95% CI 1.395–3.468, *P*=0.001) were associated with an increased overall risk of death, compared with LGJ+MMT. Previous studies have demonstrated that gastrojejunostomy can enhance compliance with chemotherapy and is associated with better nutritional and metabolic status (13–16), arguing that the primary survival advantages of this treatment model were due to more cycles of chemotherapy. In our current study, significantly increased cycles of chemotherapy were observed in patients treated with conversion therapy after LGJ (six cycles vs. two cycles vs. three cycles, *P*<0.001). However, no significant differences were found in patients receiving NAC (*P=0.251*), which may be due to the shorter time these patients needed. However, our propensity score-matched study revealed long survival in patients treated with LGJ+MMT in NAC (35.3 vs.

30.2 vs. 23.4 months, P=0.0493). This phenomenon may be due to better nutrition and inflammatory status, represented by increased PNI and decreased NLR and PLR (17–21). In particular, the difference in pathological states after treatment was not found, which can be explained by the selection bias that subsequent resection involves only those patients who respond to chemotherapy and subsequently undergo surgery. The question then arises on the optimum personalized enteral nutrition after LGJ and suitably alters the chemotherapy regimen when chemotherapy fails.

One concern with methods to alleviate GOO lies in the indications to choose surgery or endoscopy. A previous study demonstrated that stent therapy was selected for more physically deteriorated patients who underwent gastrojejunostomy in clinical settings (3). However, this result was limited to open operation and was focused on palliative purposes. In this study, LGJ+MMT was associated with a better prognosis in patients with GOO. To further evaluate the impact of treatment models on the risk of death, we performed a subgroup analysis and found that patients who underwent LGJ+MMT had a decreased risk of death in any subgroup.

This study has several limitations. First, although propensity score matching was used to balance the significant baseline characteristics of the patients, RCTs are desirable for further analysis. Moreover, this study had a relatively small sample size and a retrospective exploratory design. Second, we excluded patients with less than two cycles of chemotherapy and altered chemotherapy regimens. Since the target patients had deteriorated nutritional and metabolic status, difficulties were associated with obtaining and maintaining subsequent treatments. Finally, the follow-up period was not long enough to achieve a 5-year survival rate.

CONCLUSION

We demonstrated that in patients with GOO, LGJ+MMT improved nutritional and inflammatory status, increased subsequent resection rates, and at the 3-year of follow-up, has survival benefits compared to EMSP+MMT and MMT. In the absence of randomized controlled trials directly comparing these treatment models, we conclude that LGJ+MMT is a feasible and effective modality for treating GOO caused by AGC. Further investigations should be conducted develop personalized scheme to implement this strategy.

DATA AVAILABILITY STATEMENT

All data and materials generated during and/or analyzed during the current study are available from the corresponding author on reasonable request.

ETHICS STATEMENT

The studies involving human participants were reviewed and approved by the Ethics Committee of Fujian Provincial Hospital. Written informed consent for participation was not required for this study in accordance with the national legislation and the institutional requirements.

AUTHOR CONTRIBUTIONS

Conceptualization, WL. Methodology, CW, XZ, and SL. Formal analysis, CW, XZ, CY, BZ, YM, RY, YC, WC, XL, ST, YZ, and WL. Resources, SL, CY, BZ, and WL. Writing—original draft preparation. CW, XZ, and WL. Writing—review and editing. CW, XZ, and WL. Funding acquisition, WL. All authors have read and agreed to the published version of the manuscript.

ACKNOWLEDGMENTS

We wish to thank all colleagues and nurses who provided care to the patients in this study.

REFERENCES

1. Smyth EC, Nilsson M, Grabsch HI, van Grieken NC, Lordick F. Gastric Cancer. *Lancet (London England)* (2020) 396(10251):635–48. doi: 10.1016/s0140-6736(20)31288-5
2. Li SS, Klempner SJ, Costantino CL, Parikh A, Clark JW, Wo JY, et al. Impact of Treatment Sequencing on Survival for Patients With Locally Advanced Gastric Cancer. *Ann Surg Oncol* (2021) 28(5):2856–65. doi: 10.1245/s10434-020-09248-1
3. Haga Y, Hiki N, Kinoshita T, Ojima T, Nabeya Y, Kuwabara S, et al. Treatment Option of Endoscopic Stent Insertion or Gastrojejunostomy for Gastric Outlet Obstruction Due to Gastric Cancer: A Propensity Score-Matched Analysis. *Gastric Cancer* (2020) 23(4):667–76. doi: 10.1007/s10120-020-01040-0
4. Solaini L, Ministrini S, Bencivenga M, D'Ignazio A, Marino E, Cipollari C, et al. Conversion Gastrectomy for Stage IV Unresectable Gastric Cancer: A GIRCG Retrospective Cohort Study. *Gastric Cancer* (2019) 22(6):1285–93. doi: 10.1007/s10120-019-00968-2
5. Cunningham D, Allum WH, Stenning SP, Thompson JN, Van de Velde CJ, Nicolson M, et al. Perioperative Chemotherapy Versus Surgery Alone for Resectable Gastroesophageal Cancer. *New Engl J Med* (2006) 355(1):11–20. doi: 10.1056/NEJMoa055531
6. Fujitani K, Yang HK, Mizusawa J, Kim YW, Terashima M, Han SU, et al. Gastrectomy Plus Chemotherapy Versus Chemotherapy Alone for Advanced Gastric Cancer With a Single non-Curable Factor (REGATTA): A Phase 3, Randomised Controlled Trial. *Lancet Oncol* (2016) 17(3):309–18. doi: 10.1016/s1470-2045(15)00553-7
7. Yu Y, Fang Y, Shen Z, Wang Y, Yan M, Cao H, et al. Oxaliplatin Plus Capecitabine in the Perioperative Treatment of Locally Advanced Gastric Adenocarcinoma in Combination With D2 Gastrectomy: NEO-CLASSIC Study. *Oncol* (2019) 24(10):1311–e989. doi: 10.1634/theoncologist.2019-0416
8. Yamaguchi K, Yoshida K, Tanahashi T, Takahashi T, Matsuhashi N, Tanaka Y, et al. The Long-Term Survival of Stage IV Gastric Cancer Patients With Conversion Therapy. *Gastric Cancer* (2018) 21(2):315–23. doi: 10.1007/s10120-017-0738-1
9. Yoshida K, Yamaguchi K, Okumura N, Tanahashi T, Kodera Y. Is Conversion Therapy Possible in Stage IV Gastric Cancer: The Proposal of New Biological Categories of Classification. *Gastric Cancer* (2016) 19(2):329–38. doi: 10.1007/s10120-015-0575-z

10. Zhang F, Huang X, Song Y, Gao P, Zhou C, Guo Z, et al. Conversion Surgery for Stage IV Gastric Cancer. *Front Oncol* (2019) 9:1158. doi: 10.3389/fonc.2019.01158
11. Ministrini S, Bencivenga M, Solaini L, Cipollari C, Sofia S, Marino E, et al. Stage IV Gastric Cancer: The Surgical Perspective of the Italian Research Group on Gastric Cancer. *Cancers* (2020) 12(1):158. doi: 10.3390/cancers12010158
12. Sato Y, Ohnuma H, Nobuoka T, Hirakawa M, Sagawa T, Fujikawa K, et al. Conversion Therapy for Inoperable Advanced Gastric Cancer Patients by Docetaxel, Cisplatin, and S-1 (DCS) Chemotherapy: A Multi-Institutional Retrospective Study. *Gastric Cancer* (2017) 20(3):517–26. doi: 10.1007/s10120-016-0633-1
13. Jang S, Stevens T, Lopez R, Bhatt A, Vargo JJ. Superiority of Gastrojejunostomy Over Endoscopic Stenting for Palliation of Malignant Gastric Outlet Obstruction. *Clin Gastroenterol Hepatol* (2019) 17(7):1295–302.e1. doi: 10.1016/j.cgh.2018.10.042
14. Tanaka T, Suda K, Satoh S, Kawamura Y, Inaba K, Ishida Y, et al. Effectiveness of Laparoscopic Stomach-Partitioning Gastrojejunostomy for Patients With Gastric Outlet Obstruction Caused by Advanced Gastric Cancer. *Surg Endoscopy* (2017) 31(1):359–67. doi: 10.1007/s00464-016-4980-0
15. Wang C, Lin S, Zhang X, Yang C, Li W. Laparoscopic Gastrojejunostomy With Conversion Therapy in Gastric Outlet Obstruction Caused by Incurable Advanced Gastric Cancer. *Cancer Manage Res* (2021) 13:6847–57. doi: 10.2147/cmar.S322569
16. Wang C, Lin S, Zhang X, Li W. Laparoscopic Gastrojejunostomy Versus Endoscopic Stenting Combined With Conversion Therapy for Gastric Outlet Obstruction. *Scand J Gastroenterol* (2021) 56(10):1248–54. doi: 10.1080/00365521.2021.1956581
17. Mimatsu K, Fukino N, Ogasawara Y, Saino Y, Oida T. Utility of Inflammatory Marker- and Nutritional Status-Based Prognostic Factors for Predicting the Prognosis of Stage IV Gastric Cancer Patients Undergoing Non-Curative Surgery. *Anticancer Res* (2017) 37(8):4215–22. doi: 10.21873/anticanres.11812
18. Migita K, Matsumoto S, Wakatsuki K, Ito M, Kunishige T, Nakade H, et al. A Decrease in the Prognostic Nutritional Index is Associated With a Worse Long-Term Outcome in Gastric Cancer Patients Undergoing Neoadjuvant Chemotherapy. *Surg Today* (2017) 47(8):1018–26. doi: 10.1007/s00595-017-1469-y
19. Jagadesham VP, Lagarde SM, Immanuel A, Griffin SM. Systemic Inflammatory Markers and Outcome in Patients With Locally Advanced Adenocarcinoma of the Oesophagus and Gastro-Oesophageal Junction. *Br J Surg* (2017) 104(4):401–7. doi: 10.1002/bjs.10425
20. Gong W, Zhao L, Dong Z, Dou Y, Liu Y, Ma C, et al. After Neoadjuvant Chemotherapy Platelet/Lymphocyte Ratios Negatively Correlate With Prognosis in Gastric Cancer Patients. *J Clin Lab Anal* (2018) 32(5):e22364. doi: 10.1002/jcla.22364
21. Chen L, Hao Y, Cong X, Zou M, Li S, Zhu L, et al. Peripheral Venous Blood Platelet-To-Lymphocyte Ratio (PLR) for Predicting the Survival of Patients With Gastric Cancer Treated With SOX or XELOX Regimen Neoadjuvant Chemotherapy. *Technol Cancer Res Treat* (2019) 18:1533033819829485. doi: 10.1177/1533033819829485
22. Provenzale D, Gupta S, Ahnen DJ, Bray T, Cannon JA, Cooper G, et al. Genetic/Familial High-Risk Assessment: Colorectal Version 1.2016, NCCN Clinical Practice Guidelines in Oncology. *J Natl Compr Cancer Netw: JNCCN* (2016) 14(8):1010–30. doi: 10.6004/jnccn.2016.0108
23. Galizia G, Lieto E, Zamboli A, De Vita F, Castellano P, Romano C, et al. Neutrophil to Lymphocyte Ratio is a Strong Predictor of Tumor Recurrence in Early Colon Cancers: A Propensity Score-Matched Analysis. *Surgery* (2015) 158(1):112–20. doi: 10.1016/j.surg.2015.02.006
24. Upchurch E, Ragusa M, Cirocchi R. Stent Placement Versus Surgical Palliation for Adults With Malignant Gastric Outlet Obstruction. *Cochrane Database Syst Rev* (2018) 5(5):Cd012506. doi: 10.1002/14651858.CD012506.pub2
25. Min SH, Son SY, Jung DH, Lee CM, Ahn SH, Park DJ, et al. Laparoscopic Gastrojejunostomy Versus Duodenal Stenting in Unresectable Gastric Cancer With Gastric Outlet Obstruction. *Ann Surg Treat Res* (2017) 93(3):130–6. doi: 10.4174/astr.2017.93.3.130
26. Jang SH, Lee H, Min BH, Kim SM, Kim HS, Carriere KC, et al. Palliative Gastrojejunostomy Versus Endoscopic Stent Placement for Gastric Outlet Obstruction in Patients With Unresectable Gastric Cancer: A Propensity Score-Matched Analysis. *Surg Endoscopy* (2017) 31(10):4217–23. doi: 10.1007/s00464-017-5480-6
27. Manuel-Vázquez A, Latorre-Fragua R, Ramiro-Pérez C, López-Marcano A, la Plaza-Llamas R, Ramia JM. Laparoscopic Gastrojejunostomy for Gastric Outlet Obstruction in Patients With Unresectable Hepatopancreatobiliary Cancers: A Personal Series and Systematic Review of the Literature. *World J Gastroenterol* (2018) 24(18):1978–88. doi: 10.3748/wjg.v24.i18.1978
28. Blayney DW, Zhang Q, Feng J, Zhao Y, Bondarenko I, Vynnychenko I, et al. Efficacy of Plinabulin vs Pegfilgrastim for Prevention of Chemotherapy-Induced Neutropenia in Adults With Non-Small Cell Lung Cancer: A Phase 2 Randomized Clinical Trial. *JAMA Oncol* (2020) 6(11):e204429. doi: 10.1001/jamaoncol.2020.4429

Conflict of Interest: The authors declare that the research was conducted in the absence of any commercial or financial relationships that could be construed as a potential conflict of interest.

Publisher's Note: All claims expressed in this article are solely those of the authors and do not necessarily represent those of their affiliated organizations, or those of the publisher, the editors and the reviewers. Any product that may be evaluated in this article, or claim that may be made by its manufacturer, is not guaranteed or endorsed by the publisher.

Copyright © 2022 Wang, Zhang, Lin, Yang, Zhou, Mi, Ye, Chen, Chen, Lin, Tan, Zhou and Li. This is an open-access article distributed under the terms of the Creative Commons Attribution License (CC BY). The use, distribution or reproduction in other forums is permitted, provided the original author(s) and the copyright owner(s) are credited and that the original publication in this journal is cited, in accordance with accepted academic practice. No use, distribution or reproduction is permitted which does not comply with these terms.

frontiers in Oncology

ORIGINAL RESEARCH
published: 02 February 2022
doi: 10.3389/fonc.2021.725889

Identifying Prognostic Markers From Clinical, Radiomics, and Deep Learning Imaging Features for Gastric Cancer Survival Prediction

Degan Hao[1†], Qiong Li[2†], Qiu-Xia Feng[2], Liang Qi[2], Xi-Sheng Liu[2], Dooman Arefan[3], Yu-Dong Zhang[2] and Shandong Wu[1,3,4,5*]*

[1] Intelligent Systems Program, University of Pittsburgh, Pittsburgh, PA, United States, [2] Department of Radiology, The First Affiliated Hospital with Nanjing Medical University, Nanjing, China, [3] Department of Radiology, University of Pittsburgh, Pittsburgh, PA, United States, [4] Department of Biomedical Informatics, University of Pittsburgh, Pittsburgh, PA, United States, [5] Department of Bioengineering, University of Pittsburgh, Pittsburgh, PA, United States

Background: Gastric cancer is one of the leading causes of cancer death in the world. Improving gastric cancer survival prediction can enhance patient prognostication and treatment planning.

Methods: In this study, we performed gastric cancer survival prediction using machine learning and multi-modal data of 1061 patients, including 743 for model learning and 318 independent patients for evaluation. A Cox proportional-hazard model was trained to integrate clinical variables and CT imaging features (extracted by radiomics and deep learning) for overall and progression-free survival prediction. We further analyzed the prediction effects of clinical, radiomics, and deep learning features. Concordance index (c-index) was used as the model performance metric, and the predictive effects of multi-modal features were measured by hazard ratios (HRs) at pre- and post-operative settings.

Results: Among 318 patients in the independent testing group, the hazard predicted by Cox from multi-modal features is associated with their survival. The highest c-index was 0.783 (95% CI, 0.782-0.783) and 0.770 (95% CI, 0.769-0.771) for overall and progression-free survival prediction, respectively. The post-operative variables are significantly ($p<0.001$) more predictive than the pre-operative variables. Pathological tumor stage (HR=1.336 [overall survival]/1.768 [progression-free survival], $p<0.005$), pathological lymph node stage (HR=1.665/1.433, $p<0.005$), carcinoembryonic antigen (CEA) (HR=1.632/1.522, $p=0.02$), chemotherapy treatment (HR=0.254/0.287, $p<0.005$), radiomics signature [HR=1.540/1.310, $p<0.005$], and deep learning signature [HR=1.950/1.420, $p<0.005$]) are significant survival predictors.

OPEN ACCESS

Edited by:
Pankaj Kumar Garg, Shri Guru Ram Rai Institute of Medical and Health Sciences, India

Reviewed by:
David Akhavan, University of Kansas Medical Center, United States
Andreas Krieg, University Hospital of Düsseldorf, Germany

***Correspondence:**
Shandong Wu
wus3@upmc.edu
Yu-Dong Zhang
njmu_zyd@163.com

[†]These authors have contributed equally to this work

Specialty section:
This article was submitted to Gastrointestinal Cancers, a section of the journal Frontiers in Oncology

Received: *16 June 2021*
Accepted: *23 December 2021*
Published: *02 February 2022*

Citation:
Hao D, Li Q, Feng Q-X, Qi L, Liu X-S, Arefan D, Zhang Y-D and Wu S (2022) Identifying Prognostic Markers From Clinical, Radiomics, and Deep Learning Imaging Features for Gastric Cancer Survival Prediction. Front. Oncol. 11:725889. doi: 10.3389/fonc.2021.725889

Conclusion: Our study showed that CT radiomics and deep learning imaging features are significant pre-operative predictors, providing additional prognostic information to the pathological staging markers. Lower CEA levels and chemotherapy treatments also increase survival chances. These findings can enhance gastric cancer patient prognostication and inform treatment planning.

Keywords: gastric cancer, survival analysis (source: MeSH NLM), multi-modal data analysis, radiomics, deep learning - CNN

INTRODUCTION

Gastric cancer is one of the leading causes of death worldwide (1). Accurate survival prediction of gastric cancer patients can inform clinical decision making and benefit treatment planning (2). Since 1977, the American Joint Committee on Cancer (AJCC) staging system is the guideline for treatment allocation and prognostic prediction on gastric cancer patients (3–5). However, the staging system is hard to account for the large variations in survival outcomes.

Previous studies have reported a variety of clinical factors indicative of gastric cancer prognosis, including serum tumor markers, lymphovascular invasion, perineural invasion, histological grade, etc. (6–10). Recent studies also showed that quantitative imaging features, such as radiomics and deep learning modeling, are associated with survival/prognosis of gastric cancer patients (11, 12). Radiomics represent predefined quantitative imaging descriptors. Deep learning (13) can automatically extract imaging features from high-dimensional imaging data, but these features are less intuitive than radiomics descriptors.

It is expected that the combination of multi-modal data, such as demographic information, clinical variables, imaging data, histopathologic findings, lab measurements, therapeutic interventions, can empower survival analysis of gastric cancer (14). Currently, it lacks understanding of the interaction and relationship of the multi-modal features for predicting gastric cancer survival. The purpose of this study is to integrate clinical variables, radiomics features, and convolutional neural network (CNN)-identified deep learning features to predict overall and progression-free survival on gastric cancer patients and identify key prognostic markers from the multi-modal data modeling at pre- and post-operative settings.

MATERIALS AND METHODS

Overview

We built a machine learning prognostic model (**Figure 1**) for overall and progression-free survival prediction after gastrectomy, by integrating multi-modal data: clinical variables (including demographic information, lab tests, pathology, and treatment data), intra-tumor radiomics, and deep learning features of the tumor regions. The large set of radiomics (or deep learning) features were aggregated to generate a signature by the random survival forest method (15). We used the classic Cox proportional-hazards (Cox in short) model for data integration, survival prediction, and effect measurement.

Study Cohort

We performed a retrospective study that received approvals by a local ethics committee and an institutional review board with a waiver of written informed consent. Our study complies with the 1964 Helsinki declaration and its later amendments. Initially a total of 1,647 patients with pathologically confirmed gastric cancer during 2014 to 2018 were identified for the study. The exclusion criteria included: i) patients who failed to undergo radical surgery; ii) patients with diagnosis of other cancers in addition to gastric cancer; iii) patients with any intervention or therapy before surgery; iv) patients with poor imaging quality unacceptable for computational analysis; and v) patients without pre-operative CT imaging available. Finally, 1,061 patients were included for analysis, which were randomly split to two independent study groups: Group-A of 743 patients (70%) for model development and Group-B of 318 patients (30%) for independent evaluation. Patients were followed up every 3-6 months, starting from the time of gastrectomy and censored at the last alive contact or by the time of this study (i.e., 30 June 2019). For each patient, we collected various clinical data and a pre-operative contrast-enhanced computed tomography (CECT) scan.

Clinical Variables

We collected a set of clinical data acquired before and after the gastrectomy operation. The pre-operative variables include lab tests [e.g., serum carcinoembryonic antigen (CEA) and carbohydrate antigen 19-9 (CA19-9)], demographic variables, qualitative radiologic staging variables [e.g., tumor depth invasion (rT) and lymph node invasion (rN)], tumor location assessed by radiographic imaging and endoscopy, histologic grades by endoscopic biopsy. The post-operative data includes chemotherapy treatment information as well as surgical pathology variables [e.g., pathologic tumor staging (pT), pathologic lymph node staging (pN), Lauren classification, gross appearance, surgical histologic grade, lymphovascular invasion (LVI), perineural invasion (PNI)]. See **Supplementary** for more details on the variable measurement. We performed univariate statistical tests for each variable (chi-squared test for discrete variables and Mann-Whitney U test for continuous variables) between Group-A and Group-B to measure their properties. In order to select variables that are substantially related to survival, univariate Cox analysis (16) was performed

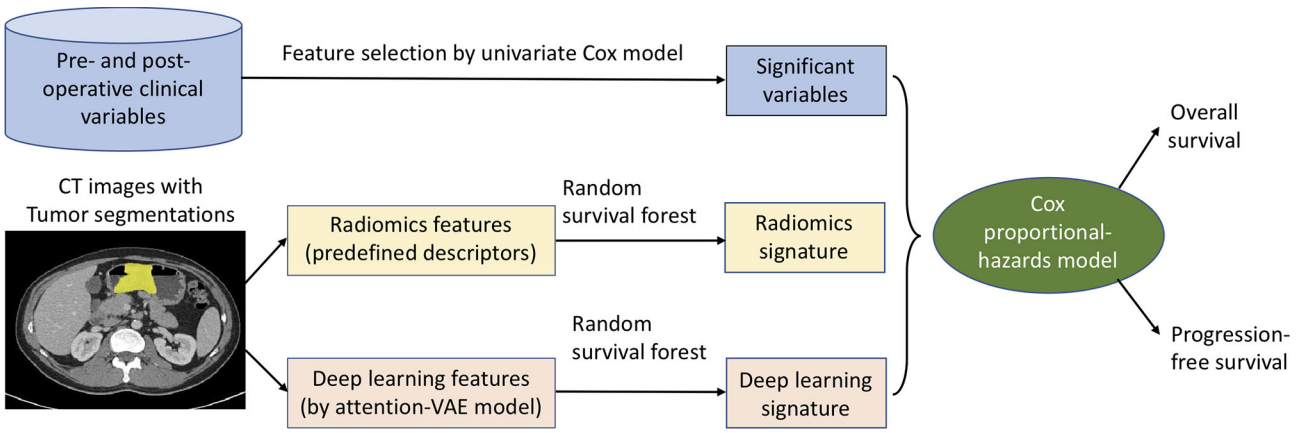

FIGURE 1 | Machine learning of multi-modal features for gastric cancer survival prediction and interpretation. The significant clinical variables, radiomics signature, and deep learning signature were integrated in the Cox model for survival prediction, and the effects of these features were measured and analyzed by hazard ratios at pre- and post-operative settings.

and those with a p-value < 0.10 were selected for subsequent joint modeling with imaging data.

Radiomics Features Extracted From 3D Intra-Tumor Volume

Quantitative radiomic features are extracted from the segmented 3D tumor volume in the CECT images. The gastric tumor was segmented slice-by-slice and semi-automatically by two radiologists (QL and QXF) using an in-house developed and validated software (ONCO IMAG ANLY v 2.0; Shanghai Key Laboratory of MRI, ECNU, Shanghai, China). QL first segmented the lesion for all cases; and one week later, QL repeated segmentation on 30 patients to evaluate intra-reader variability. To evaluate inter-observer variability, QXF performed lesion segmentation on a selected subset of 30 patients. The lesion segmentation was conducted over approximately two months. A total of 1,210 radiomic features, which describe the tumor characteristics in terms of intensity, shape, texture, etc., are extracted from the segmented gastric tumor volumes using an open-source Python package Pyradiomics (17). The robustness of each radiomic feature between readers is measured using intra-class correlation coefficient (ICC).

Deep Learning Features Extracted From the Full Images Focused on the Tumor Regions

Deep learning was used to extract potentially different features from the approximate local regions around segmented tumor. To this end, we designed an attention-guided Variational AutoEncoder (attention-guided VAE) model (**Figure 2A**) to guide the feature learning. The model was trained with the manually segmented gastric tumor masks, where an attention unit was incorporated to learn an attention map around the segmented tumor regions. At the bottleneck of this model, the hidden layer outputs a 100-dimensional vector as the deep learning features to characterize the attended tumor regions. **Figure 2B** shows several examples of the attention regions identified by the deep learning model.

Generating Aggregated Imaging Signatures by Random Survival Forest

Due to the relatively large number of radiomics features and deep learning features, direct use of the full set of features may result in overfitting in the Cox model. We employed random survival forest (15) to first select a substantially smaller subset from the 1,210 radiomic features, and from the 100 attention-VAE features, respectively. Random survival forest is an ensemble tree method that identifies a subset of outcome-correlated features based on their permutation feature importance (18). The random survival forest process produces a score indicating the survival probability and the score represents an aggregated signature of its selected features, from which we generated the radiomics signature and deep learning signature. The training of random survival forest models was performed on Group-A only and separately for the overall and progression-free survival prediction.

Evaluation and Statistical Analysis

We evaluated and compared the survival prediction effects at 4 different settings, including using pre-operative data and post-operative data, separately (Setting 1), combination of the full set of pre- and post-operative data (Setting 2), and combination of only the variables that are shown in Setting 1 to be statistically significant ($p<0.05$) (Setting 3). In addition, we performed one more round of feature selection using the random survival forest method from the full set of data at Setting 1 and only the selected variables were combined for modeling (Setting 4).

In the deep learning feature extraction, the 743 patients in Group-A were randomly split into a training set (669 patients)

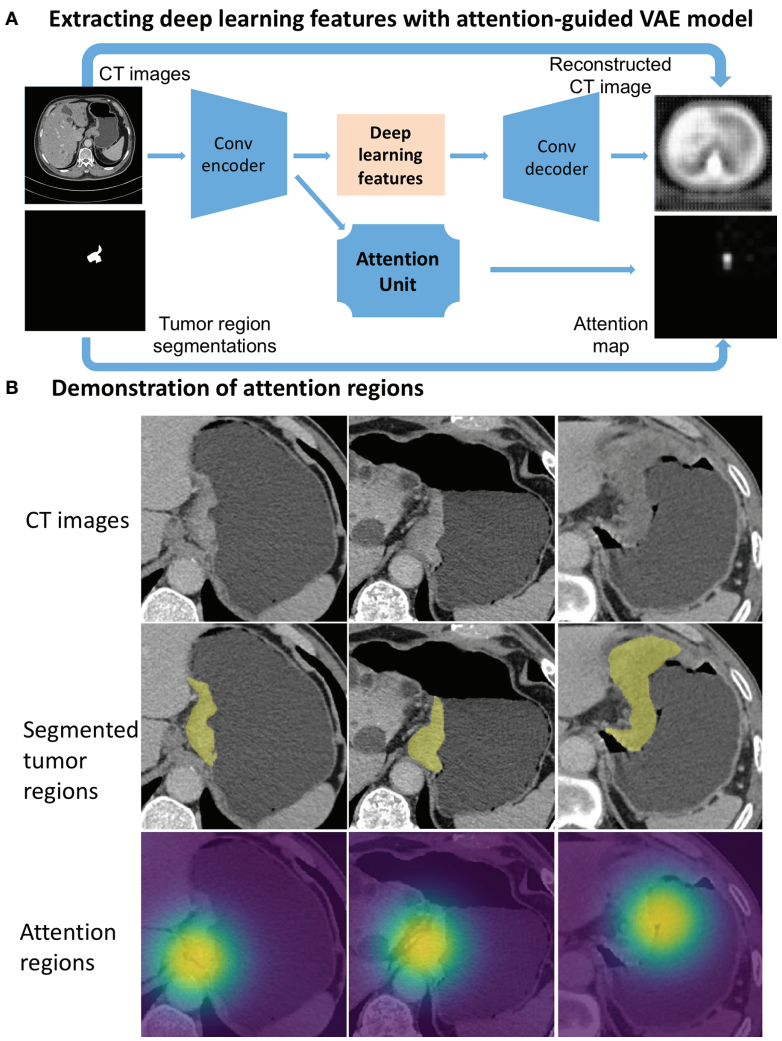

FIGURE 2 | Deep learning feature extraction from CT images through an attention-guided Variational AutoEncoder (attention-guided VAE) model. **(A)** model structure. **(B)** Gastric tumor region (yellow annotations) and the attention regions (highlighted by heatmaps) identified by the attention-guided VAE model.

and a validation set (74 patients) for model learning. The axial view CECT image with the largest cross-sectional area of tumor was selected as the input of the attention-VAE model. We used open-source software libraries PyTorch (19) to implement deep learning modeling, and scikit-survival (20) to implement random survival forest.

The model performance was measured on the independent Group-B of 318 patients using concordance index (c-index) (21). Hazard ratios were calculated to measure the effect of each individual variable/feature. In order to measure the effects more robustly, we repeated each experiment 20 times and calculated the average c-index values. We reported 95% confidence intervals of the c-index values using the non-parametric bootstrap method (22). We also conducted statistical comparisons on the model performance among Settings 1 to 4 using two-tailed Student's t-test. We performed all statistical analyses using the R software (version 3.6.1, R Project for Statistical Computing) and Python (version 3.6.8). A two-sided p value less than 0.05 is considered statistically significant.

RESULTS

Patient Characteristics

Table 1 summarizes key characteristics of the study cohort in terms of 16 clinical variables. There are 8 pre-operative and 8 post-operative variables. The percentage of the average follow-up time is 23.6 months (range 1- 65 months). The median age is 61.7 ± 10.3 years. There are 762 male patients and 299 female patients. The time interval between the CECT examination and standard gastrectomy had a median of 9 days, ranging from 6 to 14 days. Between Group-A and Group-B, all the clinical variables are statistically similar (as shown in **Table 1**, all the p values are greater than or equal to 0.05). In Group-A, 355 (48%) patients

TABLE 1 | Patient characteristics (i.e., 16 clinical variables) included for survival modeling.

Characteristic	Group-A for training (n = 743)	Group-B for independent test (n = 318)	p-value
Preoperative variables			
Age, mean ± Std	61.8 ± 9.7	62.0 ± 9.6	0.43
Sex, No. (%)			0.20
Male	541 (72.8)	221 (69.5)	
Female	202 (27.2)	97 (30.5)	
CA19-9 < 39 units/milliliter, No. (%)			0.27
Yes	94 (12.7)	35 (11.0)	
No	649 (87.3)	283 (89.0)	
CEA < 4.7 nanograms/milliliter, No. (%)			0.24
Yes	160 (21.5)	63 (19.8)	
No	583 (78.5)	255 (80.2)	
Biopsy histologic grade, No. (%)			0.63
Well/moderate	440 (59.2)	194 (61.0)	
Poor/undifferentiated	303 (40.8)	124 (39.0)	
Location, No. (%)			0.99
Upper	165 (22.2)	87 (27.4)	
Middle	232 (31.2)	96 (30.2)	
Lower	332 (44.7)	128 (40.3)	
Entire	14 (1.9)	7 (2.2)	
Radiologic T stage, No. (%)			0.05
rT1 stage	152 (20.5)	46 (14.5)	
rT2 stage	123 (16.6)	70 (22.0)	
rT3 stage	286 (38.5)	122 (38.4)	
rT4 stage	182 (24.5)	80 (25.2)	
Radiologic N stage, No. (%)			0.83
rN0 stage	281 (37.8)	113 (35.5)	
rN1 stage	196 (26.4)	81 (25.5)	
rN2 stage	134 (18.0)	65 (20.4)	
rN3 stage	70 (9.4)	34 (10.7)	
rN4 stage	62 (8.3)	25 (7.9)	
Post-operative variables			
Pathological T stage[†], No. (%)			0.99
pT1 stage	202 (27.2)	86 (27.0)	
pT2 stage	95 (12.8)	39 (12.3)	
pT3 stage	202 (27.2)	85 (26.7)	
pT4 stage	244 (32.8)	108 (34.0)	
Pathological N stage[†], No. (%)			0.69
pN0 stage	285 (38.4)	115 (36.2)	
pN1 stage	102 (13.7)	51 (16.0)	
pN2 stage	120 (16.2)	47 (14.8)	
pN3a stage	131 (17.6)	53 (16.7)	
pN3b stage	105 (14.1)	52 (16.4)	
Surgical histologic grade, No. (%)			0.44
Well/moderate	418 (56.3)	170 (53.5)	
Poor/undifferentiated	325 (43.7)	148 (46.5)	
Lauren classification, No. (%)			0.63
Intestinal type	407 (54.8)	180 (56.6)	
Diffuse/mixed type	336 (45.2)	138 (43.4)	
Gross appearance, No. (%)			0.75
Borrmann type I-III	715 (96.2)	304 (95.6)	
Borrmann type IV	28 (3.8)	14 (4.4)	
Lymphovascular invasion, No. (%)			0.51
Negative	457 (61.5)	188 (59.1)	
Positive	286 (38.5)	130 (40.9)	
Perineural invasion, No. (%)			0.86
Negative	443 (59.6)	187 (58.8)	
Positive	300 (40.4)	131 (41.2)	
Chemotherapy therapy, No. (%)			0.55
Yes	334 (45.0)	150 (47.2)	
No	409 (55.0)	168 (52.8)	

[†]*According to the eighth edition AJCC Cancer Staging Manual.*

underwent total gastrectomy while 388 (52%) patients underwent subtotal gastrectomy. In Group-B, the corresponding number was 163 (51%) and 155 (49%), respectively, for total and subtotal gastrectomy. In our cohort, there were 308 patients who did not undergo chemotherapy while they were eligible according to the National Comprehensive Cancer Network (NCCN) guideline on indications for chemotherapy (23), and there were 8 patients who underwent chemotherapy while they are ineligible per the NCCN guideline (23). The type of the chemotherapy varied across patients, including XELOX (oxaliplatin + capecitabine), SOX (S-1 + oxaliplatin), DS (docetaxel + S-1), etc. Our study cohort did not include patients who received neoadjuvant chemotherapy.

Selected Significant Variables/Features

Out of the 16 variables listed in **Table 1**, the following key variables were selected for modeling: 5 pre-operative variables (CEA, CA19-9, biopsy findings, rT, rN) and 7 post-operative variables (pT, pN, LVI, PNI, gross appearance, surgical histologic grade, and chemotherapy treatment). For the radiomics feature extraction, the average intra-observer ICC was 0.96 and the average inter-observer ICC was 0.86, indicating a good reliability. The most relevant radiomics features selected by random survival forest to generate the radiomics signatures are listed in **Table 2**, along with their respective ICC values.

Performance of the Survival Prediction Models

Table 3 shows the full survival prediction results with a comprehensive comparison under different settings. As can be seen at Setting 1, when only using the post-operative variables, the c-indexes are 0.783 for overall survival and 0.770 for progression-free survival. When only using the pre-operative

TABLE 2 | Radiomic features selected by random survival forest to generate the radiomics signatures for overall survival and progression-free survival.

Prediction	Radiomic feature name	Permutation importance	Intra-observer ICC	Inter-observer ICC
Overall survival	wavelet-HLL_firstorder_MeanAbsoluteDeviation	0.0068	0.999	0.999
	wavelet-HHH_glszm_SmallAreaLowGrayLevelEmphasis	0.0048	0.823	0.818
	log-sigma-5-0-mm-3D_glszm_SmallAreaHighGrayLevelEmphasis	0.0034	0.947	0.912
	original_shape_Maximum2DDiameterRow	0.0033	0.999	0.999
	original_glszm_ZoneVariance	0.0029	0.999	0.999
	wavelet-LLL_firstorder_Energy	0.0029	0.999	0.999
	original_shape_MajorAxis	0.0029	0.999	0.999
	wavelet-HLH_glszm_LargeAreaEmphasis	0.0028	0.987	0.977
	wavelet-HLH_glrlm_LongRunEmphasis	0.0027	0.996	0.994
	log-sigma-5-0-mm-3D_glszm_GrayLevelNonUniformity	0.0027	0.999	0.999
	wavelet-LHL_firstorder_MeanAbsoluteDeviation	0.0023	0.999	0.998
	original_shape_SurfaceVolumeRatio	0.0022	0.994	0.991
	original_glszm_SmallAreaEmphasis	0.0022	0.972	0.942
	original_firstorder_10Percentile	0.0021	0.996	0.992
	log-sigma-2-0-mm-3D_glszm_GrayLevelNonUniformity	0.0021	0.999	0.999
	wavelet-LLH_gldm_DependenceNonUniformity	0.0021	0.998	0.999
	wavelet-HLH_firstorder_Mean	0.002	0.984	0.962
	original_firstorder_Energy	0.002	0.999	0.999
	wavelet-HHL_glcm_ClusterTendency	0.0017	0.996	0.995
	wavelet-LLH_glrlm_GrayLevelNonUniformityNormalized	0.0017	0.998	0.996
Progression-free survival	original_glszm_SizeZoneNonUniformity	0.0037	0.999	0.999
	log-sigma-4-0-mm-3D_gldm_LargeDependenceHighGrayLevelEmphasis	0.0033	0.981	0.980
	wavelet-LLH_firstorder_RootMeanSquared	0.0032	0.999	0.999
	wavelet-LLH_gldm_LargeDependenceEmphasis	0.003	0.995	0.992
	original_shape_SurfaceArea	0.0029	0.999	0.999
	original_glszm_GrayLevelNonUniformity	0.0028	0.999	0.997
	log-sigma-5-0-mm-3D_glszm_LargeAreaHighGrayLevelEmphasis	0.0026	0.999	0.991
	wavelet-HHL_glcm_SumSquares	0.0025	0.999	0.999
	wavelet-HLL_glszm_ZoneVariance	0.0025	0.992	0.983
	wavelet-HHH_glszm_SmallAreaLowGrayLevelEmphasis	0.0024	0.823	0.818
	wavelet-HHH_glszm_SizeZoneNonUniformity	0.0023	0.929	0.929
	wavelet-HHL_glcm_JointEntropy	0.0022	0.999	0.999
	wavelet-LHH_firstorder_RobustMeanAbsoluteDeviation	0.002	0.999	0.999
	wavelet-LHL_glszm_LargeAreaLowGrayLevelEmphasis	0.002	0.996	0.944
	wavelet-HHL_glrlm_RunLengthNonUniformity	0.002	0.999	0.999
	wavelet-LLH_glszm_ZoneVariance	0.0018	0.998	0.997
	wavelet-HHH_glrlm_RunPercentage	0.0018	0.995	0.988
	original_firstorder_Variance	0.0018	0.995	0.991
	wavelet-HHH_glszm_SmallAreaEmphasis	0.0017	0.856	0.822
	wavelet-HHL_glszm_GrayLevelNonUniformityNormalized	0.0017	0.973	0.948

Larger permutation importance values indicate more important features for the prediction task. The intra-class correlation coefficient (ICC) values indicate reliability of the features.

TABLE 3 | Prediction performance of overall survival and progression-free survival and their comparisons at different settings.

Tasks	Variable groups	Variable names	Setting 1: Pre-operative / post-operative separate modeling			Setting 2: Combined modeling (full set of variabels in Setting 1)			Setting 3: Combined modeling (only significant variabels in Setting 1)			Setting 4: Combined modeling (applied feature selection to full set in Setting 1)		
			Hazard Ratio	p-value	C-index [95% CI]	Hazard Ratio	p-value	C-index [95% CI]	Hazard Ratio	p-value	C-index [95% CI]	Hazard Ratio	p-value	C-index [95% CI]
Overall Survival	Pre-operative variables	CEA	1.477	0.03	0.651 (0.649, 0.653)	1.405	0.06	0.703 (0.702, 0.706)	1.632	0.02	0.708 (0.706, 0.709)			0.721 (0.720, 0.722)
		CA199	0.878	0.51		0.951	0.82							
		Biopsy histologic grade	1.000	0.98		0.970	0.86							
		rT	1.051	0.65		1.020	0.90					1.03	0.65	
		rN	1.127	0.10		1.105	0.20					1.08	0.12	
		Deep learning signature	2.746	<0.005		2.612	<0.005		2.560	<0.005		1.95	<0.005	
		Radiomics signature	1.584	<0.005		1.522	<0.005		1.665	<0.005		1.540	<0.005	
	Post-operative variables	pT	1.336	<0.005	0.783 (0.782, 0.783)	0.980	0.88		1.020	0.88		1.050	0.43	
		pN	1.665	<0.005		1.197	0.05		1.139	0.17		1.120	0.05	
		LVI	0.844	0.34		0.914	0.60							
		PNI	1.323	0.10		1.419	0.05							
		Gross appearance	1.682	0.04		1.139	0.64		1.896	0.05				
		Surgical histologic grade	1.051	0.76		1.020	0.90					1.07	0.61	
		Chemotherapy	0.254	<0.005		0.440	<0.005		0.419	<0.005		0.57	<0.005	
Progression-Free Survival	Pre-operative variables	CEA	1.699	0.01	0.686 (0.685,0.687)	1.616	0.01	0.743 (0741,0.744)	1.522	0.02	0.761 (0.759, 0.762)	1.64	0.01	0.758 (0.757, 0.759)
		CA199	1.062	0.78		1.139	0.57							
		Biopsy histologic grade	1.507	0.03		1.246	0.25					1.28	0.19	
		rT	1.234	0.07		0.932	0.61					0.93	0.61	
		rN	1.162	0.06		1.105	0.22					1.11	0.26	
		Deep learning signature	1.537	<0.005		1.419	<0.005		1.42	<0.005		1.42	<0.005	
		Radiomics signature	1.419	<0.005		1.310	0.01		1.31	0.01		1.32	<0.005	

(Continued)

TABLE 3 | Continued

Tasks	Variable groups	Variable names	Setting 1: Pre-operative / post-operative separate modeling			Setting 2: Combined modeling (full set of variabels in Setting 1)			Setting 3: Combined modeling (only significant variabels in Setting 1)			Setting 4: Combined modeling (applied feature selection to full set in Setting 1)		
			Hazard Ratio	p-value	C-index [95% CI]	Hazard Ratio	p-value	C-index [95% CI]	Hazard Ratio	p-value	C-index [95% CI]	Hazard Ratio	p-value	C-index [95% CI]
	Post-operative variables	pT	1.768	<0.005	0.770 (0.769, 0771)	1.522	<0.005		1.56	<0.005		1.52	<0.005	
		pN	1.433	<0.005		1.150	0.14		1.27	<0.005		1.16	0.03	
		LVI	1.051	0.82		1.174	0.42							
		PNI	1.197	0.36		1.234	0.29							
		Gross appearance	1.716	0.07		1.105	0.76		1.24	0.48				
		Surgical histologic grade	0.741	0.09		0.763	0.14							
		Chemotherapy	0.287	<0.005		0.395	<0.005		0.37	<0.005		0.4	<0.005	

The length of the color bars in each cell represents the absolute value of the hazard ratios.

variables, the corresponding c-indexes are 0.651 and 0.686, respectively. In both cases, the post-operative variables are significantly ($p<0.001$ for both overall and progression-free survival) more predictive than the pre-operative variables.

When the full set of the pre- and post-operative variables are combined (Setting 2), the respective c-index of overall and progression-free survival is 0.703 and 0.743, both outperforming (both $p<0.001$) the pre-operative variables alone but underperforming (both $p<0.001$) the post-operative variables alone. This implies that these variables may not be optimally integrated by the Cox model in Setting 2. When combining only the significant variables (those with $p<0.05$ at Setting 1), as shown at Setting 3, the c-index increases to 0.708 for overall survival prediction, slightly higher ($p=0.19$) than using all the variables (0.703) at Setting 2, while still significantly lower ($p<0.001$) than the post-operative variables (0.783) at Setting 1; meanwhile, the progression-free survival prediction shows a similar observation at Setting 3, where the c-index increases to 0.761, which is significantly higher ($p<0.001$) than using all the variables at Setting 2 (0.743), but again, significantly lower ($p<0.001$) than the post-operative variables (0.770) at Setting 1. At Setting 4, the c-index increases to 0.721 for overall survival prediction, which is still significantly ($p<0.001$) lower than the post-operative modeling (0.783) in Setting 1, but significantly ($p<0.001$) higher than the combined full set (0.703) at Setting 2. Likewise, at Setting 4, the performance pattern of the progression-free survival is similar to that of the overall survival. The comparisons of these results indicate the following: (I) when the full set of pre- and post-operative variables are all combined (Setting 2), the c-index values increase and become closer to, but are still lower than, just using the post-operative variables; and (II) regardless of using only the significant variables with $p<0.05$ (Setting 3) or using the variables selected by a second process of feature selection (Setting 4), the c-index is improved than using the full set at Setting 2. When comparing Setting 3 and Setting 4, the c-index for overall survival is higher ($p<0.001$) at Setting 4, while the c-index for progression-free survival is higher ($p=0.02$) at Setting 3. This indicates that the two methods of selecting subset variables for modeling (i.e., Settings 3 and 4) have respective advantages for the two different survival prediction tasks.

Effect Evaluations of the Multi-Modal Features

After comparing the prediction model's performance, here we analyze the prediction effects of individual variables in terms of their hazard ratios. Here we first look at the overall survival prediction. It shows CEA (HR=1.477; $p=0.03$), deep learning signature (HR=2.746; $p<0.005$), and radiomics signature (HR=1.584; $p<0.005$) are significant variables for pre-operative prediction; for post-operative prediction, the significant variables are pT (HR=1.336; $p<0.005$), pN (HR=1.665; $p<0.005$), gross appearance (HR=1.682, $p=0.04$), and chemotherapy (HR=0.254, $p<0.005$). At Setting 2, the two imaging variables (i.e., deep learning signature and radiomics signature) remain significant with similar hazard ratios, along with the following new observations: CEA became marginal ($p=0.06$), pT became

insignificant (p=0.88)), PNI became marginally significant (p=0.05), gross appearance became insignificant (p=0.64), and chemotherapy's hazard ratio increased to 0.440 from 0.254. At Setting 3, those significant variables still remain significant except the pT and pN; it should be noted that in this case, the c-index (0.708) is much lower than the post-operative prediction (0.783), indicating very likely that the effects of pT and pN were lost in this setting. It is interesting to see that at Setting 4, rT and rN are selected in the models; however, as their p values are greater than 0.05 and the HRs are close to 1, the predictive values of rT and rN are limited when combined with other more significant variables. Comparing Setting 3 and Setting 4, CEA and gross appearance are significant in Setting 3, but they are not selected at Setting 4; in contrast, pN is marginally significant (p=0.05) at Setting 4 but is in-significant (p=0.17) at Setting 3; the two imaging signatures and chemotherapy treatment remain the significant predictors at both Setting 3 and Setting 4 for the overall survival prediction.

Similarly, we now compare the effects of these variables for the progression-free survival prediction. Specifically, for pre-operative prediction at Setting 1, the significant variables are almost the same with the overall survival prediction, except here the biopsy histologic grade is also significant (HR=1.507; p=0.03). For post-operative prediction at Setting 1, the significant variables are also almost the same with the overall survival prediction, except that gross appearance is not significant. Most significant variables at Setting 1 remain significant at Setting 2, except that biopsy histologic grade and pN became insignificant. Interestingly, when combining only the significant variables as shown at Setting 3, the significant variables are CEA, the two imaging signatures, pT, pN, and chemotherapy. Comparing Setting 3 and Setting 4, the significant predictors remain the same in the two settings.

In all the four settings, the hazard ratios for chemotherapy treatment are lower than one, indicating the chemotherapy treatment reduces the risk of death (in other words, patients benefit from receiving the treatment with an increasing survival time). The two imaging signatures play a significant prediction role of survival in all the four settings. For pT and pN, at Setting 3, they are not significant for overall survival while significantly predictive of progression-free survival; at Setting 4, pN is a significant predictor for both overall and progression-free survival, while pT is only significantly predictive for progression-free survival.

DISCUSSION

In this study, we evaluated the combination of various clinical variables and quantitative CECT imaging descriptors for overall and progression-free survival prediction on gastric cancer patients. We identified five primary prognosis factors, including two pathological staging variables, the history of chemotherapy treatment, and two aggregated signatures from radiomics and deep learning. While multi-modal data have been increasingly used in machine learning modeling, our study provides a measurement on the quantitative effects of the examined multi-modal features for gastric cancer survival analysis. This can enhance gastric cancer patient prognostication.

We found that in the models with the highest c-indices, the two pathological staging variables, pT and pN, are correlated with survival with highest hazard ratios. This suggests that the pathological staging data including both the depth of mural invasion and nodal involvement are closely indicative of patient survival. It is noted that when combined with pre-operative variables (including the imaging signatures), the effects of pT and pN are dismissed for overall survival prediction. This may have two important indications. First, because of the lower c-index at Settings 3 and 4, we suspect this may have to do with the modeling method in the Cox model, where variables are simply linearly concatenated and thus may not be optimal to capture more complicated non-linear interactions when the aggregated imaging signatures are incorporated in the model. Additional work on developing advanced modeling methods is therefore warranted. Second, at Settings 3 and 4 we found that the deep learning signature maintains high hazard ratios (like at Settings 1 and 2), while pT and pN are insignificant. This implies that the proposed deep learning model can extract quantitative imaging features that have overlapping information with pT and pN for overall survival prediction. This is a finding that highlights the important utility of pre-operative CECT imaging data coupled with the proposed deep learning modeling techniques. Interestingly, when looking at the progression-free survival at Setting 3, both the two imaging signatures and pT and pN are significant predictors with a similar magnitude of hazard ratios, which indicates that the information in the pre-operative CECT imaging signatures and the information in the pathological staging markers are complementary to each other for the progression-free survival prediction. Such complementary effects may align with the observation that CECT images can visualize the invasion of tumor into gastric wall (T stage) and the enlarged regional lymph nodes (N stage). Finally, it is not surprising to see that post-operative chemotherapy, with a hazard ratio consistently lower than one, can significantly increase survival.

Radiomics are mathematically defined descriptors while deep learning features are less intuitive because of the complexity in deep neural networks. The two aggregated imaging signatures are identified as significant factors for both overall and progression-free survival prediction. These two signatures may convey distinct information on the high-dimensional CECT images. Radiomic features/signature quantify characteristics of the segmented intratumor regions. Tumor margins, or the peri-tumorous regions, may also carry active and predictive information related to patient outcomes (24). The deep learning signature derived specifically from the attention-guided VAE model can extract additional features from the approximate tumor regions (not necessarily limited to intra-tumor). In our analysis, when the pre- and post-operative data are combined, deep learning signature shows a higher hazard ratio (i.e., importance) than the radiomic signature for overall survival prediction, and a comparable hazard ratio for the

progression-free survival prediction. This observation indicates that the radiomics features and deep learning-identified features play important yet different roles or interact distinctly in the two survival prediction tasks.

The focus of our study is to examine the effect and relationship of multi-modal features for gastric cancer survival prediction. Meanwhile, our model's c-index values are in line with previously reported studies (3, 11). For example, a deep learning-based nomogram (11) achieved c-index of 0.802 and 0.792, respectively, for overall and disease-free survival of gastric cancer. A Cox proportional hazard model with the AJCC staging system showed c-index of 0.796 for overall survival on a gastric cancer cohort (3). Although these values cannot be directly compared due to the differences on study cohort, data modality, and evaluation setting, we put these numbers in the same context for a general overview of the survival prediction model's performance. In addition, while these prediction models may not be directly used in their current capacities, the important findings of our study are the quantitative effects of the prognostic biomarkers identified from the multi-modality data, which can better inform clinicians for clinical decision-making. In particular, the pre-operative prediction of survival may provide early information to improve treatment planning and patient care.

Our study has some limitations. While our study included more than one thousand patients with complete data to enable the performed analyses, additional evaluation using external datasets will further validate our findings. The Cox model is more explainable but may be less effective to integrate non-linear interactions among multi-modal features. This study indicates the needs of developing more advanced models in future work. In addition, indications to chemotherapy were not consistently applied to the enrolled patients according to the NCCN guideline, which reflects a limitation of retrospective analysis. Finally, the tumor segmentation is semi-automated, which may have introduced certain level of dependence to the data annotators. While showing a high intra- and inter-observer agreement on segmentations, we expect to use fully automated and robust tumor segmentation methods when they become available.

CONCLUSIONS

We integrated multi-modal data for gastric cancer survival prediction and evaluated their individual and combined effects. Our study showed that quantitative radiomics and deep learning imaging features are significant pre-operative predictors of survival, providing additional prognostic information to the pathological staging markers. Lower CEA levels and chemotherapy treatments independently increase survival chances. Our findings provide quantitative effect measures on these markers in pre- and post-operative survival prediction, which will enhance gastric cancer patient prognostication and benefit treatment planning

DATA AVAILABILITY STATEMENT

The datasets presented in this article are not currently available to the public because of internal regulations and considerations of our research and publishing plans. Readers who are interested to the datasets may send a request to wus3@upmc.edu.

ETHICS STATEMENT

The studies involving human participants were reviewed and approved by an ethics committee of the First Affiliated Hospital with Nanjing Medical University (2018-SR-043) and the Institutional Review Board of University of Pittsburgh (STUDY19080135). The ethics committee waived the requirement of written informed consent for participation.

AUTHOR CONTRIBUTIONS

SW and YZ jointly conceived the concept and supervised the study. DH, YZ, and SW designed the methodology. DH implemented the models. DH and QL performed major data analysis. QL, YZ, and XL collected and pre-processed data and provided clinical expertise. LQ, QXF, and QL performed imaging data annotation and/or clinical data review/re-interpretation. DA contributed to model evaluation. All authors contributed to data analysis and result interpretation. DH, QL, YZ, and SW drafted the manuscript. All authors contributed to the article and approved the submitted version.

FUNDING

This work was supported in part by an Amazon Machine Learning Research Award.

ACKNOWLEDGMENTS

We thank the computational resource support by the Extreme Science and Engineering Discovery Environment (XSEDE), which is supported by National Science Foundation (NSF) grant number ACI-1548562. Specifically, it used the Bridges system, which is supported by NSF award number ACI-1445606, at the Pittsburgh Supercomputing Center. We thank the help of Chang Liu for the radiological staging evaluation.

SUPPLEMENTARY MATERIAL

The Supplementary Material for this article can be found online at: https://www.frontiersin.org/articles/10.3389/fonc.2021.725889/full#supplementary-material

REFERENCES

1. Chen W, Zheng R, Baade PD, Zhang S, Zeng H, Bray F, et al. Cancer Statistics in China, 2015. *CA: Cancer J Clin* (2016) 66(2):115–32. doi: 10.3322/caac.21338
2. Novotny AR, Schuhmacher C, Busch R, Kattan MW, Brennan MF, Siewert JR. Predicting Individual Survival After Gastric Cancer Resection: Validation of a US-Derived Nomogram at a Single High-Volume Center in Europe. *Ann Surg* (2006) 243(1):74. doi: 10.1097/01.sla.0000194088.81126.85
3. Son T, Sun J, Choi S, Cho M, Kwon IG, Kim HI, et al. Multi-Institutional Validation of the 8th AJCC TNM Staging System for Gastric Cancer: Analysis of Survival Data From High-Volume Eastern Centers and the SEER Database. *J Surg Oncol* (2019) 120(4):676–84. doi: 10.1002/jso.25639
4. In H, Solsky I, Palis B, Langdon-Embry M, Ajani J, Sano T. Validation of the 8th Edition of the AJCC TNM Staging System for Gastric Cancer Using the National Cancer Database. *Ann Surg Oncol* (2017) 24(12):3683–91. doi: 10.1245/s10434-017-6078-x
5. He X, Wu W, Lin Z, Ding Y, Si J, Sun L-m. Validation of the American Joint Committee on Cancer (AJCC) Stage System for Gastric Cancer Patients: A Population-Based Analysis. *Gastric Cancer* (2018) 21(3):391–400. doi: 10.1007/s10120-017-0770-1
6. Kono K, Amemiya H, Sekikawa T, Iizuka H, Takahashi A, Fujii H, et al. Clinicopathologic Features of Gastric Cancers Producing Alpha-Fetoprotein. *Digestive Surg* (2002) 19(5):359–65. doi: 10.1159/000065838
7. Adachi Y, Yasuda K, Inomata M, Sato K, Shiraishi N, Kitano S. Pathology and Prognosis of Gastric Carcinoma: Well Versus Poorly Differentiated Type. *Cancer: Interdiscip Int J Am Cancer Soc* (2000) 89(7):1418–24. doi: 10.1002/1097-0142(20001001)89:7<1418::AID-CNCR2>3.0.CO;2-A
8. Hyung WJ, Lee JH, Choi SH, Min JS, Noh SH. Prognostic Impact of Lymphatic and/or Blood Vessel Invasion in Patients With Node-Negative Advanced Gastric Cancer. *Ann Surg Oncol* (2002) 9(6):562–7. doi: 10.1007/BF02573892
9. Bilici A, Seker M, Ustaalioglu BBO, Kefeli U, Yildirim E, Yavuzer D, et al. Prognostic Significance of Perineural Invasion in Patients With Gastric Cancer Who Underwent Curative Resection. *Ann Surg Oncol* (2010) 17(8):2037–44. doi: 10.1245/s10434-010-1027-y
10. Takahashi Y, Takeuchi T, Sakamoto J, Touge T, Mai M, Ohkura H, et al. The Usefulness of CEA and/or CA19-9 in Monitoring for Recurrence in Gastric Cancer Patients: A Prospective Clinical Study. *Gastric Cancer* (2003) 6(3):142–5. doi: 10.1007/s10120-003-0240-9
11. Jiang Y, Jin C, Yu H, Wu J, Chen C, Yuan Q, et al. Development and Validation of a Deep Learning CT Signature to Predict Survival and Chemotherapy Benefit in Gastric Cancer: A Multicenter, Retrospective Study. *Ann Surg* (2020) 274(6):1153–61. doi: 10.1097/SLA.0000000000003778
12. Jiang Y, Chen C, Xie J, Wang W, Zha X, Lv W, et al. Radiomics Signature of Computed Tomography Imaging for Prediction of Survival and Chemotherapeutic Benefits in Gastric Cancer. *EBioMedicine* (2018) 36:171–82. doi: 10.1016/j.ebiom.2018.09.007
13. LeCun Y, Bengio Y, Hinton G. Deep Learning. *Nature* (2015) 521(7553):436–44. doi: 10.1038/nature14539
14. Mobadersany P, Yousefi S, Amgad M, Gutman DA, Barnholtz-Sloan JS, Vega JEV, et al. Predicting Cancer Outcomes From Histology and Genomics Using Convolutional Networks. *Proc Natl Acad Sci* (2018) 115(13):E2970–9. doi: 10.1073/pnas.1717139115
15. Ishwaran H, Kogalur UB, Blackstone EH, Lauer MS. Random Survival Forests. *Ann Appl Stat* (2008) 2(3):841–60. doi: 10.1214/08-AOAS169
16. Cox DR. Regression Models and Life-Tables. *J R Stat Society: Ser B (Methodological)* (1972) 34(2):187–202. doi: 10.1111/j.2517-6161.1972.tb00899.x
17. Van Griethuysen JJ, Fedorov A, Parmar C, Hosny A, Aucoin N, Narayan V, et al. Computational Radiomics System to Decode the Radiographic Phenotype. *Cancer Res* (2017) 77(21):e104–e7. doi: 10.1158/0008-5472.CAN-17-0339
18. Breiman L. Random Forests. *Mach Learn* (2001) 45(1):5–32. doi: 10.1023/A:1010933404324
19. Paszke A, Gross S, Massa F, Lerer A, Bradbury J, Chanan G, et al. eds. *Pytorch: An Imperative Style, High-Performance Deep Learning Library. Advances in Neural Information Processing Systems*. Vancouver, B.C., Canada: Curran Associates, Inc. (2019).
20. Polsterl S, Gupta P, Wang L, Conjeti S, Katouzian A, Navab N. Heterogeneous Ensembles for Predicting Survival of Metastatic, Castrate-Resistant Prostate Cancer Patients. *F1000Res* (2016) 5:2676. doi: 10.12688/f1000research.8231.1
21. Harrell FE Jr, Lee KL, Mark DB. Multivariable Prognostic Models: Issues in Developing Models, Evaluating Assumptions and Adequacy, and Measuring and Reducing Errors. *Stat Med* (1996) 15(4):361–87. doi: 10.1002/(SICI)1097-0258(19960229)15:4<361::AID-SIM168>3.0.CO;2-4
22. Dekking FM, Kraaikamp C, Lopuhaä HP, Meester LE. *A Modern Introduction to Probability and Statistics: Understanding Why and How*. Springer Science & Business Media (2005).
23. Ajani J, D'Amico T, Bentrem D, Chao J, Corvera C, Das P. *NCCN Clinical Practice Guidelines in Oncology: Gastric Cancer*. National Comprehensive Cancer Network (2015).
24. Chen T, Xu L, Dong X, Li Y, Yu J, Xiong W, et al. The Roles of CT and EUS in the Preoperative Evaluation of Gastric Gastrointestinal Stromal Tumors Larger Than 2 Cm. *Eur Radiol* (2019) 29(5):2481–9. doi: 10.1007/s00330-018-5945-6

Conflict of Interest: SW is a scientific consultant and stockholder of COGNISTX, Inc. SW has a research grant funded by Amazon.

The remaining authors declare that the research was conducted in the absence of any commercial or financial relationships that could be construed as a potential conflict of interest.

Publisher's Note: All claims expressed in this article are solely those of the authors and do not necessarily represent those of their affiliated organizations, or those of the publisher, the editors and the reviewers. Any product that may be evaluated in this article, or claim that may be made by its manufacturer, is not guaranteed or endorsed by the publisher.

Copyright © 2022 Hao, Li, Feng, Qi, Liu, Arefan, Zhang and Wu. This is an open-access article distributed under the terms of the Creative Commons Attribution License (CC BY). The use, distribution or reproduction in other forums is permitted, provided the original author(s) and the copyright owner(s) are credited and that the original publication in this journal is cited, in accordance with accepted academic practice. No use, distribution or reproduction is permitted which does not comply with these terms.

frontiers in Oncology

ORIGINAL RESEARCH
published: 09 February 2022
doi: 10.3389/fonc.2022.821586

The Value of Whole-Tumor Histogram and Texture Analysis Using Intravoxel Incoherent Motion in Differentiating Pathologic Subtypes of Locally Advanced Gastric Cancer

Huan-Huan Li[1†], Bo Sun[2†], Cong Tan[3], Rong Li[1], Cai-Xia Fu[4], Robert Grimm[5], Hui Zhu[1] and Wei-jun Peng[1*]*

[1] Department of Radiology, Fudan University Shanghai Cancer Center, Shanghai, China, [2] Department of Gastric Surgery, Fudan University Shanghai Cancer Center, Shanghai, China, [3] Department of Pathology, Fudan University Shanghai Cancer Center, Shanghai, China, [4] MR Applications Development, Siemens Shenzhen Magnetic Resonance Ltd, Shenzhen, China, [5] MR Applications Development, Siemens Healthcare, Erlangen, Germany

OPEN ACCESS

Edited by:
Luigi Marano, University of Siena, Italy

Reviewed by:
Giulio Bagnacci, University of Siena, Italy
Ludovico Carbone, University of Siena, Italy

***Correspondence:**
Hui Zhu
huizhu171717@163.com
Wei-jun Peng
pengweijun2017@.163.com

[†]These authors have contributed equally to this work and share first authorship

Specialty section:
This article was submitted to Gastrointestinal Cancers: Gastric & Esophageal Cancers, a section of the journal Frontiers in Oncology

Received: *24 November 2021*
Accepted: *20 January 2022*
Published: *09 February 2022*

Citation:
Li H-H, Sun B, Tan C, Li R, Fu C-X, Grimm R, Zhu H and Peng W-j (2022) The Value of Whole-Tumor Histogram and Texture Analysis Using Intravoxel Incoherent Motion in Differentiating Pathologic Subtypes of Locally Advanced Gastric Cancer. Front. Oncol. 12:821586. doi: 10.3389/fonc.2022.821586

Purpose: To determine if whole-tumor histogram and texture analyses using intravoxel incoherent motion (IVIM) parameters values could differentiate the pathologic characteristics of locally advanced gastric cancer.

Methods: Eighty patients with histologically confirmed locally advanced gastric cancer who received surgery in our institution were retrospectively enrolled into our study between April 2017 and December 2018. Patients were excluded if they had lesions with the smallest diameter < 5 mm and severe image artifacts. MR scanning included IVIM sequences (9 b values, 0, 20, 40, 60, 100, 150,200, 500, and 800 s/mm^2) used in all patients before treatment. Whole tumors were segmented by manually drawing the lesion contours on each slice of the diffusion-weighted imaging (DWI) images (with b=800). Histogram and texture metrics for IVIM parameters values and apparent diffusion coefficient (ADC) values were measured based on whole-tumor volume analyses. Then, all 24 extracted metrics were compared between well, moderately, and poorly differentiated tumors, and between different Lauren classifications, signet-ring cell carcinomas, and other poorly cohesive carcinomas using univariate analyses. Multivariate logistic analyses and multicollinear tests were used to identify independent influencing factors from the significant variables of the univariate analyses to distinguish tumor differentiation and Lauren classifications. ROC curve analyses were performed to evaluate the diagnostic performance of these independent influencing factors for determining tumor differentiation and Lauren classifications and identifying signet-ring cell carcinomas. The interobserver agreement was also conducted between the two observers for image quality evaluations and parameter metric measurements.

Results: For diagnosing tumor differentiation, the ADC_{median}, pure diffusion coefficient median ($Dslow_{median}$), and pure diffusion coefficient entropy ($Dslow_{entropy}$) showed the greatest AUCs: 0.937, 0.948, and 0.850, respectively, and no differences were found between the three

metrics, P>0.05). The 95th percentile perfusion factor (FP_{P95th}) was the best metric to distinguish diffuse-type GCs vs. intestinal/mixed (AUC=0.896). The ROC curve to distinguish signet-ring cell carcinomas from other poorly cohesive carcinomas showed that the $Dslow_{median}$ had AUC of 0.738. For interobserver reliability, image quality evaluations showed excellent agreement (interclass correlation coefficient [ICC]=0.85); metrics measurements of all parameters indicated good to excellent agreement (ICC=0.65-0.89), except for the Dfast metric, which showed moderate agreement (ICC=0.41-0.60).

Conclusions: The whole-tumor histogram and texture analyses of the IVIM parameters based on the biexponential model provided a non-invasive method to discriminate pathologic tumor subtypes preoperatively in patients with locally advanced gastric cancer. The metric FP_{P95th} derived from IVIM performed better in determining Lauren classifications than the mono-exponential model.

Keywords: gastric cancer, IVIM, pathological characterization, texture analysis, whole-tumor analysis

INTRODUCTION

In China, gastric cancer (GC) has the second-highest cancer burden and the third most common cause of cancer-related deaths (with an age-standardized rate of incidence of 20.6 per 100,000 people, an age-standardized rate of mortality 15.9 per 100,000 population), and most patients are diagnosed at advanced disease stages (1). Patients presenting with locally advanced gastric cancer (LAGC) encounter problems associated with precise diagnoses and personalized treatment plans (2, 3) since tumor differentiation, Lauren classifications, and the presence of signet-ring cells can influence prognoses and treatment determinations (4–6). Lauren classifications are convenient and easy to implement and have good interobserver agreement (7). A recent study showed that the LAGC Lauren types correlated with perioperative chemotherapy responses (6). Endoscopic biopsies are invasive procedures prone to sampling errors due to the high heterogeneity of GCs; thus, the histopathology of tumor biopsies might not be consistent with those of whole-tumor resections (8, 9). Therefore, non-invasive imaging methods that could reliably predict the histopathologic characteristics of tumors could be useful.

Texture analysis is the method by which MRI and computed tomography (CT) radiologic data are processed using special software to extract texture features, which can quantitatively reflect pathologic information (10). CT remains the primary imaging modality in GC management owing to its relatively high accuracy rates and convenience (11). Several previous studies have shown that texture analyses from CT were useful for predicting GC prognoses and evaluating responses to neoadjuvant therapy (12–14), and some other studies have reported that preoperative CT texture analysis from omentum or primary tumors can help predict occult peritoneal metastases of advanced gastric cancers (15, 16). CT exposes patients to ionizing radiation and produces poor soft-tissue contrast. However, with technologic advancements, MRI temporal and spatial resolution has improved significantly, and its accuracy for assessing GC is similar to that of CT (17). Furthermore, MRI has good soft-tissue contrast and allows for repeated examinations owing to its non-ionizing radiation. It can also yield functional imaging features and has become a promising imaging technique for GC (11). However, applying texture analyses to MRI for GC diagnostics is less common (18); A few studies have found that apparent diffusion coefficient (ADC) first-order statistical metrics might be able to predict GC nodal status and are associated with perineural and vascular invasion (19, 20). Another study exploratory showed ADC histogram data from mono-exponential could reflect different histologic grades GC (21).

Based on diffusion-weighted imaging (DWI), Le Bihan et al. (22) proposed using intravoxel incoherent motion (IVIM) model to distinguish tissue perfusion and diffusion. IVIM is performed using bi-exponential curve fitting with multiple b-values and quantitative measurements with IVIM-derived parameters. Currently, this technique has been used for tumor grading, prognostic determinations, treatment monitoring, and distinguishing benign from malignant tumors (23, 24). However, it is rarer to use IVIM parameter texture analyses to evaluate GC in clinical research (25). Therefore, in this study, we aimed to investigate if IVIM whole-tumor histogram and texture analyses could be used to predict the pathologic features of LAGC.

MATERIALS AND METHODS

Patients

The study was a retrospective, cross-sectional observational analysis. From April 2017 to December 2018, a total of 80 patients with LAGC were included. The study protocol was approved by our institutional review board. The inclusion criteria were as follows: a) patients who underwent surgery in our institution; b) patients with histologically confirmed GC; and c) patients who underwent

Abbreviations: ADC, apparent diffusion coefficient; AUC, area under the curve; Dfast, pseudo-diffusion coefficient; DWI, diffusion-weighted imaging; Dslow, pure molecular-based diffusion coefficient; FP, pseudo-diffusion perfusion factor; GC, gastric cancer; IVIM, intravoxel Incoherent Motion; ICC, interclass correlation coefficient; LAGC, locally advanced gastric cancer; P5th, 5th percentile; P95th, 95th percentile; PC, poorly cohesive carcinoma; ROC, receiver operating characteristic; SRC, signet-ring cell carcinoma.

preoperative MRI with IVIM sequences. Seventy-one patients were excluded: 1) patients had been treated before surgical interventions; 2) the time interval between MRI and surgery was ≥ 2 weeks; 3) patients failed to finish all MRI scan sequences; 4) had contraindications to raceanisodamine hydrochloride; 5) had small lesions (the smallest diameter < 5 mm); and 6) MRI images had severe artifacts (see **Figure 1**).

MRI Examinations

Examinations were performed on a 3-Tesla MR scanner (MAGNETOM Skyra; Siemens Healthcare, Erlangen, Germany). We used an integrated body coil for excitation, with a dedicated 32-channel spine coil and an 18-channel body coil for signal reception. To reduce artifacts from intestinal peristalsis, raceanisodamine hydrochloride (10 mg; Minsheng Pharmaceuticals, Hangzhou, China) was administered to patients intramuscularly 5–10 min before the MR examinations, unless contraindicated. Patients fasted for more than 6 h to ensure the stomach was empty and then drank 500-800 ml water immediately before the MR examination to distend the stomach.

IVIM acquisitions were obtained before administering contrast medium, using a single-shot echo-planar imaging sequence (SS-EPI) with diffusion gradients of 9 b-values (0, 20, 40, 60, 100, 150, 200, 500, 800 s/mm2), and a 3D-diagonal diffusion mode was applied.

Other routine sequences included axial T1-weighted imaging (T1WI; in-phase and out-of-phase), axial T2-weighted imaging (T2WI), and axial contrast-enhanced imaging using volumetric

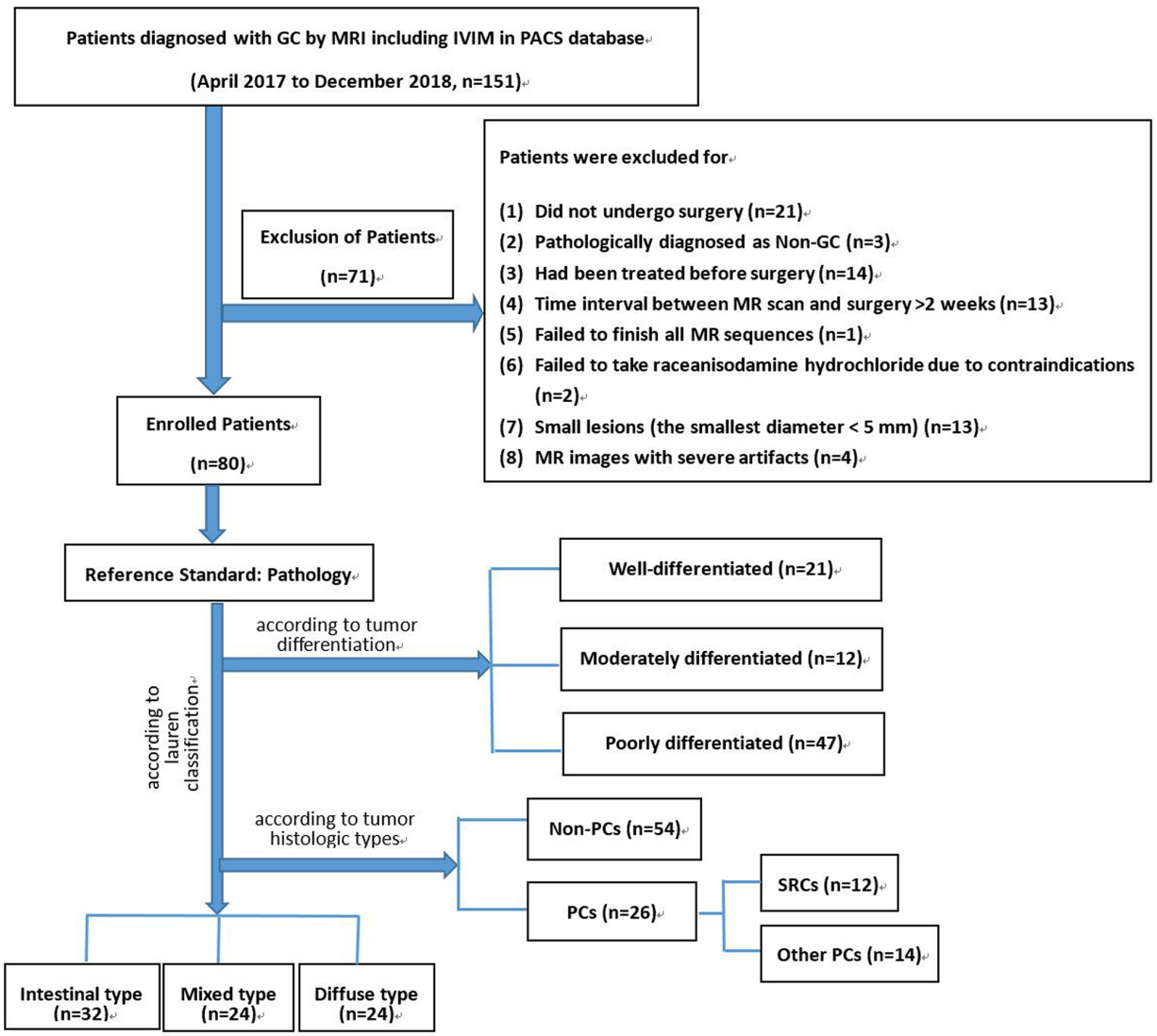

FIGURE 1 | Flow chart of our study population. GC, gastric cancer; IVIM, intravoxel incoherent motion; PACS, picture archiving and communication system; SRC, signet-ring cell carcinoma; PC, poorly cohesive carcinoma

interpolated breath-hold examinations (VIBEs). The detailed scanning parameters are shown in **Table 1**.

MR Image and Data Analyses

MR image quality was rated by two radiologists (with 5 and 10 years of abdominal diagnosis experience, respectively) according to a five-point Likert-type scale (1 = very poor, 2 = poor, 3 = moderate, 4 = good, and 5 = excellent), with a higher score indicating a better assessment.

The IVIM parameters (Dslow, pure molecular-based diffusion coefficient; Dfast, pseudo-diffusion coefficient; and FP, pseudo-diffusion perfusion factor) and ADC values were calculated using the Body Diffusion Toolbox (prototype software, Siemens Healthcare, Erlangen, Germany) based on all acquired b-values. Then, the IVIM parameter maps, ADC maps, and DWI with b=800 were imported into prototypic MR Multiparametric Analysis software (Siemens Healthcare, Erlangen, Germany). The two radiologists drew regions of interest (ROIs) manually on DWI images (with b=800), using contrast-enhanced images as references. ROIs were drawn along cancer lesion margins (excluding the areas with the highest and lowest signals to avoid partial-volume effects). After ROIs were drawn around whole tumors, based on IVIM parameters and ADC values, five histogram-derived texture metrics (median, P95th, P5th, skewness, kurtosis) and one second-order texture metric (entropy) were generated. Skewness and kurtosis reflect histogram shapes and measure parameter distribution asymmetries, and entropy represents variations in the parameter distributions of interest (26).

To evaluate interobserver agreement for image quality and data measurements, image quality scores and data analysis results of the two radiologists were tested.

Histopathologic Examinations

Histopathologic analyses were performed by a pathologist (with 10 years of clinical experience) who was blinded to IVIM parameter measurements. Tissue sections were stained with a hematoxylin and eosin (HE) stain according to routine procedures. Tumor differentiation, Lauren classifications, and the identification of poorly cohesive carcinomas (PCs) and signet-ring cell carcinomas (SRCs) on histology were evaluated and recorded according to the World Health Organization (WHO) classification (27) and Chinese national standard for GC diagnosis and treatment (28).

Statistical Analyses

The Shapiro-Wilk test and QQ plots were used to check the normality of the continuous variable distributions. The two-sample t-test or Mann-Whitney test was used to detect the metrics differences between the SRCs and other PCs. We used the one-way ANOVA and Kruskal-Wallis test to compare these metrics among the three differentiation degrees and the three Lauren classifications. Since many variables existed, logistic regression and multicollinear tests were adopted to screen out independent influencing factors for tumor differentiation and the Lauren classification. Then, screened variables were subjected to receiver operating characteristic (ROC) curve analyses, and the results were guaranteed to have practical significance due to the elimination of confounding factors. The ROC curve diagnostic accuracy was interpreted as low (area under the curve [AUC]=0.50-0.70), moderate (AUC=0.70-0.90), or high (AUC>0.90) (29). The interobserver agreement between the two radiologists was evaluated with the interclass correlation coefficient (ICC) test, which was interpreted as having a poor (ICC=0.00-0.20), fair (ICC=0.21-0.40), moderate (ICC=0.41-0.60), good 0.61-0.80, and 0.81-1.00, excellent correlations (30).

A P-value of <0.05 was considered statistically significant. ROC curve parameter comparisons were assessed using MedCalc software version 19.6.0, and other statistical analyses were performed using SPSS software version 23.0.

TABLE 1 | IVIM and routine sequence parameters.

Parameter	IVIM Sequence	T1-weighted IP and OP Sequence	T2-weighted Sequence	T1-weighted VIBE Sequence
Repetition time (msec)/echo time (msec)	5700/54	120/1.4 and 2.74	3500/83	3.9/1.89
b values (sec/mm^2)	0, 20, 40, 60, 100, 150, 200, 500, 800	—	—	—
Slice thickness (mm)	5	3.5	4	3.5
Slice gap (mm)	1	0.7	0.8	0.7
Acquisition matrix	128 × 128	320 × 240	256 × 256	320 × 240
Field of view (mm^2)	380 × 380	380 × 310	380 × 380	380 × 310
Acquisition time	3min and 9s	26s	3min and 15s	17s×3(30,60,90s)
Flip angle value	Excitation 90°	70°	91°	9°
	Refocusing 180°	—	—	—
Parallel imaging factor	2	—	—	—
Echo-planar imaging factor	115	—	—	—
No. of signals acquired	Sequentially according to b values: 2, 2, 2, 2, 3, 4, 4, 4, 6.	2	4	1

IP, in-phase; IVIM, intravoxel incoherent motion; OP, out-of-phase; and VIBE, volumetric interpolated breath-hold examination.
The acquisition planes are all axial imaging.

RESULTS

The Study Population and Interobserver Agreement

Eighty patients were finally included in the study. The average age of the patients (58 men and 22 women) was 60.7 years (range, 28–89 years). Tumors were located in the gastric cardia and fundus in 27 cases, the gastric body in 24 cases, and the gastric antrum in 29 cases. Most tumors in the cardia and fundus involved in the study were not confined to cardia or fundus, and there was no clear demarcation between the two areas. Therefore, we did not distinguish them among anatomical subtypes. For more detailed patient characteristics, see **Table 2**.

The interobserver agreement for image quality evaluations was excellent (the ICC was 0.85), so we adopted results from the first reader. Of the recruited patients, IVIM images from 26 patients were rated as 5 points (excellent), 32 patients as 4 points (good), 18 patients as 3 points (moderate), and 4 patients as 2 points (poor). We observed the IVIM image artifacts of 4 patients with 2 points, but the artifacts were on the abdominal wall and did not affect the gastric lesion conspicuity. The interobserver agreement for ADC, Dslow, and FP measurements was good to excellent (ICC=0.65-0.89), and the agreement for Dfast measurements was moderate (ICC=0.41-0.60; see **Table 3**).

TABLE 2 | Baseline and demographic data in 80 patients.

Characteristics	Value
Patient sex	
No. of men	58 (72.5%)
No. of women	22 (27.5%)
Age (y)	60.7 (28-89)
Tumor location	
Cardia and fundus	27 (33.7%)
Gastric body	24 (30.0%)
Gastric antrum	29 (36.3%)
Tumor volume (cm^3)	43.2 (3.4-200.7)
Tumor smallest diameter (mm)	16.9 (6.0-65.0)
Pathologic findings	
T staging	
T2	12 (15.0%)
T3	36 (45.0%)
T4a	32 (40.0%)
N staging	
N0	19 (23.75%)
N1	20 (25%)
N2	23 (28.75%)
N3	18 (22.5%)
Tumor differentiation	
Well-differentiated	21 (26.2%)
Moderately differentiated	12 (15.0%)
Poorly differentiated	47 (58.8%)
Lauren classification	
Intestinal type	32 (40.0%)
Mixed type	24 (30.0%)
Diffuse type	24 (30.0%)
Histologic types	
Non-PCs	54 (67.5%)
PCs	26 (32.5%)
SRCs	12 (15.0%)
Other PCs	14 (17.5%)

Continuous data are shown as means, with ranges in brackets. Categorical data are expressed as numbers of patients, with percentages in brackets.
T staging, tumor staging; N staging, lymph node staging; SRCs, signet-ring cell carcinomas; PC, poorly cohesive carcinoma.

Histograms and Texture Metrics of IVIM Parameters for Tumor Differentiation

The median, P5th, and P95th values of the ADC, Dslow, and FP parameters were higher in the well/moderately differentiated GCs compared with those in the poorly differentiated GCs(all total P-values <0.05, except the P-value for $Dslow_{P5th}$). The skewness, kurtosis, and entropy values of the ADC, Dslow, and FP parameters were lower in the well/moderately differentiated GCs compared with those in the poorly differentiated GCs (all total P-values <0.05, except P-value for $ADC_{kurtosis}$). For the Dfast parameter, none of the metric values were different among the three differentiation degrees (P >0.05); see **Table E1** (online). **Table E1** also shows the paired comparisons among the three differentiation degrees. Representative cases from the two groups are shown in **Figures 2**, **3**.

ADC_{median}, $Dslow_{median}$, $Dslow_{entropy}$, and FP_{P95th} were screened out as independent influencing factors for tumor differentiation (the cutoff values for distinguishing the well/moderately differentiated and poorly differentiated GCs were $1601.50\times10^{-6}mm^2/s$, $1356.50\times10^{-6}mm^2/s$, 3.16, and 63.15%, respectively). In ROC curve analyses, we found $Dslow_{median}$ had the largest AUC of 0.948 (P<0.001) with an accuracy of 91.3%, sensitivity of 89.4%, and specificity of 93.9%; however, these values were not statistically different from those of ADC_{median} and $Dslow_{entropy}$ (P>0.05; see **Table 4** and **Figure 4**).

Histograms and Texture Metrics of IVIM Parameters for Lauren Classifications

Except for Dfast metrics, $Dslow_{P5th}$, and $FP_{entropy}$, other metrics were statistically different among the three Lauren classifications. The median, P5th, and P95th values of the ADC, Dslow, and FP parameters were higher in the intestinal/mixed types compared with those in the diffuse-types (all total P-values <0.05, except the P-value for $Dslow_{P5th}$). The skewness, kurtosis, and entropy values of the ADC, Dslow, and FP parameters were lower in the intestinal/mixed types compared with those in the diffuse-types(all total P-values <0.05, except the P-value for $FP_{entropy}$); see **Table E2** (online). **Table E2** also shows the paired comparisons among the different Lauren classification groups.

We further screened the independent influencing factors for the different Lauren classification groups, including ADC_{median}, $Dslow_{median}$, $Dslow_{entropy}$, and FP_{P95th}. We found that FP_{P95th} had the largest AUC of 0.896 (P<0.001) with an accuracy of 77.5%, sensitivity of 95.8%, and specificity of 69.6%, with no statistical difference between the other three metrics (see **Table 5** and **Figure 5**).

Histograms and Texture Metrics of IVIM Parameters for Differentiating Signet-Ring Cell Carcinomas from the Other Poorly Cohesive Types

All SRC and other PC metrics were compared using univariate analyses. The $Dslow_{median}$ value was the only metric that showed

TABLE 3 | Interobserver agreement for parameters measurements assessed by the interclass correlation coefficient.

Variable metrics	ADC	Dslow	Dfast	FP
Median	0.82 [0.74,0.88]	0.81 [0.72,0.87]	0.60 [0.43,0.72]	0.88 [0.82,0.92]
P5th	0.85 [0.77,0.90]	0.88 [0.82,0.92]	0.58 [0.42,0.71]	0.89 [0.83,0.93]
P95th	0.78 [0.68,0.85]	0.74 [0.62,0.82]	0.49 [0.30,0.64]	0.84 [0.76,0.89]
Skewness	0.73 [0.61,0.82]	0.74 [0.63,0.83]	0.44 [0.24,0.60]	0.76 [0.65,0.84]
Kurtosis	0.79 [0.69,0.86]	0.88 [0.82,0.92]	0.45 [0.26,0.61]	0.84 [0.77,0.90]
Entropy	0.65 [0.51,0.76]	0.72 [0.60,0.81]	0.41 [0.21,0.58]	0.78 [0.67,0.85]

Data are interobserver correlation coefficients, with 95% confidence intervals in brackets.
ADC, apparent diffusion coefficient; Dslow, pure molecular-based diffusion coefficient; Dfast, pseudo-diffusion coefficient; FP, pseudo-diffusion factor given as a percentage; P5th, 5th percentile; and P95th, 95th percentile.

statistical differences between the two groups, with the SRC values being less than those of the other PC types ($P < 0.05$); see **Table E3** (online). In the ROC analyses, the $Dslow_{median}$ had an AUC of 0.738, with an accuracy of 70.4%, sensitivity of 75.0%, and specificity of 71.4%; see **Table 6** and **Figure 6**.

DISCUSSION

Our research focused on analyzing histogram and texture characteristics of IVIM parameters for LAGC with different pathological subtypes. IVIM imaging has the advantage of simultaneously obtaining diffusion and perfusion information without a co-registration processing step and the administration of contrast media (31). Many studies have reported its application in rectal tumors, concluding that IVIM parameters reflected histologic changes after treatment. Studies have also shown that IVIM parameters are associated with tumor differentiation and clinical staging (32–35). However, clinical studies looking at IVIM in patients with GC have not been commonly reported, although a few animal studies have examined chemotherapeutic efficacies (36, 37). An initial study reported the use of IVIM parameters to assess GC histotypes, but single-slice ROIs rather than whole-tumor volumetric measurements were used, and histograms and texture analyses were not applied (38). SRC is a rare type of adenocarcinoma characterized by signet-ring cells that secrete large amounts of mucin and displace the nucleus to the cell periphery (39). This cancer type is insensitive to chemoradiotherapy and has a poor prognosis in advanced stages (40). In 2010, the WHO classification defined PC as isolated or small aggregates of discohesive carcinoma cells with an infiltrative pattern, including SRCs and other cell types (27, 41).. There have only been a few previously published MRI studies on SRC, especially with respect to the difference between SRCs and other PC types. In this study, we explored the value of whole-tumor histogram and texture features for IVIM parameters in identifying GC differentiation, Lauren types, and SRC carcinomas according to ROC curve analysis.

For tumor differentiation, we found that the diffusion parameter metrics, ADC_{median}, $Dslow_{median}$, and $Dslow_{entropy}$, showed better diagnostic performance as independent influencing factors for distinguishing poorly differentiated from the well/moderately differentiated GCs (see **Figure 4**). The ADC_{median} and $Dslow_{median}$ values of poorly differentiated tumors were significantly lower than those of the well/moderately differentiated tumors. These findings were similar to a previously reported study, which showed that restricted water motion in malignant tumors was associated with tumor differentiation (21). In addition, the $Dslow_{entropy}$ value of poorly differentiated tumors was higher than that of well/moderately differentiated tumors, suggesting that poorly differentiated tumors have more radiologic heterogeneity/variability. As a perfusion parameter, the diagnostic performance of FP_{P95th} for tumor differentiation was not too bad, although the AUC was smaller than that of ADC_{median}, $Dslow_{median}$, and $Dslow_{entropy}$. In our study, the FP_{P95th} in the poorly differentiated tumor was significantly lower than that of well/moderately differentiated tumors, which could indicate that lower FP values are related to the hypoperfusion of blood caused by fewer normal glandular structures in poorly differentiated tumors (35).

Lauren classifications can reflect the biological aggressiveness of GC, in which diffuse-type GCs display a diffusely invasive growth pattern with a worse prognosis than intestinal/mixed-type (5). We found the perfusion parameter metric, FP_{P95th}, had the best diagnostic efficiency for discriminating diffuse-type GCs from intestinal/mixed-type GCs (see **Figure 5**). The FP_{P95th} values of the diffuse-type GCs were significantly lower than those of the intestinal/mixed-type GCs, which suggests that the diffuse-type GC FP histograms were less frequent at the high end of the FP values compared with intestinal/mixed-type GC FP histograms. We previously showed that diffuse-type GCs have a less glandular appearance than intestinal/mixed GCs (5), which suggests that the lower FP values of diffuse-type GCs might be due to the hypoperfusion of blood caused by fewer normal glandular structures. Diffuse-type GCs also had higher $Dslow_{entropy}$ values than intestinal/mixed-type GCs, indicating that the diffuse-type GCs have more radiologic heterogeneity/variability on the Dslow maps. A previous study reported that the ADC values from a mono-exponential model correlated with the GC Lauren classifications (42). Our research indicated that the FP_{P95th} metric performed better than ADC in determining Lauren classifications, demonstrating the advantage of using IVIM multi-parametric analyses from the biexponential model over using parametric analyses from the mono-exponential model.

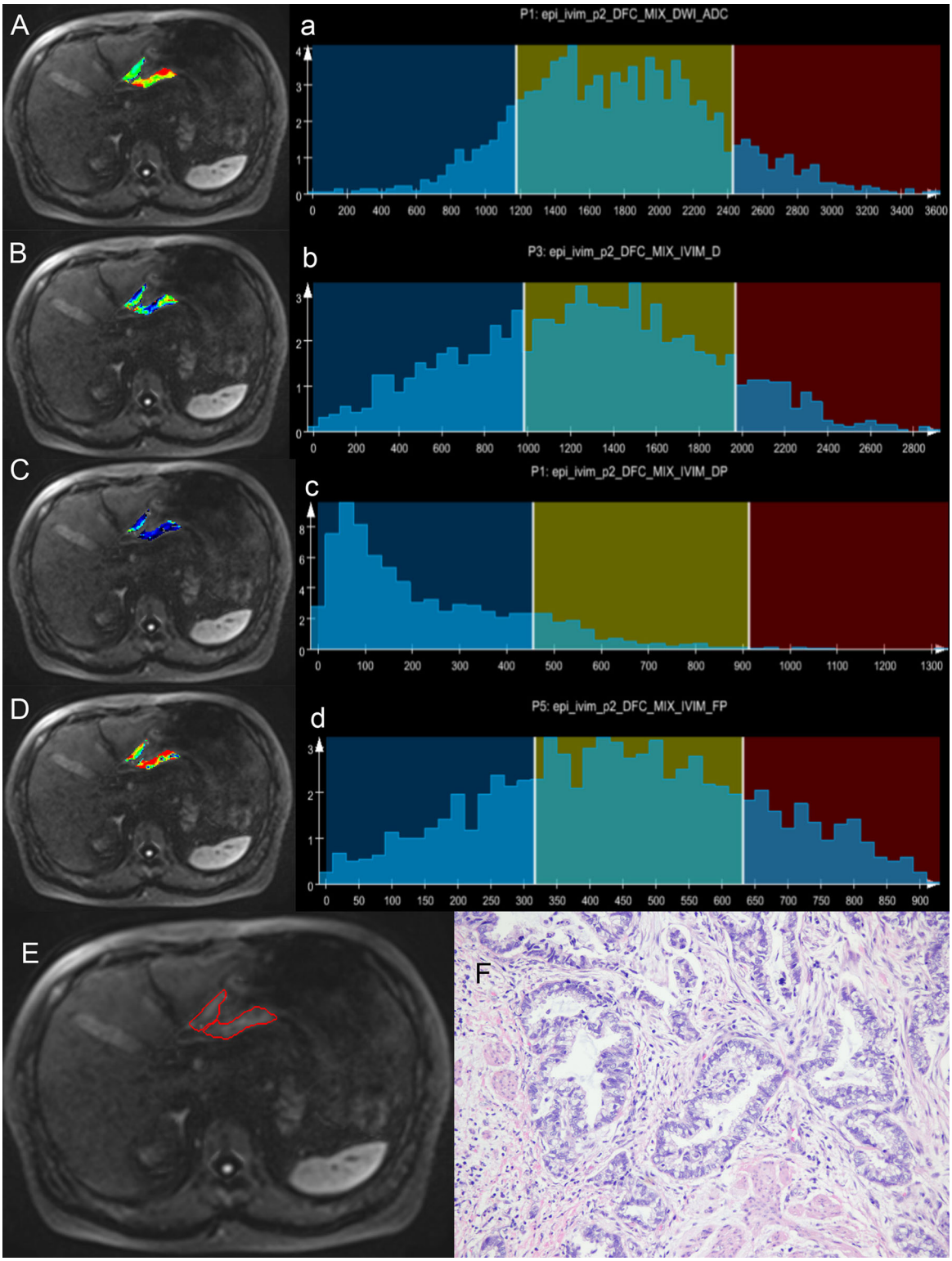

FIGURE 2 | A case of gastric antrum cancer. The colored regions in **(A–D)** represent the lesion parameters maps; **(a–d)** show histogram parameter distributions for the whole tumor (ADC, Dslow, Dfast, and FP presenting sequentially). **(E)** Shows the contour of the region of interest (ROI). **(F)** A photomicrograph of an HE stained tissue section demonstrating a moderately differentiated adenocarcinoma.

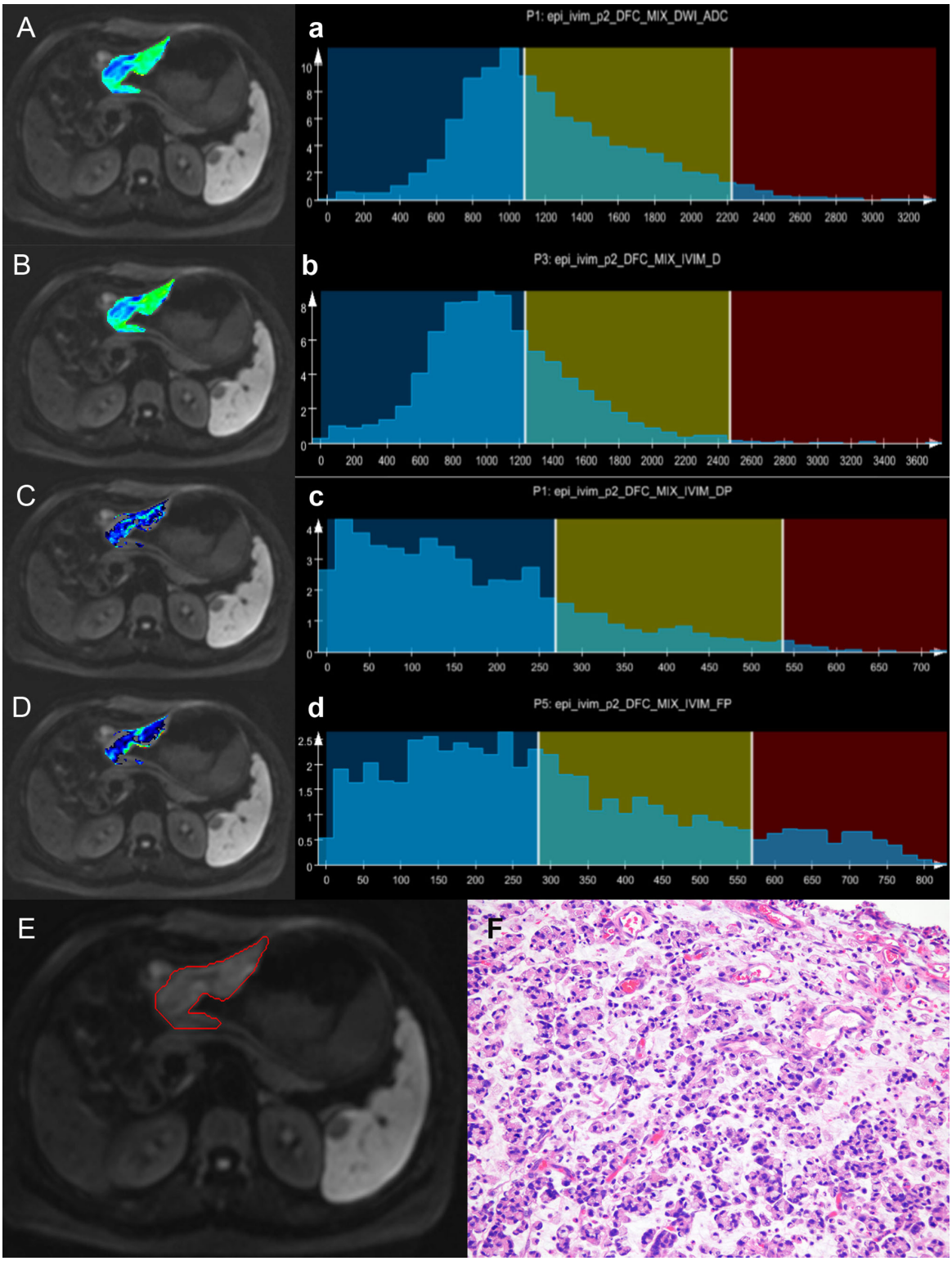

FIGURE 3 | A case of gastric body cancer. The colored regions in **(A–D)** represent the lesion parameters maps; **(a–d)** show histogram parameter distributions for the whole tumor (ADC, Dslow, Dfast, and FP presenting sequentially). **(E)** Shows the contour of the region of interest (ROI). **(F)** A photomicrograph of an HE stained tissue section demonstrating a poorly differentiated signet-ring cell carcinoma.

TABLE 4 | The diagnostic performance of the independent influencing factors for the well/moderately differentiated vs. poorly differentiated GC.

Variable metrics	Cutoff	Accuracy	Sensitivity	Specificity	PPV	NPV	AUC	P-value
ADC_{median}	1601.50[a]	90.0%	91.5%	87.9%	91.5%	87.9%	0.937 [0.874-0.985]	<0.001
$Dslow_{median}$	1356.50[a]	91.3%	89.4%	93.9%	95.5%	86.1%	0.948 [0.860-0.979]	<0.001
$Dslow_{entropy}$	3.16	78.8%	74.5%	84.8%	87.5%	70.0%	0.850 [0.749-0.918]	<0.001
FP_{P95th}	63.15%	76.3%	80.9%	69.7%	79.2%	71.9%	0.803 [0.699-0.883]	<0.001

Numbers in brackets are 95% confidence intervals (95% CI).
PPV, Positive predictive value; NPV, Negative predictive value; AUC, area under the curve; ADC, apparent diffusion coefficient; Dslow, pure molecular-based diffusion coefficient; FP, pseudo-diffusion factor given as a percentage; and P95th, 95th percentile.
a, $10^{-6}mm^2/s$.
No differences (P >0.05) were detected by paired comparisons between ADC_{median}, $Dslow_{median}$, and $Dslow_{entropy}$.

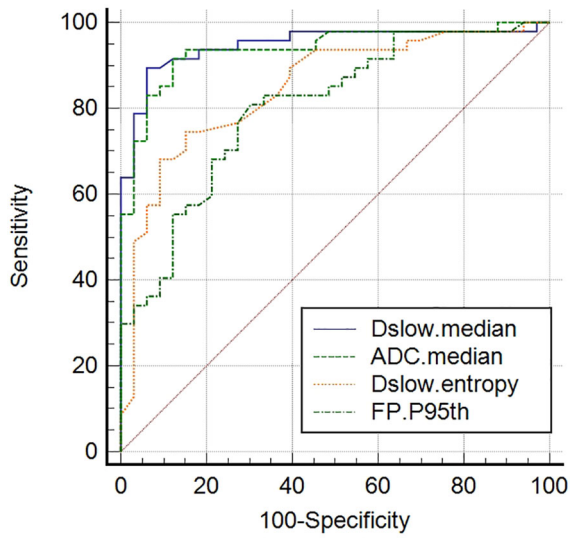

FIGURE 4 | Receiver operating characteristic (ROC) curves of screened independent influencing factors that could distinguish poorly differentiated from well/moderately differentiated GCs. ADC_{median}, $Dslow_{median}$, and $Dslow_{entropy}$ show good diagnostic performance, with AUCs of 0.937, 0.948, and 0.850, respectively. Comparisons among the four metrics determined that these values were significantly different (P <0.05), although no differences (P >0.05) were detected when paired comparisons among the ADC_{median}, $Dslow_{median}$, and $Dslow_{entropy}$ values were performed.

Our research found that the $Dslow_{median}$ values of the SRCs were lower than those of other PC types, providing moderate diagnostic efficacies for distinguishing the two types (see **Figure 6**). The parameter Dslow from the biexponential model, which separates perfusion effects, might reflect the true diffusion state within lesions better than ADC from the mono-exponential model (23, 31). In our study, $Dslow_{median}$ value was the only metric that showed statistical differences between the SRCs and other PC types, and which had greater AUC values than ADC_{median} in determining tumor differentiation and Lauren classifications. However, the differences were not statistically significant and could have been caused by the relatively small sample size of some groups and the difficulty of including additional b-values in clinical practice.

Our study used whole-tumor analysis for IVIM parameter metric measurements. This whole-tumor analysis reduced intratumoral heterogeneity influences on the measurements and provided more reproducible and reliable data than single-slice ROI analyses (33, 43). In this research, all parameter measurements had good or excellent interobserver reproducibility except for Dfast, which showed greater measurement susceptibility with moderate agreement.

There were several limitations to this study. First, early GC lesions are small and susceptible to motion artifacts and partial-volume averaging; thus, our research included only patients with LAGC (the smallest diameter of lesions≥ 5 mm). Second, we used water as the negative contrast agent to fill the stomach cavity; however, gas-liquid levels sometimes appeared near the lesions, leading to susceptibility artifacts. Future prospective studies will develop a more robust acquisition method and a special gastric filling contrast agent to minimize susceptibility artifacts. Third, there were slightly fewer cases in the diffuse group, but according to the EPV (events per variable) principle proposed by

TABLE 5 | The diagnostic performance of the independent influencing factors for the intestinal/mixed vs. diffuse-type GC.

Variable metrics	Cutoff	Accuracy	Sensitivity	Specificity	PPV	NPV	AUC	P value
ADC_{median}	1626.50[a]	62.5%	91.7%	50.0%	44.0%	93.3%	0.747 [0.637-0.838]	<0.001
$Dslow_{median}$	1437.50[a]	60.0%	95.8%	44.6%	42.6%	96.2%	0.762 [0.653-0.850]	<0.001
$Dslow_{entropy}$	3.16	68.8%	75.0%	66.1%	48.6%	86.0%	0.755 [0.646-0.844]	<0.001
FP_{P95th}	61.15%	77.5%	95.8%	69.6%	57.5%	97.5%	0.896 [0.829-0.963]	<0.001

Numbers in brackets are 95% confidence intervals.
PPV, Positive predictive value; NPV, Negative predictive value; AUC, area under the curve; ADC, apparent diffusion coefficient; Dslow, pure molecular-based diffusion coefficient; FP, pseudo-diffusion factor given as a percentage; and P95th, 95th percentile.
a = $10^{-6}mm^2/s$.
No differences (P >0.05) were detected by paired comparisons between ADC_{median}, $Dslow_{median}$, and $Dslow_{entropy}$.

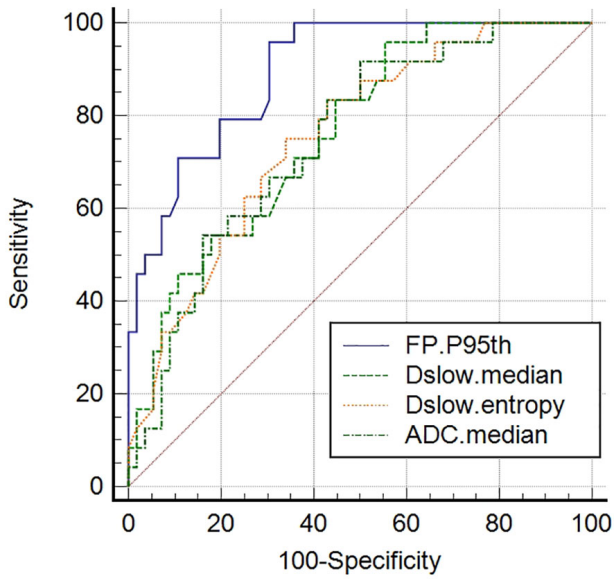

FIGURE 5 | Receiver operating characteristic (ROC) curves of screened independent influencing factors that could distinguish diffuse-type GCs from intestinal/mixed-type GCs. FP_{P95th} had the largest AUC of 0.896. Comparisons among the four metrics determined that these values were significantly different (P <0.05), although no differences (P >0.05) were detected when paired comparisons among the ADC_{median}, $Dslow_{median}$, and $Dslow_{entropy}$ values were performed.

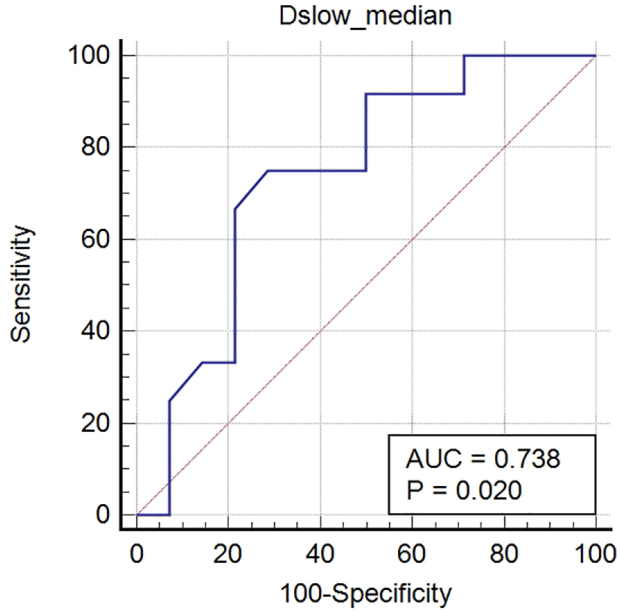

FIGURE 6 | Receiver operating characteristic (ROC) curves of $Dslow_{median}$ for distinguishing signet-ring cell carcinomas from other poorly cohesive carcinomas. The AUC of $Dslow_{median}$ was 0.738.

TABLE 6 | The diagnostic performance of $Dslow_{median}$ for discriminating SRCs and other poorly cohesive carcinomas.

Variable metrics	Cutoff	Accuracy	Sensitivity	Specificity	PPV	NPV	AUC	P value
$Dslow_{median}$	1041.00[a]	70.4%	75.0%	71.4%	69.2%	76.9%	0.738 [0.537-0.939]	0.020

Numbers in brackets are 95% confidence intervals.
PPV, Positive predictive value; NPV, Negative predictive value; AUC, area under the curve SRCs, Signet-ring cell carcinomas; ADC, apparent diffusion coefficient; and Dslow, pure molecular-based diffusion coefficient.
a =$10^{-6}mm^2/s$.
No differences (P >0.05) were detected by paired comparisons between ADC_{median} and $Dslow_{median}$.

Vittinghoff et al. (44), the sample size was sufficient for the analyses. In addition, the sample sizes of patients with SRC and other PC were small, so for these individuals, we only performed univariate analyses. Given that SRC is less common, our univariate analytic results have some significance.

Despite these limitations, our study showed the novel advantages of IVIM multi-parameter histogram and texture analyses for GC research based on the biexponential model. Moreover, IVIM provided an additional perfusion parameter, FP, which demonstrated greater potential for determining Lauren classifications than ADC from the mono-exponential model.

DATA AVAILABILITY STATEMENT

The raw data supporting the conclusions of this article will be made available by the authors, without undue reservation.

ETHICS STATEMENT

The study is approved by Fudan University Shanghai Cancer Center Institutional Review Board. Written informed consent for participation was not required for this study in accordance with the national legislation and the institutional requirements.

AUTHOR CONTRIBUTIONS

W-JP and HZ conceived this idea and managed the research project, H-HL and BS designed this study, MRI data acquisition was performed by H-HL and RL, Statistical analysis was performed by H-HL and HZ, BS was contributed to clinical data interpretation, CT performed pathological analysis. C-XF

and RG provided software analysis methods. All authors contributed to the article and approved the submitted version.

FUNDING

This work was supported by the National Natural Science Foundation of China (grant number 81902436) and the Science and Technology Commission of Shanghai Municipality (grant number STCSM18411953000).

ACKNOWLEDGMENTS

Thanks to our colleague Tian-Wen Xie for assistance with this project and valuable discussion.

SUPPLEMENTARY MATERIAL

The Supplementary Material for this article can be found online at: https://www.frontiersin.org/articles/10.3389/fonc.2022.821586/full#supplementary-material

REFERENCES

1. Qiu HB, Cao SM, Xu RH. Cancer Incidence, Mortality, and Burden in China: A Time-Trend Analysis and Comparison With the United States and United Kingdom Based on the Global Epidemiological Data Released in 2020. *Cancer Commun (Lond)* (2021) 41:1037–48. doi: 10.1002/cac2.12197
2. Mocan L. Surgical Management of Gastric Cancer: A Systematic Review. *J Clin Med* (2021) 10:2557. doi: 10.3390/jcm10122557
3. Tokunaga M, Sato Y, Nakagawa M, Aburatani T, Matsuyama T, Nakajima Y, et al. Perioperative Chemotherapy for Locally Advanced Gastric Cancer in Japan: Current and Future Perspectives. *Surg Today* (2020) 50:30–7. doi: 10.1007/s00595-019-01896-5
4. Alshehri A, Alanezi H, Kim BS. Prognosis Factors of Advanced Gastric Cancer According to Sex and Age. *World J Clin Cases* (2020) 8:1608–19. doi: 10.12998/wjcc.v8.i9.1608
5. Chen YC, Fang WL, Wang RF, Liu CA, Yang MH, Lo SS, et al. Clinicopathological Variation of Lauren Classification in Gastric Cancer. *Pathol Oncol Res* (2016) 22:197–202. doi: 10.1007/s12253-015-9996-6
6. Zurlo IV, Basso M, Strippoli A, Calegari MA, Orlandi A, Cassano A, et al. Treatment of Locally Advanced Gastric Cancer (LAGC): Back to Lauren's Classification in Pan-Cancer Analysis Era? *Cancers (Basel)* (2020) 12:1749. doi: 10.3390/cancers12071749
7. Yu Y. Evaluation of Traditional Pathological Classification at Molecular Classification Era for Gastric Cancer. *Chin J Gastrointest Surg* (2014) 17:18–20.
8. Tae CH, Lee JH, Min BH, Kim KM, Rhee PL, Kim JJ. Negative Biopsy After Referral for Biopsy-Proven Gastric Cancer. *Gut Liver* (2016) 10:63–8. doi: 10.5009/gnl14281
9. Yan H, Li M, Cao L, Chen H, Lai H, Guan Q, et al. A Robust Qualitative Transcriptional Signature for the Correct Pathological Diagnosis of Gastric Cancer. *J Transl Med* (2019) 17:63. doi: 10.1186/s12967-019-1816-4
10. Hainc N, Stippich C, Stieltjes B, Leu S, Bink A. Experimental Texture Analysis in Glioblastoma: A Methodological Study. *Invest Radiol* (2017) 52:367–73. doi: 10.1097/RLI.0000000000000354
11. Borggreve AS, Goense L, Brenkman HJF, Mook S, Meijer GJ, Wessels FJ, et al. Imaging Strategies in the Management of Gastric Cancer: Current Role and Future Potential of MRI. *Br J Radiol* (2019) 92:20181044. doi: 10.1259/bjr.20181044
12. Giganti F, Marra P, Ambrosi A, Salerno A, Antunes S, Chiari D, et al. Pre-Treatment MDCT-Based Texture Analysis for Therapy Response Prediction in Gastric Cancer: Comparison With Tumour Regression Grade at Final Histology. *Eur J Radiol* (2017) 90:129–37. doi: 10.1016/j.ejrad.2017.02.043
13. Mazzei MA, Nardone V, Di Giacomo L, Bagnacci G, Gentili F, Tini P, et al. The Role of Delta Radiomics in Gastric Cancer. *Quant Imaging Med Surg* (2018) 8:719–21. doi: 10.21037/qims.2018.07.08
14. Mazzei MA, Di Giacomo L, Bagnacci G, Nardone V, Gentili F, Lucii G, et al. Delta-Radiomics and Response to Neoadjuvant Treatment in Locally Advanced Gastric Cancer-A Multicenter Study of GIRCG (Italian Research Group for Gastric Cancer). *Quant Imaging Med Surg* (2021) 11:2376–87. doi: 10.21037/qims-20-683
15. Kim HY, Kim YH, Yun G, Chang W, Lee YJ, Kim B. Could Texture Features From Preoperative CT Image be Used for Predicting Occult Peritoneal Carcinomatosis in Patients With Advanced Gastric Cancer? *PloS One* (2018) 13:e0194755. doi: 10.1371/journal.pone.0194755
16. Liu S, He J, Liu S, Ji C, Guan W, Chen L, et al. Radiomics Analysis Using Contrast-Enhanced CT for Preoperative Prediction of Occult Peritoneal Metastasis in Advanced Gastric Cancer. *Eur Radiol* (2020) 30:239–46. doi: 10.1007/s00330-019-06368-5
17. Renzulli M, Clemente A, Spinelli D, Ierardi AM, Marasco G, Farina D, et al. Gastric Cancer Staging: Is It Time for Magnetic Resonance Imaging? *Cancers (Basel)* (2020) 12:1402. doi: 10.3390/cancers12061402
18. Sah BR, Owczarczyk K, Siddique M, Cook GJR, Goh V. Radiomics in Esophageal and Gastric Cancer. *Abdom Radiol (NY)* (2019) 44:2048–58. doi: 10.1007/s00261-018-1724-8
19. Liu S, Zhang Y, Xia J, Chen L, Guan W, Guan Y, et al. Predicting the Nodal Status in Gastric Cancers: The Role of Apparent Diffusion Coefficient Histogram Characteristic Analysis. *Magn Reson Imaging* (2017) 42:144–51. doi: 10.1016/j.mri.2017.07.013
20. Liu S, Zheng H, Zhang Y, Chen L, Guan W, Guan Y, et al. Whole-Volume Apparent Diffusion Coefficient-Based Entropy Parameters for Assessment of Gastric Cancer Aggressiveness. *J Magn Reson Imaging* (2018) 47:168–75. doi: 10.1002/jmri.25752
21. Zhang Y, Chen J, Liu S, Shi H, Guan W, Ji C, et al. Assessment of Histological Differentiation in Gastric Cancers Using Whole-Volume Histogram Analysis of Apparent Diffusion Coefficient Maps. *J Magn Reson Imaging* (2017) 45:440–9. doi: 10.1002/jmri.25360
22. Le Bihan D, Breton E, Lallemand D, Grenier P, Cabanis E, Laval-Jeantet M. MR Imaging of Intravoxel Incoherent Motions: Application to Diffusion and Perfusion in Neurologic Disorders. *Radiology* (1986) 161:401–7. doi: 10.1148/radiology.161.2.3763909
23. Iima M, Le Bihan D. Clinical Intravoxel Incoherent Motion and Diffusion MR Imaging: Past, Present, and Future. *Radiology* (2016) 278:13–32. doi: 10.1148/radiol.2015150244
24. Klauss M, Lemke A, Grünberg K, Simon D, Re TJ, Wente MN, et al. Intravoxel Incoherent Motion MRI for the Differentiation Between Mass Forming Chronic Pancreatitis and Pancreatic Carcinoma. *Invest Radiol* (2011) 46:57–63. doi: 10.1097/RLI.0b013e3181fb3bf2
25. Zuo HD, Zhang XM. Could Intravoxel Incoherent Motion Diffusion-Weighted Magnetic Resonance Imaging be Feasible and Beneficial to the Evaluation of Gastrointestinal Tumors Histopathology and the Therapeutic Response? *World J Radiol* (2018) 10:116–23. doi: 10.4329/wjr.v10.i10.116
26. Just N. Improving Tumour Heterogeneity MRI Assessment With Histograms. *Br J Cancer* (2014) 111:2205–13. doi: 10.1038/bjc.2014.512
27. Bosman FT, Carneiro F, Hruban RH, Theise ND. WHO Classification of Tumours of the Digestive System. *Lyon: IARC Press* (2010).
28. National Health Commission of the People's Republic of China. *Notice on the Issuance of "National Standard for Diagnosis and Treatment of Gastric Cancer* (2011). Available at: http://www.nhc.gov.cn/wjw/gfxwj/201304/a70adc50534148448702b9f1ab3abcf7.shtml (Accessed December 31, 2021).
29. Zhou D-Y, Zhuang C, Jiao Z-S, Ma J. Step-By-Step Examples of Data Analysis and Statistical Graphs in Clinical Researches. Beijing: Military Med Sci Press (2011). 267 p.
30. Salkind NJ. *Statistics for People Who (Think They) Hate Statistics*. Thousand Oaks CA: SAGE Publications (2016). 480 p.

31. Kim HS, Suh CH, Kim N, Choi CG, Kim SJ. Histogram Analysis of Intravoxel Incoherent Motion for Differentiating Recurrent Tumor From Treatment Effect in Patients With Glioblastoma: Initial Clinical Experience. *AJNR Am J Neuroradiol* (2014) 35:490–7. doi: 10.3174/ajnr.A3719
32. Bäuerle T, Seyler L, Münter M, Jensen A, Brand K, Fritzsche KH, et al. Diffusion-Weighted Imaging in Rectal Carcinoma Patients Without and After Chemoradiotherapy: A Comparative Study With Histology. *Eur J Radiol* (2013) 82:444–52. doi: 10.1016/j.ejrad.2012.10.012
33. Nougaret S, Vargas HA, Lakhman Y, Sudre R, Do RK, Bibeau F, et al. Intravoxel Incoherent Motion-Derived Histogram Metrics for Assessment of Response After Combined Chemotherapy and Radiation Therapy in Rectal Cancer: Initial Experience and Comparison Between Single-Section and Volumetric Analyses. *Radiology* (2016) 280:446–54. doi: 10.1148/radiol.2016150702
34. Xu Q, Xu Y, Sun H, Chan Q, Shi K, Song A, et al. Quantitative Intravoxel Incoherent Motion Parameters Derived From Whole-Tumor Volume for Assessing Pathological Complete Response to Neoadjuvant Chemotherapy in Locally Advanced Rectal Cancer. *J Magn Reson Imaging* (2018) 48:248–58. doi: 10.1002/jmri.25931
35. Sun H, Xu Y, Song A, Shi K, Wang W. Intravoxel Incoherent Motion MRI of Rectal Cancer: Correlation of Diffusion and Perfusion Characteristics With Prognostic Tumor Markers. *AJR Am J Roentgenol* (2018) 210:W139–47. doi: 10.2214/AJR.17.18342
36. Song XL, Kang HK, Jeong GW, Ahn KY, Jeong YY, Kang YJ, et al. Intravoxel Incoherent Motion Diffusion-Weighted Imaging for Monitoring Chemotherapeutic Efficacy in Gastric Cancer. *World J Gastroenterol* (2016) 22:5520–31. doi: 10.3748/wjg.v22.i24.5520
37. Cheng J, Wang Y, Zhang CF, Wang H, Wu WZ, Pan F, et al. Chemotherapy Response Evaluation in a Mouse Model of Gastric Cancer Using Intravoxel Incoherent Motion Diffusion-Weighted MRI and Histopathology. *World J Gastroenterol* (2017) 23:1990–2001. doi: 10.3748/wjg.v23.i11.1990
38. Ji C, Chen L, Guan W, Guo T, Zhang Q, Liu S, et al. Intravoxel Incoherent Motion Magnetic Resonance Imaging in Assessing Histopathological Features of Gastric Cancers: Initial Findings. *Transl Cancer Res* (2017) 6:1129– 1140. doi: 10.21037/tcr.2017.11.15
39. Arai T. Where Does Signet-Ring Cell Carcinoma Come From and Where Does It Go? *Gastric Cancer* (2019) 22:651–2. doi: 10.1007/s10120-019-00960-w
40. Chon HJ, Hyung WJ, Kim C, Park S, Kim JH, Park CH, et al. Differential Prognostic Implications of Gastric Signet Ring Cell Carcinoma: Stage Adjusted Analysis From a Single High-Volume Center in Asia. *Ann Surg* (2017) 265:946–53. doi: 10.1097/SLA.0000000000001793
41. Kwon CH, Kim YK, Lee S, Kim A, Park HJ, Choi Y, et al. Gastric Poorly Cohesive Carcinoma: A Correlative Study of Mutational Signatures and Prognostic Significance Based on Histopathological Subtypes. *Histopathology* (2018) 72:556–68. doi: 10.1111/his.13383
42. Liu S, Guan W, Wang H, Pan L, Zhou Z, Yu H, et al. Apparent Diffusion Coefficient Value of Gastric Cancer by Diffusion-Weighted Imaging: Correlations With the Histological Differentiation and Lauren Classification. *Eur J Radiol* (2014) 83:2122–8. doi: 10.1016/j.ejrad.2014.09.021
43. Zhao Q, Xie T, Fu C, Chen L, Bai Q, Grimm R, et al. Differentiation Between Idiopathic Granulomatous Mastitis and Invasive Breast Carcinoma, Both Presenting With Non-Mass Enhancement Without Rim-Enhanced Masses: The Value of Whole-Lesion Histogram and Texture Analysis Using Apparent Diffusion Coefficient. *Eur J Radiol* (2020) 123:108782. doi: 10.1016/j.ejrad.2019.108782
44. Vittinghoff E, McCulloch CE. Relaxing the Rule of Ten Events Per Variable in Logistic and Cox Regression. *Am J Epidemiol* (2007) 165:710–8. doi: 10.1093/aje/kwk052

Conflict of Interest: C-XF was employed by Siemens Shenzhen Magnetic Resonance Ltd. RG was employed by Siemens Healthcare.

The remaining authors declare that the research was conducted without any commercial or financial relationships that could be construed as a potential conflict of interest.

Publisher's Note: All claims expressed in this article are solely those of the authors and do not necessarily represent those of their affiliated organizations, or those of the publisher, the editors and the reviewers. Any product that may be evaluated in this article, or claim that may be made by its manufacturer, is not guaranteed or endorsed by the publisher.

Copyright © 2022 Li, Sun, Tan, Li, Fu, Grimm, Zhu and Peng. This is an open-access article distributed under the terms of the Creative Commons Attribution License (CC BY). The use, distribution or reproduction in other forums is permitted, provided the original author(s) and the copyright owner(s) are credited and that the original publication in this journal is cited, in accordance with accepted academic practice. No use, distribution or reproduction is permitted which does not comply with these terms.

frontiers in Oncology

ORIGINAL RESEARCH
published: 17 February 2022
doi: 10.3389/fonc.2022.802009

ω-3 and ω-6 Polyunsaturated Fatty Acids Regulate the Proliferation, Invasion and Angiogenesis of Gastric Cancer Through COX/PGE Signaling Pathway

Jiachi Ma[1], Chensong Zhang[1], Wanqing Liang[1], Lei Li[1], Jun Du[1], Chengwu Pan[1], Bangling Chen[1], Yuzhong Chen[1] and Yuanpeng Wang[2]*

[1] Department of Oncological Surgery, The First Affiliated Hospital of Bengbu Medical College, Bengbu, China,
[2] Department of General Surgery, The Second Hospital of Bengbu Medical College, Bengbu, China

OPEN ACCESS

Edited by:
Pankaj Kumar Garg,
Shri Guru Ram Rai Institute of Medical and Health Sciences, India

Reviewed by:
Ibrahim Sallam,
MISR Cancer Center, Egypt
Dharma Ram Poonia,
All India Institute of Medical Sciences Jodhpur, India
Mukurdipi Ray,
All India Institute of Medical Sciences, India

***Correspondence:**
Jiachi Ma
majiachi@bbmc.edu.cn

Specialty section:
This article was submitted to Gastrointestinal Cancers: Gastric Esophageal Cancers, a section of the journal Frontiers in Oncology

Received: *26 October 2021*
Accepted: *18 January 2022*
Published: *17 February 2022*

Citation:
Ma J, Zhang C, Liang W, Li L, Du J, Pan C, Chen B, Chen Y and Wang Y (2022) ω-3 and ω-6 Polyunsaturated Fatty Acids Regulate the Proliferation, Invasion and Angiogenesis of Gastric Cancer Through COX/PGE Signaling Pathway. Front. Oncol. 12:802009. doi: 10.3389/fonc.2022.802009

Background: This study aims to investigate the effects of ω-3, ω-6 polyunsaturated fatty acids (PUFAs), and their middle metabolites prostaglandin (PGE)2 and PGE3 on proliferation, invasion, and angiogenesis formation of gastric cancer cells and to explore associated mechanism.

Methods: RT-PCR and ELISA were used to detect the expression of cyclooxygenase (COX)-1 and COX-2 in gastric cancer cell lines. The effect of ω-3, ω-6, PGE2, and PGE3 on the proliferation, invasion, and angiogenesis of gastric cancer cells were measured by cell proliferation, invasion, and angiogenesis assay *in vitro*. COX-2 small interfering RNA (siRNA) was transfected into gastric cancer cells, and the expression of COX-2 protein was detected by Western blot. COX-2 gene silencing influencing proliferation, invasion, and angiogenesis potential of gastric cancer cells was detected by WST-1, transwell chamber, and angiogenesis assay, respectively.

Results: COX-2 was only expressed in MKN74 and MKN45 cells. In gastric cancer cell lines with positive COX-2 expression, ω-6 and PGE2 could significantly enhance the proliferation, invasion, and angiogenesis of gastric cancer cells, and after transfection with COX-2 siRNA, the effects of ω-6 and PGE2 on enhancing the proliferation, invasion, and angiogenesis of gastric cancer cells were significantly attenuated; ω-3 and PEG3 could inhibit the proliferation, invasion, and angiogenesis of gastric cancer cells. In gastric cancer cell lines with negative COX-2 expression, ω-6 and PGE2 had no significant effect on the proliferation, invasion, and angiogenesis of gastric cancer; ω-3 and PGE3 could significantly inhibit the proliferation, invasion, and angiogenesis of gastric cancer.

Conclusion: ω-6 PUFAs reinforce the metastatic potential of gastric cancer cells *via* COX-2/PGE2; ω-3 PUFAs inhibit the metastatic potential of gastric cancer *via* COX-1/PGE3 signaling axis.

Keywords: ω-3 PUFAs, ω-6 PUFAs, angiogenesis, metastasis, gastric cancer

INTRODUCTION

Gastric cancer is one of the common malignant tumors, with an incidence of 17.6/100,000 worldwide, about 1.1 million new cases per year, accounting for 5.6% of all new cases of malignant tumors and ranking fifth, and it also ranks fourth due to 770,000 deaths it causes (1). The main cause of death in patients with gastric cancer is metastasis; the liver is the most common hematogenous metastatic organ of gastric cancer, and the incidence of liver metastasis in gastric cancer ranges from 17% to 29% (2, 3). Patients with liver metastasis from gastric cancer have a very poor prognosis and a 5-year survival rate of less than 10% (4). Although there are many studies on liver metastasis of gastric cancer, the molecular mechanism of liver metastasis of gastric cancer has not been elucidated so far, and there is no effective treatment in clinical practice. Therefore, it is important to deeply study the mechanism of liver metastasis of gastric cancer and take targeted interventions to improve the survival rate and quality of life of patients with gastric cancer.

Polyunsaturated fatty acids (PUFAs) ω-3 and ω-6 are the main components of cell membrane structure, which also are essential fatty acids for human body. Recent studies have shown that ω-6 PUFAs can promote the occurrence, progression, and metastasis of malignant tumors, while ω-3 PUFAs has anticancer effects. ω-3 and ω-6 PUFAs play an important role in remodeling the microenvironment to regulate tumor metastasis, but the regulated mechanism is still unclear (5). PUFAs are a class of fatty acids containing double bonds on the carbon chain (6), which, in addition to providing energy for the body, are also involved in the composition of cell membrane lipids and are important substances in the regulation of cellular metabolism and cell signaling. PUFAs are classified into ω-3 system, ω-6 system, ω-7 system, and ω-9 system according to the position of the first double bond in the carbon chain as counted from the methyl end (7). Among them, ω-3 and ω-6 PUFAs are the most common PUFAs. The ω-3 and ω-6 PUFAs are the main components of various biofilm structures, which play an indispensable role in maintaining the normal physiological metabolism of the human body and are essential fatty acids in the human body. The ω-3 PUFAs have good immunomodulatory effects and can inhibit local chronic inflammatory responses by regulating the cell microenvironment, stabilizing cell membranes, and regulating cell proliferation and differentiation, which in turn play a role in the prevention and treatment of tumors (8–10). The applicant's previous studies have shown that, PUFAs can affect the invasion, proliferation, and angiogenesis of gastric cancer cells, and the role of PUFAs is closely related to their metabolites prostaglandin (PGE) and cyclooxygenase (COX) on the nuclear membrane of tumor cells *in vivo*, while the expression of PGE and COX is closely related to lymphatic metastasis of gastric cancer (11). The ω-3 and ω-6 PUFAs, as essential fatty acids in the human body, can play a role in inhibiting tumor invasion by reducing ω-6 PUFAs containing foods and appropriately increasing ω-3 PUFAs containing foods in the daily diet (12). COX is an essential enzyme for the synthesis of prostaglandin (PG) and a key rate-limiting enzyme in the initial step of PG synthesis. Cyclooxygenase has two isozymes, COX-1 and COX-2. COX-1 is a structural enzyme that is expressed in most normal tissues, and COX-1 promotes prostaglandin production, thereby maintaining normal human function (13); COX-2 is an inducible enzyme that is rarely expressed in normal tissues, but often highly expressed in tumor cells, such as melanoma, colon cancer, breast cancer, liver cancer, cervical cancer, esophageal cancer, pancreatic cancer, and gastric cancer (14). At present, studies have confirmed that dietary polyunsaturated fatty acid is closely related to the occurrence and metastasis of gastric cancer (15). Among them, ω-6 PUFAs (arachidonic acid) can bind to cyclooxygenase 2 (COX-2) to produce PGE2 and enhance cancer cell invasion; ω-3 PUFAs (eicosapentaenoic acid) can bind to cyclooxygenase 1 (COX-1) to produce PGE3 and inhibit the activity of COX-2, reduce the production of PGE2, and inhibit cancer cell invasion (16).

Currently, there are few studies on the role of ω-3 PUFAs and ω-6 PUFAs in gastric cancer metastasis and their mechanisms. However, the antitumor effect of ω-3 PUFAs and the tumor-promoting effect of ω-6 PUFAs are complex processes involving multiple factors and multiple levels and are interrelated, and there are still many issues to be elucidated. For this reason, this study focused on exploring the mechanism of ω-3 PUFAs, ω-6 PUFAs, and their intermediate metabolites PGE2 and PGE3 on gastric cancer progression and metastasis, elucidating the biological characteristics and mechanism of PUFAs affecting gastric cancer metastasis, exploring the molecular targets affecting gastric cancer metastasis, and providing a theoretical basis and new way for the clinical application of ω-3 and ω-6 PUFAs in the prevention and treatment of gastric cancer.

MATERIALS AND METHODS

Cell Lines and Culture

The cell lines derived from human gastric carcinoma were examined: MKN45, MKN74, and NUGC-4 cell lines were obtained from Japanese Riken Cell Bank (Tsukuba, Japan). All cell lines were maintained in RPMI 1640 (Sigma Chemical Co., St. Louis, MO, USA) added with 10% heat-inactivated fetal bovine serum (FBS). Human umbilical vein endothelial cells (HUVECs) were obtained from Kurabo Co. (Osaka, Japan). HUVECs were maintained in HuMedia-EG2 medium supplemented with 2% FBS, 5 ng/ml basic fibroblast growth factor, 10 μg/ml heparin, 10 ng/ml epidermal growth factor, and 1 μg/ml hydrocortisone according to the supplier's instructions (Kurabo Co.). All cells were incubated at 37°C in a humidified atmosphere of 5% CO_2 in air.

RT-PCR Analysis of COX-1 and COX-2 mRNA Expression

Total RNA was extracted from gastric cancer cell lines by an Isogen Kit (Nippon Gene, Tokyo, Japan), and quantities were determined spectrophotometrically. The 1 μg of total RNA aliquots was reverse-transcribed into cDNA using the SuperScript III system (Invitrogen, San Diego, CA, USA) in a PCR Thermal Cycler (model TP3000; Perkin-Elmer, Norwalk, CT, USA). Reaction mixture aliquots (1 μl) were used as

templates for PCR analysis. Amplification reactions were performed in a DNA Thermal Cycler.

The primer sequences and PCR conditions are shown in **Table 1**. The amplified DNA fragments were resolved by electrophoresis in 1.5% agarose gels containing ethidium bromide.

Enzyme-Linked Immunosorbent Assay for COX-1 and COX-2 Protein Measurement

To determinate the COX-1 and COX-2 protein measurement, HUVECs and cells of the three gastric cancer cell lines (MKN74, MKN45, NUGC-4) were seeded at a density of 2×10^5 cells/ml cells into 12-well plates and cultured overnight, following which the medium in each well was replaced and the cells cultured for a further 48 h. Cell numbers were determined, and the culture media were harvested and microfuged at 1,500 rpm for 15 min to remove the particles. The supernatant liquid were frozen at −80°C until used in ELISA assay. The concentration of COX-1 and COX-2 in supernatants of per 2×10^5/ml cells was measured by ELISA kit (R&D Systems, Minneapolis, MN, USA) according to the manufacturer's instructions.

Design and Synthesis of siRNA and Transfection Into Gastric Cancer Cells

Two specific small interfering RNAs (siRNAs) were designed based on the coding region gene sequence of the human COX-2 gene, and the COX-2 siRNA sequences were 5′-GCCAA GGAGUGC UAAAGAA-3′ and 5′-CCAACACAGAAAUUGU-3′, and the control siRNA sequences were 5′-UUCUCCGAA CGUGUCACGUTT-3′ and 5′-ACGUGACACGU CGGAGA ATT-3′. After counting the two kinds of gastric cancer cells, they were seeded in cell culture dishes with a diameter of 35 mm at a density of 2×10^5 cells/well and cultured overnight, followed by replacement with fresh culture medium containing 10% fetal bovine serum without antibiotics for another 24 h before transfection. A total of 500 μl of Opti-MEM® I-reduced serum medium was used to dilute 200 nmol/L COX-2 siRNA or control siRNA, while 10 μl of LipofectAMINE™2000 was diluted with the same reagent. After standing at room temperature for 5 min, the two were quickly mixed and then allowed to stand at room temperature for 20 min. The mixture of siRNA-Lipofect AMINE™2000 (diluted by adding 1 ml culture medium) at a concentration of 100 pmol/L was then directly added to each cultured cell, followed by mixing well and placing in an incubator at 37°C for transfection. After 48 h of transfection, cells were collected for Western blotting assay to verify the silencing effect of COX-2 gene.

Western Blot Was Used to Detect the Effect of COX-2 Gene Silencing on COX-2 Protein Expression in Gastric Cancer Cells

COX-2-expressing gastric cancer cells at 1×10^6 cells/ml in the logarithmic growth phase were aspirated, the cells were lysed with a cell-lysis buffer, total protein was extracted and centrifuged at 500×*g* for 15 min at 4°C, and then the supernatant was collected to determine the protein concentration using the Bradford method. A total of 30 μg of sample protein was mixed well with an appropriate amount of solid-phase pH gradient strip solution, and electrophoresis was performed using a 10% SDS-PAGE gel for 2 h. The proteins on the gel plate after electrophoresis were transferred to PVDF membranes, followed by blocking with 5% skimmed milk powder for 2 h at room temperature and washing the membranes three times with TBST buffer. The membrane was immersed in blocking solution containing rabbit anti-human COX-2 monoclonal antibody (dilution ratio of 1:800), followed by reaction at room temperature for 2 h and the membrane washing three times with TBST solution; then the membranes were immersed in horseradish peroxidase-labeled goat anti-rabbit or anti-mouse IgG (dilution ratio of 1:2,000) solution, respectively, followed by placement overnight at 4°C, washing three times with TBST buffer, color development by ECL method, and scanning by computer. The gray value of the target band was determined using the image analysis software Image J. The relative expression level of the target protein was expressed as the ratio of the gray value of the target protein and the internal reference protein band, followed by plotting after statistical analysis.

WST-1 Assay Examined the Effects of ω-3 PUFAs, ω-6 PUFAs, PGE2, and PGE3 on Proliferation of Gastric Cancer Cell

Gastric cancer cells expressing and not expressing COX-2 in the logarithmic growth phase were taken, and each group of cells were added to a 96-well culture plate at a density of 1×10^4 cells/100 μl, respectively, with five replicating wells in each group, and the cells were cultured overnight to adhere and grow. The culture medium was replaced, and after another 72 h of culture, 100 μl CellTiter 96 aqueous solution reagent was added to each well and placed in a 37°C incubator for 4 h of reaction, and then the absorbance (*D* value) of the cells in each well at a wavelength of 490 nm was measured with a microplate reader to reflect the proliferation of the cells. The cell growth curve was plotted with time as the abscissa and the average D-ordinate.

TABLE 1 | Primer sequence and PCR condition.

Gene Name	Primer Sequences	Tm (°C)	Cycles	Length (bp)	Accession number
COX-1	F: 5'-CTGGAGGGTGGACTTGTCAT-3' R: 5'-ACATTCTAGGTTGTCGGCCA-3'	58	35	250	NM_001003023
COX-2	F: 5'-GAGAGAAGGAAATGGCTGCG-3' R: 5'-ACACACAGCCAGTCAACGAG-3'	58	35	203	NM_001003354

Transwell Chamber Assay Examined the Effects of ω-3 PUFAs, ω-6 PUFAs, PGE2, and PGE3 on Invasion of Gastric Cancer Cell

The *in vitro* invasion assay was performed using BioCoat Matrigel Invasion Chambers (Becton Dickinson, Bedford, MA, USA) according to the manufacturer's instructions. Briefly, gastric cancer cells expressing and not expressing COX-2 in the logarithmic growth phase were used to adjust the single cell density to 2.0×10^5cells/ml with different culture media containing 5% fetal bovine serum; the cells were seeded into transwell chambers with matrigel at the bottom, and the chambers were placed in 24-well cell culture plates, with 5 replicates for each group of cells. After 12 h of culture, chambers were removed, and cells that did not cross the membrane were wiped off with a cotton swab, rinsed three times with PBS, fixed in 4% formaldehyde solution for 5 min, and stained with Diff-Quick's solution.

Result Interpretation

The number of penetrating cells within five fields was counted separately for each filter membrane under a light microscope (×100), and the average number of cells per field was calculated, in order to reflect the invasive ability of the cells.

ω-3 PUFAs, ω-6 PUFAs, PGE2, and PGE3 Influence Angiogenesis *In Vitro*

HUVECs and human fibroblasts were seeded in a 24-well culture plate in a certain proportion and cultured together. On the second day, the culture medium was replaced and ω-3 PUFAs, ω-6 PUFAs, PGE2, and PGE3 at different concentrations were added, and then a transwell chamber with 0.45 μm microwells was placed in the 24-well culture plate. The bottom of the chamber was covered with polycarbonate membrane and transwell chambers with the wells contained 2×10^4/ml gastric cancer cells to form a coculture system. The culture medium was changed every day, and after 11 days of coculture, the culture medium was removed and the culture wells were washed three times with a PBS solution and fixed with formaldehyde for 30 min, followed by vascular staining with CD31 antibody and then by natural drying. Angiogenesis in 10 different areas was photographed under a microscope and then each photograph was analyzed with vascular analysis software (Kurabo Co.); the total area or length of blood vessels in each photograph was calculated, and the standard amount of new blood vessels was expressed in pixels.

Angiogenic Activity During Cocultivation With Gastric Cancer Cells and Regulation of Polyunsaturated Fatty Acid

To further investigate the effect of different gastric cancer cells on tubule formation by HUVECs. Transfected or nontransfected gastric cancer cells (MKN45 or NUGC-4) were cocultured with HUVECs and fibroblasts using a double chamber method in 24-well plates. MKN45 or NUGC-4 cells (2×10^4 cells/ml) were planted in transwell chambers, consisting of polycarbonate membranes with 0.45 μm pores, and the cells adhere overnight. The transwell chambers were then placed in the HUVEC/fibroblast and coincubated in 24-well plates and the medium exchanged every 2 days. Cells were incubated for 12 days, and HUVEC tubule formation was determined as described above.

Statistical Analysis

Statistical comparisons were made using Student's *t*-test for paired observations or one-way ANOVA with a *post-hoc* test (Dunnett's multiple comparison) for multiple group comparisons. Statistical significance was indicated by $p < 0.05$. Data are presented as mean ± SD. Each experiment was carried out in triplicate.

RESULTS

Expression of COX-1 and COX-2 in Gastric Cancer Cells

COX-1 and COX-2 mRNA levels were determined in all gastric cancer cell lines by RT-PCR. The results showed that all gastric cancer cell lines were expressed as COX-1 mRNA. COX-2 mRNA was detected in MKN45 and MKN74 cells (**Figure 1**). Consistent with RT-PCR observations, COX-1 and COX-2 proteins secreted into cultured liquid supernatant were measured by ELISA. COX-2 proteins are 390.16 ± 22.19 and 423.05 ± 17.73 pg/ml/2×10^5 cells in MKN74- and MKN45-cultured supernatant, respectively, but not detected in NUGC-4 cell-cultured supernatant. The secreted COX-1 protein was determined in the cultured liquid supernatant of MKN45, MKN74, and NUGC-4 cells. The secreted level of COX-1 in MKN74 (560.72 ± 43.09) and MKN45 (623.15 ± 38.59) is higher than NUGC-4 cells (25.93 ± 21.05). MKN74 and MKN45 are respectively compared with control, and *p*-value is less than 0.01 (**Figure 2**).

Effect of COX-2 siRNA Transfection on Secretion of COX-2 Proteins in Gastric Cancer Cells

MKN45 and MKN74 gastric cells were transfected with siRNA, which specifically targets COX-2 genes; the expressions of COX-2 proteins were detected by immunoblotting. The results revealed that COX-2 gene silencing led to a near total loss of COX-2 expression, and compared with the untransfected and control siRNA groups and positive control β-actin, the expressions of COX-2 proteins in MKN45 and MKN74 cancer cells were significantly inhibited (**Figure 3A**). After transfecting MKN45 and MKN74 cells with COX-2 siRNA, significantly inhibited expressions of PGE2 were observed (**Figure 3B**).

Effects of ω-3 PUFAs, ω-6 PUFAs, PGE2, and PGE3 on Gastric Cancer Cell Proliferation

The gastric cancer cell line MKN45 can express COX-2. The cell proliferation curve showed that there was a difference in the proliferation of MKN45 gastric cancer cells following treatment with ω-6 and PGE2 after being cultured for 24 h; the proliferation of MKN45 cells in 0 and 50 μM of ω-6 and PGE3 group was significantly enhanced than those in the

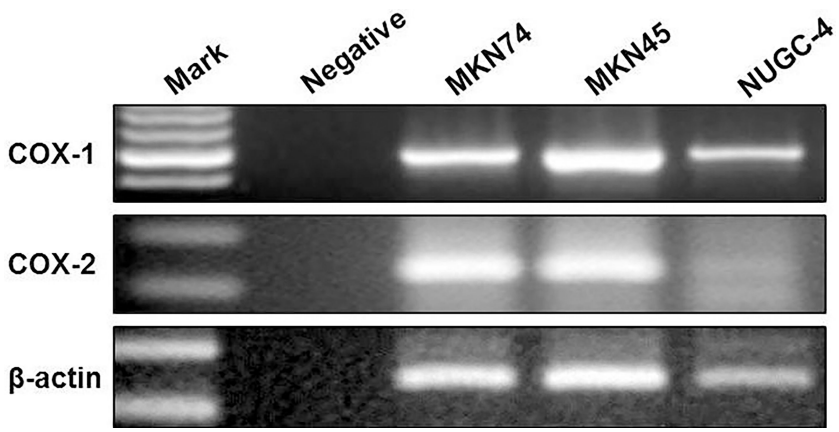

FIGURE 1 | The expression of COX-1 and COX-2 in gastric cancer cells. COX-1 and COX-2 mRNA in gastric cancer cell lines were measured by RT-PCR. PCR products stained with ethidium bromide were displayed at 1.5% agarose gel electrophoresis. β-Actin served as a loading control. The experiments were performed at least thrice.

control groups after 48, 72, 96, and 120 h (*$p < 0.01$, compared with the control groups); meanwhile, the proliferation of MKN45 cells was significantly inhibited by ω-3 and PGE3 in a concentration-dependent manner (compared with the control groups, respectively, *$p < 0.01$, as shown in **Figures 4A, B**). After being transfected with COX-2 siRNA for 24 h, the proliferation of MKN45 cells was measured by WST-1 assay. The results showed that after COX-2 gene silencing, the proliferation of MKN45 cells was significantly inhibited (compared with the control groups, *$p < 0.01$). At the same time, ω-3 and PGE3 could have also inhibited the proliferation of MKN45, but in ω-6 and PGE2, nosignificant change was observed (compared with the COX-2 siRNA groups, *$p < 0.01$, as shown in **Figures 4C, D**). The proliferation of NUGC-4 cells was significantly inhibited by the presence of ω-3 and PGE3. Moreover, there were no significant changes in the presence of ω-6 and PGE2 compared with the control groups, respectively (*$p < 0.01$, **Figures 4E, F**).

Effects of ω-3 PUFAs, ω-6 PUFAs, PGE2, and PGE3 on Gastric Cancer Cell Invasion

The results of transwell invasion assay showed that the COX-2-positive cell MKN45, ω-3, and PGE3 inhibited the invasion of MKN45 cells in a dose-dependent manner, and in ω-6 and PGE2, there was no significant effect on the invasive capability of MKN45 cells (*$p < 0.01$, **Figure 5A**). After transfecting MKN45 cells with COX-2 siRNA, there were no significant changes in the presence of ω-6 and PGE2 in the invasive ability of MKN45. PGE3 and ω-3 could significantly reduce the invasion ability of MKN45 cells compared with the control (*$p < 0.01$, as shown in **Figure 5B**). The invasion of gastric cancer cell NUGC-4 was inhibited by ω-3 and PGE2 in a concentration-dependent manner compared with the control (*$p < 0.01$), and ω-6 and PGE2 cannot significantly influence the invasiveness of NUGC-4 cells (*$p < 0.01$, as shown in **Figure 5C**).

Effect of ω-3 PUFAs, ω-6 PUFAs, PGE2, and PGE3 on HUVEC Tube Formation

To measure the role of ω-3 PUFAs, ω-6 PUFAs, PGE2, and PGE3 in tube formation by HUVECs, we examined the effect of ω-3 PUFAs, ω-6 PUFAs, PGE2, and PGE3 on HUVEC tube formation using an angiogenesis assay. The HUVEC tube formation was significantly promoted in a dose-dependent manner following the presence of ω-6 PUFAs and PGE2 (compared with the control *$p < 0.01$). On the contrary, the HUVEC tube formation was also significantly inhibited by ω-3 PUFAs and PGE3 compared with the control (*$p < 0.01$, **Figure 6A**).

Effect of Gastric Cancer Cells and Presence of ω-3 PUFAs, ω-6 PUFAs, PGE2, and PGE3 on Tube Formation

In order to further pursue the effect of PUFA and its metabolites PGE2 and PGE3 on angiogenesis, focus should be made on the interaction between tumor cell and stromal cell by characterizing the angiogenic activity in cocultured system consisting of HUVECs, fibroblasts, and MKN45 or NUGC-4 gastric cancer cells. HUVEC tube formation was significantly enhanced by coculturing with MKN45 cells compared with NUGC-4 cells (*$p < 0.01$). In MKN45 cocultured system, ω-6 PUFAs and PGE2 significantly promoted the HUVEC tube formation in a dose-dependent manner (compared with MKN45 only, *$p < 0.01$), but this promoted action was inhibited by COX-2 siRNA. Furthermore, the HUVEC tube formation was decreased by ω-6 PUFAs and PGE2 in MKN45 and NUGC-4 cocultured system (compared with the control, *$p < 0.01$, as shown in **Figures 6B, C**). To confirm the specificity of COX-2 siRNA for inhibition of COX-2 in MKN45 cells, we set control siRNA in MKN45 cells as a control. The results showed that ω-6 and PGE2 significantly enhanced angiogenesis, while ω-3 and PGE3 significantly reduced tumor angiogenesis in cocultured system (**Figure 6D**).

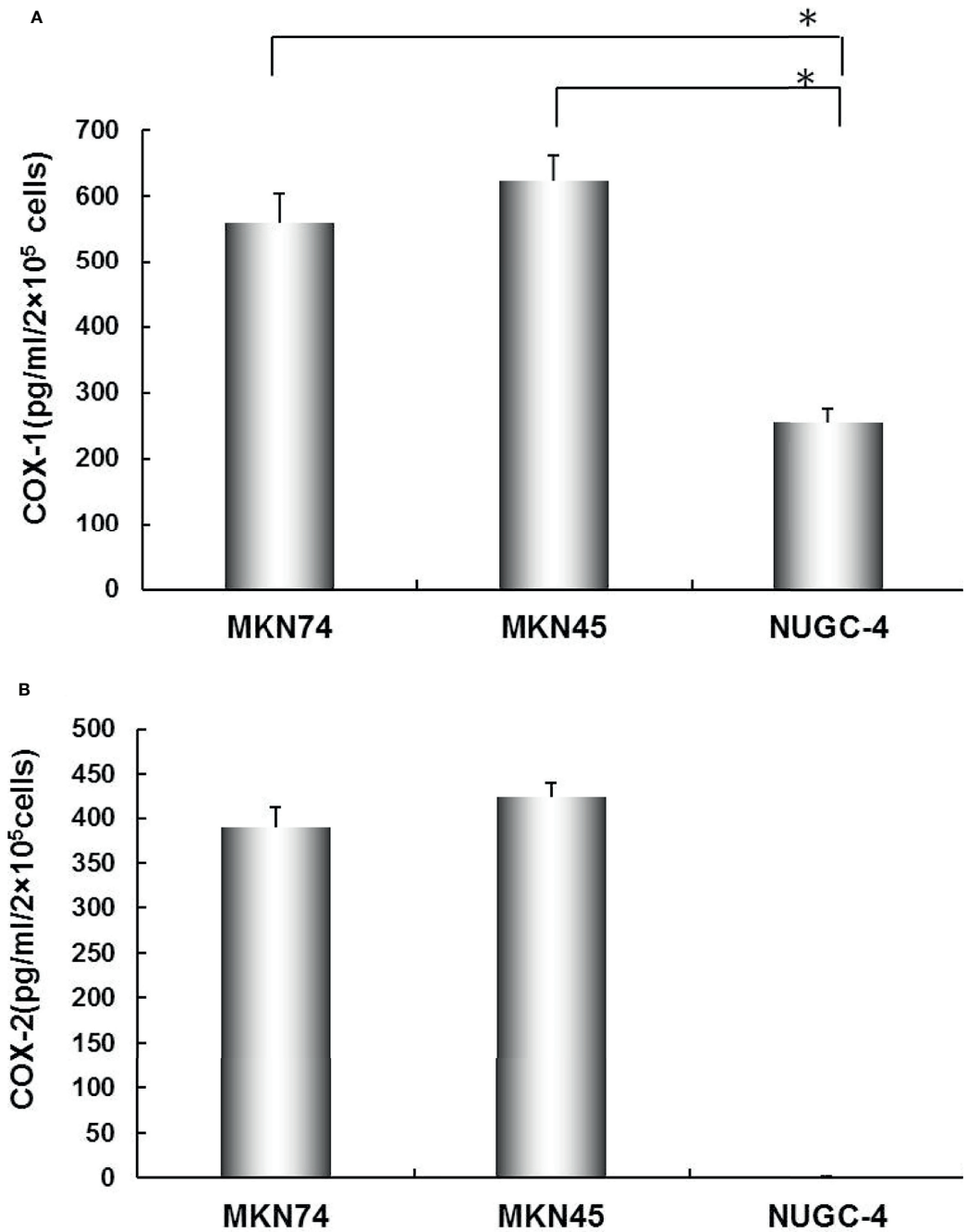

FIGURE 2 | The secreted levels of COX-1 **(A)** and COX-2 **(B)** in gastric cancer cell lines. COX-1 and COX-2 protein concentration in MKN74, MKN45, and NUGC-4 cell culture medium was determined by ELISA. The values are expressed as mean ± SD. Multiple comparisons were analyzed by one-way ANOVA followed by Student-Newman-Keuls test; *$p < 0.01$. This experiment was carried out in triplicate.

DISCUSSION

The ω-3 and ω-6 polyunsaturated fats are the most common polyunsaturated fats. They play an indispensable role in maintaining the normal physiological metabolism of the human body and are essential fatty acids for the human body. ω-3 PUFAs mainly include alpha linolenic acid (ALA) and eicosapentaenoic acid (EPA); ω-6 PUFAs mainly include linoleic acid (LA) and arachidonic acid (AA). The conversion and utilization of ω-3 PUFAs and ω-6 PUFAs in the human body is a complex process. Cyclooxygenase can promote the conversion of AA and EPA into prostaglandin, thromboxane A

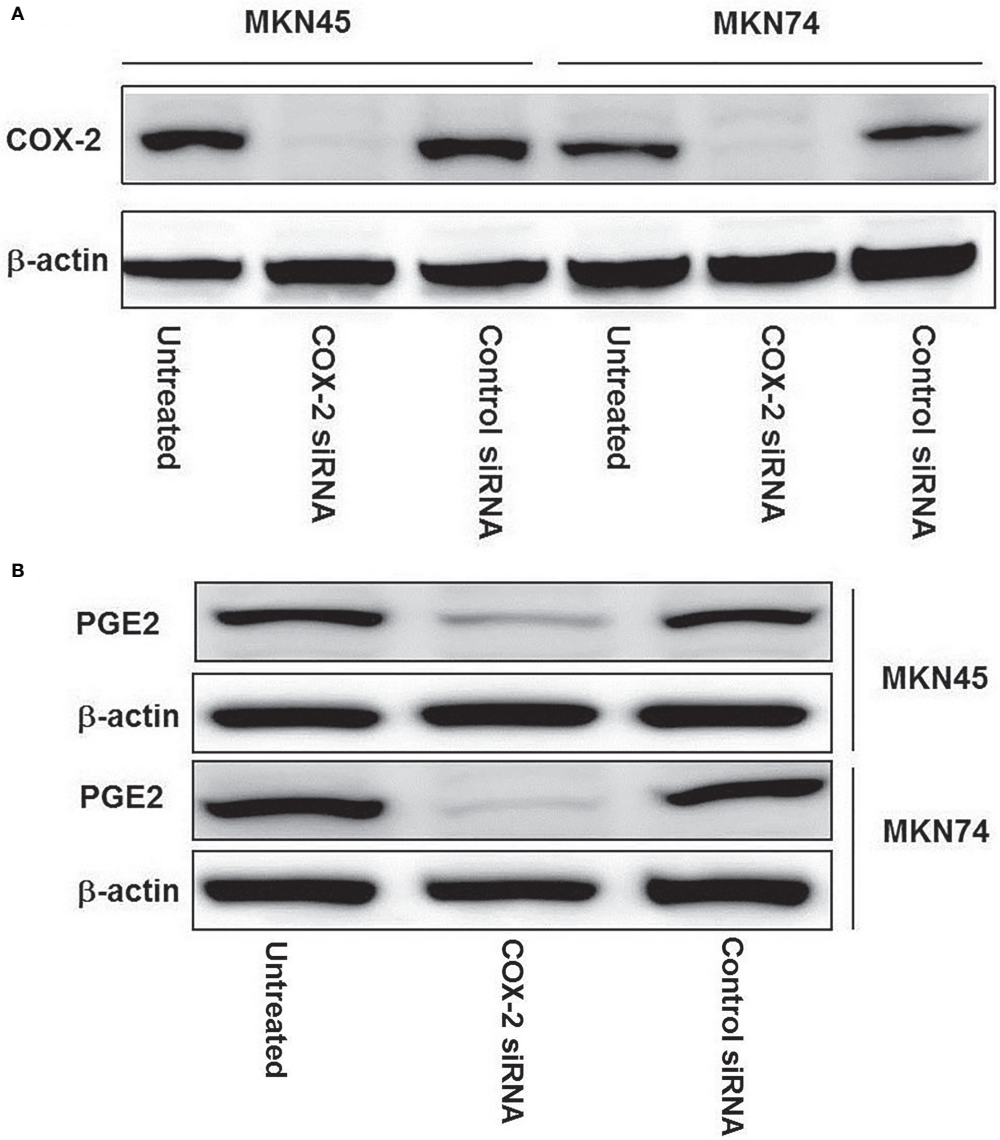

FIGURE 3 | The expression of COX-2 protein in gastric cancer cell line after silencing of CXCL12 gene. Knockdown of COX-2 by COX-2 siRNA was confirmed by immunoblotting in expressed COX-2 gastric cancer cell lines: MKN74 and MKN45. COX-2 siRNA duplex oligoribonucleotides were transfected into cells for 48 h; the proteins were extracted and then subjected to Western blotting **(A)**. After being transfected with COX-2 siRNA in MKN45 and MKN74 cells, a significant inhibited expression of PGE2 was observed **(B)**. The experiments were performed in triplicate.

(TXA), and other products (7). Recent studies have shown that ω-3 PUFAs have an inhibitory effect on the occurrence and progression of malignant tumors, while ω-6 PUFAs have a promoting effect; their mechanism of action may be related to the regulation of cyclooxygenase and prostaglandin synthetase (PGES), the main enzymes in the function and reaction of prostaglandin E3, and prostaglandin E2, and metabolites of ω-3 PUFAs and ω-6 PUFAs (17, 18). ω-6 PUFAs bind to COX-2 in the human body to generate PGE2, while PGE2 can induce cell proliferation and stimulate the expression of BLC-2 protein (BLC-2 protein inhibits apoptosis) to imbalance cell proliferation and apoptosis and promote the occurrence of tumors; PGE2 can also promote extracellular matrix degradation and produce thromboxane to promote platelet aggregation, which is conducive to the invasion and metastasis of cancer cells. While ω-3 PUFAs produce PGE3 after binding to COX-1, PGE3 can inhibit the production of PGE2 and can inhibit phospholipase A2 (PLA2), phosphatidylinositol-specific phospholipase C (PI-PLC), nuclear factor-κB, and COX-2 activities, which in turn reduce the proliferation and invasion

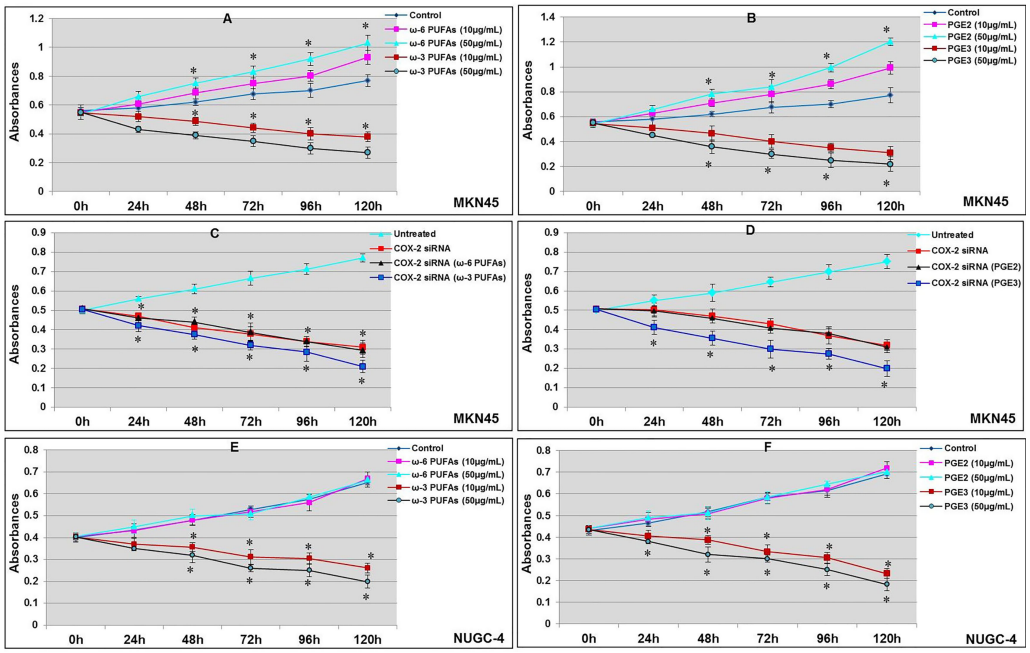

FIGURE 4 | Effects of ω-3 PUFAs, ω-6 PUFAs, PGE2, and PGE3 on proliferation of gastric cancer cell. MKN45 gastric cancer cells incubated for 24 h; the proliferation of cancer cells was measured by WST-1 assay. The proliferation of MKN45 cells in ω-3 PUFA **(A)** and PGE3 **(B)** were significantly inhibited (compared with control groups, $^*p < 0.01$); ω-6 PUFAs **(A)** and PGE2 **(B)** significantly promoted the proliferation (compared with control groups, $^*p < 0.01$). MKN45 cells were transfected with COX-2 siRNA; the proliferation of MKN45 cells were significantly inhibited (compared with control group, $^*p < 0.01$). PGE3 and ω-3 could also inhibit the proliferation of MKN45 (compared with COX-2 siRNA group, $^*p < 0.01$). However, there were no significant changes in ω-6 and PGE2 **(C, D)**. The proliferation of NUGC-4 cells was significantly inhibited by the presence of ω-3 and PGE3. Moreover, there were no significant changes in the presence of ω-6 and PGE2 (compared with the control groups, respectively, $^*p < 0.01$, **E**, **F**). Multiple comparisons used the method of one-way ANOVA and followed by the SNK test. Values are expressed as mean ± SD. Bars indicated SD, $^*p < 0.01$. The experiments were performed at least thrice.

of tumor cells and play a role in inhibiting the growth and metastasis of malignant tumors (8, 12, 19–21). Previously, we retrospectively analyzed the clinical data of 115 patients with radical resection of colorectal cancer and found that the positive rate of prostaglandin E2 expression in colorectal cancer tissues was 87.8%, which was significantly higher than that in normal colorectal mucosal tissues and correlated with the depth of invasion and lymph node and liver metastasis of colorectal cancer; it was positively correlated with the expression of cyclooxygenase 2; the 5-year cumulative survival rate was 63.6% in patients with double-negative PGE2 and COX-2 and 37.8% in patients with double-positive expression (22). Thus, PGE2 and COX-2 downstream of ω-6 PUFAs can be used as important markers for the clinical evaluation of metastasis of colorectal cancer and are important for patient prognosis assessment.

ω-6 PUFAs rely on the catalytic effect of COX-2 to generate PGE2 in the body, which can stimulate the expression of Bcl-2 protein to imbalance cell proliferation and apoptosis and thus promote tumor progression. PGE2 can also enhance the degradation of extracellular matrix, which further promotes the invasion and metastasis of cancer cells (18). ω-6 PUFAs in the microenvironment can upregulate PGE2 production in colorectal cancer cells and promote the transformation of myeloid-inhibiting cells (MDSC) into M2 macrophages (23); hypoxia-inducible factor-1α (HIF-1α) secreted by M2 macrophages promotes tumor invasion and metastasis by inducing the expression of COX-2 and PGE2 in stromal cells and tumor cells in the hypoxic microenvironment (24). HIF-1α derived from M2 macrophages elevates the secretion of CXCR4 in cancer cells to promote colorectal liver metastasis (25). While ω-3 PUFAs produce prostaglandin E3 (PGE3) in response to COX-1, PGE3 inhibits the proliferation and invasion of tumor cells by downregulating the expression of phospholipase A2 phosphatidylinositol-specific phospholipase C (PI-PLC), nuclear factor (NF-κB), and COX-2. PGE3 can also inhibit the metastasis of colorectal cancer by downregulating colorectal cell adhesion factors and the formation of new blood vessels, and ω-3 PUFAs upstream of PGE3 have a potential application value in the treatment of colorectal cancer as a target of antitumor angiogenesis (26, 27).

On the basis of previous studies, this experiment focused on exploring the role of ω-3, ω-6, PGE2, and PGE3 in gastric cancer metastasis, and the results showed that the expression of PGE2 and COX-2 in gastric cancer cell lines was closely related to their liver metastasis, that is, PGE2 and COX-2 were expressed in cell lines MKN45 and MKN74 with high liver metastasis, while PGE3

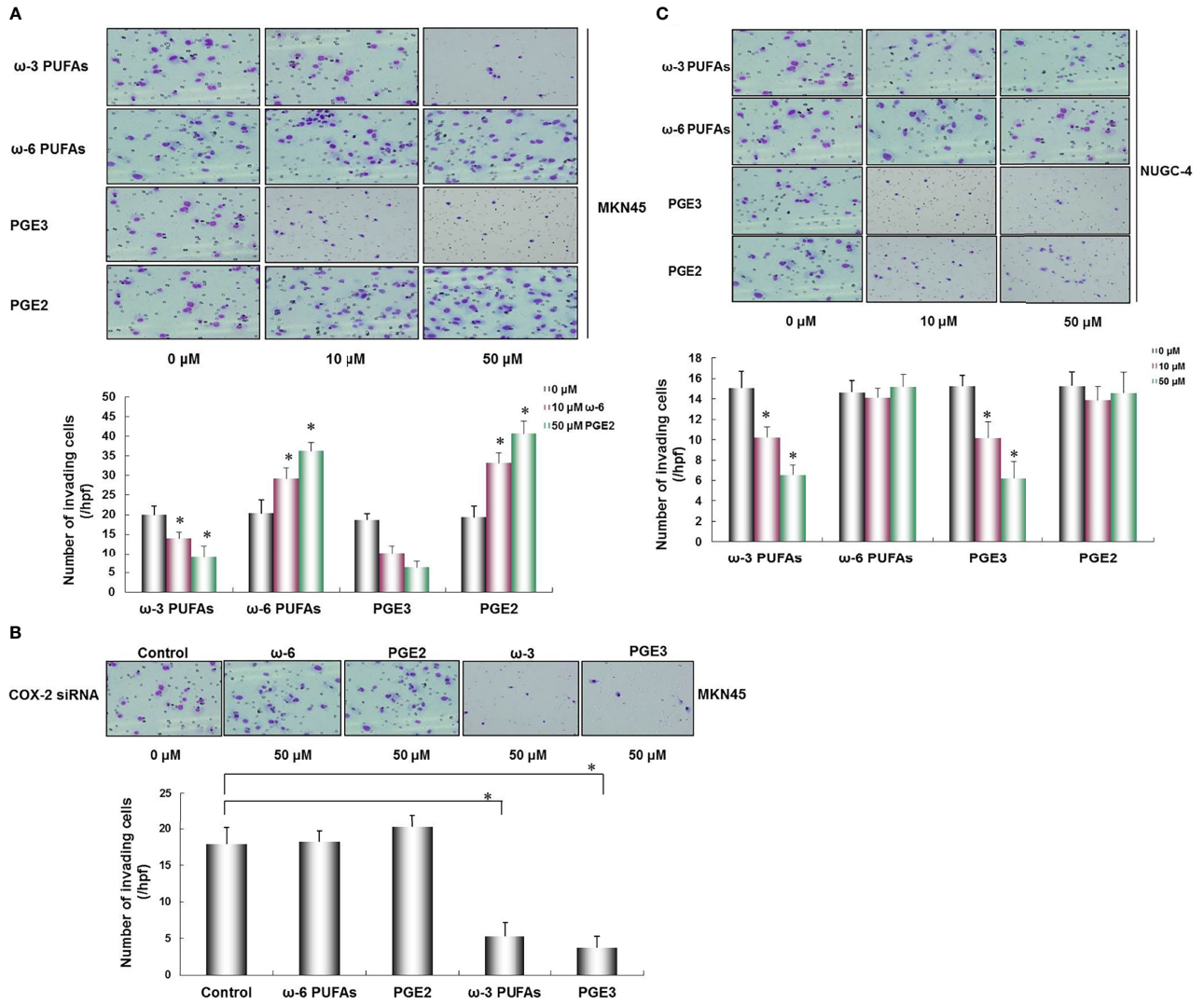

FIGURE 5 | Effects of ω-3 PUFAs, ω-6 PUFAs, PGE2, and PGE3 on gastric cancer cell invasion. PGE3 and ω-3 inhibited the invasion of MKN45 cells, and as for ω-6 and PGE2, there was no significant effect on the invasive ability of MKN45 cells **(A)**. In the MKN45 cells transfected with COX-2 siRNA, no significant changes were found in the presence of ω-6 and PEG2 in MKN45 cells. PGE3 and ω-3 could significantly reduce the invasion capability of MKN45 cells compared with the control **(B)**. The invasion of NUGC-4 cells was inhibited by ω-3 and PGE2 in a concentration-dependent manner compared with the control (*$p < 0.01$) and ω-6 and PGE2 cannot significantly influence the invasiveness of NUGC-4 cells **(C)**. Multiple comparisons used the method of one-way ANOVA followed by the SNK test. Columns, relative invading number. Bars indicate SD, *$p < 0.01$. The experiment was carried out in triplicate.

and COX-1 were expressed in cell lines with high and low liver metastases. The ω-6 PUFAs in the tumor microenvironment is converted into PGE2 that promotes tumor growth by binding to COX-2 in gastric cancer cells, and PGE2 can progressively enhance the proliferation, invasion, and angiogenesis of gastric cancer cells over the increase of concentration. On the one hand, ω-3 PUFAs can inhibit the activity of COX-2 and reduce the production of PGE2, thereby inhibiting the proliferation, invasion, and angiogenesis of tumor cells; on the other hand, ω-3 PUFAs can compete with ω-6 PUFAs to bind to COX-1 to produce PGE3, which can significantly inhibit the proliferation, invasion, and angiogenesis of tumor cells. In addition, after silencing COX-2 gene, ω-6 inhibits the proliferation, invasion, and angiogenesis of gastric cancer cells. In order to detect the effect of unsaturated fatty acids in tumor microenvironment on gastric cancer angiogenesis, we used gastric cancer cells and stromal cells to construct a coculture system to culture angiogenesis *in vitro* and detected the effect of gastric cancer cells with a different expression of COX-2 on angiogenesis. The effect of MKN45 on the angiogenesis of HUVEC in COX-2-positive gastric cancer cells was significantly stronger than that in COX-2-negative gastric cancer cells (NUGC-4); ω-6 PUFAs could promote the angiogenesis of COX-2-positive gastric cancer cells, while ω-3 PUFAs could inhibit the angiogenesis of COX-1-

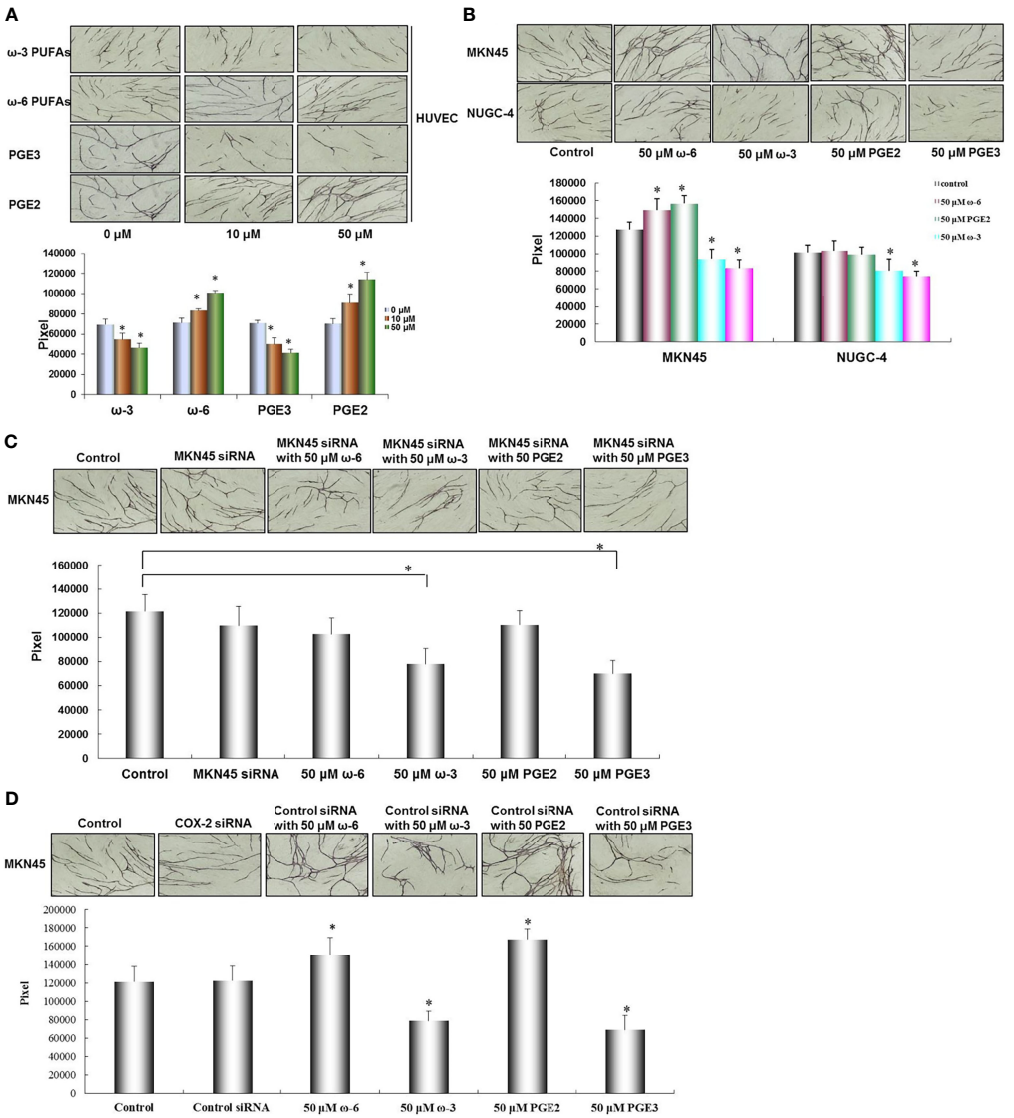

FIGURE 6 | Effect of ω-3, ω-6 PUFAs, PGE2, PGE3, and gastric cancer cells on HUVEC tube formation. HUVEC tube formation was significantly promoted by ω-6 PUFAs and PGE2. On the contrary, HUVEC tube formation was also significantly inhibited by ω-3 PUFAs and PGE3 **(A)**. HUVEC tube formation was significantly enhanced by coculture with MKN45 cells compared with NUGC-4 cells. In MKN45 cocultured system, ω-6 PUFAs and PGE2 significantly promoted HUVEC tube formation, but this promoted action was inhibited by COX-2 siRNA. HUVEC tube formation was decreased by ω-6 PUFAs and PGE2 in MKN45 and NUGC-4 cocultured system **(B, C)**. To confirm the specificity of COX-2 siRNA for inhibition of COX-2 in MKN45 cells, control siRNA was set as a control in the MKN45 cells. The results showed that ω-6 and PGE2 significantly enhanced angiogenesis, while ω-3 and PGE3 significantly reduced tumor angiogenesis in cocultured system **(D)**. Multiple comparisons used the method of one-way ANOVA followed by the SNK test. Bars indicate SD, $^*p < 0.01$. The experiments were performed in triplicate.

positive gastric cancer cells. The above results demonstrated that the effect of ω-3 and ω-6 PUFAs on gastric cancer metastasis was mainly achieved by regulating the physiological functions of COX and PGE. ω-6 enhances the metastatic potential energy of gastric cancer cells by being converted into PGE2 that promotes tumor growth after binding to COX-2; ω-3 can inhibit the activity of COX-2 and reduce the production of PGE2 on the one hand, thereby inhibiting the metastatic potential energy of gastric cancer; on the other hand, ω-3 can compete with ω-6 to bind to COX-1 to produce PGE3 so as to inhibit the metastatic potential energy of gastric cancer. Taking PUFAs and its intermediate metabolites as interference factors, the *in vitro* simulation experiment and exploration experiment of tumor internal environment using a coculture system can more objectively and truly reproduce and observe the effect of PUFAs on the microenvironment of gastric cancer cells, which plays an irreplaceable important role in understanding the specific growth, invasion, and metastasis mechanism of tumor cells, and also plays an important theoretical foundation for the next *in vivo* experiment and clinical trials.

At present, there are a few studies on ω-3 PUFAs, ω-6 PUFAs, PGE2, and PGE3 in gastric cancer, and the mechanism and clinical significance of the effect of polyunsaturated fatty acids on the occurrence, development, and metastasis of gastric cancer remain to be more deeply and comprehensively studied. Through further *in vitro* and *in vivo* experiments at a later stage, our team will find a suitable ratio of two fatty acids or a suitable concentration of COX-2 inhibitor, in order to inhibit the invasion and metastasis of tumor cells, finally providing a new way for clinical prevention and treatment of gastric cancer.

DATA AVAILABILITY STATEMENT

The original contributions presented in the study are included in the article/supplementary material. Further inquiries can be directed to the corresponding author.

AUTHOR CONTRIBUTIONS

JM, CZ, and WL designed the project. JM and CZ wrote the manuscript. LL, JD, and CP finished **Figures 1**, **2**. BC finished **Figure 3**. YC finished **Figure 4**. JM and YW finished **Figures 5**, **6**. All authors reviewed the manuscript. All authors listed have made a substantial, direct, and intellectual contribution to the work and approved it for publication.

FUNDING

This work was supported by Grants from the Natural and Science Foundation of China (Grant No. 81260325), Key Natural Science Research Projects in Universities of Anhui Province (Grant No. KJ2019A0396), and Bengbu Medical College Gastric Cancer Multidisciplinary Diagnosis and Treatment Innovation Team Project (Grant No. BYKC 201907).

REFERENCES

1. Sung H, Ferlay J, Siegel RL, Laversanne M, Soerjomataram I, Jemal A, et al. Global Cancer Statistics 2020: GLOBOCAN Estimates of Incidence and Mortality Worldwide for 36 Cancers in 185 Countries. *CA Cancer J Clin* (2021) 71(3):209–49. doi: 10.3322/caac.21660
2. Li SC, Lee CH, Hung CL, Wu JC, Chen JH. Surgical Resection of Metachro-Nous Hepatic Metastases From Gastric Cancer Improves Long-Termsurvival: A Population-Based Study. *PloS One* (2017) 12(7):e0182255. doi: 10.1371/journal.pone.0182255
3. Qiu JL, Deng MG, Li W, Zou RH, Li BK, Zheng Y, et al. Hepatic Resection for Synchronous Hepatic Metastasis From Gastric Cancer. *Eur J Surg Oncol* (2013) 39(7):694–700. doi: 10.1016/j.ejso.2013.03.006
4. Kakeji Y, Morita M, Maehara Y. Strategies for Treating Liver Metastasis from Gastric Cancer. *Surg Today* (2010) 40(4):287–94. doi: 10.1007/s00595-009-4152-0
5. Huerta-Yépez S, Tirado-Rodriguez AB, Hankinson O. Role of Diets Rich in Omega-3 and Omega-6 in the Development of Cancer. *Bol Med Hosp Infant Mex* (2016) 73(6):446–56. doi: 10.1016/j.bmhimx.2016.11.001
6. Hidaka A, Shimazu T, Sawada N, Hidaka A, Shimazu T, Sawada N, et al. Fish, N-3 PUFA Consumption, and Pancreatic Cancer Risk in Japanese: A Large, Population-Based, Prospective Cohort Study. *Am J Clin Nutr* (2015) 102 (6):1490–7. doi: 10.3945/ajcn.115.113597
7. Elsherbiny ME, Chen H, Emara M, Godbout R. Omega-3 and Omega-6 Fatty Acids Modulate Conventional and Atypical Protein Kinase C Activities in a Brain Fatty Acid Binding Protein Dependent Manner in Glioblastoma Multiforme. *Nutrients* (2018) 10(4):454. doi: 10.3390/nu10040454
8. Abel S, Riedel S, Gelderblom WC. Dietary PUFA and Cancer. *Proc Nutr Soc* (2014) 73(3):361–8. doi: 10.1017/S0029665114000585
9. Hofmanova J, Vaculova A, Kozubik A. Polyunsaturated Fatty Acids Sensitize Human Colon Adenocarcinoma HT-29 Cells to Death Receptor Mediated Apoptosis. *Cancer Lett* (2005) 218(1):33–41. doi: 10.1016/j.canlet.2004.07.038
10. Otto C, Kaemmerer U, Iller B, Muehling B, Pfetzer N, Wittig R, et al. Growth of Human Gastric Cancer Cells in Nude Mice Is Delayed by a Ketogenic Diet Supplemented With Omega-3 Fat Ty Acids an D Medium-Chain Triglycerides. *BMC Cancer* (2008) 8:122–34. doi: 10.1186/1471-2407-8-122
11. Ma J, Ma Y, Guo T, Chen Q, Li Y, Su H, et al. Effect of Polyunsaturated Fatty Acids ω-3 and ω-6 on Angiogenesis Formation in Human Gastric Cancer. *Zhonghua Wei Chang Wai Ke Za Zhi* (2017) 20(1):84–9.
12. Hanson S, Thorpe G, Winstanley L, Abdelhamid AS, Hooper LPUFAH group. Omega-3, Omega-6 and Total Dietary Polyunsaturated Fat on Cancer Incidence: Systematic Review and Meta-Analysis of Randomised Trials. *Br J Cancer* (2020) 122(8):1260–70. doi: 10.1038/s41416-020-0761-6
13. Ye Y, Wang X, Jeschke U, von Schönfeldt V. COX-2-PGE2-EPs in Gynecological Cancers. *Arch Gynecol Obstet* (2020) 301(6):1365–75. doi: 10.1007/s00404-020-05559-6
14. Hashemi Goradel N, Najafi M, Salehi E, Farhood B, Mortezaee K. Cyclooxygenase-2 in Cancer: A Review. *J Cell Physiol* (2019) 234(5):5683–99. doi: 10.1002/jcp.27411
15. Lee JY, Nam M, Son HY, Hyun K, Jang SY, Kim JW, et al. Polyunsaturated Fatty Acid Biosynthesis Pathway Determines Ferroptosis Sensitivity in Gastric Cancer. *Proc Natl Acad Sci USA* (2020) 117(51):32433–42. doi: 10.1073/pnas.2006828117
16. de Bus I, Zuilhof H, Witkamp R, Balvers M, Albada B. Novel COX-2 Products of *N*-3polyunsaturated Fatty Acid-Ethanolamine-Conjugates Identified in RAW264. *7 Macrophages J Lipid Res* (2019) 60(11):1829–40. doi: 10.1194/jlr.M094235
17. Bonafini S, Giontella A, Tagetti A, Marcon D, Montagnana M, Benati M, et al. Possible Role of CYP450 Generated Omega-3/Omega-6 PUFA Metabolites in the Modulation of Blood Pressure and Vascular Function in Obese Children. *Nutrients* (2018) 10(11):1689. doi: 10.3390/nu10111689
18. Araujo P, Belghit I, Aarsæther N, Espe M, Lucena E, Holen E. The Effect of Omega-3 and Omega-6 Polyunsaturated Fatty Acids Onthe Production of Cyclooxygenase and Lipoxygenase Metabolites by Human Umbilical Vein Endothelial Cells. *Nutrients* (2019) 11(5):966. doi: 10.3390/nu11050966
19. Han YM, Jeong M, Park JM. The Omega-3 Polyunsaturated Fatty Acids Prevented Colitis-Associated Carcinogenesis Through Blocking Dissociation of Beta-Catenin Complex, Inhibiting COX-2 Through Repressing NF-Kappa B, and Inducing 15-Prostaglandin Dehydrogenase. *Oncotarget* (2016) 7 (39):63583–95. doi: 10.18632/oncotarget.11544
20. Han YM, Park JM, Cha JY. Endogenous Conversion of Omega-6 to Omega-3 Poly Unsaturated Fatty Acids in Fat-1 Mice Attenuated Intestinal Polyposis by Either Inhibiting COX-2/Beta-Catenin Signaling or Activating 15-PGDH/IL-18. *Int J Cancer* (2016) 138(9):2247–56. doi: 10.1002/ijc.29956
21. Defago MD, Perovic NR, Valentich MA, Repossi G, Actis AB. Omega-3 and Omega-6 Salivary Fatty Acids as Markers of Dietary Fat Quality: A Cross-Sectional Study in Argentina. *Acta Odontol Latinoam* (2018) 31(2):97–103. doi: 10.18632/oncotarget.11544
22. Ma JC, Zhao XD, Qi JB, Guo QJ, Chen XC. Expression of PGE2 and COX-2 in Colorectal Cancer and the Clinical Significance. *Chin J Gen Surg* (2018) 33 (4):322–5. doi: 10.1002/ijc.29956
23. Yan G, Zhao H, Zhang Q, Zhou Y, Wu L, Lei J, et al. A RIPK3-PGE2 Circuit Mediates Myeloid-Derived Suppressor Cell-Potentiated Colorectal Carcinogenesis. *Cancer Res* (2018) 78(19):5586–99. doi: 10.1158/0008-5472.CAN-17-3962
24. Saha J, Sarkar D, Pramanik A, Mahanti K, Adhikary A, Bhattacharyya S. PGE2-Hif1α Reciprocal Induction Regulates Migration, Phenotypic Alteration and Immunosuppressive Capacity of Macrophages in Tumor Microenvironment. *Life Sci* (2020) 253:117731. doi: 10.1016/j.lfs.2020.117731
25. Romain B, Hachet-Haas M, Rohr S, Brigand C, Galzi JL, Gaub MP, et al. Hypoxia Differentially Regulated CXCR4 and CXCR7 Signaling in Colon Cancer. *Mol Cancer* (2014) 13:58. doi: 10.1186/1476-4598-13-58

26. Liang P, Henning SM, Guan J, Grogan T, Elashoff D, Cohen P, et al. Effect of Dietary Omega-3 Fatty Acids on Castrate-Resistant Prostate Cancer and Tumor-Associated Macrophages. *Prostate Cancer Prostatic Dis* (2020) 23 (1):127– 135. doi: 10.1038/s41391-019-0168-8
27. Calviello G, Di Nicuolo F, Gragnoli S, Piccioni E, Serini S, Maggiano N, et al. N-3 PUFAs Reduce VEGF Expression in Human Colon Cancer Cells Modulating the COX-2/PGE2 Induced ERK-1 and -2 and HIF-1alpha Induction Pathway. *Carcinogenesis* (2004) 25(12):2303–10. doi: 10.1093/carcin/bgh265

Conflict of Interest: The authors declare that the research was conducted in the absence of any commercial or financial relationships that could be construed as a potential conflict of interest.

Publisher's Note: All claims expressed in this article are solely those of the authors and do not necessarily represent those of their affiliated organizations, or those of the publisher, the editors and the reviewers. Any product that may be evaluated in this article, or claim that may be made by its manufacturer, is not guaranteed or endorsed by the publisher.

Copyright © 2022 Ma, Zhang, Liang, Li, Du, Pan, Chen, Chen and Wang. This is an open-access article distributed under the terms of the Creative Commons Attribution License (CC BY). The use, distribution or reproduction in other forums is permitted, provided the original author(s) and the copyright owner(s) are credited and that the original publication in this journal is cited, in accordance with accepted academic practice. No use, distribution or reproduction is permitted which does not comply with these terms.

frontiers in Oncology

METHODS
published: 28 February 2022
doi: 10.3389/fonc.2022.802683

Comparison of the Efficacy of D2 Gastrectomy Plus Liver Radiofrequency Combined With Chemotherapy Versus Chemotherapy Alone in the Treatment of Advanced Gastric Cancer With Unresectable Synchronous Liver Metastases: A Multicenter Randomized Controlled Trial Protocol

Weidong Wang, Ruiqi Gao, Pengfei Yu, Zhenchang Mo, Danhong Dong, Xisheng Yang, Xiaohua Li and Gang Ji**

Department of Digestive Surgery, Xijing Hospital, Air Force Military Medical University, Xi'an, China

Background: Whether patients with advanced gastric cancer with unresectable synchronous liver metastases require surgical treatment remains a controversial topic among surgeons. Recently, an open-label multicenter, international RCT study show that compared with chemotherapy alone, gastric resection combined with chemotherapy had no survival advantage for advanced gastric cancer with unresectable synchronous liver metastases. A limitation of this study was that gastrectomy for gastric cancers was restricted to D1 lymphadenectomy and no metastatic lesions were removed. Whether D2 gastrectomy plus liver radiofrequency plus postoperative chemotherapy could provide benefits to these patients is worthy of further confirmation by high-level evidence-based medicine.

Methods/Design: This study will investigate the efficacy of D2 gastrectomy plus liver radiofrequency plus postoperative chemotherapy compared to chemotherapy alone in a prospective, multicenter, randomized controlled trial that will enroll 200 patients who have advanced gastric cancer with unresectable synchronous liver metastases. The patients will be randomly divided into two groups: the test group (D2 gastrectomy plus liver radiofrequency plus postoperative chemotherapy, n=100) and the control group (chemotherapy alone, n=100). The patients' general information, past medical history, laboratory tests, imaging results, surgery details, and chemotherapy details will be recorded and analysed. The overall survival (OS) will be recorded as primary endpoints.

OPEN ACCESS

Edited by:
Pankaj Kumar Garg, Shri Guru Ram Rai Institute of Medical and Health Sciences, India

Reviewed by:
Ramses Aguilera, Civil Hospital of Guadalajara, Mexico
Andrea Cossu, San Raffaele Hospital (IRCCS), Italy
Rahul Kumar, All India Institute of Medical Sciences, Rishikesh, India

***Correspondence:**
Xiaohua Li
xjyylixiaohua@163.com
Gang Ji
Jigang@fmmu.edu.cn

Specialty section:
This article was submitted to Gastrointestinal Cancers: Gastric and Esophageal Cancers, a section of the journal Frontiers in Oncology

Received: *27 October 2021*
Accepted: *09 February 2022*
Published: *28 February 2022*

Citation:
Wang W, Gao R, Yu P, Mo Z, Dong D, Yang X, Li X and Ji G (2022) Comparison of the Efficacy of D2 Gastrectomy Plus Liver Radiofrequency Combined With Chemotherapy Versus Chemotherapy Alone in the Treatment of Advanced Gastric Cancer With Unresectable Synchronous Liver Metastases: A Multicenter Randomized Controlled Trial Protocol. Front. Oncol. 12:802683. doi: 10.3389/fonc.2022.802683

Progression-free survival (PFS) and the total incidence of complications will be recorded as secondary endpoints.

Discussion: This study is to establish a multicentre randomized controlled trial to compare the efficacy of D2 gastrectomy plus liver radiofrequency combined with postoperative chemotherapy versus chemotherapy alone.

Trial Registration: Chinese Clinical Trial Registry, Approved No. of ethics committee: ChiECRCT20200331. Registered on 15 November 2020. Registration number: ChiCTR2000039964. The study has received full ethical and institutional approval.

Advantages and Limitations of this Study: This is the first clinical trial that will provide evidence on the efficacy of D2 gastrectomy plus liver radiofrequency combined with chemotherapy versus chemotherapy alone for the treatment of advanced gastric cancer with unresectable synchronous liver metastases. A prospective RCT with 200 patients who have advanced gastric cancer with unresectable synchronous liver metastases.

Clinical Trial Registration: [https://www.chictr.org.cn/], identifier ChiCTR2000039964.

Keywords: gastric cancer, synchronous liver metastasis, chemotherapy, radiofrequency, protocol

BACKGROUND

Gastric cancer (GC) ranks fifth in incidence and third in mortality among all cancers worldwide each year (1). Synchronous liver metastasis occurs in 3%-14% of GC patients and has a very poor prognosis (2, 3). Currently, chemotherapy is recommended as the standard treatment for advanced gastric cancer with unresectable synchronous liver metastasis (GCLM) by Japanese, American, and international guidelines (4, 5). Although the therapeutic effect has been improved to a certain extent due to the continuous improvement in chemotherapy in the past decade, patients with GCLM have a poor prognosis under this treatment (6, 7). Therefore, there is an urgent need for a new therapeutic strategy to improve survival and prognosis in patients with GCLM.

Previous studies (8–10) showed that palliative gastrectomy combined with chemotherapy could improve the survival of patients with GCLM. However, a recent multicenter randomized controlled study (11) published in Lancet Oncology reported that gastrectomy plus chemotherapy did not provide a survival advantage in the treatment of GCLM compared with chemotherapy alone. However, the method of GC surgery in this study was D1 lymphadenectomy in gastrectomy for primary gastric tumors, which was performed in patients who received chemotherapy after gastrectomy. The surgical methods used in our study will be D2 lymphadenectomy in gastrectomy for primary gastric tumors, a more thorough dissection for the possible occurrence of lymph node metastasis in patients with GC.

Most of the current clinical studies are retrospective cohort studies (12, 13), so the current evidence is not sufficient to support a treatment strategy of D2 gastrectomy plus liver radiofrequency plus postoperative chemotherapy for standardized treatment of patients with GCLM. At the same time, there is also a lack of prospective studies on the efficacy of D2 gastrectomy plus liver radiofrequency plus postoperative chemotherapy versus chemotherapy alone for treatment in China. If the results obtained in this study are in line with our expectations, this study will supplement the existing deficiency of treatment regimens for GCLM, which is of great significance for improving the prognosis of patients with GCLM in clinical practice, and even for the development of a new, more feasible and effective standardized treatment strategy for patients with GCLM.

METHODS/DESIGN

This study will be a multicenter RCT in which 200 patients will be enrolled from November 2020 to November 2022. They will be randomly designated to the test group or the control group in a 1:1 distribution ratio. The test flow chart is shown in **Figure 1**.

Main Objective

According to the process shown in **Figure 1**, 200 patients with GCLM will be grouped to explore a comparison of the OS of D2 gastrectomy plus liver radiofrequency plus postoperative chemotherapy versus chemotherapy alone.

Secondary Objectives

- To compare the PFS of patients in the treatment of D2 gastrectomy plus liver radiofrequency plus postoperative chemotherapy to those treated with chemotherapy alone

Abbreviations: GC, gastric cancer; GCLM, advanced gastric cancer with unresectable synchronous liver metastasis; RCT, randomized controlled study; WHO, World Health Organization; CRF, Case Report Form; EMR, endoscopic mucosal resection; PS, performance status; RFA, radiofrequency ablation; PFS, progression-free survival; OS, overall survival.

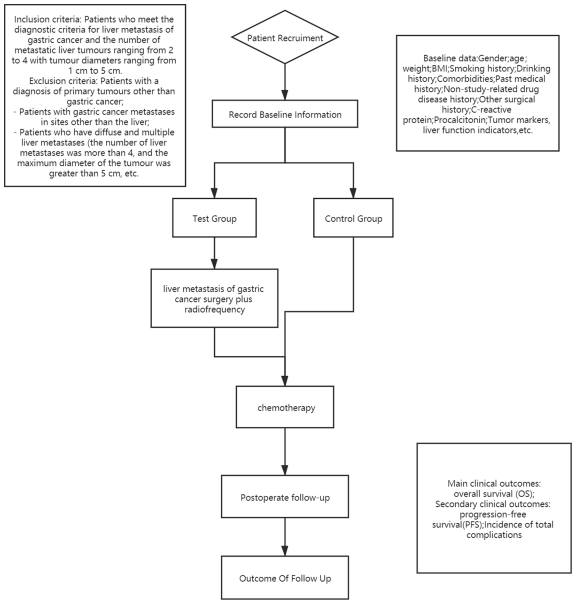

FIGURE 1 | This is the whole flow diagram of the test.

- To explore a comparison of the total incidence of complications of D2 gastrectomy plus liver radiofrequency plus postoperative chemotherapy to those of chemotherapy alone

Patient Recruitment and Characteristics

The recruitment method will be to collect patients during routine procedures who were screened by investigators against the exclusion criteria. The researchers will have them sign the informed consent form. The above procedures conform to the provisions of the Measures for Ethical Review of Biomedical Research Involving Human Beings (Trial), the Declaration of Helsinki v.08 and the International Ethical Guidelines for Biomedical Research Involving Human Beings.

Inclusion Criteria

Patients will be included when they meet all of the following conditions:

- Patients who are male or female, aged 20 to 75 years;
- Patients who were diagnosed histologically with primary gastric adenocarcinoma;
- Patients diagnosed with clinical T1–3 disease by laparotomy or laparoscopy (for T1-T3 patients with the node positive, in order to eliminate the inter group differences, they were randomly divided into control group or experimental group according to the clinical nodal status (further subgroup: N0–1 vs N2–3). For patients with para-aortic lymph node metastasis above the coeliac axis or below the inferior mesenteric artery (lymph node 16a1/b2 of maximum diameter ≥1 cm), or both, or T4 patients with the node positive, according to the NCCN diagnosis and treatment guidelines for gastric cancer and the recommendations of our multidisciplinary diagnosis and treatment team, neoadjuvant therapy was first chosen) (11);
- Patients who will undergo diagnostic laparoscopic exploration combined with peritoneal lavage cytology to exclude peritoneal disseminated implant metastasis that is not visible to the naked eye (14);
- Patients who will be examined for the molecular profile of the tumors (HER2, PDL1, MSI and MMR expression) [patients with HER2-positive advanced gastric cancer were excluded since trastuzumab in combination with chemotherapy has become the standard treatment for these patients (15)];
- Patients with distant metastases that were limited to synchronous liver metastases confirmed by both laparotomy and CT scan;
- Patients with metastatic liver tumor ranging from 2 to 4 with tumor diameters ranging from 1 cm to 5 cm (11) (In order to avoid the omission of potential liver metastases, we used contrast-enhanced liver ultrasound as one of the means of further screening. Considered that unless data are now available from ongoing trials, ablation for resectable liver metastasis lesions should not be used in radiofrequency of liver resection. We recommend all patients to multidisciplinary tumor boards to determine whether the liver metastasis is actually unresectable);
- Patients whose PS (performance status) was from 0 to 1;
- Patients who have not previously been treated for gastric cancer other than EMR;
- Patients who have not previously received radiation therapy or chemotherapy for any other malignancy;
- Patients who have no contraindications to treatment (surgery, radiofrequency ablation, and chemotherapy);
- Patients and their families voluntarily participated in the study and signed the informed consent form.

Exclusion Criteria

Patients will be excluded when they meet any of the following conditions:

- Patients with a diagnosis of primary tumors other than gastric cancer;
- Patients who have gastric cancer metastases in sites other than the liver;
- Patients who have coagulation dysfunction that cannot be corrected;
- Patients with viral hepatitis and cirrhosis;
- Patients with diabetes mellitus, uncontrolled or controlled with insulin;
- Patients treated with systemic steroids;
- Patients suffering from psychosis;
- Patients with heart, lung, liver, brain, kidney or other organ failure;
- Patients who have ascites and cachexia preoperatively, and their general conditions are poor;

- Patients who refuse to sign the informed consent to take part in this study;
- Female patients who are during pregnancy or breast-feeding (except for those women who are breast feeding but consenting to surgery and chemotherapy).

Terminating Study Criteria

The terminating study criteria are as follows:

- Patients are unable to undergo surgery for various reasons after enrollment (reasons need to be recorded);
- The researchers consider that the patients are not suitable to continue the clinical trial (the reason for withdrawal should be recorded);
- Patients with serious complications or unbearable adverse reactions;
- Patients request that the trial be terminated;
- Patients violated the treatment principles (violation of injection and discharge standards, disobedience to the study chemotherapy arrangement, etc.)

We will terminate the study for individual patients once they meet the termination criteria and their data will not be included in the final analysis. Other patients who meet the criteria for admission but do not meet the criteria for termination will continue to participate in our study.

Participating Entities

This clinical trial is a multicenter study. The institutions are as follows: the First Affiliated Hospital of Air Force Military Medical University, The Second Affiliated Hospital of Air Force Medical University, The First Affiliated Hospital of Xi'an Jiaotong University, Zhongshan Hospital Affiliated to Fudan University and West China Hospital of Sichuan University. The above institutions all have sufficient experience in the diagnosis and treatment of gastrointestinal tumors.

Randomization Procedure

Eligible participants will be randomly designated to either the test group or the control group in a 1:1 distribution ratio. First, all enrolled patients were tested the molecular profile of the tumors, such as HER2, PDL1, MSI and MMR expression. And after the patient underwent molecular profile testing, patients with HER2-positive advanced gastric cancer were excluded since trastuzumab in combination with chemotherapy has become the standard treatment for these patients. For the rest of the other patients, follow up treatment protocols could be adjusted according to the patients' molecular profile, such as immunotherapeutic antibody PD-1 or PD-L1, and so on. Accordingly, in the statistical analysis of data, different patients also need to conduct subgroup hierarchical analysis according to the molecular detection results of tumors to reduce data error. Biostatisticians not involved in this study will use SAS software 9.2 (SAS Institute, Cary, NC, USA) to generate random sequences. A research assistant not participating in the recruitment process will seal the random list in sequentially numbered nontransparent envelopes stored in a cabinet that is double-locked. The research assistant will store the randomly assigned envelopes separately. Data collection and data analysis will be blinded, except that the intervention is not blinded to participants and clinicians (16).

Treatment Protocols

All eligible patients will be randomly divided into a test group or a control group according to a 1:1 distribution ratio. The test group will receive D2 gastrectomy plus liver radiofrequency plus postoperative chemotherapy. In the test group, only open surgery is allowed. The control group will receive chemotherapy alone. The chemotherapy regimens of the two groups are the same (11), S-1 plus cisplatin. S-1 will be given orally 80-120 mg/m^2 per day for the first 3 weeks of every 5-week cycle. The dose of S-1 will be given according to the patients' body surface area (less than 1.25 m^2, 80 mg; 1.25–1.5 m^2, 100 mg; and greater than 1.5 m^2, 120 mg). Patients will receive cisplatin 60 mg/m^2 on Day 8 of every 5-week cycle *via* intravenous infusion. **Table 1** shows the treatments applied in this study. **Table 2** shows the medication and usage in this experiment. Because all enrolled patients are tested for the molecular profile of the tumors, such as HER2, PDL1, MSI and MMR expression, follow up treatment protocols could be adjusted according to the patients' molecular profile, such as trastuzumab or immunotherapeutic antibody. Accordingly, in the statistical analysis of data, different patients also require conduct subgroup hierarchical analysis according to the molecular detection results of tumors to reduce data error.

Clinical Data

Clinical data from the patients will be obtained by medical staff and recorded on an online electronic platform (http://www.medresman.org.cn) and in the CRF table. The samples will be coded, and the patients' identity will be known only by the attending physician. The clinical data will include the following: general patient information, past medical history, past surgical history, laboratory examination results, imaging results, surgery details, PFS and OS. The timing and processing of the above recorded contents will be reflected in the CRF table, and the laboratory examinations will mainly assess preoperative and

TABLE 1 | The treatments applied in this study.

	gastrectomy (total gastrectomy, distal or proximal gastrectomy plus D2 lymph node dissection)	liver radiofrequency	chemotherapy (S-1 + cisplatin)
test group	√	√	√
control group	—	—	√

TABLE 2 | The medication and usage in this experiment.

Chemotherapy drugs	dose	Timing of the drugs (a total of 35 days/cycle)			
		Day 1-7/cycle	Day 8/cycle	Day 9-21/cycle	Day 22-35/cycle
S-1	80-120 mg/m² (oral)	√	√	√	—
cisplatin	60 mg/m² (intravenous infusion)	—	√	—	—

postoperative routine blood, liver function, tumor markers, and inflammatory indicators. The prognosis of GC with liver metastasis (GCLM) was very poor, with a 5-year survival rate of <10% (17). Patients will be assessed at least monthly from baseline for adverse events *via* verbal interview, physical examination, and blood tests, including a complete blood cell count and assessments of liver and renal function, until disease progression. Abdominal CT and measurements of tumor markers, such as carcinoembryonic antigen, carbohydrate antigen 199, carbohydrate antigen 125, carbohydrate antigen 153 and alpha fetoprotein, were done every 3 months.

A detailed description of the above data is shown in the CRF table. **Table 3** shows the test and data acquisition schedule for this experiment.

Collection and Storage Management of Biochemical Specimens

For this study, blood samples, tissue samples of GC, and tissue samples of liver metastasis from the participants will be collected and subsequently tested by the laboratories and pathology departments. As previously reported (18), the collection and testing techniques for the above samples are quite mature. All blood samples will be destroyed after the test without preservation. GC specimens and liver metastatic tissue specimens will be sent to the pathological examination for timely preservation. They will be separated into cryopreservation tubes, and the separated tissues will be stored in liquid nitrogen tanks. They will be stored for five years and then destroyed six months after the end of the study.

Evaluation of Technology Effectiveness

Contrast enhanced CT and tumor marker testing were performed in the first month after D2 gastrectomy and RFA treatment to evaluate the effectiveness of the technique and as a new baseline for future comparison. Every 2 to 4 months, additional CT examinations were performed to assess the progression of the disease. For patients who cannot be evaluated by enhanced CT, additional Hepatic contrast-enhanced ultrasonography, MRI or PET/CT can be used for further evaluation.

For the definition of effective rate of D2 gastrectomy, according to NCCN guidelines for diagnosis and treatment of gastric cancer, tumor clearance effectiveness is defined as that the tumor markers are not increased compared with the baseline data, and CT does not find the recurrence of new tumor or metastatic lymph nodes, or potential metastases in other parts and organs (19, 20).

For the definition of effective rate of RFA treatment, according to standardized terminology and reporting criteria for tumor ablation, technique effectiveness is defined as no evidence of residual tumor within 1 cm of the ablation defect; local tumor progression (LTP) is defined as any new peripheral or nodular enhancement within 1 cm or enlargement of the baseline ablation defect (21, 22).

Sample Size Estimate and Statistical Analysis

The aim of REGATTA study (11) was to establish whether the addition of gastrectomy to standard chemotherapy improves survival among patients with advanced gastric cancer with a single non-curable factor. A single non-curable factor was defined as hepatic metastasis (H1; two to four lesions of maximum diameter ≤5 cm and minimum diameter ≥1 cm); peritoneal metastasis (P1) in the diaphragm or peritoneum caudal to the transverse colon without massive ascites or intestinal obstruction. However, our study was to compare the

TABLE 3 | The test and data acquisition schedule for this experiment.

Stage	Pre-operation	Intra-operation	Postoperation					Unplanned follow-up
Follow up period	14-1 days		0-12 month	13-24 month	25-36 month	37-48 month	49-60 month	
Baseline data collected	√	—	—	—	—	—	—	—
Inclusion and exclusion	√	—	—	—	—	—	—	—
Sign informed consent	√	—	—	—	—	—	—	—
Group determination	√	—	—	—	—	—	—	—
Fill in the basic information	√	—	—	—	—	—	—	—
Physical examination	√	—	√	√	√	√	√	—
Imaging examination	√	—	√	√	√	√	√	if necessary
Laboratory examination	√	—	√	√	√	√	√	—
Operation information	—	√	—	—	—	—	—	—
Postoperative pathology	—	√	—	—	—	—	—	if necessary
Safety observation	√	—	√	√	√	√	√	if necessary
Record adverse events	√	—	√	√	√	√	√	if necessary
Other works	√	√	√	√	√	√	√	if necessary

efficacy of D2 gastrectomy plus liver radiofrequency combined with chemotherapy versus chemotherapy alone in the treatment of advanced gastric cancer with unresectable synchronous liver metastases. Because there is a lack of international large-sample studies on the efficacy comparison of D2 gastrectomy plus liver radiofrequency plus postoperative chemotherapy versus chemotherapy alone, we can only estimate the sample size based on the correlation data according to the REGATTA study. The REGATTA study showed that adverse events occurred in 5 of 7 the patients with gastric cancer with liver metastases in chemotherapy group and 9 of 11 the patients with gastric cancer with liver metastases in chemotherapy plus gastrectomy group, which indicated that the incidence of adverse events in gastrectomy plus chemotherapy group was 60%, and that of chemotherapy group was 81.8%. Therefore, the incidence of adverse events in patients with gastric cancer with liver metastasis under the two treatment regimens in the REGATTA study was used to estimate the sample size.

To verify the comparison of the efficacy of D2 gastrectomy plus liver radiofrequency plus postoperative chemotherapy versus chemotherapy alone for patients with GCLM, we designed a superiority study with a superiority margin of 5% (α= 0.05, β= 0.20, 80% power). With a standard error of 0.05 and a confidence interval of 80%, a sample size of 178 is necessary. To minimize sampling error and account for the rate of loss to follow-up for various reasons, we determined the sample size to be 200 participants. Standard descriptive statistics will be used to analyze qualitative and quantitative variables such as relative and absolute frequencies, frequency tables, means, medians, standard deviations, ranges, and quartiles. A 95% confidence level will be considered appropriate for analysis. Descriptive statistics will also be used to describe the most relevant clinical parameter measurements. Analysis of categorical variables will be performed by two-sample t tests or Fisher's exact test. If there is no significant difference in the response rate to D2 gastrectomy plus liver radiofrequency plus postoperative chemotherapy versus chemotherapy alone, then the result will be negative, that is, the difference is not related to whether to apply the treatment strategy of D2 gastrectomy plus liver radiofrequency plus postoperative chemotherapy for patients with GCLM; otherwise, there is a relationship.

Study Endpoints

In this study, the primary endpoint will be the OS. The secondary endpoints PFS and total complication rate. The total complications will include postoperative and chemotherapy complications. Postoperative complications were defined as events occurring within 30 days after the procedure, the severity of which was assessed by the ClavienDindo classification system (23, 24). Postoperative complications will include surgical site infection (SSI refers to the infection that occurs in the incision, deep organ or cavity during the perioperative period. It is mainly divided into superficial wound tissue infection, deep wound tissue infection and organ/cavity infection); anastomotic leaks and duodenal blow-out (identified clinically or radiographically); Chylous fistula (defined as milky white liquid in peritoneal drainage fluid after the start of enteral nutrition); respiratory complications (defined as clinical manifestation of pneumonia or bronchopneumonia confirmed by computed tomographic scan); and other complications (such as: delayedgastricemptying, intestinal obstruction, anastomotic and/or abdominal bleeding, abdominal abscess, pancreatic fistula, pancreatitis and so on.). Postoperative mortality was defined as all-cause death occurring within 30 days after the procedure. Chemotherapy complications refer to the side effects of chemotherapy, such as ototoxicity and nephrotoxicity. For those patients delayed postoperative systemic radiotherapy and/or chemotherapy after 4 weeks of surgery due to surgery and its complications, their clinical data were recorded in detail and analyzed by subgroup stratification.

Adverse events are adverse medical events that occur after surgical and medical treatment in patients in clinical trials. Adverse events, whether treatment-related or not, will be considered from the date participants sign informed consent until 5 years after the end of treatment in this study. The nature and severity of adverse events will be assessed in accordance with "expert consensus on diagnostic criteria for postoperative complications of gastrointestinal cancer in China". The investigator will determine if the adverse event is clinically significant, and if so, it will be identified as an adverse event. The investigators will assess possible relationships among the adverse events, the investigational drugs and the surgery to assess adverse events and their causal relationship to treatment. Adverse reactions include those results recorded as positive, correlated, and possibly correlated. The investigators will keep a full record of serious adverse events from the start of the surgery to the end of the study. All serious adverse events will be reported regardless of whether they are related to the use of drugs or surgery in the study. It is the responsibility of the investigators to notify independent ethics committees or governmental regulatory authorities related to adverse events.

Follow-up

When patients are discharged from the hospital, the first follow-up is to be performed on the 14th day after surgery. The patients will be given physical examination, imaging examination and laboratory examination to determine the postoperative complications of the patients during the follow-up period. The next chemotherapy plan will be formulated for the patients according to the above results. Physical examination and laboratory examination will be performed at least monthly on all enrolled patients. Imaging examinations will be performed every three months. The patients will be followed up by researchers every month to every 3 months. In addition to the above, the complications of chemotherapy will be examined. Recurrence, metastasis, death, and dates of patients will be recorded. The contents of each follow-up will be collated and combined. The follow-up contents will be recorded in **Table 3**.

Patient Protection/Written Informed Consent Forms

Both parties will ensure the protection of the patient's personal records. Except for documents where it is required by law, patient names will not be included in any form in tabular

reports, publications, or any type of research-related document. Informed consent will be formulated in strict accordance with Chinese laws and regulations. Written informed consent, including all changes made throughout the study, must be preapproved by the IRB/ICB before inclusion in the study. Medical staff will obtain a signature with written informed consent from each patient (if the patient is unable to make their own decision for various reasons, the immediate family will decide on their behalf) prior to any specific activities related to the study. Researchers will submit and keep original copies of all written informed consent forms signed by patients and provide additional copies to patients or their immediate family members for their records.

Monitoring of the Study

Before the start of the study, the personnel of the project unit will visit all of the research centers and discuss with the researcher (and/or other research-related personnel) the responsibility of the researcher for the research program and the responsibility of the project undertaking unit or representative.

During the study period, the project undertaker or the supervisor representing the project undertaker will regularly contact the research center for a number of reasons, including the following: providing information and technical support; establishing randomized grouping as required; confirming that the investigator complies with the study plan, that the data on the CRFs are accurately recorded, and the dosage of drugs being used is checked; and carrying out original data analysis (e.g., the data on CRFs are related to the records of patients in the hospital, and the research will compare these with other records). This requires direct access to the original records of each patient (e.g., clinical charts).

The interim analysis will be performed when half of the planned sample size is enrolled. The prespecified stopping criteria in the study protocol are as follows: if D2 gastrectomy plus liver radiofrequency combined with chemotherapy is superior to chemotherapy alone, and the analysis is statistically significant, study termination will be considered, and subsequent patients will receive D2 gastrectomy plus liver radiofrequency combined with chemotherapy. However, if the efficacy of D2 gastrectomy plus liver radiofrequency combined with chemotherapy is not superior to chemotherapy alone, and the analysis results are statistically significant, the study will be considered as invalid and the subsequent enrolled patients will receive chemotherapy alone. The Data and Safety Monitoring Committee of the China Clinical Trial Registry independently reviewed the interim analysis protocol and may decide to terminate the study early with the approval of the ethics committee of each center.

Representatives authorized by project undertakers, regulatory departments, and independent ethics committees may visit the center for inspections, including verifying the original data. The purpose of the inspections of the site and personnel is to systematically and independently examine all research-related behaviors and documents, to determine that these behaviors have been managed and that the data have been analyzed, recorded, and accurately reported in accordance with the research program, GCP, ICH guidelines and other regulatory requirements.

Patient and Public Involvement

Patients and the public will not participate in the design, implementation, dissemination, or reporting of our studies.

Ethical Approval and Consent to Participate

This trial is a prospective multicenter randomized controlled study designed to explore the best strategy for the treatment of gastric cancer with unresectable synchronous liver metastasis. This study will strictly abide by all legal requirements, regulations and general principles formulated by international agencies concerning ethical conduct in human biomedical research and by the Declaration of Helsinki and the International Ethical Guidelines for Biomedical Research Involving Human Beings. This study protocol was approved by the Chinese Registered Clinical Trial Ethics Committee (Hong Kong Center, China Clinical Trial Registry, Kowloon Pond Baptist University Road, Hong Kong Special Administrative Region, China, Approval No. ChiECRCT20200331, Resolution 15 November 2020). The ERC is obliged to evaluate the progress of the study periodically. As soon as any adverse event (AES) occurs, the relevant information will be reported to the IRB.

DISCUSSION

At present, chemotherapy, as a treatment strategy for patients with GCLM, has been recommended as the standard treatment for such patients by Japanese, American and international guidelines (4, 5). With the continuous improvement of chemotherapy schemes, the prognosis of patients with GCLM has been improved to a certain extent (7, 25). A phase 3, randomized controlled trial (11), conducted in 2016, showed that compared to chemotherapy alone, chemotherapy after gastrectomy did not show any survival benefit. However, Fujitani et al. performed D1 lymphadenectomy in gastrectomy for primary gastric cancers and did not remove metastatic lesions in livers in their study. Therefore, whether more thorough D2 lymphadenectomy in gastrectomy for primary gastric cancers plus radiofrequencies for liver metastases plus postoperative chemotherapy can improve the prognosis of patients with GCLM deserves further high-level evidence-based medical evidence.

However, there remains a lack of multicenter randomized controlled trials on D2 gastrectomy plus liver radiofrequency plus postoperative chemotherapy versus chemotherapy alone. The aim of the study was to establish a multicenter randomized controlled trial to evaluate the efficacy of D2 gastrectomy plus liver radiofrequency plus postoperative chemotherapy versus chemotherapy alone. OS and PFS will be taken as the main indicators to study a comparison of the efficacy of two treatment strategies for GCLM in this study. This study will be the first prospective multicenter randomized controlled study comparing the efficacy of D2 gastrectomy plus liver radiofrequency plus postoperative chemotherapy versus chemotherapy alone in China, which may change the selection of standard treatment strategies for GCLM worldwide.

If the results of this study meet our expectations, it will be a great encouragement for health care providers to improve the prognosis of patients with GCLM. We hope to collect lessons and suggestions from this study and integrate them into clinical practice to improve clinical treatments, to further improve the quality of life, and to change the standard treatment strategy for these patients.

DATA AVAILABILITY STATEMENT

The original contributions presented in the study are included in the article/supplementary material. Further inquiries can be directed to the corresponding authors.

ETHICS STATEMENT

The studies involving human participants were reviewed and approved by Chinese Clinical Trial Registry. The patients/participants provided their written informed consent to participate in this study.

AUTHOR CONTRIBUTIONS

Concept Proposal: XL. Survey and Data Summary: WW. Data Collection, analysis and statistics: WW, RG, PY, DD, and ZM. Specific scheme implementation GJ, XL, PY, DD, ZM, XY, RG, and WW. Research Regulatory: GJ and XL. Writing – Draft: WW. Writing-Proofreading and Editing: XL and WW. All authors have approved the final version of this manuscript.

FUNDING

This work is supported by grants from the National Natural Science Foundation of China (Key Program 82100680) by PFY and GJ. This work is also supported by grants from the Shaanxi Innovation Team(2021-TD-43) by XL and GJ.

ACKNOWLEDGMENTS

The authors thank all patients who will participate in this study and the medical staff of the hospital.

REFERENCES

1. Guan K, Liu X, Li J, Ding Y, Li J, Cui G, et al. Expression Status And Prognostic Value Of M6A-Associated Genes in Gastric Cancer. *J Cancer* (2020) 11(10):3027–40. doi: 10.7150/jca.40866
2. Saiura A, Umekita N, Inoue S, Maeshiro T, Miyamoto S, Matsui Y, et al. Clinicopathological Features and Outcome of Hepatic Resection for Liver Metastasis From Gastric Cancer. *Hepatogastroenterology* (2002) 49(46):1062–5. doi: 10.1136/gut.51.suppl_1.i63
3. Kim HR, Cheon SH, Lee KH, Ahn JR, Jeung HC, Lee SS, et al. Efficacy and Feasibility of Radiofrequency Ablation for Liver Metastases From Gastric Adenocarcinoma. *Int J Hyperthermia* (2010) 26(4):305–15. doi: 10.3109/02656730903555696
4. Japanese Gastric Cancer Association. Japanese Gastric Cancer Treatment Guidelines 2010 (Ver. 3). *Gastric Cancer* (2011) 14(2):113–23. doi: 10.1007/s10120-011-0042-4
5. Strong VE, D'Amico TA, Kleinberg L, Ajani J. Impact of the 7th Edition AJCC Staging Classification on the NCCN Clinical Practice Guidelines in Oncology for Gastric and Esophageal Cancers. *J Natl Compr Canc Netw* (2013) 11(1):60–6. doi: 10.6004/jnccn.2013.0009
6. Ohtsu A, Shimada Y, Shirao K, Boku N, Hyodo I, Saito H, et al. Randomized Phase III Trial of Fluorouracil Alone Versus Fluorouracil Plus Cisplatin Versus Uracil and Tegafur Plus Mitomycin in Patients With Unresectable, Advanced Gastric Cancer: The Japan Clinical Oncology Group Study (Jcog9205). *J Clin Oncol* (2003) 21(1):54–9. doi: 10.1200/JCO.2003.04.130
7. Koizumi W, Narahara H, Hara T, Takagane A, Akiya T, Takagi M, et al. S-1 Plus Cisplatin Versus S-1 Alone for First-Line Treatment of Advanced Gastric Cancer (SPIRITS Trial): A Phase III Trial. *Lancet Oncol* (2008) 9(3):215–21. doi: 10.1016/S1470-2045(08)70035-4
8. Bonenkamp JJ, Sasako M, Hermans J, van de Velde CJ. Tumor Load and Surgical Palliation in Gastric Cancer. *Hepatogastroenterology* (2001) 48(41):1219–21. doi: 10.1002/hed.1116
9. Koga S, Kawaguchi H, Kishimoto H, Tanaka K, Miyano Y, Kimura O, et al. Therapeutic Significance of Noncurative Gastrectomy for Gastric Cancer With Liver Metastasis. *Am J Surg* (1980) 140(3):356–9. doi: 10.1016/0002-9610(80)90167-1
10. Haugstvedt T, Viste A, Eide GE, Söreide O. The Survival Benefit of Resection in Patients With Advanced Stomach Cancer: The Norwegian Multicenter Experience. *Norwegian Stomach Cancer Trial World J Surg* (1989) 13(5):617–21; discussion 621-2. doi: 10.1007/BF01658884
11. Fujitani K, Yang HK, Mizusawa J, Kim YW, Terashima M, Han SU, et al. Gastrectomy Plus Chemotherapy Versus Chemotherapy Alone for Advanced Gastric Cancer With a Single Non-Curable Factor (REGATTA): A Phase 3, Randomised Controlled Trial. *Lancet Oncol* (2016) 17(3):309–18. doi: 10.1016/S1470-2045(15)00553-7
12. Yu P, Zhang Y, Ye Z, Chen X, Huang L, Du Y, et al. Treatment of Synchronous Liver Metastases From Gastric Cancer: A Single-Center Study. *Cancer Manag Res* (2020) 12:7905–11. doi: 10.2147/CMAR.S261353
13. Chen L, Song MQ, Lin HZ, Hao LH, Jiang XJ, Li ZY, et al. Chemotherapy and Resection for Gastric Cancer With Synchronous Liver Metastases. *World J Gastroenterol* (2013) 19(13):2097–103. doi: 10.3748/wjg.v19.i13.2097
14. Kuramoto M, Shimada S, Ikeshima S, Matsuo A, Yagi Y, Matsuda M, et al. Extensive Intraoperative Peritoneal Lavage as a Standard Prophylactic Strategy for Peritoneal Recurrence in Patients With Gastric Carcinoma. *Ann Surg* (2009) 250(2):242–6. doi: 10.1097/SLA.0b013e3181b0c80e
15. Bang YJ, Van Cutsem E, Feyereislova A, Chung HC, Shen L, Sawaki A, et al. Trastuzumab in Combination With Chemotherapy Versus Chemotherapy Alone for Treatment of HER2-Positive Advanced Gastric or Gastro-Oesophageal Junction Cancer (ToGA): A Phase 3, Open-Label, Randomised Controlled Trial. *Lancet* (2010) 376(9742):687–97. doi: 10.1016/S0140-6736(10)61121-X
16. Higgins JE. *Cochrane Handbook for Systematic Reviews of Interventions* (2008). Available at: https://handbook-5-1.cochrane.org/ (Accessed 25 Mar 2018).
17. Kakeji Y, Morita M, Maehara Y. Strategies for Treating Liver Metastasis From Gastric Cancer. *Surg Today* (2010) 40(4):287–94. doi: 10.1007/s00595-009-4152-0
18. Fan XS, Chen J, Xue WC. Accurate Diagnosis and Individualized Treatment of Advanced Gastric Cancer: Pathological Detection of Biomarkers Based on Cancer Tissue Samples. *Zhonghua Bing Li Xue Za Zhi* (2021) 50(2):84–9. doi: 10.3760/cma.j.cn112151-20200701-00517
19. Tang K, Zhang B, Dong L, Wang L, Tang Z. Radiofrequency Ablation Versus Traditional Liver Resection and Chemotherapy for Liver Metastases From Gastric Cancer. *J Int Med Res* (2020) 48(7):300060520940509. doi: 10.1177/0300060520940509

20. Lee JW, Choi MH, Lee YJ, Ali B, Yoo HM, Song KY, et al. Radiofrequency Ablation for Liver Metastases in Patients With Gastric Cancer as an Alternative to Hepatic Resection. *BMC Cancer* (2017) 17(1):185. doi: 10.1186/s12885-017-3156-1
21. Goldberg SN, Grassi CJ, Cardella JF, Charboneau JW, Dodd GD 3rd, Dupuy DE, et al. Image-Guided Tumor Ablation: Standardization of Terminology and Reporting Criteria. *J Vasc Interv Radiol* (2005) 16(6):765–78. doi: 10.1097/01.RVI.0000170858.46668.65
22. Ahmed M, Solbiati L, Brace CL, Breen DJ, Callstrom MR, Charboneau JW, et al. Image-Guided Tumor Ablation: Standardization of Terminology and Reporting Criteria–a 10-Year Update. *Radiology* (2014) 273(1):241–60. doi: 10.1148/radiol.14132958
23. Clavien PA, Sanabria JR, Strasberg SM. Proposed Classification of Complications of Surgery With Examples of Utility in Cholecystectomy. *Surgery* (1992) 111(5):518–26.
24. Dindo D, Demartines N, Clavien PA. Classification of Surgical Complications: A New Proposal With Evaluation in a Cohort of 6336 Patients and Results of a Survey. *Ann Surg* (2004) 240(2):205–13. doi: 10.1097/01.sla.0000133083.54934.ae
25. Boku N, Yamamoto S, Fukuda H, Shirao K, Doi T, Sawaki A, et al. Fluorouracil Versus Combination of Irinotecan Plus Cisplatin Versus S-1 in Metastatic Gastric Cancer: A Randomized Phase 3 Study. *Lancet Oncol* (2009) 10(11):1063–9. doi: 10.1016/S1470-2045(09)70259-1

Conflict of Interest: The authors declare that the research was conducted in the absence of any commercial or financial relationships that could be construed as a potential conflict of interest.

Publisher's Note: All claims expressed in this article are solely those of the authors and do not necessarily represent those of their affiliated organizations, or those of the publisher, the editors and the reviewers. Any product that may be evaluated in this article, or claim that may be made by its manufacturer, is not guaranteed or endorsed by the publisher.

Copyright © 2022 Wang, Gao, Yu, Mo, Dong, Yang, Li and Ji. This is an open-access article distributed under the terms of the Creative Commons Attribution License (CC BY). The use, distribution or reproduction in other forums is permitted, provided the original author(s) and the copyright owner(s) are credited and that the original publication in this journal is cited, in accordance with accepted academic practice. No use, distribution or reproduction is permitted which does not comply with these terms.

frontiers in Oncology

ORIGINAL RESEARCH
published: 04 March 2022
doi: 10.3389/fonc.2022.854408

Laparoscopic Gastrectomy for Cancer: Cut Down Complications to Unveil Positive Results of Minimally Invasive Approach

Milos Bjelovic[1,2]*, *Milan Veselinovic*[1,2], *Dragan Gunjic*[1], *Zoran Bukumiric*[2,3], *Tamara Babic*[1], *Radmila Vlajic*[1] and *Dario Potkonjak*[1]

[1] Department for Minimally Invasive Upper Digestive Surgery, Hospital for Digestive Surgery, Clinical Center of Serbia, Belgrade, Serbia, [2] School of Medicine, University of Belgrade, Belgrade, Serbia, [3] Institute for Medical Statistics, Belgrade, Serbia

OPEN ACCESS

Edited by:
Andreas Brandl,
Champalimaud Foundation, Portugal

Reviewed by:
Filipe De Castro E. Borges,
Champalimaud Foundation, Portugal
Giovanni Maria Garbarino,
Sapienza University of Rome, Italy

***Correspondence:**
Milos Bjelovic
milos.bjelovic@gmail.com

Specialty section:
This article was submitted to Gastrointestinal Cancers: Gastric Esophageal Cancers, a section of the journal Frontiers in Oncology

Received: 13 January 2022
Accepted: 09 February 2022
Published: 04 March 2022

Citation:
Bjelovic M, Veselinovic M, Gunjic D, Bukumiric Z, Babic T, Vlajic R and Potkonjak D (2022) Laparoscopic Gastrectomy for Cancer: Cut Down Complications to Unveil Positive Results of Minimally Invasive Approach. Front. Oncol. 12:854408. doi: 10.3389/fonc.2022.854408

Several randomized controlled trials and meta-analyses have confirmed the advantages of laparoscopic surgery in early gastric cancer, and there are indications that this may also apply in advanced distal gastric cancer. The study objective was to evaluate the safety and effectiveness of laparoscopic gastrectomy (LG), in comparison to open gastrectomy (OG), in the management of locally advanced gastric cancer. The single-center, case–control study included 204 patients, in conveyance sampling, who underwent radical gastrectomy for locally advanced gastric cancer. Out of 204 patients, 102 underwent LG, and 102 patients underwent OG. The primary endpoints were safety endpoints, i.e., complication rates, reoperation rates, and 30-day mortality rates. The secondary endpoints were efficacy endpoints, including perioperative characteristics and oncological outcomes. Even though the overall complication rate was higher in the OG group compared to the LG group (30.4% and 19.6%, respectively), the difference between groups did not reach statistical significance ($p = 0.075$). No significant difference was identified in reoperation rates and 30-day mortality rates. Time spent in the intensive care unit (ICU) and overall hospital stay were shorter in the LG group compared to the OG group ($p < 0.001$). Although the number of retrieved lymph nodes is oncologically adequate in both groups, the median number is higher in the OG group (35 vs. 29; $p = 0.024$). Resection margins came out to be negative in 92% of patients in the LG group and 73.1% in the OG group ($p < 0.001$). The study demonstrated statistically longer survival rates for the patients in the laparoscopic group, which particularly applies to patients in the most prevalent, third stage of the disease. When patients with the Clavien–Dindo grade ≥II were excluded from the survival analysis, further divergence of survival curves was observed. In conclusion, LG can be safely performed in patients with locally advanced gastric cancer and accomplish the oncological standard with short ICU and

overall hospital stay. Since postoperative complications could affect overall treatment results and diminish and blur the positive effect of the minimally invasive approach, further clinical investigations should be focused on the patients with no surgical complications and on clinical practice to cut down the prevalence of complications.

Keywords: gastrectomy, advanced gastric cancer (AGC), laparoscopic gastrectomy (LG), minimally invasive surgery, postoperative complications

INTRODUCTION

When Erich Muhe and Phillipe Mouret first described laparoscopic cholecystectomy in 1985 and 1987, respectively, no one believed that large and demanding surgical procedures would be treated the same way in the future. But back in 1993, Juan Santiago Azagra performed the first laparoscopic-assisted total gastrectomy for gastric cancer.

In 1994, Kitano performed the first laparoscopic-assisted distal gastrectomy with a modified D1 lymph node dissection for the treatment of early gastric cancer, with a high risk of lymph node metastasis. Yasuhiro Kodera et al. heralded a whole new perspective for laparoscopic gastrectomy (LG) in 2010. They performed a meta-analysis, enrolling 6 randomized controlled trials and 666 patients, and they concluded that laparoscopic surgery with D2 lymphadenectomy for early gastric cancer is feasible and safe and adheres to the oncological principles (1).

Later on, several randomized controlled trials and meta-analyses have confirmed the advantages of laparoscopic surgery in early gastric cancer, and there are indications that this may also apply in advanced distal gastric cancer (1–3). However, in Western countries, the majority of patients still present with advanced stages of the disease. Locally advanced tumors require a more technically demanding procedure, especially in the case of total gastrectomy with intracorporeal esophagojejunal anastomosis. Nevertheless, laparoscopic surgery for gastric cancer has increased in popularity during the last two decades, in both the East and the West (4, 5). In addition, recent European-based studies found treatment results comparable with their Asian counterpart (6–8).

The study objective was to evaluate the safety and effectiveness of LG, in comparison to open gastrectomy (OG), in the management of locally advanced gastric cancer.

MATERIALS AND METHODS

The single-center, case–control study included 204 patients, in the convenience sampling, who underwent gastrectomy with a curative intention for locally advanced gastric cancer, between March 2013 and May 2021. Out of 204 patients, 102 underwent LG, and 102 patients underwent OG. Perioperative and postoperative data for the patients treated with LG were collected from a prospectively developed database. The OG group was a historical cohort. The study was reviewed and approved by the Clinical Centre of Serbia Institutional Review Board (decision number 187/15 dated October 20, 2016).

Through strategic change management, over the observed period, we have gradually increased the proportion of patients operated using the laparoscopic approach and decreased the proportion of patients operated using the open approach. Preoperative data did not influence the operative approach. Subsequent comparative analysis of the preoperative data did not indicate selection bias or potential confounding.

Inclusion criteria were as follows:

- patient's age ≥18 and ≤80 years
- patients able to undergo general anesthesia and major surgery and are suitable laparoscopic surgical candidates
- patients who provided written informed consent after being informed of the study procedure and risks prior to any study-related events
- patients with documented locally advanced gastric cancer

Patients with other synchronous or metachronous neoplasms, preoperatively confirmed metastatic disease, histology other than adenocarcinoma, and poor general status with severe comorbidities were excluded from the study.

Study Procedures

The study plan included a preoperative/baseline visit, a surgical procedure phase with hospital stay until discharge, and follow-up visits.

At the preoperative/baseline visit, the eligibility of subjects to receive treatment was determined. Before surgery, all patients underwent multidisciplinary team consultation with diagnostic and therapeutic workout according to the European Society for Medical Oncology (ESMO) recommendations (9).

Eligible subjects then undergo gastrectomy for cancer with curative intent. In the LG group, the positions of the patient and trocars were adopted from Luketich et al. (10); at the end of the procedure, the surgical specimen is placed in an extraction bag and removed from the abdomen through a 5-cm-long Pfannenstiel incision. A standard approach included omentectomy, D2 lymph node dissection, and total or subtotal gastrectomy, according to the criteria of the Japanese Gastric Cancer Association (JGCA) (9). Standard reconstruction after total gastrectomy was circular stapled esophagojejunal anastomosis utilizing double stapling technique with transabdominally inserted anvil (reverse-penetrating technique). In the laparoscopic approach, the insertion site of the stapler is in the left upper abdomen (11). The continuity of the digestive tube, in the patients with subtotal gastrectomy, was provided by forming retrocolic, inframesocolic hand-sewn gastro-jejunal anastomosis (Billroth II reconstruction–Finsterer-Hofmeister modification).

All patients underwent antibiotics and thromboembolic prophylaxis, as well as early mobilization after surgery. Control barium radiography was performed routinely on the fifth postoperative day after total gastrectomy, followed by a clear liquid diet. However, a control barium meal was not routinely performed after subtotal gastrectomy, and these patients began with the clear liquid diet on postoperative day three.

The specimen assessment was conducted through specified pathologists according to the 8th edition of the American Joint Committee on Cancer protocol from 2017. Localization and cell type of the tumor, as well as TNM status, were evaluated. Furthermore, the number of the harvested lymph nodes and the R status were assessed as key features of the oncological outcome of the methods in use (12).

After a discharge from the hospital, the first follow-up visits were at intervals of 3–4 months for the first year, six-monthly reviews for the second year, and annually thereafter.

Study Endpoints

The primary endpoints were safety endpoints: non-inferiority of the LG group, compared to OE group, in the onset of

- •total number and the most prevalent early postoperative complications (13, 14)
- •complication classified according to the Clavien–Dindo classification (15)
- •complications grade according to Comprehensive Complication Index (CCI) (16)
- •reoperation rates and 30-day mortality rates

The secondary endpoints were efficacy endpoints, including perioperative characteristics and oncological outcomes:

- •reduction in the LG group, compared to the OG group, in the intensive care unit (ICU) and overall hospital stay
- •non-inferiority of the oncological outcomes of the LG group, compared to the OG group, based on the number of harvested lymph nodes, R status, and short-term survival.

Statistical Analysis

Depending on the type of variables and the normality of the distribution, the data description is here presented as n (%), arithmetic means ± SD, or median (range, min–max). Among the methods for testing statistical hypotheses, the following were used: t-test, Mann–Whitney test, chi-square test, and Fisher's test of exact probability. Logistic regression was used to analyze the relationship between binary outcomes and potential predictors. The Kaplan–Meier method was used to analyze the survival of patients with cancer, the log-rank test was used to assess the survival function of these patients depending on the type of surgery, and the Cox regression model with a 95% CI was used to find an independent predictor of death.

The data were censored for the following reasons: the respondent survived the entire follow-up period or was lost from the records. Statistical hypotheses were tested at the level of statistical significance (alpha level) of 0.05.

The results are presented in tables and graphs. All data were processed in the IBM SPSS Statistics 22 (SPSS Inc., Chicago, IL, USA) software package.

RESULTS

Patient Characteristics, Surgical Procedures, and Tumor Characteristics

Two groups were homogenous in respect to average patients' age, sex, body mass index (BMI), and American Society of Anesthesiologists physical status score (ASA score). They did not differ in respect to the type and duration of surgery, as well (**Table 1**).

While tumor localization and stage of the disease have no significant difference between groups, the size of the tumor was statistically larger in the OG group (p = 0.023). The average tumor diameter in the LG group was 60 mm and in the OG group 70 mm. Observed groups did not differ in respect to the T stage (p = 0.107). T1 stage of the disease was found only in 12.1% of patients in the LG group and 15.2% in the OG group. In addition, more than three-quarters of all patients had ≥T3 tumor at the time of surgery (**Table 2**). Groups did not differ in respect to the N stage as well (p = 0.669). Negative lymph nodes, at the time of surgery, were observed in 32.3% of patients treated utilizing the minimally invasive (MI) approach and 30.3% of patients treated using the open approach.

Safety Endpoints (Prevalence of Significant Early Postoperative Complications)

Even though the overall complication rate was higher in the OG group, compared to the LG group (30.4% and 19.6% respectively), the difference between groups did not reach statistical significance (p = 0.075).

The statistics did not reach a significant difference even when each complication was analyzed individually. One of the most frequent complications was wound infection. Almost 3 times higher relative frequency of wound infections was identified in the OG group, compared to the LG group (8.8% vs. 2.9%). Nevertheless, due to low frequencies of outcomes of interest, no statistical significance was achieved (p = 0.074) (**Table 3**). The same is with other complications, including major postoperative

TABLE 1 | Patient characteristics, perioperative data, and surgical procedures.

	Laparoscopic (n = 102)	*Open* (n = 102)	p
Age[a] (years)	63 (25–87)	64 (18–84)	0.595
Sex, males: n (%)	68 (66.7)	66 (64.7)	0.768
BMI[a,b](kg/m^2)	24.6 (16.8–46.6)	24.4 (16.2–35.4)	0.710
ASA[c] score[a]			0.129
1: n (%)	40 (39.2)	30 (29.4)	
2: n (%)	42 (41.2)	46 (45.1)	
3: n (%)	20 (19.6)	26 (25.5)	
Extent of gastrectomy: n (%)			0.066
Total gastrectomy	52 (51.0)	65 (63.7)	
Subtotal gastrectomy	50 (49.0)	37 (36.3)	
Duration of surgery (min)[a]	290 (180–420)	270 (90–510)	0.058
Hospital stay (days)[a]	10 (4–27)	11 (6–26)	**<0.001**
ICU[d] stay (days)[a]	1 (0–7)	1 (1–8)	**<0.001**

[a]*Data shown represent median (range).*
[b]*BMI, body mass index.*
[c]*ASA, American Society of Anesthesiologists.*
[d]*ICU, intensive care unit.*
In bold: statistically significant.

TABLE 2 | Histopathological findings.

	Laparoscopic	Open	p
Tumor localization			0.**022**
Upper third: n (%)	13 (12.7)	31 (30.4)	
Middle third: n (%)	33 (32.4)	26 (25.5)	
Lower third: n (%)	44 (43.1)	37 (36.3)	
Pangastric: n (%)	12 (11.8)	8 (7.8)	
Diameter of tumor (mm)[a]	60.0 (10–180)	70.0 (15–300)	0.**023**
R status			**<**0.**001**
R0 resection: n (%)	92 (92.0)	68 (73.1)	
R1 resection: n (%)	8 (8.0)	25 (26.9)	
T stage			0.107
T1: n (%)	12 (12.1)	15 (15.2)	
T2: n (%)	12 (12.1)	3 (3.0)	
T3: n (%)	40 (40.4)	33 (33.3)	
T4: n (%)	35 (35.4)	48 (48.5)	
N stage			0.669
N0: n (%)	32 (32.3)	30 (30.3)	
N1: n (%)	15 (15.2)	13 (13.1)	
N2: n (%)	18 (18.2)	20 (20.2)	
N3: n (%)	34 (34.3)	36 (36.4)	
Lymph nodes retrieved[a]	29 (15–74)	35 (15–81)	0.**024**
Positive lymph nodes[a]	3 (0–38)	4 (0–59)	0.487
AJCC[b] pathological stage			0.259
I stage: n (%)	18 (18.2)	17 (17.2)	
II stage: n (%)	26 (26.3)	18 (18.2)	
III stage: n (%)	53 (53.5)	61 (61.6)	
IV stage: n (%)	2 (2.0)	3 (3.0)	

[a]*Data shown represent median (range).*
[b]*American Joint Committee on Cancer, 8th edition.*
In bold: statistically significant.

TABLE 3 | Postoperative complications.

	Laparoscopic (n = 102)	*Open* (n = 102)	p
Overall complications: n (%)	20 (19.6)	31 (30.4)	0.075
• Wound infection: n (%)	3 (2.9)	9 (8.8)	0.074
• Diarrhea: n (%)	3 (2.9)	9 (8.8)	0.074
• Transient hepatic function damage: n (%)	1 (1.0)	0 (0)	1.000
• Intraabdominal bleeding: n (%)	2 (2.0)	1 (1.0)	1.000
• Intraabdominal collection: n (%)	0 (0)	1 (1.0)	1.000
• Neurological: n (%)	2 (2.0)	1 (1.0)	1.000
• Urinary tract infection: n (%)	2 (2.0)	2 (2.0)	1.000
• Urinary retention: n (%)	1 (1.0)	1 (1.0)	1.000
• Prolonged bowel paresis: n (%)	1 (1.0)	2 (2.0)	1.000
• Leukopenia: n (%)	0 (0)	1 (1.0)	1.000
• Thrombocytosis: n (%)	0 (0)	2 (2.0)	0.498
• Fever: n (%)	2 (2.0)	7 (6.9)	0.170
• Pneumonia: n (%)	1 (1.0)	2 (2.0)	1.000
• Biliary fistula: n (%)	1 (1.0)	0 (0)	1.000
• Ileus: n (%)	1 (1.0)	0 (0)	1.000
• Anastomotic leak: n (%)	0 (0)	1 (1.0)	1.000
• Respiratory failure: n (%)	0 (0)	2 (2.0)	0.498
• Pulmonary embolism: n (%)	1 (1.0)	0 (0)	1.000
Clavien–Dindo: n (%)			0.067
0	82 (80.4)	71 (69.6)	
I	9 (8.8)	11 (10.8)	
II	8 (7.8)	16 (15.7)	
III	2 (2.0)	1 (1.0)	
IV	1 (1.0)	2 (2.0)	
V	0 (0)	1 (1.0)	
CCI[a,b]	3.6 (0–42.4)	6.7 (0–100)	0.060
MPPC[c]: n (%)	0 (0)	2 (2.0)	0.498
Reoperation: n (%)	2 (2.0)	1 (1.0)	1.000
30-day mortality: n (%)	0 (0)	1 (1)	1.000

[a]*Data shown represent median (range).*
[b]*CCI, Comprehensive Complication Index.*
[c]*MPPC, major postoperative pulmonary complications.*

pulmonary complications (MPPC) and anastomotic leakage. One patient in the OG group had type 2 leakage of the esophagojejunal anastomosis, and 2 patients in the OG group had MPPC. No such complications are observed in the LG group (**Table 3**).

By analyzing complications according to the Clavien–Dindo classification (CDC) and CCI, no statistically significant difference between the two groups was observed (**Table 3**). Complications classified as the Clavien–Dindo grade ≥II had 10.8% patients in the LG group and 19.7% in the OG group (p = 0.067). In addition, although 80.4% of patients in the LG group had a CCI score of 0, compared to 69.6% of patients in the OG group, no statistically significant difference between groups was achieved (p = 0.060).

Based on the analysis, no statistically significant difference was identified in reoperation rates and 30-day mortality rates (**Table 3**).

Perioperative Characteristics

Time spent in the ICU was significantly shorter in the LG group with an average value of 1.0 compared to 1.5 days for the OG group (p < 0.001). A statistically significant difference is also observed in the length of hospital stay (10 vs. 11 days) (p < 0.001) (**Table 1**). In the group of laparoscopically treated patients, there were no conversions to open surgery.

Oncological Outcomes

Although the number of retrieved lymph nodes is oncologically adequate in both groups, the median number is significantly higher in the OG group (35 vs. 29; p = 0.024). Resection margins came out to be negative in 92% of patients in the LG group and 73.1% in the OG group (p < 0.001). The vast majority of these patients in the OG group had a positive circumferential resection margin.

Follow-Up

The estimated mean survival in all treated patients was 37.4 months (95% CI 34.0–40.8) (**Figure 1**). The estimated mean survival in the LG group was 41.8 months (95% CI 36.9–46.7), while in the OG group, it was 33.8 months (95% CI 29.2–38.4) (p = 0.018).

By analyzing mean survival rates only for the patients who had stage I and II disease, no statistical significance was found (p = 0.566): 49.8 months in the LG group (95% CI 43.6–56.0) and 52.6 months in the OG group (95% CI 47.5–57.8) (**Figure 2**). For the patients with stage III disease, the median survival rate in the LG group was 26.6 months (95% CI 12.8–40.4) and in the OG group 16.1 months (95% CI 14.4–17.8), which is statistically significant (p = 0.014) (**Figure 3**).

The multivariate Cox regression model included predictors of death after surgery, which were statistically significant in

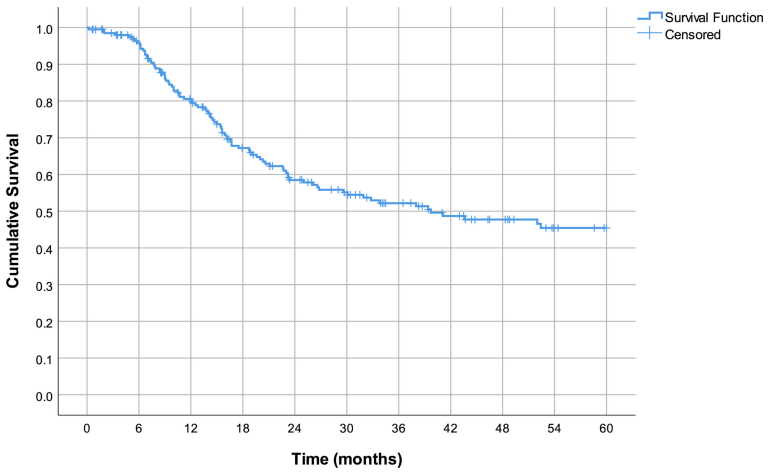

FIGURE 1 | Estimated mean overall survival.

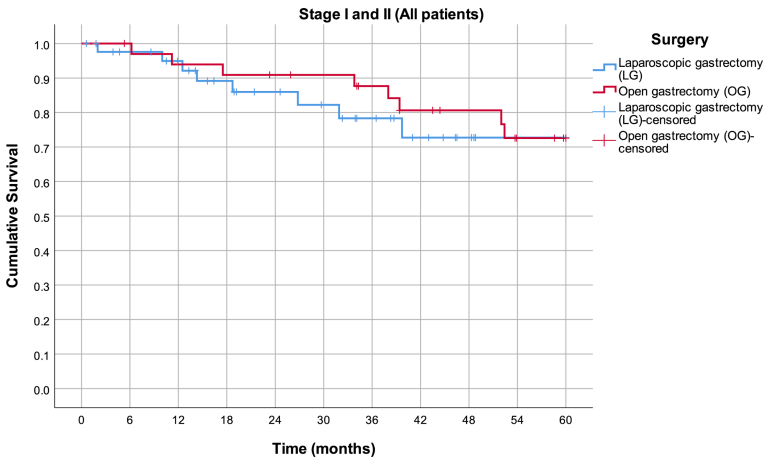

FIGURE 2 | Estimated mean survival for the patients in stage I and II disease, in respect to the operative approach.

univariate regression models, at a significance level of 0.05 (**Table 4**). In this model, the variables associated with increased mortality hazard are presence of the surgical complications (Clavien–Dindo grade ≥II (B = 2.100; p = 0.001)) and higher stage of the disease (higher T stage (B = 0.394; p = 0.018), higher N stage (B = 0.384; p = 0.002), and metastatic disease (B = 1.768; p < 0.001)). Even though surgical access in the multivariate model did not reach statistical significance, the hazard ratio (HR) for open surgery compared to laparoscopy is 1.5.

By excluding patients who had complications grade ≥II according to the Clavien–Dindo classification, a further divergence of survival curves is observed (**Figure 4**). In the third stage of the disease, the mean survival rate in the LG group is 36.3 months (95% CI 29.0–43.6), while in the OG group, it is 22.0 months (95% CI 16.7–27.4) (p = 0.002).

DISCUSSION

Several randomized controlled trials and meta-analyses have confirmed the advantages of LG, compared to OG, in the treatment of early gastric cancer (1–3). However, in Western countries, the vast majority of patients still present with advanced stages of the disease and often with proximal tumor localization. Thus, despite that laparoscopic surgery has increased in popularity, uptake of the MI approach in the treatment of gastric cancer in Europe is relatively slow. Nevertheless, Hawerkamp et al. in 2016 and later on Chevallay, Bracale, and others demonstrated that European-based studies found that LG can be performed in Western European patients with locally advanced gastric cancer and meets the oncological standard with a short hospital stay when performed by trained surgeons (6–8).

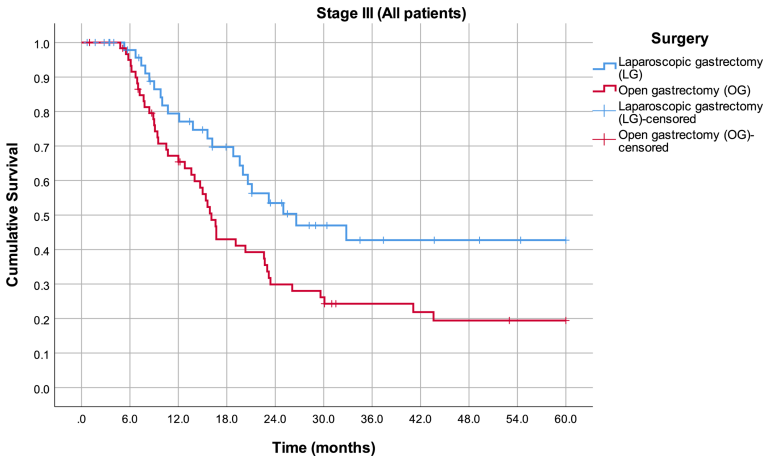

FIGURE 3 | Estimated mean survival for the patients in stage III disease, in respect to the operative approach.

TABLE 4 | Multivariate Cox regression model.

	B	p	HR	95.0% CI for Exp(B)	
				Lower	Upper
Surgical access	0.403	0.095	1.50	0.933	2.402
Sex	0.340	0.220	0.71	0.414	1.225
Clavien–Dindo	2.100	**0.001**	8.17	2.254	29.586
Tumor diameter	0.001	0.815	1.00	0.994	1.007
R status	0.218	0.450	1.24	0.706	2.190
T stage	0.394	**0.018**	1.48	1.071	2.055
N stage	0.384	**0.002**	1.47	1.149	1.877
M stage	1.768	**<0.001**	5.86	2.178	15.750

HR, hazard ratio.
In bold: statistically significant.

This study analyzed the safety and efficacy of LG for locally advanced gastric cancer in a tertiary referral center in Serbia. In this single-center, case–control study, observed groups were homogenous in respect to patient demographic characteristics, type of surgery, tumor localization, and stage of the disease. All patients in this trial were initially diagnosed with locally advanced tumors. After neoadjuvant treatment, patients were operated on, and definitive histology was clarified according to the final histopathological findings (PH). In the final analysis, there was a subgroup of patients with T1 tumors. One of many possible explanations is that clinical TNM did not match ideally with the pathological TNM staging. Another could be that, to some point, regression of the tumor could be expected with neoadjuvant treatment, but the correlation between the clinical and pathological treatment response is weak. At the end of the day, some patients with T1 (especially T1b) tumors were node positive.

This study demonstrated evidently lower complication rates in the MI group, yet not reaching a statistically significant difference (19.6% vs. 30.4%; p = 0.075). The study by Van der

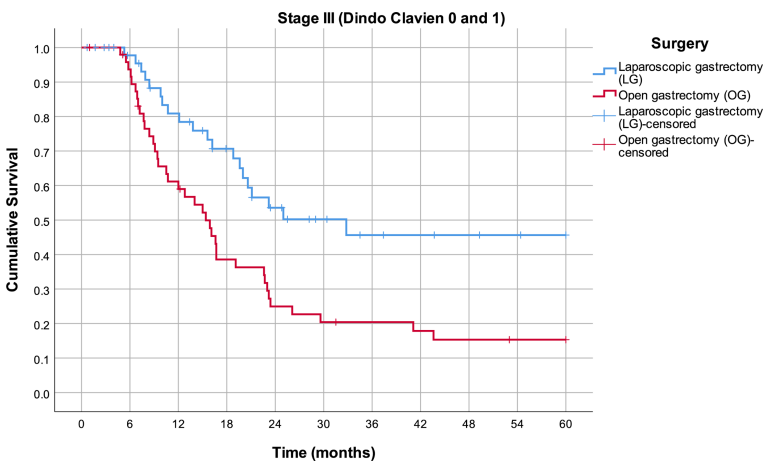

FIGURE 4 | Estimated mean survival for the Clavien–Dindo group 0 and 1 patients in stage III disease, in respect to the operative approach.

Wielen et al. (17) analyzed the outcome differences between East and West in MI gastrectomy versus OG. They found that the overall complication rates for the LG group were 21.69% and for OG 30.80% in the Western studies. Differently, the rates in Asian studies showed complication rates of 12.23% in the LG group and 15.79% in the OG group. Recently published Western trials found results comparable with those of the Asian counterpart. To our knowledge, the lowest quoted overall complication rate, after LG for cancer, was 15.8% (18).

The most frequent complication, in our study, was wound infection. Although statistically not significant, it was 3 times more common in the OG group compared to the LG group (2.9% vs. 8.8%). One of the most fearsome complications is anastomotic leakage. There was one patient in the OG group with type 2 leakage of the esophagojejunal anastomosis, a rate that is comparable to that of most Western and Eastern studies (6, 19). No difference was observed in MPPC, reoperation, and 30-day mortality rates.

In most trials, the number of overall complications matches complication rates according to the Clavien–Dindo classification. However, Clavien–Dindo classification does not sum up all of the complications that occurred, but only the gravest. Thus, a limitation of this classification is that events of lesser severity may not be considered, leading to an underestimation of the true overall postoperative morbidity. The CCI has been shown to yield a substantial additional value to the Clavien–Dindo classification in patients with more than 1 complication.

Prevalence of complications defined as the Clavien–Dindo grade ≥II is almost two times lower in the LG group, compared to the OG group (10.8% and 19.7% respectively); nevertheless, the difference did not reach statistical significance ($p = 0.067$). Similar results have been achieved when the severity of complications, with grade according to the CCI, was analyzed. The mean CCI index was 3.6 in the LG group and 6.7 in the OG group, yet not reaching the level of statistical significance.

When we look beyond the percentage of specific complications, we can find that Tsukada et al. have reported that elevated levels of inflammatory mediators like cytokines could be the cause of complications following major cancer surgery (20). When the production of cytokines was evaluated in patients undergoing major cancer surgery, lower production of cytokines was noted in the group of patients treated by utilizing the MI approach, compared to the open approach. In order to measure the invasiveness of MI esophagectomy (MIE), it might be necessary to evaluate other parameters in addition to morbidity rates. Moreover, there is a possibility that the overall number of cases in our study was too small to reach statistical significance.

The mean duration of surgery for the LG group and OG group was 290 and 270 min, respectively, and is comparable to that in most Western series (6, 7, 17) and slightly longer than that in the Asian studies (17, 21). Introducing technically demanding procedure needs must not unduly prolong operations. The effects of the learning curve in our opinion were minimized with excessive experience in other advanced upper gastrointestinal laparoscopic and thoracoscopic procedures with the same surgical team performing all operations.

The duration of routine postoperative ICU stay/recovery and hospital stay, although unreliable as a criterion of outcome among centers, is a useful parameter of the severity of the postoperative course and complication within a single center, particularly when there are defined protocols and discharge policy (15). Nevertheless, in our study, the average ICU stay and length of hospital stay were significantly reduced in the LG group when compared to the OG group, suggesting an earlier recovery in the case of LG.

Regarding oncological outcomes, significantly more lymph nodes were retrieved in the OG group, compared to the LG group, even though the mean number of harvested lymph nodes in the LG group also met the criteria for adequate radical lymphadenectomy. Our results were more comparable to those reported in Eastern studies and somewhat better than in Western studies (17, 22). Data also revealed a higher R0 rate in the LG group (92% vs. 73.1%), which can be justified by a more advanced T category and mean tumor size in the open group, with the majority of R1 resections at circumferential resection margin.

Numerous Western and Eastern studies demonstrated that the long-term survival and recurrence rates of laparoscopic gastric cancer surgery are comparable to those of open surgery for the treatment of both early and advanced stage gastric cancer (23–26). Garbarino et al., comparing laparoscopic versus open distal gastrectomy for locally advanced gastric cancer, pointed out completely different survival results. Patients with N0 or stage IB-II had better survival after LG. On the contrary, N+ and stage III patients had no survival benefit due to the laparoscopic approach (27). Observing the late outcome, our study demonstrated statistically longer survival rates for the patients in the laparoscopic group, which particularly applies to patients in the most prevalent, third stage of the disease. However, the survival inferiority of the OG group is probably related to the more advanced tumor, rather than the operative approach itself. The analyzed groups did not differ statistically in respect to the T, N, and M status and tumor stage. Nevertheless, due to the small sample size, patients were classified into the single-stage III rather than stage IIIA, IIIB, or IIIC. Out of the total number of patients in the stage III disease, in the OG group, more than 27% were in stage IIIC, while in the laparoscopic group, there were only 18% in this most advanced III stage. This observation is further supported by the multivariate statistics where survival is influenced by the stage of the disease and the presence of the surgical complications, rather than the surgical approach. Nevertheless, in the multivariate model, HR for open surgery compared to laparoscopy is 1.5. In addition, a significant difference was observed in respect to the tumor size and R status, and possible oncological impact of the higher R1 status on the OG patients should not be underestimated.

To check to what extent postoperative complications influence the positive effects of the MI approach, all patients with the Clavien–Dindo grade ≥II were excluded from the survival analysis, and further divergence of survival curves was observed. That could mean that postoperative complications could adversely affect the positive effects of the MI approach when the total population of patients is analyzed.

Our study showed that postoperative complications could diminish and blur the positive effect of the laparoscopic approach. Thus, future research focused on the evaluation of the MI approach in major cancer surgery should be focused on the patients with no complications. In addition, clinical practice should be focused on complication prediction and prevention to reduce their clinical and oncological impact.

The study has several limitations. First, the sample size is relatively small and has limited power to compare low frequencies of outcomes of interest. Second, this is a case–control study with a historical cohort and is subjected to selection biases. The importance of the MI approach in the treatment of locally advanced gastric cancer should be further tested in future, single-institution, randomized controlled trials. We strongly suggest testing the benefit of the MI approach separately in the subpopulation of patients with no significant surgical complications.

CONCLUSION

In conclusion, LG can be safely performed in patients with locally advanced gastric cancer and accomplish the oncological standard with short ICU and overall hospital stay, when performed by surgeons trained in gastric cancer and advanced laparoscopic surgery. Since postoperative complications could affect overall treatment results and diminish and blur the positive effect of the MI approach, further clinical investigations should be focused on the patients with no surgical complications and clinical practice to cut down the prevalence of complications.

DATA AVAILABILITY STATEMENT

The original contributions presented in the study are included in the article/supplementary material. Further inquiries can be directed to the corresponding author.

ETHICS STATEMENT

The studies involving human participants were reviewed and approved by the Clinical Centre of Serbia Institutional Review Board (decision number 187/15 dated October 20, 2016). The patients/participants provided their written informed consent to participate in this study.

AUTHOR CONTRIBUTIONS

MB contributed to the conception and design of the study. MV organized the database. ZB performed the statistical analysis. MV wrote the first draft of the manuscript. DG, TB, RV, and DP wrote sections of the manuscript and participated in data collection. All authors contributed to manuscript revision and read and approved the submitted version.

ACKNOWLEDGMENTS

Special thanks to James D. Luketic for the master coaching. It was a real honor to learn from an extraordinary and dedicated teacher and surgeon.

REFERENCES

1. Kodera Y, Fujiwara M, Ohashi N, Nakayama G, Koike M, Morita S, et al. Laparoscopic Surgery for Gastric Cancer: A Collective Review With Meta-Analysis of Randomized Trials. *J Am Coll Surg* (2010) 211(5):677–86. doi: 10.1016/j.jamcollsurg.2010.07.013
2. Kim H-H, Han S-U, Kim M-C, Kim W, Lee H-J, Ryu SW, et al. Effect of Laparoscopic Distal Gastrectomy vs Open Distal Gastrectomy on Long-Term Survival Among Patients With Stage I Gastric Cancer: The KLASS-01 Randomized Clinical Trial. *JAMA Oncol* (2019) 5(4):506–13. doi: 10.1001/jamaoncol.2018.6727
3. Lee H-J, Hyung WJ, Yang H-K, Han SU, Park Y-K, An JY, et al. Short-Term Outcomes of a Multicenter Randomized Controlled Trial Comparing Laparoscopic Distal Gastrectomy With D2 Lymphadenectomy to Open Distal Gastrectomy for Locally Advanced Gastric Cancer (KLASS-02-RCT). *Ann Surg* (2019) 270(6):983–91. doi: 10.1097/SLA.0000000000003217
4. Lee H-J, Yang H-K. Laparoscopic Gastrectomy for Gastric Cancer. *Dig Surg* (2013) 30(2):132–41. doi: 10.1159/000350884
5. Strong VE, Devaud N, Karpeh M. The Role of Laparoscopy for Gastric Surgery in the West. *Gastric Cancer Off J Int Gastric Cancer Assoc Jpn Gastric Cancer Assoc* (2009) 12(3):127–31. doi: 10.1007/s10120-008-0516-1
6. Chevallay M, Jung M, Berlth F, Seung-Hun C, Morel P, Mönig S. Laparoscopic Surgery for Gastric Cancer: The European Point of View. *J Oncol* (2019) 2019:8738502. doi: 10.1155/2019/8738502
7. Haverkamp L, Ruurda JP, Offerhaus GJA, Weijs TJ, van der Sluis PC, van Hillegersberg R. Laparoscopic Gastrectomy in Western European Patients With Advanced Gastric Cancer. *Eur J Surg Oncol J Eur Soc Surg Oncol Br Assoc Surg Oncol* (2016) 42(1):110–5. doi: 10.1016/j.ejso.2015.09.018
8. Bracale U, Merola G, Pignata G, Andreuccetti J, Dolce P, Boni L, et al. Laparoscopic Gastrectomy for Stage II and III Advanced Gastric Cancer: Long–Term Follow–Up Data From a Western Multicenter Retrospective Study. *Surg Endosc* (2021). doi: 10.1007/s00464-021-08505-y
9. . Japanese Gastric Cancer Association. Japanese Gastric Cancer Treatment Guidelines 2018 (5th Edition). *Gastric Cancer* (2021) 24(1):1–21. doi: 10.1007/s10120-020-01042-y
10. Pennathur A, Awais O, Luketich JD. Technique of Minimally Invasive Ivor Lewis Esophagectomy. *Ann Thorac Surg* (2010) 89(6):S2159–2162. doi: 10.1016/j.athoracsur.2010.03.069
11. Kawaguchi Y, Shiraishi K, Akaike H, Ichikawa D. Current Status of Laparoscopic Total Gastrectomy. *Ann Gastroenterol Surg* (2019) 3(1):14–23. doi: 10.1002/ags3.12208
12. *TNM Classification of Malignant Tumours, 8th Edition | Wiley [Internet]. Wiley.Com.* Available at: https://www.wiley.com/en-ru/TNM+Classification+of+Malignant+Tumours%2C+8th+Edition-p-9781119263579 (Accessed 2021 Nov 1).
13. Baiocchi GL, Giacopuzzi S, Marrelli D, Reim D, Piessen G, Matos da Costa P, et al. International Consensus on a Complications List After Gastrectomy for Cancer. *Gastric Cancer Off J Int Gastric Cancer Assoc Jpn Gastric Cancer Assoc* (2019) 22(1):172–89. doi: 10.1007/s10120-018-0839-5
14. Low DE, Alderson D, Cecconello I, Chang AC, Darling GE, D'Journo XB, et al. International Consensus on Standardization of Data Collection for Complications Associated With Esophagectomy: Esophagectomy Complications Consensus Group (ECCG). *Ann Surg* (2015) 262(2):286–94. doi: 10.1097/SLA.0000000000001098
15. Dindo D, Demartines N, Clavien P-A. Classification of Surgical Complications: A New Proposal With Evaluation in a Cohort of 6336 Patients and Results of a Survey. *Ann Surg* (2004) 240(2):205–13. doi: 10.1097/01.sla.0000133083.54934.ae
16. Slankamenac K, Nederlof N, Pessaux P, de Jonge J, Wijnhoven BPL, Breitenstein S, et al. The Comprehensive Complication Index: A Novel and

More Sensitive Endpoint for Assessing Outcome and Reducing Sample Size in Randomized Controlled Trials. *Ann Surg* (2014) 260(5):757–62; discussion 762-763. doi: 10.1097/SLA.0000000000000948
17. van der Wielen N, Straatman J, Cuesta MA, Daams F, van der Peet DL. Short-Term Outcomes in Minimally Invasive Versus Open Gastrectomy: The Differences Between East and West. A Systematic Review of the Literature. *Gastric Cancer Off J Int Gastric Cancer Assoc Jpn Gastric Cancer Assoc* (2018) 21(1):19–30. doi: 10.1007/s10120-017-0747-0
18. Lin J-X, Lin J-P, Desiderio J, Xie J-W, Gemini A, Wang J-B, et al. Difference in the Short-Term Outcomes of Laparoscopic Gastrectomy for Gastric Carcinoma Between the East and West: A Retrospective Study From the IMIGASTRIC Trial. *J Cancer* (2019) 10(17):4106–13. doi: 10.7150/jca.31192
19. Małczak P, Torbicz G, Rubinkiewicz M, Gajewska N, Sajuk N, Rozmus K, et al. Comparison of Totally Laparoscopic and Open Approach in Total Gastrectomy With D2 Lymphadenectomy - Systematic Review and Meta-Analysis. *Cancer Manag Res* (2018) 10:6705–14. doi: 10.2147/CMAR.S182557
20. Tsukada K, Hasegawa T, Miyazaki T, Katoh H, Yoshikawa M, Masuda N, et al. Predictive Value of Interleukin-8 and Granulocyte Elastase in Pulmonary Complication After Esophagectomy. *Am J Surg* (2001) 181(2):167–71. doi: 10.1016/S0002-9610(00)00558-4
21. Tanaka R, Lee S-W, Imai Y, Honda K, Matsuo K, Tashiro K, et al. Advantages of Laparoscopic Surgery for Gastric Cancer in Elderly Patients Aged Over 80 Years: A Propensity Score Matching Analysis. *World J Surg* (2021) 45 (9):2830–9. doi: 10.1007/s00268-021-06157-6
22. Li B, Yu-Hong Wong I, Siu-Yin Chan F, Chan KK, Lai-Yin Wong C, Law T-T, et al. Comparison of Laparoscopic Versus Open Gastrectomy for Gastric Cancer. *Surg Oncol* (2020) 35:14–21. doi: 10.1016/j.suronc.2020.06.008
23. Kostakis ID, Alexandrou A, Armeni E, Damaskos C, Kouraklis G, Diamantis T, et al. Comparison Between Minimally Invasive and Open Gastrectomy for Gastric Cancer in Europe: A Systematic Review and Meta-Analysis. *Scand J Surg SJS Off Organ Finn Surg Soc Scand Surg Soc* (2017) 106(1):3–20. doi: 10.1177/1457496916630654
24. Chen X-Z, Wen L, Rui Y-Y, Liu C-X, Zhao Q-C, Zhou Z-G, et al. Long-Term Survival Outcomes of Laparoscopic Versus Open Gastrectomy for Gastric Cancer: A Systematic Review and Meta-Analysis. *Med (Baltimore)* (2015) 94 (4):e454. doi: 10.1097/MD.0000000000000454
25. Hyung WJ, Yang H-K, Park Y-K, Lee H-J, An JY, Kim W, et al. Long-Term Outcomes of Laparoscopic Distal Gastrectomy for Locally Advanced Gastric Cancer: The KLASS-02-RCT Randomized Clinical Trial. *J Clin Oncol Off J Am Soc Clin Oncol* (2020) 38(28):3304–13. doi: 10.1200/JCO.20.01210
26. van der Wielen N, Straatman J, Daams F, Rosati R, Parise P, Weitz J, et al. Open Versus Minimally Invasive Total Gastrectomy After Neoadjuvant Chemotherapy: Results of a European Randomized Trial. *Gastric Cancer Off J Int Gastric Cancer Assoc Jpn Gastric Cancer Assoc* (2021) 24(1):258–71. doi: 10.1007/s10120-020-01109-w
27. Garbarino GM, Costa G, Laracca GG, Castagnola G, Mercantini P, Di Paola M, et al. Laparoscopic Versus Open Distal Gastrectomy for Locally Advanced Gastric Cancer in Middle-Low-Volume Centers in Western Countries: A Propensity Score Matching Analysis. *Langenbecks Arch Surg* (2020) 405 (6):797–807. doi: 10.1007/s00423-020-01951-7

Conflict of Interest: The authors declare that the research was conducted in the absence of any commercial or financial relationships that could be construed as a potential conflict of interest.

Publisher's Note: All claims expressed in this article are solely those of the authors and do not necessarily represent those of their affiliated organizations, or those of the publisher, the editors and the reviewers. Any product that may be evaluated in this article, or claim that may be made by its manufacturer, is not guaranteed or endorsed by the publisher.

Copyright © 2022 Bjelovic, Veselinovic, Gunjic, Bukumiric, Babic, Vlajic and Potkonjak. This is an open-access article distributed under the terms of the Creative Commons Attribution License (CC BY). The use, distribution or reproduction in other forums is permitted, provided the original author(s) and the copyright owner(s) are credited and that the original publication in this journal is cited, in accordance with accepted academic practice. No use, distribution or reproduction is permitted which does not comply with these terms.

frontiers in Oncology

SYSTEMATIC REVIEW
published: 07 March 2022
doi: 10.3389/fonc.2022.831207

Comparison of Treatment Efficacy and Survival Outcomes Between Asian and Western Patients With Unresectable Gastric or Gastro-Esophageal Adenocarcinoma: A Systematic Review and Meta-Analysis

Zhening Zhang[1,2†], *Zining Liu*[1,3†] *and Zeyang Chen*[1*]

[1] Department of General Surgery, Peking University First Hospital, Beijing, China, [2] Department of Gastrointestinal Oncology, Key Laboratory of Carcinogenesis and Translational Research, Peking University Cancer Hospital and Institute, Beijing, China, [3] Department of Gastrointestinal Cancer Center, Key Laboratory of Carcinogenesis and Translational Research, Peking University Cancer Hospital and Institute, Beijing, China

OPEN ACCESS

Edited by:
Luigi Marano,
University of Siena, Italy

Reviewed by:
Ludovico Carbone,
University of Siena, Italy
Sally Lau,
NYU Grossman School of Medicine, United States

***Correspondence:**
Zeyang Chen
chenzeyang_pku@163.com

[†]These authors have contributed equally to this work

Specialty section:
This article was submitted to Gastrointestinal Cancers: Gastric & Esophageal Cancers, a section of the journal Frontiers in Oncology

Received: 08 December 2021
Accepted: 15 February 2022
Published: 07 March 2022

Citation:
Zhang Z, Liu Z and Chen Z (2022) Comparison of Treatment Efficacy and Survival Outcomes Between Asian and Western Patients With Unresectable Gastric or Gastro-Esophageal Adenocarcinoma: A Systematic Review and Meta-Analysis. Front. Oncol. 12:831207. doi: 10.3389/fonc.2022.831207

Background: Gastric cancer and gastro-esophageal adenocarcinoma are geographically heterogeneous diseases. Previous studies suggested that Asian and Western patients with late-stage gastric or gastro-esophageal adenocarcinoma possess distinct survival outcomes. However, the interregional differences of multiple systemic therapies in unresectable diseases have not been comprehensively described.

Materials and Methods: We searched PubMed-MEDLINE, Embase, Web of Science and Cochrane Library from inception to 31 October 2021 and reviewed major conference abstracts for controlled trials of systemic therapies in unresectable gastric or gastro-esophageal adenocarcinoma that reported hazard ratios stratified by geographical region. The primary measurements were overall survival and progression-free survival. The pooled hazard ratios and 95% confidence intervals for overall survival and progression-free survival in Asian and Western populations were calculated using a random effect model. A linear regression model was adopted to compare the overall survival and progression-free survival between Asian and Western patients.

Results: A total of 9033 patients from 20 studies were included for analysis. Immunotherapy was associated with an improvement in the overall survival for both Asian (hazard ratio, 0.80; 95% confidence interval, 0.65–0.98) and Western (hazard ratio, 0.90; 95% confidence interval, 0.81–1.00) patients, with no significant difference between the two groups (P = 0.32). Trends of survival benefit with anti-HER2 therapy and anti-angiogenic therapy versus control were observed in both Asian and Western patients, although statistical significance was not denoted. Subgroup analyses yielded a statistically superior overall survival of Asian versus Western patients in trials that investigated first-line

immunotherapy (P = 0.04). Due to the linear regression analyses with scatter plot graphs, Asian patients showed a higher overall survival, but not progression-free survival, than Western patients irrespective of treatment type.

Conclusion: Asian and Western patients with unresectable gastric or gastro-esophageal adenocarcinoma show similar responses to systemic therapies with limited interregional differences. Exceptionally, first-line immunotherapy could elicit superior survival among Asian populations. In addition, Asian patients with gastric or gastro-esophageal adenocarcinoma display a superior OS compared with Western counterparts.

Keywords: gastric cancer, gastro-esophageal adenocarcinoma, immunotherapy, anti-angiogenic therapy, anti-HER2 therapy, overall survival, progression-free survival, regional difference

1 INTRODUCTION

Gastric cancer (GC) and gastro-esophageal adenocarcinoma (GEA) are the fourth cause of cancer mortality worldwide (1). The incidence of GC/GEA varies across regions, with the highest estimated rate in Asia/Pacific and the lowest in North America (2). Despite a decline in global incidence within the past few decades, a substantial proportion of unresectable GCs remain incurable and portend dismal prognosis. For a long time, the mainstay chemotherapy regimen for unresectable GCs encompasses first-line platinum-based doublet and second-line taxanes (3–5). Nevertheless, treatment modalities for advanced/metastatic GC have undergone drastic evolution in recent years. Novel medications emerge exponentially, including immunotherapy, which predominantly exerts immune checkpoint blockade, antiangiogenic therapy, which ameliorates vascular remodeling, and growth factor receptor-targeted therapy, which counteracts aberrant cancer signaling, equipping oncologists with a vast number of robust weapons against late-stage GCs (6–8).

Notably, GC/GEA are highly heterogeneous diseases regarding geographic locality. According to previous studies, Asian (comprised of Japan, China, and South Korea) and Western (mainly Caucasians from North America or West/North Europe) GC patients have distinct prognoses even if balanced by stage. Asian patients are reported to possess longer PFS and OS according to subgroup analyses of multinational RCTs. By contrast, Western patients suffer from shorter survival and prone to show poorer responses to systemic therapies (9–14). It has been considered that the variation of both genetic and sociocultural factors contributes to the disparities. In terms of molecular patterns, somatic gene mutation or amplification rates in oncogenes such as HER2, EGFR, and KRAS are similar across regions. Nevertheless, Western GCs present molecular signatures regarding inflammation and T cell function, while Asian GCs do not (15–17). Taking into account the selective nature of targeted therapies and immunotherapy, we reasonably infer that the efficacy of various systemic therapies might differ between Asian and Western populations.

Uncovering the discrepancies of survival outcomes and treatment efficacy is critical for clinicians, as they can identify beneficiaries more efficiently and might develop strategies to eliminate disparities. However, the variety and volume of existing studies restrict clinicians to precisely make a judgment. Therefore, in this research, we aimed to quantificationally evaluate whether various systematic therapies exhibit different efficacies in Asian and Western patients with unresectable GC or GEA, measured in terms of OS and PFS. We also attempt to verify the correlation between survival parameters and geographic locality.

2 MATERIALS AND METHODS

2.1 Literature Review and Inclusion Criteria

An electronic literature search with language limited to English was conducted utilizing PubMed-MEDLINE, EMBASE, Web of Science and the Cochrane Library to identify clinical trials published from inception to October ^{31}, 2021. In addition, we reviewed conference abstracts from the Annual Meetings of the American Society of Clinical Oncology (ASCO) and the European Society of Medical Oncology (ESMO) during the last 20 years (2001-2021). Potentially relevant studies were retrieved with their references manually checked. Separately published subgroup analyses were also screened as the supporting data source. Detailed search algorithms are presented in **Supplementary Table 1**. Our meta-analysis followed the Preferred Reporting Items for Systematic Reviews and Meta-analyses (PRISMA) guidelines (18).

Eligibility criteria were as follows: 1) randomized or nonrandomized controlled clinical trials that recruited both Asian and Western patients (defined as patients from North America, Oceania or West/North Europe) with pathologically confirmed unresectable GC or GEA; 2) investigated the clinical benefit of systematic therapies (including chemotherapy, targeted therapy, immunotherapy or any of the combinations); and 3) reported subgroup survival outcomes (OS or PFS) stratified by geographical regions (including Asia). Exclusion criteria were as follows: 1) trials with single-arm design; 2) either Asian or Western participants were not enrolled; 3) subgroup analyses were lacking; 4) non-systemic interventions were investigated (e.g., local radiotherapy, debulking surgery). For trials that did not report subgroup outcomes, we tried to contact the corresponding author for integrated data.

2.2 Overall Design of the Meta-Analysis

The analyses contained two parts. In the first part, a meta-analysis investigating the interregional differences in treatment efficacy was performed. In the second part, OS and PFS between Asian and Western populations with unresectable GC/GEA were compared.

2.3 Data Extraction

Data extraction was performed independently by two investigators, ZZ and ZL. Discrepancies were consulted and resolved by the senior author ZC. Trial name, name of first author, year of publication, treatment regimen, treatment line and the number of participants in each cohort were recorded. Median OS, median PFS, hazard ratios (HRs) for OS and PFS by regional subgroups, and their 95% CIs were extracted.

2.4 Quality Assessment

The quality of enrolled studies was evaluated using the Cochrane Collaboration tool and scored through the following domains: selection bias, performance bias, detection bias, attrition bias, reporting bias and other biases (19). The risk level of each domain was rated as high, low or unclear. Publication bias was evaluated *via* funnel plots.

2.5 Statistical Analysis

First, extracted HRs and CIs from individual studies were pooled utilizing generic inverse variance. In studies that did not have a single "Asia" or "Western" subgroup, we used fixed effect models to generate the pooled estimates of region-specific survival HRs. Then, random effects models were used considering heterogeneity due to different trial designs, and forest plots were generated. Statistically significant heterogeneity was considered when $I^2 > 50\%$. We also conducted an interaction test to determine the correlation of effect modifiers with regions and pooled HRs. Prespecified categories included line of therapy (first-line versus second-line or beyond) and combination strategy (monotherapy versus combination therapy).

Second, the correlation of median OS and median PFS from both experimental and control arms between Asian and Western populations was analyzed using a linear regression model, weighted by the sample size of each comparison. Pearson correlation coefficients (r) and their 95% CIs were calculated. In studies with more than one experimental arm, multiple separate comparisons were conducted.

All meta-analyses were conducted by RevMan 5.3 (The Cochrane Collaboration, Copenhagen, Denmark). Stata 16.0 (StataCorp, Texas, USA) was used for the regression analyses and subsequent graph plotting. All reported *P* values were 2-sided, and statistical significance was defined as $P < 0.05$.

3 RESULTS

3.1 Study Selection and Characteristics

A total of 1654 potentially relevant publications were obtained from the literature search. After initial abstract review and duplicate removal, 20 original studies were considered eligible, comprising 9,033 patients for final analysis (**Figure 1**). The baseline characteristics of the 20 included studies are indicated in **Table 1**.

Seventeen out of 20 studies were phase III clinical trials, and the remaining 3 were phase II trials. In terms of regional distribution, most trials were roughly balanced, while the TRIO-013 and REGARD trials predominantly enrolled Asian and Western participants, respectively. All 20 studies investigated nonconventional therapies: fourteen studies investigated the efficacy of targeted therapy (5 on VEGF, 4 on HER2, 1 on EGFR, 1 on MET, 1 on mTOR, and 1 on AKT); six studies focused on immunotherapy; and only one study explored the efficacy of a cytotoxic agent (TAS-102). Among all studies, eleven investigated first-line therapy, two investigated first-line maintenance therapy, and the remaining 7 were conducted at second- or later-line therapy. All trials were two-arm except KEYNOTE-062, which had a three-arm design.

3.2 Quality Assessments

All clinical trials conducted well-organized random sequence generation and allocation concealment (**Figure S1**). Eight trials did not blind the treatment allocation to participants or personnel, leading to a high risk of performance bias. Blinding of outcome assessment was not implemented in 7 trials, leading to risk of detection bias. No trial was at high risk of attrition and reporting bias. The funnel plots did not suggest significant publication bias (**Figure S2**).

3.3 Quantitative Analyses of the Overall Populations

Eighteen and 9 studies investigated the OS and PFS of systemic therapies stratified by region, respectively. Each of the included studies compared the efficacy of certain types of systemic therapy with standard-of-care treatment. The HRs of individual studies and the pooled results are summarized in **Supplementary Figure 3**. The overall estimated HR for OS among Asian patients was 0.89 with a 95% CI of 0.80–0.99 with nonsignificant heterogeneity (I^2 = 36%, P = 0.06, **Supplementary Figure 3A**), demonstrating an 11% reduction in the hazard of death credited with experimental treatment. Similarly, among Western patients, our meta-analysis indicated that experimental treatment could decrease the risk of death by 14% (HR = 0.86; 95% CI, 0.80–0.93, **Supplementary Figure 3B**) without interstudy heterogeneity (I^2 = 21%, P = 0.20).

The HRs for PFS of the individual studies and the pooled results are summarized in **Supplementary Figure 4**. In contrast with OS, our meta-analysis failed to suggest any survival benefit of experimental treatment versus control in terms of PFS in both Asian and Western patients (HR = 0.71; 95% CI, 0.48–1.04; HR = 0.80; 95% CI, 0.62–1.04 for Asian and Western patients, respectively).

3.4 Comparison of Efficacy Between Asian and Western Patients Stratified by Treatment Type

In view that most of the included studies explored targeted therapy and immunotherapy where HRs for OS stratified by

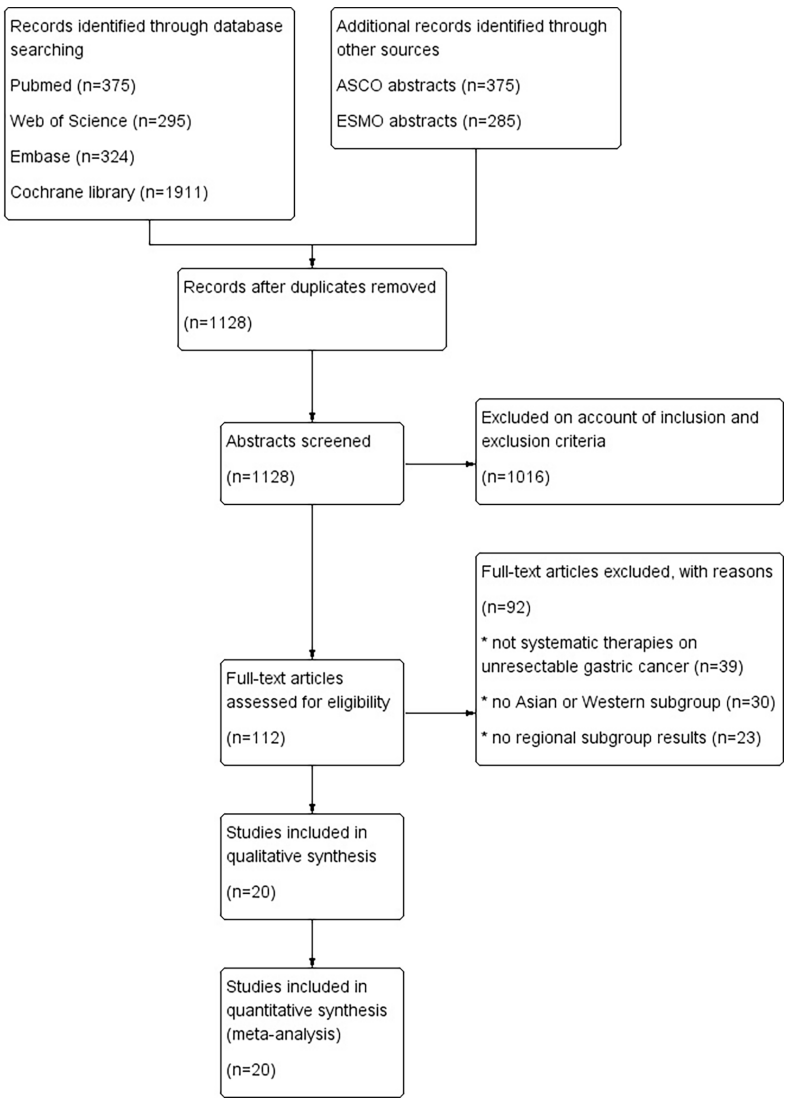

FIGURE 1 | PRISMA flow diagram for the meta-analysis.

region were accessible, we pooled these data to make interregional comparisons classified by treatment categories (**Figure 2**). It should be mentioned that published subgroup data regarding HRs for PFS were incomplete. PFS was generally a secondary endpoint in clinical trials; therefore, the relevant subgroup analyses were frequently unimplemented. In that case, we did not perform the same analyses on PFS.

3.4.1 Immunotherapy: Overall

In the 6 studies focusing on immunotherapy that reported subregional OS, there was no difference in OS between Asian and Western (P for interaction = 0.32) patients (**Figure 2A**). The application of immunotherapy elicited an improvement in OS in both Asians (HR, 0.80; 95% CI, 0.65–0.98) and Westerns (HR, 0.90; 95% CI, 0.81–1.00) compared with controls.

3.4.2 Immunotherapy: Line of Therapy

Among trials investigating immunotherapy, two were conducted in the first-line setting. Further subgroup analysis by treatment line in terms of OS suggested significant interregional differences (**Figure 3**). In the first-line setting, Asians displayed an improved OS (HR, 0.65; 95% CI, 0.53–0.79), while Westerns did not gain such benefit (HR, 0.86; 95% CI, 0.72–1.04), with P for interaction = 0.04 (**Figure 3A**). In regard to second-line treatment or beyond, neither Asian (HR, 0.98; 95% CI, 0.78–1.23) nor Western (HR, 0.92; 95% CI, 0.83–1.06) patients derived survival benefits from immunotherapy (P for interaction = 0.66) (**Figure 3B**).

3.4.3 Immunotherapy: Combination Strategy

Among trials investigating immunotherapy, five investigated monotherapies, while two sought combination therapy

TABLE 1 | Major characteristics of the eligible studies.

No.	Study Name	Year of publication	Name of first author	Treatment line	Phase	No. of Asian patients	No. of Western patients	Experimental arm	Control arm	Constituents of Asian populations	Constituents of Western populations
1	ToGA	2010	Yung-Jue Bang	1	III	319	190	CAPE/5-FU + DDP + Trastuzumab	CAPE/5-FU + DDP	China, Japan, South Korea	Europe
2	AVAGAST	2011	Atsushi Ohtsu	1	III	376	398	5-FU + DDP + BEV	5-FU + DDP	Japan, South Korea	Europe, Pan-America
3	EXPAND	2013	Florian Lordick	1	III	339	490	CAPE + DDP + Cetuximab	CAPE + DDP	South Korea	Europe
4	GRANITE-1	2013	Atsushi Ohtsu	2 or 2+	III	377	241	Everolimus	Placebo	China, Japan, South Korea	West Europe
5	REGARD	2014	Charles S Fuchs	2	III	26	245	RAM	Placebo	South Korea	North America, Europe, Australia, New Zealand
6	RAINBOW	2014	Hansjochen Wilke	2	III	223	398	PTX + RAM	PTX	South Korea, Japan, Taiwan, Hong Kong, Singapore	North America, West Europe
7	INTEGRATE	2016	Nick Pavlakis	1 or 2	II	54	93	Regorafenib	Placebo	South Korea	Canada, Australia, New Zealand
78	TRIO-013	2016	J. Randolph Hecht	1	III	193	17	CAPE + OXA + Lapatinib +	CAPE + OXA	China, South Korea, Hong Kong, Taiwan, Thailand	North America
9	GATSBY	2017	Peter C Thuss-Patience	2	III	157	188	Trastuzumab	PTX	Japan, South Korea	North America, West Europe
10	METGastric	2017	Manish A. Shah	1	III	183	379	5-FU + LV + OXA + Onartuzumab	5-FU + LV + OXA	South Korea, China	North America, Europe
11	N/A	2017	Yung-Jue Bang	1 MN	II	61	51	Ipilimumab	Placebo	South Korea	Europe
12	JACOB	2018	Josep Tabernero	1	III	369	266	Trastuzumab + DDP + CAPE/5-FU + Pertuzumab	Trastuzumab + DDP + CAPE/5-FU	Japan, China, South Korea, Taiwan, Thailand, Malesia	North America, West Europe
13	KEYNOTE-061	2018	Kohei Shitara	2	III	104	263	PEM	PTX	Japan, Hong Kong, South Korea, Taiwan, Malesia	North America, Europe, Australia, Israel
14	TAGS	2018	Kohei Shitara	3 or 3+	III	73	434	TAS-102	Placebo	Japan	North America, Europe
15	JAVELIN Gastric-300	2018	Yung-Jue Bang	3	III	93	278	Avelumab	PTX/IRI/Placebo	Japan, South Korea	Europe, North America, South America
16	RAINFALL	2019	Charles S Fuchs	1	III	69	520	5-FU + DDP + RAM	5-FU + DDP	Japan	Europe, Pan-America
17	N/A	2019	Yung-Jue Bang	1	III	86	67	LV + 5-FU + OXA + Ipatasertib	LV + 5-FU + OXA	South Korea, Singapore	North America, UK
18	KEYNOTE-062	2020	Kohei Shitara	1	III	123	295	DDP + 5-FU/CAPE + PEM	DDP + 5-FU/ CAPE	Japan, South Korea	North America, Europe, Australia
19	JAVELIN Gastric-100	2020	Markus Moehler	1 MN	III	114	385	Avelumab	OXA + LV + 5-FU/CAPE	South Korea, Japan	North America, Europe (majority)
20	CheckMate-649	2020	Markus Moehler	1	III	236	135	OXA + LV + 5-FU/CAPE + NIVO	OXA + LV + 5-FU/CAPE	China, Japan, South Korea, Hong Kong, Taiwan, Singapore	North America

(MN, maintenance; CAPE, capecitabine; DDP, cisplatin; 5-FU, fluorouracil; BEV, bevacizumab; RAM, ramucirumab; PTX, paclitaxel; OXA, oxaliplatin; PEM, pembrolizumab; TAS-102, trifluridine/tipiracil; IRI, irinotecan; LV, leucovorin; NIVO, nivolumab).

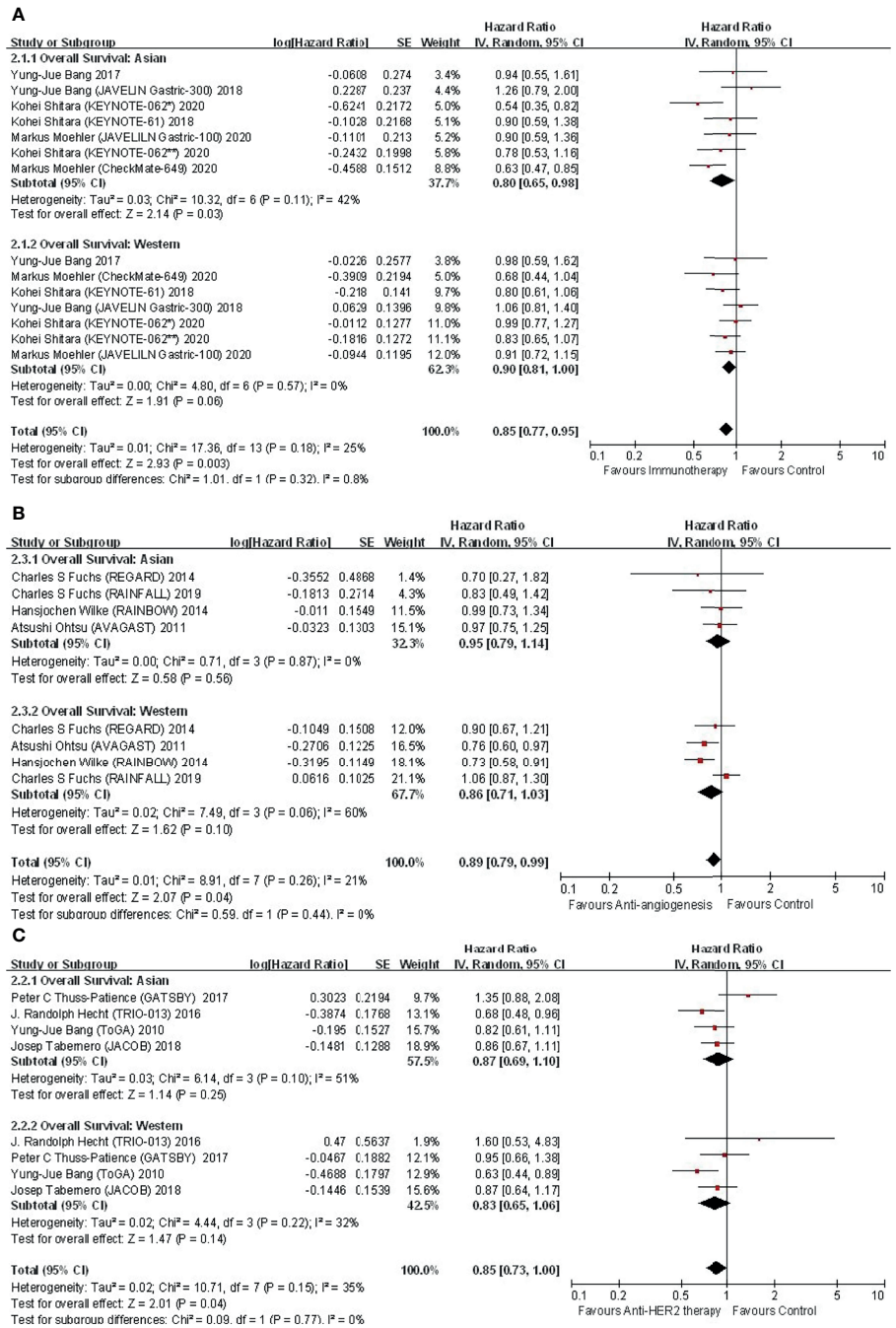

FIGURE 2 | Comparison of regional subgroup differences in OS benefit with **(A)** immunotherapy; **(B)** anti-angiogenic therapy; and **(C)** anti-HER2 therapy.

(immunotherapy or immunotherapy plus chemotherapy were compared with chemotherapy alone in KEYNOTE-062) (**Supplementary Figure 5**). In the monotherapy subgroup, neither Asian (HR, 0.87; 95% CI, 0.66–1.14) nor Western (HR, 0.94; 95% CI, 0.83–1.06) patients exhibited a prolonged OS, indicating limited interregional variance (P for interaction = 0.60). Instead, in the combination subgroup, combination immunotherapy significantly improved OS in both Asian (HR, 0.56; 95% CI, 0.54–0.87) and Western (HR, 0.77; 95% CI, 0.63–0.93) patients (P for interaction = 0.22).

3.4.4 Anti-Angiogenic Therapy: Overall

In the 4 studies focusing on antiangiogenic therapy that reported subgroup data, the OS benefit in Asian and Western patients was

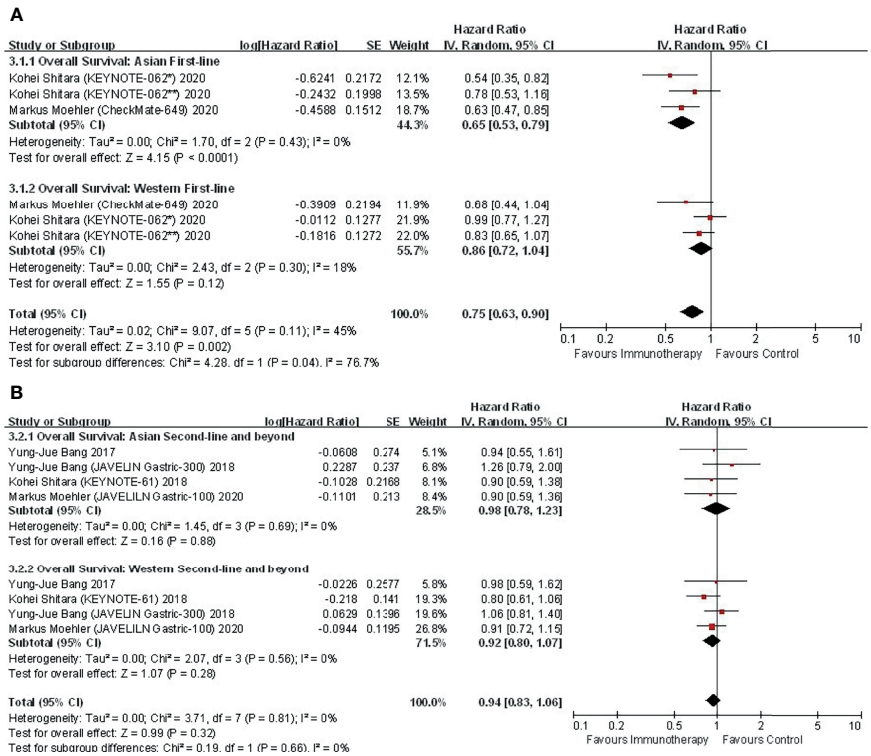

FIGURE 3 | Comparison of regional subgroup differences in OS according to first versus subsequent lines of immunotherapy. **(A)** first-line; **(B)** second-line and beyond.

proportional (P for interaction = 0.44) (**Figure 2B**). Compared with the control, antiangiogenic therapy was not superior in either Asian (HR, 0.95; 95% CI, 0.79–1.14) or Western (HR, 0.86; 95% CI, 0.71–1.03) patients. Nevertheless, a trend of OS benefit with antiangiogenic therapy was shown.

3.4.5 Anti-Angiogenic Therapy: Line of Therapy

Among trials investigating antiangiogenic therapies, two were conducted in the first-line setting, while the remaining two were conducted in the second-line setting (**Supplementary Figure 6**). Neither Asian (HR, 0.94; 95% CI, 0.75–1.19) nor Western (HR, 0.91; 95% CI, 0.66–1.26) patients yielded a survival benefit from first-line treatment (P for interaction = 0.85). In terms of second-line treatment, Western patients receiving antiangiogenic agents indicated prolonged survival (HR, 0.79; 95% CI, 0.64–0.97), while Asians (HR, 0.96; 95% CI, 0.72–1.28) did not, although the interregional difference was not statistically significant (P for interaction = 0.29).

3.4.6 Anti-HER2 Therapy: Overall

In the 4 studies focusing on anti-HER2 therapy that reported subregional OS, anti-HER2 therapy did not significantly improve OS in either Asian (HR, 0.87; 95% CI, 0.69–1.10) or Western (HR, 0.83; 95% CI, 0.65–1.06) populations, although a trend of survival benefit with anti-HER2 therapy versus control was yielded (**Figure 2C**). Interregional disparity was not discovered (P for interaction =0.77). Subgroup analyses were unable to be carried out due to similar designs.

3.5 Comparison and Correlation Between Survival Parameters in Asian and Western Populations

Eleven eligible studies provided 22 pairs of median OS data for Asian and Western patients, consisting of 11 experimental arms and 11 control arms. The bar chart comparing median OS between Asian and Western populations is presented in **Supplementary Figure 7A**. The correlation of the median OS between Asian and Western patients was strong and statistically significant ($r = 0.867$, $p < 0.001$; **Supplementary Figure 7B**). According to the weighted linear regression analysis and the scatter plot, the majority of dots were located beyond the reference line y=x, indicating that Asian patients had a longer OS than Western patients.

Five eligible studies provided 10 pairs of median PFS data for Asian and Western patients, consisting of 5 experimental arms and 5 control arms. The bar chart comparing the median PFS between Asian and Western populations is presented in **Supplementary Figure 8A**. The correlation of the median PFS between Asian and Western patients was strong and statistically significant ($r = 0.942$, $p < 0.001$; **Supplementary Figure 8B**). According to the weighted linear regression analysis and the scatter plot, the dots were uniformly distributed on both sides of

the reference line y=x, suggesting that Asian patients had a similar PFS to Western patients.

4 DISCUSSION

Asian race has long been considered a favorable prognostic factor of late-stage GCs (4, 11, 20). Previous clinical studies mainly considered chemotherapy (11, 21). Nevertheless, as novel treatment means for advanced/metastatic GC/GEA are applied in clinical practice, whether they act consistently between Asian and Western patients remains undefined because confounding factors often impede researchers from making direct comparisons of intertrial numerical data.

This is the first meta-analysis that comprehensively compares the efficacy of multiple therapies in patients with unresectable GC or GEA from different regions. Our meta-analysis of 20 clinical trials indicates that both Asian and Western patients benefit from immunotherapy, anti-HER2, and anti-angiogenic therapies with no interregional differences in efficacy. Nonetheless, Asian patients benefit more from first-line immunotherapy in terms of OS. Asian patients with late-stage GC/GEA also have a remarkably longer OS than their Western counterparts.

The strength of our meta-analysis is the strict inclusion criteria that require both PFS and OS of regional subgroups in global trials, rather than solitary survival data. By pooling regional subgroup data from individual studies, we conducted more reliable comparisons where patients from different districts could be allocated evenly in each trial. Avoidance of direct comparison of survival data from single-site studies also considerably eliminated interstudy heterogeneity.

There are possible explanations for the little interregional differences of therapeutic effects with immunotherapy, anti-HER2 therapy and anti-angiogenic therapy. It has been acknowledged that responses to either immunotherapy or targeted therapy are biomarker determinative. From one perspective, hallmarks such as PD-L1 and HER2 are expressed equivalently among Asian and Western GCs (22). From another perspective, although there might be undiscovered factors exerting an impact on prognosis, the complex regulation system of the tumor microenvironment attenuates their single function. Multiple predictors could counteract one another, leading to similar treatment responses (23, 24).

Interestingly, Asian patients seem to be more sensitive to first-line immunotherapy, as suggested by the pooled results of two large RCTs, CheckMate-649 and KEYNOTE-062, which is in line with data from clinical trials regarding a few other cancer types (25, 26). However, it is challenging to interpret these results.

Previous studies have proposed the regional disparities of GC/GEA in clinicopathological characteristics. Proximal tumors are more common in Western patients, while antral tumors are dominant in Asians (4, 27). For Lauren classification, the proportion of intestinal-type is higher in Asians (4). In regard to molecular subtyping, the distribution proportion of 4 GC subtypes proposed by TCGA (EBV-positive, genomically stable, microsatellite instable and chromosomal instable) is similar in the East and the West, with Korea being an outlier at prominently higher rates of GCs being MSI- or EBV-positive (28–30). However, the somatic mutation or gene amplification rates of several driver genes, including APC, ARIDIA, PIK3CA, PTEN and KRAS, vary greatly across races (31). Genetic polymorphisms and epigenome properties are also regional (32, 33). Reportedly, the presence of certain oncogenic mutations or promotor alternations is associated with resistance to immunotherapy (34–36). In addition, the diversity of dietary structures between Asian and Western regions might affect constituents of gut microbiota, exerting an impact on the efficacy of immunotherapy in gastrointestinal cancers (37, 38). All these factors could account for the interregional disparity in sensitivity to immunotherapy.

On all accounts, the prognosis of GC/GEA should be judged with caution. According to the results of CheckMate-649 and KEYNOTE-062, responses to immunotherapy could not be explained merely by conventional indicators such as PD-L1 level or TMB. These two biomarkers are far from faultless for screening out immunotherapy-sensitive populations. A vast number of patients in CheckMate-649 and KEYNOTE-062 with PD-L1-negative or TMB-low tumors generated anomalous durable responses. Given that antitumor immunity differs across untreated and heavily treated patients, we boldly speculate that an undiscovered Asian signature might reside in a treatment-naïve immune context and favors first-line immunotherapy. This possible ethnic-specific signature could be exploited to assist prognosis stratification together with traditional indicators such as PD-L1 and TMB. From our perspective, the development of new hallmarks for predicting responses to immunotherapy must take into account the unique immunogenomic features that Asian and Western patients do not share (39, 40). As immune checkpoint inhibitors play an increasingly critical role in the treatment of multiple advanced cancers, the correlation between geographic locality and treatment responses warrants further investigations (41).

According to our results, Asian patients with unresectable GC/GEA present a longer OS than Western patients regardless of treatment type, which is highly in accordance with previous records. Intriguingly, PFS is similar across two populations. One possible explanation is that immunotherapy could impose a lasting antitumor effect in treatment-sensitive patients even after radiographic progression, leading to a longer post-progression survival. In addition, Asian patients with advanced/metastatic GC/GEA generally receive more cytotoxic therapies and palliative care after disease progression (evidenced in RAINBOW and AVAGAST trials), possibly contributing to a superior OS among Asians (12, 42). In addition, Asian patients show better baseline physical status than their Western counterparts, which might portend better tolerance and reactivity to subsequent therapies. However, the hypotheses presented above need to be examined in prospective studies with further analyses.

The limitations of our studies are as follows. First, due to the variation of disease prevalence, the definition of "Asian" or "Western" is inconsistent across studies. Although we regrouped the data of each trial, the scope of these two terms was not uniform in the strict sense. Second, eligible studies investigating cytotoxic agents are scarce. On the one hand, the standard treatment regimen of GC/GEA is different between the East and the West. Thus, it is difficult to conduct a chemotherapy trial with the same interventions on participants of different districts. On the other hand, a substantial number of excluded clinical trials did not perform subgroup analyses, making a portion of survival data inaccessible. Third, inclusion criteria with respect to biomarkers differ across studies, which is inevitable but could bias our pooled analyses (e.g., PD-L1 CPS ≥1 or CPS ≥5; HER2 IHC 3+ or 2+).

In conclusion, although Asian and Western patients with unresectable GC/GEA possess different clinical and genetic profiles, they respond similarly to systemic therapies with limited interregional differences. Exceptionally, Asian patients indicate a superior responsiveness to first-line immunotherapy. In addition, Asian patients also present a higher OS, rather than PFS, than Western patients. These results may be implicated in the design of multinational clinical trials. For example, if geographic heterogeneity of drug efficacy is found, research directors are amenable to determine the minimal sample size for each participant district, ensuring consistency of regional outcome in accordance with the global tendencies. This process could tremendously improve work efficiency and conserve resources, including time and funds.

DATA AVAILABILITY STATEMENT

The original contributions presented in the study are included in the article/**Supplementary Material**. Further inquiries can be directed to the corresponding author.

AUTHOR CONTRIBUTIONS

ZZ, ZL, and ZC contributed to conception and design of the study. ZZ and ZL conducted the literature search, extracted the data and performed the statistical analysis. ZZ wrote the first draft of the manuscript. ZL and ZC contributed to manuscript revision, read, and approved the submitted version.

SUPPLEMENTARY MATERIAL

The Supplementary Material for this article can be found online at: https://www.frontiersin.org/articles/10.3389/fonc.2022.831207/full#supplementary-material

Supplementary Figure 1 | Risk of bias summary **(A)** and bias graph **(B).**

Supplementary Figure 2 | Funnel plots: OS **(A)** and PFS **(B)** in Asian populations; OS **(C)** and PFS **(D)** in Western populations.

Supplementary Figure 3 | HRs of OS in patients receiving systemic therapies versus controls in Asian and Western populations. Each study was shown by the study name and year of publication. For each trial, the position of the square denoted the HR value, horizontal lines represented 95% CIs, and diamond plots represented overall results. **(A)** HRs of OS in the Asian population; **(B)** HRs of OS in Western patients.

Supplementary Figure 4 | Hazard ratios of PFS in patients receiving exploratory therapies versus controls in Asian and Western populations. Each study was shown by the study name and year of publication. For each trial, the position of the square denoted the HR value, horizontal lines represented 95% CIs, and diamond plots represented overall results. **(A)** HRs of PFS in the Asian population; **(B)** HRs of PFS in Western patients.

Supplementary Figure 5 | Comparison of regional subgroup differences in OS according to single versus combination immunotherapy. **(A)** monotherapy; **(B)** combination therapy.

Supplementary Figure 6 | Comparison of regional subgroup differences in OS according to first versus subsequent lines of antiangiogenic therapy. **(A)** first-line; **(B)** second-line.

Supplementary Figure 7 | Bar chart **(A)** and scatter plot with linear regression analysis **(B)** of median OS between Asian and Western patients. Pearson correlation coefficients (r) and correlation equations are shown. The red line represents the reference line y=x, suggesting equivalent OS between Asian and Western patients.

Supplementary Figure 8 | Bar chart **(A)** and scatter plot with linear regression analysis **(B)** of median PFS between Asian and Western patients. Pearson correlation coefficients (r) and correlation equations are shown. The red line represents the reference line y=x, suggesting equivalent PFS between Asian and Western patients.

REFERENCES

1. Sung H, Ferlay J, Siegel RL, Laversanne M, Soerjomataram I, Jemal A, et al. Global Cancer Statistics 2020: GLOBOCAN Estimates of Incidence and Mortality Worldwide for 36 Cancers in 185 Countries. *CA Cancer J Clin* (2021) 71:209–49. doi: 10.3322/caac.21660
2. Yamaoka Y, Kato M, Asaka M. Geographic Differences in Gastric Cancer Incidence can be Explained by Differences Between Helicobacter Pylori Strains. *Intern Med* (2008) 47:1077–83. doi: 10.2169/internalmedicine.47.0975
3. Wagner AD, Syn NL, Moehler M, Grothe W, Yong WP, Tai B-C, et al. Chemotherapy for Advanced Gastric Cancer. *Cochrane Database Syst Rev* (2017) 8:D4064. doi: 10.1002/14651858.CD004064.pub4
4. Russo AE, Strong VE. Gastric Cancer Etiology and Management in Asia and the West. *Annu Rev Med* (2019) 70:353–67. doi: 10.1146/annurev-med-081117-043436
5. Baden LR, Swaminathan S, Angarone M, Blouin G, Camins BC, Casper C, et al. Prevention and Treatment of Cancer-Related Infections, Version 2.2016, NCCN Clinical Practice Guidelines in Oncology. *J Natl Compr Canc Netw* (2016) 14:882–913. doi: 10.6004/jnccn.2016.0093
6. Wei SC, Duffy CR, Allison JP. Fundamental Mechanisms of Immune Checkpoint Blockade Therapy. *Cancer Discovery* (2018) 8:1069–86. doi: 10.1158/2159-8290.CD-18-0367
7. Oono Y, Kuwata T, Takashima K, Shinmura K, Hori K, Yoda Y, et al. Human Epidermal Growth Factor Receptor 2-, Epidermal Growth Factor Receptor-, and Mesenchymal Epithelial Transition Factor-Positive Sites of Gastric Cancer Using Surgical Samples. *Gastric Cancer* (2019) 22:335–43. doi: 10.1007/s10120-018-0853-7
8. Huang Y, Yuan J, Righi E, Kamoun WS, Ancukiewicz M, Nezivar J, et al. Vascular Normalizing Doses of Antiangiogenic Treatment Reprogram the Immunosuppressive Tumor Microenvironment and Enhance

Immunotherapy. *Proc Natl Acad Sci USA* (2012) 109:17561–6. doi: 10.1073/pnas.1215397109
9. Shitara K, Honma Y, Omuro Y, Yamaguchi K, Chin K, Muro K, et al. Efficacy of Trastuzumab Emtansine in Japanese Patients With Previously Treated HER2-Positive Locally Advanced or Metastatic Gastric or Gastroesophageal Junction Adenocarcinoma: A Subgroup Analysis of the GATSBY Study. *Asia Pac J Clin Oncol* (2020) 16:5–13. doi: 10.1111/ajco.13243
10. Satoh T, Xu R, Chung HC, Sun G-P, Doi T, Xu J-M, et al. Lapatinib Plus Paclitaxel Versus Paclitaxel Alone in the Second-Line Treatment of HER2-Amplified Advanced Gastric Cancer in Asian Populations: TyTAN–a Randomized, Phase III Study. *J Clin Oncol* (2014) 32:2039–49. doi: 10.1200/JCO.2013.53.6136
11. Zhang G, Zhao X, Li J, Yuan Y, Wen M, Hao X, et al. Racial Disparities in Stage-Specific Gastric Cancer: Analysis of Results From the Surveillance Epidemiology and End Results (SEER) Program Database. *J Investig Med* (2017) 65:991–8. doi: 10.1136/jim-2017-000413
12. Sawaki A, Yamada Y, Yamaguchi K, Nishina T, Doi T, Satoh T, et al. Regional Differences in Advanced Gastric Cancer: Exploratory Analyses of the AVAGAST Placebo Arm. *Gastric Cancer* (2018) 21:429–38. doi: 10.1007/s10120-017-0773-y
13. Chung HC, Kok VC, Cheng R, Hsu Y, Orlando M, Fuchs C, et al. Subgroup Analysis of East Asian Patients in REGARD: A Phase III Trial of Ramucirumab and Best Supportive Care for Advanced Gastric Cancer. *Asia Pac J Clin Oncol* (2018) 14:204–9. doi: 10.1111/ajco.12829
14. Muro K, Oh SC, Shimada Y, Lee K-W, Yen C-J, Chao Y, et al. Subgroup Analysis of East Asians in RAINBOW: A Phase 3 Trial of Ramucirumab Plus Paclitaxel for Advanced Gastric Cancer. *J Gastroenterol Hepatol* (2016) 31:581–9. doi: 10.1111/jgh.13153
15. Cancer Genome Atlas Research NetworkComprehensive Molecular Characterization of Gastric Adenocarcinoma. *Nature* (2014) 513:202–9. doi: 10.1038/nature13480
16. Lin SJ, Gagnon-Bartsch JA, Tan IB, Earle S, Ruff L, Pettinger K, et al. Signatures of Tumour Immunity Distinguish Asian and Non-Asian Gastric Adenocarcinomas. *Gut* (2015) 64:1721–31. doi: 10.1136/gutjnl-2014-308252
17. van Grieken NCT, Aoyama T, Aoyma T, Chambers PA, Bottomley D, Ward LC, et al. KRAS and BRAF Mutations are Rare and Related to DNA Mismatch Repair Deficiency in Gastric Cancer From the East and the West: Results From a Large International Multicentre Study. *Br J Cancer* (2013) 108:1495–501. doi: 10.1038/bjc.2013.109
18. Liberati A, Altman DG, Tetzlaff J, Mulrow C, Gøtzsche PC, Ioannidis JPA, et al. The PRISMA Statement for Reporting Systematic Reviews and Meta-Analyses of Studies That Evaluate Healthcare Interventions: Explanation and Elaboration. *BMJ* (2009) 339:b2700. doi: 10.1136/bmj.b2700
19. Higgins JPT, Altman DG, Gøtzsche PC, Jüni P, Moher D, Oxman AD, et al. The Cochrane Collaboration's Tool for Assessing Risk of Bias in Randomised Trials. *BMJ* (2011) 343:d5928. doi: 10.1136/bmj.d5928
20. Kim J, Sun C-L, Mailey B, Prendergast C, Artinyan A, Bhatia S, et al. Race and Ethnicity Correlate With Survival in Patients With Gastric Adenocarcinoma. *Ann Oncol* (2010) 21:152–60. doi: 10.1093/annonc/mdp290
21. Hsu C, Shen Y-C, Cheng C-C, Cheng A-L, Hu F-C, Yeh K-H, et al. Geographic Difference in Safety and Efficacy of Systemicchemotherapy for Advanced Gastric or Gastroesophagealcarcinoma: A Meta-Analysis and Meta-Regression. *Gastric Cancer* (2012) 15:265–80. doi: 10.1007/s10120-011-0106-5
22. Van Cutsem E, Bang Y, Feng-Yi F, Xu JM, Lee K-W, Jiao S-C, et al. HER2 Screening Data From ToGA: Targeting HER2 in Gastric and Gastroesophageal Junction Cancer. *Gastric Cancer* (2015) 18:476–84. doi: 10.1007/s10120-014-0402-y
23. Montfort A, Colacios C, Levade T, Andrieu-Abadie N, Meyers N, Ségui B, et al. The TNF Paradox in Cancer Progression and Immunotherapy. *Front Immunol* (2019) 10:1818. doi: 10.3389/fimmu.2019.01818
24. Barham W, Gicobi JK, Yan Y, Dronca RS, Dong H. Paradox-Driven Adventures in the Development of Cancer Immunology and Immunotherapy. *Genes Dis* (2019) 6:224–31. doi: 10.1016/j.gendis.2019.07.001
25. Kiyota N, Hasegawa Y, Takahashi S, Yokota T, Yen C-J, Iwae S, et al. A Randomized, Open-Label, Phase III Clinical Trial of Nivolumab vs. Therapy of Investigator's Choice in Recurrent Squamous Cell Carcinoma of the Head and Neck: A Subanalysis of Asian Patients Versus the Global Population in Checkmate 141. *Oral Oncol* (2017) 73:138–46. doi: 10.1016/j.oraloncology.2017.07.023
26. Nishio M, Sugawara S, Atagi S, Akamatsu H, Sakai H, Okamoto I, et al. Subgroup Analysis of Japanese Patients in a Phase III Study of Atezolizumab in Extensive-Stage Small-Cell Lung Cancer (Impower133). *Clin Lung Cancer* (2019) 20:469–76. doi: 10.1016/j.cllc.2019.07.005
27. Wang J, Sun Y, Bertagnolli MM. Comparison of Gastric Cancer Survival Between Caucasian and Asian Patients Treated in the United States: Results From the Surveillance Epidemiology and End Results (SEER) Database. *Ann Surg Oncol* (2015) 22:2965–71. doi: 10.1245/s10434-015-4388-4
28. Liao P, Jia F, Teer JK, Knepper C, Zhou H-H, He Y-J, et al. Geographic Variation in Molecular Subtype for Gastric Adenocarcinoma. *Gut* (2019) 68:1340–1. doi: 10.1136/gutjnl-2018-316605
29. Sohn BH, Hwang J-E, Jang H-J, Lee H-S, Oh SC, Shim J-J, et al. Clinical Significance of Four Molecular Subtypes of Gastric Cancer Identified by The Cancer Genome Atlas Project. *Clin Cancer Res* (2017) 23:4441–9. doi: 10.1158/1078-0432.CCR-16-2211
30. Furukawa K, Hatakeyama K, Terashima M, Nagashima T, Urakami K, Ohshima K, et al. Molecular Classification of Gastric Cancer Predicts Survival in Patients Undergoing Radical Gastrectomy Based on Project HOPE. *Gastric Cancer* (2022) 25:138–48. doi: 10.1007/s10120-021-01242-0
31. Jia F, Teer JK, Knepper TC, Lee JK, Zhou H-H, He Y-J, et al. Discordance of Somatic Mutations Between Asian and Caucasian Patient Populations With Gastric Cancer. *Mol Diagn Ther* (2017) 21:179–85. doi: 10.1007/s40291-016-0250-z
32. Loh M, Koh KX, Yeo BH, Song CM, Chia KS, Zhu F, et al. Meta-Analysis of Genetic Polymorphisms and Gastric Cancer Risk: Variability in Associations According to Race. *Eur J Cancer* (2009) 45:2562–8. doi: 10.1016/j.ejca.2009.03.017
33. Mocellin S, Verdi D, Pooley KA, Nitti D. Genetic Variation and Gastric Cancer Risk: A Field Synopsis and Meta-Analysis. *Gut* (2015) 64:1209–19. doi: 10.1136/gutjnl-2015-309168
34. Hastings K, Yu HA, Wei W, Sanchez-Vega F, DeVeaux M, Choi J, et al. EGFR Mutation Subtypes and Response to Immune Checkpoint Blockade Treatment in Non-Small-Cell Lung Cancer. *Ann Oncol* (2019) 30:1311–20. doi: 10.1093/annonc/mdz141
35. Zaretsky JM, Garcia-Diaz A, Shin DS, Escuin-Ordinas H, Hugo W, Hu-Lieskovan S, et al. Mutations Associated With Acquired Resistance to PD-1 Blockade in Melanoma. *N Engl J Med* (2016) 375:819–29. doi: 10.1056/NEJMoa1604958
36. Sundar R, Huang KK, Qamra A, Kim K-M, Kim ST, Kang WK, et al. Epigenomic Promoter Alterations Predict for Benefit From Immune Checkpoint Inhibition in Metastatic Gastric Cancer. *Ann Oncol* (2019) 30:424–30. doi: 10.1093/annonc/mdy550
37. Peng Z, Cheng S, Kou Y, Wang Z, Jin R, Hu H, et al. The Gut Microbiome is Associated With Clinical Response to Anti-PD-1/PD-L1 Immunotherapy in Gastrointestinal Cancer. *Cancer Immunol Res* (2020) 8:1251–61. doi: 10.1158/2326-6066.CIR-19-1014
38. Garajová I, Balsano R, Wang H, Leonardi F, Giovannetti E, Deng D, et al. The Role of the Microbiome in Drug Resistance in Gastrointestinal Cancers. *Expert Rev Anticancer Ther* (2021) 21:165–76. doi: 10.1080/14737140.2021.1844007
39. Mao C, Ma L, Huang Y, Yang X, Huang H, Cai W, et al. Immunogenomic Landscape and Immune-Related Gene-Based Prognostic Signature in Asian Gastric Cancer. *Front Oncol* (2021) 11:750768. doi: 10.3389/fonc.2021.750768
40. Zeng D, Wu J, Luo H, Li Y, Xiao J, Peng J, et al. Tumor Microenvironment Evaluation Promotes Precise Checkpoint Immunotherapy of Advanced Gastric Cancer. *J Immunother Cancer* (2021) 9:e002467. doi: 10.1136/jitc-2021-002467
41. Ayers KL, Mullaney T, Zhou X, Liu JJ, Lee K, Ma M, et al. Analysis of Real-World Data to Investigate the Impact of Race and Ethnicity on Response to Programmed Cell Death-1 and Programmed Cell Death-Ligand 1 Inhibitors in Advanced Non-Small Cell Lung Cancers. *Oncologist* (2021) 26:e1226–39. doi: 10.1002/onco.13780
42. Shitara K, Muro K, Shimada Y, Hironaka S, Sugimoto N, Komatsu Y, et al. Subgroup Analyses of the Safety and Efficacy of Ramucirumab in Japanese and Western Patients in RAINBOW: A Randomized Clinical Trial in Second-Line Treatment of Gastric Cancer. *Gastric Cancer* (2016) 19:927–38. doi: 10.1007/s10120-015-0559-z

Conflict of Interest: The authors declare that the research was conducted in the absence of any commercial or financial relationships that could be construed as a potential conflict of interest.

Publisher's Note: All claims expressed in this article are solely those of the authors and do not necessarily represent those of their affiliated organizations, or those of the publisher, the editors and the reviewers. Any product that may be evaluated in

this article, or claim that may be made by its manufacturer, is not guaranteed or endorsed by the publisher.

Copyright © 2022 Zhang, Liu and Chen. This is an open-access article distributed under the terms of the Creative Commons Attribution License (CC BY). The use, distribution or reproduction in other forums is permitted, provided the original author(s) and the copyright owner(s) are credited and that the original publication in this journal is cited, in accordance with accepted academic practice. No use, distribution or reproduction is permitted which does not comply with these terms.

frontiers in Oncology

ORIGINAL RESEARCH
published: 08 March 2022
doi: 10.3389/fonc.2022.852559

Conversion Surgery in Gastric Cancer Carcinomatosis

Paolo Morgagni[1], Leonardo Solaini[1,2], Luca Saragoni[3], Manlio Monti[4], Martina Valgiusti[4], Giovanni Vittimberga[1], Giovanni Luca Frassineti[4], Massimo Framarini[1] and Giorgio Ercolani[1,2]*

[1] General and Oncologic Surgery, "Morgagni-Pierantoni" Hospital, Forlì, Italy, [2] Department of Medical and Surgical Sciences, University of Bologna, Bologna, Italy, [3] Pathology Unit, "Morgagni-Pierantoni" Hospital, Forlì, Italy, [4] Department of Medical Oncology, IRCCS Istituto Romagnolo per lo Studio dei Tumori (IRST) "DinoAmadori", Meldola, Italy

Background: After the REGATTA trial, patients with stage IV gastric cancer could only benefit from chemotherapy (CHT). However, some of these patients may respond extraordinarily to palliative chemotherapy, converting their disease to a radically operable stage. We present a single centre experience in treating peritoneal carcinomatosis from gastric cancer.

Methods: All patients with stage IV gastric cancer with peritoneal metastases as a single metastatic site operated at a single centre between 2005 and 2020 were included. Cases were grouped according to the treatment received.

Results: A total of 118 patients were considered, 46 were submitted to palliative gastrectomy (11 were considered M1 because of an unsuspected positive peritoneal cytology), and 20 were submitted to Hyperthermic Intraperitoneal Chemotherapy (HIPEC) because of a <6 Peritoneal Cancer Index (PCI). The median overall survival (OS) after surgery plus HIPEC was 46.7 (95% CI 15.8–64.0). Surgery (without HIPEC) after CHT presented a median OS 14.4 (8.2–26.8) and after upfront surgery 14.7 (10.9–21.1). Patients treated with upfront surgery and considered M1 only because of a positive cytology, had a median OS of 29.2 (25.2–29.2). The OS of patients treated with surgery plus HIPEC were 60.4 months (9.2–60.4) in completely regressed cancer after chemotherapy and 31.2 (15.8–64.0) in those partially regressed ($p = 0.742$).

Conclusions: Conversion surgery for peritoneal carcinomatosis from gastric cancer was associated with long survival and it should always be taken into consideration in this group of patients.

Keywords: gastric cancer, conversion surgery, HIPEC, positive peritoneal cytology, metastatic disease

OPEN ACCESS

Edited by:
Luigi Marano, University of Siena, Italy

Reviewed by:
Fausto Rosa, Catholic University of the Sacred Heart, Rome, Italy
Chukwuemeka Ihemelandu, MedStar Washington Hospital Center, United States

***Correspondence:**
Manlio Monti
manlio.monti@irst.emr.it

Specialty section:
This article was submitted to Gastrointestinal Cancers: Gastric and Esophageal Cancers, a section of the journal Frontiers in Oncology

Received: *11 January 2022*
Accepted: *08 February 2022*
Published: *08 March 2022*

Citation:
Morgagni P, Solaini L, Saragoni L, Monti M, Valgiusti M, Vittimberga G, Frassineti GL, Framarini M and Ercolani G (2022) Conversion Surgery in Gastric Cancer Carcinomatosis. Front. Oncol. 12:852559. doi: 10.3389/fonc.2022.852559

INTRODUCTION

Peritoneal carcinomatosis is the most frequent metastatic site in gastric cancer (1). The findings from the REGATTA trial (2) indicate that patients with stage IV gastric cancer could only benefit from chemotherapy, regardless of the metastatic site; however, in other studies, these patients may respond extraordinarily to palliative chemotherapy, converting their disease to a radically operable stage (3) and showing promising results in a much selected group (3–8).

Considering the peritoneal metastatic site, a radical procedure associated with Hyperthermic Intraperitoneal Chemotherapy (HIPEC) seemed to be a valuable option to improve survival (6). However, the Japanese PHOENIX trial, which reported results comparing intraperitoneal/intravenous versus intravenous preoperative treatment failed to find significant differences between these procedures (9).

Interestingly, there is a different approach to HIPEC or conversion surgery by Eastern and Western authors; whereas Eastern authors presented studies where gastrectomy was proposed after chemotherapy and only if a second laparoscopy could confirm the absence of carcinomatosis, the Western ones considered HIPEC in cases which presented a minimal carcinomatosis [peritoneal cancer index (PCI) <6)] after palliative chemotherapy (10).

In this context, this study aims to present an Italian single center experience on patients with peritoneal carcinomatosis as the single metastatic site.

MATERIAL AND METHODS

Patient Recruitment

Between 2005 and 2020, 913 patients were operated on for gastric cancer at the "Morgagni-Pierantoni" General Hospital, in Forlì. Of these, 118 presented peritoneal metastases as a single metastatic site. These cases were all regularly discussed at multidisciplinary meetings during which different approaches were explored from the upfront surgery to conversion according to the guidelines in force at that time

These 118 patients were grouped according to the treatment received: a) patients submitted to upfront surgery and b) patients submitted to palliative chemotherapy and then surgically re-evaluated for resection alone or resection plus HIPEC (11). The peritoneal status was measured with the PCI. Patients with non-peritoneal distant metastases were excluded. Morbidity was classified in accordance with the Clavien–Dindo classification (12).

All surgically treated patients were then submitted to post-operative chemotherapy. Tumor stage was presented according to the Union for International Cancer Control (UICC)/ American Joint Committee on Cancer (AJCC) (13).

All procedures performed in this study were in accordance with the ethical standard of the Area Vasta Romagna Ethics Committee (approval n° 5707/2020-I.5/264 on July 3, 2020), with the 1964 Declaration of Helsinki and its later amendments, and with the Good Clinical Practice (GCP) guidelines. Informed consent from patients was collected as instructed.

Statistical Analysis

Continuous data was presented as the median and interquartile range (IQR). Fisher's exact test was used to compare categorical variables which were presented as numbers and percentages. The Kaplan–Meier curve was used to calculate survival rates, and differences in survival rates between subgroups were assessed by the log-rank test. Overall survival was defined as the time between surgery and death or last follow-up. The median follow-up and IQR was found using the Kaplan–Meier function as suggested by Schemper and Smith (14). A 95% confidence interval (CI) was reported when required. Analyses were performed with MedCalc® for Windows® (version 10.2.0.0; MedCalc Software, Ostend, Belgium).

RESULTS

In total, 118 patients with peritoneal carcinomatosis as the exclusive metastatic site were included in the study. The type of treatment received is shown in the flow-chart, **Figure 1**. Clinicopathological characteristics and operative details are presented in **Table 1**.

Of the 79 patients treated with upfront surgery, 33 received only an exploratory laparoscopy because of diffuse carcinomatosis, and 46 had palliative gastrectomy. Eleven of these upfront surgery patients were considered M1 only because of a positive peritoneal cytology without macroscopic carcinomatosis (**Figure 1**).

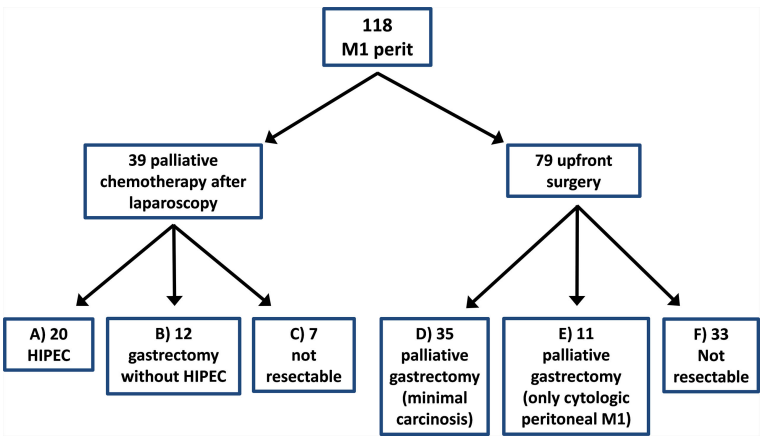

FIGURE 1 | Flow-chart shows the types of treatment.

TABLE 1 | Patients' characteristics.

Variables	Palliative CT+ HIPEC (No. = 20)	CT+ surgery No. = 12	Upfront surgery No. = 46	Explorative laparotomy No. = 40
Gender				
Male	13	8	34	22
Female	7	4	12	18
Age	61.05 (range 29–78)	66.5 (range 53–77)	76.7 (range 61–90)	67.7 (range 37–89)
T stage				
cT2	0	1	–	–
cT3	2	0	–	–
cT4a	15	10	–	–
cT4b	3	1	–	–
yT0	3	1	0	0
yT1	3	0	0	0
yT2	1	0	0	0
yT3	4	4	10	0
yT4a	9	6	32	13
yT4b	0	1	4	27
N stage				
cN0	0	2	–	–
cN+	11	7	–	–
Nx	9	3	–	–
yN0	8	3	1	–
yN1	4	3	6	–
yN2	3	1	8	–
yN3a	2	3	14	–
yN3b	3	2	17	–
Lauren histotype				
Intestinal	14	5	26	20
Diffuse	3	6	15	20
Mixed	3	1	5	
Site				
cardias	5	–	9	7
fundus	3	1	6	4
corpus	4	4	8	11
antrum	6	5	18	10
all	2	2	5	10
Regression (Becker)				
1a	3	0	–	–
1b	4	3	–	–
2	3	1	–	–
3	10	8	–	–
Gastrectomy				
Subtotal	5	4	20	0
Total	15	8	26	0
Explorative	0	0	0	40
Cytology				
Pretreatment pos	20	2	–	–
Pretreatment neg	0	4	–	–
Pretreatment Not det	0	6	–	–
Surgery pos	10	4	16	18
Surgery neg	10	5	4	2
Surgery not det	0	3	26	20

Thirty-nine patients were submitted to an explorative approach and then proposed for oncologic treatment before re-evaluation. Induction chemotherapy included FOLFOX (5-fluorouracile, leucovorin ed oxaliplatin) in 12 cases (30.8%), PELF (Cisplatin, Epirubicin, Leukovorin, 5-Fluoruracil) in 12 (30.8%), FLOT (Fluorouracil, Leucovorin, Oxaliplatin and Docetaxel) in 11 (28.2%) and other different treatments in the remaining 4 cases (10.2%). At re-evaluation, twenty of these were found as partially (n = 10) or totally regressed (n = 10) and were submitted to surgery plus HIPEC; twelve patients were submitted to palliative surgery and seven could not be operated on because of progression during treatment.

Clavien–Dindo >2 complications rate was 20.0 (n = 4) in patients treated with HIPEC and 13 (37.1%) in patients who had upfront surgery (p = 0.234). Mortality was similar between the groups (1 death after pancreatitis and leakage vs. 2 deaths due to leakage/bleeding and perforation).

Kaplan–Meier curves are shown in **Figure 2**. Patients who had surgery plus HIPEC after chemotherapy had a median OS of 46.7

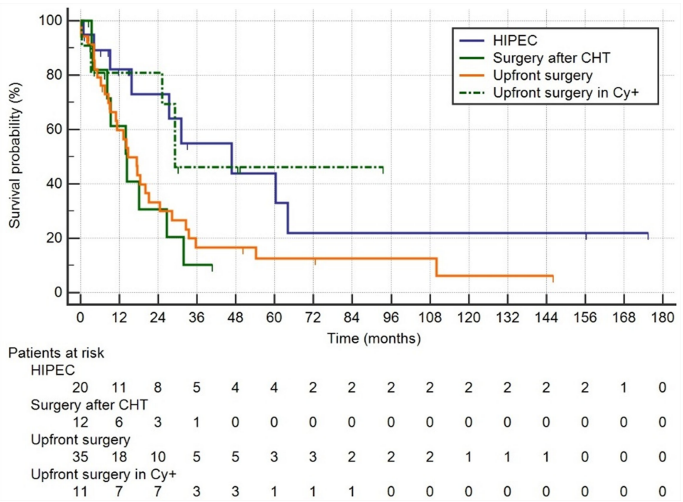

FIGURE 2 | Group1: HIPEC, palliative chemotherapy followed by surgery plus HIPEC; Group 2: surgery after CTH without HIPEC; Group 3: upfront surgery; Group 4: upfront surgery in positive Cy+ only.

months (95% CI 15.8–64.0), those who had surgery after CHT 14.4 (8.2–26.8), those after upfront surgery 14.7 (10.9–21.1), and finally those who had upfront surgery for positive peritoneal cytology had a median survival of 29.2 months (14.7–29.2) (p = 0.050). Median follow-up was 50 months (IQR 15–110).

Among the 20 patients who had R0 surgery plus HIPEC median survival was 60.4 (9.2–60.4) months in the group (n = 10) who had surgery plus HIPEC after a complete regression of peritoneal carcinomatosis (and peritoneal cytology) following chemotherapy (CR-HIPEC) versus 31.2 (15.8–64.0) in the patients (n = 10) who had a PCI <6 or positive peritoneal cytology after chemotherapy followed by surgery plus HIPEC (PR-HIPEC) (p = 0.742) (**Figure 3**).

DISCUSSION

The treatment of peritoneal carcinomatosis from gastric cancer represents the most challenging and intriguing treatment frontier and only a multidisciplinary approach may help in achieving the best results.

In 2016, Yoshida et al. classified all metastatic patients into four classes, differentiating macroscopic peritoneal involvement

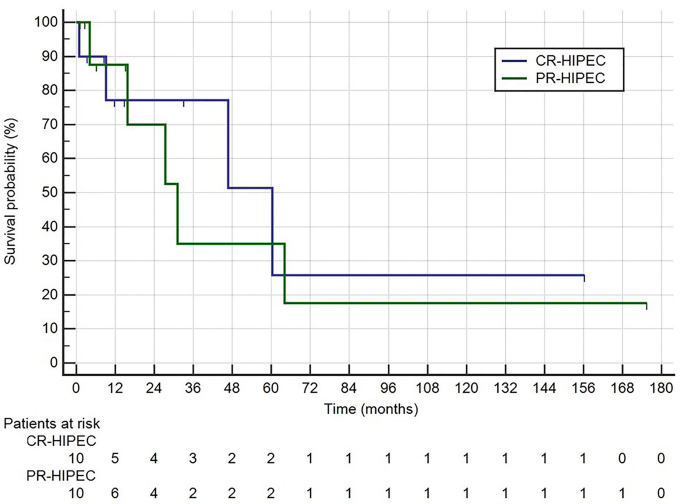

FIGURE 3 | Survival rates for Group 1: CR-HIPEC, completely regressed followed by surgery plus HIPEC; Group 2: PR-HIPEC, partially regressed followed by surgery plus HIPEC.

or not, and proposing conversion surgery especially for patients without peritoneal involvement (3). The worst results, nonetheless, sometimes gave positive outcomes, as observed by the same author in a selected group of patients with peritoneal involvement with a median survival time of 31.0 for category three (previously unresectable except for local palliation) and 24.7 for category four (previously non curable metastases) (15).

The Korean and Japanese REGATTA trial indicated only chemotherapy for stage IV, and this is currently proposed in Korean guidelines (16).

In Japan some patients can be considered for surgery after chemotherapy and some promising results have been reported with conversion surgery after S1 or intraperitoneal paclitaxel; Yasufuku et al. reported a three-year survival rate of 76.9% in positive cytology patients (4), and Ishigami et al. reported 30.5 months median survival time after chemotherapy and preoperative HIPEC (5).

Unfortunately, in the West, gastric cancer treatments without the S1 option were associated with the worst results. Peritoneum represents a sort of barrier for chemotherapy and its involvement cannot be approached using conventional treatments. Rau et al., showed a median survival of 18 months in patients treated with surgery plus HIPEC (6) and Passot et al. showed similar results (17).

This poor prognosis is generally due to late diagnosis; early stage carcinomatosis, which could give some hope for cure, is difficult to be diagnosed as staging laparoscopy, which can help in defining the peritoneal involvement, is rarely performed.

Moreover, peritoneal carcinomatosis can be associated with other hidden metastatic sites often not detected at diagnosis and these metastases cannot be cured with a local peritoneal treatment.

Intraperitoneal hyperthermic chemotherapy failed to show clear benefits in patients with massive involvement and its use has also been discussed for gastric cancer at early stages (10).

In the Japanese trial PHOENIX, HIPEC was preoperatively proposed as intraperitoneal weekly chemotherapy through a port associated with intravenous treatment. In the second arm of this trial, patients received only intravenous chemotherapy; results did not find any advantages for preoperative HIPEC.

Of the specific treatments proposed such as HIPEC, bidirectional, and PIPAC, these probably present some results only for a subset of patients; for the other patients there is sometimes only a lesser amount of ascites (9, 18).

Our experience collected patients over a long period of time and some of the approaches were changed; in the last ten years, we generally proposed HIPEC for a very selected group of patients with positive cytology or small carcinomatosis detected at laparoscopy and always performed before preoperative treatment.

All the patients were firstly submitted to systemic palliative chemotherapy, generally with FOLFOX treatment and this was usually performed by our oncologist for metastatic treatment. This approach, which postponed surgery for a median of 3 months, improved the selection of those patients with rapidly advancing cancer by treating them only with chemotherapy and avoiding unnecessary surgery.

Responder patients if not R0, but potentially radically resectable with a PCI <6, were submitted to surgical treatment with gastrectomy and HIPEC.

The most interesting result of our study was that survival rates after HIPEC did not significantly differ from patients submitted to surgery and completely regressed after palliative preoperative treatment and those patients operated on even if with only a few carcinomatosis, that is: if R0 could be reached, HIPEC was also proposed to patients with small areas of resectable carcinomatosis. These patients presented results as good as those completely regressed after preoperative chemotherapy.

This approach is completely different from the Asian experience which recommended surgery only to patients with complete regression and it also differs from some Western experiences, which presented extended indications for surgery plus HIPEC (10).

Another surprising result was the good survival rates of patients with positive cytology treated without HIPEC, but with upfront surgery. These patients presented promising outcomes with a median survival of 29.2 months (14.7–29.2).

Considering patients M1 only because of peritoneal positive cytology, good survival rates have been presented also by other authors: in 2019, Kim et al. proposed to classify positive cytology in a particular subset with massive lymphatic involvement (N3b) patients because of unlike other stage IV carcinosis; these patients present similar survival rates (19).

Even if we generally think that patients with advanced carcinomatosis may be better treated with oncologic treatment as proposed by the Korean REGATTA trial, we could, perhaps, select a subset of patients suitable for good surgical results by using a real multimodal approach.

Our study has a few limitations. First, it is a retrospective study and it carries the bias linked to its nature. Second, during the fifteen year-long study interval, several major changes in the management of stage IV gastric cancer have been introduced and this resulted in the heterogeneity of treatment seen in our analysis. As such, staging laparoscopy was not routinely performed as it was after 2013 (20, 21) and this may have had an impact on the type of treatment received. Finally, it must be observed that the upfront surgery group may have included a higher rate of symptomatic cases and/or elderly patients who were not fit for preoperative treatment. Those factors should be taken into account in the interpretation of the survival curves.

CONCLUSION

Prognosis in peritoneal metastasis is generally poor; however, the good results observed in the HIPEC subset of patients, gives hope that it will be possible to select some patients fit for surgery and stimulate research in this direction.

DATA AVAILABILITY STATEMENT

The raw data supporting the conclusions of this article will be made available by the authors, without undue reservation.

ETHICS STATEMENT

The studies involving human participants were reviewed and approved by the Area Vasta Romagna Ethics Committee (approval n° 5707/2020-I.5/264 on July 3rd, 2020). The patients/participants provided their written informed consent to participate in this study.

AUTHOR CONTRIBUTIONS

PM designed the study. LSo performed the statistical analysis. PM, LSo, and MM wrote the paper with input from all authors. All authors listed have made a substantial, direct, and intellectual contribution to the work and approved it for publication.

REFERENCES

1. Marrelli D, De Stefano A, de Manzoni G, Morgagni P, Di Leo A, Roviello F. Prediction of Recurrence After Radical Surgery for Gastric Cancer: A Scoring System Obtained From a Prospective Multicenter Study. *Ann Surg* (2005) 241:247–55. doi: 10.1097/01.sla.0000152019.14741.97
2. Fujitani K, Yang HK, Mizusawa J, Kim YW, Terashima M, Han SU, et al. REGATTA Study Investigators. Gastrectomy Plus Chemotherapy Versus Chemotherapy Alone for Advanced Gastric Cancer With a Single Non-Curable Factor (REGATTA): A Phase 3, Randomized Controlled Trial. *Lancet Oncol* (2016) 17:309–18. doi: 10.1016/S1470-2045(15)00553-7
3. Yoshida K, Yamaguchi K, Okumura N, Tanahashi T, Kodera Y. Is Conversion Therapy Possible in Stage IV Gastric Cancer: The Proposal of New Biological Categories of Classification. *Gastric Cancer* (2016) 19:329–38. doi: 10.1007/s10120-015-0575-z
4. Yasufuku I, Nunobe S, Ida S, Kumagai K, Ohashi M, Hiki N, et al. Conversion Therapy for Peritoneal Lavage Cytology-Positive Type 4 and Large Type 3 Gastric Cancer Patients Selected as Candidates for R0 Resection by Diagnostic Staging Laparoscopy. *Gastric Cancer* (2020) 23:319–27. doi: 10.1007/s10120-019-00994-0
5. Ishigami H, Yamaguchi H, Yamashita H, Asakage M, Kitayama J. Surgery After Intraperitoneal Chemotherapy for Gastric Cancer With Peritoneal Metastasis or Positive Peritoneal Cytology Findings. *Gastric Cancer* (2017) 20(Suppl. 1):128–34. doi: 10.1007/s10120-016-0684-3
6. Rau B, Brandl A, Thuss-Patience P, Bergner F, Raue W, Arnold A, et al. The Efficacy of Treatment Options for Patients With Gastric Cancer and Peritoneal Metastasis. *Gastric Cancer* (2019) 22:1226–37. doi: 10.1007/s10120-019-00969-1
7. Ministrini S, Bencivenga M, Solaini L, Cipollari C, Sofia S, Marino E, et al. Stage IV Gastric Cancer: The Surgical Perspective of the Italian Research Group on Gastric Cancer. *Cancers (Basel)* (2020) 12:158. doi: 10.3390/cancers12010158
8. Solaini L, Ministrini S, Bencivenga M, D'Ignazio A, Marino E, Cipollari C, et al. Conversion Gastrectomy for Stage IV Unresectable Gastric Cancer: A GIRCG Retrospective Cohort Study. *Gastric Cancer* (2019) 22:1285–93. doi: 10.1007/s10120-019-00968-2
9. Ishigami H, Fujiwara Y, Fukushima R, Nashimoto A, Yabusaki H, Imano M, et al. Phase III Trial Comparing Intraperitoneal and Intravenous Paclitaxel Plus S1 Versus Cisplatin Plus S1 in Patients With Gastric Cancer With Peritoneal Metastasis: Phoenix GC Trial. *J Clin Oncol* (2018) 36:1922–30. doi: 10.1200/JCO.2018.77.8613
10. Rau B, Brandl A, Piso P, Pelz J, Busch P, Demtröder C, et al. Peritoneum Surface Oncology Group and Members of the StuDoQ|Peritoneum Registry of the German Society for General and Visceral Surgery (DGAV). Peritoneal Metastasis in Gastric Cancer: Results From the German Database. *Gastric Cancer* (2020) 23:1–22. doi: 10.1007/s10120-019-00978-0
11. Sugarbaker PH. Peritonectomy Procedures. *Ann Surg* (1995) 221:29–42. doi: 10.1097/00000658-199501000-00004
12. Dindo D, Demartines N, Clavien PA. Classification of Surgical Complications: A New Proposal With Evaluation in a Cohort of 6336 Patients and Results of a Survey. *Ann Surg* (2004) 240:205–13. doi: 10.1097/01.sla.0000133083.54934.ae
13. Edge S, Byrd D, Compton C. *AJCC Cancer Staging Manual, Edn 7*. New York: Springer (2010).
14. Schemper M. Smith TL. A Note on Quantifying Follow-Up in Studies of Failure Time. *Control Clin Trials* (1996) 17:343–6. doi: 10.1016/0197-2456(96)00075-x
15. Yamaguchi K, Yoshida K, Tanahashi T, Takahashi T, Matsuhashi N, Tanaka Y, et al. The Long-Term Survival of Stage IV Gastric Cancer Patients With Conversion Therapy. *Gastric Cancer* (2018) 21:315–23. doi: 10.1007/s10120-017-0738-1
16. Guideline Committee of the Korean Gastric Cancer Association (KGCA) and Development Working Group & Review Panel. Korean Practice Guideline for Gastric Cancer 2018: An Evidence-Based, Multi-Disciplinary Approach. *J Gastric Cancer* (2019) 19:1–48. doi: 10.5230/jgc.2019.19.e8
17. Passot G, Vaudoyer D, Villeneuve L, Kepenekian V, Beaujard AC, Bakrin N, et al. What Made Hyperthermic Intraperitoneal Chemotherapy an Effective Curative Treatment for Peritoneal Surface Malignancy: A 25-Year Experience With 1,125 Procedures. *J Surg Oncol* (2016) 113:796–803. doi: 10.1002/jso.24248
18. Gockel I, Jansen-Winkeln B, Haase L, Rhode P, Mehdorn M, Niebisch S, et al. Pressurized Intraperitoneal Aerosol Chemotherapy (PIPAC) in Gastric Cancer Patients With Peritoneal Metastasis (PM): Results of a Single-Center Experience and Register Study. *J Gastric Cancer* (2018) 18:379–91. doi: 10.5230/jgc.2018.18.e37
19. Kim SH, Lee HJ, Park JH, Choi JH, Park SH, Choe HN, et al. Proposal of a New TNM Classification for Gastric Cancer: Focusing on Pn3b and Cytology-Positive (CY1) Disease. *J Gastric Cancer* (2019) 19:329–43. doi: 10.5230/jgc.2019.19.e33
20. Solaini L, Bencivenga M, D'ignazio A, Milone M, Marino E, De Pascale S, et al. Which Gastric Cancer Patients Could Benefit From Staging Laparoscopy? A GIRCG Multicenter Cohort Study. *Eur J Surg Oncol* (2022). doi: 10.1016/j.ejso.2022.01.020
21. De Manzoni G, Marrelli D, Baiocchi GL, Morgagni P, Saragoni L, Degiuli M, et al. The Italian Research Group for Gastric Cancer (GIRCG) Guidelines for Gastric Cancer Staging and Treatment: The Italian Research Group for Gastric Cancer (GIRCG) Guidelines for Gastric Cancer Staging and Treatment: 2015. *Gastric Cancer* (2017) 20:20–30. doi: 10.1007/s10120-016-0615-3. 2015

Conflict of Interest: The Handling Editor declared a past co-authorship with the authors GE, LS and PM.

Publisher's Note: All claims expressed in this article are solely those of the authors and do not necessarily represent those of their affiliated organizations, or those of the publisher, the editors and the reviewers. Any product that may be evaluated in this article, or claim that may be made by its manufacturer, is not guaranteed or endorsed by the publisher.

Copyright © 2022 Morgagni, Solaini, Saragoni, Monti, Valgiusti, Vittimberga, Frassineti, Framarini and Ercolani. This is an open-access article distributed under the terms of the Creative Commons Attribution License (CC BY). The use, distribution or reproduction in other forums is permitted, provided the original author(s) and the copyright owner(s) are credited and that the original publication in this journal is cited, in accordance with accepted academic practice. No use, distribution or reproduction is permitted which does not comply with these terms.

frontiers | Frontiers in Oncology

ORIGINAL RESEARCH
published: 20 April 2022
doi: 10.3389/fonc.2022.851522

Cost-Effectiveness of Nivolumab Plus Chemotherapy vs. Chemotherapy as First-Line Treatment for Advanced Gastric Cancer/Gastroesophageal Junction Cancer/Esophagel Adenocarcinoma in China

Yamin Shu[1], *Yufeng Ding*[1] *and Qilin Zhang*[2]*

[1] Department of Pharmacy, Tongji Hospital, Tongji Medical College, Huazhong University of Science and Technology, Wuhan, China, [2] Department of Pharmacy, Union Hospital, Tongji Medical College, Huazhong University of Science and Technology, Wuhan, China

OPEN ACCESS

Edited by:
Pankaj Kumar Garg, Shri Guru Ram Rai Institute of Medical and Health Sciences, India

Reviewed by:
Amit Sehrawat, All India Institute of Medical Sciences, India
Pallvi Kaul, Shri Guru Ram Rai Education Mission, India

***Correspondence:**
Qilin Zhang
qilinzhang88@163.com

Specialty section:
This article was submitted to Gastrointestinal Cancers: Gastric Esophageal Cancers, a section of the journal Frontiers in Oncology

Received: *10 January 2022*
Accepted: *25 March 2022*
Published: *20 April 2022*

Citation:
Shu Y, Ding Y and Zhang Q (2022) Cost-Effectiveness of Nivolumab Plus Chemotherapy vs. Chemotherapy as First-Line Treatment for Advanced Gastric Cancer/Gastroesophageal Junction Cancer/Esophageal Adenocarcinoma in China. Front. Oncol. 12:851522. doi: 10.3389/fonc.2022.851522

Objective: The purpose of this study was to evaluate the cost-effectiveness of nivolumab plus chemotherapy vs. chemotherapy as first-line therapy in patients with advanced gastric cancer/gastroesophageal junction cancer/esophageal adenocarcinoma from the perspective of the Chinese healthcare system.

Methods: This economic evaluation used a state-transition Markov model to assess the cost and effectiveness of nivolumab plus chemotherapy vs. chemotherapy as first-line treatment for advanced gastric cancer/gastroesophageal junction cancer/esophageal adenocarcinoma. The characteristics of patients in the model came from a phase 3 open-label randomized clinical trial (CheckMate 649). Key clinical data were based on the CheckMate 649 trial conducted from March 2017 to April 2019, and costs and utilities were collected from the published literature. The total cost of treatment per patient, quality-adjusted life-years (QALYs), and incremental cost-effectiveness ratio (ICER) were calculated for the two treatment strategies. Deterministic sensitivity analysis and probabilistic sensitivity analysis were performed.

Results: In the baseline analysis, the incremental effectiveness and cost of nivolumab plus chemotherapy vs. chemotherapy were 0.28 QALYs and $78,626.53, resulting in an ICER of $278,658.71/QALY, higher than the willingness-to-pay (WTP) threshold of China ($31,498.70/QALY). The model was sensitive to the duration of progression-free survival (PFS) for the nivolumab plus chemotherapy group, the cost of nivolumab per 100 mg, and the utility of PFS.

Conclusion: Nivolumab plus chemotherapy was clearly not a cost-effective treatment strategy compared with chemotherapy as first-line therapy for patients with advanced gastric cancer/gastroesophageal junction cancer/esophageal adenocarcinoma in China. Reducing the price of nivolumab may improve its cost-effectiveness.

Keywords: cost-effectiveness analysis, gastric cancer/gastroesophageal junction cancer/esophageal adenocarcinoma, nivolumab, CheckMate 649 trial, first-line treatment

INTRODUCTION

Gastric cancer (GC), including gastroesophageal junction cancer (GEJC), is the fifth most common cancer and is the fourth leading cause of cancer mortality worldwide (1, 2). In China, the morbidity and mortality of GC rank second among malignant tumors. Approximately 80% of patients diagnosed with GC are advanced metastatic disease, which have a very poor prognosis, with a 5-year survival rate of only about 5% (3, 4). Fluoropyrimidine plus platinum-based chemotherapy remains the standard first-line therapy for patients with non-operative radical or human epidermal growth factor 2 (HER2)-negative advanced or metastatic GC/GEJC by the National Comprehensive Cancer Network (NCCN), the European Society for Medical Oncology (ESMO), and the Chinese Society of Clinical Oncology (CSCO) (5–7), despite poor efficacy. For HER2-positive GC/GEJC, a targeted agent such as trastuzumab is recommended as first-line therapy, but the known incidence of HER2-positive in GC/GEJC was only about 20% (8, 9). The majority of patients with advanced GC/GEJC still lack innovative treatment options.

Nivolumab, a fully human IgG4 monoclonal antibody, can block the binding of programmed death-1 (PD-1) with its ligand PD-L1 and restore the function of T cell activation and cytokine production, thus achieving excellent antitumor effects. It has been proved to prominently provide improved survival benefits and quality of life for patients with non-small cell lung cancer (NSCLC), renal cancer, head and neck cancer, melanoma, and other cancers who previously had few treatment options (10–13). PD-L1 expression on tumor cells and tumor-associated immune cells (combined positive score [CPS]) showed better efficacy than PD-L1 expression on tumor cells of immune checkpoint inhibitors in the treatment of advanced GC/GEJC/esophageal adenocarcinoma (9).

The world's first global multicenter, randomized, open-label, phase 3 clinical study of the first-line immunotherapy combined with chemotherapy for patients with previously untreated, unresectable advanced, or metastatic GC/GEJC/esophageal adenocarcinoma is the CheckMate 649 trial, which is designed to evaluate the efficacy of nivolumab plus chemotherapy compared with chemotherapy alone (9). Results were published in July 2021 and demonstrated that nivolumab plus chemotherapy resulted in significant improvements in overall survival (OS) (14.4 vs. 11.1 months, hazard ratio (HR) = 0.71, 98.4% CI, 0.59–0.86, $p < 0.0001$) and progression-free survival (PFS) (7.7 vs. 6.05 months, HR = 0.68, 98% CI, 0.56–0.81, $p < 0.0001$) when compared with chemotherapy alone in PD-L1 CPS ≥5 GC/GEJC/esophageal adenocarcinoma patients (9).

Based on the CheckMate 649 study, on April 16, 2021, the Food and Drug Administration (FDA) approved nivolumab in combination with fluorouracil and platinum agents as the new first-line treatment strategy for patients with advanced or metastatic GC/GEJC/esophageal adenocarcinoma, regardless of PD-L1 expression status, followed by NCCN Guidelines (2021 edition) recommended. Just over 4 months later, on August 31, 2021, the National Medical Products Administration (NMPA) approved the same indication in China. In the CheckMate 649 trial, the Chinese population showed a trend of greater benefit as compared with the global population, for example, 39% vs. 20% reduction in the risk of death and 43% vs. 23% reduction in the risk of disease progression or death. The first-line treatment of HER2-negative advanced GC patients in China has been facing a huge gap in innovative treatment for a long time. The emergence of nivolumab has brought an unprecedented breakthrough in this field. Therefore, nivolumab immunotherapy combined with chemotherapy has been recommended as the first-line therapy for HER2-negative advanced or metastatic GC with PD-L1 CPS ≥5 in the latest CSCO (2021 edition) guidelines.

Despite the longer survival benefit of nivolumab, its high cost also increases the economic burden on patients' families and society. The cost-effectiveness of first-line treatment of advanced GC/GEJC with nivolumab plus chemotherapy has not, to our knowledge, been evaluated in China and other countries. The primary objective of this study was to estimate the cost-effectiveness of nivolumab plus chemotherapy compared with chemotherapy alone as first-line treatment for advanced or metastatic PD-L1 CPS ≥5 GC/GEJC/esophageal adenocarcinoma patients from the perspective of the Chinese healthcare system.

METHODS

Model Structure

This economic evaluation used a state-transition Markov model to estimate the cost and effectiveness associated with nivolumab plus chemotherapy vs. chemotherapy as first-line treatment for advanced GC/GEJC/esophageal adenocarcinoma in China (**Figure 1**). Patients were simulated through three mutually exclusive health states: PFS, progressive disease (PD), and death. All began in PFS with advanced disease, and patients either remained in their assigned health state or progressed to a new health state during each Markov cycle. It was assumed that all patients received first-line treatment until disease progression, and both groups could receive second-line treatment until death.

The time horizon of the model simulation was 5 years, and each Markov cycle represented 1 month in the model. The primary endpoints of the model were the total cost of treatment per patient, quality-adjusted life-years (QALYs), and incremental cost-effectiveness ratio (ICER). The formula used to calculate the ICER is as follows: ICER = [Cost (nivolumab plus chemotherapy) − Cost (chemotherapy)]/[QALY (nivolumab plus chemotherapy) − QALY (chemotherapy)]. The future costs and survival estimates were adjusted at a discount rate of 3% per year according to the WHO guidelines for pharmacoeconomic evaluations (14). ICER was compared with a willingness-to-pay (WTP) threshold of 3× the per-capita gross domestic product (GDP) of China in 2020 ($31,498.70). All costs had been adjusted to 2020 prices according to the local Consumer Price Index and were presented in US dollars ($1 = ¥6.9). The Markov model was performed in TreeAge Pro 2019 software (Williamstown, MA, USA), and statistical analyses were performed in R software (version 4.0.5, Vienna, Austria). This economic analysis was based on a published randomized clinical trial, and a mathematical model was used. Thus, the study did not require approval from an institutional review board or ethics committee.

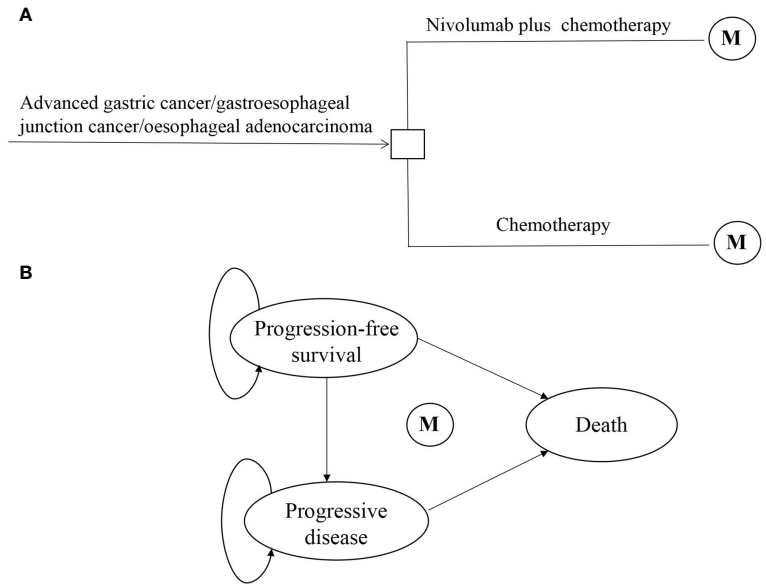

FIGURE 1 | Model structure of a decision tree combining the Markov state transition model with the 3 health states. **(A)** Decision tree. **(B)** Markov state transition model. M, Markov node.

Clinical Data and Transition Probabilities

The survival benefits and safety data of nivolumab plus chemotherapy and chemotherapy were based on the results of the CheckMate 649 trial (ClinicalTrials.gov number, NCT02872116), a multicenter, randomized, open-label, phase 3 trial (9). Eligible patients conformed to the following conditions: 1) 18 years of age or older, with previously untreated, unresectable advanced, or metastatic GC/GEJC/esophageal adenocarcinoma, regardless of PD-L1 expression; 2) measurable (at least one lesion) or evaluable disease per Response Evaluation Criteria in Solid Tumors (RECIST), version 1.1, and Eastern Cooperative Oncology Group performance status of 0 or 1; 3) adequate organ function and availability to provide a fresh or archival tumor sample to evaluate PD-L1; and 4) patients with prior adjuvant or neoadjuvant chemotherapy, radiotherapy, and/or chemoradiotherapy (administered at least 6 months before randomization) were allowed. Patients were randomly assigned in a 1:1 ratio to nivolumab plus chemotherapy (PD-L1 CPS ≥5, n = 473) or chemotherapy alone (PD-L1 CPS ≥5, n = 482). Patients were administered nivolumab (360 mg every 3 weeks or 240 mg every 2 weeks) plus chemotherapy (XELOX [capecitabine 1,000 mg/m^2 twice daily, days 1 to 14 and oxaliplatin 130 mg/m^2, day 1, every 3 weeks] or FOLFOX [leucovorin 400 mg/m^2, day 1; fluorouracil 400 mg/m^2, day 1 and 1200 mg/m^2, days 1 and 2; and oxaliplatin 85 mg/m^2, day 1, every 2 weeks]) or chemotherapy alone. Treatment continued until disease progression or unacceptable toxicity. The median OS was 14.4 months (95% CI, 13.1–16.2) in the nivolumab plus chemotherapy group and 11.1 months (95% CI, 10.0–12.1) in the chemotherapy group. The median PFS was 7.7 months (95% CI, 7.0–9.2) in the nivolumab plus chemotherapy group and 6.05 months (95% CI, 5.6–6.9) in the chemotherapy group.

The Kaplan–Meier survival curves from the CheckMate 649 trial were used to estimate transition probabilities between different health states. First, OS and PFS data points were extracted from the corresponding Kaplan–Meier survival curves using the GetData Graph Digitizer software (version 2.26), which digitized data points from an image file. Second, virtual data comprised follow-up time and the same initial number at risk, which closely reproduced the digitized Kaplan–Meier curves, and R software was used to reconstruct the Kaplan–Meier curve of the obtained data (**Figure 2**). Third, to predict survival beyond the observation period, the proportions of patients with PFS and OS were calculated by using the Weibull distribution. Finally, the Weibull distribution parameters, scale (λ) and shape (γ) parameters, SE, and 95% CI were computed using R (**Table 1**). Formula $S(t) = \exp(-\lambda t^{\gamma})$ was used to calculate the survival probability at time t, and the transition probabilities between different health states at a given cycle t were estimated by formula $P(t) = 1 - \exp[\lambda(t-1)^{\gamma} - \lambda t^{\gamma}]$ (15, 16). The background mortality rate from PFS to death state was derived from the natural death rate of the Chinese population in 2020 (0.707%) (17).

Costs and Utilities

Costs were estimated from the perspective of the Chinese healthcare system. The direct medical cost components, that is, the costs of first-line and subsequent treatment, management of treatment-related grade 3–4 serious adverse events (SAEs), laboratory tests and radiological examinations, best supportive care (BSC), cost of salvage therapy per cycle, routine follow-up, and terminal care in end of life, were included in the model (**Table 2**). In calculating dosage amounts, a body weight of 65 kg

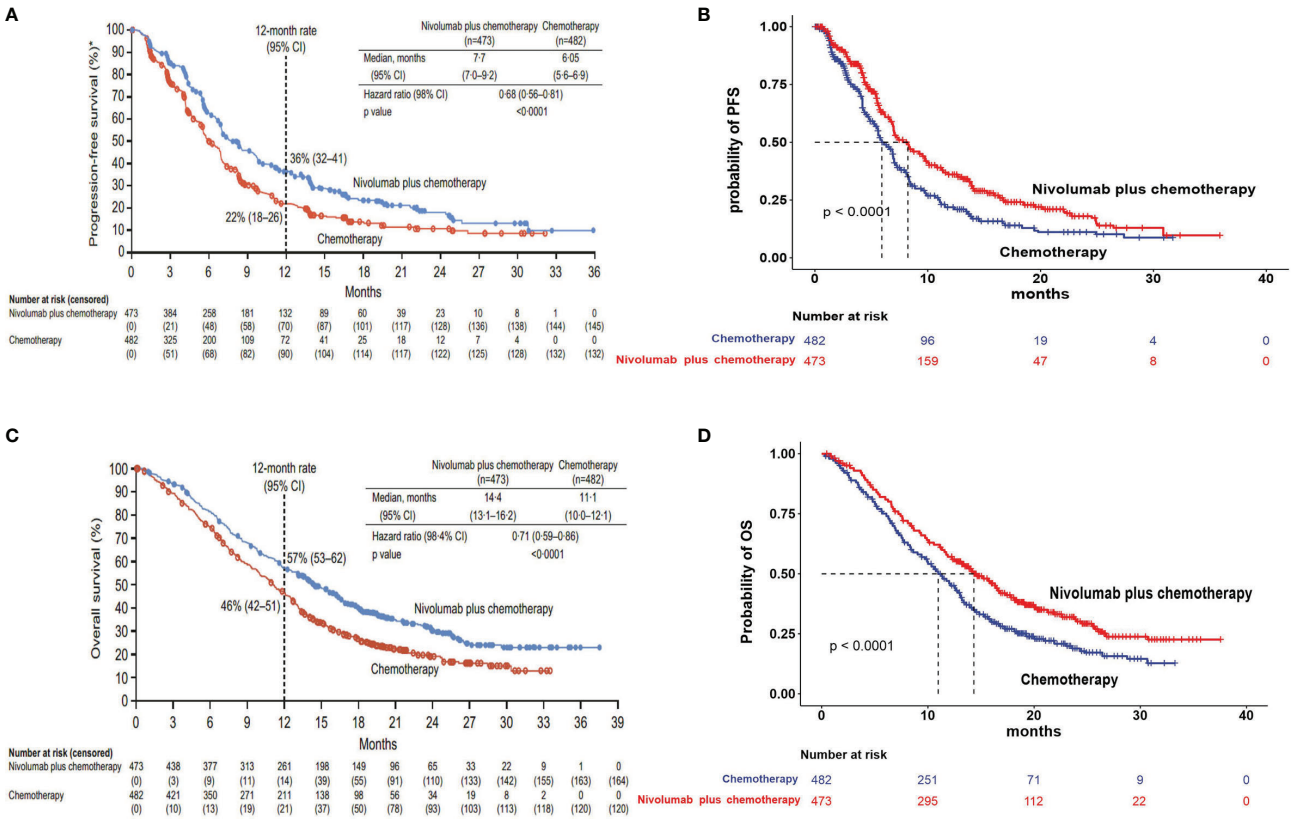

FIGURE 2 | Model estimated PFS and OS were plotted, together with the original Kaplan–Meier PFS and OS curves from the CheckMate 649 trial, respectively. **(A)** Kaplan–Meier curve of the progression-free survival from the CheckMate 649 trial. **(B)** Simulate progression-free survival curve for the nivolumab plus chemotherapy and chemotherapy. **(C)** Kaplan–Meier curve of overall survival from the CheckMate 649 trial. **(D)** Simulate overall survival curve for the nivolumab plus chemotherapy and chemotherapy. PFS, progression-free survival; OS, overall survival.

TABLE 1 | Weibull parameters of model estimated for progression-free and overall survival curves.

Group		Parameter	Mean	SE	95% CI	
					Low	Up
Nivolumab plus chemotherapy	PFS	Scale (λ)	0.047288	0.006835	0.035621	0.062776
		Shape (γ)	1.186735	0.051729	1.089558	1.292580
	OS	Scale (λ)	0.021699	0.004037	0.015069	0.031245
		Shape (γ)	1.267705	0.061001	1.153611	1.393084
Chemotherapy	PFS	Scale (λ)	0.073625	0.009085	0.057809	0.093768
		Shape (γ)	1.170952	0.047834	1.080855	1.268560
	OS	Scale (λ)	0.031801	0.005104	0.023217	0.043558
		Shape (γ)	1.267607	0.055288	1.163747	1.380736

PFS, progression-free survival; OS, overall survival.

and a height of 1.64 m were used, resulting in a body surface area of 1.72 m^2 for typical patients (24). In addition, to better reflect the cost of first-line treatment in real-world settings, the duration of these treatments was adjusted based on the median treatment cycles reported in the CheckMate 649 trial. Only grade 3 or higher SAEs with an incidence of >5% at least in one group were incorporated into the model, including anemia, decreased neutrophil count, neutropenia, and increased lipase. The costs related to SAEs were calculated by multiplying the incidence of the SAEs by the costs of managing the SAEs per event. After disease progression, patients could subsequently receive salvage chemotherapy and supportive care. All costs were derived from local hospitals or previously published literature (18–22).

The CheckMate 649 trial had evaluated the health-related quality of life (HRQoL), but it has not been published. The baseline utility estimates for PFS and PD health states were

TABLE 2 | Model economic parameters and the range of the sensitivity analysis.

Variables	Base case (range)	Distribution	Source
Costs ($)			
Nivolumab (100 mg)	1,342.03 (1,073.62–1,610.44)	Triangle	Local charge
Oxaliplatin (100 mg)	90.00 (72.00–108.00)	Triangle	Local charge
Capecitabine (1,000 mg)	6.38 (5.10–7.66)	Triangle	Local charge
Leucovorin (100 mg)	2.22 (1.78–2.66)	Triangle	Local charge
Fluorouracil (1,000 mg)	26.67 (21.34–32.00)	Triangle	Local charge
Cost of salvage therapy per cycle	478.82 (383.06–574.58)	Triangle	Local charge
Routine follow-up cost per cycle	80.71 (64.57–96.85)	Triangle	(18)
Cost of tests and radiological examinations per cycle	141.29 (113.03–169.55)	Triangle	(19)
Cost of supportive care per cycle	164.57 (131.66–197.48)	Triangle	(18)
Cost of terminal care in end of life	1,460.30 (1,168.24–1,752.36)	Triangle	(18)
Costs of serious adverse events			
Anemia	508.20 (381.2–635.3)	Triangle	(20)
Neutrophil count decreased	534.40 (427.52–641.28)	Triangle	(21)
Neutropenia	466.00 (372.80–559.20)	Triangle	(20)
Lipase increased	44.30 (35.44–53.16)	Triangle	(22)
Risks of serious adverse events in nivolumab plus chemotherapy group (grade 3 or 4) %			
Anemia	6.46 (5.17–7.75)	Beta	(9)
Neutrophil count decreased	11.40 (9.12–13.68)	Beta	(9)
Neutropenia	16.21 (12.97–19.45)	Beta	(9)
Lipase increased	6.18 (4.94–7.42)	Beta	(9)
Risks of serious adverse events in chemotherapy group (grade 3 or 4) %			
Anemia	2.74 (2.19–3.29)	Beta	(9)
Neutrophil count decreased	8.74 (6.99–10.49)	Beta	(9)
Neutropenia	12.13 (9.70–14.56)	Beta	(9)
Lipase increased	2.09 (1.67–2.51)	Beta	(9)
Utility value			
PFS	0.797 (0.638–0.956)	Beta	(23)
PD	0.577 (0.462–0.692)	Beta	(23)
Body surface area (m^2)	1.72 (1.38–2.06)	Triangle	(24)
Discount rate (%)	3 (0–8)	Fixed in PSA	(14)

PFS, progression-free survival; PD, progressive disease; PSA, probabilistic sensitivity analyses.

derived from previously published literature (23), with 0 indicating death and 1 indicating perfect health. To simplify the model, the disutility of SAEs in the model was not considered, as the effect of SAEs was assumed to be captured in the utility values. Furthermore, a half-cycle correction was implemented to the outcomes, according to the TreeAge Pro 2019 manual and Guidelines for pharmacoeconomic evaluation in China.

Sensitivity Analyses

To assess the robustness of the model and the uncertainty in parameter estimation, deterministic sensitivity analysis and probabilistic sensitivity analysis were performed in this research. In the deterministic sensitivity analysis, relevant variables were tested one by one at the upper and lower limits of plausible ranges, to explore the impact of each parameter on ICER. The result of the deterministic sensitivity analysis is presented in a tornado diagram. To determine the effect of variation in multiple parameters simultaneously, a probabilistic sensitivity analysis with 1,000 Monte Carlo simulations was performed, in which the parameters were changed with a specific pattern of distribution. A cost-effectiveness acceptability curve and probabilistic scatter plot were given to show the probability of the cost-effectiveness simulations at various WTP thresholds.

To investigate the uncertainty of economic outcomes caused by the differences in race, exploratory subgroup analyses were performed for the prespecified subgroup that was reported in PD-L1 CPS ≥5 GC/GEJC/esophageal adenocarcinoma patients in the CheckMate 649 trial by varying the HR for OS.

RESULTS

Incremental Cost-Effectiveness Ratios

The primary analysis results of the model are listed in **Table 3**. In the base case, first-line treatment with nivolumab plus chemotherapy resulted in a cost of $88,190.33 and survival of 1.11 QALYs per patient. Treatment with chemotherapy resulted in a cost of $9,563.80 and survival of 0.82 QALYs. Nivolumab plus chemotherapy provided an additional $78,626.53 and conferred an additional 0.28 QALYs, leading to an ICER of $278,658.71/QALY. At the Chinese cost-effectiveness WTP threshold of $31,498.70/QALY, nivolumab plus chemotherapy was clearly not a cost-effective treatment strategy compared with chemotherapy.

Sensitivity Analyses

The results of one-way sensitivity analyses are shown in a tornado diagram (**Figure 3**). The variables that had the

TABLE 3 | The cost and outcome results of the cost-effectiveness analysis.

Parameters	Nivolumab plus chemotherapy	Chemotherapy
Costs ($)		
PFS state	83,110.53	5,183.48
PD state	5,079.79	4,380.32
Total cost	88,190.33	9,563.80
Incremental costs ($)	78,626.53	/
Effectiveness (QALYs)		
PFS state	0.82	0.59
PD state	0.28	0.23
Total effectiveness	1.11	0.82
Incremental effectiveness (QALYs)	0.28	/
ICER ($/QALY)	278,658.71	/

PFS, progression-free survival; PD, progressive disease; QALYs, Quality-adjusted life-years; ICER, incremental cost-effectiveness ratios.

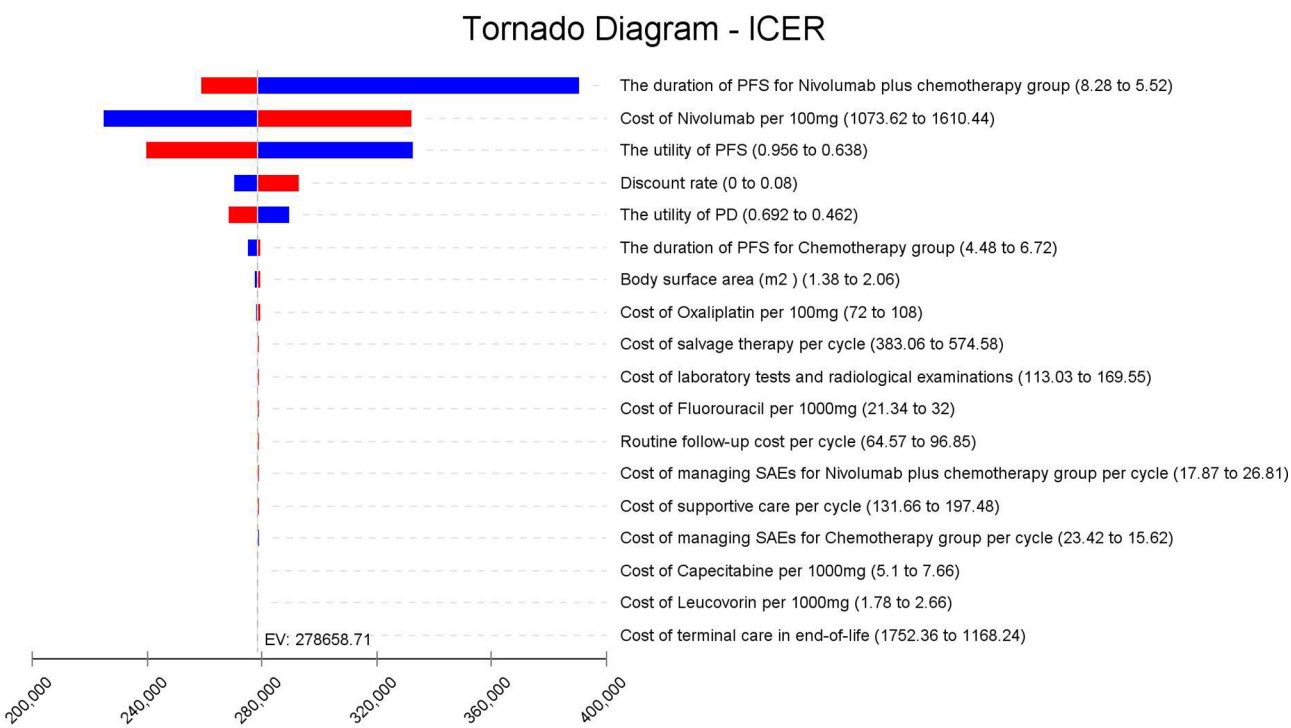

FIGURE 3 | Tornado diagram of one-way sensitivity analysis. It summarizes the results of one-way sensitivity analysis, which lists influential parameters in descending order according to their effect on the ICER over the variation of each parameter value. ICER, incremental cost-effectiveness ratios; PFS, progression-free survival; PD, progressive disease; SAEs, serious adverse events.

greatest influence on the ICER were the duration of PFS for the nivolumab plus chemotherapy group, the cost of nivolumab per 100 mg, and the utility of PFS. Other parameters such as discount rate, body surface area (m^2), and costs of SAEs had a moderate or mild impact on ICER. However, any of the tested variables' upper or lower limits were unable to change the cost-effective treatment strategy from chemotherapy to nivolumab plus chemotherapy, with the ICERs below the thresholds. The probabilistic sensitivity analysis of the primary analysis revealed that the probability of nivolumab plus chemotherapy being cost-effective was 0% at the WTP threshold of $31,498.70/QALY (**Figures 4**, **5**). Treatment with nivolumab plus chemotherapy had a 50% probability to be cost-effective at a WTP threshold of approximately $280,000/QALY, and this probability increased with the rising WTP thresholds (**Figure 4**). According to the sensitivity analyses, the results of the model were very robust. Although our study was based on the subgroup of PD-L1 CPS ≥5, due to the small difference in survival benefit of each subgroup, the results could be generalized to other subgroups regardless of the PD-L1 CPS

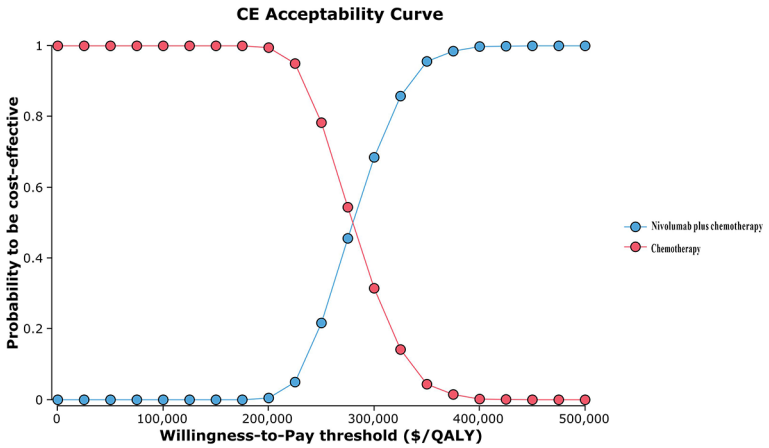

FIGURE 4 | Cost-effectiveness acceptability curve. QALY, quality-adjusted life-year; CE, cost-effectiveness.

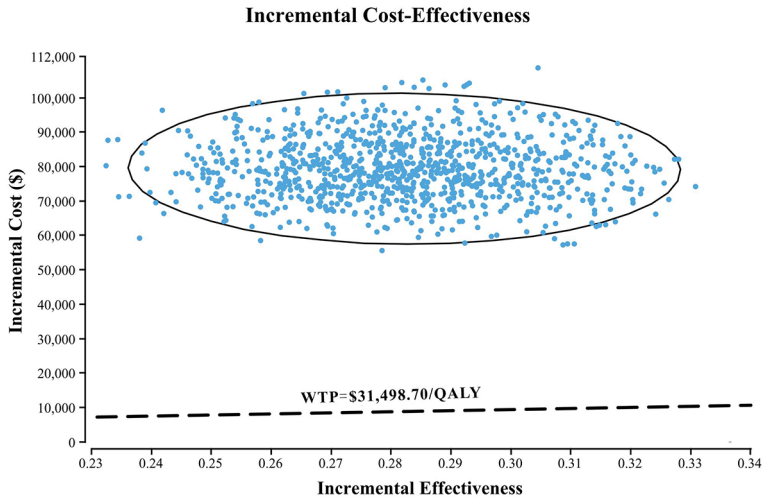

FIGURE 5 | A probabilistic scatter plot of the ICER between the nivolumab plus chemotherapy and chemotherapy. Each dot represents the ICER for 1 simulation. An ellipse means 95% CI. Dots that are located below the ICER threshold represent cost-effective simulations. WTP, willingness to pay; QALY, quality-adjusted life-year; ICER, incremental cost-effectiveness ratios.

expression level in the CheckMate 649 trial. However, in comparison with chemotherapy, nivolumab plus chemotherapy was associated with an ICER of $240,678.12/QALY in the Asian population subgroup of PD-L1 CPS ≥5, which was lower than the overall population.

DISCUSSION

The average early diagnosis rate of GC in China is only about 10%, resulting in a large proportion of patients with advanced GC. The prognosis of advanced GC is relatively poor, and the curative effect is not ideal. CheckMate 649 is the only study to date in the treatment of advanced GC to confirm the dual benefit of PFS and OS achieved by immunotherapy combined with chemotherapy. So far, CheckMate 649 was the largest randomized, global multicenter phase 3 study, which enrolled 2,032 patients at 176 centers in the first-line treatment of advanced GC/GEJC/esophageal adenocarcinoma based on immune checkpoint inhibitors and was published in *Lancet* (9). With 208 participants, China has the highest percentage (13.4%) of patients among all countries; hence, results can be extrapolated to the Chinese population to a large extent.

Nivolumab is the first and currently the only PD-1 inhibitor approved for first-line therapy of advanced GC in China. With the widespread use of nivolumab, the substantial increase in

financial burden has become an important concern for decision makers. An economic evaluation of nivolumab has become an urgent need. To our knowledge, this study is the first to evaluate the cost-effectiveness of nivolumab plus chemotherapy as first-line treatment for advanced PD-L1 CPS ≥5 GC/GEJC/esophageal adenocarcinoma patients as recommended by the latest clinical guidelines (7), and our results are of great significance in both China and other countries.

On the basis of the simulated survival model, our analysis showed that nivolumab plus chemotherapy demonstrated an average of 1.11 QALYs, while chemotherapy demonstrated 0.82 QALYs. Nivolumab plus chemotherapy was more effective than chemotherapy by 0.28 QALYs. Furthermore, nivolumab plus chemotherapy was also more expensive with the cost of $88,190.33 compared to $9,563.80 for chemotherapy (+$78,626.53), resulting in an ICER of $278,658.71/QALY, much higher than the WTP value ($31,498.70/QALY) in China. In our study, the subgroup with PD-L1 CPS ≥5 was selected for analysis, because the PFS and OS of this subgroup had the highest survival benefits. At the same cost, since the subgroup with PD-L1 CPS ≥5 was not economical, the other groups were even less economical. In summary, it means that regardless of PD-L1 CPS expression level, nivolumab plus chemotherapy regimen as first-line treatment of advanced GC/GEJC/esophageal adenocarcinoma is not cost-effective in China, despite having a greater survival benefit as evaluated by QALYs.

In the one-way sensitivity analysis, the duration of PFS for the nivolumab plus chemotherapy group, the cost of nivolumab per 100 mg, and the utility of PFS were the most sensitive parameters, which had the greatest influence on the model results. However, within the variation range of each parameter, the ICER value was always higher than the WTP value, which had no influence on the final outcomes, proving the stability of the model. The cost of nivolumab was much higher than the placebo, which was the main reason why it was not cost-effective. We obtained an economical price of nivolumab by changing the price of nivolumab so that ICER was close to or equal to the WTP ($31,498.70/QALY) in China. According to the one-way sensitivity analysis (**Figure 3**), when the price of nivolumab is reduced by 90%, with an ICER of $30,843.63/QALY, it is lower than the WTP in China, and it becomes cost-effective, further supporting the view that nivolumab is currently costly for its clinical value. However, in the Asian population subgroup of PD-L1 CPS ≥5, it becomes cost-effective in China when the price of nivolumab is reduced by 83% (ICER = $31,016.44/QALY). But it does not mean the nivolumab plus chemotherapy in Asians was more cost-effective than in non-Asians because the WTP was varied in different countries. Probability sensitivity analysis showed that the probability of nivolumab plus chemotherapy being cost-effective relative to chemotherapy (ICER below $31,498.70/QALY) was 0%. Nivolumab plus chemotherapy would only be more cost-effective than chemotherapy if WTP exceeded approximately $280,000/QALY. It should be noted that the per-capita GDP of different regions in China varies greatly, among which the WTP of economically developed cities and provinces, such as Beijing, Shanghai, Jiangsu, Fujian, and Zhejiang, are $72,886.96/QALY, $69,297.83/QALY, $55341.30/QALY, $48,046.09/QALY, and $48,021.74/QALY, respectively. However, the nivolumab plus chemotherapy regimen is still not cost-effective in these areas. Additionally, ICER in the nivolumab plus chemotherapy group was higher than the threshold recommended by wealthier developed countries, such as £20,000–30,000 per QALY proposed by the National Institute for Health and Care Excellence (NICE) in the United Kingdom and $150,000 per QALY in the United States (25, 26). It suggests that nivolumab plus chemotherapy may also not be cost-effective as first-line therapy for patients with advanced GC/GEJC/esophageal adenocarcinoma in other developed countries.

At present, most of the pharmacoeconomic studies on advanced GC focused on screening, surgical techniques, and chemoradiation, and few studies focused on immunotherapy (27–30). Moreover, economic studies of nivolumab have also been limited to advanced renal cell carcinoma, NSCLC, and melanoma (31–33). Only one Japanese study showed that the QALYs and expected costs per patient were 0.5295 and JPY 5,018,148 ($45,620) for nivolumab and 0.4379 and JPY 2,054,625 ($18,678) for trifluridine/tipiracil, respectively, for patients with heavily pretreated metastatic GC (34). The ICER of nivolumab vs. trifluridine/tipiracil was JPY 32,352,489 ($294,113) per QALY gained, much higher than the WTP of Japan. Accordingly, nivolumab is not cost-effective compared to trifluridine/tipiracil.

In fact, due to the limited survival, small incremental effect, and high incremental cost of patients with advanced GC, many antitumor drugs are not considered economical. Shiroiwa (23) reported that trastuzumab plus chemotherapy for HER2-positive advanced GC was not cost-effective based on the ToGA trial. Chen et al. (35) conducted a cost-effectiveness analysis of apatinib in patients with advanced GC in China and found that apatinib was not cost-effective with an ICER of $90,154/QALY (WTP = $23,700/QALY). Pharmacoeconomic studies in both China and other countries have found that ramucirumab alone or in combination with paclitaxel does not have a cost-effectiveness advantage in second-line therapy for advanced GC/GEJC (4, 36, 37). Another research demonstrated that among six possible second-line treatment options for patients with advanced GC who have failed previous chemotherapy—irinotecan, docetaxel, paclitaxel, ramucirumab, paclitaxel plus ramucirumab, and palliative care—irinotecan alone appears to be the most cost-effective. Both paclitaxel alone and the combination of paclitaxel and ramucirumab were not cost-effective with ICER values being $86,815/QALY and $1,056,125/QALY, respectively, more than $50,000/QALY (36). Consistently, nivolumab does not achieve cost-effectiveness compared to placebo for chemotherapy-refractory advanced GC in the current healthcare environment in China (38). Generally, the cost of PD-1 inhibitors is higher in China than in conventional chemotherapy. Based on previous studies and our results, it is suggested that nivolumab plus chemotherapy may not be cost-effective compared to chemotherapy in both first-line and second-line treatment of advanced GC/GEJC/esophageal adenocarcinoma from the perspective of the Chinese healthcare system. As far as we know, since the official establishment of the National Healthcare Security Administration (NHSA) in May 2018, there have been several rounds of negotiations with pharmaceutical

companies on the price of cancer drugs, aiming to relieve the medical burden of cancer patients through national strategic procurement (24, 39). At present, the NHSA of China is making great efforts for the successful entry of nivolumab into the negotiation list for the first-line treatment of advanced GC/GEJC/esophageal adenocarcinoma.

Our study has some limitations. First, the model based on the clinical trial and the use of a two-parameter Weibull survival model to extrapolate the long-term PFS and OS beyond the experimental observation time may not accurately reflect the disease course in the real world. Future studies are expected to confirm the cost-effectiveness of nivolumab plus chemotherapy vs. chemotherapy when the clinical data are mature. Second, the HRQoL data for patients were unavailable in the CheckMate 649 trial, and health state utilities used in our study were derived from published literature, which might lead to bias in the model outcomes. However, the result of the sensitivity analysis found that varying the health state utilities in the sensitivity analysis did not substantially change our results. Third, we only considered the most common grade 3/4 SAEs in the model. We hypothesized that low-probability adverse events would not change the final conclusions of the study, and the sensitivity analysis showed that the result was not sensitive to SAE-related parameters. Fourth, according to the guidelines, we assumed all patients subsequently received paclitaxel as salvage chemotherapy, which may not reflect the current Chinese clinical practice situation precisely because patients might choose different treatment options upon further progression. Finally, due to the strict eligible conditions of clinical trials and the unbalanced economic development in various regions of China, the applicability of this study may be limited.

CONCLUSION

In conclusion, nivolumab plus chemotherapy is unlikely to be considered cost-effective compared with chemotherapy alone in the first-line therapy for advanced or metastatic PD-L1 CPS ≥5 GC/GEJC/esophageal adenocarcinoma from the perspective of the Chinese healthcare system. However, if the cost is reduced by 90%, nivolumab may be a cost-effective and effective treatment option. Our results may be helpful to provide guidance for GC/GEJC/esophageal adenocarcinoma treatment decisions by physicians and healthcare requests in China.

DATA AVAILABILITY STATEMENT

The original contributions presented in the study are included in the article/supplementary material. Further inquiries can be directed to the corresponding author.

ETHICS STATEMENT

This article does not contain any studies with human participants or animals performed by any of the authors.

AUTHOR CONTRIBUTIONS

YS and QZ made a significant contribution to the work in the conception, study design, execution, acquisition of data, analysis, and interpretation. All authors took part in drafting, revising, or critically reviewing the article and gave final approval of the version to be published.

FUNDING

This work was supported by the National Natural Science Foundation of China (No. 82104476).

REFERENCES

1. Sung H, Ferlay J, Siegel RL, Laversanne M, Soerjomataram I, Jemal A, et al. Global Cancer Statistics 2020: GLOBOCAN Estimates of Incidence and Mortality Worldwide for 36 Cancers in 185 Countries. *CA: Cancer J Clin* (2021) 71(3):209–49. doi: 10.3322/caac.21660
2. *Stomach, Globocan 2018 Lyon: Global Cancer Observatory* (2019). Available at: http://gco.iarc.fr/today/data/factsheets/cancers/7-Stomach-fact-sheet.pdf (Accessed 25 April 2019).
3. Cancer Research UK. *Stomach Cancer Mortality Statistics* (2012). Cancer Research UK. Available at: http://www.cancerresearchuk.org/health-professional/cancer-statistics/statistics-by-cancer-type/stomach-cancer/mortality (Accessed 08 Aug 2016).
4. Büyükkaramikli NC, Blommestein HM, Riemsma R, Armstrong N, Clay FJ, Ross J, et al. Ramucirumab for Treating Advanced Gastric Cancer or Gastro-Oesophageal Junction Adenocarcinoma Previously Treated With Chemotherapy: An Evidence Review Group Perspective of a NICE Single Technology Appraisal. *PharmacoEconomics* (2017) 35(12):1211–21. doi: 10.1007/s40273-017-0528-y
5. Ajani JA, D'Amico TA, Bentrem DJ, Chao J, Cooke D, Corvera C, et al. Gastric Cancer, Version 2.2022, NCCN Clinical Practice Guidelines in Oncology. *J Natl Compr Cancer Network: JNCCN* (2022) 20(2):167–92. doi: 10.6004/jnccn.2022.0008
6. Muro K, Van Cutsem E, Narita Y, Pentheroudakis G, Baba E, Li J, et al. Pan-Asian Adapted ESMO Clinical Practice Guidelines for the Management of Patients With Metastatic Gastric Cancer: A JSMO-ESMO Initiative Endorsed by CSCO, KSMO, MOS, SSO and TOS. *Ann Oncology: Off J Eur Soc Med Oncol* (2019) 30(1):19–33. doi: 10.1093/annonc/mdy502
7. Wang FH, Zhang XT, Li YF, Tang L, Qu XJ, Ying JE, et al. The Chinese Society of Clinical Oncology (CSCO): Clinical Guidelines for the Diagnosis and Treatment of Gastric Cancer, 2021. *Cancer Commun (Lond Engl)* (2021) 41(8):747–95. doi: 10.1002/cac2.12193
8. Bang YJ, Van Cutsem E, Feyereislova A, Chung HC, Shen L, Sawaki A, et al. Trastuzumab in Combination With Chemotherapy Versus Chemotherapy Alone for Treatment of HER2-Positive Advanced Gastric or Gastro-Oesophageal Junction Cancer (Toga): A Phase 3, Open-Label, Randomised Controlled Trial. *Lancet (Lond Engl)* (2010) 376(9742):687–97. doi: 10.1016/s0140-6736(10)61121-x
9. Janjigian YY, Shitara K, Moehler M, Garrido M, Salman P, Shen L, et al. First-Line Nivolumab Plus Chemotherapy Versus Chemotherapy Alone for Advanced Gastric, Gastro-Oesophageal Junction, and Oesophageal Adenocarcinoma (Checkmate 649): A Randomised, Open-Label, Phase 3

Trial. *Lancet (Lond Engl)* (2021) 398(10294):27–40. doi: 10.1016/s0140-6736(21)00797-2
10. Borghaei H, Paz-Ares L, Horn L, Spigel DR, Steins M, Ready NE, et al. Nivolumab Versus Docetaxel in Advanced Nonsquamous Non-Small-Cell Lung Cancer. *New Engl J Med* (2015) 373(17):1627–39. doi: 10.1056/NEJMoa1507643
11. Motzer RJ, Escudier B, McDermott DF, George S, Hammers HJ, Srinivas S, et al. Nivolumab Versus Everolimus in Advanced Renal-Cell Carcinoma. *New Engl J Med* (2015) 373(19):1803–13. doi: 10.1056/NEJMoa1510665
12. Janjigian YY, Bendell J, Calvo E, Kim JW, Ascierto PA, Sharma P, et al. Checkmate-032 Study: Efficacy and Safety of Nivolumab and Nivolumab Plus Ipilimumab in Patients With Metastatic Esophagogastric Cancer. *J Clin Oncol Off J Am Soc Clin Oncol* (2018) 36(28):2836–44. doi: 10.1200/jco.2017.76.6212
13. Larkin J, Chiarion-Sileni V, Gonzalez R, Grob JJ, Cowey CL, Lao CD, et al. Combined Nivolumab and Ipilimumab or Monotherapy in Untreated Melanoma. *New Engl J Med* (2015) 373(1):23–34. doi: 10.1056/NEJMoa1504030
14. Murray CJ, Evans DB, Acharya A, Baltussen RM. Development of WHO Guidelines on Generalized Cost-Effectiveness Analysis. *Health economics* (2000) 9(3):235–51. doi: 10.1002/(sici)1099-1050(200004)9:3<235::aid-hec502>3.0.co;2-o
15. Diaby V, Adunlin G, Montero AJ. Survival Modeling for the Estimation of Transition Probabilities in Model-Based Economic Evaluations in the Absence of Individual Patient Data: A Tutorial. *PharmacoEconomics* (2014) 32(2):101–8. doi: 10.1007/s40273-013-0123-9
16. Liu M, Zhang L, Huang Q, Li N, Zheng B, Cai H. Cost-Effectiveness Analysis of Ceritinib and Alectinib Versus Crizotinib in the Treatment of Anaplastic Lymphoma Kinase-Positive Advanced Non-Small Cell Lung Cancer. *Cancer Manage Res* (2019) 11:9195–202. doi: 10.2147/cmar.S223441
17. Shu Y, Zhang Q, He X, Chen L. Cost-Effectiveness Analysis of Gefitinib Plus Chemotherapy Versus Gefitinib Alone for Advanced Non-Small-Cell Lung Cancer With EGFR Mutations in China. *Cancer Manage Res* (2021) 13:8297–306. doi: 10.2147/cmar.S334643
18. Wu B, Li T, Cai J, Xu Y, Zhao G. Cost-Effectiveness Analysis of Adjuvant Chemotherapies in Patients Presenting With Gastric Cancer After D2 Gastrectomy. *BMC Cancer* (2014) 14:984. doi: 10.1186/1471-2407-14-984
19. He J, Wen F, Yin X, Zhang P, Du Z, He X, et al. Cost Analysis of S1 and XELOX as Adjuvant Therapy for Gastric Cancer. *Anti-cancer Drugs* (2013) 24(7):754–8. doi: 10.1097/CAD.0b013e328361bef2
20. Zhang PF, Xie D, Li Q. Cost-Effectiveness Analysis of Nivolumab in the Second-Line Treatment for Advanced Esophageal Squamous Cell Carcinoma. *Future Oncol (Lond Engl)* (2020) 16(17):1189–98. doi: 10.2217/fon-2019-0821
21. Li S, Peng L, Tan C, Zeng X, Wan X, Luo X, et al. Cost-Effectiveness of Ramucirumab Plus Paclitaxel as a Second-Line Therapy for Advanced Gastric or Gastro-Oesophageal Cancer in China. *PloS One* (2020) 15(5):e0232240. doi: 10.1371/journal.pone.0232240
22. Wu B, Ye M, Chen H, Shen JF. Costs of Trastuzumab in Combination With Chemotherapy for HER2-Positive Advanced Gastric or Gastroesophageal Junction Cancer: An Economic Evaluation in the Chinese Context. *Clin Ther* (2012) 34(2):468–79. doi: 10.1016/j.clinthera.2012.01.012
23. Shiroiwa T, Fukuda T, Shimozuma K. Cost-Effectiveness Analysis of Trastuzumab to Treat HER2-Positive Advanced Gastric Cancer Based on the Randomised Toga Trial. *Br J Cancer* (2011) 105(9):1273–8. doi: 10.1038/bjc.2011.390
24. Qiao L, Zhou Z, Zeng X, Tan C. Cost-Effectiveness of Domestic PD-1 Inhibitor Camrelizumab Combined With Chemotherapy in the First-Line Treatment of Advanced Nonsquamous Non-Small-Cell Lung Cancer in China. *Front Pharmacol* (2021) 12:728440. doi: 10.3389/fphar.2021.728440
25. London: National Institute for Health and Care Excellence (NICE). *Guide to the Methods of Technology Appraisal*. London: National Institute for Health and Care Excellence (NICE). Process and Methods Guides (2013)
26. Marseille E, Larson B, Kazi DS, Kahn JG, Rosen S. Thresholds for the Cost-Effectiveness of Interventions: Alternative Approaches. *Bull World Health Organ* (2015) 93(2):118–24. doi: 10.2471/blt.14.138206
27. Saumoy M, Schneider Y, Shen N, Kahaleh M, Sharaiha RZ, Shah SC. Cost Effectiveness of Gastric Cancer Screening According to Race and Ethnicity. *Gastroenterology* (2018) 155(3):648–60. doi: 10.1053/j.gastro.2018.05.026
28. Zhang M, Wen F, He X, Zhang W, Hu J, Li Q. Adjuvant Chemoradiotherapy for Gastric Cancer: Efficacy and Cost-Effectiveness Analysis. *Front Oncol* (2019) 9:1357. doi: 10.3389/fonc.2019.01357
29. Huang HL, Leung CY, Saito E, Katanoda K, Hur C, Kong CY, et al. Effect and Cost-Effectiveness of National Gastric Cancer Screening in Japan: A Microsimulation Modeling Study. *BMC Med* (2020) 18(1):257. doi: 10.1186/s12916-020-01729-0
30. Wang H, Hao Q, Wang M, Feng M, Wang F, Kang X, et al. Esophagojejunostomy After Laparoscopic Total Gastrectomy by Orvil™ or Hemi-Double Stapling Technique. *World J Gastroenterol* (2015) 21(29):8943–51. doi: 10.3748/wjg.v21.i29.8943
31. Wan X, Zhang Y, Tan C, Zeng X, Peng L. First-Line Nivolumab Plus Ipilimumab vs Sunitinib for Metastatic Renal Cell Carcinoma: A Cost-Effectiveness Analysis. *JAMA Oncol* (2019) 5(4):491–6. doi: 10.1001/jamaoncol.2018.7086
32. Hu H, She L, Liao M, Shi Y, Yao L, Ding D, et al. Cost-Effectiveness Analysis of Nivolumab Plus Ipilimumab vs. Chemotherapy as First-Line Therapy in Advanced Non-Small Cell Lung Cancer. *Front Oncol* (2020) 10:1649. doi: 10.3389/fonc.2020.01649
33. Gorry C, McCullagh L, Barry M. Economic Evaluation of Systemic Treatments for Advanced Melanoma: A Systematic Review. *Value Health J Int Soc Pharmacoeconomics Outcomes Res* (2020) 23(1):52–60. doi: 10.1016/j.jval.2019.07.003
34. Takushima Y, Igarashi A, Yoshihara H, Shitara K, Doi T. Cost-Effectiveness of Trifluridine/Tipiracil Against Nivolumab for Heavily Pretreated Metastatic Gastric Cancer in Japan. *Japanese J Clin Oncol* (2021) 51(9):1383–90. doi: 10.1093/jjco/hyab086
35. Chen HD, Zhou J, Wen F, Zhang PF, Zhou KX, Zheng HR, et al. Cost-Effectiveness Analysis of Apatinib Treatment for Chemotherapy-Refractory Advanced Gastric Cancer. *J Cancer Res Clin Oncol* (2017) 143(2):361–8. doi: 10.1007/s00432-016-2296-z
36. Lam SW, Wai M, Lau JE, McNamara M, Earl M, Udeh B. Cost-Effectiveness Analysis of Second-Line Chemotherapy Agents for Advanced Gastric Cancer. *Pharmacotherapy* (2017) 37(1):94–103. doi: 10.1002/phar.1870
37. Kimura M, Usami E, Teramachi H, Yoshimura T. Cost-Effectiveness and Safety of Ramucirumab Plus Paclitaxel Chemotherapy in the Treatment of Advanced and Recurrent Gastric Cancer. *J Oncol Pharm Pract Off Publ Int Soc Oncol Pharm Practitioners* (2018) 24(6):403–11. doi: 10.1177/1078155217707335
38. Han J, She L, Yao L, Huang J. Cost-Effectiveness Analysis of Nivolumab in Treatment of Chemotherapy-Refractory Advanced Gastric Cancer Based on Markov Model. *Chin J Gen Surg* (2019) 28(3):327–34. doi: 10.1177/1078155217707335
39. NHSA. *Notice of the National Healthcare Security Administration on Bringing 17 Kinds of Anticancer Drugs Into the Category B of National Basic Medical Insurance, Industrial Injury Insurance and Maternity Insurance Drug* (2018). Available at: http://www.nhsa.gov.cn/art/2018/10/10/art_19_397.html.

Conflict of Interest: The authors declare that the research was conducted in the absence of any commercial or financial relationships that could be construed as a potential conflict of interest.

Publisher's Note: All claims expressed in this article are solely those of the authors and do not necessarily represent those of their affiliated organizations, or those of the publisher, the editors and the reviewers. Any product that may be evaluated in this article, or claim that may be made by its manufacturer, is not guaranteed or endorsed by the publisher.

Copyright © 2022 Shu, Ding and Zhang. This is an open-access article distributed under the terms of the Creative Commons Attribution License (CC BY). The use, distribution or reproduction in other forums is permitted, provided the original author(s) and the copyright owner(s) are credited and that the original publication in this journal is cited, in accordance with accepted academic practice. No use, distribution or reproduction is permitted which does not comply with these terms.

frontiers | Frontiers in Oncology

ORIGINAL RESEARCH
published: 02 May 2022
doi: 10.3389/fonc.2022.877493

Patterns of Multimodality Management of Gastric Cancer—Single Institutional Experience of 372 Cases From a Tertiary Care Center in North India

Sunil Kumar[1], Naveen Kumar[1], Suryanarayana Deo[1], Sandeep Bhoriwal[1], Amitabha Mandal[1], Atul Sharma[2], Sushmita Pathy[3], Prasenjit Das[4], Sanjay Thulkar[5] and Sushma Bhatnagar[6]*

[1] Department of Surgical Oncology, DR. Bhim Rao Ambedkar Institute Rotary Cancer Hospital (DRBRAIRCH), All India Institute of Medical Sciences, New Delhi, India, [2] Department of Medical Oncology, DR. Bhim Rao Ambedkar Institute Rotary Cancer Hospital (DRBRAIRCH), All India Institute of Medical Sciences, New Delhi, India, [3] Department of Radiation Oncology, DR. Bhim Rao Ambedkar Institute Rotary Cancer Hospital (DRBRAIRCH), All India Institute of Medical Sciences, New Delhi, India, [4] Department of Pathology, All India Institute of Medical Sciences, New Delhi, India, [5] Department of Oncoradiology, DR. Bhim Rao Ambedkar Institute Rotary Cancer Hospital (DRBRAIRCH), All India Institute of Medical Sciences, New Delhi, India, [6] Department of Oncoanasthesia, DR. Bhim Rao Ambedkar Institute Rotary Cancer Hospital (DRBRAIRCH), All India Institute of Medical Sciences, New Delhi, India

OPEN ACCESS

Edited by:
Pankaj Kumar Garg,
Shri Guru Ram Rai Institute of Medical and Health Sciences, India

Reviewed by:
Ajeet Kumar Tiwari,
Sir Ganga Ram Hospital, India
Rajesh Pasricha,
All India Institute of Medical Sciences Bhopal, India

***Correspondence:**
Suryanarayana Deo
svsdeo@yahoo.co.in

Specialty section:
This article was submitted to Gastrointestinal Cancers: Gastric and Esophageal Cancers, a section of the journal Frontiers in Oncology

Received: 16 February 2022
Accepted: 25 March 2022
Published: 02 May 2022

Citation:
Kumar S, Kumar N, Deo S, Bhoriwal S, Mandal A, Sharma A, Pathy S, Das P, Thulkar S and Bhatnagar S (2022) Patterns of Multimodality Management of Gastric Cancer—Single Institutional Experience of 372 Cases From a Tertiary Care Center in North India. Front. Oncol. 12:877493. doi: 10.3389/fonc.2022.877493

Introduction: Worldwide gastric cancer is the 5th most commonly diagnosed cancer and the leading cause of gastrointestinal cancer-related deaths. Alone surgery provides long-term survival improvements in 20% of the patients with local advanced gastric cancer. The results can be improved considering multimodal management including chemotherapy and radiotherapy. However, in low middle-income countries like India, multimodal management is challenging. Herein, we evaluated the experience of multimodal management of gastric cancer and the long-term outcome.

Methods: Retrospective analysis of the data of 372 patients was done from a prospectively maintained computerized database from 1994 to 2021. Records were analyzed for demographic details, treatment patterns, recurrences, and long-term outcomes (DFS and OS). Statistical analysis was done with the package SPSS version 26 (IBM Corp, Chicago, Illinois, USA).

Results: This study included 372 patients. The mean age of the patients was 54.07. A total of 307 patients (82.5%) were operated upfront, 45 (12%) received NACT, and 20 (5.5%) underwent the palliative procedure. A total of 53.2% underwent curative resection. R0 resection rate was achieved in 95% of patients. A total of 72.58% of patients required adjuvant treatment, and the majority of the patients underwent chemoradiotherapy. The most common site of metastasis was the liver. Median follow-up was 50.16 months. The 3-year disease-free survival and overall survival were 36.28% and 67.8%, and the 5-year disease-free survival and overall survival were 30.15% and 37.7%, respectively.

Conclusion: Our study suggested that multimodal management is required in locally advanced gastric cancer to achieve good long-term outcomes. The treatment sequence can be tailored based on the available resources.

Keywords: gastric cancer, multimodal, outcomes, survival, India

INTRODUCTION

Worldwide gastric cancer is the 5th most commonly diagnosed cancer and ranks 3rd in cancer-related death (1). Although gastric cancer was the leading cause of cancer death till the 1980s, the incidence has declined rapidly since the last few decades in most parts of the world (2–4). The decline in gastric cancer incidence was due to identifying *Helicobacter pylori* as a risk factor and modifying dietary factors. The rate of decline of gastric cancer is more profound in the United Kingdom, whereas in a country like Japan with a very high incidence of gastric cancer, the decline rate is slower. Almost two-thirds of the gastric patients are found with advanced stage, whereas 50% of patients are detected at the early stage in East Asian countries like Japan and Korea because of the endoscopic screening program (5, 6).

Gastric cancer is a lethal disease with persistently high mortality due to its presence in the advanced stage and change in the distribution of tumor location from pylorus and antrum to body and cardia (7). Despite the aggressive nature of the disease, the prognosis of gastric cancer had improved significantly in the last two decades due to improvement in surgical management and multimodal therapy. If it is diagnosed in the early stage, very good survival outcomes can be achieved with multimodal management (8). Multimodal management includes surgical management, ranging from endoscopic mucosal resection to gastrectomy, lymph node dissection, neoadjuvant chemotherapy (NACT), perioperative chemotherapy, adjuvant chemoradiation, and adjuvant chemotherapy. Advanced stage disease has a very dismal prognosis; multimodal treatment approach may prolong the survival. This study aims to evaluate the basic demographic characteristic, multimodal approach to gastric cancer, resectability rate, the response of neoadjuvant therapy, recurrence pattern, and long-term survival of gastric cancer in a high-volume tertiary cancer care center in North India.

MATERIALS AND METHODS

Retrospective analysis of the data of 372 patients was done from a prospectively maintained computerized database from 1994 to 2021. All the gastric patients were registered in the gastrointestinal cancer clinic. Multimodal management was planned. Upper gastrointestinal endoscopy (UGIE) and biopsy were done in all patients for diagnosis and extent of intraluminal disease. Contrast-enhanced computed tomography (CECT) of the chest, abdomen, and pelvis was done for the staging of the disease.

Treatment Protocol

Before the neoadjuvant era, upfront surgery was offered in all potentially operable cases and neoadjuvant chemotherapy was only offered to the patients who were initially unresectable or locally advanced without evidence of distant metastasis. Adjuvant therapy was given to patients with a pathological T3 or above and node-positive disease.

In the last decade, neoadjuvant chemotherapy has gained ground significantly and now it is a standard treatment in locally advanced gastric cancer after the results of several randomized trials (9, 10). We followed the same treatment protocol. In all locally advanced tumors (T3/T4 or node positive), neoadjuvant chemotherapy followed by surgery was done. Upfront surgery was performed in only emergency indications like bleeding or gastric outlet obstruction.

Neoadjuvant Chemotherapy Regimens

We used epirubicine, cisplatin, and 5-FU (ECF); folinic acid, fluorouracil, and oxaliplatin (FOLFOX); and capecitabine and oxaliplatine (CAPOX) before FLOT era. After the FLOT4-AIO trial, 5-fluorouracile, leucovorin, oxaliplatin, and docetaxel (FLOT) regimen was an integral part of our NACT schedule for patients with good performance status (ECOG 0 or 1), and FOLFOX for poor performance status patients (2 or 3).

Adjuvant Treatment

Adjuvant treatment was offered to patients with pathological T3/T4 or node-positive disease. Adjuvant chemotherapy alone was given to the patients with adequate lymph node dissection (D2 lymphadenectomy), and optimum lymph node was evaluated in histopathological examination (16 nodes). Adjuvant chemoradiation as per McDonald's protocol (chemotherapy: fluorouracil and leucovorin; radiotherapy: 45 Gy of radiation at 1.80 Gy per day, 5 days per week for 5 weeks, with intensity-modulated radiation therapy technique) was given to those patients who had inadequate lymph node dissection (less than D2 dissection) and less than 16 nodes evaluated in the pathological examination.

Statistical Analysis

Categorical variables were expressed in percentages and frequencies. A chi-square test was used for group comparison of categorical variables. The software package SPSS version 26 (IBM Corp, Chicago, Illinois, USA) was used for the statistical analysis. All values of $p < 0.05$ were taken as statistical significance. Disease-free survival (DFS) was calculated from the date of completion of the treatment to recurrence or death, whichever comes earlier. Overall survival (OS) was calculated

from the date of registration to death or lost to follow up, whichever comes earlier. Kaplan–Meier estimate was used for survival analysis.

RESULTS

This study included 372 patients. The mean age of the patients was 54.07 (range 17–84 years), with male predominance. Pain in the abdomen was the most common presenting symptom followed by anorexia and weight loss. The antropyloric region was the most common site of tumor occurrence. The majority of the patients were presented with locally advanced stages (stage II and stage III). The demographic profile of the patients is shown in **Table 1**. Among all the patients, 63 (16.9%), 39 (10.5%), and 36 patients (9.7%) were smokers, alcoholics, and tobacco chewers, respectively. Most of the patients were presented with good performance status (**Table 1**).

A total of 307 patients (82.5%) were operated upfront, 45 (12%) patients were planned for neoadjuvant chemotherapy (NACT) followed by reassessment for surgery, and 20 (5.5%) cases underwent the palliative procedure. Among NACT patients, complete response (CR) and partial response (PR) were noted in 1 (0.5%) and 24 (6.5%) respectively; 17 (4.6%) patients had stable disease and 2 (0.5%) had progressive disease. Curative resection was done in 19 patients (42.2%) after NACT, and the rest of the 26 patients were unresectable on exploration and underwent palliative surgery.

The curative resection rate in this study was 53.4% (199 patients). The most commonly performed surgical procedure was distal radical gastrectomy followed by total gastrectomy. Clavien Dindo grade 3–4 was seen in 16 (7.5%) patients. R0 resection rate was achieved in 95% of the patients. The mean node harvested was 15, ranging from 6 to 32, and the mean pathological node involvement was 3 (range 1–16). Surgical details are shown in **Table 2**. After palliative surgery, 51 (13.3%) patients did not receive any form of palliative therapy, 102 (27.4%) patients received palliative chemotherapy, 2 (0.5%) patients received palliative radiotherapy, and the remaining 18 patients (4.8%) received the best supportive care.

After curative resection, 143 (72.58%) patients received adjuvant therapy, and 54 (27.4%) did not receive any adjuvant therapy. Out of 143 patients, 30 (15.2%) patients received adjuvant chemotherapy and 103 (52.3%) patients received adjuvant chemoradiotherapy. Palliative RT and palliative chemotherapy were offered to 3 (1.5%) patients each, whereas 1 patient went for the best supportive therapy; the remaining 18 patients (9.13%) lost their follow-up. The majority of the patients developed systemic recurrence, and the liver was the most common site of systemic recurrence. Systemic, local, and locoregional recurrence occurred in 72 patients (36.2%), 16 patients (8%), and 13 patients (6.5%), respectively. Among all systemic recurrences, 33 (16.6%) patients had liver metastasis followed by peritoneum in 29 (14.6%) patients.

Survival analysis was done for only those patients who underwent curative resection. The median follow-up was

TABLE 1 | Demographic profile and baseline characteristics of the patients.

Sl N	Parameters	Variables	No. of patients (n = 372)	Percentage
1	**Sex**	Male	274	(73.3%)
		Female	98	(26.7%)
2	**Symptoms**	Pain	222	59.7%
		Anorexia	106	28.5%
		Weight loss	104	28%
		Dyspepsia	68	18.3%
		Vomiting	65	17.5%
		Malena	10	4.3%
		Hematemesis	6	1.9%
		GOO	81	21.8%
		Abdominal mass	54	14.5%
3	**Location**	Antropyloric	230	61.8%
		Body	111	29.8%
		Cardia	24	6.5%
		GE Junction	7	1.9%
4	**CT findings**	Perigastric node	107	28.7%
		Ascites	12	3.2%
		Omental nodule	4	1.1%
		Peritoneal deposit	1	0.3%
		Liver mets	1	0.3%
5	**Clinical stage**	Stage 1	17	4.6%
		Stage 2	76	20.4%
		Stage 3	217	58.3%
		Stage 4A	28	7.5%
		Stage 4B	34	9.1%
6	**ECOG**	0	22	5.9%
		1	270	72.6%
		2	58	15.6%
		3	22	5.9%

TABLE 2 | Surgical details and pathological parameters.

Sl N	Parameters	Variables	No. of patients (*n* = 372)	Percentage
1	**Type of surgery**	Curative resection	199	53.4%
		Unresectable on exploration	93	25.1%
		Palliative procedure	80	21.5%
2	**Surgical procedure**	Distal radical gastrectomy (DRG)	119	31.6%
		Total gastrectomy	46	12.4%
		Subtotal gastrectomy	31	8.4%
		Esophago-gastrectomy	1	0.3%
		Wedge resection	2	0.5%
		Palliative procedure (Unresectable + palliative surgery)	173	46.8%
3	**Exploration findings**	Omental deposits	74	19.9%
		Peritoneal deposits	68	18.3%
		Liver metastasis	37	9.9%
		Colonic involvement	37	9.9%
		Pancreas involvement	37	9.9%
		Ascites	37	9.9%
		Mesenteric deposits	25	6.7%
		Duodenal involvement	29	7.8%
		Celiac axis involvement	18	4.8%
4	**Margin positivity**	Proximal margin	4	1.1%
		Distal margin	6	1.6%
		Final margin positivity	10	5.1%
5	**Pathological stage**	Stage 0	3	1.5%
		Stage 1	14	7.1%
		Stage 2	85	42.7%
		Stage 3	90	45.2%
		Stage 4	7	3.5%

50.166 months. The 3-year DFS and OS were 36.28% and 67.8%, respectively. The 3-year median DFS and OS were 61 (95% CI, 46.6–75.3) and 84 (95% CI, 85.1–103.1) months (**Figure 1**). The 5-year DFS and OS were 30.15% and 37.7%, respectively, and the 5-year median DFS and OS were 63 months (95% CI, 96.2–119.7) and (95% CI, 52.7–73.2) (**Figure 2**).

DISCUSSION

Although the incidence of gastric cancer has declined in most countries, it is still a major cause of cancer-related mortality (2, 7). The lethality of gastric cancer lies in its presentation in late stage, due to vague symptomatology. Until or unless there are features of gastric outlet obstruction, hematemesis, abdominal lump, or gross weight loss, the disease does not attract the attention of the patients (11, 12). In this study, the most common symptom was pain in the abdomen. Worldwide, the incidence of stomach cancer has declined significantly, mainly in European countries, due to modification in dietary factors and identification of *H. pylori* as a risk factor. Other risk factors are smoking, alcohol intake, and tobacco chewing (13). In our study, almost 35% of the patients were associated with predisposing factors.

In the last two decades, the trends of the location of the tumor in the stomach have shifted more proximally from the location in the distal stomach (14). In the current study, the distal stomach is the most common site of cancer.

Traditionally, the staging of gastric cancer is done with a CT scan; however, various studies have been conducted to see the role of 18-FDG PET scan. PET scan has certain limitations in diagnosing gastric cancer because the normal gastric mucosa and benign lesions take FDG uptake and are difficult to differentiate with pathological uptake. Few studies have reported a limited role in stage IV disease (peritoneal carcinomatosis) with low sensitivity (range: 9%–50%; median: 32.5%) and marginal higher specificity (63%–99%; median: 88.5%) (15). Thus, the role of PET scan is still evolving. At our center, a PET scan is advised only in recurrent or stage IV cases to prognosticate the disease.

The sequence of choice of the multimodal treatment depends on various factors like patient's performance status (ECOG performance status), comorbidity, and site and stage of the disease. Treatment options for early gastric cancer are eradication of *H. pylori*, endoscopic therapy, gastrectomy, and adjuvant therapy (16). In developing countries, endoscopic resection expertise is still lesser, and gastrectomy is commonly preferred. In our study, only 4.6% of the patients presented with early gastric cancer and all patients underwent gastrectomies.

Locally advanced gastric cancer requires multimodal management. Many randomized trials and one meta-analysis proved that using NACT or perioperative chemotherapy has a survival advantage over upfront surgery for potentially resectable gastric cancer (9, 17). In our study, more than 50% of patients had a locally advanced stage and required multimodal management. The resectability rate after NACT was 42.2%, which is a bit lower than other studies. The pathological CR rate is lower (0.5%) in this study as compared to literature (5%–15%) (18, 19). This difference was seen because of the advanced stage at the presentation.

Gastrectomy with adequate lymph node dissection (at least 16 nodes) is the surgical procedure of choice for operable gastric cancer with good quality of life. Proximal tumors involving cardia, fundus, and GE junction are treated with total

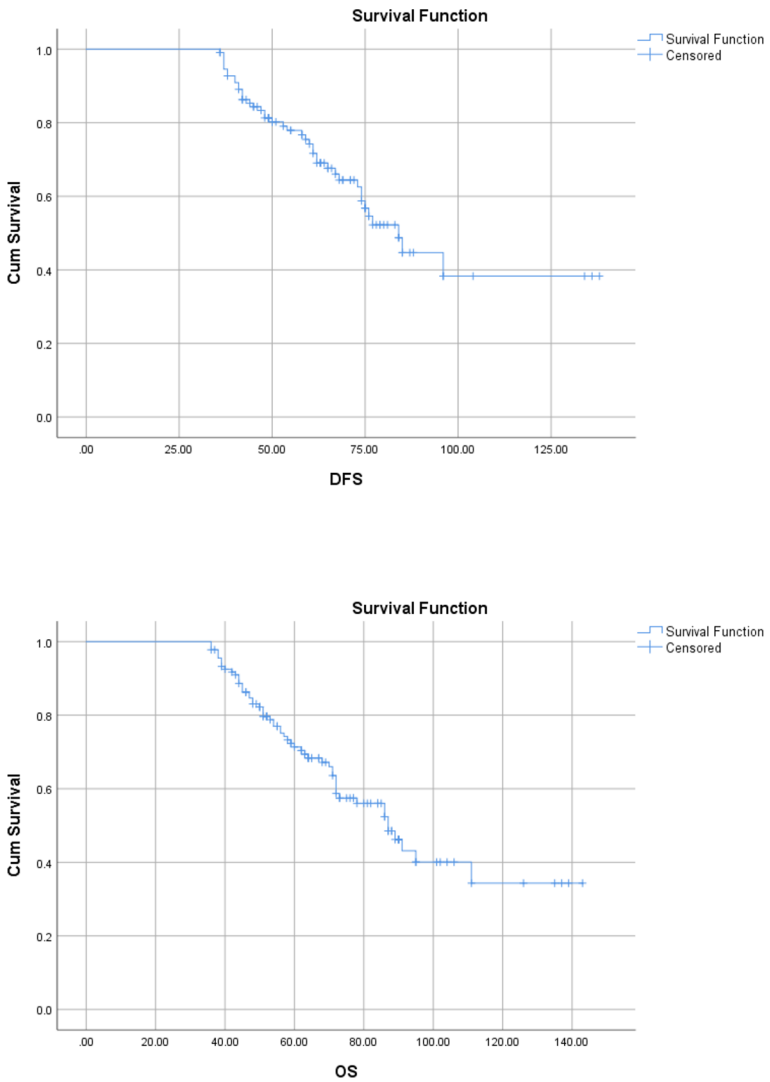

FIGURE 1 | Kaplan–Meier curve showing 3-year disease-free and overall survival.

gastrectomy and distal tumors (body, antropyloric area) with subtotal or distal gastrectomy. In our series, most of the patients underwent distal radical gastrectomy since the majority of the patients had distal gastric cancer and total gastrectomy was only performed for proximal tumors or involvement of the whole stomach. In the literature, two major trials compared subtotal with total gastrectomy for distal gastric cancer without any significant survival advantage in favor of total gastrectomy (20, 21). In this study, distant metastasis, involvement of celiac axis, hepatic artery, and aorta were considered as unresectable diseases, and require palliative surgery (56%) in the form of feeding jejunostomy or gastrojejunostomy.

The extent of lymphadenectomy is an area of active debate for a long time. Various types of lymph node dissection is described in the literature, D1 (Station 1-6), D1+ (Station 1-6, and 8a, 9, 11), D2 (Station 1-12a), and D3 (Station 1-16 or D2+ paraaortic node dissection). Japanese and Korean surgeons preferred more aggressive lymph node dissection, whereas according to current NCCN guidelines, spleen and pancreas preserving D2 lymphadenectomy with at least 15 nodes for histopathological examination is the standard of care (22–24). In the current study, all the patients underwent D2 lymph node dissection and the complication rate is comparable. Most of the prospective randomized trials have failed to demonstrate the survival advantage of D2 over D1 lymphadenectomy. The two largest prospective randomized trials (MRC, Dutch), which are debated the most, also did not find any significant survival advantage of D2 over D1 lymphadenectomy; however, long-term analysis of these studies had shown disease-specific survival benefits (25–28).

Targeted therapy such as trastuzumab has been established for unresectable and metastatic HER2 positive gastric cancer. Many trials like ToGA, LOGiC, and TyTNHA showed an improvement in survival after using the HER2-targeted

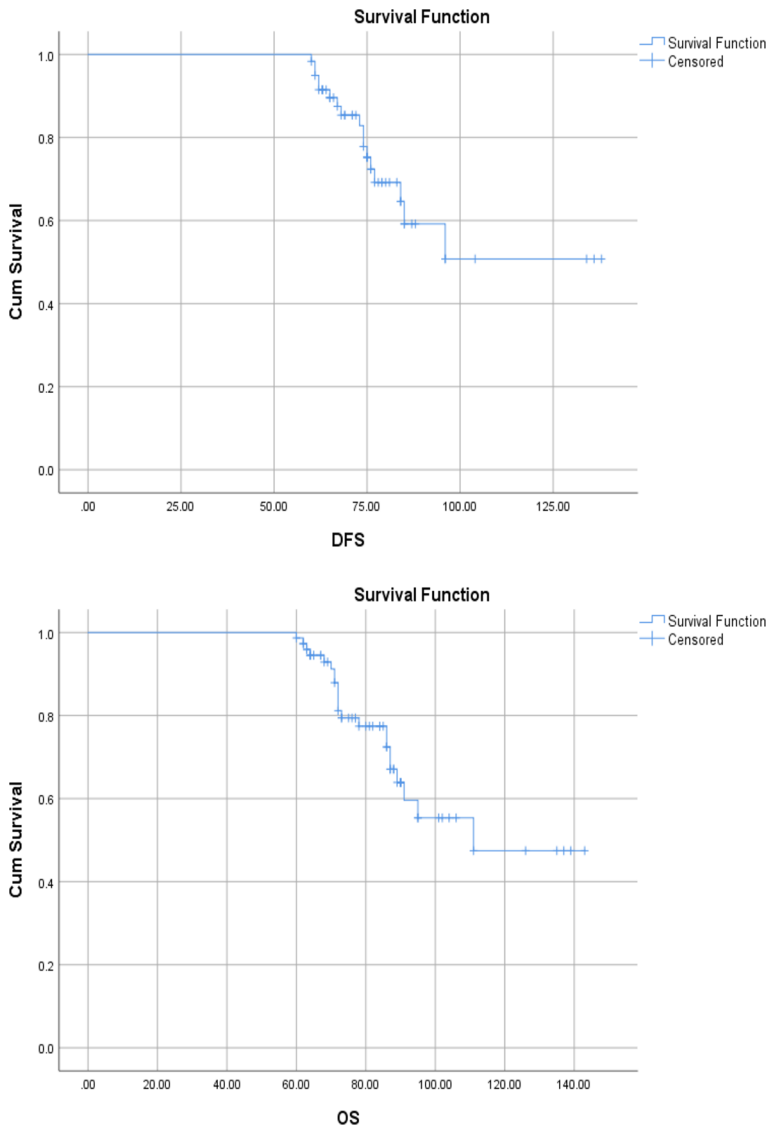

FIGURE 2 | Kaplan–Meier curve showing 5-year disease-free and overall survival.

therapy. Various phase III trials are ongoing to explore other targeted therapies based on epidermal growth factor receptor (EGFR), vascular endothelial growth factor (VEGF)/vascular endothelial growth factor receptor (VEGFR), MET, or the mechanistic target of rapamycin (mTOR) (29).

Systemic and locoregional recurrence are the two forms of recurrence in gastric cancer, where systemic is common. In one study, systemic and locoregional recurrences were 60% and 40%, respectively (30). Another study quoted locoregional recurrence rate in 15% of cases; peritoneal, 49%; nonperitoneal distant recurrence, 54%; and liver metastasis, 20% (31). Another study evaluated the recurrence pattern in proximal gastric cancer and found a recurrence rate of 85.9% within 2 years, where locoregional recurrence was the most common pattern followed by hematogenous. Among them, liver was the most common organ for systemic recurrence followed by the peritoneum (32). In this current study, systemic recurrence (36.2%) was the most common form of relapse and liver was the most common site.

Survival after curative resection depends on stage, location, and ethnicity. The Asian population has better survival than the Western population (32). In the literature, 5-year survival of locally advanced gastric cancer is reported with a range of 40%–60% after multimodal management (25, 26, 33). Our study has shown almost similar outcomes.

CONCLUSION

Although the incidence of gastric cancer has been decreased in the Indian population, it is still a deadly disease, because of its

aggressive biology and late presentation. Our study suggested that optimal outcomes of gastric cancer in low middle-income countries can be achieved based on the best available resources using a multimodal treatment approach.

DATA AVAILABILITY STATEMENT

The original contributions presented in the study are included in the article/supplementary material. Further inquiries can be directed to the corresponding author.

ETHICS STATEMENT

Ethical review and approval were not required for the study on human participants in accordance with the local legislation and institutional requirements. Written informed consent for participation was not required for this study in accordance with the national legislation and the institutional requirements.

AUTHOR CONTRIBUTIONS

SD started the surgical program and provided extensive guidance in making the manuscript. NK and AM analyzed the data and wrote the manuscript. SK and SBho reviewed the manuscript and added their inputs. AS were the lead medical oncologist and added the inputs. SP was a lead radiation oncologist and PD was the lead pathologist and they added their inputs. All authors contributed to the article and approved the submitted version.

REFERENCES

1. Bray F, Ferlay J, Soerjomataram I, Siegel RL, Torre LA, Jemal A. Global Cancer Statistics 2018: GLOBOCAN Estimates of Incidence and Mortality Worldwide for 36 Cancers in 185 Countries. *CA Cancer J Clin* (2018) 68 (6):394–424. doi: 10.3322/caac.21492
2. Pisani P, Parkin DM, Ferlay J. Estimates of the Worldwide Mortality From Eighteen Major Cancers in 1985. Implications for Prevention and Projections of Future Burden. *Int J Cancer* (1993) 55(6):891–903. doi: 10.1002/ijc.2910550604
3. Zhu AL, Sonnenberg A. Is Gastric Cancer Again Rising? *J Clin Gastroenterol* (2012) 46(9):804–6. doi: 10.1097/MCG.0b013e3182604254
4. Fitzsimmons D, Osmond C, George S, Johnson CD. Trends in Stomach and Pancreatic Cancer Incidence and Mortality in England and Wales, 1951-2000. *Br J Surg* (2007) 94(9):1162–71. doi: 10.1002/bjs.5751
5. Ahn HS, Lee H-J, Yoo M-W, Jeong S-H, Park D-J, Kim H-H, et al. Changes in Clinicopathological Features and Survival After Gastrectomy for Gastric Cancer Over a 20-Year Period. *Br J Surg* (2011) 98(2):255–60. doi: 10.1002/bjs.7310
6. Rausei S, Boni L, Rovera F, Dionigi G. Locally Advanced Gastric Cancer: A New Definition to Standardise. *J Clin Pathol* (2013) 66(2):164–5. doi: 10.1136/jclinpath-2012-201176
7. Fuchs CS, Mayer RJ. Gastric Carcinoma. *N Engl J Med* (1995) 333(1):32–41. doi: 10.1056/NEJM199507063330107
8. Cellini F, Morganti AG, Di Matteo FM, Mattiucci GC, Valentini V. Clinical Management of Gastroesophageal Junction Tumors: Past and Recent Evidences for the Role of Radiotherapy in the Multidisciplinary Approach. *Radiat Oncol* (2014) 9(1):45. doi: 10.1186/1748-717X-9-45
9. *Perioperative Chemotherapy Versus Surgery Alone for Resectable Gastroesophageal Cancer|NEJM*. Available at: https://www.nejm.org/doi/full/10.1056/nejmoa055531.
10. Al-Batran S-E, Homann N, Pauligk C, Goetze TO, Meiler J, Kasper S, et al. Perioperative Chemotherapy With Fluorouracil Plus Leucovorin, Oxaliplatin, and Docetaxel Versus Fluorouracil or Capecitabine Plus Cisplatin and Epirubicin for Locally Advanced, Resectable Gastric or Gastro-Oesophageal Junction Adenocarcinoma (FLOT4): A Randomised, Phase 2/3 Trial. *Lancet Lond Engl* (2019) 393(10184):1948–57. doi: 10.1016/S0140-6736(18)32557-1
11. Quadri HS, Smaglo BG, Morales SJ, Phillips AC, Martin AD, Chalhoub WM, et al. Gastric Adenocarcinoma: A Multimodal Approach. *Front Surg* (2017) 4:42. doi: 10.3389/fsurg.2017.00042
12. Dicken BJ, Bigam DL, Cass C, Mackey JR, Joy AA, Hamilton SM. Gastric Adenocarcinoma: Review and Considerations for Future Directions. *Ann Surg* (2005) 241(1):27–39. doi: 10.1097/01.sla.0000149300.28588.23
13. Rawla P, Barsouk A. Epidemiology of Gastric Cancer: Global Trends, Risk Factors and Prevention. *Przeglad Gastroenterol* (2019) 14(1):26–38. doi: 10.5114/pg.2018.80001
14. Crew KD, Neugut AI. Epidemiology of Gastric Cancer. *World J Gastroenterol* (2006) 12(3):354–62. doi: 10.3748/wjg.v12.i3.354
15. Dascălu R-I, Păduraru DN, Bolocan A, Ion D, Andronic O. The Role of PET-CT in Gastric Cancer – A Narrative Review. *Sudan J Med Sci (SJMS)* (2020) 15 (3):332–44. doi: 10.18502/sjms.v15i3.7749
16. Espinel J, Pinedo E, Ojeda V, del Rio MG. Treatment Modalities for Early Gastric Cancer. *World J Gastrointest Endosc* (2015) 7(12):1062–9. doi: 10.4253/wjge.v7.i12.1062
17. Xiong B-H, Cheng Y, Ma L, Zhang C-Q. An Updated Meta-Analysis of Randomized Controlled Trial Assessing the Effect of Neoadjuvant Chemotherapy in Advanced Gastric Cancer. *Cancer Invest* (2014) 32 (6):272–84. doi: 10.3109/07357907.2014.911877
18. Gallardo-Rincón D, Oñate-Ocaña LF, Calderillo-Ruiz G. Neoadjuvant Chemotherapy With P-ELF (Cisplatin, Etoposide, Leucovorin, 5-Fluorouracil) Followed by Radical Resection in Patients With Initially Unresectable Gastric Adenocarcinoma: A Phase II Study. *Ann Surg Oncol* (2000) 7(1):45–50. doi: 10.1007/s10434-000-0045-6
19. Yoshikawa T, Sasako M, Yamamoto S, Sano T, Imamura H, Fujitani K, et al. Phase II Study of Neoadjuvant Chemotherapy and Extended Surgery for Locally Advanced Gastric Cancer. *Br J Surg* (2009) 96(9):1015–22. doi: 10.1002/bjs.6665
20. Robertson CS, Chung SC, Woods SD, Griffin SM, Raimes SA, Lau JT, et al. A Prospective Randomized Trial Comparing R1 Subtotal Gastrectomy With R3 Total Gastrectomy for Antral Cancer. *Ann Surg* (1994) 220(2):176. doi: 10.1097/00000658-199408000-00009
21. Bozzetti F, Marubini E, Bonfanti G, Miceli R, Piano C, Gennari L. Subtotal Versus Total Gastrectomy for Gastric Cancer: Five-Year Survival Rates in a Multicenter Randomized Italian Trial. Italian Gastrointestinal Tumor Study Group. *Ann Surg* (1999) 230(2):170–8. doi: 10.1097/00000658-199908000-00006
22. Japanese Gastric Cancer Association. Japanese Gastric Cancer Treatment Guidelines 2018 (5th Edition). *Gastric Cancer* (2021) 24(1):1–21. doi: 10.1007/s10120-020-01042-y
23. Degiuli M, De Manzoni G, Di Leo A, D'Ugo D, Galasso E, Marrelli D, et al. Gastric Cancer: Current Status of Lymph Node Dissection. *World J of Gastroenterol* (2016) 22(10):2875–93. doi: 10.3748/wjg.v22.i10.2875
24. Sasako M, Sano T, Yamamoto S, Kurokawa Y, Nashimoto A, Kurita A, et al. D2 Lymphadenectomy Alone or With Para-Aortic Nodal Dissection for Gastric Cancer. *N Engl J Med* (2008) 359(5):453–62. doi: 10.1056/NEJMoa0707035
25. Cuschieri A, Weeden S, Fielding J, Bancewicz J, Craven J, Joypaul V, et al. Patient Survival After D1 and D2 Resections for Gastric Cancer: Long-Term Results of the MRC Randomized Surgical Trial. Surgical Co-Operative Group. *Br J Cancer* (1999) 79(9–10):1522–30. doi: 10.1038/sj.bjc.6690243
26. Songun I, Putter H, Kranenbarg EM-K, Sasako M, van de Velde CJH. Surgical Treatment of Gastric Cancer: 15-Year Follow-Up Results of the Randomised Nationwide Dutch D1D2 Trial. *Lancet Oncol* (2010) 11(5):439–49. doi: 10.1016/S1470-2045(10)70070-X

27. Degiuli M, Sasako M, Ponti A, Vendrame A, Tomatis M, Mazza C, et al. Randomized Clinical Trial Comparing Survival After D1 or D2 Gastrectomy for Gastric Cancer. *Br J Surg* (2014) 101(2):23–31. doi: 10.1002/bjs.9345
28. Information NC for B, Pike USNL of M 8600 R and MD B, Usa 20894. A Meta-Analysis of D1 Versus D2 Lymph Node Dissection. In: *Database of Abstracts of Reviews of Effects (DARE): Quality-Assessed Reviews*. UK: Centre for Reviews and Dissemination (2012). Available at: https://www.ncbi.nlm.nih.gov/books/NBK127357/.
29. Kiyozumi Y, Iwatsuki M, Yamashita K, Koga Y, Yoshida N, Baba H. Update on Targeted Therapy and Immune Therapy for Gastric Cancer, 2018. *J Cancer Metastasis Treat* (2018) 4:31. doi: 10.20517/2394-4722.2017.77
30. Wanebo HJ, Kennedy BJ, Chmiel J, Steele G, Winchester D, Osteen R. Cancer of the Stomach. A Patient Care Study by the American College of Surgeons. *Ann Surg* (1993) 218(5):583–92. doi: 10.1097/00000658-199321850-00002
31. Elimova E, Slack RS, Chen H-C, Planjery V, Shiozaki H, Shimodaira Y, et al. Patterns of Relapse in Patients With Localized Gastric Adenocarcinoma Who Had Surgery With or Without Adjunctive Therapy: Costs and Effectiveness of Surveillance. *Oncotarget* (2017) 8(46):81430–40. doi: 10.18632/oncotarget.19226
32. Cao L, Selby LV, Hu X, Zhang Y, Janjigian YY, Tang L, et al. Risk Factors for Recurrence in T1-2n0 Gastric Cancer in the United States and China. *J Surg Oncol* (2016) 113(7):745–9. doi: 10.1002/jso.24228
33. *Stomach (Gastric) Cancer Survival Rates*. Available at: https://www.cancer.org/cancer/stomach-cancer/detection-diagnosis-staging/survival-rates.html.

Conflict of Interest: The authors declare that the research was conducted in the absence of any commercial or financial relationships that could be construed as a potential conflict of interest.

Publisher's Note: All claims expressed in this article are solely those of the authors and do not necessarily represent those of their affiliated organizations, or those of the publisher, the editors and the reviewers. Any product that may be evaluated in this article, or claim that may be made by its manufacturer, is not guaranteed or endorsed by the publisher.

Copyright © 2022 Kumar, Kumar, Deo, Bhoriwal, Mandal, Sharma, Pathy, Das, Thulkar and Bhatnagar. This is an open-access article distributed under the terms of the Creative Commons Attribution License (CC BY). The use, distribution or reproduction in other forums is permitted, provided the original author(s) and the copyright owner(s) are credited and that the original publication in this journal is cited, in accordance with accepted academic practice. No use, distribution or reproduction is permitted which does not comply with these terms.

frontiers | Frontiers in Oncology

REVIEW
published: 26 May 2022
doi: 10.3389/fonc.2022.864647

Gastric Cancer With Peritoneal Metastasis—A Comprehensive Review of Current Intraperitoneal Treatment Modalities

Aruna Prabhu[1]*, *Deepti Mishra*[1], *Andreas Brandl*[2,3] and *Yutaka Yonemura*[4,5,6]

[1] Department of Surgical Oncology, Thangam Cancer Center, Namakkal, India, [2] Digestive Unit, Champalimaud Foundation, Lisbon, Portugal, [3] Department of Surgery, Campus Virchow-Klinikum, Charité-Universitätsmedizin Berlin, Berlin, Germany, [4] Department of Regional Cancer therapy, Peritoneal Surface Malignancy Centee, Kishiwada Tokushukai Hospital, Kishiwada, Japan, [5] Japanese/Asian School of Peritoneal Surface Oncology, Osaka, Japan, [6] Department of Regional Cancer therapy, Peritoneal Surface Malignancy Center, Kusatsu General Hospital, Shiga, Japan

OPEN ACCESS

Edited by:
Alberto Biondi,
Agostino Gemelli University Polyclinic (IRCCS), Italy

Reviewed by:
Dario Baratti,
Fondazione IRCCS Istituto Nazionale Tumori, Italy
Carlo Abatini,
Agostino Gemelli University Polyclinic (IRCCS), Italy

***Correspondence:**
Aruna Prabhu
dranuprabhu.surgeon@gmail.com

Specialty section:
This article was submitted to Gastrointestinal Cancers: Gastric and Esophageal Cancers, a section of the journal Frontiers in Oncology

Received: 31 January 2022
Accepted: 22 April 2022
Published: 26 May 2022

Citation:
Prabhu A, Mishra D, Brandl A and Yonemura Y (2022) Gastric Cancer With Peritoneal Metastasis—A Comprehensive Review of Current Intraperitoneal Treatment Modalities. Front. Oncol. 12:864647. doi: 10.3389/fonc.2022.864647

The treatment of patients with peritoneal metastasis from gastric cancer continues to evolve. With various forms of intraperitoneal drug delivery available, it is now possible to reach the sites of peritoneal metastases, which were otherwise sub-optimally covered by systemic chemotherapy, owing to the blood peritoneal barrier. We conducted a narrative review based on an extensive literature research, highlighting the current available intraperitoneal treatment options, which resulted in improved survival in well-selected patients of peritoneally metastasized gastric cancer. Intraperitoneal chemotherapy showed promising results in four different treatment modalities: prophylactic, neoadjuvant, adjuvant, and palliative. It is now possible to choose the type of intraperitoneal treatment/s in combination with systemic treatment/s, depending on patients' general condition and peritoneal disease burden, thus providing individualized treatment to these patients. Randomized controlled trials for the different treatment modalities were mainly conducted in Asia and lack further validation in the other parts of the world. Most recent application tools, such as pressurized intraperitoneal aerosol chemotherapy, seem promising and need to pass the ongoing clinical trials.

Keywords: gastric cancer, peritoneal metastases, intraperitoneal chemotherapy, cytoreductive surgery, HIPEC, PIPAC

1 INTRODUCTION

Gastric cancer (GC) is the third leading cause of cancer-related deaths worldwide with peritoneal metastases (PM) from GC associated with poorer median survival, ranging from 4 to6 months (1–3). In last two decades, however, with the advent of cytoreductive surgery (CRS) and hyperthermic intraperitoneal chemotherapy (HIPEC), there is increasing evidence of improvement in survival in well-selected patients of peritoneally metastasized GC. Other than intraoperative HIPEC, normothermic intraperitoneal chemotherapy in the form of EPIC (early postoperative

intraperitoneal chemotherapy), SIPC (sequential intraperitoneal chemotherapy), neoadjuvant systemic and intraperitoneal chemotherapy (NIPS), and pressurized intraperitoneal aerosolized chemotherapy (PIPAC) are the various ways in which the intraperitoneal route is being utilized for better drug delivery to the sites of PM, wherein the reach of systemic chemotherapy is known to be suboptimal, owing to the blood peritoneal barrier.

2 TREATMENT MODALITIES OF INTRAPERITONEAL CHEMOTHERAPY

Similar to the different types of application, evidence has been created for the respective treatment modalities, such as *prophylactic* for patients with absence but high risk for PM, *neoadjuvant*, and *adjuvant* for patients after complete CRS, and *palliative* over the past two decades. To shed more light on these various clinical indications, they will be separately listed and discussed in the following sections.

2.1 Prophylactic

Metachronus PM have been reported to occur in 15%–46% of patients with locally advanced GC even after a R0 resection and are the most common cause of death in these patients (2, 4). Even with advances in perioperative multimodality treatment regimens, the proportion of patients developing metachronus PM remains high. Risk factors for the development of metachronus PM are T3/4 tumors, lymph node positivity status, higher grade of tumor (grades 3/4), signet ring cell (SRC) histology, and diffuse infiltrative growth pattern. Several studies since 1994 (**Table 1**), including the meta-analysis by Xu et al., Yan et al., and Sun et al. have reported on the beneficial use of prophylactic HIPEC in these patients with higher risk of developing PM (5–7, 9–12, 15–17, 20).

The most recent data on use of prophylactic HIPEC has been reported by Yarema et al. and Beeharry et al. both in 2019. The study by Yarema et al. included 37 patients treated with radical surgery followed by prophylactic HIPEC (13). Out of the 37 patients, 29 had pT4a and eight had pT4b disease. The median OS was 34 months; 1-year OS was 91.7% and DFS was 82.3%. Level I evidence has been reported by Beeharry et al., who conducted a randomized controlled trial (RCT) on 80 consecutive patients of locally advanced GC (18. Patients were separated into two groups: prophylactic HIPEC group (Radical D2 gastrectomy + intraoperative HIPEC with cisplatin 50 mg/m^2 for 60 min) and control group (Radical D2 gastrectomy only). The HIPEC group experienced a significantly better 3-year DFS (93% versus 65%, $p = 0.005$) and lower peritoneal recurrence rate (3% versus 23%, $p < 0.05$).

In a systematic review and random effect analysis of the role of adjuvant IP chemotherapy in resectable GC, reported by Feingold et al., maximal benefit was noted with intra-operative delivery and possibly with the use of Mitomycin C (MMC) (18). The meta-analysis by Desiderio et al. includes 1,810 patients with advanced GC [from nine RCTs and nine non randomized controlled trials (NRCTs)]; 731 undergoing gastrectomy + HIPEC and 1,079 undergoing standard gastrectomy alone, although no significant difference was noted in 1-year OS, the OS at 3 and 5 years did show a statistically significant difference favoring the HIPEC arm (RR 0.71, $p = 0.03$ and RR 0.82, $p = 0.01$) (19), which is in line with previous studies. In addition, HIPEC proved advantageous in preventing peritoneal recurrences (RR 0.63, $p < 0.01$). However, no benefit was reported in local, lymph nodal, liver, or other sites of distant recurrences.

2.1.1 Ongoing Studies

The GASTRICHIP study (a prospective, open, RCT; NCT01882933) is currently accruing patients with resectable T3/4 GC with or without lymph nodal involvement and with or without positive peritoneal cytology at washing, treated with perioperative systemic chemotherapy and D1/D2 gastrectomy, to oxaliplatin HIPEC or not (21). The primary outcome is OS at 5 years with secondary outcome being RFS, morbidity, mortality, and quality of life.

The PREVENT trial (open-label, RCT; NCT04447352) including a total of 200 patients with localized and locally advanced diffuse or mixed type (Laurens' classification) adenocarcinoma of the stomach and Type II/III GEJ (22). All included patients will receive three to six pre-operative cycles of docetaxel, oxaliplatin, leucovorin, and 5-fluorouracil (FLOT) and will be randomized 1:1 to receive surgery only and postoperative FLOT or surgery plus HIPEC (Cis 75 mg/m^2 for 90 min) and postoperative FLOT. The primary endpoint is PFS/DFS.

2.2 Neoadjuvant

Studies focusing on the neoadjuvant, meaning IP use of chemotherapy before CRS, were mainly conducted in the eastern world using IP port systems. During the last years, evidence is growing in the western world, using mainly laparoscopic HIPEC, and most recently pressurized intraperitoneal chemotherapy (PIPAC) for chemotherapeutic administration. Studies using normothermic intraperitoneal chemotherapy (NIPEC) or HIPEC are illustrated in **Table 2**.

In 2006, the concept of neoadjuvant systemic and intraperitoneal chemotherapy (NIPS) was introduced by Yonemura et al. (29) NIPS comprises of oral S1 (tegafur/gimeracil/oteracil) of 60 mg/m^2, from days 1 to 21, followed by 1-week rest. On days 1, 8, and 15 after the start of oral S1, cisplatin of 30 mg/m^2, and docetaxel of 30 mg/m^2 in 500 ml of saline are introduced intraperitoneally through an intraperitoneal (IP) port placed under local anaesthesia. Usuall8y, CRS and HIPEC is performed after five to six cycles of NIPS and 5 to 6 weeks after the last cycle of NIPS.

A new bidirectional intraperitoneal and systemic induction chemotherapy (BISIC) has been reported in 2014 by the same group, wherein 60 mg/m^2 of oral S1 was administered on days 1 to 14 followed by 1-week rest. Cisplatin of 30 mg/m^2 and docetaxel of 30 mg/m^2 were administered by IP infusion, as in NIPS, on day 1, and docetaxel and cisplatin are then administered intravenously (IV) on day 8 (30). In 71.1% of patients, a positive cytology became negative after BISIC, and a

TABLE 1 | Studies on prophylactic IP chemotherapy on patients with locally advanced GC.

Year and Author	Study Design	No. of Patients	Study Group	Group/s Studied	Survival	Morbidity and Mortality
HIPEC						
1994 Hamazoe et al. (5)	RCT	82	Serosal invasion	Sx+ HIPEC (MMC 10 mg/ ml × 50–60 min) vs. Sx alone	5-year OS (NS): 64.3% vs. 52.5% Median OS: 77 m vs. 66 m	Morbidity (Leak): 4.8% vs. 7.5% Mortality: 0% vs. 0%
1994 Fujimura et al. (6)	RCT	58	Serosal invasion	Sx+ HIPEC (300-mg Cis + 30-mg MMC at 41° C–42°C × 60 min) vs. Sx + CNPP (at 37°C–38°C × 60 min) vs. Sx alone	1-, 2-, and 3-year OS: 95%, 89%, and 68% vs. 81%, 75%, and 51% vs. 43%, 23%, and 23%	Morbidity: 36.3% vs. 39.1% vs. NK Mortality: 0% vs. 0% vs. NK
1995 Ikeguchi et al. (7)	RCT	174	Serosal invasion	Sx + HIPEC (MMC, 80–100 mg/m^2) vs. Sx alone	5-year OS – 51 vs. 46% (NS) (1–9 LNs positive: 66 vs. 44%)	Morbidity: 1.2% vs. 2.1%
1995 Takahashi et al. (8)	RCT	113	Serosal invasion	Sx + MMC CH (50-mg MMC) vs. Sx alone	3-year OS: 38 vs. 20% ($p < 0.05$)	Morbidity: 40.4% vs. 7.1% Mortality: 0% vs. 0%
1999 Fujimoto et al. (9)	RCT	141	Serosal invasion	Sx + HIPEC (MMC, 10 mg/ ml) vs. Sx alone	2-, 4-, and 8-year OS: 88%, 76%, and 62% vs. 77%, 58%, and 49% ($p = 0.03$)	Morbidity: 2.8% vs. 2.8% Mortality: 0% vs. 0%
2001 Kim et al. (10)	Pros Case-Control	103	Serosal invasion	Sx + HIPEC (MMC, 10 µg/ml × 120 min) vs. Sx alone	5-year OS: 32.7% vs. 27.1%	Morbidity: 36.5% vs. 33.3%
2001 Yonemura et al. (11)	RCT	139	T2-T4	Sx + HIPEC (30-mg MMC + 300-mg Cis at 42°C–43°C) vs. Sx + CNPP (at 37°C) vs. Sx alone	5-year OS 61 vs. 43 vs. 42%	Morbidity: 19 vs. 14 vs. 19% Mortality: 4 vs. 0 vs. 4%
2006 Zhu et al. (12)	Pros Case - Control	118	Serosal invasion	Sx + HIPEC (30-mg MMC + 300-mg Cis) vs. Sx alone	Mean OS: 61 vs. 43 m 2-, 4-, and 6 -year OS: 83%, 70.5%, and 67.9% vs. 63.7%, 52.1%, and 37.7%	Morbidity: 23.1% vs. 12.2% Mortality: 0% vs. 0%
2019 Yarema et al. (13)	Retro	37	Serosal invasion	Sx + HIPEC	Mean OS: 34m 1-year OS:	Morbidity: 29.1% Mortality: 5.1%
2019 Beeharry et al. (14)	RCT	80	Locally advanced cT3/4	Sx + HIPEC (Cis of 50 mg/m^2; 60 min) vs. Sx alone	3-year DFS 93% vs. 65% ($p = 0.0054$)	Morbidity: 7.5% vs. 15% Mortality-: 0% vs. 0%
2004 Xu et al. (15)	Meta-analysis	1161: 11 studies	Locally advanced GC	Sx + IP chemotherapy in GC vs. Sx alone	Pooled Odds ratio: 0.51	–
2007 Yan et al. (16)	Meta-analysis	1,648: 13 studies	Locally advanced GC	Sx + IP chemotherapy in GC vs. Sx alone	HIPEC: HR, 0.60; HIPEC + EPIC: HR, 0.45	IP chemotherapy-Intra-abdominal abscess: HR, 2.37; Neutropenia: HR, 4.33
2012 Sun et al. (17)	Meta-analysis	1,062: 10 studies	Locally advanced GC	Sx + HIPEC vs. Sx alone	HIPEC with: MMC-RR, 0.75; 5FU-RR, 0.69; Overall RR, 0.73	BM suppression: RR, 1.68; Anastomotic leak: RR, 0.52; Bowel fistula: RR, 1.38, Adhesive ileus: RR, 0.79 Liver dysfunction: RR, 1.47 (all NS)
2016 Feingold et al. (18)	systematic review	2,029: 17 studies	locally advanced GC	Sx + HIPEC vs. Sx alone	HIPEC: 5-year OR 0.65 ($p = 0.0015$)	
2017 Desiderio et al. (19)	Meta-analysis	1,810:18 studies	advanced GC	Sx + HIPEC vs. Sx alone	HIPEC: 3-year OS RR 0.71 ($p = 0.03$) 5-year OS RR 0.82 ($p = 0.01$)	

Sx, Surgery; CNPP, continuous normothermic peritoneal perfusion; LNs, lymph nodes; CH, activated charcoal particles; BM, bone marrow; NS, not significant; RR, risk ratio; NK, not known; MMC, mitomycin C; Cis, cisplatin; 5FU, 5 fluro-uracil; OS, overall survival; DFS, disease-free survival.

complete cytoreduction was possible in 64% of the patients. Grades 3 and 4 morbidity were reported in 9% and 6.8% of patients with operative mortality of 4.5%. Patient selection is of utmost importance for gaining maximum benefit from these comprehensive treatment options.

The same group published long-term survival of patients with PM from GC, with the above multimodality treatment (27). Out of the 419 patients treated with NIPS/BISIC, a CC0 resection was possible in 266 (63.5%) with resultant 10-year survival of 8.3% and median OS of 20.5 months. They identified that Peritoneal Cancer Index (PCI) before NIPS ≤ 13, after NIPS ≤ 11, small bowel PCI ≤ 2, ≤ 5 involved peritoneal sectors, negative pre- and post-NIPS cytology, and complete cytoreduction were all associated with significantly favorable prognosis.

TABLE 2 | Studies on neoadjuvant IP chemotherapy in patients with PM from GC.

Year and Author	Study Design	No. of Patients	Study Group	IP Treatment	Response Rate (%)	Median Overall Survival	Morbidity and Mortality
NIPEC							
2012 Fujiwara et al. (23)	Phase II	18	Cyto pos/PM	DOC: 40–60 mg/m^2	62.5–78	24.6	
2013 Fushida et al. (24)	Phase II	27	PM	DOC: 35–50 mg/m^2	22–51.9	16.2	
2013 Yamaguchi et al. (25)	Phase II	35	PM	PTX: 20 mg/m^2	68–97	17.6	
2017 Ishigami et al. (26)	Phase II	100	Cyto pos/PM	PTX: 20 mg/m^2	64	30.5	
2020 Yonemura et al. (27)	Pros case control	419	Cyto pos/PM	DOC: 30 mg/m^2 CIS: 30 mg/m^2	64.1	CC-0: 20.5 CC-1: 12.0	
HIPEC							
2017 Yonemura et al. (28)	Pros case control	53	PM	DOC: 30 mg/m^2 CIS: 30 mg/m^2	PCI regression	14.4m 19.2m	Morbidity: 22.2% Mortality: 3.7%
2021 Badgwell et al. (32)	Phase II	20	Cyto pos/PM	MMC: 30 mg CIS: 200 mg	n.a.	24.2 post CRS: 16.1	Grade III/IV: 25% Mortality: 0%

NIPEC, normothermic intraperitoneal chemotherapy; HIPEC, hyperthermic intraperitoneal chemotherapy; Cyto pos, positive cytology; PM, peritoneal metastasis; DOC, docetaxel; PTX, paclitaxel; CIS, cisplatin; MMC, mitomycin C; CC, completeness of cytoreduction; CRS, cytoreductive surgery; n.a., not available.

IP paclitaxel has also been evaluated in a prospective phase II study by Chia et al., in combination with systemic capecitabine and oxaliplatin (XELOX) in patients with GCPM (31). Forty-four patients were treated with IP paclitaxel (40 mg/m^2 on days 1 and 8), intravenous oxaliplatin (100 mg/m^2 on day 1), and oral Capecitabine (1,000 mg/m^2 from days 1 to 14). Responders underwent CRS and HIPEC. On comparing with a retrospective historical cohort of 39 patients treated with systemic chemotherapy (SC) alone, the median OS for the IP and SC groups was 14.6 and 10.6 months, p = .002. The 1-year OS was 67.8% in the IP group and 32.3% in the SC group, p <0.001. The median PFS for the IP and SC group was 9.5 and 4.4 months, respectively, p <0.001.

After the initial experience of neoadjuvant laparoscopic hyperthermic intraperitoneal chemoperfusion (NLHIPEC) from Yonemura et al. (28), who showed a significant decrease in PCI from 14.8 ± 11.4 to 9.9 ± 11.3 (p < 0.0001) in patients with PM of GC, Badgwell et al. conducted a phase II trial using laparoscopic HIPEC with 200 mg of cisplatin and 30 mg of MMC in a neoadjuvant modality (32). Patients reached median overall survival rates of 16.1 months after CRS + HIPEC with a morbidity of 25% (grade III/IV) and mortality of 0% (**Table 2**).

2.3 Adjuvant

2.3.1 Cytoreductive Surgery and HIPEC

After the first publication by Fujimoto et al. (4) in 1988, reporting on the successful use of hyperthermic chemotherapy in patients with GC with PM, there have been several reports confirming the benefit of CRS and HIPEC in well-selected patients of PM from GC (**Table 3**) (12, 36–42, 50, 51).

2.3.2 PCI Threshold for CRS

Strict patient selection is of utmost importance, to ensure maximum benefit from these comprehensive treatment options. One of the important aspects in selection of patients for CRS and HIPEC is the disease burden. For patients with PM from GC, a PCI of maximum 10 to 12 has been suggested (52, 53). Even with complete CRS, benefit in OS is seldomly seen in patients with PCI > 12. Recent studies have suggested more stringent PCI cut offs; ≤ 6.

Chia et al. reported on 81 patients, from five French institutions who underwent CRS and HIPEC for PM from GC (43). Of the 81 patients, 59 had a complete cytoreduction with median PCI of 6 in these patients. The 5-year OS was 18% with nine patients disease free at 5 years (cure rate of 11%).

2.3.3 Recent Literature

Recent data on the effectiveness of CRS and HIPEC on patients with GC exist from across the world with studies from high-volume centers and multicenter data pooling, along with RCTs and systematic reviews and meta-analysis.

There are data on CRS and HIPEC in patients from Central and Eastern European population by Yarema et al. (13). In all, 70 patients of PM from GC were treated with CRS and HIPEC at six of the Central and Eastern European HIPEC centers. The mean peritoneal carcinomatosis index (PCI) was 5.6. Complete cytoreduction was achieved in 71.4% of the patients. After CRS and HIPEC, 44 were treated with adjuvant systemic chemotherapy. The median OS was 12.6 months, and 1 year OS was 53.8%.

Despite most recent studies, it seems worthwhile mentioning the two largest studies from the western world, i.e., France and Germany. The CYTO-CHIP (Cytoreductive surgery versus Cytoreductive surgery and Hyperthermic Intraperitoneal Therapy) is an observational study of patients with GC with limited PM across 19 French treatment centers that were part of the BIG-RENAPE and/or the FREGAT groups (46). Patients with histologically proven PM and/or positive peritoneal cytology and/or ovarian metastases who had undergone CC0/1 were only included for the analysis. The inverse probability of treatment weighting (IPTW) approach was used to ensure that the two groups were similar in the observable characteristics. Except the median PCI that remained higher in the CRS-HIPEC

TABLE 3 | Studies on adjuvant IP chemotherapy in patients with PM from GC.

Year and Author	Study Design	No. of Patients	Study Group	Disease Burden	CC0/1	Group/s Studied	Survival	Morbidity and Mortality
2011 Yang et al (33)	RCT	68	GC PM	Median PCI: 15	58.8%	CRS alone vs. CRS + HIPEC (120-mg Cis + 30-mg MMC)	Median OS: 6.5 m vs. 11 m 3-year OS: 5.9%	Morbidity: 11.7%
2014 Rudloff et al. (34)	RCT	9	GC PM	Mean PCI: 9.3	77.8%	CRS + HIPEC vs. systemic chemotherapy alone	Median OS: 11.3 m vs. 4.3 m	Morbidity: 77.8% Mortality: 11%
2021 Rau et al. (35)	RCT	105	GC PM	n.s.	n.s.	CRS alone vs. CRS + HIPEC (Cis of 75 mg/m^2; MMC of 15mg/m^2)	median OS 14.9m vs. 14.9m	Morbidity: 43.6% vs. 38.1% Mortality: n.s.
1996 Yonemura et al. (36)	Pros	83	GC PM	P1/2: 40 P3: 43	33.8%	CRS + HIPEC (30-mg MMC +500-mg Cis +150-mg etoposide) × 60 min	1-year OS: 43% 5-year OS: 11% **In CC0/1**-1-year OS: 61% 5-year OS: 17%	Morbidity: 7.2%
2004 Glehen et al. (37)	Pros	49	GC PM	Gilly Stage: I: 13 II: 5 III: 12 IV: 19	48.8%	CRS + HIPEC (MMC, 40–60 mg) × 90 min	Med OS: 10.3m **In CCR0/1** Med OS: 21.3 m 5-year OS: 16%	Morbidity: 27% 30-day Mortality: 4%
2004 Hall et al. (38)	Pros Case control	74	GC PM	Gilly Stage I–III: 5 vs. 29, Stage IV: 29 vs. 9	35.3% vs. 62.5%	CRS + HIPEC (40-mg MMC) × 120 min vs. Radical Sx	Median OS: 8 m vs. 7.8 m **HIPEC group**: Med OS: R0: 23.3 m, R1: 11.2 m, R2: 4.6 m	Morbidity: 35% vs. 17.5% 30-day Mortality: 0% vs. 15%
2005 Yonemura et al. (39)	Retro	107	GC PM	P1/2: 35 P3: 72	69% vs. 28%	CRS + HIPEC (30-mg MMC + 300-mg Cis + 150-mg Etoposide) × 60 min vs. Conv Sx + HIPEC	**For all patients**: Median OS: 11 m, 5-year OS: 6.7% **For CRS group**: Median OS: 19.2 m (CC0/1) vs. 7.8 m (CC2/3)	Morbidity: 43% vs. 8% Mortality: 7% vs. 0%
2006 Zhu et al. (12)	Pros Case control	22	GC PM	NK	NK	Sx + HIPEC (50-μg/ml Cis + 5 μg/ml MMC) × 60 min vs. Sx alone	Median OS: 10 m vs. 5 m	Morbidity: NK, Mortality: 0%
2008 Scaringi et al. (20)	Retro	26	GC PM	Gilly stage III–IV: 81%	30.8%	CRS + HIPEC (MMC of 120 mg MMC + Cis of 200 mg/m^2) × 90–120 min	Median OS: 6.6m CC0: 15 m vs. ≥CC1: 3.9 m	Morbidity: 27% Mortality: 3.8%
2010 Glehen et al. (40)	Retro	159	GC PM	Mean PCI: 9.4	CC0: 56%, CC1: 25.2%	CRS + HIPEC ± EPIC (HIPEC- MMC of 30–50 mg/m^2 ± Cis of 50–100 mg/m^2 × 60–120 min OR Oxali of 360–460 mg/m^2 ± Irino of 100–200 mg/m^2 ± IV 5FU/LV × 30 min)	Median OS: 9.2 m, 1-, 3-, and 5-year OS: 43%, 18%, and 13% **CC0/1 group**: Median OS: 15 m, 1-, 3-, and 5-year OS: 61%, 30%, and 23%	Morbidity: 27.8% Mortality: 6.5%
2010 Yang et al. (41)	Pros	28	GC PM ± Ascitis	Median PCI: 12	CC0: 39.2% CC1: 21.4%	CRS + HIPEC (MMC 30 mg + Cis 120 mg) × 90–120 min	Estimated Med OS: CC0/1: 43.4 m CC2: 9.5 m CC3: 7.5 m	Morbidity: 14.3% Mortality: 0%
2013 Hultman et al (10)	Pros	18	GC PM (all treated with NACT)	Median PCI: 12 (8 patients)	CC0:75% CC1: 12.5%	CRS + HIPEC + EPIC (8 patients) (HIPEC - Cis of 50 mg/m^2 + Doxo of 15 mg/m^2 × 90 min OR Oxali of 460 mg/m^2 + IV5FU/ LV of 500 mg/m^2 × 30 min	Median OS: 14.3 m (8 patients) **CC0 patients**: Median OS: 19.1 m	Morbidity: 62.5% 90-day Mortality: 10%
2014 Magge et al. (42)	Pros	23	GC PM	Median PCI: 10.5	CC0/1: 95.7%	CRS + HIPEC (MMC of 40 mg) × 100 min	Median OS: 9.5 m 3-year OS: 18%	Morbidity: 52.2% Mortality: 4.3%
2016 Chia et al. (43)	Retro	81	GC PM	Median PCI: 6	100%	MMC or Cis or Oxali × 90 min	5-year OS: 18%	Morbidity: 44% Mortality: 6.2%

(Continued)

TABLE 3 | Continued

Year and Author	Study Design	No. of Patients	Study Group	Disease Burden	CC0/1	Group/s Studied	Survival	Morbidity and Mortality
2018 Rihuete Caro et al. (44)	Retro	35	Cyto pos/GC PM	Median PCI: 8	94%	Cis: 100 mg/m^2 Doxo: 15 mg/m^2	Median OS: 16 m 3-year OS: 21.3%	Morbidity: 25.7% Mortality: 5.7%
2019 Yarema et al. (13)	Retro	70	GC PM	Mean: PCI 5.6	71.4%	MMC or Cis or Oxali or Doxo	Median OS: 12.6 m 3-year OS: 21.3%	Morbidity: 29.1% Mortality: 5.1%
2019 Rau et al. (45)	Retro	58	GC PM	Mean: PCI 8.3	79.3%	Cis: 75 mg/m^2 MMC: 15 mg/m^2	Median OS 9.8 m 3-year OS: 17.5%	Morbidity: 22.4% Mortality: 1.7%
2019 Bonnot et al. (46)	Retro	180	GC PM	Median PCI 6	CCO: 76.7% CC1: 23.3%	Various	Median OS: 18.4 m 3-year OS: 27.1%	Morbidity: 53.7% Mortality: 7.4%
2020 Rau et al. (47)	Retro	235	GC PM	Median PCI 8	CCO: 71.6%	Various	Median OS: 13 m 5-year OS: 6%	Morbidity: 17.0% Mortality: 5.1%

Pros, prospective study; Retro, retrospective study; Cis, cisplatin; MMC, mitomycin C; Oxali, oxaliplatin; Doxo, doxorubicin; 5FU, 5 fluro-uracil; LV, leucovorin; Sx, surgery.
Japanese staging system for PM (48).
P1: Peritoneal dissemination limited to the adjacent peritoneum of the stomach.
P2: Several scattered metastases in the distant peritoneum.
P3: Numerous metastases to the distant peritoneum.
Gilly's staging system for PM (49).
Gilly stage 1: Malignant tumor nodules <5 mm in diameter, localized in one part of the abdomen.
Gilly stage II: Tumor nodules < 5 mm in diameter, diffuse to the whole abdomen.
Gilly stage III: Tumor nodules 5 mm to 2 cm in diameter.
Gilly stage IV: Large malignant nodules (>2 cm in diameter).

group (6 versus 2, p= 0.003), the other parameters were balanced between the two study groups, after the IPTW adjustment. In total, 277 patients were included for the analysis; 180 underwent CRS and HIPEC, and 97 CRS alone. The median OS was 18.8 vs. 12.1 months in the CRS-HIPEC compared to the CRS alone groups, respectively; with 3- and 5-year OS rates being 26.2% and 19.9% versus 10.8% and 6.4% (adjusted HR, 0.60, p = 0.005), and 3-and 5-year recurrence-free survival (RFS) rates were 20.4% and 17.1% versus 5.9% and 3.8% (p = 0.001), respectively. No significant differences were noted between the two groups regarding the 90-day mortality (7.4% versus 10.1%, p = 0.820) or major complication rate (53.7% versus 55.3%, p = 0.496). The study results affirm the benefit of HIPEC in addition to CRS, in improving both OS and RFS in patients with limited PM from GC, without added morbidity.

Rau et al. reported on the effectiveness of CRS and HIPEC in 315 patients, of peritoneally metastasized GC, from the national German HIPEC registry initiated by the German Society of General and Visceral surgery (DGAV) (47). Patients with pathologically confirmed synchronous PM of GC from 2011 to 2016 were included in this analysis. Preoperative chemotherapy was used in majority of the patients (74%). A complete cytoreduction was possible in 121 patients (71.6%). The median OS was 13 months and 5-year OS was 6% for the entire study cohort. PCI was noted to significantly influence the median OS; PCI of 0–6: 18 months; PCI of 7–15: 12 months; and PCI of 16–39: 5 months (p = 0.002). This study stressed on the proper selection of patients with the use of staging laparoscopy for selecting patients for CRS and HIPEC.

Regarding long-term survival or even cure, an analysis by Brandl et al. shed more light on this topic in a multi-institutional cohort study from PSOGI including 28 patients (out of 448), with histologically proven PM of GC, treated with CRS and HIPEC, between 1994 and 2014 (54). The median OS was 11.0 years. The mean PCI was 3.3% and 78.6% of these patients had CC0 with PCI < 6. Thus, stating that long-term survival and even cure is possible in appropriately selected patients of PM from GC (54).

Most recently, the results of the GASTRIPEC trial, which was prematurely stopped due to slow recruitment, were published, in which a total of 105 patients were randomized to be treated either with CRS alone or CRS and HIPEC (35). The median OS for both groups was 14.9 months without any significant difference between both groups (14.9 versus 14.9 months; p = 0.165). While the treatment related morbidity was similar (grade >3 adverse events during NACT and 30 post-op days were similar in both groups; 46% and 43.6% in the CRS and HIPEC group, 62% and 38.1% in CRS alone group; p = 0.160 and p = 0.79, respectively), the PFS was significantly improved from 3.5 months (95% CI, 3.0–7.0) in the CRS alone group to 7.1 months (95% CI, 3.7–10.5; p = 0.047) in the CRS and HIPEC group (35).

2.3.4 Ongoing Trials

The Dutch PERISCOPE II trial (NCT03348150) investigates the effect of CRS + HIPEC with oxaliplatin (460 mg/m^2) for 30 min at 41°C–42°C, followed by docetaxel (50 mg/m^2) for 90 min at 37°C in patients with limited PM (PCI < 7) compared to systemic chemotherapy (55). The inclusion of a total of 182 patients are intended; primary endpoint is 5-year overall survival.

2.4 Palliative

On the basis of the thesis of an improved efficacy using bidirectional chemotherapy (intravenously and intraperitoneally), several studies investigated the additional benefit on patient survival using IP chemotherapy in palliative indication, which are illustrated in **Table 4**.

2.4.1 Role of NIPEC

After the successful results of phase II (25, 60) studies, demonstrating efficacy and safety of IP paclitaxel, in 2018, Ishigami et al. reported on the first RCT, comparing combined IP paclitaxel and systemic chemotherapy with systemic chemotherapy in patients with PM from GC (56). The combination arm consisted of IP paclitaxel of 20 mg/m^2 and IV paclitaxel of 50 mg/m^2 on days 1 and 8 plus oral S1 of 80 mg/m^2 daily from days 1 to 14 at 3 weekly intervals. The systemic chemotherapy arm consisted of daily oral S1 from days 1 to 21 with cisplatin of 60mg/m^2 on day 8 at 5 weekly intervals. The treatment was continued, until disease progression, unacceptable toxicity, investigator decision or patient withdrawal. The median duration of treatment was 39 weeks in the IP arm and 15 weeks in the systemic chemotherapy arm. The median survival was 17.7 months in the IP arm versus 15.2 months in the systemic chemotherapy arm, not statistically significant (p = 0.080). However, after adjusting for baseline ascites, the HR was 0.59 (p = 0.008). The authors concluded that the efficacy of the IP regimen was underestimated by the primary analysis owing to the unexpected imbalance in the amount of ascites and the crossover from systemic to IP chemotherapy arms.

2.4.2 Role of HIPEC

Control of malignant ascites can be achieved by HIPEC. Several reports along with a systematic review have shown ascites control in 95% of patients with the use of laparoscopic HIPEC (61–63). Recently, Yarema et al. reported on use of HIPEC to control malignant ascites in 10 patients. Mean volume of ascitic fluid was 5.5 liters ± 1.4 (3.5–8), and the mean PCI was 30.6 ± 6.1 (15–39). Although ascites elimination was achieved in all patients, giving symptomatic relief, this group, as expected, had poor median OS and DFS; 3.5months and 2.5 months respectively (13).

2.4.3 Role of PIPAC

Pressurized intraperitoneal chemotherapy (PIPAC) using aerosolized system of drug delivery in the setting of capnoperitoneum has been increasingly used in the setting of unresectable PM and malignant ascites. Initial reports on the use of PIPAC in 24 patients of PM from GC, by Reymond et al., showed objective tumor response in 50% of the patients with PIPAC with 25% patients, having complete pathological response (64).

Alyami et al. reported on the use of PIPAC in 42 patients with unresectable PM, who were treated with PIPAC (cisplatin and doxorubicin) (59). The morbidity was low (6.1%), and a median overall survival of 19.1 months was reached.

Another study by Di Giorgio et al. reported on the safety and efficacy of PIPAC in 28 consecutive patients of GC PM from a single center, from September 2017 to September 2019 (58). Forty-six PIPAC procedures were performed with a mean of 1.7 PIPAC per patient. Pathological response was noted in 61.5% of patients (one with complete and seven with partial response). The median OS was 12.3 months for the entire cohort and 15 months in patients undergoing >1 PIPAC procedure (58).

TABLE 4 | Studies on IP chemotherapy as palliative treatment in patients with PM from GC.

Year and Author	Study Design	No. of Patients	Study Group	Group/s Studied	Median Overall Survival	Morbidity and Mortality
NIPEC						
2013 Yamaguchi et al. (25)	Phase II	35	GC PM	IP + IV + S1	17.6 m	Morbidity: 34%
2018 Ishigami et al. (56)	RCT Phase III	164	GC PM	IP + IV + S1 IV + S1	17.7 m 15.2 m 3-year OS: 21.9% vs. 6.0%	Morbidity: 50% Mortality: 0%
PIPAC						
2017 Alyami et al (48)	Retro	73	GC PM	Cis: 7.5 mg/m^2 Doxo: 1.5 mg/m^2	Decreased PCI: 64.5%	Morbidity: 9.7% Mortality: 6.8%
2018 Khomyakov et al (49)	Phase II	31	GC PM	Cis: 7.5 mg/m^2 Doxo: 1.5 mg/m^2	13m major pathol. Response 60%	Morbidity: 0%
2019 Struller et al (57)	Phase II	25	GC PM	Cis: 7.5 mg/m^2 Doxo: 1.5 mg/m^2	6.7m pathol Response / Stable 40%	Morbidity: 0%
2020 di Giorgio et al (58)	Phase II	28	GC PM	Cis: 7.5 mg/m^2 Doxo: 1.5mg/m^2	12.3m pathol response 61.5%	Morbidity: 4% Mortality: 4%
2021 Alyami et al. (59)	Retro	42	GC PM	Cis: 7.5 mg/m^2 Doxo: 1.5 mg/m^2	19.1m	Morbidity: 6.1% Mortality: 4.7%

IP, intraperitoneal; IV, intravenously; S1, tegafur/gimeracil/oteracil; Retro, retrospective study; Cis, cisplatin; Doxo, doxorubicin; GC PM, gastric cancer peritoneal metastasis.

Presently, there are several studies reporting on the safety, feasibility, and the effectiveness of PIPAC procedure with low-dose cisplatin (7.5 mg/m^2) and doxorubicin (1.5 mg/m^2) in patients with unresectable PM from GC (59, 65, 66). A systematic review by Garg et al. identified a total of 129 patients with GC PM treated with PIPAC (10 studies; two with an exclusive cohort of patients with GC and eight with a heterogeneous population with only a small proportion of GC patients). The review concluded that PIPAC is a safe and well-tolerated procedure with minimal peri-operative morbidity, with the potential to contain the spread of PM, at the same time improving or stabilizing the patients QoL (67).

2.4.4 Ongoing Trials

Research on the further safety and efficacy of PIPAC procedure, drugs to be used, the optimal dose of drugs, etc., continue. The results of PIPAC EstoK 01—a prospective, open, randomized multicenter phase II study on patients with PM with GC, with PCI > 8—are awaited (68). Patients are being treated with either three cycles of PIPAC with oxaliplatin + systemic chemotherapy (one PIPAC then two IV chemotherapy) versus systemic chemotherapy alone. Two dose escalation studies on oxaliplatin PIPAC are also currently ongoing to determine the optimal dose to be used during PIPAC (69, 70). PIPAC GA 01 is yet another PIPAC trial on patients with recurrent GC, to evaluate the safety and efficacy of PIPAC with doxorubicin and cisplatin (three single doses in 6-week interval) (71).

3 SPECIFIC SUBTYPES

3.1 P0/Cy1

Patients with positive peritoneal fluid cytology without evidence of visible PM (P0/Cy1) need a special mention, because in spite of a curative resection, the median survival of these patients is similar to patients with obvious PM (14, 72). The AJCC (seventh edition) has also classified the presence of positive peritoneal cytology as M1 disease (73). These patients have been either treated with gastrectomy followed by adjuvant treatment (resulting in high rates of peritoneal recurrence) or with palliative intent chemotherapy. The effectiveness of neoadjuvant intraperitoneal chemotherapy on patients with positive peritoneal cytology has been demonstrated by studies on patients with PM and positive peritoneal cytology by Yonemura et al. (29, 30). These studies have reported positive cytology reverting to negative in 56% and 70% of the patients after neoadjuvant IP treatment, respectively. There are very few studies looking specifically at treatment of patients with only positive peritoneal cytology, as this factor is usually considered as an exclusion criteria.

In the study by Kuramoto et al., 88 patients of P0/Cy1 were randomized into three groups: surgery alone, surgery with IP chemotherapy, and surgery with extensive intraperitoneal lavage (EIPL) and IP chemotherapy (74). All patients were treated with adjuvant 5FU derivatives × 2 years. The 5-year OS was significantly higher in the surgery + EIPL+ IP chemotherapy group (44%) than in the surgery + IP chemotherapy (5%) and surgery alone group (0%). Similarly, the peritoneal recurrence was significantly lower in the EIPL group; 40%, 79%, and 90%, respectively. Thus, EIPL and IPC during surgery have shown beneficial effects in this group of patients. In another study, Imano et al. reported 100% conversion of positive cytology to negative with improved 5-year survival (5-year OS rate: 25%), for patients of P0/Cy1, treated with gastrectomy and EPIC using paclitaxel (75).

Ishigami et al. reported on the effectiveness of NIPS (IP and intravenous paclitaxel with oral S1), on patients with GC with PM or positive peritoneal cytology (26). Although the number of patients with only positive peritoneal cytology in their study was only 8, in comparison to the entire cohort of 100 patients, they did demonstrate improved median OS with this neoadjuvant treatment.

The recently reported CYTO-CHIP study by Bonnot et al. included 46 patients with PCI 0 (46). However, they also included patients with microscopic PM at the time of pathological examination or isolated ovarian Krukenberg tumors along with patients with positive peritoneal cytology as PCI 0. Of the 46 patients, 16 patients were treated with CRS-HIPEC and 30 with CRS alone. The median OS was 22.8 versus 12.9 months, respectively, a difference of 9.9 months, although not statistically significant due to small sample size.

In a review of various studies on patients of GC with P0/Cy1, Taniguchi et al. have concluded that postoperative oral S1, NIPS, or EPIC can result in cure in 25% to 44% patients by eradicating intraperitoneal micrometastasis (76).

Thus, these patients with only positive peritoneal cytology in the absence of obvious PM need to be identified by preoperative ascitic fluid or peritoneal wash cytology, so as to cater appropriate treatment, with the use of IP chemotherapy in some form along with CRS and HIPEC, to improve their prognosis.

3.2 Her2-Positive Gastric Cancer With PM

Her2 positivity has been identified in 13%–22% of all patients with GC (77, 78). In patients with PM from GC, the frequency of Her2 positivity has been found to be extremely low in the range of 2%–3% (79). Trastuzumab in combination with chemotherapy in patients with advanced gastric and gastro-esophageal cancers has shown survival advantage in this otherwise poor prognostic sub-group (80). Very few studies have been reported on the use of trastuzumab in patients with GCPM, considering the low frequency of Her2 positivity in this subgroup.

In 2014, Berretta et al., for the first time, reported on the use of IP Trastuzumab in a 61-year-old lady with pleural and peritoneal disease progression in a previously treated patient of advanced GC (81). The patient was initially treated with systemic chemotherapy with Trastuzumab along with weekly intra-pleural cisplatin, which resulted in complete pathological response at the pleural site of disease. IP Trastuzumab was then administered weekly at a dose of 150 mg for six cycles (after paracentesis). The patient had symptomatic relief without any local complications due to the IP Trastuzumab along with a stable peritoneal disease.

Recently, Li et al. reported on the use of α-emitting Trastuzumab in a mice model with PM of Her2 positive GC (82). Biodistribution analysis in the mouse model showed that IP administration of the α-emitting Trastuzumab was more

uniform than IV administration and showed prolonged survival time as compared to the controls (two of six mice had complete response and three of six had good partial response).

3.3 Signet Ring Subtype of Gastric Cancer

SRC histology is known to be an aggressive subtype with poor prognosis. In comparison to appendicular and colorectal cancers, GC is more likely to have SRC subtype; 3.4% to 32.5% of all gastric cancers (83–85). The role of CRS and HIPEC in patients with PM from SRC GC is unclear.

In 2014, Konigsrainer et al. retrospectively analyzed 18 patients of SRC GC with synchronous PM treated with four to six cycles of neoadjuvant chemotherapy (5FU, folinic acid, docetaxel, and oxaliplatin) followed by CRS and HIPEC (cisplatin of 50 mg/m^2 for 90 min at 42°C) (86). CC0/1 was achievable in 72% of patients. At a median follow-up of 6.6 months, the median OS was 8.9 months for patients with CC0/1, as opposed to 1.1 month for CC2/3. The PFS in patients with CC0/1 was 6.2 months. They concluded that prognosis of patients with PM from SRC GC remains poor, in spite of CRS and HIPEC and only a highly selected subgroup of patients after confirming response and resectability by a prior staging laparoscopy, should be subjected to this multimodality treatment to achieve any OS advantage.

Daniel et al. have reported on 204 patients with SRC histology from various primary gastrointestinal malignancies, treated with complete CRS followed by HIPEC from 2007 to 2016 (87). Of the 204 patients, 18 patients had primary GC. The median OS was 12 months for the patients with SRC GC, as compared to 27 months for SRC appendicular cancers and 18 months for the SRC colorectal cancers. Multivariate analysis of all 204 patients with SRC subtype showed GC origin to negatively influence survival (HR 4.59, p = 0.008) (87).

In the CYTO-CHIP study (previously mentioned), 188 of 277 patients had SRC (88). Median PCI was highest in the SRC-CRS + HIPEC group (median PCI of 7). The 3-year OS (after CRS ± HIPEC) was poor in the SRC group as compared to the non-SRC group (14% versus 38.4%, p < 0.001). However, within the SRC group, HIPEC was associated with better OS on multivariate analysis, than CRS alone (median OS 16.3 months versus 11 months, p = 0.003). They concluded that in well-selected patients of SRC GC with resectable PM, HIPEC is a valuable option.

Recent studies by Alyami et al. (59) and Bonnot et al. (65) on the use of PIPAC in patients with diffuse and unresectable PM from GC had significant number of patients with SRC histology; 33 of 42 patients and 79 of 91 patients, respectively. The median OS for the whole cohort was 19.1 and 15.1 months, respectively, thus indicating that PIPAC alternating with systemic chemotherapy may be the treatment of choice in future for this poor prognostic subgroup followed by reassessment for CRS and HIPEC in responding patients.

In addition, targeting tumor cells with loss of E-cadherin due to epithelial mesenchymal transition (EMT), which plays a central role in the loss of cohesiveness and increased chances of peritoneal dissemination in SRC cancers, is an interesting area of research in this subgroup of patients, which may eventually help improving their prognosis (89).

4 DISCUSSION

The treatment armamentarium of patients with GC PM continues to expand. In these patients who had only systemic chemotherapy or best supportive care as their treatment options, in the past, they now can be treated with a wide variety of multimodality treatments.

With the advent of CRS and HIPEC, improved median OS has been reported, ranging from 11 to 23 months (13, 36–,12, 38, 44–47). The improvement in median OS is more pronounced in well-selected patients (good pre-operative functional reserve), absence of diffuse peritoneal involvement (PCI ≤ 12 or ≤ 6), absence of extraperitoneal metastasis, and when CC0/1 resection is possible. In a highly selected cohort study from PSOGI of 28 patients with >5-year OS, the median OS was reported to be 11.0 years (54). The mean PCI was 3.3% and 78.6% of these patients had CC0 resection with PCI < 6. Thus, in well-selected patients of PM from GC, even cure is a possibility.

When intraperitoneal chemotherapy is used in the neoadjuvant setting in conjunction with systemic chemotherapy (NIPS/BISIC), there is remarkable number of patients in whom CC0/1 resection may become feasible. This concept was first introduced by Yonemura et al. (29) and is now being widely used to downstage patients with diffuse peritoneal involvement, making them amenable to CRS and HIPEC. Several studies have shown significant decrease in PCI with combined IP/IV treatments, as well as conversion of ascitic fluid cytology from positive to negative with acceptable grade 3 and 4 morbidity and mortality (25, 27, 30, 31, 56, 60, 90). Various regimens are available and very well summarized by Brandl et al. with suggestions of regimens toward the latter part of the article with the intention to standardize these treatment protocols (53).

Metachronous development of PM occurs in 15%–45% of patients with locally advanced GC (T3/4 tumors, N2/3 lymph node positivity, high grade tumors, and SRC histology). Several studies, including systematic reviews and meta-analyses, have reported improved DFS and OS with prophylactic HIPEC (5–7, 9–12, 14–18, 91). The results of the GASTRICCHIP study, a prospective RCT on prophylactic HIPEC is eagerly awaited, before routine use of prophylactic HIPEC, across the world (21).

Patients with positive ascitic fluid cytology or peritoneal washings in the absence of obvious PM need to be treated aggressively with some form of IP chemotherapy, as we have studies demonstrating high chances of peritoneal recurrence when treated with surgery with or without systemic chemotherapy. Use of NIPS, EIPL, CRS and HIPEC, EPIC or post- operative prolonged S1 have shown to result in cure in 25% to 44% of patients by eradicating intraperitoneal micrometastasis (76).

Similarly, well-selected patients of the SRC histology (patients responding to neoadjuvant treatment, having limited PM, limited small bowel involvement) can have improved outcome with CRS and HIPEC. With the advent of PIPAC, even patients with diffuse peritoneal involvement may become amenable to complete CRS if good response to PIPAC alternating with systemic chemotherapy is noted in this otherwise poor prognostic subgroup (59, 65).

There is an overwhelming increase in data on the safety, feasibility, and efficacy of PIPAC in patients with diffuse PM from GC. In highly selected patients, initially deemed unresectable, a secondary CRS and HIPEC may become possible after repeated PIPAC cycles (92). Thus, patients who are not candidates for CC0/1 resection either upfront or after some form of neoadjuvant treatment may be considered for studies on PIPAC.

5 CONCLUSION

Thus, a favorable survival in patients with PM from GC has been seen with the various forms of IP chemotherapy. Proper patient selection in terms of patient fitness and peritoneal disease burden are key to maximize the benefit and minimize the morbidity and mortality from these available multimodality comprehensive treatment options. The importance of multidisciplinary team and treatment in high volume centers has also been time and again demonstrated to be of importance while treating patients with this aggressive disease. Further research in molecular subtypes of GC with multiplex profiling of PM from GC may eventually provide us with targets to provide more individualized treatment for these patients and thus result in favorable outcomes.

AUTHOR CONTRIBUTIONS

AP and DM: Data acquisition, manuscript preparation, and manuscript editing and review. AB and YY: Manuscript editing and review. All authors contributed to the article and approved the submitted version.

ACKNOWLEDGMENTS

Contribution from all authors is acknowledged.

REFERENCES

1. Bray F, Ferlay J, Soerjomataram I, Siegel RL, Torre LA, Jemal A. Global Cancer Statistics 2018: GLOBOCAN Estimates of Incidence and Mortality Worldwide for 36 Cancers in 185 Countries. *CA Cancer J Clin* (2018) 68 (6):394–424. doi: 10.3322/caac.21492
2. Chu DZ, Lang NP, Thompson C, Osteen PK, Westbrook KC. Peritoneal Carcinomatosis in Nongynecologic Malignancy. A Prospective Study of Prognostic Factors. *Cancer* (1989) 63:364–7. doi: 10.1002/1097-0142(19890115)63:2%3C364::aid-cncr2820630228%3E3.0.co;2-v
3. Thomassen I, van Getsel YR, van Ramshorst B, Luyer MD, Bosscha K, Neinhuijs SW, et al. Peritoneal Carcinomatosis of Gastric Origin: A Population-Based Study on Incidence, Survival and Risk Factors. *Int J Cancer* (2014) 134(3):622–8. doi: 10.1002/ijc.28373
4. Fujimoto S, Shrestha RD, Kokubun M, Ohta M, Takahashi M, Kobayashi K, et al. Intraperitoneal Hyperthermic Perfusion Combined With Surgery Effective for Gastric Cancer Patients With Peritoneal Seeding. *Ann Surg* (1988) 208(1):36–41. doi: 10.1097/00000658-198807000-00005
5. Hamazoe R, Maeta M, Kaibara N. Intraperitoneal Thermochemotherapy for Prevention of Peritoneal Recurrence of Gastric Cancer. Final Results of a Randomized Controlled Study. *Cancer* (1994) 73(8):2048–52. doi: 10.1002/1097-0142(19940415)73:8%3C2048::aid-cncr2820730806%3E3.0.co;2-q
6. Fujimura T, Yonemura Y, Muraoka K, Takamura H, Hirono Y, Sahara H, et al. Continuous Hyperthermic Peritoneal Perfusion for the Prevention of Peritoneal Recurrence of Gastric Cancer: Randomized Controlled Study. *World J Surg* (1994) 18(1):150–5. doi: 10.1007/bf00348209
7. Ikeguchi M, Kondou A, Oka A, Tsujitani S, Maeta M, Kaibara N. Effects of Continuous Hyperthermic Peritoneal Perfusion on Prognosis of Gastric Cancer With Serosal Invasion. *Eur J Surg* (1995) 161(8):581–6.
8. Takahashi T, Hagiwara A, Shimotsuma M, Sawai K, Yamaguchi T. Prophylaxis and Treatment of Peritoneal Carcinomatosis: Intraperitoneal Chemotherapy With Mitomycin C Bound to Activated Carbon Particles. *World J Surg* (1995) 19(4):565–9. doi: 10.1007/BF00294724
9. Fujimoto S, Takahashi M, Mutou T, Kobayashi K, Toyosawa T. Successful Intraperitoneal Hyperthermic Chemoperfusion for the Prevention of Postoperative Peritoneal Recurrence in Patients With Advanced Gastric Carcinoma. *Cancer* (1999) 85(3):529–34. doi: 10.1002/(SICI)1097-0142(19990201)85:3<529::AID-CNCR3>3.0.CO;2-9
10. Kim JY, Bae HS. A Controlled Clinical Study of Serosa-Invasive Gastric Carcinoma Patients Who Underwent Surgery Plus Intraperitoneal Hyperthermo-Chemo-Perfusion (IHCP). *Gastric Cancer* (2001) 4(1):27–33. doi: 10.1007/s101200100013
11. Yonemura Y, de Aretxabala X, Fujimura T, Fushida S, Katayama K, Bandou E, et al. Intraoperative Chemohyperthermic Peritoneal Perfusion as an Adjuvant to Gastric Cancer: Final Results of a Randomized Controlled Study. *Hepato-Gastroenterol* (2001) 48(42):1776–82.
12. Zhu ZG, Tang R, Yan M, Chen J, Yang QM, Li C, et al. Efficacy and Safety of Intraoperative Peritoneal Hyperthermic Chemotherapy for Advanced Gastric Cancer Patients With Serosal Invasion. A Long-Term Follow-Up Study. *Dig Surg* (2006) 23(1–2):93–102. doi: 10.1159/000093778
13. Yarema R, Mielko J, Fetsych T, Ohorchak M, Skorzewska M, Rawicz-Pruszynski K, et al. Hyperthermic Intraperitoneal Chemotherapy (HIPEC) in Combined Treatment of Locally Advanced and Intraperitoneally Disseminated Gastric Cancer: A Retrospective Cooperative Central-Eastern European Study. *Cancer Med* (2019) 8:2877–85. doi: 10.1002/cam4.2204
14. Beeharry MK, Zhu Z-L, Liu W-T, Yao X-X, Yan M, Zhu Z-G. Prophylactic HIPEC With Radical D2 Gastrectomy Improves Survival and Peritoneal Recurrence Rates for Locally Advanced Gastric Cancer: Personal Experience From a Randomized Case Control Study. *BMC Cancer* (2019) 19:932. doi: 10.1186/s12885-019-6125-z
15. Xu DZ, Zhan YQ, Sun XW, Cao SM and Geng QR. Meta-Analysis of Intraperitoneal Chemotherapy for Gastric Cancer. *World J Gastroenterol* (2004) 10:2727–30. doi: 10.3748/wjg.v10.i18.2727
16. Yan TD, Black D, Sugarbaker PH, Zhu J, Yonemura Y, Petrou G, et al. A Systematic Review and Meta-Analysis of the Randomized Controlled Trials on Adjuvant Intraperitoneal Chemotherapy for Resectable Gastric Cancer. *Ann Surg Oncol* (2007) 14:2702–13. doi: 10.1245/s10434-007-9487-4
17. Sun J, Song Y, Wang Z, Gao P, Chen X, Xu Y, et al. Benefits of Hyperthermic Intraperitoneal Chemotherapy for Patients With Serosal Invasion in Gastric Cancer: A Metaanalysis of the Randomized Controlled Trials. *BMC Cancer* (2012) 12:526. doi: 10.1186/1471-2407-12-526
18. Feingold PL, Kwong MLM, Davis JL, Rudolf U. Adjuvant Intraperitoneal Chemotherapy for the Treatment of Gastric Cancer at Risk for Peritoneal Carcinomatosis: A Systematic Review. *J Surg Oncol* (2017) 115(2):192–201. doi: 10.1002/jso.24476
19. Desiderio J, Chao J, Melstrom L, Warner S, Tozzi F, Fong Y, et al. The 30-Year Experience-A Meta-Analysis of Randomised and High-Quality non-Randomised Studies of Hyperthermic Intraperitoneal Chemotherapy in the Treatment of Gastric Cancer. *Eur J Cancer* (2017) 79:1–14. doi: 10.1016/j.ejca.2017.03.030
20. Scaringi S, Kianmanesh R, Sabate JM, Facchiano E, Jouet P, Coffin B, et al. Advanced Gastric Cancer With or Without Peritoneal Carcinomatosis Treated With Hyperthermic Intraperitoneal Chemotherapy: A Single Western Center Experience. *Eur J Surg Oncol* (2008) 34(11):1246–52. doi: 10.1016/j.ejso.2007.12.003
21. Glehen O, Passot G, Villeneuve L, Vaudoyer D, Bin-Dorel S, Boschetti G, et al. GASTRICHIP: D2 Resection and Hyperthermic Intraperitoneal Chemotherapy in Locally Advanced Gastric Carcinoma: A Randomized and

Multicenter Phase III Study. *BMC Cancer* (2014) 14:183. doi: 10.1186/1471-2407-14-183

22. Gotze TO, Piso P, Lorenzen S, Bankstahl US, Pauligk C, Elshafei M, et al. Preventive HIPEC in Combination With Perioperative FLOT Versus FLOT Alone for Resectable Diffuse Type Gastric and Gastroesophageal Junction Type II/III Adenocarcinoma - the Phase III "PREVENT"- (FLOT9) Trial of the AIO /CAOGI /ACO. *BMC Cancer* (2021) 21(1):1158. doi: 10.1186/s12885-021-08872-8
23. Fujiwara Y, Takiguchi S, Nakajima K, Miyata H, Yamasaki M, Kurokawa Y, et al. Intraperitoneal Docetaxel Combined With S-1 for Advanced Gastric Cancer With Peritoneal Dissemination. *J Surg Oncol* (2012) 105, Issue 1:38–42. doi: 10.1002/jso.22057
24. Fushida S, Kinoshita J, Kaji M, Goda F, Oyama K, Sudo Y, et al. Phase I/II Study of Intraperitoneal Docetaxel Plus S-1 for the Gastric Cancer Patients With Peritoneal Carcinomatosis. *Cancer Chemother Pharmacol* (2013) 71 (5):1265–72. doi: 10.1007/s00280-013-2122-0
25. Yamaguchi H, Kitayama J, Ishigami H, Emoto S, Yamashita H, Watanabe T. : A Phase 2 Trial of Intravenous and Intraperitoneal Paclitaxel Combined With S-1 for Treatment of Gastric Cancer With Macroscopic Peritoneal Metastasis. *Cancer* (2013) 119:3354–8. doi: 10.1002/cncr.28204
26. Ishigami H, Yamaguchi H, Yamashita H, Asakage M, Kitayama J. Surgery After Intraperitoneal and Systemic Chemotherapy for Gastric Cancer With Peritoneal Metastasis or Positive Peritoneal Cytology Findings. *Gastric Cancer* (2017) 20:128–34. doi: 10.1007/s10120-016-0684-3
27. Yonemura Y, Prabhu A, Sako S, Ishibashi H, Mizumoto A, Takao N, et al. Long Term Survival After Cytoreductive Surgery Combined With Perioperative Chemotherapy in Gastric Cancer Patients With Peritoneal Metastasis. *Cancers* (2020) 12:116. doi: 10.3390/cancers12010116
28. Yonemura Y, Ishibashi H, Hirano M, Mizumoto A, Takeshita K, Noguchi K, et al. Effects of Neoadjuvant Laparoscopic Hyperthermic Intraperitoneal Chemotherapy and Neoadjuvant Intraperitoneal/Systemic Chemotherapy on Peritoneal Metastases From Gastric Cancer. *Ann Surg Oncol* (2017) 24:478–85. doi: 10.1245/s10434-016-5487-6
29. Yonemura Y, Bandou E, Sawa T, Yoshimitsu Y, Endou Y, Sasaki T, et al. Neoadjuvant Treatment of Gastric Cancer With Peritoneal Dissemination. *Eur J Surg Oncol* (2006) 32:661–5. doi: 10.1016/j.ejso.2006.03.007
30. Yonemura Y, Canbay E, Endou Y, Ishibashi H, Mizumoto A, Li Y, et al. A New Bidirectional Intraperitoneal and Systemic Induction Chemotherapy (BISIC) for the Peritoneal Metastasis From Gastric Cancer in Neoadjuvant Setting. *Integr Cancer Sci Ther Vol* (2014) 1(2):26–9. doi: 10.15761/ICST.1000106
31. Chia D, Sundar R, Kim GW, Ang J, Lum J, Ngoi N, et al. Outcomes of a Phase II Study of Intraperitoneal Paclitaxel Plus Systemic Capecitabine and Oxaliplatin (XELOX) for Gastric Cancer With Peritoneal Metastases. *J Clin Oncol* (2021) 39.3_suppl.165:165. doi: 10.1200/JCO.2021.39.3_suppl.165
32. Badgwell B, Ikoma N, Murphy MB, Wang X, Estrella J, Chowdhuri SR, et al. A Phase II Trial of Cytoreduction, Gastrectomy, and Hyperthermic Intraperitoneal Perfusion With Chemotherapy for Patients With Gastric Cancer and Carcinomatosis or Positive Cytology. *Ann Surg Oncol* (2021) 28 (1):258–64. doi: 10.1245/s10434-020-08739-5
33. Yang XJ, Huang CQ, Suo T, Mei LJ, Yang GL, Cheng FL, et al. Cytoreductive Surgery and Hyperthermic Intraperitoneal Chemotherapy Improves Survival of Patients With Peritoneal Carcinomatosis From Gastric Cancer: Final Results of a Phase III Randomized Clinical Trial. *Ann Surg Oncol* (2011) 18:1575–81. doi: 10.1245/s10434-011-1631-5
34. Rudloff U, Langan RC, Mullinax JE, Beane JD, Steinberg SM, Beresnev T, et al. Impact of Maximal Cytoreductive Surgery Plus Regional Heated Intraperitoneal Chemotherapy (HIPEC) on Outcome of Patients With Peritoneal Carcinomatosis of Gastric Origin: Results of the GYMSSA Trial. *J Surg Oncol* (2014) 110:275–84. doi: 10.1002/jso.23633
35. Rau B, Lang H, Konigsrainer A, Gockel I, Rau HG, Seeliger H, et al. 1376o The Effect of Hyperthermic Intraperitoneal Chemotherapy (HIPEC) Upon Cytoreductive Surgery (CRS) in Gastric Cancer (GC) With Synchronous Peritoneal Metastasis (PM): A Randomized Multicentre Phase III Trial (GASTRIPEC-I-Trial). *ESMO* (2021) 32, supplement 5:s1040. doi: 10.1016/j.annonc.2021.08.1485
36. Yonemura Y, Fujimura T, Nishimura G, Falla R, Sawa T, Katayama K, et al. Effects of Intraoperative Chemohyperthermia in Patients With Gastric Cancer With Peritoneal Dissemination. *Surgery* (1996) 119(4):437–44. doi: 10.1016/s0039-6060(96)80145-0
37. Glehen O, Schreiber V, Cotte E, Beaujard ACS, Osinsky D, Freyer G, et al. Cytoreductive Surgery and Intraperitoneal Chemohyperthermia for Peritoneal Carcinomatosis Arising From Gastric Cancer. *Arch Surg* (2004) 139(1):20–6. doi: 10.1001/archsurg.139.1.20
38. Hall JJ, Loggie BW, Shen P, Beamer S, Douglas Case L, McQuellon R, et al. Cytoreductive Surgery With Intraperitoneal Hyperthermic Chemotherapy for Advanced Gastric Cancer. *J Gastrointest Surg* (2004) 8(4):454–63. doi: 10.1016/j.gassur.2003.12.014
39. Yonemura Y, Kawamura T, Bandou E, Takahashi S, Sawa T, Matsuki N. Treatment of Peritoneal Dissemination From Gastric Cancer by Peritonectomy and Chemohyperthermic Peritoneal Perfusion. *Br J Surg* (2005) 92:370–5. doi: 10.1002/bjs.4695
40. Glehen O, Gilly FN, Arvieux C, Ctte E, Boutitie F, Mansvelt B, et al. Peritoneal Carcinomatosis From Gastric Cancer: A Multi-Institutional Study of 159 Patients Treated by Cytoreductive Surgery Combined With Perioperative Intraperitoneal Chemotherapy. *Ann Surg Oncol* (2010) 17(9):2370–7. doi: 10.1245/s10434-010-1039-7
41. Yang XJ, Li Y, Yonemura Y. Cytoreductive Surgery Plus Hyperthermic Intraperitoneal Chemotherapy to Treat Gastric Cancer With Ascites and/or Peritoneal Carcinomatosis: Results From a Chinese Centre. *J Surg Oncol* (2010) 101:457–64. doi: 10.1002/jso.21519
42. Magge D, Zenati M, Mavanur A, Winer J, Ramalingam L, Jones H, et al. Aggressive Locoregional Surgical Therapy for Gastric Peritoneal Carcinomatosis. *Ann Surg Oncol* (2014) 21:1448–55. doi: 10.1245/s10434-013-3327-5
43. Chia CS, You B, Decullier E, Vaudoyer D, Lorimier G, Abboud K, et al. Patients With Peritoneal Carcinomatosis From Gastric Cancer Treated With Cytoreductive Surgery and Hyperthermic Intraperitoneal Chemotherapy: Is Cure a Possibility? *Ann Surg Oncol* (2016) 23:1971–9. doi: 10.1245/s10434-015-5081-3
44. Rihuete C, Manzanedo I, Pereira F, Carrion-Alvarez L, Serrano Á, Pérez-Viejo E. Cytoreductive Surgery Combined With Hyperthermic Intraperitoneal Chemotherapy (HIPEC) in Patients With Gastric Cancer and Peritoneal Carcinomatosis. *Eur J Surg Oncol* (2018) 44(11):1805–10. doi: 10.1016/j.ejso.2018.06.036
45. Rau B, Brandl A, Thuss-Patience P, Bergner F, Raue W, Arnold A, et al. The Efficacy of Treatment Options for Patients With Gastric Cancer and Peritoneal Metastasis. *Gastric Cancer* (2019) 22(6):1226–37. doi: 10.1007/s10120-019-00969-1
46. Bonnot P-E, Piessen G, Kepenekian V, Decullier E, Pocard M, Meunier B, et al. Cytoreductive Surgery With or Without Hyperthermic Intraperitoneal Chemotherapy for Gastric Cancer With Peritoneal Metastases (CYTO-CHIP Study): A Propensity Score Analysis. *J Clin Oncol* (2019) 37(23):2028–40. doi: 10.1200/jco.18.01688
47. Rau B, Brandl A, Piso P, Pelz J, Busch P, Demtroder C, et al. Peritoneal Metastasis in Gastric Cancer: Results From the German Database. *Gastric Cancer* (2020) 2311-22(1):11–22. doi: 10.1007/s10120-019-00978-0
48. Alyami M, Gagniere J, Sgarbura O, Cabelguenne D, Villeneuve L, Pezet D, et al. Multicentric Initial Experience With the Use of the Pressurized Intraperitoneal Aerosol Chemotherapy (PIPAC) in the Management of Unresectable Peritoneal Carcinomatosiseur. *J Surg Oncol EJSO* (2017) 43:2178–83. doi: 10.1016/j.ejso.2017.09.010
49. Khomyakov V, Ryabov A, Ivanov A, Bolotina L, Utkina A, Volchenko N, et al. Bidirectional Chemotherapy in Gastric Cancer With Peritoneal Metastasis Combining Intravenous XELOX With Intraperitoneal Chemotherapy With Low-Dose Cisplatin and Doxorubicin Administered as a Pressurized Aerosol: An Open-Label, Phase-2 Study (PIPAC-Ga2). *Pleura Peritoneum* (2016) 1 (3):159–66. doi: 10.1515/pp-2016-0017
50. Sugarbaker PH, Yonemura Y. Clinical Pathway for the Management of Resectable Gastric Cancer With Peritoneal Seeding: Best Palliation With a Ray of Hope for Cure. *Oncology* (2000) 58(2):96–107. doi: 10.1159/000012086
51. Hultman B, Lind P, Glimelius B, Sundbom M, Nygren P, Haglund U, et al. Phase II Study of Patients With Peritoneal Carcinomatosis From Gastric Cancer Treated With Preoperative Systemic Chemotherapy Followed by Peritonectomy and Intraperitoneal Chemotherapy. *Acta Oncol* (2013) 52:824–30. doi: 10.3109/0284186x.2012.702925

52. Bozzetti F, Yu W, Baratti D, Kusamura S, Dearco M. Locoregional Treatment of Peritoneal Carcinomatosis From Gastric Cancer. *J Surg Oncol* (2008) 98 (4):273–6. doi: 10.1002/jso.21052
53. Brandl A, Prabhu A. Intraperitoneal Chemotherapy in the Treatment of Gastric Cancer Peritoneal Metastases: An Overview of Common Therapeutic Regimens. *J Gastrointest Oncol* (2021) 12(Suppl 1):S32–44. doi: 10.21037/jgo-2020-04
54. Brandl A, Yonemura Y, Glehen O, Sugarbaker P, Rau B. Long Term Survival in Patients With Peritoneal Metastasised Gastric Cancer Treated With Cytoreductive Surgery and HIPEC: A Multi-Institutional Cohort From PSOGI. *Eur J Surg Oncol* (2021) 47(1):172–80. doi: 10.1016/j.ejso.2020.10.006
55. Koemans WJ, van der Kaaji RT, Boot H, Buffart T, Veenhof AAFA, Hartemink KJ, et al. Cytoreductive Surgery and Hyperthermic Intraperitoneal Chemotherapy Versus Palliative Systemic Chemotherapy in Stomach Cancer Patients With Peritoneal Dissemination, the Study Protocol of a Multicentre Randomised Controlled Trial (PERISCOPE Ii). *BMC Cancer* (2019) volume 19:420. doi: 10.1186/s12885-019-5640-2
56. Hironori I, Yoshiyuki F, Ryoji F, Nashimoto A, Yabusaki H, Imano M, et al. Phase III Trial Comparing Intraperitoneal and Intravenous Paclitaxel Plus S-1 Versus Cisplatin Plus S-1 in Patients With Gastric Cancer With Peritoneal Metastasis: PHOENIX-GC Trial. *J Clin Oncol* (2018) 36:1922–9. doi: 10.1200/jco.2018.77.8613
57. Struller F, Horvath P, Solass W, Weinreich FJ, Strumberg D, Kokkalis MK, et al. Pressurized Intraperitoneal Aerosol Chemotherapy With Low-Dose Cisplatin and Doxorubicin (PIPAC C/D) in Patients With Gastric Cancer and Peritoneal Metastasis: A Phase II Study. *Ther Adv Med Oncol* (2019) 11:1758835919846402. doi: 10.1177/1758835919846402
58. Di Giorgio A, Schena CA, El Halabeih MA, Abatini C, Vita E, Strippoli A, et al. Systemic Chemotherapy and Pressurized Intraperitoneal Aerosol Chemotherapy (PIPAC): A Bidirectional Approach for Gastric Cancer Peritoneal Metastasis. *Surg Oncol* (2020) 34:270–5. doi: 10.1016/j.suronc.2020.05.006
59. Alyami M, Bonnot PE, Mercier F, Laplace N, Villeneuve L, Passot G, et al. Pressurized Intraperitoneal Aerosol Chemotherapy (PIPAC) for Unresectable Peritoneal Metastasis From Gastric Cancer. *Eur J Surg Oncol* (2021) 47 (1):123–7. doi: 10.1016/j.ejso.2020.05.021
60. Ishigami H, Kitayama J, Kaisaki S, Hidemura A, Kato M, Otani K, et al. Phase II Study of Weekly Intravenous and Intraperitoneal Paclitaxel Combined With S-1 for Advanced Gastric Cancer With Peritoneal Metastasis. *Ann Oncol* (2010) 21:67–70. doi: 10.1093/annonc/mdp260
61. Facchiano E, Scaringi S, Kianmanesh R, Sabate JM, Castel B, Flamant Y, et al. Laparoscopic Hyperthermic Intraperitoneal Chemotherapy (HIPEC) for the Treatment of Malignant Ascites Secondary to Unresectable Peritoneal Carcinomatosis From Advanced Gastric Cancer. *Eur J Surg Oncol* (2008) 34 (2):154–8. doi: 10.1016/j.ejso.2007.05.015
62. Facchiano E, Risio D, Kianmanesh R, Msika S. Laparoscopic Hyperthermic Intraperitoneal Chemotherapy: Indications, Aims, and Results: A Systematic Review of the Literature. *Ann Surg Oncol* (2012) 19(9):2946–50. doi: 10.1245/s10434-012-2360-0
63. Valle M, van der Speeten K, Garofalo A. Laparoscopic Hyperthermic Intraperitoneal Peroperative Chemotherapy (HIPEC) in the Management of Refractory Malignant Ascites: A Multi-Institutional Retrospective Analysis in 52 Patients. *J Surg Oncol* (2009) 100(4):331–4. doi: 10.1002/jso.21321
64. Nadiradze G, Giger-Pabst U, Zieren J, Strumberg D, Solass W, Reymond M-A. Pressurized Intraperitoneal Aerosol Chemotherapy (PIPAC) With Low-Dose Cisplatin and Doxorubicin in Gastric Peritoneal Metastasis. *J Gastrointest Surg* (2016) 20:367–73. doi: 10.1007/s11605-015-2995-9
65. Bonnot PE, Rabel T, Lintis A, Laplace N, Bakrin N, Kepenekian V, et al. Pressurized Intraperitoneal Aerosol Chemotherapy (PIPAC) Associated to Systemic Chemotherapy for Gastric Cancer With Diffuse Peritoneal Metastases in a Palliative Setting. *J Clin Oncol* (2020) 38, Issue 15 suppl. doi: 10.1200/JCO.2020.38.15_suppl.e16538
66. Ellebaek SB, Graverson M, Detlefsen S, Lundell L, Fristrup CW, Pfeiffer P, et al. Pressurized Intraperitoneal Aerosol Chemotherapy (PIPAC) of Peritoneal Metastasis From Gastric Cancer: A Descriptive Cohort Study. *Clin Exp Metastasis* (2020) 37(2):325–32. doi: 10.1007/s10585-020-10023-5
67. Garg PK, Jara M, Alberto M, Rau B. The Role of Pressurized IntraPeritoneal Aerosol Chemotherapy in the Management of Gastric Cancer: A Systematic Review. *Pleura Peritoneum* (2019) 2019:20180127. doi: 10.1515/pp-2018-0127
68. Eveno C, Jouvin I, Pocard M. PIPAC EstoK 01: Pressurized Intraperitoneal Aerosol Chemotherapy With Cisplatin and Doxorubicin (PIPAC C/D) in Gastric Peritoneal Metastasis: A Randomized and Multicenter Phase II Study. *Pleura Peritoneum* (2018) 3:20180116. doi: 10.1515/pp-2018-0116
69. Kim G, Tan Hon L, Chen E, Teo SC, Jia Min Jang C, Ho J, et al. Study Protocol: Phase 1 Dose Escalating Study of Pressurized Intra-Peritoneal Aerosol Chemotherapy (PIPAC) With Oxaliplatin in Peritoneal Metastasis. *Pleura Peritoneum* (2018) 3:20180118. doi: 10.1515/pp-2018-0118
70. Dumont F, Senellart H, Pein F, Campion L, Glehen O, Goere D, et al. Phase I/II Study of Oxaliplatin Dose Escalation *via* a Laparoscopic Approach Using Pressurized Aerosol Intraperitoneal Chemotherapy (PIPOX Trial) for Nonresectable Peritoneal Metastases of Digestive Cancers (Stomach, Small Bowel and Colorectal): Rationale and Design. *Pleura Peritoneum* (2018) 3:20180120. doi: 10.1515/pp-2018-0120
71. Struller F, Horvath P, Solass W, Weinreich FJ, Strumberg D, Kokkalis MK, et al. Feasibility, Efficacy and Safety of Pressurized Intraperitoneal Aerosol Chemotherapy (PIPAC) With Cisplatin and Doxorubicin in Patients With Gastric Cancer and Peritoneal Carcinomatosis: An Open-Label, Single-Arm, Phase II Clinical Trial (PIPAC-Ga01). *Ther Adv Med Oncol* (2019) 11:1758835919846402. doi: 10.1177/1758835919846402
72. Suzuki O, Fukuchi M, Mochiki E, Ishiguro T, Sobajima J, Onozawa H, et al. Prognostic Role of Gastrectomy in Patients With Gastric Cancer With Positive Peritoneal Cytology. *Int Surg* (2014) 99:830–4. doi: 10.9738/intsurg-d-14-00119.1
73. Edge SB, Compton CC. *AJCC Cancer Staging Manual, 7th Ed*. New York: Springer (2010). doi: 10.1245/s10434-010-0985-4
74. Kuramoto M, Shimada S, Ikeshima S, Matsuo A, Yagi Y, Matsuda M, et al. Extensive Intraoperative Peritoneal Lavage as a Standard Prophylactic Strategy for Peritoneal Recurrence in Patients With Gastric Carcinoma. *Ann Surg* (2009) 250(2):242–6. doi: 10.1097/sla.0b013e3181b0c80e
75. Imano M, Imamoto H, Itoh T, Satou T, Peng YF, Yasuda A, et al. Impact of Intraperitoneal Chemotherapy After Gastrectomy With Positive Cytological Findings in Peritoneal Washings. *Eur Surg Res* (2011) 47:254–9. doi: 10.1159/000333803
76. Taniguchi K, Yonemura Y, Ishibashi H, Mizumoto A, Wakama S, Coccolini F, et al. Recent Advances in the Treatment of Peritoneal Metastasis Form Gastric Cancer. *Cancer Rep Rev* (2018). doi: 10.15761/CRR.1000148
77. Sukanya JS, Vittal Raj P and Thanka J. Role of HER2neu Expression in Gastric Cancer. *Ind J Path Micro* (2021) 64(1):58–64. doi: 10.4103/ijpm.ijpm_835_19
78. Van Cutsem E, Bang YJ, Feng-Yi F, Xu JM, Lee KW, Jiao SC, et al. HER2 Screening Data From ToGA: Targeting HER2 in Gastric and Gastroesophageal Junction Cancer. *Gastric Cancer* (2015) 18:476–84. doi: 10.1007/s10120-014-0402-y
79. Imano M1, Satou T, Itoh T, Yasuda A, Kato H, Shinkai M, et al. Peritoneal Metastatic Lesions of Gastric Cancer Exhibit Low Expression of Human Epidermal Growth Factor Receptor 2. *Target Oncol* (2012) 7(4):213–6. doi: 10.1007/s11523-012-0223-z
80. Bang YJ, Van Cutsem E, Feyereislova A, Chung HC, Shen L, Sawaki A, et al. Trastuzumab in Combination With Chemotherapy Versus Chemotherapy Alone for Treatment of HER2-Positive Advanced Gastric or Gastro-Oesophageal Junction Cancer (ToGA): A Phase 3, Open-Label, Randomised Controlled Trial. *Lancet* (2010) 376:687–97. doi: 10.1016/s0140-6736(10)61121-x
81. Berretta M, Fisichella R, Borsatti E, Lleshi A, Lofferdo S, Meneguzzo N, et al. Feasibility of Intraperitoneal Trastuzumab Treatment in a Patient With Peritoneal Carcinomatosis From Gastric Cancer. *Eur Rev Med Pharmacol Sci* (2014) 18(5):689–92.
82. Li HK, Morokoshi Y, Nagatsu K, Kamada T, Hasegawa S. Locoregional Therapy With Alpha-Emitting Trastuzumab Against Peritoneal Metastasis of Human Epidermal Growth Factor Receptor 2-Positive Gastric Cancer in Mice. *Cancer Sci* (2017) 108:1648–56. doi: 10.1111/cas.13282
83. Liu X, Cai H, Sheng W, Yu L, Long Z, Shi Y, et al. Clinicopathological Characteristics and Survival Outcomes of Primary Signet Ring Cell Carcinoma in the Stomach: Retrospective Analysis of Single Center Database. *PLoS One* (2015) 10:e0144420. doi: 10.1371/journal.pone.0144420
84. Piessen G, Messager M, Leteurtre E, Jean-Pierre T, Mariette C. Signet Ring Cell Histology is an Independent Predictor of Poor Prognosis in Gastric Adenocarcinoma Regardless of Tumoral Clinical Presentation. *Ann Surg* (2009) 250:878–87. doi: 10.1097/sla.0b013e3181b21c7b

85. Taghavi S, Jayarajan SN, Davey A, Willis AI. Prognostic Significance of Signet Ring Gastric Cancer. *J Clin Oncol* (2012) 30:3493–8. doi: 10.1200/jco.2012.42.6635
86. Königsrainer I, Horvath P, Struller F, Königsrainer H, Beckert S. Initial Clinical Experience With Cytoreductive Surgery and Hyperthermic Intraperitoneal Chemotherapy in Signet-Ring Cell Gastric Cancer With Peritoneal Metastases. *J Gastric Cancer* (2014) 14(2):117–22. doi: 10.5230/jgc.2014.14.2.117
87. Daniel S, DeNicola N, Feingold D, Liu PH, Aycart S, Golas BJ, et al. Signet Ring Cell Features With Peritoneal Carcinomatosis in Patients Undergoing Cytoreductive Surgery and Hyperthermic Intraperitoneal Chemotherapy are Associated With Poor Overall Survival. *J Surg Oncol* (2019) 119(6):758–65. doi: 10.1002/jso.25379
88. Bonnot P-E, Piessen G, Mercier F, Pocard M, Meunier B, Marc J, et al. Is Cytoreductive Surgery and Hyperthermic Intraperitoneal Chemotherapy Reasonable Treatment for Gastric Signet-Ring Cell Adenocarcinoma and Linitis Plastica With Peritoneal Metastasis? CYTO-CHIP Study—Ancillary Results. *J Clin Oncol* (2018) 36,no.15_suppl:4073–3. doi: 10.1200/JCO.2018.36.15_suppl.4073
89. Ghoorun RA, Liao Y, Chen C, Li S, Lin F, Yang Z. Current Concepts in Gastric Signet Ring Cell Carcinoma. *Ann Clin Lab Res ISSN 2386-5180* (2015) Vol.3 No, 3:29.
90. Canbay E, Torun BC, Cosarcan K, Altunal C, Gurbuz B, Bilgic C, et al. Surgery With Hyperthermic Intraperitoneal Chemotherapy After Response to Induction Chemotherapy in Patients With Peritoneal Metastasis of Gastric Cancer. *J Gastrointest Oncol* (2021) 12(Suppl 1):S47–56. doi: 10.21037/jgo-20-121
91. Coccolini F, Cotte E, Glehen O, Lotti M, Poiasina E, Catena F, et al. Intraperitoneal Chemotherapy in Advanced Gastric Cancer. Meta-Analysis of Randomized Trials. *Eur J Surg Oncol* (2014) 40:12–26. doi: 10.1016/j.ejso.2013.10.019
92. Alyami M, Mercier F, Siebert M, Bonnot PE, Laplace N, Villeneuve L, et al. Unresectable Peritoneal Metastasis Treated by Pressurised Intraperitoneal Aerosol Chemotherapy (PIPAC) Leading to Cytoreductive Surgery and Hyperthermic Intraperitoneal Chemotherapy. *Eur J Surg Oncol* (2019) 47(1):128-33. doi: 10.1016/j.ejso.2019.06.028

Conflict of Interest: The authors declare that the research was conducted in the absence of any commercial or financial relationships that could be construed as a potential conflict of interest.

Publisher's Note: All claims expressed in this article are solely those of the authors and do not necessarily represent those of their affiliated organizations, or those of the publisher, the editors and the reviewers. Any product that may be evaluated in this article, or claim that may be made by its manufacturer, is not guaranteed or endorsed by the publisher.

Copyright © 2022 Prabhu, Mishra, Brandl and Yonemura. This is an open-access article distributed under the terms of the Creative Commons Attribution License (CC BY). The use, distribution or reproduction in other forums is permitted, provided the original author(s) and the copyright owner(s) are credited and that the original publication in this journal is cited, in accordance with accepted academic practice. No use, distribution or reproduction is permitted which does not comply with these terms.

frontiers | Frontiers in Oncology

TYPE Original Research
PUBLISHED 22 July 2022
DOI 10.3389/fonc.2022.899966

Check for updates

OPEN ACCESS

EDITED BY
Luigi Marano,
University of Siena, Italy

REVIEWED BY
Xiaoyu Xi,
China Pharmaceutical University, China
Longjiang She,
First People's Hospital of Foshan, China
George Gourzoulidis,
Health Through Evidence, Greece

*CORRESPONDENCE
Shunping Li
lishunping@sdu.edu.cn

SPECIALTY SECTION
This article was submitted to Gastrointestinal Cancers: Gastric & Esophageal Cancers, a section of the journal Frontiers in Oncology

RECEIVED 19 March 2022
ACCEPTED 27 June 2022
PUBLISHED 22 July 2022

CITATION
Liu S, Dou L, Wang K, Shi Z, Wang R, Zhu X, Song Z and Li S (2022) Cost-effectiveness analysis of nivolumab combination therapy in the first-line treatment for advanced esophageal squamous-cell carcinoma. *Front. Oncol.* 12:899966. doi: 10.3389/fonc.2022.899966

COPYRIGHT
© 2022 Liu, Dou, Wang, Shi, Wang, Zhu, Song and Li. This is an open-access article distributed under the terms of the Creative Commons Attribution License (CC BY). The use, distribution or reproduction in other forums is permitted, provided the original author (s) and the copyright owner(s) are credited and that the original publication in this journal is cited, in accordance with accepted academic practice. No use, distribution or reproduction is permitted which does not comply with these terms.

Cost-effectiveness analysis of nivolumab combination therapy in the first-line treatment for advanced esophageal squamous-cell carcinoma

Shixian Liu[1,2,3], Lei Dou[1,2,3], Kaixuan Wang[1,2,3], Zhao Shi[1,2,3], Ruixue Wang[1,2,3], Xiaohong Zhu[1,2,3], Zehua Song[1,2,3] and Shunping Li[1,2,3]*

[1]Centre for Health Management and Policy Research, School of Public Health, Cheeloo College of Medicine, Shandong University, Jinan, China, [2]National Health Commission (NHC) Key Laboratory of Health Economics and Policy Research, Shandong University, Jinan, China, [3]Center for Health Preference Research, Shandong University, Jinan, China

Objective: We aimed to investigate the cost-effectiveness of nivolumab plus chemotherapy and nivolumab plus ipilimumab versus chemotherapy in the first-line treatment for advanced esophageal squamous-cell carcinoma (ESCC) patients from a healthcare system perspective in China.

Methods: On the basis of the CheckMate 648 trial, a partitioned survival model was constructed to estimate economic costs and health outcomes among overall and PD-L1-positive advanced ESCC patients over a 10-year lifetime horizon. The health-related costs and utilities were obtained from the local charges and published literature. The lifetime costs, life-years, quality-adjusted life-years (QALYs), and incremental cost-effectiveness ratio (ICER) were measured. One-way and probabilistic sensitivity analyses (PSA) were performed to assess the robustness of the model.

Results: In the base-case analysis, in overall and PD-L1-positive advanced ESCC patients, the ICERs were $415,163.81/QALY and $216,628.00/QALY for nivolumab plus chemotherapy, and$430,704.11/QALY and $185,483.94/QALY for nivolumab plus ipilimumab, respectively, compared with chemotherapy. One-way sensitivity analyses revealed that patients' weight was the most influential parameter on ICER. The PSA demonstrated that the probability of nivolumab combination therapy being cost-effective was 0% over chemotherapy at the current price and willingness-to-pay threshold ($38,351.20/QALY). When the price of nivolumab and ipilimumab decreased 80%, the cost-effective probability of nivolumab plus ipilimumab increased to 40.44% and 86.38% in overall and PD-L1-positive advanced ESCC patients, respectively.

Conclusion: Nivolumab combination therapy could improve survival time and health benefits over chemotherapy for advanced ESCC patients, but it is unlikely to be a cost-effective treatment option in China.

KEYWORDS

nivolumab, ipilimumab, chemotherapy, cost-effectiveness, esophageal squamous-cell carcinoma, first-line treatment

Introduction

Esophageal cancer ranks seventh in terms of incidence (604, 000 new cases) and sixth in mortality (544, 000 deaths) worldwide, and East Asian countries were with the highest incidence rates, in part because of the enormous burden in China (1). Nearly half of the esophageal cancer across the world were in China, and the prevention of esophageal cancer has become an important goal for the Chinese government (2). Esophageal squamous-cell carcinoma (ESCC) and esophageal adenocarcinoma are the two major histological types of esophageal cancer, the former accounts for approximately 85% of the cases (3). Standard platinum plus fluorouracil or paclitaxel-based chemotherapy are the recommended first-line treatment option for patients with unresectable advanced, recurrent or metastatic ESCC (4, 5). Although chemotherapy has been widely used as first-line treatment for decades, survival improvement in these patients remains poor (median survival, <1 year) (6, 7), and novel treatment strategies are urgently needed.

Nivolumab, a human monoclonal anti-PD-1 antibody, has been demonstrated to improve the survival benefits for the treatment of several solid tumors in previously published studies (8–10). Programmed death ligand 1 (PD-L1) expression is enriched in ESCC, with expression ranging from 15% to 83% in tumor cells, and from 13% to 31% in immune cells (11). Recently, the results of CheckMate 648 trial, which compared nivolumab plus chemotherapy, nivolumab plus the monoclonal antibody ipilimumab, and chemotherapy in patients with unresectable advanced, recurrent, or metastatic ESCC, have revealed that overall survival (OS) was significantly longer with nivolumab plus chemotherapy than with chemotherapy alone in the overall population (median, 13.2 vs. 10.7 months; hazard ratio [HR], 0.74; 99.1% confidence interval [CI], 0.58-0.96; P=0.002) and also among patients with tumor-cell PD-L1 expression of 1% or greater (median, 15.4 vs. 9.1 months, HR, 0.54; 99.5% CI, 0.37-0.80; P<0.001) (12). A significant OS benefit was also seen with nivolumab plus ipilimumab over chemotherapy alone in overall and PD-L1-positive advanced ESCC patients (12). The CheckMate 648 trial indicated that nivolumab combination therapy could be considered as novel standard first-line treatment options to clinicians and decision-makers for the treatment of advanced ESCC patients, and these treatments has been recommended by the Chinese Society of Clinical Oncology (CSCO) Guidelines of Esophageal Cancer (13).

Significant costs always accompany the research and development of innovative drugs (14). The high cost of nivolumab and ipilimumab may limit its availability and impose a substantial financial burden on the national healthcare system. Although previous economic evidence demonstrated that nivolumab was unlikely to be cost-effective compared with chemotherapy in the second-line treatment of advanced ESCC patients from the perspective of Chinese society (15), the cost-effectiveness of nivolumab plus chemotherapy and nivolumab plus ipilimumab was not clear yet. Therefore, the objective of this study was to assess the cost-effectiveness of nivolumab combination therapy as first-line management for advanced ESCC patients in China. Such evidence may better inform clinical practice and reimbursement policy to optimize resource utilization.

Methods

Patients and intervention

This economic evaluation study was based on the CheckMate 648 trial (12), and the ethical approval of the institutional review board was exempted because no real human participants were involved. This study followed the Consolidated Health Economic Evaluation Reporting Standards 2022 (CHEERS 2022) reporting guidelines (**Supplementary Table 1**) (16). The target patient population was kept with the cohort included in the CheckMate 648 trial, an open-label, phase 3 trial conducted at 182 sites in 26 countries. Eligible patients were at least 18 years of age and had been confirmed unresectable advanced, recurrent, or metastatic ESCC, regardless of PD-L1 expression status, according to Response Evaluation Criteria in Solid Tumors (12).

Included patients were randomly assigned in a 1:1:1 ratio to receive nivolumab (240 mg intravenously on day 1 and day 15 every 4 weeks) plus chemotherapy (consisting of fluorouracil at a dose of 800 mg per square meter of the body-surface area on days 1 through 5 and cisplatin at a dose of 80 mg per square meter on day 1 each 4-week); nivolumab (3 mg per kilogram of body weight every 2 weeks) plus ipilimumab (1 mg per kilogram every 6 weeks); or chemotherapy alone until disease progression, unacceptable toxicity or other reasons (12). Patients were permitted to receive nivolumab or nivolumab plus ipilimumab up to a maximum of 2 years in line with package insert information and published resource. Subsequently, patients were managed with chemotherapy until progression.

Model structure

A partitioned survival model was developed using Microsoft Excel 2019 to compare the cost and effectiveness of the three competing regimens mentioned above among patients with advanced ESCC. The model was composed of three mutually exclusive health states: progression-free survival (PFS), progressed disease (PD) and death (**Figure 1**). The initial health state of all patients was PFS state, and that they could maintain their assigned health state or redistribute to another health state during each cycle. The proportion of patients in the PFS state at each time point was estimated as the area under the curve (AUC) for the PFS, while the proportion of patients in the death state was calculated by 1 minus the OS curve. The AUC between the PFS and OS curves was the PD state. The cycle length of the model was set at 4 weeks to facilitate parameter calculation. The time horizon was ten years to ensure that ESCC patients fully entered the terminal state.

This study was conducted from a Chinese healthcare system perspective. The primary outcomes of the model were total cost, life-years, quality-adjusted life-years (QALYs), and incremental cost-effectiveness ratio (ICER) between the treatment strategies. ICER was described as the additional cost required for each additional QALY. A half-cycle correction was implemented to improve the accuracy of the results. According to China Guidelines for Pharmacoeconomic Evaluations, a 5% annual discount rate was applied for all costs and QALYs (17). Based on the local Consumer Price Index, all costs were adjusted to 2022 prices and converted into US dollars (1$=6.33 CNY). As recommended by the World Health Organization, we used three times of the per capita gross domestic product (GDP) of China in 2021 ($38,351.20) as the willingness-to-pay (WTP) threshold to determine the cost-effectiveness of treatment regimens (18–21). Treatment options were considered highly cost-effective when the ICER was less than 1 times GDP per capita, while treatment options were considered cost-effective when the ICER was less than 3 times the GDP per capita (18). This WTP threshold has been widely employed in health technology assessment within low- and middle-income countries (20).

Clinical data

The clinical efficacy and safety data were derived from the CheckMate 648 trial (12). As individual patient data (IPD) was not available, the GetData Graph Digitizer 2.26 (http://www.getdata-graph-digitizer.com/) was used to extract PFS and OS data points from the corresponding Kaplan–Meier survival curves. Different parametric distributions, including Exponential, Weibull, Log-logistic, Log-normal, and Gompertz, were fitted to extrapolate the survival curves beyond the follow-up duration of the clinical trials (22). The distribution with the best fit was evaluated based on graphical validation, Akaike information criterion (AIC) and Bayesian information criterion (BIC) (**Supplementary Tables 2, 3**) (23). The AIC and BIC were calculated using survival analyses with Stata 15.1. As for the long-tail curve, we used the sub-optimal or Weibull distribution for extrapolation to avoid overestimating the survival time (24).

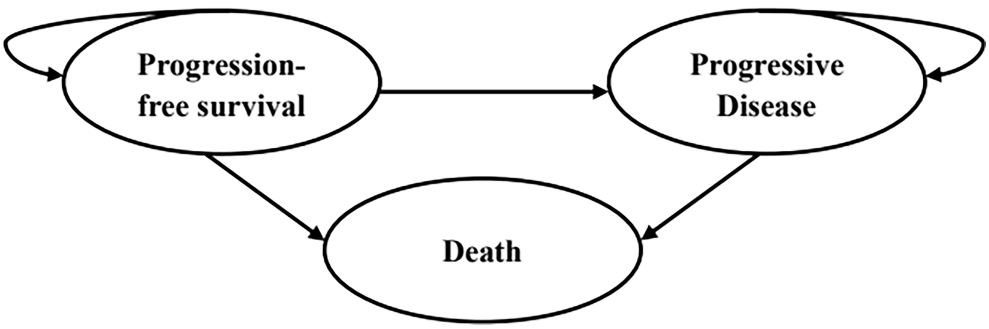

FIGURE 1
The structure of the partitioned survival model.

A total of 12 parametric survival curves were modeled, including the PFS and OS of overall and PD-L1-positive advanced ESCC patients (**Supplementary Figures 1–12**). The estimated scale (λ) and shape (γ) parameters of the fitting model are presented in **Table 1**.

Costs

Only direct medical costs were considered, including costs for drugs, laboratory tests and radiological examinations, routine follow-up, management of treatment-related severe adverse events (AEs), salvage therapy, best supportive care, and terminal care in end-of-life. The drug administration schedules were in accordance with the CheckMate 648 trial. To estimate the dosage of chemotherapy agents, a typical patient weighed 65 kg and had a height of 1.64 m was assumed, resulting in a body surface area of 1.72 m^2 (25). The model included management costs associated with grade 3-4 AEs that occurred in 3% or greater of patients as they have a substantial effect on the survival and costs. In this condition, our analysis calculated the costs of nausea, decreased appetite, stomatitis, anemia, neutropenia, fatigue, and vomiting. The treatment of neutropenia covered that of leukopenia, so that the cost of leukopenia was not included based on expert consensus (26). Furthermore, owing to the unavailability of cost and disutility values, mucosal inflammation was not considered either. All costs were acquired from local hospitals or previously published literature (27–30). The nivolumab patient assistance program (PAP) was currently implemented in patients with advanced or recurrent gastric or gastro-oesophageal junction adenocarcinoma, so we only considered the effection of price reductions for nivolumab and ipilimumab.

Utilities

Each health state was assigned a utility value anchored in 0 (death) and 1 (perfect health) in this partitioned survival model. QALYs were measured to determine health outcomes, namely, the utility values in a particular health state multiplied by the years of the corresponding state lasted. As the CheckMate 648 trial did not report the utility values of different health states, we obtained from another published study, a global, randomized, double-blind phase III trial, in which the utility values were measured by the EuroQol five dimensions health status questionnaire (EQ-5D-3L) and the UK-specific value algorithm (31, 32). In addition, we considered the disutility values caused by grade 3-4 AEs according to the relevant literature (33–35). All costs and utilities are shown in **Table 2**.

Scenario analysis

Our analyses covered two scenarios. In the first scenario, we assumed that nivolumab and ipilimumab were reduced to 80%, 60%, 40% or 20% of the current price to explore the cost-effectiveness of nivolumab combination therapy, respectively. In addition, we evaluated the impact of a longer or shorter time horizon of simulation on ICERs.

Sensitivity analyses

In order to evaluate the robustness of the model and identify the variables that have considerable impacts on the analysis results, we performed one-way and probabilistic sensitivity analyses (PSA) for input parameters. In the one-

TABLE 1 Optimal distribution of progression-free and overall survival curves.

Group		Shape	Scale	Distribution
Overall advanced ESCC patients				
Chemotherapy	PFS	1.670192	-0.081726	Log-normal
	OS	2.450230	-0.620517	Log-logistic
Nivolumab plus chemotherapy	PFS	1.908558	-0.514040	Log-logistic
	OS	2.659128	-0.598290	Log-logistic
Nivolumab plus ipilimumab	PFS	1.364702	-0.329654	Log-logistic
	OS	2.604049	-0.305029	Log-logistic
Advanced ESCC patients with PD-L1-positive status				
Chemotherapy	PFS	1.539710	-0.162895	Log-normal
	OS	2.431702	-0.627434	Log-logistic
Nivolumab plus chemotherapy	PFS	1.996054	0.103059	Log-normal
	OS	2.845191	0.070365	Log-normal
Nivolumab plus ipilimumab	PFS	1.657211	0.379699	Log-normal
	OS	2.809128	0.381912	Log-normal

ESCC, esophageal squamous-cell carcinoma; PFS, progression-free survival; OS, overall survival.

TABLE 2 Basic parameters input to the model and the ranges of the sensitivity analysis.

Parameters	Baseline value	Range		Distribution	Reference
		Minimum	Maximum		
Cost inputs (US $)					
Nivolumab (40 mg)	724.11	579.29	868.93	Gamma	Local estimate
Fluorouracil (250 mg)	31.42	25.13	37.70	Gamma	Local estimate
Cisplatin (10 mg)	1.47	1.18	1.77	Gamma	Local estimate
Ipilimumab (50 mg)	4,420.38	3,536.30	5,304.45	Gamma	Local estimate
Laboratory tests and radiological examinations	357.34	285.87	428.81	Gamma	(27)
Routine follow-up per cycle	73.72	58.98	88.47	Gamma	(27)
Salvage therapy	639.75	511.80	767.70	Gamma	(27)
Beat supportive care per cycle	182.23	145.78	218.68	Gamma	(27)
Terminal care in end-of-life	1,460.30	1,055.30	2,085.70	Gamma	(28)
Nausea per event	71.00	56.80	85.20	Gamma	(29)
Decreased appetite per event	115.00	92.00	138.00	Gamma	(29)
Stomatitis per event	46.54	37.23	55.85	Gamma	(30)
Anemia per event	523.36	418.69	628.03	Gamma	(30)
Decreased neutrophil count per event	454.26	363.41	545.11	Gamma	(30)
Fatigue per event	113.59	90.87	136.31	Gamma	(30)
Vomiting per event	71.00	56.80	85.20	Gamma	(29)
Utility inputs					
Progression-free survival	0.75	0.60	0.90	Beta	(31, 32)
Progressive Disease	0.60	0.48	0.72	Beta	(31, 32)
Disutility inputs					
Nausea	-0.13	-0.10	-0.15	Beta	(33)
Decreased appetite	-0.07	-0.05	-0.08	Beta	Assumption
Stomatitis	-0.15	-0.12	-0.18	Beta	(34)
Anemia	-0.07	-0.06	-0.09	Beta	(35)
Decreased neutrophil count	-0.20	-0.16	-0.24	Beta	(33)
Fatigue	-0.07	-0.05	-0.08	Beta	(33)
Vomiting	-0.13	-0.10	-0.16	Beta	(33)
Risk of severe adverse events in chemotherapy group					
Nausea	3.00%	2.40%	3.60%	Beta	(12)
Decreased appetite	3.00%	2.40%	3.60%	Beta	(12)
Anemia	6.00%	4.80%	7.20%	Beta	(12)
Decreased neutrophil count	8.00%	6.40%	9.60%	Beta	(12)
Fatigue	4.00%	3.20%	4.80%	Beta	(12)
Vomiting	3.00%	2.40%	3.60%	Beta	(12)
Risk of severe adverse events in Nivolumab plus chemotherapy group					
Nausea	4.00%	3.20%	4.80%	Beta	(12)
Decreased appetite	4.00%	3.20%	4.80%	Beta	(12)
Stomatitis	6.00%	4.80%	7.20%	Beta	(12)
Anemia	10.00%	8.00%	12.00%	Beta	(12)
Decreased neutrophil count	8.00%	6.40%	9.60%	Beta	(12)
Proportion of patients receivied subsequent therapy					
Chemotherapy	59.57%	47.65%	71.48%	Beta	(12)
Nivolumab plus chemotherapy	57.32%	45.86%	68.79%	Beta	(12)
Nivolumab plus ipilimumab	53.54%	42.83%	64.25%	Beta	(12)

(Continued)

TABLE 2 Continued

Parameters	Baseline value	Range		Distribution	Reference
		Minimum	Maximum		
Others					
Discount rate	5.00%	0.00%	8.00%	Fixed	(17)
Patient weight (kg)	65.00	52.00	78.00	Gamma	(25)
Body surface area (m^2)	1.72	1.38	2.06	Gamma	(25)

ESCC, esophageal squamous-cell carcinoma; PFS, progression-free survival; OS, overall survival.

way sensitivity analysis, input parameters were adjusted one-by-one to their respective minimum and maximum values, with a range of the 95% confidence intervals reported in the referenced literature or a ± 20% change from the base-case value, in order to ascertain the variables that significantly influenced the economic outcomes. The range of discount rate was 0%-8%. Tornado diagram was used to present the results. A Monte Carlo simulation of 10,000 iterations was conducted for PSA by simultaneously sampling all input parameters from the pre-specified distributions. All the costs were sampled from Gamma distribution. The utility values and probabilities were sampled from Beta distribution. Cost-effectiveness acceptability curves (CEAC) were plotted based on the outcomes from 10,000 iterations to illustrate the probability of cost-effectiveness of nivolumab plus chemotherapy and nivolumab plus ipilimumab against chemotherapy alone at various WTP thresholds.

Results

Base-case results

The base-case results are presented in Table 3. Over the lifetime horizon of 10 years, compared with chemotherapy, nivolumab plus chemotherapy or ipilimumab as first-line therapy for overall advanced ESCC patients provided an incremental cost of $78,349.01 and $63,058.82 with additional 0.19 QALYs and 0.15 QALYs, respectively, resulting in an ICER of $415,163.81/QALY and $430,704.11/QALY. Compared with chemotherapy, nivolumab plus chemotherapy or ipilimumab as first-line therapy for PD-L1-positive advanced ESCC patients generated an incremental cost of $ 88,366.61 and $ 89,257.72 with additional 0.41 QALYs and 0.48 QALYs, respectively, resulting in an ICER of $216,628.00/QALY and $185,483.94/QALY. In the pairwise comparison between the two nivolumab combination therapies, nivolumab plus ipilimumab increased the cost by $891.12 with the augments of 0.07 QALYs against nivolumab plus chemotherapy for PD-L1-positive advanced ESCC patients, and the ICER ($12,157.66/QALY) was lower than the WTP threshold.

Scenario analysis results

The results of the scenario analysis are shown in Supplementary Tables 4, 5. As the price of nivolumab and ipilimumab decreased or the time horizon of simulation increased, the ICER of nivolumab combination therapy over chemotherapy gradually decreased. With 80% price reduction of nivolumab and ipilimumab, the ICER ($29,649.50/QALY) of nivolumab plus ipilimumab versus chemotherapy was below the WTP threshold in the treatment of PD-L1-positive advanced ESCC patients.

One-way sensitivity analysis

The top 10 parameters that most influenced the base-case analysis of overall advanced ESCC patients are presented in Tornado diagrams (Figures 2–4). Patients' weight, utility values, and the prices of nivolumab and ipilimumab greatly influenced the model results. Similar results were obtained in PD-L1-positive advanced ESCC patients (Supplementary Figures 13–15).

Probabilistic sensitivity analysis

At the base-case WTP threshold and current price, the CEAC demonstrated that the probability of nivolumab combination therapy strategies being cost-effective was 0% in overall and PD-L1-positive ESCC patients (Figures 5, 6). As the price of nivolumab and ipilimumab decreased, the results of the PSA have changed. When the price of nivolumab and ipilimumab reduced 80%, the probability of being cost-effective increased to 0% and 7.85% for nivolumab plus chemotherapy and 40.44% and 86.38% for nivolumab plus ipilimumab in overall and PD-L1-positive advanced ESCC patients, respectively. In the pairwise comparison between the two nivolumab combination therapies, the probability of nivolumab plus chemotherapy being cost-effectiveness was 4.72% and 41.26% in overall and PD-L1-positive advanced ESCC patients at the WTP threshold of $38,351.20 per QALY, respectively, compared with nivolumab plus ipilimumab (Supplementary Figures 16, 17).

TABLE 3 Base case results.

Parameters	Overall advanced ESCC patients			Advanced ESCC patients with PD-L1-positive status		
	Chemotherapy	Nivolumab plus chemotherapy	Nivolumab plus ipilimumab	Chemotherapy	Nivolumab plus chemotherapy	Nivolumab plus ipilimumab
Cost ($)						
Drug	6,952.79	88,285.53	72,568.91	5,781.46	96,689.13	97,103.71
Follow-up and tests	1,009.81	1,439.20	1,069.46	839.69	1,602.10	1,594.97
Adverse events	29.13	35.22	6.69[#]	24.22	39.33	14.10[#]
PFS state	7,991.72	89,759.94	73,645.06	6,645.37	98,330.56	98,712.79
PD state	5,047.23	1,628.02	2,452.71	5,605.15	2,286.57	2,795.46
Terminal care	1,460.30	1,460.30	1,460.30	1,460.30	1,460.30	1,460.30
Total Cost	14,499.25	92,848.26	77,558.07	13,710.82	102,077.43	102,968.54
LYs						
PFS state	0.62	0.91	0.68	0.51	1.02	1.04
PD state	0.45	0.45	0.69	0.84	1.13	1.53
Total LYs	1.08	1.36	1.38	1.35	2.15	2.57
QALYs						
PFS state	0.45	0.64	0.48	0.37	0.72	0.71
PD state	0.24	0.24	0.36	0.27	0.34	0.41
Total QALYs	0.70	0.88	0.84	0.65	1.05	1.13
ICER ($/LYs)		272,390.06	208,386.78		110,465.61	73,402.85
			-1,021,434.44*			2,141.84*
ICER ($/QALY)		415,163.81	430,704.11		216,628.00	185,483.94
			361,388.00*			12,157.66*

[#]Management costs associated with adverse events caused by chemotherapy after two years of treatment with nivolumab plus ipilimumab; *nivolumab plus chemotherapy versus nivolumab plus ipilimumab; ESCC, esophageal squamous-cell carcinoma; PFS, progression-free survival; OS, overall survival; LYs, lifeyears; QALYs, Quality-adjusted life years; ICER, Incremental cost-effectiveness ratio.

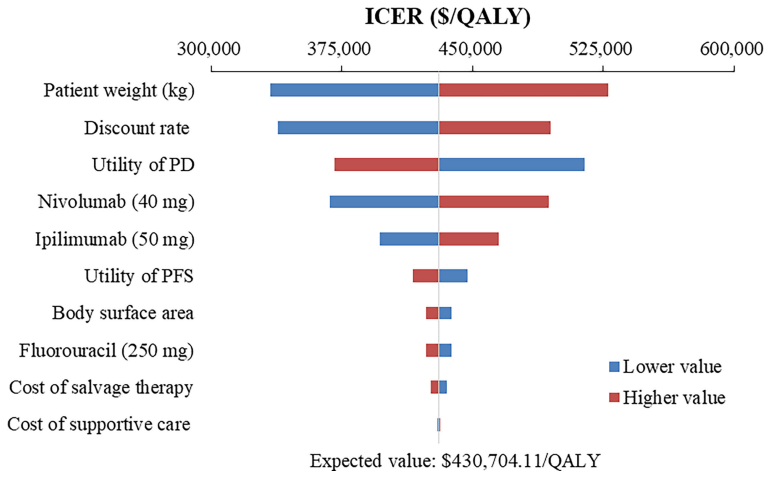

FIGURE 2
Tornado diagram of one-way sensitivity analysis of Nivolumab plus ipilimumab versus Chemotherapy in the treatment of overall advanced ESCC patients. ICER, incremental cost-effectiveness ratio; QALY, quality-adjusted life year; PFS, progression-free survival; PD, progressive disease.

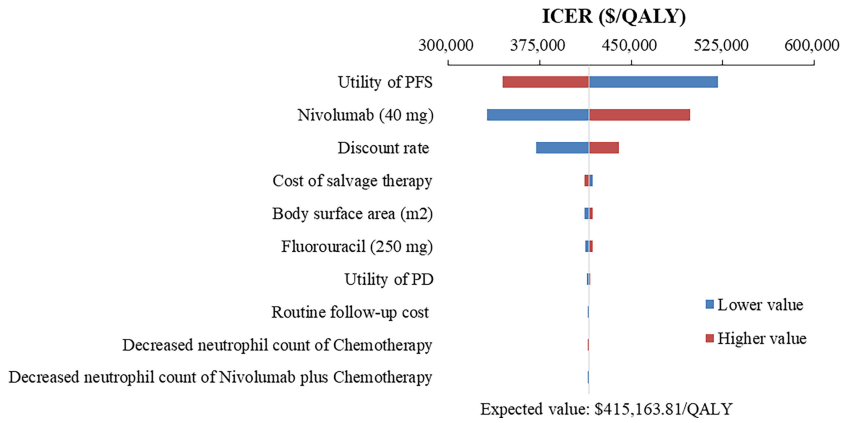

FIGURE 3
Tornado diagram of one-way sensitivity analysis of Nivolumab plus chemotherapy versus Chemotherapy in the treatment of overall advanced ESCC patients. ICER, incremental cost-effectiveness ratio; QALY, quality-adjusted life year; PFS, progression-free survival; PD, progressive disease.

Discussion

To our knowledge, this study was the first modeling analysis to examine the cost-effectiveness of nivolumab combination therapy in the treatment of advanced ESCC patients by incorporating the latest evidence from a Chinese healthcare system perspective. The results revealed that nivolumab combination therapy could provide higher health outcomes with higher cost expenditures, the ICER well above the WTP threshold based on the latest GDP. Sensitivity analyses confirmed that the model results were robust. Considering the implementation of the national price negotiation policy in China (36, 37), we assumed that nivolumab and ipilimumab were reduced to 40% or 20% of the current price, respectively, to explore the optimal treatment options. The results of PSA indicated that when the price of nivolumab and ipilimumab at 20% price, the cost-effective probability of nivolumab plus ipilimumab improved from 0% to 40.44% and 86.38% in overall and PD-L1-positive advanced ESCC patients, respectively, otherwise chemotherapy was dominant at a WTP threshold of $38,351.20/QALY.

Regardless of the overall or PD-L1-positive advanced ESCC patients, nivolumab combined with chemotherapy or ipilimumab yielded near-equal health outcomes over a 10-year lifetime horizon estimation. In the PFS state, the QALYs produced by nivolumab plus ipilimumab were much lower than that of nivolumab plus chemotherapy for overall advanced ESCC patients, while there was

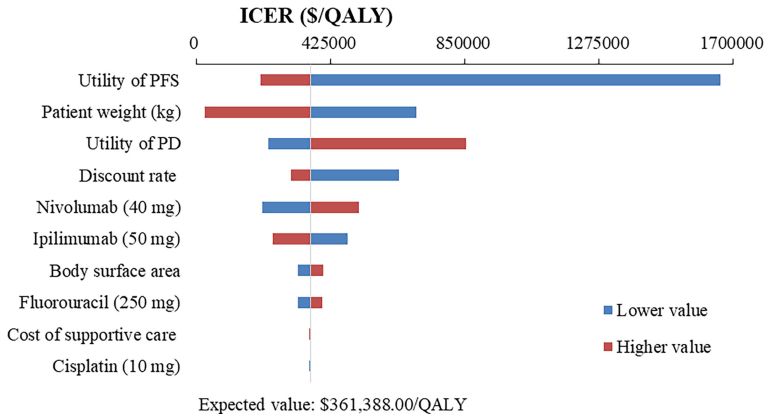

FIGURE 4
Tornado diagram of one-way sensitivity analysis of Nivolumab plus chemotherapy versus Nivolumab plus ipilimumab in the treatment of overall advanced ESCC patients. ICER, incremental cost-effectiveness ratio; QALY, quality-adjusted life year; PFS, progression-free survival; PD, progressive disease.

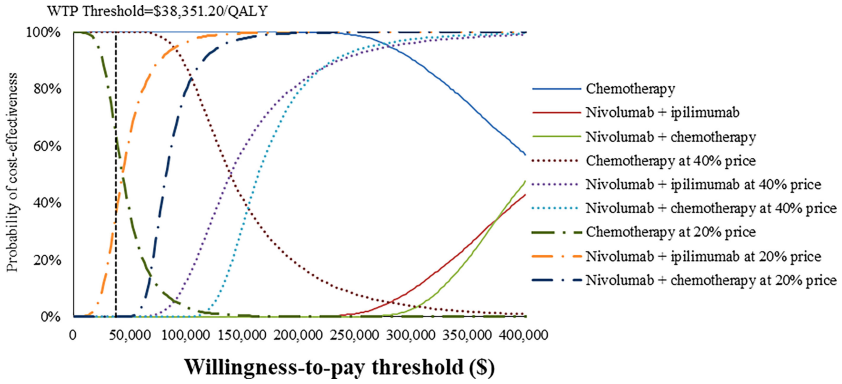

FIGURE 5
Cost-effectiveness acceptability curves of nivolumab plus ipilimumab and nivolumab plus chemotherapy versus chemotherapy in the treatment of overall advanced ESCC patients from the Chinese healthcare perspective.

almost identity between the two treatment regiments for PD-L1 positive ESCC patients. In the PD state, with the increase of time horizon, nivolumab plus ipilimumab could accumulate more QALYs than nivolumab plus chemotherapy, which benefited from the improvement of overall survival time. As such, the cost-effectiveness advantage of nivolumab plus ipilimumab compared with nivolumab plus chemotherapy progressively emerged as the simulation time increased. It was worth mentioning that these results should be interpreted with caution, due to the lack of sufficient data on the cost and disutility values of treatment-related AEs in the nivolumab plus ipilimumab group.

Due to the dramatically increasing cost and the uncertainty of survival benefits, innovative drugs combined with existing treatment schemes often have lower cost-effective probabilities than standard treatment regimens (14). Although the survival benefits of nivolumab combination therapy were superior to chemotherapy in the treatment of advanced ESCC, the higher expenditures and limited improvement in health outcomes were such that substantial price reductions still could not salvage its cost-effectiveness. Previous economic evidence suggested that nivolumab was not a cost-effective treatment option compared with chemotherapy in the second-line treatment of advanced ESCC patients from the perspective of Chinese society (15, 38). Our findings were consistent with those of previous economic evaluations, and the total cost and QALYs were different, which might be caused by various treatment schedules, modeling techniques, and cost measurements used in the two studies.

Among patients with advanced ESCC, the addition of camrelizumab (an anti-PD-1 antibody) to chemotherapy also significantly improved PFS (6.9 vs. 5.6 months; HR for progression or death, 0.56; 95% CI, 0.46-0.68; P<0.001) and OS (15.3 vs. 12.0 months; HR for death, 0.70; 95% CI, 0.56-0.88;

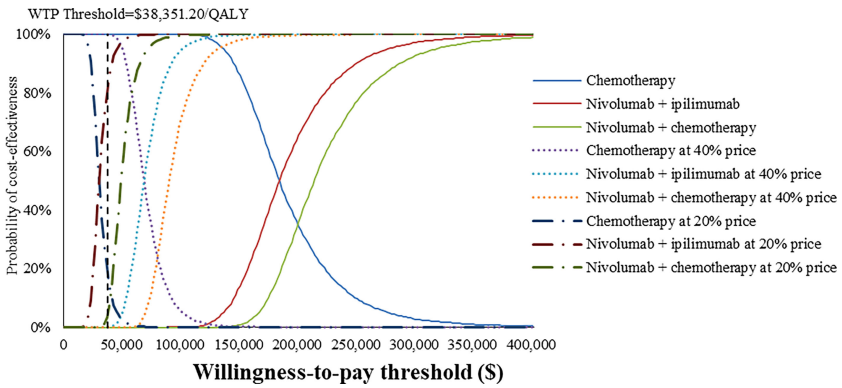

FIGURE 6
Cost-effectiveness acceptability curves of nivolumab plus ipilimumab and nivolumab plus chemotherapy versus chemotherapy in the treatment of PD-L1-positive advanced ESCC patients from the Chinese healthcare perspective.

P=0.001) in comparison with single-agent chemotherapy (39). Similarly, the latest cost-effectiveness analysis has shown that camrelizumab plus chemotherapy was unlikely to be cost-effective versus chemotherapy in patients with advanced or metastatic ESCC over a 5-year lifetime horizon estimation in China (27). However, after a price reduction of 85.2% through China's drug price negotiation mechanism, camrelizumab was a cost-effective treatment regimen against chemotherapy for advanced or metastatic ESCC patients (35). Consequently, in the absence of further breakthroughs in efficacy at this time, a substantial price reduction is the key to ensuring cost-effectiveness and affordability of treatment options, especially in countries with a huge cancer burden and limited medical resources (40). Our sensitivity analyses also indicated that drug price was an important variable affecting ICER, and price reduction could improve the cost-effective probability of nivolumab combination therapy. In addition, equitable and niche-targeting PAP can yet be regarded as a shortcut to improve affordability.

In addition to the price of nivolumab and ipilimumab, sensitivity analyses demonstrated that patients' weight and utility values for PFS and PD state were the most influential parameter within the model. We used the default body weight to estimate the dosage of the therapeutic agents in the base-case analysis, which limited the transferability and representativeness of specific population, such as the over-weight (41, 42). Therefore, weight-specific economic evaluations warranted further studies to best inform cancer precision medicine and reimbursement policy (43). Furthermore, the quality of life research of esophageal neoplasms has been available in China (44, 45), but these still cannot meet the urgent needs of health technology assessment, especially the lack of utility and disutility values associated with various health states and treatment regimens. Hence, developing health utility values based on realistic modeling needs remains a priority.

As model assumptions and limited data, several potential limitations should be considered in the current economic evaluation. First, we reconstructed IPD rather than actual data from the CheckMate 648 trial because the original data were unavailable from the published literature. Although this approach was not perfect, it approximately reflected the actual survival data observed in the clinical trials so as to guarantee the credibility of this simulation. Second, since the quality of life was not reported in the CheckMate 648 trial, we obtained utility values from the published literature. That might lead to some deviations between the simulation results and actual health outcomes. Therefore, we used a wide range (± 20%) of utility values to examine the effect of changes on outcomes in the sensitivity analysis, which did not substantially impact the base-case results. Third, we only considered disutility values and costs related to grade 3-4 AEs of chemotherapy and nivolumab plus chemotherapy group, as these were difficult to define and obtain in the nivolumab plus ipilimumab group. Fourth, some important cost variables were derived from published economic evaluations rather than the real-world medical data, although one-way sensitivity analysis proved that these costs exerted minimal influence on the model results, except for the costs of nivolumab and ipilimumab. Fifth, we assumed that the best supportive care was administrated after the progression of nivolumab combination therapy, which might differ from the actual treatment options.

Conclusion

In summary, nivolumab combination therapy was unlikely to be a cost-effective treatment regimen compared with chemotherapy in the first-line treatment of patients with advanced ESCC in China. When the price of nivolumab and ipilimumab decreased 80%, nivolumab plus ipilimumab was the optimal treatment option among PD-L1-positive advanced ESCC patients in China.

Data availability statement

The original contributions presented in the study are included in the article/**Supplementary Material**. Further inquiries can be directed to the corresponding author.

Author contributions

SXL, SPL, and LD were responsible for study design, model building and statistical analysis. SXL prepared the manuscript. KW, ZS, RW, XZ, and ZHS searched literatures and collected data. All authors critically reviewed the model structure, verified results and revised the manuscript.

Conflict of interest

The authors declare that the research was conducted in the absence of any commercial or financial relationships that could be construed as a potential conflict of interest.

Publisher's note

All claims expressed in this article are solely those of the authors and do not necessarily represent those of their affiliated organizations, or those of the publisher, the editors and the reviewers. Any product that may be evaluated in this article, or claim that may be made by its manufacturer, is not guaranteed or endorsed by the publisher.

Supplementary material

The Supplementary Material for this article can be found online at: https://www.frontiersin.org/articles/10.3389/fonc.2022.899966/full#supplementary-material

References

1. Sung H, Ferlay J, Siegel RL, Laversanne M, Soerjomataram I, Jemal A, et al. Global cancer statistics 2020: Globocan estimates of incidence and mortality worldwide for 36 cancers in 185 countries. *CA Cancer J Clin* (2021) 71(3):209–49. doi: 10.3322/caac.21660

2. Li SB, Chen H, Man JY, Zhang TC, Yin XL, He QF, et al. Changing trends in the disease burden of esophageal cancer in China from 1990 to 2017 and its predicted level in 25 years. *Cancer Med* (2021) 10(5):1889–99. doi: 10.1002/cam4.3775

3. Arnold M, Ferlay J, Henegouwen MIV, Soerjomataram I. Global burden of oesophageal and gastric cancer by histology and subsite in 2018. *Gut* (2020) 69 (9):1564–71. doi: 10.1136/gutjnl-2020-321600

4. Lordick F, Mariette C, Haustermans K, Obermannova R, Arnold D, Comm EG. Oesophageal cancer: Esmo clinical practice guidelines for diagnosis, treatment and follow-up. *Ann Oncol* (2016) 27(suppl 5):v50–7. doi: 10.1093/annonc/mdw329

5. Kitagawa Y, Uno T, Oyama T, Kato K, Kato H, Kawakubo H, et al. Esophageal cancer practice guidelines 2017 edited by the Japan esophageal society: Part 2. *Esophagus* (2019) 16(1):25–43. doi: 10.1007/s10388-018-0642-8

6. Bleiberg H, Conroy T, Paillot B, Lacave AJ, Blijham G, Jacob JH, et al. Randomised phase ii study of cisplatin and 5-fluorouracil (5-fu) versus cisplatin alone in advanced squamous cell oesophageal cancer. *Eur J Cancer* (1997) 33 (8):1216–20. doi: 10.1016/s0959-8049(97)00088-9

7. Lee SJ, Kim S, Kim M, Lee J, Park YH, Im YH, et al. Capecitabine in combination with either cisplatin or weekly paclitaxel as a first-line treatment for metastatic esophageal squamous cell carcinoma: A randomized phase ii study. *BMC Cancer* (2015) 15:693. doi: 10.1186/s12885-015-1716-9

8. Hellmann MD, Paz-Ares L, Bernabe Caro R, Zurawski B, Kim SW, Carcereny Costa E, et al. Nivolumab plus ipilimumab in advanced non-Small-Cell lung cancer. *N Engl J Med* (2019) 381(21):2020–31. doi: 10.1056/NEJMoa1910231

9. Janjigian YY, Shitara K, Moehler M, Garrido M, Salman P, Shen L, et al. First-line nivolumab plus chemotherapy versus chemotherapy alone for advanced gastric, gastro-oesophageal junction, and oesophageal adenocarcinoma (Checkmate 649): A randomised, open-label, phase 3 trial. *Lancet* (2021) 398 (10294):27–40. doi: 10.1016/s0140-6736(21)00797-2

10. Wolchok JD, Chiarion-Sileni V, Gonzalez R, Grob JJ, Rutkowski P, Lao CD, et al. Long-term outcomes with nivolumab plus ipilimumab or nivolumab alone versus ipilimumab in patients with advanced melanoma. *J Clin Oncol* (2022) 40 (2):127–37. doi: 10.1200/jco.21.02229

11. Kato K, Cho BC, Takahashi M, Okada M, Lin CY, Chin K, et al. Nivolumab versus chemotherapy in patients with advanced oesophageal squamous cell carcinoma refractory or intolerant to previous chemotherapy (Attraction-3): A multicentre, randomised, open-label, phase 3 trial. *Lancet Oncol* (2019) 20 (11):1506–17. doi: 10.1016/s1470-2045(19)30626-6

12. Doki Y, Ajani JA, Kato K, Xu J, Wyrwicz L, Motoyama S, et al. Nivolumab combination therapy in advanced esophageal squamous-cell carcinoma. *N Engl J Med* (2022) 386(5):449–62. doi: 10.1056/NEJMoa2111380

13. CSCO. *Guidelines of Chinese society of clinical Oncologhy(Csco) esophageal cancer*. Beijing: People's Medical Publishing House (2022).

14. Sullivan R, Peppercorn J, Sikora K, Zalcberg J, Meropol NJ, Amir E, et al. Delivering affordable cancer care in high-income countries. *Lancet Oncol* (2011) 12 (10):933–80. doi: 10.1016/s1470-2045(11)70141-3

15. Zhang P-F, Xie D, Li Q. Cost-effectiveness analysis of nivolumab in the second-line treatment for advanced esophageal squamous cell carcinoma. *Future Oncol* (2020) 16(17):1189–98. doi: 10.2217/fon-2019-0821

16. Husereau D, Drummond M, Augustovski F, De Bekker-Grob E, Briggs AH, Carswell C, et al. Consolidated health economic evaluation reporting standards (Cheers) 2022 explanation and elaboration: A report of the ispor cheers ii good practices task force. *Value Health* (2022) 25(1):10–31. doi: 10.1016/j.jval.2021.10.008

17. Liu G, Hu S, Wu J, Wu J. *China guidelines for pharmacoeconomic evaluations*. Beijing: China Market Press (2020) 1–8.

18. Ochalek J, Wang H, Gu Y, Lomas J, Cutler H, Jin C. Informing a cost-effectiveness threshold for health technology assessment in China: A marginal productivity approach. *Pharmacoeconomics* (2020) 38(12):1319–31. doi: 10.1007/s40273-020-00954-y

19. Cameron D, Ubels J, Norstrom F. On what basis are medical cost-effectiveness thresholds set? clashing opinions and an absence of data: A systematic review. *Glob Health Action* (2018) 11(1):1447828. doi: 10.1080/16549716.2018.1447828

20. Thokala P, Ochalek J, Leech AA, Tong T. Cost-effectiveness thresholds: The past, the present and the future. *Pharmacoeconomics* (2018) 36(5):509–22. doi: 10.1007/s40273-017-0606-1

21. Tzanetakos C, Stefanou G, Gourzoulidis G. Does a standard willingness-To-Pay threshold exist in Greece? *Value Health* (2019) 22:S772–S3. doi: 10.1016/j.jval.2019.09.1963

22. Ishak KJ, Kreif N, Benedict A, Muszbek N. Overview of parametric survival analysis for health-economic applications. *Pharmacoeconomics* (2013) 31(8):663–75. doi: 10.1007/s40273-013-0064-3

23. Latimer NR. Survival analysis for economic evaluations alongside clinical trials-extrapolation with patient-level data: Inconsistencies, limitations, and a practical guide. *Med Decis Making* (2013) 33(6):743–54. doi: 10.1177/0272989x12472398

24. Ball G, Levine M, Thabane L, Tarride J-E. Onwards and upwards: A systematic survey of economic evaluation methods in oncology. *Pharmacoecon Open* (2021) 5(3):397–410. doi: 10.1007/s41669-021-00263-w

25. Wu B, Dong B, Xu Y, Zhang Q, Shen J, Chen H, et al. Economic evaluation of first-line treatments for metastatic renal cell carcinoma: A cost-effectiveness analysis in a health resource-limited setting. *PloS One* (2012) 7(3):e32530. doi: 10.1371/journal.pone.0032530

26. Zhang Y, Zeng X, Deng H, Ma F, Peng Y, Yi L, et al. Cost-effectiveness analysis of adding palbociclib as a second-line endocrine therapy for Hr+/Her2(-) metastatic breast cancer from the us and Chinese perspectives. *Clin Ther* (2019) 41 (6):1175–85. doi: 10.1016/j.clinthera.2019.04.033

27. Zhang Q, Wu P, He X, Ding Y, Shu Y. Cost-effectiveness analysis of camrelizumab vs. placebo added to chemotherapy as first-line therapy for advanced or metastatic esophageal squamous cell carcinoma in China. *Front Oncol* (2021) 11:790373(1). doi: 10.3389/fonc.2021.790373

28. Wu B, Li T, Cai J, Xu Y, Zhao G. Cost-effectiveness analysis of adjuvant chemotherapies in patients presenting with gastric cancer after D2 gastrectomy. *BMC Cancer* (2014) 14(1):984. doi: 10.1186/1471-2407-14-984

29. Yang F, Fu Y, Kumar A, Chen M, Si L, Rojanasarot S. Cost-effectiveness analysis of camrelizumab in the second-line treatment for advanced or metastatic esophageal squamous cell carcinoma in China. *Ann Transl Med* (2021) 9(15):1226. doi: 10.21037/atm-21-1803

30. Shi G, Park SH, Ren H, Xue M, Lu X, Dong P, et al. Cost analysis for different sequential treatment regimens for metastatic renal cell carcinoma in China. *J Med Econ* (2018) 21(12):1150–8. doi: 10.1080/13696998.2018.1515769

31. Al-Batran SE, Van Cutsem E, Oh SC, Bodoky G, Shimada Y, Hironaka S, et al. Quality-Of-Life and performance status results from the phase iii rainbow study of ramucirumab plus paclitaxel versus placebo plus paclitaxel in patients with previously treated gastric or gastroesophageal junction adenocarcinoma. *Ann Oncol* (2016) 27(4):673–9. doi: 10.1093/annonc/mdv625

32. Wilke H, Muro K, Van Cutsem E, Oh S-C, Bodoky G, Shimada Y, et al. Ramucirumab plus paclitaxel versus placebo plus paclitaxel in patients with previously treated advanced gastric or gastro-oesophageal junction adenocarcinoma (Rainbow): A double-blind, randomised phase 3 trial. *Lancet Oncol* (2014) 15(11):1224–35. doi: 10.1016/s1470-2045(14)70420-6

33. Nafees B, Lloyd AJ, Dewilde S, Rajan N, Lorenzo M. Health state utilities in non-small cell lung cancer: An international study. *Asia Pac J Clin Oncol* (2017) 13 (5):E195–203. doi: 10.1111/ajco.12477

34. Lloyd A, Nafees B, Narewska J, Dewilde S, Watkins J. Health state utilities for metastatic breast cancer. *Br J Cancer* (2006) 95(6):683–90. doi: 10.1038/sj.bjc.6603326

35. Cai H, Xu B, Li N, Zheng B, Zheng Z, Liu M. Cost-effectiveness analysis of camrelizumab versus chemotherapy as second-line treatment of advanced or metastatic esophageal squamous cell carcinoma. *Front Pharmacol* (2021) 12:732912(1) (2021) in press. doi: 10.3389/fphar.2021.732912

36. Huang C, Ung COL, Wushouer H, Bai L, Li XY, Guan XD, et al. Trends of negotiated targeted anticancer medicines use in China: An interrupted time series analysis. *Int J Health Policy Manage*. doi: 10.34172/ijhpm.2021.47

37. Li H, Liu GG, Wu J, Wu J-H, Dong C-H, Hu S-L. Recent pricing negotiations on innovative medicines pilot in China: Experiences, implications, and suggestions. *Value Health Reg Issues* (2018) 15(1):133–7. doi: 10.1016/j.vhri.2018.01.009

38. Kudo T, Hamamoto Y, Kato K, Ura T, Kojima T, Tsushima T, et al. Nivolumab treatment for oesophageal squamous-cell carcinoma: An open-label, multicentre, phase 2 trial. *Lancet Oncol* (2017) 18(5):631–9. doi: 10.1016/s1470-2045(17)30181-x

39. Luo HY, Lu J, Bai YX, Mao T, Wang J, Fan QX, et al. Effect of camrelizumab vs placebo added to chemotherapy on survival and progression-free survival in patients with advanced or metastatic esophageal squamous cell carcinoma: The escort-1st randomized clinical trial. *JAMA* (2021) 326(10):916–25. doi: 10.1001/jama.2021.12836

40. Wu Q, Qin Y, Liao W, Zhang M, Yang Y, Zhang P, et al. Cost-effectiveness of enfortumab vedotin in previously treated advanced urothelial carcinoma. *Ther Adv Med Oncol* (2022) 14(1):17588359211068733. doi: 10.1177/17588359211068733

41. Steffen A, Huerta JM, Weiderpass E, Bueno-de-Mesquita HB, May AM, Siersema PD, et al. General and abdominal obesity and risk of esophageal and

gastric adenocarcinoma in the European prospective investigation into cancer and nutrition. *Int J Cancer* (2015) 137(3):646–57. doi: 10.1002/ijc.29432

42. Cho JH, Shin CM, Han KD, Yoon H, Park YS, Kim N, et al. Abdominal obesity increases risk for esophageal cancer: A nationwide population-based cohort study of south Korea. *J Gastroenterol* (2020) 55(3):307–16. doi: 10.1007/s00535-019-01648-9

43. Li H. Cancer precision medicine in China. *Genomics Proteomics Bioinf* (2016) 14(5):325–8. doi: 10.1016/j.gpb.2016.10.002

44. Liu Q, Zeng H, Xia R, Chen G, Liu S, Zhang Z, et al. Health-related quality of life of esophageal cancer patients in daily life after treatment: A multicenter cross-sectional study in China. *Cancer Med* (2018) 7(11):5803–11. doi: 10.1002/cam4.1817

45. Wang H, Pan Y, Guo C, Li F, Xu R, Liu M, et al. Health-related quality of life among rural residents aged 45-69 years in hua county, henan province, China: Results of esecc trial for esophageal cancer screening with endoscopy. *Chin J Cancer Res* (2018) 30(2):240–53. doi: 10.21147/j.issn.1000-9604.2018.02.07

frontiers | Frontiers in Oncology

TYPE Systematic Review
PUBLISHED 13 October 2022
DOI 10.3389/fonc.2022.963091

Check for updates

OPEN ACCESS

EDITED BY
Chiara Bazzichetto,
Regina Elena National Cancer Institute (IRCCS), Italy

REVIEWED BY
Baoguang Hu,
Binzhou Medical University Hospital, China
Kai Cui,
Shandong Cancer Hospital, Shandong University, China

*CORRESPONDENCE
Jing Yang
21634604@qq.com

SPECIALTY SECTION
This article was submitted to Gastrointestinal Cancers: Gastric and Esophageal Cancers, a section of the journal Frontiers in Oncology

RECEIVED 07 June 2022
ACCEPTED 29 August 2022
PUBLISHED 13 October 2022

CITATION
Li Z, Song M, Han S, Jin C and Yang J (2022) The prognostic role of circulating tumor cells in gastric cancer: A meta-analysis. *Front. Oncol.* 12:963091. doi: 10.3389/fonc.2022.963091

COPYRIGHT
© 2022 Li, Song, Han, Jin and Yang. This is an open-access article distributed under the terms of the Creative Commons Attribution License (CC BY). The use, distribution or reproduction in other forums is permitted, provided the original author(s) and the copyright owner(s) are credited and that the original publication in this journal is cited, in accordance with accepted academic practice. No use, distribution or reproduction is permitted which does not comply with these terms.

The prognostic role of circulating tumor cells in gastric cancer: A meta-analysis

Zuxi Li[1,2,3], Meijuan Song[1,2,3], Shangjun Han[1,2,3], Chuanwei Jin[1,2,3] and Jing Yang[1,2,3]*

[1]The First Clinical School of Gansu University of Chinese Medicine, Lanzhou, China, [2]General Surgery Clinical Medical Center, Gansu Provincial Hospital, Lanzhou, China, [3]Gansu Provincial Key Laboratory of Molecular Diagnosis and Precision Therapy of Surgical Tumors, Gansu Provincial Hospital, Lanzhou, China

Objective: We conducted a meta-analysis to evaluate the relationship between circulating tumor cells (CTC) and the prognosis of patients with gastric cancer.

Materials and methods: The cohort studies reporting on the relationship between CTC and prognosis of gastric cancer were collected from Pubmed, Cochrane, Embase, CNKI, WanFang Data, and VIP databases. The two researchers independently screened the literature, extracted the data, and evaluated the bias risk of the included literature. The data were analyzed by Revman software (Review Manager version 5.4).

Result: A total of 14 retrospective cohort studies with 1053 patients were included. The results showed that the overall survival time (OS) and progression-free survival time (PFS) of CTC-positive patients were shorter compared to CTC-negative patients. Taking into consideration the critical value of CTC positive patients, country of origin, sample size, treatment mode, and study time, the subgroup analysis showed that CTC-positive was related to the shortening of OS in patients with gastric cancer. Based on the subgroup analysis of the factors such as CTC positive critical value < 2.8, sample size ≥ 75, mixed therapy, longer study duration, country, and immunofluorescence detection of CTC, it was found that OS in CTC positive group was shorter than that in CTC-negative group (all $P<0.05$), while the critical value of positive CTC ≥ 2.8, sample size ≥ 75, choice of treatment only for operation or non-operation, short study time and molecular detection of CTC were not associated with OS (all $P>0.05$). In addition, CTC-positive patients had a more advanced TNM staging, poorer tumor differentiation, and earlier distant metastasis.

Conclusion: CTC can be used as a prognostic indicator of gastric cancer. Gastric cancer patients with positive CTC may have a poorer prognosis compared to those with CTC-negative tumors.

Systematic Review Registration: https://www.crd.york.ac.uk/PROSPERO/, identifier CRD42022323155.

KEYWORDS

gastric cancer, circulating tumor cell, CTC, prognosis, meta-analysis

Introduction

Gastric cancer is one of the most common malignant tumors (1) and the second deadliest tumor worldwide (2). Smoking tobacco, age over 60, *Helicobacter pylori* infection, alcohol consumption, and obesity are the main causes leading to a gastric tumor (3). Surgery is the most effective treatment, yet patients present with an advanced stage at the time of diagnosis, losing their chance to undergo surgical resection (4). Chemotherapy and immunotherapy are the most common treatment methods for advanced-stage gastric tumors (5). Still, most gastric patients develop metastasis after therapy and have a poor prognosis.

In recent years, with the development of liquid biopsy technology, several new biomarkers have been discovered for accurately predicting the prognosis of gastric cancer and effectively evaluating the efficacy of chemotherapy for gastric cancer. For example, circulating tumor cells (CTC), i.e., tumor cells that detach from the primary or metastatic focus of the tumor and enter the blood, have recently attracted interest as biomarkers of cancer metastases (6–9). At present, existing studies have shown that CTC has an important role in the diagnosis of early gastric cancer (10), the guidance of chemotherapy, and analysis of chemotherapy efficacy (11–15), chemotherapy resistance (16), and prognosis (17, 18). Clinically, CTC has incomparable potential value in evaluating the prognosis of tumors. Given the important value of CTC in evaluating the prognosis of malignant tumors, we performed a meta-analysis in order to determine the relationship between baseline CTC and the prognosis of patients with gastric cancer and objectively evaluate its prognostic value in gastric cancer.

Materials and methods

Retrieval strategy

Six electronic databases were explored: Pubmed, Cochrane, Embase, CNKI, WanFang Data, and VIP. The cohort studies reporting on the relationship between CTC and prognosis of gastric cancer were collected from the establishment of the database to December 26, 2021. The following key words were used (Pubmed database): Neoplasm Circulating Cells, Neoplasm Circulating Cell, Circulating Neoplastic Cells, Circulating Neoplastic Cell, Circulating Tumor Cells, Circulating Tumor Cell, Embolic Tumor Cell, Embolic Tumor Cells, Tumor Embolism, Tmor Embolisms, CTC, Stomach Neoplasms, Stomach Neoplasm, Gastric Neoplasms, Gastric Neoplasm, Cancer of Stomach, Stomach Cancers, Gastric Cancer, Gastric Cancers, Stomach Cancer, Cancer of the Stomach, Prognosis, Prognoses, Prognostic Factors, Prognostic Factor. Chinese keywords include: circulating tumor cells, CTC, gastric cancer, and prognosis. This study has been registered on PROSPERO platform (Registration number: CRD42022323155).

Inclusion and exclusion criteria

Inclusion criteria for research literature were (1): studies evaluating the relationship between CTC expression and prognosis of gastric cancer (2); dividing patients into high expression group and low expression group of CTC (3); describing effective prognostic indicators (OS, DFS, RFS, and PFS) or related clinicopathological parameters (tumor size, differentiation, depth of infiltration, lymph node metastasis, distant metastasis, and tumor stage) (4); enough data to calculate the hazard ratio (HR) or odds ratio (OR) and 95% confidence interval (95%CI) (5); patients did not receive any treatment at baseline (6); blood was collected and CTC were tested before treatment.

Exclusion criteria were (1): case reports, conference summaries, reviews, editorials, and non-human studies (2); repeated publication (3); lack of HR or Tumor and its 95%CI, or unable to estimate these parameters.

Literature screening and data extraction

Two researchers (ZL and MS) independently reviewed and analyzed the title and abstract of the study, screened the search results, and evaluated the full text of the research literature that met the inclusion criteria. All differences were resolved through group discussion or by inviting a third researcher (JY). Two researchers (ZL and MS) independently extracted the following data from each

study: title, first author, year of publication, study time, country, sample size, sex, treatment, follow-up time, CTC positive threshold, outcome indicators, and outcome measurements.

Evaluation of research quality

The included study was independently assessed for bias risk according to the Newcastle-Ottawa quantity (NOS). A study with a score of 6 or more was defined as a high-quality study (19).

Statistical analysis

Revman software (Review Manager version 5.4) was used for statistical analysis, and Stata software (Stata12.0 version) was used for sensitivity analysis and publication bias. In order to evaluate the effect of CTC on the prognosis of gastric cancer, the standard errors of risk ratio (HR), OS, or PFS were extracted from the included literature. HR > 1 indicates that the prognosis of the positive group is worse than that of the negative group. The inverse variance method was used to combine HRs in the Revman software. Considering the heterogeneity between studies, the literature heterogeneity was judged by I^2 statistics and the Q test. When $P < 0.1$ or $I^2 > 50\%$, the heterogeneity was significant, and the random effect model was used for meta-analysis; on the contrary, the fixed effect model was used for meta-analysis (20). Publication bias was tested by the Beg method and the Egger method (test level $\alpha = 0.05$) (21).

Results

Data screening process and results

A total of 758 original studies were retrieved in the preliminary screening, 515 articles were obtained after deduplication, those that did not meet the inclusion criteria were excluded, and the full text was excluded after reading and evaluation. Finally, 14 retrospective cohort studies were included in the analysis (Figure 1).

Basic characteristics of the included study

A total of 14 retrospective cohort studies were included (22–35), including 1053 patients. These studies were published from 2007 to 2021 (3 articles (23, 29, 35) were published in 2021). Six studies (23, 25, 26, 32, 34, 35) were conducted in China; others were carried out in Poland (22), Brazil (24), Germany (28), South Korea (29), Japan (27, 30, 31, 33) and other countries. Ten studies (22, 23, 26, 27, 29, 30, 32–35) reported the relationship between CTC and OS in gastric cancer patients, 3 (25, 28, 31) reported the relationship between CTC and OS or PFS in patients with gastric cancer, and 1 study (24) reported the relationship between CTC and PFS in patients with gastric cancer. The critical value of CTC positive was between 1 and 7.5. The NOS scores of the included studies were all above 6, indicating that the quality of the included studies was high (Table 1).

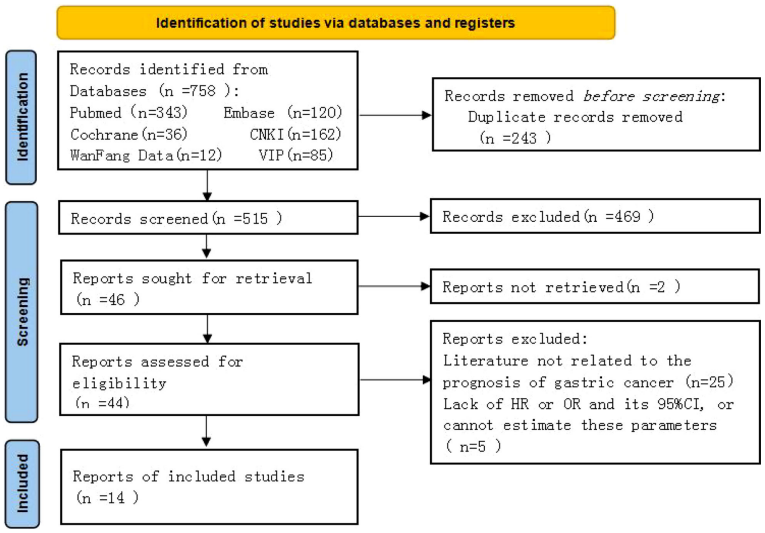

FIGURE 1
Literature screening process and results.

TABLE 1 Basic characteristics of the included study.

Included in the study	Research time (year)	Country	Sample size (n)	Male/ female (n)	Mode of treatment	Follow-up time (months)	CTC detection method	Critical value of CTC positive	Outcome index	TNM staging	NOS score
Anna Pituch-Noworolska 2007	1997-1999	Poland	57	44/13	Operation	60	Immunofluorescence	3	OS	I-IV	8
Chengcheng Qian 2021	2016-2020	China	72	49/23	Mixed therapy	50	Immunofluorescence	1	OS	I-IV	8
Emne A.Abdallah 2019	2016-2017	Brazil	55	33/22	Mixed therapy	15	Immunofluorescence	2.8	PFS	I-IV	7
Huang Wei2019	2016-2017	China	28	16/12	Non-Operation	11	Immunofluorescence	4	OS、PFS	III-IV	7
Han Hongbing2015	2011-2013	China	60	36/24	Operation	18	Immunofluorescence	1	OS	I-IV	8
Hiroaki Ito 2016	2010-2011	Japan	65	46/19	Operation	60	Immunofluorescence	5	OS	I-IV	8
Ilja Kubisch 2015	2010-2011	Germany	62	39/23	Non-Operation	17	Molecular detection	1	OS、PFS	–	8
Joon Hyung Jhi 2021	2017-2018	South Korea	31	22/9	Non-Operation	12	Immunofluorescence	7.5	OS	–	7
Kunihiko Hiraiwa 2008	–	Japan	27	–	Mixed therapy	–	Immunofluorescence	2	OS	I-III	7
Okabe, H 2015	2008-2013	Japan	136	87/49	Mixed therapy	26	Immunofluorescence	1	OS、PFS	I-III	8
Qiyue Zhang 2018	2013-2014	China	93	68/25	Operation	36	Immunofluorescence	5	OS	I-III	8
Yoshikazu Uenosono 2013	2005-2012	Japan	148	99/49	Operation	60	Immunofluorescence	1	OS	I-IV	8
Yang Han2020	2014-2017	China	103	74/29	Mixed therapy	16.3	Immunofluorescence	2	OS	I-IV	7
Yinxing Zhu 2021	2015-2018	China	116	89/27	Mixed therapy	14.5	Molecular detection	3	OS	I-IV	7

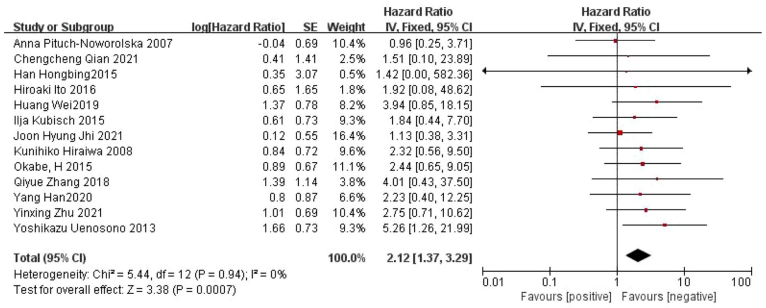

FIGURE 2
Meta-analysis of the relationship between CTC and OS.

Meta-analysis results

Relationship between CTC and OS in patients with gastric cancer

A total of 13 articles (22, 23, 25–35) reported on the relationship between CTC and OS in patients with gastric cancer. There was no heterogeneity between the studies (I^2 =0%, P=0.94), and a fixed effect model was used. Meta-analysis showed that the OS was shorter in CTC-positive patients than in CTC-negative patients (*HR*=2.12, 95% *CI*= [1.37, 3.29], *P*=0.0007) (Figure 2).

Relationship between CTC and PFS in patients with gastric cancer

A total of 4 articles (24, 25, 28, 31) reported on the relationship between CTC and PFS in patients with gastric cancer. There was no heterogeneity between the studies (I^2 =0%, P=0.95), and a fixed effect model was used. Meta-analysis showed that the PFS was shorter in CTC-positive patients than in CTC-negative patients *(HR*=2.54, 95% *CI*= [1.14, 5.63], *P*=0.02) (Figure 3).

Subgroup analysis

In order to further analyze the prognostic effect of CTC on patients with gastric cancer, this study conducted a subgroup analysis taking into consideration the critical value, country, sample size, treatment mode, and research time of CTC positive. Subgroup analysis showed that when the critical value of CTC positive was < 2.8, the OS of the CTC positive group was shorter than that of a CTC-negative group; when the critical value of CTC was ≥ 2.8, there was no significant relationship between CTC and OS (all P<0.05). In addition, when the sample size was ≥ 75, the OS of the CTC-positive group was shorter than that of the CTC-negative group (P<0.05); when the sample size was < 75, there was no significant relationship between CTC and OS (P>0.05).

When the gastric cancer patients were treated with mixed therapy, the OS of the CTC-positive group was shorter than that of the CTC-negative group. When surgery or a non-operative approach was used, the relationship between CTC and OS was not statistically significant (P>0.05). The positive rate of CTC was associated with shorter OS in longer study time (P<0.05). When the study time was short, the relationship between CTC and OS was not statistically significant (P>0.05).

In the subgroup analysis of national factors, it was found that CTC positive was associated with shorter OS. By performing a subgroup analysis of CTC assays, it was found that by applying immunofluorescence assays, CTC positivity was associated with a shorter OS (Table 2).

Relationship between CTC and clinicopathological features of patients with gastric cancer

This study explored the relationship between CTC and clinicopathological features of gastric cancer patients from the aspects of age, sex, TNM stage, tumor differentiation, distant metastasis, Lauren classification, and CEA (Table 3). The heterogeneity of each study was small. The results of the meta-analysis showed that the CTC-positive patients had a higher TNM stage (*OR*=3.50, 95% *CI*=[2.21,5.54], *P*<0.00001), poorer tumor differentiation (*OR*=2.49, 95% *CI*=[1.54,4.03], *P*=0.0002), and earlier distant metastasis (*OR*=2.03, 95% *CI*=[1.36,3.04], *P*=0.0006); while the positive rate of CTC was not related to age, sex, Lauren classification and CEA (P>0.05).

Sensitivity analysis

Single studies were excluded one by one for sensitivity analysis. The results showed that the results of a meta-analysis analyzing the relationship between CTC and OS or PFS were stable (OS: *HR*= 0.67- 0.86; PFS: *HR*=0.93- 1.10) (Figure 4).

Publication bias

The publication bias of the relationship between CTC and OS was evaluated by the Begg test (*Z*=0.34, *P*=0.732) and Egger test (*t*=0.75, *P*=0.468). The publication bias of the relationship between CTC and PFS was analyzed by Begg test (*Z* =-0.24, *P* = 1.000) and Egger test (*t* = 0.33, *P* = 0.762). The results showed less possibility of publication bias in the included study (Figure 5).

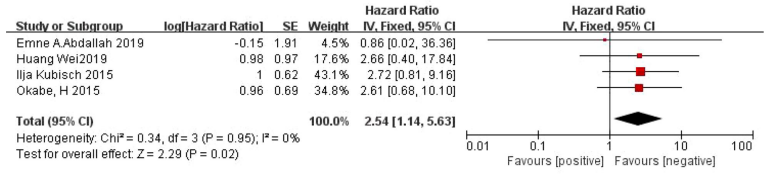

FIGURE 3
Meta-analysis of the relationship between CTC and PFS.

TABLE 2 Subgroup analysis of the relationship between CTC and OS in patients with gastric cancer.

Subgroup analysis	Research number (n)	Sample size (n)	Model	*HR* (95% *CI*)	*P*	Heterogeneity	
						I^2 (%)	P_h
Critical value of CTC positive							
≥2.8	7	445	Fixed effect model	1.76 (0.96~3.21)	0.07	0	0.73
<2.8	7	608	Fixed effect model	2.54 (1.36~4.74)	0.003	0	0.97
Country							
China	6	472	Fixed effect model	2.85 (1.32~6.16)	0.008	0	0.99
Other	8	581	Fixed effect model	1.82 (1.08~3.08)	0.03	0	0.76
Sample size							
≥75	5	596	Fixed effect model	3.09 (1.56~6.09)	0.001	0	0.93
<75	9	457	Fixed effect model	1.61 (0.92~2.83)	0.10	0	0.95
Mode of treatment							
Operation	5	423	Fixed effect model	2.31 (0.98~5.45)	0.06	0	0.53
Non-operation	3	121	Fixed effect model	1.74 (0.82~3.69)	0.15	0	0.42
Mixed therapy	6	509	Fixed effect model	2.30 (1.17~4.52)	0.02	0	0.99
Research time							
≥2.5 year	5	575	Fixed effect model	2.88 (1.44~5.74)	0.003	0	0.90
<2.5 year	8	451	Fixed effect model	1.62 (0.88~2.96)	0.12	0	0.88
CTC detection method							
Immunofluorescence	12	875	Fixed effect model	2.06 (1.27~3.34)	0.003	0	0.91
Molecular detection	2	178	Fixed effect model	2.27 (0.85~6.07)	0.1	0	0.69

Discussion

As a new prognostic marker, CTC has the biological characteristics of the primary tumor and strong invasive ability (7). The release of CTCs from the tumor into the circulating blood occurs through the epithelial-mesenchymal transition (EMT) and non-EMT-mediated invasion (36). As a non-invasive and simple "fluid biopsy" technique, CTC detection is a simple procedure (37). Herein, we conducted a meta-analysis to evaluate the relationship between circulating tumor cells (CTC) and the prognosis of patients with gastric cancer. This study included the original studies from Chinese and English databases, including South Korea, Japan, China, and other Asian countries with a high incidence of gastric cancer, in order to improve the scientific and reliable conclusion of the relationship between CTC and the prognosis of patients with gastric cancer. Fourteen retrospective cohort studies with 1053 patients were included to explore the prognostic role of CTC in gastric cancer. The results showed that the positive rate of CTC was associated with shorter OS and PFS. CTC are tumor cells that detach from the primary or metastatic focus of the tumor and enter the blood (38). In recent years, CTC has been used as an important prognostic marker for many solid tumors, including lung cancer (39), breast cancer (40), prostate cancer (41), nasopharyngeal cancer (42), rectal cancer (43), and so on. CTC detection can effectively make up for the deficiency of imaging, serum markers, and tissue samples in the evaluation of the prognosis of patients with gastric cancer, providing qualitative, specific, and dynamic evaluation, and avoiding temporal and spatial heterogeneity of tumors. CTC can be

TABLE 3 Relationship between CTC and clinicopathological features of patients with gastric cancer.

Pathological features	Research number (*n*)	Sample size (*n*)	Model	*OR* (95% *CI*)	*P*	Heterogeneity	
						I^2 (%)	P_h
Age (high vs. low)	7	548	Fixed effect model	1.02 [0.67,1.55]	0.92	0	0.55
Gender (male vs. female)	9	741	Fixed effect model	1.20 [0.82,1.78]	0.35	0	1
TNM (III-IV vs. I-II)	7	684	Fixed effect model	3.50 [2.21,5.54]	<0.00001	49	0.07
Differentiation (poor vs. good)	6	517	Fixed effect model	2.49 [1.54,4.03]	0.0002	0	0.85
Distant metastasis (yes vs. no)	9	741	Fixed effect model	2.03 [1.36,3.04]	0.0006	17	0.29
Lauren (diffuse vs. no-diffuse)	4	317	Fixed effect model	1.53 [0.82,2.85]	0.18	45	0.14
CEA(high expression vs. low expression)	4	375	Fixed effect model	1.54 [0.89,2.66]	0.12	0	0.48

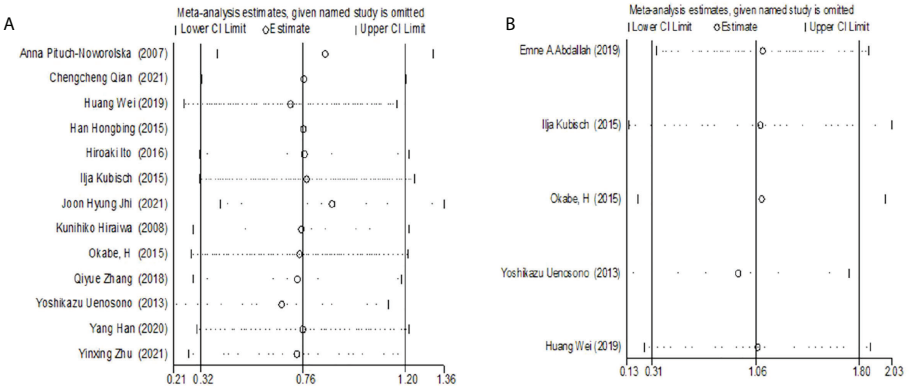

FIGURE 4
(A) Sensitivity Analysis of the relationship between CTC and OS. **(B)** Sensitivity analysis of the relationship between CTC and PFS.

directly detected through blood samples, which is helpful for clinicians to systematically and effectively evaluate the progression of tumors so as to provide scientific and reasonable treatment.

In this study, subgroup analysis indicated that critical value of CTC positive < 2.8, sample size ≥ 75, mixed therapy, long study time, and using immunofluorescence assay were associated with shorter OS in CTC-positive patients. However, the critical value of positive CTC ≥ 2.8, sample size < 75, simple surgical or non-operative treatment, short research time, and molecular detection method had no significant relationship with OS. This may be the reason why the small sample size and short research time could not reveal the real results, but it also shows that mixed treatment is the best choice for patients with gastric cancer.

After analyzing the subgroups of different countries, it was found that the positive rate of CTC was related to the shorter OS. There was no heterogeneity in the whole subgroup analysis (I^2 = 0%), ensuring the reliability of the research results. In addition, this study also explored the relationship between CTC and clinicopathological features of gastric cancer patients. CTC-positive patients had an advanced TNM stage, poorer tumor differentiation, and were more prone to distant metastasis than those with CTC-negative patients. These clinical parameters, which are closely related to the progression of malignant tumors, are correlated with CTC, which proves that the positive expression of CTC is an important index for evaluating the prognosis of patients with gastric cancer, which also indicates that the change of CTC in the process of tumor development may be the key factor causing tumor recurrence and metastasis, which is consistent with previous study (44).

This study has some limitations. First, only a few literature and retrospective cohort studies were included; also, there is a lack of data support for large samples of randomized controlled trials. At present, there is no unified positive standard of CTC in gastric cancer, which may lead to bias. In subgroup analysis, all heterogeneities could not be explored. Because only the baseline CTC count was collected in the included studies, the

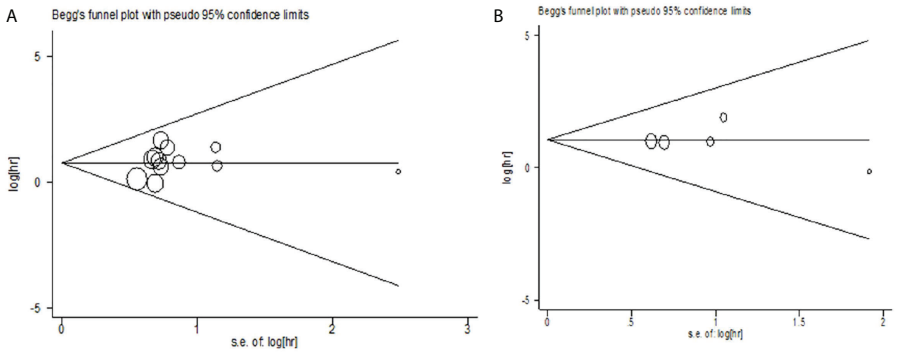

FIGURE 5
(A) The relationship between CTC and OS. **(B)** The relationship between CTC and PFS.

changes in CTC after an intervention such as surgery and chemotherapy were not analyzed, and it was impossible to evaluate the effect of treatment intervention on the prognosis of patients with gastric cancer. In their large sample size meta-analysis, Zou *et al.* (45) found that high CTC counts before and during chemotherapy were significantly correlated with poor OS, PFS, and disease control rates (DC) in patients with advanced gastric cancer. Moreover, Yue *et al.* (46) found that the dynamic changes in CTC and prognosis were also affected by the study of the relationship between gastrointestinal tumors and CTC.

Conclusion

The existing evidence shows that CTC can be used as an effective index to evaluate the prognosis of gastric cancer. However, due to the research quantity and quality limitation, larger, high-quality studies are needed to further verify the above conclusions.

Data availability statement

The original contributions presented in the study are included in the article/supplementary material. Further inquiries can be directed to the corresponding author.

Author contributions

JY contributed to study design. ZL were responsible for literature search, data extraction and analysis and wrote the manuscript. MS, CJ and SH contributed to study selection. All authors contributed to the article and approved the submitted version.

Funding

Natural Science Foundation of Gansu provincial (No. 21JR1RA017); Natural Science Foundation of Gansu provincial hospital (No. 21GSSYB-5).

Conflict of interest

The authors declare that the research was conducted in the absence of any commercial or financial relationships that could be construed as a potential conflict of interest.

Publisher's note

All claims expressed in this article are solely those of the authors and do not necessarily represent those of their affiliated organizations, or those of the publisher, the editors and the reviewers. Any product that may be evaluated in this article, or claim that may be made by its manufacturer, is not guaranteed or endorsed by the publisher.

References

1. Smyth EC, Lordick F, Nilsson M, Grabsch HI, van Grieken NCT, Lordick F. Gastric cancer. *Lancet* (2020) 396(10251):635–48. doi: 10.1016/S0140-6736(20)31288-5

2. Ang TL, Fock KM. Clinical epidemiology of gastric cancer. *Singapore Med J* (2014) 55(12):621. doi: 10.11622/smedj.2014174

3. Yuxia Y, Lili M, Yan G, Jufang B, Youhua Z, Lingling Q, et al. The relationship between hp infection and the expression of MUC2, MUC5AC, MUC6 and CD10 in gastric cancer and precancerous lesions. *Chin J Hosp infect* (2022) (05):721–5. doi: 10.11816/cn.ni.2022-210601

4. Leja M, Linē A. Early detection of gastric cancer beyond endoscopy-new methods. *Best Pract Res Clin Gastroenterol* (2021) 50:101731. doi: 10.1016/j.bpg.2021.101731

5. Machlowska J, Baj J, Sitarz M, Maciejewski R, Sitarz R. Gastric cancer: epidemiology, risk factors, classification, genomic characteristics and treatment strategies. *Int J Mol Sci* (2020) 21(11):4012. doi: 10.3390/ijms21114012

6. Vasseur A, Kiavue N, Bidard FC, Pierga JY, Cabel L. Clinical utility of circulating tumor cells: An update. *Mol Oncol* (2021) 15(6):1647–66. doi: 10.1002/1878-0261.12869

7. Micalizzi DS, Maheswaran S, Haber DA. A conduit to metastasis: Circulating tumor cell biology. *Genes Dev* (2017) 31(18):1827–40. doi: 10.1101/gad.305805.117

8. Schuster E, Taftaf R, Reduzzi C, Albert MK, Romero-Calvo I, Liu H. Better together: Circulating tumor cell clustering in metastatic cancer. *Trends cancer.* (2021) 7(11):1020–32. doi: 10.1016/j.trecan.2021.07.001

9. Francart ME, Lambert J, Vanwynsberghe AM, Thompson EW, Bourcy M, Polette M, et al. Epithelial–mesenchymal plasticity and circulating tumor cells: travel companions to metastases. *Dev Dynamics.* (2018) 247(3):432–50. doi: 10.1002/dvdy.24506

10. Lee M, Kim G, Jeon H, Park S. Clinical application of circulating tumor cells in gastric cancer. *Gut liver.* (2019) 13(4):394–401. doi: 10.5009/gnl18484

11. Franses JW, Philipp J, Missios P, Bhan I, Liu A, Yashaswini C, et al. Pancreatic circulating tumor cell profiling identifies LIN28B as a metastasis driver and drug target. *Nat Commun* (2020) 11(1):1–12. doi: 10.1038/s41467-020-17150-3

12. Gorges TM, Pantel K. Circulating tumor cells as therapy-related biomarkers in cancer patients. *Cancer Immunol Immunother* (2013) 62(5):931–9. doi: 10.1007/s00262-012-1387-1

13. Bidard F-C, Jacot W, Kiavue N, Dureau S, Kadi A, Brain E, et al. Efficacy of circulating tumor cell count–driven vs clinician-driven first-line therapy choice in hormone receptor–positive, ERBB2-negative metastatic breast cancer: The STIC CTC randomized clinical trial. *JAMA Oncol* (2021) 7(1):34–41. doi: 10.1001/jamaoncol.2020.5660

14. Chen Y, Zhu M, Shen J, He W, Qiu L, Xu R. Chemosensitivity evaluation using circulating tumor cells predicts chemotherapy outcomes in patients with advanced cancer. *Clin Lab* (2022) 68(1):10.7754/Clin.Lab.2021.210218. doi: 10.7754/Clin.Lab.2021.210218

15. Zhao Y, Han L, Zhang W, Shan L, Wang Y, Song P, et al. Preoperative chemotherapy compared with postoperative adjuvant chemotherapy for squamous cell carcinoma of the thoracic oesophagus with the detection of circulating tumour cells randomized controlled trial. *Int J Surg* (2020) 73:1–8. doi: 10.1016/j.ijsu.2019.11.005

16. Labib M, Kelley SO. Circulating tumor cell profiling for precision oncology. *Mol Oncol* (2021) 15(6):1622–46. doi: 10.1002/1878-0261.12901

17. Nanduri LK, Hissa B, Weitz J, Schoelch S, Bork U. The prognostic role of circulating tumor cells in colorectal cancer. *Expert Rev Anticancer Ther* (2019) 19 (12):1077–88. doi: 10.1080/14737140.2019.1699065

18. Liang D, Hall C, Lucci A. Circulating tumor cells in breast cancer. *Recent results Cancer Res Fortschr der Krebsforschung Progres dans les recherches sur le cancer.* (2020) 215:127–45. doi: 10.1007/978-3-030-26439-0_7

19. Stang A. Critical evaluation of the Newcastle-Ottawa scale for the assessment of the quality of nonrandomized studies in meta-analyses. *Eur J Epidemiol* (2010) 25(9):603–5. doi: 10.1007/s10654-010-9491-z

20. Barili F, Parolari A, Kappetein PA, Freemantle N. Statistical primer: heterogeneity, random-or fixed-effects model analyses? *Interact Cardiovasc Thorac Surg* (2018) 27(3):317–21. doi: 10.1093/icvts/ivy163

21. Herrmann D, Sinnett P, Holmes J, Khan S, Koller C, Vassar M. Statistical controversies in clinical research: Publication bias evaluations are not routinely conducted in clinical oncology systematic reviews. *Ann Oncol* (2017) 28(5):931–7. doi: 10.1093/annonc/mdw691

22. Pituch-Noworolska A, Kolodziejczyk P, Kulig J, Drabik G, Szczepanik A, Czupryna A, et al. Circulating tumour cells and survival of patients with gastric cancer. *Anticancer Res* (2007) 27(1B):635–40.

23. Qian C, Cai R, Zhang W, Wang J, Hu X, Zhang Y, et al. Neutrophil-lymphocyte ratio and circulating tumor cells counts predict prognosis in gastrointestinal cancer patients. *Front Oncol* (2021) 11. doi: 10.3389/fonc.2021.710704

24. Abdallah EA, Braun AC, Flores BC, Senda L, Urvanegia AC, Calsavara V, et al. The potential clinical implications of circulating tumor cells and circulating tumor microemboli in gastric cancer. *oncol* (2019) 24(9):e854–e63. doi: 10.1634/theoncologist.2018-0741

25. Huang W, Xuan Q, Wu Y, Liu D, Xue J. Study on the relationship between peripheral circulating tumor cells and blood hypercoagulable state and prognosis in advanced gastric cancer. *J Oncol* (2019) 25(08):691–7 .doi: 10.11735/j.issn.1671-170X.2019.08.B003

26. Han H, Li Z, Liu S, Dong S. Detection of circulating tumor cells in peripheral blood of patients with gastric cancer and its clinical significance. *Chin J basic Clin Gen Surg* (2015) 22(07):840–3. doi: 10.7507/1007-9424.20150217

27. Ito H, Sato J, Tsujino Y, Yamaguchi N, Kimura S, Gohda K, et al. Long-term prognostic impact of circulating tumour cells in gastric cancer patients. *World J gastroenterol* (2016) 22(46):10232. doi: 10.3748/wjg.v22.i46.10232

28. Kubisch I, de Albuquerque A, Schuppan D, Kaul S, Schaich M, Stölzel U. Prognostic role of a multimarker analysis of circulating tumor cells in advanced gastric and gastroesophageal adenocarcinomas. *Oncology* (2015) 89(5):294–303. doi: 10.1159/000437373

29. Jhi JH, Kim GH, Park SJ, Kim DU, Lee MW, Lee BE, et al. Circulating tumor cells and TWIST expression in patients with metastatic gastric cancer: A preliminary study. *J Clin Med* (2021) 10(19):4481. doi: 10.3390/jcm10194481

30. Hiraiwa K, Takeuchi H, Hasegawa H, Saikawa Y, Suda K, Ando T, et al. Clinical significance of circulating tumor cells in blood from patients with gastrointestinal cancers. *Ann Surg Oncol* (2008) 15(11):3092–100. doi: 10.1245/s10434-008-0122-9

31. Okabe H, Tsunoda S, Hosogi H, Hisamori S, Tanaka E, Tanaka S, et al. Circulating tumor cells as an independent predictor of survival in advanced gastric cancer. *Ann Surg Oncol* (2015) 22(12):3954–61. doi: 10.1245/s10434-015-4483-6

32. Zhang Q, Shan F, Li Z, Gao J, Li Y, Shen L, et al. A prospective study on the changes and clinical significance of pre-operative and post-operative circulating tumor cells in resectable gastric cancer. *J Trans Med* (2018) 16(1):1–12. doi: 10.1186/s12967-018-1544-1

33. Uenosono Y, Arigami T, Kozono T, Yanagita S, Hagihara T, Haraguchi N, et al. Clinical significance of circulating tumor cells in peripheral blood from patients with gastric cancer. *Cancer* (2013) 119(22):3984–91. doi: 10.1002/cncr.28309

34. Han Y, Yizhang C, Xiaowen C, Nan C, Cuiju T. Study on circulating tumor cells, blood coagulation and prognosis in patients with gastric cancer. *J Pract Cancer* (2020) 35(04):615–9. doi: 10.3969 /j.issn.1001-5930.2020.04.025

35. Zhu Y, Chen N, Chen M, Cui X, Yang H, Zhu X, et al. Circulating tumor cells: A surrogate to predict the effect of treatment and overall survival in gastric adenocarcinoma. *Int J Biol Markers* (2021) 36(1):28–35. doi: 10.1177/1724600820981972

36. Chiang SP, Cabrera RM, Segall JE. Tumor cell intravasation. *Am J Physiol-Cell Physiol* (2016) 311(1):C1–C14. doi: 10.1152/ajpcell.00238.2015

37. Jacot W, Mazel M, Mollevi C, Pouderoux S, D'Hondt V, Cayrefourcq L, et al. Clinical correlations of programmed cell death ligand 1 status in liquid and standard biopsies in breast cancer. *Clin Chem* (2020) 66(8):1093–101. doi: 10.1093/clinchem/hvaa121

38. Castro-Giner F, Aceto N. Tracking cancer progression: From circulating tumor cells to metastasis. *Genome Med* (2020) 12(1):1–12. doi: 10.1186/s13073-020-00728-3

39. Maly V, Maly O, Kolostova K, Bobek V. Circulating tumor cells in diagnosis and treatment of lung cancer. *vivo.* (2019) 33(4):1027–37. doi: 10.21873/invivo.11571

40. Agrawal N, Punia RS, Handa U, Attri AK. Isolation and morphology of circulating tumor cells by cell block technique in breast cancer. *Indian J Pathol Microbiol* (2021) 64(2):329. doi: 10.4103/IJPM.IJPM_855_20

41. Hayes B, Brady L, Sheill G, Baird A-M, Guinan E, Stanfill B, et al. Circulating tumour cell numbers correlate with platelet count and circulating lymphocyte subsets in men with advanced prostate cancer: Data from the ExPeCT clinical trial (CTRIAL-IE 15-21). *Cancers* (2021) 13(18):4690. doi: 10.3390/cancers13184690

42. Yu Y, Lin Z-X, Li H-W, Luo H-Q, Yang D-H, Zhou H-C, et al. Circulating tumor cells and fibronectin 1 in the prognosis of nasopharyngeal carcinoma. *Technol Cancer Res Treat* (2020) 19:1533033820909911. doi: 10.1177/1533033820909911

43. Shen F, Zhu Y, Wang F, Cai X, Ding H, Zhou F, et al. Clinical significance of circulating tumour cells and tumour marker detection in the chemotherapeutic evaluation of advanced colorectal cancer. *Colorectal Dis* (2022) 24(1):68–76. doi: 10.1111/codi.15939

44. Gkountela S, Castro-Giner F, Szczerba BM, Vetter M, Landin J, Scherrer R, et al. Circulating tumor cell clustering shapes DNA methylation to enable metastasis seeding. *Cell* (2019) 176(1-2):98–112. e14. doi: 10.1016/j.cell.2018.11.046

45. Zou K, Yang S, Zheng L, Wang S, Xiong B. Prognostic role of the circulating tumor cells detected by cytological methods in gastric cancer: a meta-analysis. *BioMed Res Int* (2016) 2016:2765464. doi: 10.1155/2016/2765464

46. Yue C, Jiang Y, Li P, Wang Y, Xue J, Li N, et al. Dynamic change of PD-L1 expression on circulating tumor cells in advanced solid tumor patients undergoing PD-1 blockade therapy. *Oncoimmunology* (2018) 7(7):e1438111. doi: 10.1080/2162402X.2018.1438111

Frontiers in Oncology

Advances knowledge of carcinogenesis and tumor progression for better treatment and management

The third most-cited oncology journal, which highlights research in carcinogenesis and tumor progression, bridging the gap between basic research and applications to imrpove diagnosis, therapeutics and management strategies.

Discover the latest Research Topics

See more →

Frontiers

Avenue du Tribunal-Fédéral 34
1005 Lausanne, Switzerland
frontiersin.org

Contact us

+41 (0)21 510 17 00
frontiersin.org/about/contact